TD

Nutraceuticals and Functional Foods for Diabetes and Obesity Control

DOCTORAL THESIS

Vítor Agostinho Rodrigues Spínola

DOCTORAL DEGREE IN CHEMISTRY
SPECIALTY IN BIOCHEMISTRY

UNIVERSIDADE da MADEIRA
A Nossa Universidade
www.uma.pt

March | 2018

Nutraceuticals and Functional Foods for Diabetes and Obesity Control

DOCTORAL THESIS

Vítor Agostinho Rodrigues Spínola
DOCTORAL DEGREE IN CHEMISTRY
SPECIALTY IN BIOCHEMISTRY

SUPERVISOR
Paula Cristina Machado Ferreira Castilho

NUTRACEUTICALS AND FUNCTIONAL FOODS FOR DIABETES AND OBESITY CONTROL

This thesis was conducted at the Organic Chemistry and Natural Products Laboratory of the Madeira Chemistry Center (CQM), University of Madeira, under the supervision of Professor Paula Cristina Machado Ferreira Castilho. The financial support was provided by Fundação para a Ciência e a Tecnlogia (SFRH/BD/84672/2012). This thesis is presented to the University of Madeira, in order to fulfill the requirements necessary to obtain a Doctor Degree (Bologna 3rd Cycle) in Chemistry.

Vítor Agostinho Rodrigues Spínola

March 2018

Funchal, Madeira - Portugal


UNIVERSIDADE da MADEIRA


CQM
CENTRO DE QUÍMICA
DA MADEIRA

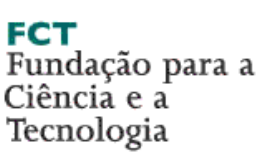
FCT
Fundação para a
Ciência e a
Tecnologia


RNE
Portuguese Mass
Spectrometry Network

Dedication

To my Mom.

"*and I needed you tonight, but you've gone to heaven*

and if you could see me now, would you remember

how you use to hold me close

how you always felt like home

and I know I feel alone

but there's an angel looking out for me tonight"

Heaven (Carolina Deslandes)

"Somos do tamanho dos nossos sonhos."

Fernando Pessoa

Acknowledgments

First of all, I thank the Centro de Química da Madeira (CQM) and the University of Madeira for the welcoming me and ensuring the necessary conditions/tools for full compliance of all my experiment and written work for my doctoral project.

I would like to express my warmest gratitude to Professor Doctor Paula Cristina M. F. Castilho, my supervisor, for giving me the opportunity to do this work, for the scientific guidance, healthy and rewarding discussions we had and valuable advices that contributed greatly to my scientific development. It has been a long journey since my supervised internship. I am very grateful for her support and for giving me the encouragement to continue on those particular difficult moments and opportunities that you have provided.

To Professor Doctor Helena Tomás for receiving me well in Biochemistry and Cell Culture Laboratory (CQM).

To Madeira Botanical Garden, in particular, Dr. Francisco Fernandes, Dr. José Augusto Carvalho and Dr. Carlos Lobo for the supply, identification and voucher numbers of plants species used in this study.

To Funchal Ecological Park, in particular, Dr. António Ferro Pereira Olival for the license to collect some plant species in their protected area.

To Esmeralda Dias from "A Quintinha das Aromáticas" (Funchal, Madeira) for the kindly supply of autumn olive (*Elaeagnus umbellata*) samples used in this research.

To Cândida Dias for the collection and supply of wax-myrtle (*Myrica faya*) and Azores blueberry (*V. cylindraceum*) samples from the Azores archipelago.

To Professor Doctor María Luisa Fernández-de Córdova, Doctor Lucía Molina-García from the Department of Physical and Analytical Chemistry, University of Jaén, for having contributed with the HPLC-MS analysis for the phytochemical characterization of plant extracts. A special thanks to Professor Doctor Eulogio J. Llorent-Martínez, also from University of Jáen, for all the support, teaching, friendship and fruitful partnership. It has been great doing research with you and I hope we can continue collaborating and publishing in the times to come.

To Professor Doctor Clévio Nóbrega, from the Department of Biomedical Sciences and Medicine, University of Algarve, for kindly providing the NADPH for the human aldose reductase assay, when it was most necessary. Also, many thanks for all those articles sent that I had not access from UMa.

To Doctor Rosa Perestrelo very special thanks for all the support with the HPLC-MS equipment. Thank you also for your teaching and technical help with the HS-SPME/GC-qMs analysis of ceriman (*Monstera deliciosa*) fruit and principal component analysis (PCA) of obtained data in all research.

To Fundação para a Ciência e Tecnologia (FCT) for the Ph.D. grant (SFRH/BD/84672/2012). Funding is also acknowledged to FCT through the Portuguese Government (Project PEst-OE/QUI/UI0674/2013) and the Portuguese National Mass Spectrometry Network (contract RNEMREDE/1508/REM/2005). The projects PROEQUIPRAM-Reforço do Investimento em Equipamentos e Infraestruturas Científicas na Região Autónoma da Madeira (RAM) (M1420-01-0145-FEDER-000008) and Centro de Química da Madeira – CQM+ (M1420-01-0145-FEDER-000005, ARDITI), funded by Madeira Regional Operational Programme (MADEIRA 1420) is also acknowledged.

I would also like to acknowledge ASAC (Austrian Society for Analytical Chemistry) for a travel grant to participate in the ISC2014 – 30th International Symposium of Chromatography (Salzburg, Austria).

I want also to show my gratitude to my NATLab colleagues, in particular, Joana Pinto and João Serina for your fellowship and help. A special thank you goes to Gonçalo Martins and Núria Fernandes, for all your patience, support, friendship and great environment. Thank you for the late afternoons moments that we shared and for making me laugh when I needed the most, making this a special journey and much easier to ride.

To Ana Cristina Olival for all your cakes, laughs and good environment. Also thank you for all your assistance with the cell cultures.

I am grateful to Doctor Carla Alves and Rita Castro for the help, availability, and valuable teaching about cell culture procedures and cytotoxicity measurements.

I also acknowledge the help of laboratory technicians Paula Andrade and Paula Vieira for their essential assistance with reagents, materials, equipment and availability.

To my friend Pedro Andrade, thank you for support and dedication shown (even being thousands of kilometers away). Thank you for every word and for every gesture that were essential throughout this last year.

To Elodie Rodrigues and André Lima, a meaningful and big “Thank you” for all your companionship, friendship, help with the collection of plant samples in the wild, all good moments that we shared and thank you for showing me what it’s like to be family. Thank you.

I want to thank my loving parents Agostinho Spínola and Fátima Spínola. Thank you for all your unconditional love, enthusiasm, unmatched care, and for always believing in me. Thank you for my education, transmitted values and work ethics, for pushing me to do better, for being an example, in conclusion, for helping to build the person that I am today.

Finally, a heartfelt and special thanks to Ricardo Garcês for your companionship, huge patience, in good and bad moments, always with a word of encouraging. Thank you for being by my side through this last decade and for never having stopped believing. All the love, continuous affection and support was essential to the completion of this long and arduous task.

Abstract

The aim of this work was to study the anti-diabetic potential of different berry-producing plants. Their mineral and phytochemical composition was studied by inductively coupled plasma - mass spectrometry and high-performance liquid chromatography/electrospray ionization tandem mass spectrometry analysis, respectively. A static model to simulate gastrointestinal digestion was employed to analyse the stability of phenolic compounds from targeted species. The mechanism of hypoglycaemic activity was evaluated in terms of *in vitro* inhibitory action on key digestive enzymes linked to type-2 diabetes (α-,β-glucosidases and α-amylase) and obesity (pancreatic lipase). Additionally, the inhibitory effect towards human aldose reductase and protein glycation, associated with long-term diabetic complications, was determined. The antioxidant activity of methanolic extracts was investigated using four different free radicals ($ABTS^{\bullet+}$, $DPPH^{\bullet}$, $NO^{\bullet}$ and $O_2^{\bullet-}$). Finally, the cytotoxicity of analysed species was assessed in Caco-2 cells by the resazurin reduction fluorescence method.

Berry species proved to be good sources of essential minerals, some of which, are known to possess hypoglycaemic effects. Analysed extracts showed diverse phytochemical profiles, anthocyanins, hydroxycinnamic acids, flavonols, flavan-3-ols and ellagitannins being the dominant compounds. Extracts showed a stronger inhibition towards glucosidases and were moderate inhibitors of α-amylase and pancreatic lipase. Potent inhibitory effects were observed in aldose reductase assay and towards formation of advanced glycation end-products. Additionally, good antioxidant activities were observed. Preliminary cytotoxicity measurements revealed that plant extracts can be considered safe for human consumption. The phenolic content and biological activities were substantially affected by the simulated *in vitro* digestion. Still, positive health effects were verified for digested samples.

The generated data about these berry-producing plants and their potential effect on the management/control of type-2 diabetes and prevention of associated complications may be useful in designing future dietary/nutraceutical strategies aimed at alleviating hyperglycaemia.

Keywords: Type-2 Diabetes; Berry-producing plants; Phenolic Compounds; Enzyme inhibition; Anti-glycation; Antioxidant activities.

Resumo

O objectivo deste trabalho foi estudar o potencial antidiabético de diferentes plantas produtoras de bagas. A composição mineral e fitoquímica foi estudada recorrendo, respectivmente, a plasma indutivamente acoplado a espectrometria de massa e cromatografia líquida de alta eficiência com espectrometria de massa. Um modelo estático para simular a digestão gastrointestinal foi utilizado para analisar a estabilidade dos compostos fenólicos das espécies alvo. A actividade hipoglicémica foi avaliada *in vitro* em enzimas digestivas ligadas à diabetes tipo-2 (α, β-glucosidases e α-amilase) e à obesidade (lípase pancreática). O efeito inibitório sob a actividade da aldose reductase e a glicação de proteínas, associadas a complicações diabéticas, foi também determinado. A actividade antioxidante dos extratos foi investigada usando quatro radicais livres diferentes ($ABTS^{\bullet+}$, $DPPH^{\bullet}$, $NO^{\bullet}$ e $O_2^{\bullet-}$). Finalmente, a citotoxicidade das espécies analisadas foi avaliada em células Caco-2 pelo método da redução da resasurina.

As bagas mostraram ser boas fontes de minerais essenciais, alguns com atribuídas capacidades hipoglicémicas. Os extratos analisados apresentaram perfis fitoquímicos diversos, sendo as antocianinas, os ácidos hidroxicinâmicos, os flavonóis, os flavan-3-oís, e os elagitaninos os compostos dominantes. Os extratos demostraram fortes inibições para as glucosidases e foram inibidores moderados da α-amilase e da lipase pancreática. Foram observados potentes efeitos inibitórios no ensaio da aldose reductase e na glicação de proteínas. Adicionalmente, observaram-se boas actividades antioxidantes. A avaliação preliminar da citotoxicidade dos extractos, revelou que são seguros para o consumo humano. O conteúdo fenólico e as atividades biológicas foram substancialmente afectados pela simulação *in vitro* do processo de digestão. Contudo, foram verificados efeitos positivos para a saúde nas amostras sujeitas à digestão.

Os dados gerados sobre as plantas produtoras de bagas analisadas relativamente ao potencial controlo da diabetes tipo-2 e prevenção de complicações associadas podem ser úteis no desenvolvimento de futuras estratégias dietéticas/nutracêuticas destinadas a aliviar a hiperglicemia.

Palavras-chave: Diabetes tipo-2; Plantas produtoras de bagas; Compostos fenólicos; Inibição enzimática; Anti-glicação; Actividade antioxidante.

Preamble

The present work was developed in the Laboratory of Natural Products and Organic Chemistry (NatLab) of the Madeira Chemistry Centre (CQM), University of Madeira (Portugal).

This study arises from the need to investigate the potential effects of edible and non-edible plants on the control/management of type-2 diabetes and obesity, as an alternative to current pharmaceutical drugs. The phytochemical profiles, ability to inhibit key digestive enzymes and protein glycation, and antioxidant activities were studied. The initial work plan of this Ph.D. project consisted of a list of more than 30 plants. Considering the results of an initial screening (yeast α-glucosidase and α-amylase assays), the plant list was shortened and we decided to focus the investigation on berry-producing plants regarding their higher inhibitory activities towards key carbohydrate-hydrolysing enzymes.

For a better understanding, the dissertation is organized in six parts. In Chapter I – Introduction, a general contextualization on the scientific topics addressed in the dissertation is given. Afterwards, Chapter II – Materials and Methods provides an explanation of the procedures and analytical assays conducted in this study. Chapter III – Results and discussion is organized in five sub-chapters: (A) addresses the phytochemical profiles (mineral and phenolic composition) of berry-producing plants under study; (B) concerns the ability of analysed extracts to inhibit the activity of key digestive enzymes linked to type-2 diabetes and obesity; (C) the inhibitory capacity of human aldose reductase activity and bovine-serum albumin glycation by fructose and ribose were assessed; (D) the antioxidant activity of plant extracts was determined against four free radicals by colorimetric assays; (E) a preliminary evaluation of the cytotoxic effects of selected extracts was assessed in Caco-2 cells. Chapter IV – Conclusions and Future Perspective is devoted to the final considerations of this project. Finally, the dissertation is completed with the references used, as well as complementary data.

The central part of this dissertation is formed by four already published scientific papers (I to IV - List of publications). The remaining data are being prepared to submit for publication in international, peer-reviewed journals in the near future. Throughout this study, other articles were published referring to the plant species not included in this dissertation, which are listed in the *Curriculum Vitae* of the author.

List of publications

A. Research Papers

I. **Spínola V.**, Pinto J., Castilho P. C. (2018) Hypoglycemic, anti-glycation and antioxidant *in vitro* properties of two *Vaccinium* species from Macaronesia: a relation to their phenolic composition. *Journal of Functional Foods*, 40: 595 – 605.

II. Pinto J., **Spínola V.**, Llorent-Martínez E. J. et al., (2017) Polyphenolic profile and antioxidant activities of Madeiran elderberry (*Sambucus lanceolata*) as affected by simulated *in vitro* digestion. *Food Research International*, 100P3: 404 – 410.

III. Llorent-Martínez E. J., **Spínola, V.**, Castilho P. C. (2017) Evaluation of the inorganic content of six underused wild berries from Portugal: Potential new sources of essential minerals. *Journal of Food Composition and Analysis*, 59: 153 – 160.

IV. **Spínola, V.**, Llorent-Martínez E. J., Gouveia S., Castilho P. C. (2014) *Myrica faya*: a new source of antioxidant phythochemicals. *Journal of Agricultural and Food Chemistry*, 62, 9722-9735.

V. **Spínola V.**, Pinto J., Castilho P. C. Evaluation of wild blackberries (*Rubus grandifolius* L.) functions targeting dietary management of type-2 diabetes: inhibitory activity towards digestive enzymes, protein glycation and antioxidant activities using *in vitro* models (ready to submit).

VI. **Spínola V.**, Castilho P. C. Polyphenols of *Myrica faya* inhibit key enzymes linked to type II diabetes and obesity and glycation of proteins (*in vitro*): potential role in the prevention of diabetic complications (ready to submit).

B. Oral communications

- **Spínola. V.**, Llorent-Martínez E. J., Castilho, P. C. Inhibition of human aldose reductase by berries polyphenos: their potential role in the prevention of diabetic complications. 5th CQM Annual Meeting, 1st -3rd February 2018, Funchal, Portugal
- **Spínola V.**, Pinto J., Castilho P. C. Phenolic composition and *in vitro* inhibitory activities of plant-producing berries on the generation of advanced glycation end-products. 10th World Congress on Polyphenols Applications, 29th June – 1st July 2016, Porto, Portugal.
- **Spínola V.**, Pinto J., Castilho P. C. Berries from Macaronesia: bioactive components and their antihyperglycaemia effects. EuroFoodChem XVIII, 13rd – 16th October 2015, Madrid, Spain.
- **Spínola V.**, Llorent-Martínez E. J., Gouveia S., Castilho P. C.; Phenolic characterization of *Myrica faya* and its relation with antioxidant activity, 1st CQM Annual Meeting, 30th – 31st January 2014, Funchal, Portugal.

C. Posters Communications

- Spínola V., Llorent-Martínez E. J., Gouveia S., Castilho P. C.; *Myrica faya*: phenolic characterization and antioxidant activity, 8th World Congress on Polyphenols Applications, 4-6th June, Lisbon, Portugal, 2014.

General Index

Index of Figures

Index of Tables

Abbreviations

A	
ABTS	2,2′-Azinobis-(3-ethylbenzthiazoline-6-sulfonic acid)
AGEs	Advanced glycation end-products
AGLU	α-Glucosidase
ALX	Allozan
AMG	Aminoguanidine
AMPK	5' Adenosine monophosphate-activated protein kinase
AMY	α-Amylase
ANTCs	Anthocyanins
AOA	Antioxidant activity
APCI	Atmospheric pressure chemical ionization
AR	Aldose reductase
ASJ	Arco de São Jorge
B	
BGLU	β-Glucosidase
BPPs	Berry-producing plants
BSA	Bovine serum albumin
BV	Boaventura
C	
CAT	Catalase
CBE	Conduritol B epoxide
CEL	Carboxyethyl-lysine
C3G	Cyanidin-3-*O*-glucoside
CI	Chemical ionization
ClO^-	Hypochlorite
CML	Carboxymethyl-lysine
COX	Cyclooxygenase
CQAs	Caffeoylquinic acids
CQM	Centro de Química da Madeira
D	
DE	Dry extract
3-DG	3-Deoxyglucosone
DM	Diabetes mellitus
1-DNJ	1-Deoxynojirimycin

DPP-4	Dipeptidyl peptidase-4
DPPH	2,2-Diphenyl-1-picrylhydrazyl
E	
ECG	(Epi)catechin-O-gallate
ECGC	(Epi)gallocatechin-O-gallate
EDTA	Ethylenediaminetetraacetic acid
ESI	Electrospray ionization
F	
FAs	Fatty acids
FAB	Fast atom bombardment ionization
FBS	Fetal bovine serum
FCR	Folin-Ciocalteu's reagent
FFAs	Free fatty acids
FL	Faial
FW	Fresh weight
FX	Funchal
G	
GC	Gas chromatography
GI	Gastrointestinal
GID	Gastrointestinal digestion
GIP	Glucose-dependent insulinotopic peptide
GLP-1	Glucagon-like peptide-1
GLUTs	Glucose transporters
GO	Glyoxal
GOLD	Glyoxal lysine dimer
GPx	Glutathione peroxidase
GRx	Glutathione reductase
H	
HAR	Human aldose reductase
HbA1C	Hemoglobin A1C
HBAs	Hydroxybenzoic acids
HCAs	Hydroxycinnamic acids
HPLC	High performance liquid chromatography
HPLC-DAD	High performance liquid chromatography with diode-array detector
HPLC-DAD-ESI/MS^n	High performance liquid chromatography with diode-array and electrospray ionization mass spectrometric detection

HSCCC	High speed counter current chromatography
HO	Hemeoxygenase
H_2O_2	Hydrogen peroxide
I	
ICP-MS	Inductively coupled plasma-mass spectrometry
IGF	Insulin-like growth factor
IL-6	Interleukin-6
IPC	Individual phenolic content
IRs	Insulin receptors
M	
MAE	Microwave-assisted extraction
MALDI	Matrix-assisted laser desorption/ionization
MCT	Myricitrin (myricetin-*O*-deoxyhexoside)
MEM	Minimum essential medium
MGO	Methylglyoxal
MPO	Myeloperoxidase
MS	Mass spectrometer
MX	Machico
N	
NADH	β-Nicotinamide adenine dinucleotide reduced
NADPH	Nicotinamide adenine dinucleotide phosphate
NBT	Nitroblue tetrazolium chloride
NEAA	Non-essential aminoacids
NEDA	N-(1-Naphthyl)ethylene-diamine dihydrochloride
NMR	Nuclear magnetic resonance
NO	Nitric oxide
NOS	Nitric oxide synthase
NOX	NADPH oxidase
p-NPB	*p*-Nitrophenyl butyrate
α-*p*-NPG	*p*-Nitrophenyl-α-D-glucopyranoside
β-*p*-NPG	*p*-Nitrophenyl-β-D-glucopyranoside
NF-kB	Nuclear factor-kappa B
O	
$O_2^{\bullet-}$	Superoxide anion radical
OH^-	Hydroxyl radical
$ONOO^-$	Peroxynitrite

P

PACs	Proanthocyanidins
PCs	Phenolic compounds
PDA	Photo-diode array
PL	Pancreatic lipase
PM	Porto Moniz
PMS	Phenazine methosulfate
PPAR-γ	Peroxisome proliferator-activated receptor gamma

R

RDA	Recommended dietary allowance
RJ	Ribeira da Janela
RNS	Reactive nitrogen species
ROS	Reactive oxygen species

S

SDG	Sorbitol dehydrogenase
SCF	Supercritical fluid chromatography
SGLUTs	Sodium-dependent glucose transporters
SOD	Superoxide dismutase
STZ	Streptotozin
SX	Seixal

T

TAC	Total anthocyanins content
TC	Terceira Island
T1DM	Type-1 diabtes mellitus
T2DM	Type-2 diabtes mellitus
TFC	Total flavonoid content
TGF-β	Transforming growth factor-β
TIPC	Total individual phenolic content
TLC	Thin-layer chromatography
TNF-α	Tumor necrosis factor-alpha
TPC	Total phenolic content
Trolox	6-Hydroxy-2,5,7,8-tetramethylchroman-2-carboxylic acid

U

UAE	Ultrasound-assisted extraction
UP	Ultra-pure
UV	Ultraviolet

UV-vis	Ultraviolet-visible

Chapter I - Introduction

1. Diabetes

Diabetes mellitus (DM) is becoming one of the most common chronic metabolic disorders worldwide (**Figure 1**) that results from disturbances in glucose homeostasis [1–6]. The global prevalence of DM in 2017 was 425 million among adults and it is estimated to affect almost 630 million people by 2045 (**Figure 1**), becoming the 7th leading cause of death in developed countries [7,8]. In Portugal, the estimated prevalence of DM in 2015 was 13.3%, that is, more than 1 million Portuguese in the 20-79 age group had DM [9]. Due to its high incidence and the vast range of associated health complications, this disease presents a significant burden in health care systems [2,5,8–10].

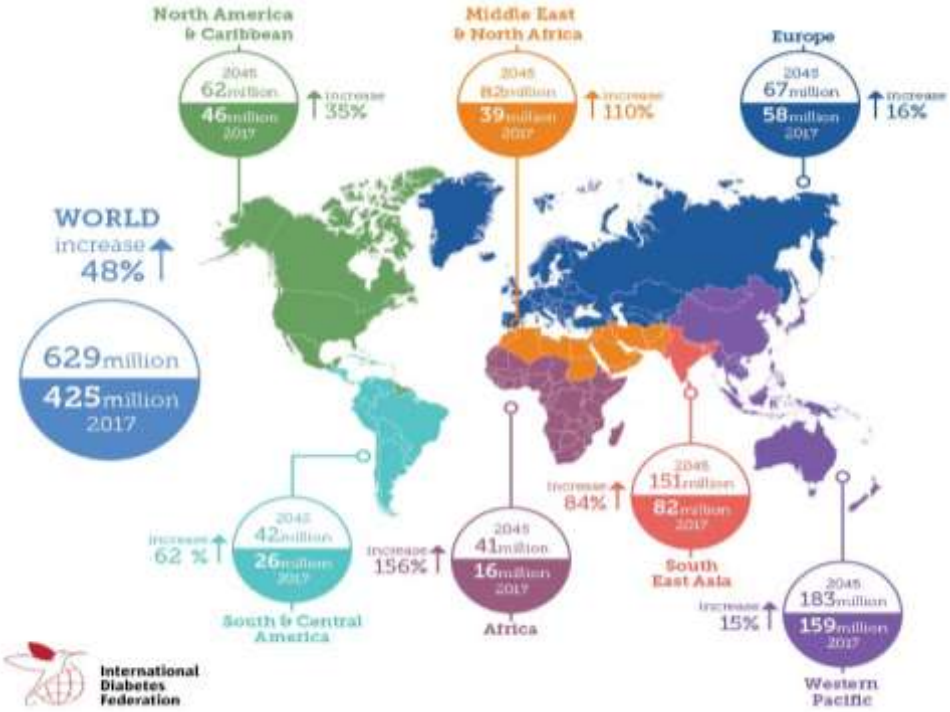

Figure 1 – Prevalence of Diabetes mellitus (DM) worldwide and per region in 2017 and 2045 (20 – 79 age group) (adapted from [8]).

DM is associated with deficiency or abnormalities in insulin secretion, or insensitivity/resistance to the metabolic action of this hormone in its target tissues, which results in raised blood sugar levels (hyperglycaemia) [3,11–13]. Lack of insulin leads to an improper balance of glucose homeostasis and disturbances of lipid and protein metabolism [1,3,14,15]. Failure of control of glucose homeostasis results in the metabolic syndrome, which comprises hyperglycaemia, glucose intolerance, chronic inflammation, dyslipidaemia and hypertension. This combination of pathological conditions leads to changes in the structure and function of major organs and tissues, especially the eyes, kidneys, nerves, heart and blood vessels. Overall, this condition diminished the patient quality of life and can lead to life-threatening complications

(neuropathy, nephropathy, retinopathy, artherosclerosis, macro- an microvascular damage, etc) and ultimately pre-mature death [3,4,14–16].

DM is commonly categorized into two main groups: type 1 diabetes (T1DM) (insulin-dependent DM) and type 2 diabetes (T2DM) (non-insulin dependent DM) [1–4,16]. The first case is characterized by insufficient or no endogenous insulin production and it accounts for 5 - 10% of the total cases, showing a higher incidence in children and adolescents. T1DM arises by autoimmune processes or infections, where pancreatic β-cells are destroyed and fail to produce insulin [1–3,5]. Hence, treatment of T1DM involves the administration of exogeneous insulin [2–4]. In the second category, the produced insulin by pancreatic β-cells is ineffective and insulin-dependent tissues (muscle, adipose tissue, liver, etc) show variable degrees of resistance to the insulin action [1–3,5,15]. T2DM is the predominant form (approximately 90 - 95% of all cases) and is generally related with older age, calorie overload, overweight, obesity, sedentary lifestyle and genetic factors [1–3,10,17].

T2DM is considered a "sneaky condition" since its harmful long-term complications develop slowly over many years before it is diagnosed [2]. "Pre-diabetes" is an intermediate stage for individuals with higher blood glucose or glycated hemoglobin A1C (HbA1C) levels than normal, but not high enough to meet the diagnostic criteria for T2DM [2,8,10]. Pre-diabetes is a warning status to the predisposition of developing T2DM and increases the risk of developing retinopathy, nephropathy, neuropathy, cardiovascular diseases and stroke [2,5,8,10]. Unlike T1DM, this condition can be controlled and even reverted with the right lifestyle alterations, including regular physical activity and weight loss and dietary intervention, by increasing consumption of fruits and vegetables, whole grains and nuts in appropriate amounts [1–4,16,18]. It has been suggested that 90% of T2DM cases could be potentially prevented [1]. This reversible particularity has made it a popular target of research, in order to find new ways to prevent/control or even avoid the onset of T2DM [2].

1.1. Carbohydrate Metabolism and Glucose homeostasis

At normal physiological state, glucose homeostasis is maintained by the peptide hormones insulin and glucagon, which tightly control blood glucose levels after ingestion of carbohydrate-rich meals [2,3,5].

1.1.1. Carbohydrate Digestion and Absorption

In humans, complex dietary carbohydrates (starch, sucrose, maltose, lactose, etc) are broken down into smaller molecules (glucose, fructose, etc) in the gastrointestinal (GI) tract before absorption [2,19,20]. α-Amylase (AMY) and α-glucosidase (AGLU) are the key enzymes in the digestion of dietary carbohydrates [2,16,19,20].

1.1.1.1. α-Amylase

AMY (α-1,4-glucan 4-glucanohydrolase; EC 3.2.1.1) (aprox. 55 kDa) performs the first step in the digestion of dietary polysaccharides, hydrolysing the α-1,4-glycosidic linkages of starch, glycogen, amylose and amylopectin [2,3,16,19]. Digestion of carbohydrates begins in the mouth. However, the action of salivary AMY is limited by the short time that food remains in this stage (about 5 % of carbohydrate digestion). Digestion by salivary AMY continues after the food reach the stomach, as long as 30 minutes. Then, its activity is stopped due to the high-acidic environment of the stomach. At the small intestinal, pancreatic AMY catalyses the hydrolysis of the remaining starch (about 70% of overall digestion) [19,20]. Maltose, isomaltose, maltotriose, and α-dextrins are the major products of AMY digestion and AGLU enzymes substrates [2–4,16,18,20].

1.1.1.1. Glucosidases

Glucosidase enzymes (including isoforms lactase, maltase, and sucrase) (260 kDa) are located in the brush border membrane of small intestine cells (enterocytes) [18–20]. Glucosidases complete the hydrolysis of oligosaccharides to monomer units [2,4,16,20]. Sucrose is hydrolysed by sucrase (sucrose alpha-glucosidase; EC 3.2.1.48) into glucose and fructose, while isomaltose is converted into glucose units by sucrase-isomaltase (oligo-1,6-glucosidase; EC 3.2.1.10). Maltose is hydrolysed by maltase (or maltase-glucoamylase; EC 3.2.1.20) [2,19,20]. All these enzymes present AGLU activity, which is the hydrolysis of (1->4)-α-glucosidic bonds [2,16,19,20]. β-Glucosidases (BGLUs) are brush border enzymes that hydrolyses (1->4)-β-glucosidic linkages, such as those found in lactose. Lactase (β-galactosidase, EC 3.2.1.108) is responsible for the hydrolysis of lactose resulting in galactose and glucose units [19].

Among all the enzymes involved in the carbohydrate digestion process, AGLU enzymes seem the most important due to the rate-limiting step in sugar hydrolysis [14,20].

Glucose, the main product of carbohydrate digestion, is highly hydrophilic and its intra-cellular transportation must be aided by specific glucose transporters (GLUTs) [3,5,19]. Glucose is actively taken up in the intestinal lumen against its concentration gradient (active transport) by the sodium-dependent glucose transporter-1 (SGLUT-1) located in the brush border of the enterocytes [2,3,5,16,19]. Then, glucose is passively released (facilitated diffusion) into the blood circulation via the glucose transporter-2 (GLUT-2), present in the basal and lateral membranes of enterocytes [2,3,5,19].

1.1.2. Glucose Homeostasis

When glucose enters the pancreas via GLUT-2, it is metabolized for energy production (glycolysis and Krebs cycle) which signals β-cells to produce and secrete insulin and suppress glucagon production by α-cells (**Figure 2**) [2,3,16,19]. Then, insulin controls the rise of blood glucose by promoting the uptake of glucose in peripheral tissues (muscle, liver and adipocytes) through translocation of GLUT-4 to the plasma membrane, enhancing glucose utilization/storage in the muscle and liver (glycolysis/glycogenesis) and inhibiting lipolysis and promoting lipogenesis in adipocytes (**Figure 2**) [2,3,5,16,19].

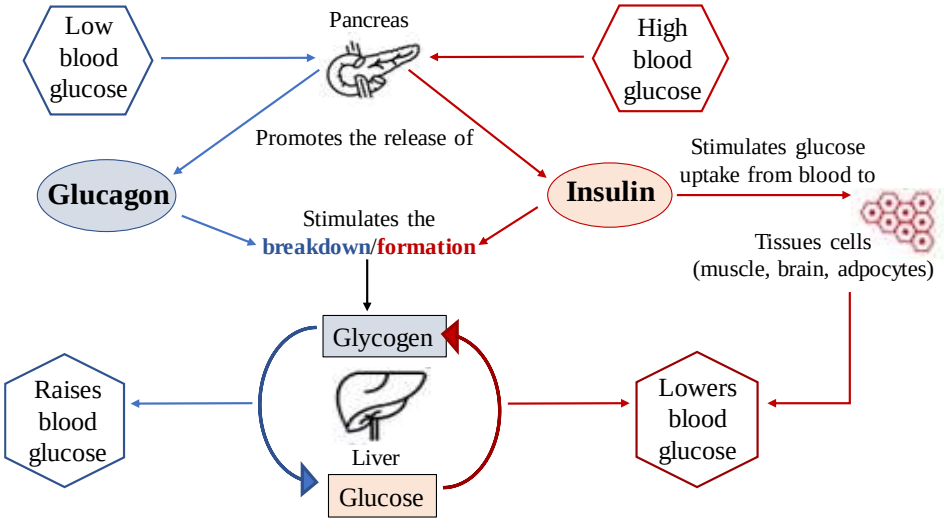

Figure 2 – Maintenance of glucose homeostasis by insulin and glucagon regulatory action (adapted from[8]).

Under fasting or between meals, blood glucose concentrations decrease to under a particular level (< 4 mM) and pancreatic α-cells secrete glucagon (**Figure 2**) [2,3]. This counterregulatory hormone acts initially on the liver, activating catabolic pathways (glycogenolysis and gluconeogenesis) to raise blood glucose to normal levels (**Figure 2**) [3,16]. Any metabolic dysregulation, associated with absolute or relative deficiency in insulin secretion or action, contributes to the development of hyperglycaemia due to depletion of glycogen storage and increased gluconeogenesis [1–3,16]. Uncontrolled or poorly managed hyperglycaemia leads, ultimately, to the onset of DM [3].

Since T2DM is the predominant form of DM [1–3], it will be the main focus of the present work.

1.2. Pathogenesis of Type-2 Diabetes

Over the past few decades, lifestyles changes characterized by excessive calorie intake (sugars and saturated-fats rich foods) and sedentary life have promoted overweight and obesity [1,5,18,21]. Obesity is a debilitating condition characterized by excess body fat accumulation, and is a key contributing risk factor for cardiovascular disease and T2DM [1,5,21–23].

Obesity-linked T2DM is associated with dyslipidemia, low-grade inflammation due to increased release and action of proinflammatory cytokines from adipose tissue (interleukin (IL)-6), nuclear factor-kappa B (NF-kB) and tumor necrosis factor-alpha (TNF-α) and activation of inflammatory signaling pathways, which impede insulin action in peripheral tissues [1,16,17,23]. Insulin resistance usually precedes and predicts the onset of T2DM (pre-diabetes) and is characterized by the reduction of glucose uptake in peripheral tissues (**Figure 3**) [2,3]. As a mechanism of compensation, there is an increased secretion of insulin by the pancreas (hyperinsulinemia) through which normal glucose tolerance is preserved [4–6]. Overtime, insulin-dependent cells become desensitized to insulin and β-cells fail to produce more insulin due to exhaustion (dysfunction), resulting in chronic hyperglycaemia [3] (**Figure 3**). In addition, activation of hepatic glucose production (glycogenolysis and gluconeogenesis) contributes to fasting hyperglycaemia. In this scenario, the muscle glucose uptake is reduced and glycogenolysis and muscle proteolysis are also enhanced. Similarly, there is activation of lipolysis in adipose tissue with elevation of fatty acids (FAs) and glycerol in the bloodstream (**Figure 3**).

Hyperglycaemia is a pre-requisite for the development of T2DM and is mainly caused by insulin resistance and impaired insulin secretion due to β-cell dysfunction [2,3,5,13,15]. Chronic exposure to glucose (glucotoxicity), free fatty acids (FFAs) (lipotoxicity) as well as increased secretory need for insulin, due to insulin resistance, lead to the diminution of pancreatic β-cell mass and further continues the progression of diabetes and its complications (retinopathy, nephropathy, neuropathy, cardiovascular disease, etc) (**Figure 3**) [2,3,16].

1.3. Oxidative stress and Type-2 Diabetes

Under normal homeostatic conditions, reactive oxygen and nitrogen species (ROS and RNS, respectively) like superoxide anion ($O_2^{\bullet-}$), hydrogen peroxide (H_2O_2), hydroxyl radical ($OH^{\bullet-}$), nitric oxide ($NO^{\bullet}$) and peroxynitrite ($ONOO^-$) are involved in important physiological processes, including defence against infections, regulation of certain biological processes (vascular tone and blood pressure) and key cellular functions (gene expression, cellular growth, differentiation, mitochondrial function and apoptosis) [2,12,24–28]. They are highly unstable and reactive oxidized molecules due to one or more unpaired electrons [2]. During the normal aerobic metabolism, ROS are mainly generated by the mitochondrial respiratory chain and inflammation processes [12]. Additionally, exogeneous sources like ultra-violet (UV) and gamma radiation

exposure, xenobiotic agents (toxins, pesticids, herbicids), polluents, drugs and diet can induce ROS [4,17].

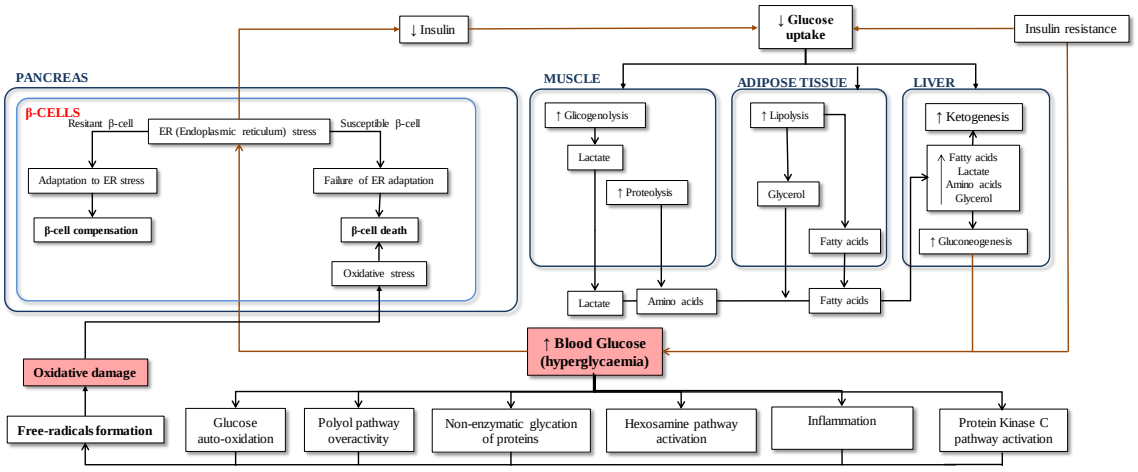

Figure 3 – Overall pathophysiology of T2DM development, with hyperglycaemia and oxidative stress as the key central mechanisms responsible for the development and progression of diabetic complications.

At normal conditions, the human organism naturally defends itself from ROS/RNS with endogenous antioxidants, including superoxide dismutase (SOD), catalase (CAT), glutathione peroxidase (GPx), glutathione reductase (GRx) and hemeoxygenase (HO)[4,12,15,17,26]. Non-enzymatic antioxidants include gluthatione, bilirubinuric acid, coenzyme Q, melanin and lipoic acid [12,17,26]. Additionally, diet can provide exogeneous antioxidants like vitamins (A, C, E), phenolic compounds (PCs), carotenoids, tocopherols and minerals [2,12,26].

Antioxidants are effective to neutralize the toxic effects of ROS/RNS [2,26,27]. However, the imbalance between these reactive species and the antioxidant defences, due to an overproduction or reduction in the removal of free radicals from cells, may cause structural deterioration and instability of macromolecules (proteins, membrane lipids, nucleic acids) resulting in cellular oxidative damage and eventually apoptosis [2–4,17,24,26]. This condition is referred to as "oxidative stress" (OS) and is considered a deleterious factor in the occurrence of several chronic pathologies (cardiovascular, neurodegenerative, cancer, etc) including pre-diabetes and onset of late complications [2,3,12,15,17,24,27].

It seems that hyperglycaemia alone is not exclusively responsible for the later diabetic complications since usually hyperglycaemia is not detected until severe complications become clinically evident [2,4]. In fact, a loop between hyperglycaemia and OS plays a pivotal role in the initiation, promotion, and progression of T2DM (**Figure 3**) [2–4,12,13,15]. Hyperglycaemia triggers glucose autoxidation, increased flux through polyol and hexosamine pathways, activation of protein kinase C (PKC) and increased formation of advanced glycation end-products (AGEs) [1,3,12–14,17]. All these detrimental pathways increases the generation of ROS which further enhances OS, contributing to various diabetic complications (**Figure 3**) [3,4,12,13].

The major cellular OS comes from overactivation of xanthine oxidase and NADPH oxidases enzymes, but mainly from mitochondrial respiration (electron transport chain complex). Hyperglycaemia condition leads to an overproduction of mitochondrial $O_2^{\bullet-}$, which is the key event for the activation of other detrimental pathways involved in oxidative stress-related diabetic complications [12,13,17]. Additionally, the combination of excessive $O_2^{\bullet-}$ and NO leads to the formation of $ONOO^-$, a powerful oxidant responsible for lipid peroxidation [2,12,17,27]. When occurring, lipid peroxidation exert cellular damages associated with pathophysiology of inflammation, atherosclerosis, etc [12,17,29]. OS activates intracellular stress-signaling pathways (via NF-kB) and contribute to the expression of transforming growth factor-β (TGF-β), insulin-like growth factor (IGF) and TNF-α, which are involved in insulin resistance [2,5,13,15,17]

Due to the low antioxidant enzymes levels (CAT, GPx, SOD) and large swings in protein flux through its secretory pathways, pancreatic β-cells are exquisitely sensitive to ROS/RNS [2,14,17]. Hyperglycemia-induced OS is an important factor in pancreatic β-cells dysfunction and destruction in T2DM [3,5,12,15,17]. Therefore, OS is associated with the decrease in insulin secretion and its action on target tissues, accelerating disease progression from insulin resistance, impaired glucose tolerance and ultimately T2DM.

1.4. Treatment of Type -2 Diabetes

1.4.1. Conventional therapy

At early stage (pre-diabetes), the slight hyperglycaemia can be controlled through lifestyle modification (diet restriction and physical activity) [2–4,17]. Generally, prescription of anti-diabetic drugs are needed for patients who fail the preliminary therapy [2,3]**.** The main pharmacological intervention includes a wide variety of oral anti-diabetic agents (AMY and AGLU inhibitors, biguanides, thiazolidinediones, sulfonylureas, etc) with the aim of improving glycemic control and prevention of diabetes complications (**Table 1**). Their main therapeutic mechanisms include inhibition of glucose digestion, reduction of hepatic glucose production, enhancement of pancreatic insulin secretion and peripheral glucose uptake [1–4,13,15,17]. Glucagon-like peptide-1 (GLP-1) receptor agonists, GLUTs-2 and dipeptidyl peptidase-4 (DPP-4, EC 3.4.14.5) inhibitors are more recent therapies [2,4,11,14,17,30].

Due to the multifactorial pathogenicity of T2DM, the available therapeutics are used mostly in combination to restore normal glucose levels in blood [4,14]. However, none of these approaches can be termed as an ideal one, due to some undesirable side effects (**Table 1**), high costs, and often response decrease after prolonged use. To overcome the adverse effects, there is a demand to research for novel targets and safer and more effective hypoglycemic agents [2–4,14]. In such context, plants have long been considered a target for source of new anti-diabetic

agents based on their traditional use, less side effects and economic viability [11,13,31]. In fact, current medicines today were based on natural products properties [2,4].

1.4.1.1. Inhibition of digestive enzymes

In diabetic patients, the rapid digestion and absorption of carbohydrates is not desirable. Post-prandial hyperglycemia plays an important role in the incidence of T2DM and related complications [2,3]. Therefore, controlling post-prandial hyperglycaemia, by slowing down glucose metabolism via inhibition of the activities of AGLU enzymes, is a key strategy to manage this disease [1,4,14,15,18].

The use of synthetic drugs that inhibit digestive enzymes (AGLU, AMY and PL) has been proposed as a treatment for T2DM and obesity [3,14,19,20]. Acarbose **(**Glucobay®, Precose®, Prandase®) (**Figure 4**), isolated from *Steptomyces spp*., is the most prescribed drug for inhibition of AMY and AGLU [2,20]. Other employed medication include miglitol (Glyset®) (**Figure 5**) and voglibose (Glasen®) (**Table 1**). These drugs delay the digestion of complex carbohydrates, thus decreasing the post-prandial hyperglycaemia. However, these medications produce undesirable GI disturbances (**Table 1**) [2,20].

In humans, 50-70% of dietary lipids are mainly hydrolysed by pancreactic lipase (PL) (E.C. 3.1.1.3; triacylglycerol acyl hydrolase) (50 kDa) in the small intestine, yielding glycerol and FAs as main products [18,20,21]. Inhibition of PL activity is a therapeutic approach used to reduce calorie intake, promote weight loss and combat obesity in diabetic patients [18,22,23]. Orlistat (Xenical®, Alli®) (**Figure 4**), a synthetic derivative of a lipostatin produced by *Streptomyces toxytricini*, was the first effective PL inhibitor approved as anti-obesity drug [20,21,32]. However, oily spotting, severe evacuations myocardial infarction have been reported from this drug intake [20].

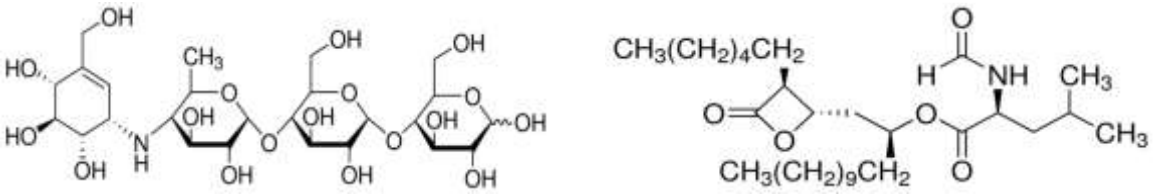

1 **2**

Figure 4 - Chemical structure of acarbose (**1**) and orlistat (**2**).

Table 1 - Main oral anti-diabetic drugs, their mechanisms of action and side effects.

Categories	Target	Mechanism	Example	Main Side Effects
AMY and AGLU inhibitors	Small intestine	Reduce carbohydrate digestion and absorption	Acarbose, Miglitol, Voglibose	Diarrhea, nausea, abdominal bloating, flatulence
Biguanides	Liver, muscle and adipocytes	Reduce hepatic glucose production (gluconeogenesis) and promotes peripheral glucose uptake (reduce insulin resistance via AMPK[1] activation)	Metmorfin, Phenformin	Diarrhea, nausea, abdominal pain, lactic acidosis
DPP-4 inhibitors	Small intestine	Reduce glucagon and glycaemic levels by inhibiting DPP-4 enzyme[2]	Sitagliptin, Vidagliptin, Saxagliptin, Linagliptin, Gemigliptin, Teneligliptin	Nasopharyngitis, headache, vomiting, nausea, pancreatitis, hypersensitivity, skin reactions
Sulfonylureas	Pancreas	Stimulate pancreatic insulin production	Glibenclamine, Glipizide, Tolbutamine, Chlorpropamide	Hypoglycaemia, weight gain, skin rash or itching
Thiazolidinediones	Liver, muscle and adipocytes	Reduce hepatic glucose production (gluconeogenesis) and promotes peripheral glucose uptake (reduce insulin resistance via PPAR-γ[3] activation)	Rosiglitazone	Hepatotoxicity, edema, increased risk of heart failure, weight gain, anemia

[1]AMPK (5' adenosine monophosphate-activated protein kinase, EC 2.7.11.31) has a key role in glucose and lipid homeostasis control [1,2,15,23]. Activation of this pathway in adipose tissue and skeletal muscle increases GLUT4 expression and membrane translocation, which provides a greater uptake and utilization of glucose through insulin-independent mechanisms; and simultaneously inhibits hepatic gluconeogenesis, which results in lower glucose blood circulation [1,2,5,15,16,23]. [2]DPP-4 is a serine exopeptidase responsible for the degradation of incretins (GLP-1 and glucose-dependent insulinotopic peptide, GIP) which maintain glucose balance by stimulation of insulin secretion. Inhibition of DPP-4 will prologue the half-life of incretins (~ 2 min) and, consequently, inhibit glucagon secretion and elevate insulin levels in human body [2,4,14,17,30]. [3]PPAR-γ (peroxisome proliferator-activated receptor gamma) is a major regulator of fatty acid storage and glucose metabolism in adipocytes. Activation of PPAR-γ lowers blood glucose levels, by improving the insulin action and glucose uptake, without increasing pancreatic insulin secretion [1,3,4,14].

1.4.2. Medicinal Plants and Phytotherapy

Since ancient times, edible and non-edible plants are used in traditional medicine throughout the world to treat T2DM and related complications [2,4,11,13,14]. Currently, approximately 800 plant species and their active extracts are still relevant for their anti-diabetic properties [11,14]. Plants are rich in unique secondary metabolites such as phenolic compounds (PCs), alkaloids, terpenoids, polysaccharides, phytosterols, etc, that have been regognized for their beneficial health effects [4,13,14]. Flavonoids, terpenoids and phenolic acids constitute the most studied and effective compounds for attenuation of diabetic complications [2,13]. As a result, plant extracts have drawn the attention of the scientific community due to their efficiency and fewer toxic and side effects [11,13]. Additionally, in developing countries where conventional drugs pose an economic burden for rural population, plants offer a cheaper and, in the case of T2DM, effective alternative [3,11,13].

There are some natural isolated compounds that possess higher therapeutic potential than synthetic drugs [11]. For example, 1-deoxynojirimycin (1-DNJ) or moranoline (**Figure 5**), isolated from mulberry (*Morus spp*.), is a more effective AGLU inhibitor than acarbose [14,33]. Miglitol (Glyset™) (**Figure 5**) is a synthetic N-hydroxyethyl derivative of 1-DNJ used in the treatment of T2DM (**Table 1**). In this view, natural products are potential sources of new anti-diabetic drugs either by providing lead molecules or as natural herbal products (infusions, teas, tinctures, poultices, powders, etc) [2,3,22].

Detailed revision about plant extracts and bioactive compounds with reported *in vitro* and *in vivo* anti-diabetic properties is documented in several works [4,11,13,14].

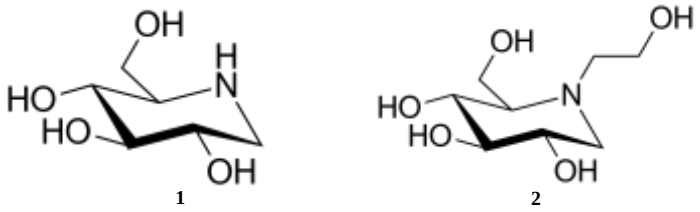

Figure 5 - Chemical structures of 1-deoxynojirimycin (**1**) and miglitol (**2**).

2. Phenolic Compounds and Type-2 Diabetes

Plant-derived products (i.e. fruit, vegetables, herbs, medicinal plants) are considered valuable sources of health-promoting phytochemicals [1,3,13,15,16,22]. In fact, a long-term consumption of fruit and vegetables has been associated with a low risk of development of T2DM, obesity, cancers, cardiovascular and neurodegenerative diseases [1,5,16,18,26,34,35]. Within secondary metabolites, PCs stand out due to their several biological activities and positive health effects (antioxidant, anti-inflammatory, anti-viral, antibacterial, anti-atherosclerotic, anti-proliferative, etc)[1,2,15,36,37]. Hence, PCs constitute a dietary resource for prevention of OS-induced diseases, such as T2DM [2,18].

2.1. Phenolic Compounds

PCs are a heterogeneous class of low to high molecular weight secondary metabolites that result from shikimate, acetate and mevalonate pathways [2,16,37,38]. These are synthesized during normal plant development (growth, reproduction) but are mostly involved in response to abiotic and biotic stress conditions like sun UV radiation, infection by pathogens (bacteria, fungi), attack by herbivores and wounding [1–3,20,39]. Additionally, this class of compounds is responsible for the organoleptic properties (flavour, bitterness, astringency, pigmentation) of plants [2,3,5,37,38,40]. PCs are practically ubiquitous in medicinal and edible plants, being the main group of secondary metabolites in human diet [2,15,37,40].

PCs are characterized by having at least one aromatic ring with one or more hydroxyl groups attached (**Figure 6**)[2,20,36,38,40,41]. They can be found in the free form (aglycones) but are generally conjugated to sugars (hexosides, pentosides, glucuronides), organic acids (citric, malic, quinic, shikimic acids) or acylated with other PCs [1,2]. This contributes to their complexity and the large number of identified individual molecules (> 8000) [1,16,37,38].

These compounds are mainly divided into two main groups, non-flavonoids and flavonoids, based on their chemical structure (**Figure 6**). The simplest PCs are phenolic acids, which are subdivided into two classes: hydroxybenzoic acids (HBAs) and hydroxycinnamic acids (HCAs). Flavonoids are more complex molecules and there are six main sub-groups: flavonols, flavones, isoflavones, flavanones, flavan-3-ols and anthocyanidins (**Figure 6**) [1–3,15,16,20,36–38,40]. Aurones, chalcones, flavan-3,4-diols, coumarins, lignans, and stilbenes (e.g. resveratrol) comprises other classes of non-flavonoids [1,3,15,16,20,37,41]. In this work, the focus will be on phenolic acids and flavonoids since they are the most relevant dietary groups of phenolics.

2.1.1. Phenolic acids (non-flavonoids)

Phenolic acids are composed by a single phenolic ring and classified as HBAs (C6-C1) and HCAs (C6-C3) (**Figure 6**) [2,15,20,40]. The most common HBAs are *p*-hydroxybenzoic, protocatechuic, gallic, vanilic and syringic acids, present in berries (cranberries, raspberries) and nuts [2,15,37]. Gallic acid can be converted to ellagic acid, which is the basic structure of hydrolysable tannins. These molecules consist of a polyol central core (e.g. D-glucose, flavonoid) and the hydroxyl groups are partially or totally esterified with gallic acid (gallotannins) or ellagic acid (ellagitannins) [1,2]. Hydrolysable tannins are common in pomegranate, strawberries, blackberries and raspberries [2,35].

The most common HCAs are *p*-coumaric, ferulic, sinapic and caffeic acids, the latter most often esterified with quinic acid as in caffeoylquinic acids (CQAs) (**Figure 6**). HCAs are significative in berries, apples, cereals, coffee and green-leafy vegetables [2,15,37,40].

2.1.2. Flavonoids

Flavonoids are the largest and most studied group of dietary PCs (> 4000 molecules) [2,15,37,38,40]. Their basic structure (C6-C3-C6) contains two phenolic rings (A- and B-rings), which are linked by a three-carbon chain that forms an oxygenated heterocycle (C-ring). Based on the substitution patterns of C-ring (oxygenation, alkylation, glycosylation, acylation, etc), flavonoids can be divided into six main sub-classes: flavonols, flavones, flavanones, isoflavones, flavan-3-ols and anthocyanidins (**Figure 6**) [1,5,15,20,38,40]. Flavonoids are usually associated to sugar moieties (glycosides) or other compounds, with the conjugation occurring at the 3- and 7-positions [2,37].

2.1.2.1. Flavonols

Flavonols are structurally characterized by a 3-hydroxy pyran-4-one group on the position 3- of the C-ring and a 2,3-double bound (**Figure 6**). They are the most abundant flavonoids, especially in fruits, vegetables (onions, spinach, broccoli) and tea. Quercetin, kaempferol and myricetin are representative of this class (**Figure 6**) [2,15,37,38].

2.1.2.2. Flavones

Flavones are structurally similar to flavonols, but they lack 3-hydroxygroup on the C-ring (**Figure 6**). They are not so common in human diet, but are present in grains, herbs, peppers, parsley and celery. Apigenin and luteolin are the most abundant dietary flavones [2,15,37].

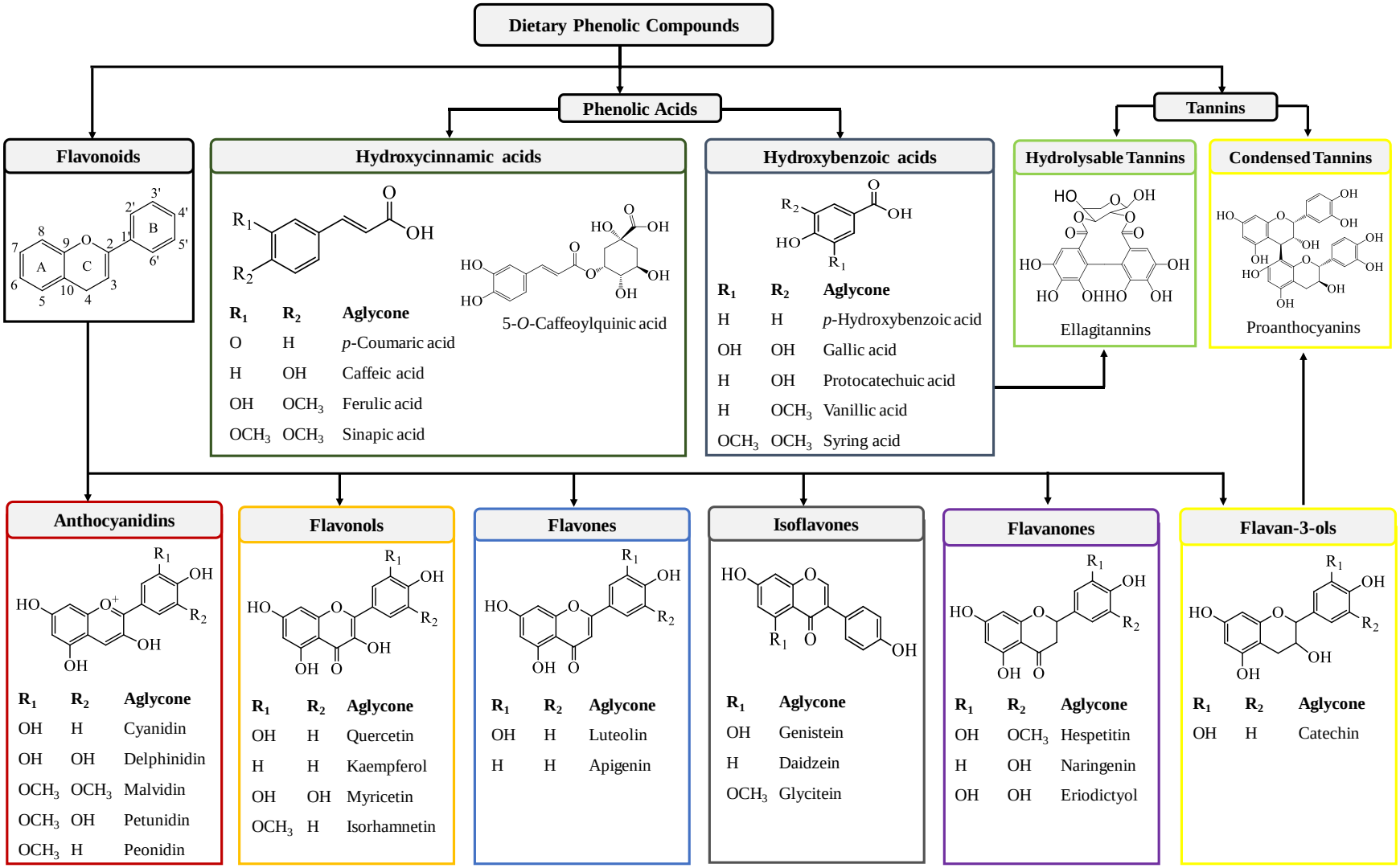

Figure 6 – Basic chemical structures of main dietary of phenolic compounds.

2.1.2.3. Isoflavones

Isoflavones possess the B-ring attached to the C-3, rather than in the position 2 (as in flavones) (**Figure 6**). The most significant amounts of isoflavones are found in soybean and its by-products (milk, miso, tofu), green beans, lentils, chickpeas and peanuts. Genistein, glycitein and daidzein are the three main isoflavones aglycones [2,15,37].

2.1.2.4. Flavan-3-ols

Flavan-3-ols are characterized by the absence of the pyran-4-one structure and the C-2,3-double bond (**Figure 6**). These flavonoids vary from the simple monomer form (catechin and (-)-epicatechin) to oligomers and polymers (proanthocyanidins, PACs) (**Figure 6**). The structure of PACs, also known as condensed tannins, is dependent on the kind of monomer (catechin, (epi)-catechin) and the type of connection between units (**Figure 6**) [1,2,37]. Tea, red wine, beans, apricots, apples, cherries, chocolate, and cinnamon are among the richest sources of flavan-3-ols [1,2].

2.1.2.5. Flavanones

Flavanones are characterized by a saturated 2,3- bond in the C-ring (**Figure 6**). These compounds are mainly found in citrus fruits (lemons, oranges, grapefruits), mint and tomatoes. The most common dietary flavanones are eriodictyol, hesperitin, and naringenin [2,15,38].

2.1.2.6. Anthocyanidins

Anthocyanidins are the most important pigments in plant foods. They are widely distributed in red fruits (berries, plums, cherries, grapes) and certain dark coloured vegetables (cabbage, beans, onions)[2,5,15,36–38,42]. Their colour can range from blue, purple and red, depending on the pH and their structural composition. This property is related to the presence of a flavylium ion on the C-ring [36,42,43]. The most important dietary anthocyanidins are cyanidin, delphinidin, malvidin, pelargonidin, peonidin, and petunidin (**Figure 6**) [2,15,42,43]. When aglycones are conjugated to a sugar moiety, they are denominated as anthocyanins (ANTCs) [2,36,37,42].

2.2. Digestion, Absorption and Metabolism of Phenolic Compounds

To exert their beneficial properties, PCs must be first delivered to and absorbed in the GI tract and transported in the bloodstream to reach tissues and organs [40,44,45]. During digestion, PCs undergo several transformations due to physical, chemical and biochemical conditions, thereby, affecting their bioavailability[1] [40,46–49]. Hence, determination of PCs content directly from foodstuff is not enough for the prediction of potential *in vivo* effects. Metabolites formed from PCs may be different from their original compounds as a result of an intensive metabolism during digestion [40,41]. This is why data from animal studies or human interventions are not as promising as those from *in vitro* studies [3,16,27,35,47].

Digestion starts in the mouth, where mastication and saliva action enable the release of food constituents [44,45,50,51]. Decreasing the particle size enlarges the contact area available for the attack by digestive enzymes, thus increasing the overall digestion efficiency. Once in the stomach, the mixing and acidic conditions have low impact on PCs [41,44,48,49,52–55]. In the small intestine, PCs undergo substantial modifications (hydrolysis, oxidation, epimerization and/or degradation) since they are highly unstable in alkaline environments [40,41,44,47,49,56]. Food matrix and co-consumed foods, basic structure, molecular size, polymerization, glycosylation, and solubility of PCs greatly determine their absorption in the lumen [1,2,16,41,44,50]. Dosage, prior diet, gender and differences in the gut microbial populations are also important factors [1,35,45]. While aglycones and some simple phenolic acids can be directly absorbed in the small intestine, large and polymerised PCs are not readily uptaken [2,40,41]. Gallic acid and isoflavones are best absorbed and in decreasing order so are flavones, catechins, quercetin glycosides and flavanones. The weakest absorption was reported for PACs, (epi)catechin-gallate (ECG) and ANTCs [1,40,41]. Therefore, the most abundant PCs in human diet are not necessarily those with the highest bioavailability [2,40,41]**.**

Phase I of PCs metabolism is the cleavage and release of the aglycone moiety for absorption, which takes place on the surface of enterocytes by the action of endogenous cytosolic BGLU (EC 3.2.1.21) and lactase-phlorizin hydrolase (EC 3.2.1.108; 3.2.1.62) [1,2,15,35,40,41,45]. However, only a small amount of PCs (5 - 10%) is absorbed in the small intestine [1,16]. The majority of the ingested PCs reach the colon, where they undergo intensive microbiota metabolism prior to

[1]In nutrition, bioavailability of a nutritional or non-nutritional compound includes its gastrointestinal digestion (GID), absorption, metabolism, tissue distribution and bioactivity. Bioaccessibility and bioactivity are the most important factors determining the bioavailability of a substance. Bioacessibility refers to the quantity or fraction of a compound that is released from food matrix, during gastrointestinal digestion (GID), and becomes potentially available for further uptake and absorption. Bioactivity is the specific physiological effect (antioxidant, anti-inflammatory, etc) upon exposure to a compound [41,47].

absorption [1,2,15,16,35,40,45]. Colonical bacterial enzymes catalyse deglycosylations, dehydroxylations, and fermentation that leads to aromatic ring-fission products (phenolic acids, catechols, among others metabolites) [1,2,35,40,45,52].

After absorption, uptaken molecules undergo intensive phase II transformations, which accounts for the absence or low concentrations of aglycones in blood [1,2,40,41,45]. These processes occur mainly in the liver and involve methylation, glucuronidation and sulfuronidation of aglycones, resulting in conjugated forms [1,2,15,16,40,47]. Metabolites are, then, transferred to the bloodstream and delivered to peripheral tissues where may exert their beneficial effects [16,40,44,45]. Phase II metabolism is responsible for increasing the hydrophilicity of PCs, which facilitates their excretion through the urine and bile (feces) [1,45].

The low absorption of PCs, extensive metabolism in the gut and rapid elimination from the body are greatly responsible for their low bioavailability after consumption [1,2,15,40,45,47].

2.2.1. *In Vitro* Models for Simulation of Phenolic Compounds Digestion

Methods for determining bioavailability and/or bioaccessibility of food components involve *in vitro* or animal/human (*in vivo*) models [44,46,57]. The latter provide the most accurate results and have been used for a great variety of compounds and foodstuffs [46,58]. However, these are lengthy, costly, and due to ethical restrictions and severe protocols, their use is limited [44,46]. As a result, much effort has been directed to the development of *in vitro* procedures that enable the prediction of PCs stability during digestion [41,47,57].

In vitro digestive models are a useful alternative by simulating the putative behaviour of food components in the GI tract since they are simple, rapid, less expensive and not subject to restrictions [44,46,57,58]. Despite their limitation regarding the significance of generated data [41,44,46,47,57], similar trends for digestion of PCs are obtained by *in vitro* and *in vivo* models [59].

GI models try to reproduce the physiological conditions in the mouth, stomach, small intestine, and occasionally large intestinal fermentation [46,47,57]. The digestion process is simulated under controlled conditions (temperature, pH, digestion time, salt concentrations, bile acids, etc) using commercial digestive enzymes (*e.g.* AMY, pepsin, pancreatin, PL, etc) while the final absorption process is commonly assessed using Caco-2 cell cultures or colonic fermentation [41,44,51,52]. In general, *in vitro* models can be divided in two categories: static models, where the products of digestion remain largely immobile and do not mimic physical processes such as shear, mixing, hydration, and so on; dynamic models try to include physical and mechanical processes (mechanical forces, continuous changes in pH, secretion flow rates) and temporal changes to mimic

in vivo conditions [44,47,57]. However, these latter models are much more labor- and cost-intensive than the static ones [47], which are the most widely used for screening PCs bioaccessibility [41].

2.3. Phenolic Compounds as Potential Anti-diabetic Agents

Intake of PCs-rich foods and/or supplementation (nutraceuticals and functional foods) has been suggested as prophylactic therapy against T2DM and latter complications [2,5,15,16,18]. Additionally, due to their safety and fewer secondary effects, PCs can be used synergistically with pharmaceuticals and reduce their dose or intake [2,3,15,60,61]. Therefore, PCs have become popular emerging sources of natural anti-diabetic drugs discovery and development [1–3,15].

The glycaemic control is putatively achieved by dietary PCs due to the integration of multiple and complementary mechanisms to improve glucose homeostasis (**Figure 7**): modulation of glucose digestion and absorption, regulation of the carbohydrate homeostasis, protection and restoration of β-cells integrity, stimulation of insulin release and improvement of glucose peripheral uptake through regulation of insulin dependent and independent signalling pathways. Additionally, PCs can also inhibit aldose reductase (AR) activity, prevent the formation AGEs and alleviate OS and inflammatory status, associated with the development of long-term diabetic complications [1–3,5,6,15,16].

Dietary human interventions are scarce, therefore, most of scientific evidence arises from *in vitro* or animal studies [3,5,16]. The most common *in vitro* models include inhibition of standard enzymes (AMY, AGLU, PL, etc) commercially available using specific probes as substrates (reducing sugars or synthetic molecules) accompanied by spectrophotometric measurements [18,19,22]. In addition to enzymatic assays, cellular models (Caco-2, HepG2, etc) are often used to evaluate glucose uptake or the effect of OS-induced toxicity [5,11,19,23,62,63]. Animal models provide more accurate results and use rats and mice with diet or chemical induced-diabetes [11,13,14]. In the latter case, pancreatic β-cells are destroyed by allozan (ALX) or streptotozin (STZ) treatment resulting in insulin deficiency, thereby resembling the T2DM in humans [14]. Overall, most epidemiological and intervention studies showed that dietary PCs were associated with a lower risk of T2DM, but these have not been as successful as *in vitro* and animal studies have pointed out [16]. Further investigation and new approaches are needed to clarify the inconsistent results and confirm the beneficial effects of dietary PCs [1,3,6,16].

In the following sub-sections, the main mechanisms involved in the potential anti-diabetic properties of PCs are summarised.

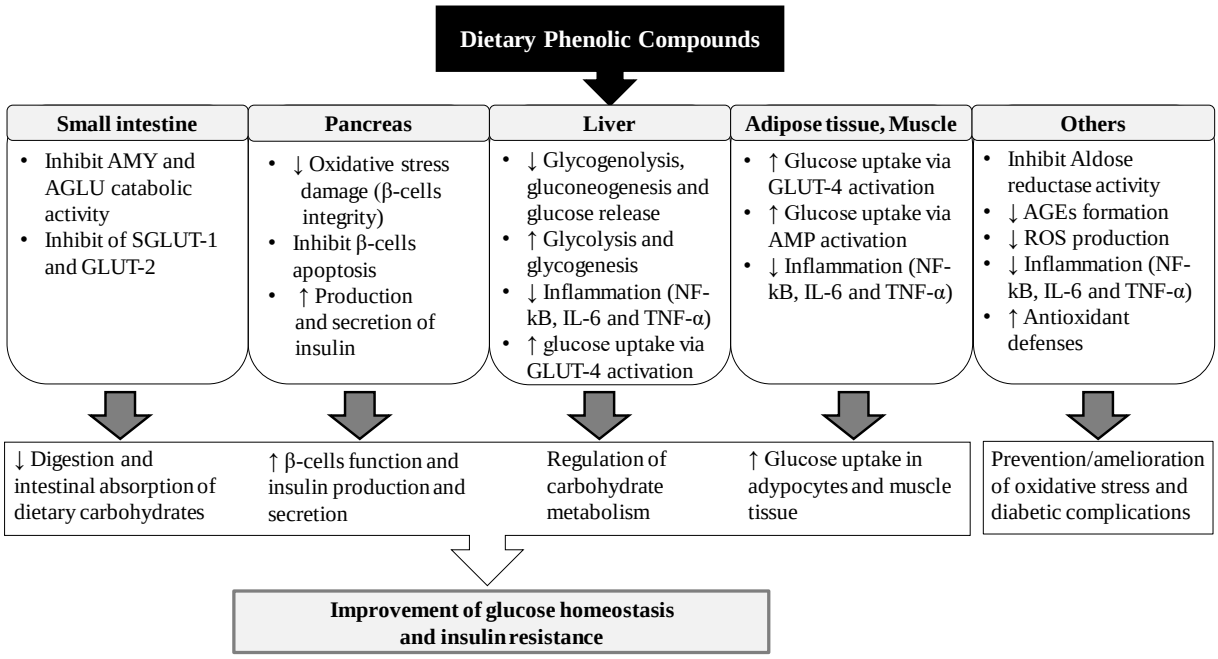

Figure 7 – Potential health benefits of phenolic compounds on management/control of hyperglycaemia in T2DM (adapted from [16]).

2.3.1. Inhibition of Carbohydrate Digestion, Absorption and Metabolism

Due to their importance in carbohydrate metabolism, AMY and AGLU enzymes are the first therapeutic target for T2DM [15,20]. Inhibition of their hydrolysing activity by PCs is considered an effective therapeutic tool to reduce post-prandial hyperglycaemia since it can limit the digestion of carbohydrates and, therefore, reduce their absorption (**Figure 7**)[1–3,5,18]. Phenolic acids (CQAs, rosmarinic acid), flavonoids (quercetin, luteolin, catechins and ANTCs) and tannins have been reported as effective carbohydrate-digestive enzymes inhibitors [1–3,15,16,18,21,61,64,65].

When insulin resistance occurs, T2DM progresses, and the risk for developing hypertension, obesity and cardiovascular diseases increases greatly [1,2]. CQAs, ANTCs and tannins are also capable to modulate lipid metabolism by inhibition of PL activity [15,18,20,21,23]. This could potentially help to prevent diabetes-induced obesity and cardiovascular pathogenesis by promoting weight loss and improving dyslipidemia [15,18].

Inhibition of GLUTs is another target for glycaemia control since it prevents glucose absorption, thereby avoiding the increase in post-prandial glucose (**Figure 7**) [2,3,15,16]. Phloridzin, flavan-3-ols (ECG and gallo(epi)catechin-*O*-gallate, EGCG), flavonols (quercetin, myricetin, isorhamnetin) naringenin and phenolic acids (CQAs, caffeic acid, ferulic acid) can limit glucose absorption via interaction with SGLUT-1 and GLUT-2 [2,3,15,16].

Another therapeutic mechanism is the suppress of hepatic glucose production by inhibition of glycogenolysis and gluconeogenesis routes (**Figure 7**) [2,3,5,15,16]. Diosmin, narigenin, isoflavones (genistein and daidzein), ferulic acid, hesperidin, EGCG, and 5-*O*-CQA presented positive inhibitory effects towards enzymes involved in these pathways (pyruvate carboxylase (EC 6.4.1.1), phosphoenolpyruvate carboxykinase (EC 4.1.1.32), fructose-1,6-bisphosphatase (EC 3.1.3.11), and glucose-6-phosphatase (EC 3.1.3.9)) and simultaneously enhanced hepatic glucose uptake and glucogenesis [1–3,15,16].

2.3.2. Protection of Pancreatic β-Cells Integrity and Enhancement of Insulin Secretion

Hyperglycaemia, hyperlipidaemia, increased ROS production and inflammation exert deleterious effects on β-cells function, ultimately leading to their failure and/or destruction [1,3,16]. PCs contribute to the protection of β-cells by alleviating glucolipotoxicity, ROS/RNS action and cells apoptosis and increasing the defence capacity of β-cells (**Figure 7**)[1–3,5,15]. Simultaneously, PCs promote β-cell proliferation and stimulates insulin production and secretion [1,3,5]. Resveratrol, flavones (diosmin, apigenin, luteolin), flavonols (quercetin, rutin) and flavan-3-ols ((epi)-catechin and ECGC) effectively prevent β-cells dysfunction and failure and, at the same time, they promote insulin secretion [3,15].

2.3.3. Improvement of Insulin Activity and enhancement of Glucose Uptake

PCs contribute to the increase of insulin sensitivity and enhancement of peripheral glucose tissue uptake through modulation of both insulin sensitive and non-insulin sensitive signalling pathways (**Figure 7**)[2,3,5,15,16].

These phytochemicals can influence insulin action by activating PPAR-γ, which improves the sensitivity of membrane insulin receptors (IRs). Consequently, insulin binding to target receptors increases the expression of GLUT-4, the main glucose membrane transporter in adipocytes and skeletal and cardiac muscles. This facilitates glucose uptake into these tissues and consequent clearance from the blood through insulin-dependent mechanisms (**Figure 7**) [1–3,42]. Alternatively, when insulin is low/absent, PCs can also promote glucose uptake *via* activation of AMPK signalling pathway accompanied by translocation of GLUT-4 to plasma membrane (**Figure 7**)[3,5,16,23]. Therefore, increase of GLUT-4 expression is considered an attractive target for developing new treatments for T2DM, but also for obesity and metabolic syndrome [2,3,15,16,23]. The improvement of glucose uptake through GLUT-4 by HCAs (CQAs, ferulic acid), flavan-3-ols (PACs, EGCG), quercetin, isoflavones and resveratrol is comparable to the performance of biguanides and thiazolodinediones, main oral hypoglycemic drugs (**Table 1**)[1–3,5,15,16].

In addition, quercetin, kaempferitin and catechin showed the ability to mimic the action of insulin by interfering with IRs and consequently stimulate glucose uptake [3].

2.3.4. Inhibition of Human Aldose Reductase (HAR) Activity

Human aldose reductase (EC: 1.1.1.21, HAR) is the first enzyme in the polyol pathway. Under normal physiological conditions, its substrate affinity to glucose is very low and primarily reduces toxic aldehydes and carbonyls (**Figure 8**) [3,12,66]. But, in hyperglycaemia conditions, this enzyme reduces the excessive glucose to sorbitol, which is further metabolized to fructose by sorbitol dehydrogenase (EC: 1.1.1.14, SDG) (**Figure 8**) [4,12,17,67]. Overactivity of HAR is an important factor in the pathogenesis of retinopathy, neuropathy, nephropathy and cataract [3,12,66–68]. It is also associated with increased OS due to enhancement of ROS production and depletion of cellular NADPH that leads to low GSH levels (**Figure 8**) [4,12,17,67].

Currently, inhibition of HAR activity by PCs has gained importance in T2DM treatment (**Figure 7**)[3,6,67,68]. HBAs (gallic, vanillic, syringic, and protocatechuic acids), CQAs, ferulic acid, flavonols (quercetin, quercitrin and myrciarin IV), EGCG and ellagic acid have been reported as effective HAR inhibitors [3,67,69].

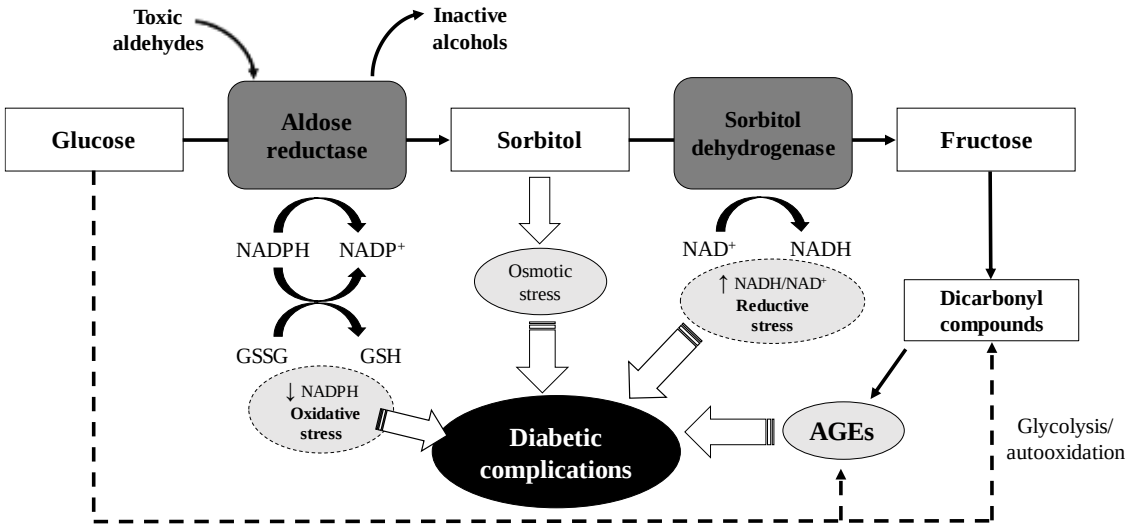

Figure 8 – The polyol pathway flux. In hyperglycaemia conditions, glucose is sequentially reduced to sorbitol and fructose by the combined action of human aldose reductase (HAR) and sorbitol dehydrogenase (SDG) (adapted from [66,67]).

2.3.5. Inhibition of Advanced Glycation End-Products (AGEs) Formation

The elevated blood glucose levels cause also the generation of AGEs through non-enzymatic Maillard or "browning" reaction [3,12,66]. These adducts are originated via binding of carbonyl groups (ketones or aldehydes) of reducing sugars (glucose, fructose, ribose) to free amino groups of proteins. **Figure 9** summarises the non-enzymetic reactions that leads to AGEs generation. The first product of the glycation reaction is the fast and highly reversible Schiff base intermediates, which are further converted to more stable Amadori products. These molecules undergo a series of reactions (dehydration, oxidation, rearrangement) resulting in carbonyl compounds such as glyoxal (GO), methylglyoxal (MGO), 3-deoxyglucosone (3-DG). These compounds are highly reactive and act as reaction propagators, finally leading to the generation of AGES (**Figure 9**) [17,70–72]. These molecules are classified into three groups: fluorescent crosslinking AGEs (crossline and pentosidine); non-fluorescent cross- linking AGEs (imidazolium dilysine crosslinks) and non-fluorescent non-crosslinking AGEs (N3-carboxyethyllysine (CEL) and N3-carboxymethyl-lysine (CML) [70,72,73].

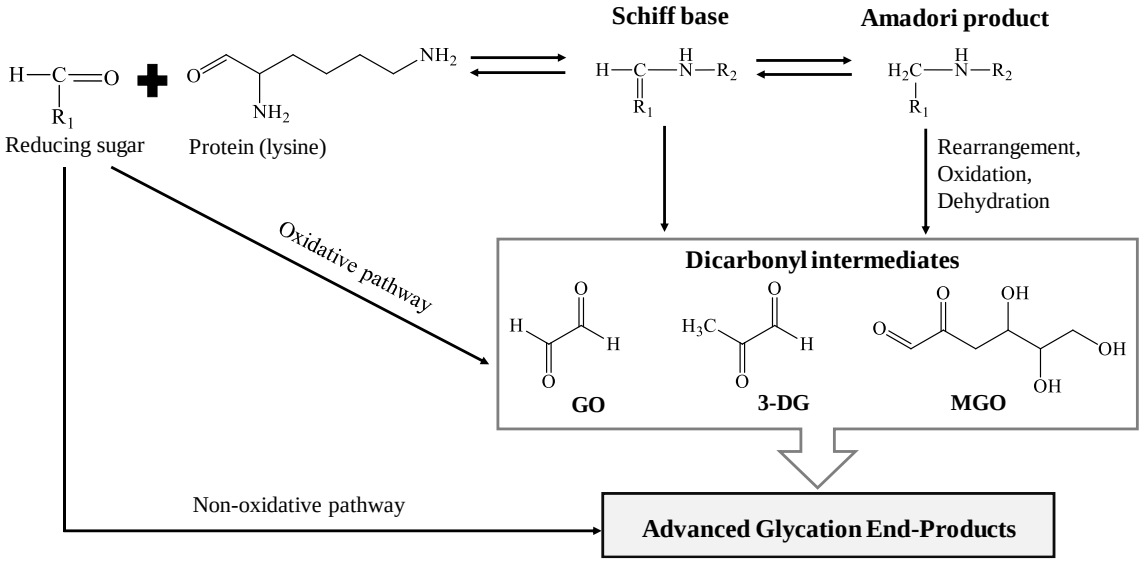

Figure 9 – Non-enzymatic protein glycation pathways leading to formation of advanced glycation end-products (AGEs) adducts. GO: glyoxal; 3-DG: 3-deoxyglucosone; MGO: methylglyoxal (adapted from [66,70,72]).

AGEs accumulation lead to structural and functional changes in cellular and tissues components, such as proteins (collagen, elastin and albumin), DNA and lipids. Hence, AGEs have been implicated in the pathogenesis of angiopathy, neuropathy, nephropathy and retinopathy (**Figure 8**) [66,70,72,74]. Additionally, binding of AGEs to specific AGEs receptors (RAGEs) may further increase the production of ROS and subsequent activates the expression of NF-kB and pro-inflammatory mediators (TNF-α, VEGF) [4,12,17].

Therefore, inhibition of AGEs formation by PCs may be a basis for a unique therapeutic approach for delaying and/or alleviating some diabetic complications (**Figure 7**)[3,15]. CQAs, ANTCs, catechin and PACs exert potent inhibitory effects on AGEs generation [3,70,74–77].

2.3.6. Alleviation of Oxidative Stress

Hyperglycaemia and increased production of ROS are crucial contributors for increased OS [1,3,15,17]. OS has been implicated in the development of T2DM, since it is responsible for insulin resistance and tissue damage that leads to several pathophysiological conditions [2–4,12,13].

Dietary PCs, due to their potent antioxidant effects, are effective in neutralizing or trapping ROS/RNS and inhibiting lipid peroxidation (**Figure 7**)[1,2,15,16]. PCs restore the chemical balance in these reactive molecules due to their ability to provide the electrons that they are lacking [2,26,27].

PCs also attenuate the production of pro-inflammatory cytokines (such as C-reactive protein, IL-6, and TNF-α) contributing to alleviate low-grade inflammatory processes associated with T2DM (**Figure 7**)[1,15,16,37]. Furthermore, PCs can enhance the cellular defence capacity through stimulation of synthesis or regeneration of antioxidant enzymes (SOD, CAT, GPx and GRx)[1,2,15,37]. Therefore, PCs can potentially prevent oxidative damage and related diabetic complications (**Figure 7**)[2,3,15].

Flavan-3-ols, resveratrol, quercetin and ANTCs showed promising results and might play a role in the treatment of T2DM [1,3,15,16,42].

2.3.7. Other anti-diabetic mechanisms

Insulin secretion by β-cells is mainly regulated by glucose, but intestinal incretins (GIP and GLP-1) play also a role in stimulation of glucose-dependent insulin secretion [2,17]. Moreover, incretins inhibit glucagon secretion, attenuate gastric emptying, and decrease appetite/weight gain [2,4,17]. CQAs, PACs, ANTCs and resveratrol are able to stimulate incretins secretion, resulting in the elevation of insulin levels [2,15]. However, incretins are rapidly inactivated by DPP-4 enzyme [2,4,14,17]. In order to extend the effects of incretins, DPP-4 inhibition has become one of the newest targets for the development of anti-diabetic drugs [4,14,17] (Table 4). Resveratrol, ANTCs, flavones (luteolin, apigenin, flavone), kaempferol, flavanones (hesperidin, naringenin), and genistein showed potent DPP-4 inhibitory effects [30].

3. Berries

Fruits, vegetables, legumes, cereal grains, spices and some beverages (tea, coffee, red wine) are major sources of PCs in the human diet [2,16,78]. Increasing evidence suggests favourable effects between fruit consumption and prevention/management of various diseases and disorders, including T2DM [1,2,5,18,35,39]. Hence, a dietary intervention could play an important role in preventing/managing T2DM or at least slowing down the rate of development of diabetes complications [2,5,18].

In addition to basic nutrition (vitamins, sugars, minerals), fibers and low energy density, fruits also contain a wide variety of non-essential compounds, such as PCs, carotenoids, etc [5,34,35]. Among fruits, berries (or berry fruits) stand out due to their unique and appreciable phenolic content (**Figure 10**) and significant health benefits (antioxidant, anti-inflammatory, anti-proliferative, anti-diabetic, etc)[5,16,34,35,39]. In this sense, there has been a growing trend in the popularity of berries consumption or as ingredients in dietary supplements and nutraceuticals, being recently recognized as "superfoods" [34,39]. Consumers are highly attracted to berries mainly because of their brightly and sharp colours (red-blue-purple), delicate taste and unique flavour [5,35,39]. Berries could be cultivated or collected from the wild and are commonly consumed fresh and in processed forms (beverages, jams, jellies, smoothies, yogurts, etc) [34,35].

Recently, leaves from berry-producing plants (BPPs) have also gained attention due to their traditional medicinal use against several diseases (colds, inflammation, diabetes, and ocular dysfunction) [34]. The phenolic composition of leaves is higher and richer than of berries, suggesting their use as alternative sources of PCs for the development of food supplements, nutraceuticals, or functional foods [34,79–81].

3.1. Phenolic Compounds in Berries

Berries represent a quite diverse group of the so-called "soft fruits" that include blackberries, blueberries, strawberries, currants, gooseberries, raspberries, etc, belonging to several botanical families (**Table S 1 -** Supplementary Material) [5,34,35].

Botanically, berries are known as simple (*e.g.* blueberry, cranberry) or composite (*e.g.* strawberry, mulberry, raspberry, blackberry, wax-myrtle) small fleshy fruits produced from single or multiple fused ovaries, respectively [5,35].

The total amounts of PCs can vary largely between different species and cultivars (**Figure 10**). Edaphoclimatic and growing conditions, degree of ripening and post-harvest treatments and processing operations also impact the phenolic profiles [5,35,39]. The phenolic composition of berries

is associated with their organoleptic properties but it also influences greatly their potential health benefits [5,18,34,35].

The red-to-blue-purple coloration of berries is due to the significant amounts of ANTCs in epidermal tissues (skin), making them the richest dietary source of ANTCs [5,34]. Cyanidin, delphinidin, malvidin, pelargonidin, peonidin, and petunidin are the most common anthocyanidins in berries (**Figure 6**) [5,34,35].

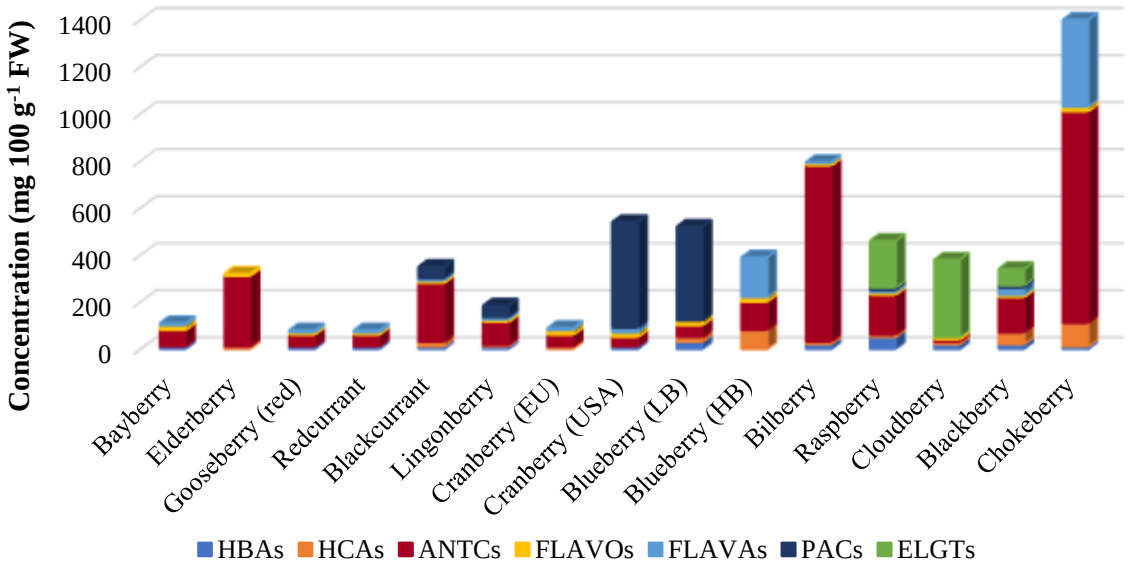

Figure 10 – The phenolic composition of some berries (adapted from [34,82]). EU: European, USA: American; LB: Low-bush; HB: High-bush. HBAs: Hydroxybenzoic acids; HCAs: Hydroxycinnamic acids; ANTCs: Anthocyanins; PACs: Proanthocyanidins. For nomenclature of berries species please check (**Table S 1** – Supplementary Material).

Strawberries are composed mainly of pelargonidin conjugates, while deep purple-black berries (*e.g.* blueberries, blackberries, elderberries, chokeberries, lingonberries) possess high amounts of delphinidin and cyanidin derivatives [34,35,83]. Sugars (glucose, rhamnose, arabinose, rutinose, sambubiose, etc) or other organic compounds (acetic, malonic, malic and phenolic acids) are the main residues associated with berry anthocyanidins [35].

Besides ANTCs, berries contain also other flavonoids, phenolic acids, and tannins (**Figure 10**) [5,34,35,39]. Ferulic, caffeic and *p*-coumaric acids and CQAs are the most common HCAs in berries, being very abundant in *Vaccinium spp*. (**Figure 10**) [34,35,63,84,85]. *O*-and *C*-glycosides of flavonols (quercetin, kaempferol and myricetin) are present in high amounts in blackcurrants, blueberries, cranberries, chokeberries, and lingonberries (**Figure 10**) [34,35,86]. *Rubus* berries

(raspberry, cloudberry and blackberry) present the most diverse phenolic composition, being particularly rich in ellagitannins (**Figure 10**) [34,35,87,88]. This class of compounds is also found in strawberries [34,35]. Chokeberries are rich sources of HBAs and condensed tannins (**Figure 10**). PACs are significant in high- and low-bush blueberries and cranberries (**Figure 10**) [34,35].

3.2. Anti-diabetic Potential of Berries

The anti-diabetic activity of the berries has been demonstrated by *in vitro* studies, animal and human models, largely attributed to their phenolic composition [5,16,18,21,23,63,64,77,89,90]. PCs from berries exert their favourable effects by regulating glucose digestion and absorption, enhancing insulin production and reducing apoptosis and promoting proliferation of pancreatic β-cells via reduction of OS and inflammation and by enhancing peripheral tissue glucose uptake [5,15,16,34]. Other targets include inhibition of AR activity and AGEs generation (**Table 2**). Hence, berries consumption may offer a non-toxic, dietary approach to manage hyperglycaemia linked to T2DM [5,18,21]. Even though berries present a fair content of total sugars (7-10 g/100 g), these are mainly free glucose and fructose with very little contents of sucrose compared to other fresh fruits of similar total sugars, which make them valuable for diabetic patients. Additionally, the high fiber content of berries is important since pectin is a intestinal regulator [39].

Information regarding animal models or human intervention studies displaying the anti-diabetic effect of berries is summarised in recent reviews [5,16].

Table 2 - Summary of *in vitro* studies showing the potential anti-diabetic effect of different berries. For berries nomenclature please check Table S1 (Supplementary Material).

Berry species	Target/Mechanism	Main agents	References
Black currants, cloudberries, rowanberries and blueberries	Inhibition of AGLU activity	Anthocyanins, phenolic acids and chlorogenic acids	[85,89,91,92]
Strawberries, black currants, arctic brambles, cloudberries, blueberries and rowanberries	Inhibition of AMY, AGLU and PL activity	Ellagitannins, proanthocyanidins and anthocyanins	[93]
Raspberries and rowanberries	Inhibition of AMY activity	Ellagitannins and proanthocyanidins	[61]
Blue honeysuckle, lingonberries and red gooseberries	Inhibition of AMY, AGLU and PL activity	Anthocyanins, ellagitannins and proanthocyanidins	[18]
Blueberries, black currants, strawberries and raspberries	Inhibition of AMY and AGLU activity	Ellagitannins and anthocyanins	[94]
Red and yellow raspberries	Inhibition of AMY and AGLU activity	Anthocyanins and tannins	[90]

Bayberries	Inhibition of AGLU activity	Cyanidin-3-*O*-glucoside, myricitrin, quercetin-3-*O*-galactoside and quercetin-3-*O*-rhamnoside	[65]
Whortleberry (berries and leaves)	Inhibition of AMY activity	Malvidin-3-*O*-glucoside, quercetin	[95,96]
Black chokeberries	Inhibition of AGLU, AMY and PL activity	Anthocyanins (cyanidin-3-O-glucoside), phenolic acids (CQAs)	[97]
Raspberries	Inhibition of AGLU activity	Ellagic acid, cyanidin-diglucoside, pelargonidin-3-*O*-rutinoside and catechin	[98]
Bayberries (leaves)	Inhibition of PL activity; improvement of glucose uptake by HepG2 cells (activation of AMPK pathway)	Epigallocatechin-3-*O*-gallate polymers	[23]
Lingonberry, arctic bramble cloudberry, strawberry and raspberry.	Inhibition of PL activity	Ellagitannins and proanthocyanidins	[64]
High-bush blueberry and blackberry	Inhibition of DPP-4	Cyanidin-3-glucoside, cyanidin and malvidin	[30]
Bayberries	Prevention of pancreatic β-cells H_2O_2-induced apoptosis, increased cellular viability, and decreased mitochondrial ROS production	Anthocyanins (cyanidin-3-*O*-glucoside)	[99]
Low-bush blueberry (berries, leaves, roots)	Enhancement of deoxyglucose uptake in C2C12 muscle cells and 3T3-L1 adipocytes; protection of PC12 cells against glucotoxicity: stimulation of insulin secretion and proliferation of pancreatic β-cells	-	[63]
Bayberries	Enhancement of glucose uptake in HepG2 cells	Cyanidin-3-*O*-glucoside, quercetin-3-*O*-galactoside, quercetin-3-*O*-glucoside, and quercetin-3-*O*-rhamnoside	[62]
Indian gooseberry	Inhibition of AR activity	Gallo- and ellagitannins (emblicanin A and B, punigluconin and pedunculagin)	[100]
Lingonberry	Inhibition of AGEs formation	Catechin, quercetin-3-*O*-galactoside and cyanidin-3-*O*-glucoside	[77]
Cranberry	Inhibition of AGEs formation	Proanthocyanidins	[76]
Low-bush blueberry (leaves and stems)	Inhibition of AGEs formation	Caffeoylquinic acids and proanthocyanidins	[75]

Blueberries, blackberries, strawberries, raspberries and cranberries	Inhibition of AGEs formation	Proanthocyanidins and anthocyanins	[74]

3.3. Berries from Madeira Archipelago

The vascular flora of Madeira archipelago (Portugal) (**Figure 11**), includes some endemic BPPs, such as *M. faya*, *R. grandifolius*, *S. lanceolata* and *V. padifolium* [101]. The study of these wild berries is relevant since it can provide information about new medicinal applications that would result in higher concern about its cultivation and/or collection. This would possibly increase their market penetration and consumers awareness/interest with some economic benefit.

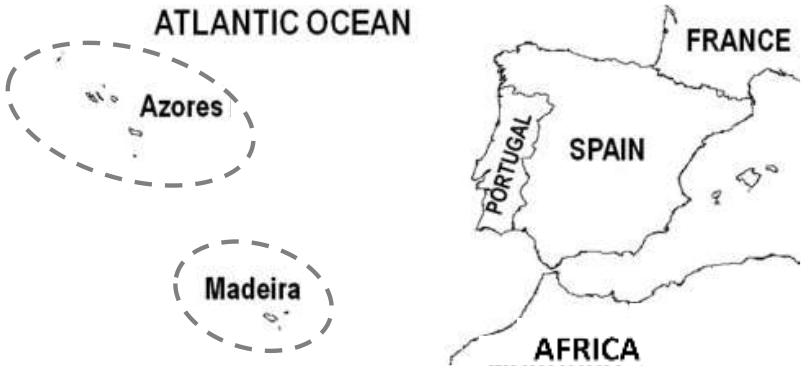

Figure 11 - Location of Madeira and Azores archipleagos in the North Atlantic Ocean.

3.3.1. *Elaeagnus umbellata*

E. umbellata Thunb (Elaeagnaceae), commonly known as autumn olive or Japanese silverberry (**Figure 12**), is a introduced (non-native) species that grows well in Madeira Island. This species is indigenous to Eastern Asia and is characterized as a deciduous shrub or small tree, typically up to 3.5 m tall. It grows small, round edible berries, which ripen to red, dotted with silver or brown color [102–104]. Berries are included in the diet of most Asian countries, but are also used to produce beverages, sauces, jams, or other products, like powders or extracts for food industry [104].

E. umbellata extracts have putative health benefits against hepatitis, fracture, injury and diarrhea [104]. Several phytochemicals have been reported in this species, namely PCs (catechins, PACs), L-ascorbic acid, α- and γ-tocopherol and appreciable amounts of carotenoids (in particular lycopene) [104,105].

Figure 12 – *Elaeagnus umbellata* (Autumn olive).

3.3.2. *Myrica faya*

M. faya Aiton (Myricaceae) or wax-myrtle (locally called "amorinhos") is native to Macaronesia region [101] (**Figure 13**). The plant is an evergreen shrub or small tree, usually about 8 m tall. Its fruits are small edible berries, red to purple in color when ripe [101]. They can be directly consumed but, due to their astringency which limits their palatability, they are mainly used to produce jams, liquors and to add colour to homemade wine. Formerly, wax was extracted from the berries for candles production and also for skin care products [106].

A previous study developed by our work group [106] reported ANTCs (in particular cyanidin-3-*O*-glucoside, C3G) and flavonoids (flavonols and flavan-3-ols) as the main compounds of wax-myrtle berries and leaves, respectively. To our best knowledge, no medicinal properties have been yet documented for this species.

Figure 13 – *Myrica faya* (wax-myrtle, fire tree)

3.3.3. *Rubus grandifolius*

R. grandifolius Lowe (Rosaceae) or wild blackberries is an endemic plant to Madeira Archipelago (Portugal), which inhabits in moist and shady areas (**Figure 14**)[101,107]. Its berries, known as "amoras", are physically similar to other blackberries, and become black when rippen. These are consumed fresh or processed as jam, juice or liquor [107]. The leaves, shoots and fruits are described in the folk medicine as astringent for children and also as remedy for diabetes, depurative, diuretic and to relieve sore throat as herbal teas or alcoholic infusions [108].

Previously [107], our research group has identified ANTCs, flavonoids and HCAs in berries and leaves of this species.

Figure 14 – *Rubus grandifolius* (wild blackberries).

3.3.4. *Sambucus lanceolata*

S. lanceolata R. Br. in Buch (Adoxaceae) (Madeira elderberry) or "sabugueiro" is a small tree or shrub, up to 7 m tall, endemic to Madeira Island (Portugal) (**Figure 15**). Berries are small yellowish round edible fruits that get dark-purple when ripe in the late Summer [101]. Infusion made of berries have been used in folk medicine to relieve colds, diarrhea and menstrual pains. Additionally, flowers are used as diuretic and emollient, while leaves are applied in poultices on bruises, wounds and sores [108]. To our best knowledge, no phytochemical studies on this species have been conducted so far.

Figure 15 - *Sambucus lanceolata* (Madeira elderberry)

3.3.5.*Vaccinium cylindraceum*

V. cylindraceum J.E. Sm (Ericaceae), locally known as "uveira" or "uva-da-serra" (Azores blueberry)(**Figure 16**) is a deciduous shrub endemic to the Azores archipelago (Portugal) (**Figure 11**). This species is not found in Madeira Island but it was included in this study for comparison purposes. It grows as a semi-evergreen shrub or small tree, up to 5 m tall, in some rural areas (above 300 m of altitude) in all the Azores Islands (except Graciosa) [109,110]. In the late summer, these plants produce ovoid-shape berries of blue-black colour, when ripe, which are consumed fresh or used to make candy and jams [110].

Previously [109], twenty-four ANTCs were identified in *V. cylindraceum* berries, mainly glycosides of malvidin, delphinidin, cyanidin, petunidin and peonin.

Figure 16 – *Vaccinium cylindraceum* (Azores blueberry) (photo reproduced from [111]).

3.3.6. *Vaccinium padifolium*

V. padifolium Sm (Ericaceae) is endemic to Madeira Island (Portugal), where is commonly called "uveira" or "uva-da-serra" (Madeira blueberry) (**Figure 17**) [101,112,113]. This small tree can grow up to 3 m tall and is physically similar to the previous described species. It grows only at high altitudes (above 1300 m) and its edible berries are used for jams, liquors and as food preserves [101,112,113]. Additionally, they are used in local ethnopharmacology for cough, colds, bronchitis and dysentery, and exported for commercial production of ophthalmic specialities [108].

Previously [112,113], twenty-five ANTCs were identified in *V. padifolium*, glycosides of malvidin, delphinidin and petunidin being the main compounds of berries.

Figure 17 – *Vaccinium padifolium* (Madeira blueberry).

4. Extraction and Characterization of Phenolic Compounds

Accumulative data showed that PCs, due to their biological and pharmacological properties, may offer prophylactic or complementary treatments for various aspects of T2DM as dietary agents or nutraceuticals and functional foods [3,15].

To benefit from their health-promoting properties, PCs must be first extracted from plant matrices to obtain a phenolic-rich concentrate (extract) for nutraceutical/pharmaceutical applications [29,36,37]. The main goal is to obtain the maximum extraction yield, and, therefore, more benefits to human health [36]. Further steps in PCs analysis include their separation, characterization, quantification and determination of their physiological properties (antioxidant, anti-inflammatory, anti-proliferative, etc) [36,37,78].

4.1. Sample preparation

Before extraction of PCs, plant samples should be collected, reserved and properly prepared [78]. To avoid degradation of PCs, samples are often preserved at low temperatures and/or dried (air, oven, lyophilization) before extraction [78]. Dried samples are then milled or ground to obtain a smaller particle sizes, while liquid samples are treated by filtration, centrifugation and pre-concentration/purification [38,78] .

4.2. Extraction

The next step to separate PCs from other substances in the matrix is their extraction, which usually involves using solvents (organic or inorganic), supercritical fluids, microwave procedures, ultrasonics, among others [36–38,78]. Several parameters like extraction time, temperature, solvent-to-sample ratio, particle size, the number of repetitions, pH and solvent type are known to influence the extraction yield [38,78]. Ethanol, methanol, propanol, ethyl acetate, acetone and their combination with different proportions of water are the most common solvents for PCs extraction [36,37,43,78]. Most extractions are carried out under acidic conditions because PCs are generally more stable in low pH. Usually weak organic acids (acetic, formic, citric, etc) are used at low concentrations to avoid hydrolysis of glycosides [36,43,78]. In general, increasing time and temperature promote higher extraction efficiencies; however, PCs can undergo degradation, hydrolyzation or oxidation reactions [38,78].

Conventional solvent extraction is the most widespread technique which applies a solvent to release/separate a desired component (the solute) from solid (solid-liquid) or liquid matrix (liquid-liquid) [36–38]. Maceration and solvent extraction are frequently used to extracts PCs from a solid matrix [36,78]. These extraction techniques are based in the same mass transfer phenomena, but heat

and/or stirring are applied in the latter case to faster the process [36,37]. These methods are simple, require relatively cheap apparatus and result in satisfactory extraction rates [36,78]. However, some disadvantages include the need to use a great amount of resources (energy and solvents) and long extraction periods [36,37,78].

New alternative methods have emerged as "environmentally friendly", namely ultrasound-assisted extraction (UAE), microwave-assisted extraction (MAE), and pressure assisted extractions [36–38,78]. These are faster, relatively simple to perform and most importantly reduce energy and solvent requirements in comparison with conventional techniques [36,38,78].

UAE is a simple, fast, efficient and inexpensive alternative to conventional solvent extraction [36–38,78]. It is a non-thermal technique in which ultrasound waves (≥ 20 kHz) causes cell wall disruption and release of cell contents, thereby facilitating the mass transfer from the matrix to the solvent [36,78,114].

MAE has been commonly used in the extraction of PCs due to low amounts of solvent, faster extraction times and increased extraction yields compared to traditional methods [36–38,78]. In this technique, cells are damaged by microwaves (non-ionizing radiation), which result in sample heating, and enhance the release of intracellular content to the solvent [36,78].

Extraction with supercritical fluids (SCF) has become increasingly popular. SCF extraction use solvents in their supercritical states (high temperature and pressure), which enables high mass transfer rates [36,37]. As a result, the extraction is more efficient, fast and selective. Also, SCF extraction requires small amounts of sample and solvent and no additional clean-up step [36–38,78]. CO_2 is the most common solvent due to its stability, low toxicity and price and non-flammability [38,78]. However, CO_2 is a non-polar molecule, and small amounts of polar solvents (modifiers) have to be added to enhance the extraction of PCs [36–38,78]. The main disadvantage of this technique is the high price of equipment [38,78].

4.3. Isolation, fractionation and purification

Extraction techniques are not selective and imply the co-extraction of non-phenolic compounds (sugars, organic acids and proteins), which sometimes requires subsequent purification processes [38,43]. Isolation and purification of PCs from crude sample extracts can be achieved by column chromatography, high-speed counter-current chromatography (HSCCC), solid-phase extraction (SPE), ultrafiltration, among others. In these techniques, PCs are separated into several fractions according to their physical properties (weight, solubility and polarity) using partitionable solvents and different resins (Sephadex LH-20, EXA-31, XAD 4, XAD16, EXA-90, etc) [37,38,78,115]. However, these methods are time-consuming, labor intensive and expensive, thereby,

used only when strictly necessary to study isolated compounds or partial concentration prior to chromatographic analysis [37,78].

4.4. Determination of Phenolic Compounds

There are several developed techniques for the quantification of PCs, present in crude extracts or isolated from plant matrices: spectrophotometry, chromatography, capillary electrophoresis, nuclear magnetic resonance (NMR), among others [36–38,78]. In the following sub-sections, the focus will be on spectrophotometric and chromatographic methods since are the most used and applied in this work for identification and quantification of PCs from crude extracts.

4.4.1. Spectrophotometric methods

Colorimetric methods, such as total phenolic content (TPC), total flavonoids content (TFC) and total anthocyanin content (TAC) are simple, low-cost, reproductible and fast spectrophotometric assays routinely used for qualitative and quantitative estimation of PCs in plant-based extracts [29,36,38,78]. However, these methods are not specific, being affected also by vitamin C, sugars, and aromatic proteins, which leads to overestimation of PCs amounts [29,36,78]. Additionally, these assays do not separate or quantify PCs individually[38,47,78].

TPC involves the reduction of Folin-Ciocalteu reagent (FCR) by PCs, under alkaline conditions [29,36,78]. FCR is composed by complexes of phosphomolibdic/phosphotungstic acid, which form blue coloured complexes around 760 nm [29,36,78]. Usually, gallic acid is used as a reference standard [29,36].

TFC measurements by the $AlCl_3$ method are based on the complexation of flavonoids with Al(III) in the range of 410 – 423 nm [38,78].

4.4.2. Chromatographic methods

In order to separate and accurately quantify individual PCs, these compounds must be separated first [78]. Chromatographic techniques for analysis of PCs include thin-layer chromatography (TLC), gas chromatography (GC) and high-performance liquid chromatography (HPLC), high speed counter current chromatography (HSCCC) and supercritical fluid chromatography (SFC) [37,38,78].

Due to its precision, reproducibility and versatility, HPLC is the dominating analytical tool for separation and quantification of PCs [37,38,78]. Generally, reverse-phase C18 columns are preferred along with a binary mobile phase system containing acidified water (acetic, formic and phosphoric acid) and polar organic solvent (methanol or acetonitrile), possibly acidified, in order to

avoid the ionization of PCs during analysis [37,43,78]. A gradient elution system is more frequent than isocratic mode [78]. Ultraviolet-visible (UV–vis), photo-diode array (PDA), fluorimetric and electrochemical detectors are normally coupled to HPLC. However, these tools are not enough for the complete identification of the composition of plant extracts [26,37,38,78]. The use of mass spectrometry (MS) detectors coupled to HPLC (HPLC-MS) have become very popular as it is a powerful analytical tool and very effective for structural characterization and identification of different PCs [26,38,78]. These equipments separate ionized atoms or molecules according to their difference in mass to charge ratio (m/z)[37]. The main ionization sources reported in the analysis of PCs are electrospray ionization (ESI), chemical ionization (CI), atmospheric pressure chemical ionization (APCI), matrix-assisted laser desorption/ionization (MALDI) and fast atom bombardment ionization (FAB) [37,38,78]. Nowadays, HPLC-MS is the best analytical technique to identify PCs in plant extracts due to its high selectivity, sensitivity, robustness and specificity [37,38,78]. Configurations that allow for multiple fragmentation, such as ion trap detectors, are particularly useful since fragments provide precious information for the identification of multiple isomers, so common among PCs.

4.5. Antioxidant Activity (AOA) Evaluation of Phenolic Compounds

Antioxidant molecules are a heterogeneous category of molecules, that include PCs, carotenoids, vitamins C and E, minerals, etc [35,37]. These compounds interact with free radicals and reduce, control or prevent cellular oxidative processes and inflammation before vital molecules are damaged [2,27,37].

PCs are the most abundant dietary antioxidants and are especially important due to their aromatic rings and the highly conjugated system with multiple hydroxyl groups, which allows them to act as reducing agents or hydrogen donors [2,38]. The arrangement and number of hydroxyl groups determine greatly the antioxidant potency of PCs [2,35]. These compounds alleviate OS through varied mechanisms (**Figure 18**): (A) inhibition of pro-oxidative enzymes and modulation of redox cell signalling and gene expression, chelating metal ions, (B) enhancing antioxidant and detoxifying enzymes expression and (C) neutralization/reduction of ROS/RNS formation [1,2,15,27,29,37].

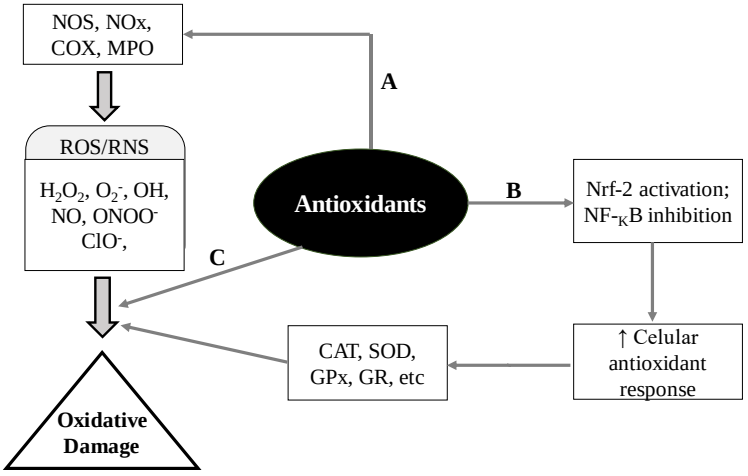

Figure 18 – Different mechanisms of action of phenolic compounds: (A) inhibition of oxidant enzymes (NOS: nitric oxide synthase; NOx: NADPH oxidase; COX: cyclooxygenase; MPO: myeloperoxidase), that translate in a decrease in ROS/RNS production; (B) interaction with cellular signalling pathways that translate in cellular antioxidant response; (C) direct scavenging of ROS/RNS (adapted from [12,27]).

In this context, it has been suggested that an intake of a phenolic-rich diet may be of great value in the prevention of the on-set and/or progression of OS-associate diseases (including T2DM), particularly due to their antioxidant activity (AOA) [2,5,16,18,27,37]. Therefore, a lot of interest is focused on the determination of AOA of isolated PCs or plant extracts [27]. Different *in vitro* methodologies, based on different strategies, have been developed for this aim [26,27,29,36]. Considering the complexity of the involved mechanisms/variables, it is recommended to conduct several tests to evaluate and compare the AOA of natural products [26,27,35].

4.5.1. *In Vitro* Assays to Determine Antioxidant Activity

The most widely *in vitro* assays used for evaluation of AOA are: $ABTS^{\bullet+}$ (2,2-azino-bis(3-ethylbenzothiazoline-6-sulfonic acid) scavenging activity, $DPPH^{\bullet}$ (1,1-diphenyl-2-picrylhydrazyl) scavenging activity, FRAP (ferric ion reducing/antioxidant power) and ORAC (oxygen radical absorbance capacity) [2,27,36,37]. These methods involve the reactions of PCs with free radicals and the complex formed is UV-Vis spectrophotometrically detected at a certain wavelength in the case of colour complex ($ABTS^{\bullet+}$, $DPPH^{\bullet}$ and FRAP) or fluorescence decay (ORAC assay). Results from radical scavenging assays can be expressed in different units, Trolox equivalents (TE), inhibition % or IC_{50} value [27,29,36,37]. *In vitro* assays are simple, quick, low-cost, high-throughput and very useful for screening of antioxidant activities [27,29]. However, they have been designed for the use of synthetic radicals that lack biological relevance, therefore, not reflecting the situation *in vivo*

[26,27,29]. Hence, other methodologies have been proposed, aiming to evaluate scavenging activity toward ROS/RNS formed *in vivo* like $O_2^{\bullet-}$, OH^-, $ONOO^-$, ClO^- (hypochlorite) and NO [26,27].

Since it is difficult to conduct studies involving animals or humans, cell-based models emerge as very attractive, cheaper and intermediate alternative to assess *in vitro* AOAs [23,27,29,35,116,117]. These assays are biologically more relevant than "test tubes" since they take into consideration some aspects of the bioavailability of PCs within the cells (absorption, distribution, and metabolism) [26,27,29,35]. Therefore, they provide a more comprehensive understanding of AOA at cellular level [26,27,29]. Different cell types have been used for these biological assays: erythrocytes, liver cancer line HepG2, Caco-2 intestinal cancer cells, human gastric adenocarcinoma cells AGS, vascular endothelial cells EA.hy926, human macrophages RAW264.7, human lung fibroblasts (WI38, IMR-90), etc [27,29]. One of the main drawbacks of these assays is related to the dosage of PCs which may be too high to achieve physiologically upon intake [5,16,26,35].

Still, *in vitro* tests are limited and the obtained data cannot be extrapolated to *in vivo* performance [26,27,29,35]. The *in vivo* antioxidant status is mainly dependent of absorption/adsorption, bioavailability, stability, and metabolism of the dietary PCs in the body [26,27,35]. Nevertheless, chemical methods are very helpful and should be considered for initial screening before clinical studies, since they provide important ranking information about the capacity of PCs to neutralize ROS/RNS, under comparable test conditions with minimum environmental interference [27,29].

The following sub-sections explain in detail the *in vitro* assays used in this work for evaluation of AOA of plant extracts.

4.5.1.1. ABTS radical ($ABTS^{\bullet+}$) scavenging assay

$ABTS^{\bullet+}$ scavenging assay is as a simple and convenient *in vitro* method widely applied for total antioxidant capacity assessment [27,29,36]. $ABTS^{\bullet+}$ is generated from ABTS by strong oxidizing agents (potassium persulfate, manganese dioxide or peroxyl radicals) [27,29,118]. In the presence of antioxidants, the blue green $ABTS^{\bullet+}$ solution (pH 7.4) is discoloured and the scavenging efficiency is measured by the decrease in absorption of the chromophore at 734 nm [27,29,118,119]**.**

4.5.1.2. $DPPH^{\bullet}$ radical scavenging assay

$DPPH^{\bullet}$ radical scavenging assay is among the most frequently used *in vitro* methods [27,29]. $DPPH^{\bullet}$ is a stable, commercially available free radical with a deep purple colour. It is a simple and fast test based on the neutralization of $DPPH^{\bullet}$ radical by antioxidants through electron donation

[27,29,36]. This reduction is measured spectrophotometrically (around 517 nm) by discoloration of the DPPH$^{\bullet}$ solution, which acts as an indicator of the antioxidant efficacy [27,29,119].

4.5.1.3. Nitric Oxide ($NO^{\bullet}$) Radical Scavenging assay

NO is produced in biological systems by specific nitric oxide synthases [12,17]**.** $NO^{\bullet}$ can be generated *in vitro* from sodium nitroprusside. This compound decomposes in aqueous solutions (pH 7.2 - 7.4) to yield $NO^{\bullet}$. Under aerobic conditions, the principal end-product of $NO^{\bullet}$ autooxidation is nitrite (NO^{-}_{2}) [26]. After addition of the Griess reagent, the absorbance of the chromophore formed during the diazotization of NO^{-}_{2} with sulfanilamide and subsequent coupling with naphthyl-ethylenediamine is measured spectrophotometrically around 560 nm [26,28]. The Griess reaction is also used in enzymes or cells models to measure NO^{-}_{2} as an indicator of OS condition [25,26].

4.5.1.4. Superoxide Anion ($O_2^{\bullet-}$) Radical Scavenging assay

The mitochondrial production of superoxide anion ($O_2^{\bullet-}$) is a major cause of cellular OS [12,13,17,26]. $O^{\bullet}_{2}{}^{-}$ is mainly generated *in vitro* by the hypoxanthine−xanthine oxidase system and, in minor extent, by the phenazine methosulfate-β-nicotinamide adenine dinucleotide (PMS-NADH) model (non-enzymatic) [26,27,120]. The inhibition of $O_2^{\bullet-}$ production by PCs is followed with the use of probes such as ferricytochrome-c or nitroblue tetrazolium (NBT) [26,27]. The reduction of the probes by O_2^{-} can be measured spectrophotometrically at 560 nm [26,27,120].

Chapter II – Materials and Methods

1. Materials

1.1. Plant Material

Six different berry-producing plants (BPPs) were studied in this work: four endemic species from Madeira Island (*M. faya*, *R. grandifolius*, *S. lanceolata* and *V. padifolium*), one endemic to Azores archipelago (*V. cylindraceum*) and one non-native species (*E. umbellata*). These plants are presented in **Table 3** and their origin/collection areas are marked in **Figure 19** and **Figure 20**. Identification of plant material was carried out by Dr. Francisco Carvalho and Dr. José Augusto Carvalho from Madeira Botanical Garden (Funchal, Madeira). Voucher specimens have been stored at Madeira Botanical Garden Herbarium.

E. umbellata **(1)** samples were collected at "A Quintinha das Ervas Aromáticas" (Funchal, Madeira Island) in two consecutive years (October 2013 and 2014) (**Table 3**). This species is the only one that is not native to Macaronesia region and did not grown in the wild.

M. faya was collected in the wild at seven different locations **(2 - 8)** in Madeira Island during July – September 2014 (**Table 3**). An additional sample was collected in Terceira Island **(9)** (Azores archipelago), shipped in styrofoam boxes over dry ice and delivered to Centro de Química da Madeira (CQM), within 3 days.

Plant material of *R. grandifolius* was collected in the wild at two different location in Madeira Island: **(10)** Pico do Arieiro (Funchal) and **(11)** Santo António da Serra (Machico) in September 2014 (**Table 3**).

S. lanceolata **(12)** was collected in the wild at Pico das Pedras (Santana, Madeira Island) in October 2014 (**Table 3**).

Two *Vaccinium* species endemic to Macaronesia region were studied in this work (**Table 3**). *V. cylindraceum* was collected in the wild at Flores Island (**13**) (Azores archipelago) by Cândida Dias. Plant material was send by air transportation to Madeira Island, the day after collection, in styrofoam boxes over dry ice and delivered to CQM, within 3 days (**Table 3**). *Vaccinium padifolium* was collected in the wild at Pico do Arieiro **(14)** (Funchal, Madeira Island) in two consecutive years (September 2013 and 2014) (**Table 3**).

Figure 19 - Collection area of analyzed berry-plant species from Madeira Island. A green-pine symbol marks the collection area. Sample number identification is shown in **Table 3**.

Figure 20 - Collection area of *M. faya* (**9**) and *V. cylindraceum* (**13**) from Azores archipelago. A green-pine symbol marks the collection area. Sample number identification is shown in **Table 3**.

Table 3 – Information of berry-producing plants under study (origin, collection date, voucher numbers).

Plant Species/Family	Common name	Collection area		Collection date	Voucher number
***E. umbellata*[1]** (Elaeagnaceae)	Autumn olive	**(1) Funchal** (32° 38' 54.20"N, 16° 55' 44.71"W)	Madeira Archipelago	October 2013, 2014	MADJ12164
***Myrica faya*[2]** (Myricaceae)	Wax-myrtle; Fire tree	**(2) Machico** (32° 44' 18.75"N, 16° 47' 37.92"W)	Madeira Archipelago	July 2013, 2014	MADJ13165
		(3) Faial (32° 46' 53.23"N, 16° 51' 47.34"W)	Madeira Archipelago	July 2014	MADJ13239
		(4) Arco de São Jorge (32° 49' 19.10"N, 16° 57' 2.21"W)	Madeira Archipelago	July 2014	MADJ13237
		(5) Boaventura (32° 49' 8.33"N, 16° 58' 33.28"W)	Madeira Archipelago	July 2014	MADJ13235
		(6) Seixal (32° 48' 10.45"N, 17° 6' 51.23"W)	Madeira Archipelago	July 2014	MADJ13236
		(7) Ribeira da Janela (32° 50' 26.02"N, 17° 10' 4.19"W)	Madeira Archipelago	July 2014	MADJ13238
		(8) Porto Moniz (32° 51' 17.15"N, 17° 10' 33.27"W)	Madeira Archipelago	August 2014	MADJ13280
		(9) Terceira Island (38º 43' 0'N, 27º 4' 0'W)	Azores Archipelago	September 2014	MADJ 14337
***R. grandifolius*[2]** (Rosaceae)	Wild blackberry	**(10) Pico do Arieiro, Funchal** (32° 42' 50.72"N, 16° 55' 55.07"W)	Madeira Archipelago	September 2014	MADJ08618
		(11) Santo da Serra, Machico (32° 43' 13.72"N, 16° 51' 2.43"W)	Madeira Archipelago	September 2014	MADJ05179

***S. lanceolata*[2]** (Adoxaceae)	Madeira elderberry	**(12) Pico das Pedras, Santana** (32° 46' 54.96"N, 16° 54' 21.85"W)	Madeira Archipelago	October 2014	MADJ13284
***V. cylindraceum*[3]** (Ericaceae)	Azores blueberry	**(13) Flores Island** (39º 26' 26"N, 31º 13' 9" W)	Azores Archipelago	August 2014	MADJ13281
***V. padifolium*[2]** (Ericaceae)	Madeira blueberry	**(14) Pico do Arieiro, Funchal** (32° 42' 50.72"N, 16° 55' 55.07"W)	Madeira Archipelago	September 2013, 2014	MADJ13283

[1]introduced in Madeira Island; [2]endemic to Madeira archipelago; [2]endemic to Azores archipelago.

Collected plant material of each species was separated into leaves and fruits (fully ripe), destemmed, washed and frozen at -80 ºC in sealed plastic bags. In the case of *V. padifolium*, leaves were divided in two groups: young leaves (red colored tips) and mature leaves (fully green). This was not verified for the other berry-producing plants, being considered only leaves (fully green) and berries. Then, samples were freeze-dried (Christ Alpha 1-2 LD plus), ground to powder using a mechanic grinder, and stored at -20 ºC in sealed plastic bags until further analysis (**Figure 21**).

1.2. Chemicals and reference compounds

Standard compounds and specific reagents used in the experimental procedures are listed in **Table S 2** (Supplementary Material).

2. Methods

In **Figure 21** is summarised the procedures and assays carried out in the present work.

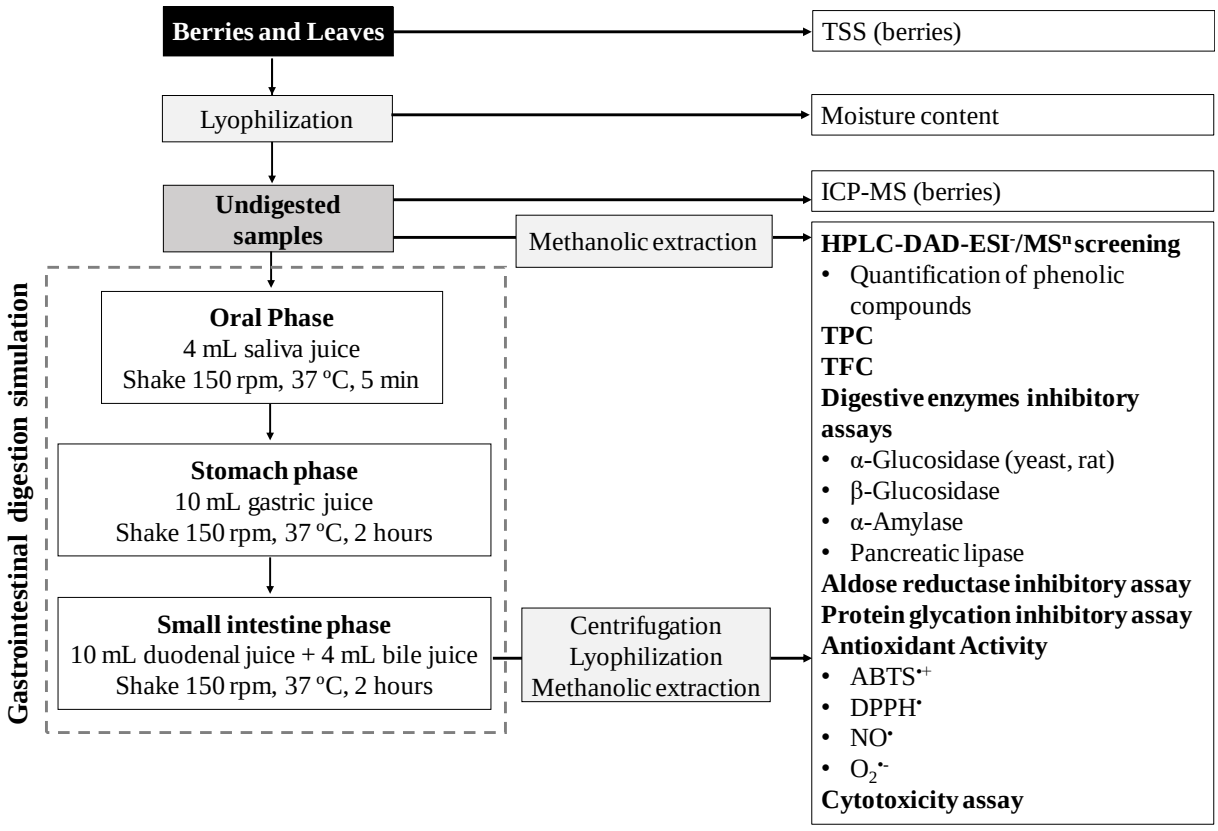

Figure 21 – Overview of the work carried out in this thesis. TSS: Total soluble solids. ICP-MS: inductively coupled plasma-mass spectrometry. HPLC-DAD-ESI$^-$/MS^n: High performance liquid chromatography with diode-array and electrospray ionization mass spectrometric detection; HPLC-DAD: High performance liquid chromatography with diode-array detector. TPC: Total phenolic content; TFC: Total flavonoids content.

2.1. Total soluble solids (TSS) determination

The total soluble solids (TSS) content, measured in Brix degree (°Brix), was determined for fresh berries. The fresh fruit was placed in a blender (Kenwood Excel) and reduced to pulp. After centrifugation (4000 rpm, 20 min) (Sigma 3K30), the supernatant was analyzed on a refractometer (ATAGO RX-1000; Tokyo, Japan). A calibration curve of sucrose (1 - 200 g L^{-1}) was prepared and results were express as gram of sucrose equivalents per liter of pulp.

2.2. Moisture content determination

For determination of moisture content, fresh plant material (berries and leaves) was weighted before and after freeze-drying (-52 ºC, 0.72 atm) (Christ Alpha 1-2 LD plus). The percentage (%) of moisture was calculated based on the following equation:

$$Moisture\ content\ (\%) = \left[1 - \left(\frac{m_{pre}}{m_{post}}\right)\right] \times 100 \qquad \textbf{(Equation 1)}$$

where m_{pre} and m_{post} were the mass of fresh plant material pre- and post-freeze drying.

2.3. Determination of mineral content by inductively coupled plasma-mass spectrometry (ICP-MS)[2]

This part of the work has been already published [121], and so it will only be briefly explained in the following sub-sections.

2.3.1. Sample preparation and microwave digestion

Samples of freeze-dried berries were shipped to University of Jáen (Spain). Briefly, 0.25 g of sample, 6 mL HNO_3 and 1 mL H_2O_2 were added to 50 mL PFA vessels. After 30 min, they were placed in an ultra-high throughput microwave digestion system (MARSXpress, CEM; Gilson, Madrid, Spain) and the temperature was increased to 200 ºC in 15 min, and maintained at 200 ºC for 15 min. The power of the microwave oven was set at 1000 W. After cooling at room temperature, all the digestion solutions were quantitatively transferred into plastic containers and diluted to 60 mL with ultra-pure (UP) water.

2.3.2. ICP-MS analysis

For determination of mineral content of berries, a quadrupole Agilent 7500a (Agilent Technologies, CA, USA) ICP-MS equipped with a Babington nebuliser, a Peltier-cooled quartz spray chamber and a standard torch (2.5 mm i.d.) was used. The operation conditions and validation parameters are summarised in (**Table S 3** - Supplementary Material)[3]. The mineral content was expressed as micrograms of mineral per gram of fresh weight (µg g^{-1} FW) of berries.

[2]This experimental part was performed by Doctor Eulogio J. Llorent-Martínez, Department of Physical and Analytical Chemistry, University of Jaén, Campus Las Lagunillas S/N, E-23071 Jaén, Spain.
[3]For more details please check reference [121].

2.4. Preparation of methanolic extracts

Extraction of phenolic compounds (PCs) followed a previous protocol [106]: 1 g of lyophilized material was extracted with 25 mL of methanol (in a 100 mL Erlenmeyer wrapped in foil) in an ultra-sonic bath (Bandelin Sonorex, Germany) at 35 kHz and 200 W for 60 min (22 ± 2 ºC). For berries, an extraction solution composed of MeOH/H_2O (acidulated with 7% acetic acid) (80:20, v/v) was used. After sonication, solutions were filtered through Whatman No.1 filter papers, concentrated to dryness under reduced pressure in a rotary evaporator (Buchi Rotavapor R-114; USA) at 40 ºC (under reduced light). Duplicate extractions were made for each sample and the resulting dry extracts (DE) were stored in 5 mL capped flasks at 4 ºC until further analysis (**Figure 21**).

In the case of leaves, an extra step was used for removal of chlorophylls. After the first filtration step, a small amount of activated charcoal was added to the liquid extract and, after mixing for a few seconds, the solution was filtered. Then, it was concentrated to dryness and stored as aforementioned.

2.5. *In vitro* simulation of gastrointestinal digestion

A static model that simulated, sequentially, mouth, stomach and small intestine digestion was employed [122], with slight adjustments [123]. Lyophilized berries and leaves (approximately 2 g) were added, separately, to 50 mL Falcon tubes. The digestion started with the addition of 4 mL of salivary juice and incubation at 37 ºC in a water bath (Heidolph MR Hei-Standard) with agitation (150 rpm), protected from light. Then, 10 mL of gastric juice was added to the mixture and further incubated for an additional 2 h. After this period, 10 mL of duodenal and 4 mL of bile juices are added and the solution was mixed for 2 hours. At the end of the simulation digestion process, solutions were centrifuged and supernatants were frozen at -20 ºC, lyophilized, submitted to extraction (*section* **2.4**), and stored until analysis (**Figure 21**). All experiments were performed in duplicate for each sample. The detailed composition of digestive juices (salivary, gastric, intestine and bile) is given in **Table 4**. The pH of the simulated digestive juices was adjusted with 1 M HCl or 1 M NaOH.

Table 4 - Composition of simulated gastrointestinal juices (adapted from [122]).

Stock solutions	*Saliva*	*Gastric*	*Duodenal*	*Bile*
Distilled water	500 mL	500 mL	500 mL	500 mL
NaCl	58.50 mg	2.75 g	7.03 g	5.27 g
KCl	74.50 mg	0.82 g	0.57 g	0.38 g
$NaHCO_3$	1.06g	-	3.39 g	5.79g
$CaCl.2H_2O$	-	0.40 g	-	-
NaH_2PO_4	-	0.266 g	-	-
KH_2PO_4	-	-	80.30 mg	-
NH_4Cl	-	0.306 g	-	-
$MgCl_2$	-	-	50.40 mg	-
Urea	0.20 g	0.09 g	0.10 g	0.26 g
Concentrated HCl	-	6.50 mL	0.15 mL	0.15mL
Adjuncts	0.50 g mucin 1.06g α-amylase	2.50 g pepsin 3.00 g mucin	9.02 g pancreatin 1.50 g lipase	12.01 g bile salts -
pH	6.8 ± 0.2	1.30 ± 0.02	8.1 ± 0.2	8.2 ± 0.2

2.6. HPLC-DAD-ESI/MS^n analysis of methanolic extracts

2.6.1. Sample preparation

Extract solutions with concentration of 5 mg mL^{-1} were prepared by dissolving each dry extract (DE) in the initial HPLC mobile phase (UP H2O:ACN; 80:20, v/v). These extract solutions were filtered through 0.45 µM PTFE micropore membranes prior to use.

2.6.2. Liquid chromatography-mass spectrometry analysis

The HPLC-DAD-ESI/MS^n analysis was performed on a Dionex ultimate 3000 series instrument (Thermo Scientific Inc., California, USA) equipped with a binary pump, an autosampler, a column compartment, a diode-array detector hyphenated to an ion trap mass detector (Bruker Esquire model 6000; Bremen, Germany) equipped with an ESI source. Separation of PCs was achieved using the chromatographic conditions summarised in **Table 5**. Each extract solution was injected and analyzed in triplicate.

Table 5 – Operation conditions of HPLC-DAD-ESI/MS^n analysis. This method was previously optimized for the analysis of phenolic compounds [107].

HPLC conditions	
Column	Phenomenex Gemini C_{18} column (5 µm, 250 x 3.0 mm i.d.)
Mobile phase flow	0.4 mL min^{-1}
Injection volume	5 µL
Column temperature	30 ºC
Mobile phase	A: acidified ultra-pure (UP) water (with 0.1% formic acid, v/v)
	B: Acetonitrile
Gradient elution	20% B (0 min), 25% B (10 min), 25% A (20 min), 50% B (40 min),
	100% B (42 – 47 min), 20% B (49 – 55 min)
Detection	DAD (210 – 520 nm)
	MS^n (ESI^-, ESI^+)

2.6.2.1. Mass spectrometry analysis

For this analysis, a coupled Bruker Esquire model 6000 (Bremen, Germany) ion trap MS equipped with an ESI source was used. Mass spectrometry analysis was performed in negative (phenolic acids and non-anthocyanins flavonoids) and positive (anthocyanins, ANTCs) modes and scan range was set at m/z 100–1000 with a speed of 13,000 Da s^{-1}. The ESI conditions were as follows: drying and nebulizer gas (N_2) flow rate and pressure, 10 mL min^{-1} and 50 psi; capillary temperature, 325 ºC; capillary voltage, 4.5 keV; collision gas (He) pressure and energy, 1 × 10−5 mbar and 40 eV. Data acquisition was made in auto MS^n mode, with an isolation width of 4.0 m/z, and a fragmentation amplitude of 1.0 V (MS^n up to MS^4). Esquire control and Data Analysis softwares (Bremen, Germany) were used for the data acquisition and processing, respectively.

2.6.3. HPLC-DAD quantification of phenolic compouds in the methanolic extracts

Quantitative determination of phenolic compounds was carried out *via* HPLC–DAD analysis. For this, one PC was selected as the standard for each group/family of PCs, based on the structural similarities, and used to determinate relative individual concentrations [84]. Caffeic and protocatechuic acids were selected as the external standards for quantification of hydroxycinnamic acids (HCAs) and hydroxybenzoic acids (HBAs), respectively. ANTCs standard was cyanidin-3-*O*-glucoside (C3G). Quercetin dihydrate, (+)-catechin hydrate, apigenin, ellagic acid and hesperidin were the standards used for the flavonols, flavan-3-ols, flavones, ellagitannins and flavanones, respectively. Myricitrin (MCT) was used for the relative quantification of myricetin derivatives.

Stock standard solutions (1000 mg L^{-1}) were freshly prepared in methanol and stored at -20 ºC until use. Six different concentration levels (5 - 100 mg L^{-1}) were prepared by dilution with the initial eluent gradient (UP H_2O:ACN; 80:20, v/v) and analysed under previous conditions (*section* **2.6.2**), to obtain the respective calibration curve, plotting HPLC chromatogram peak area versus concentrations of the standard solutions. A linear regression equation was calculated by the least squares method. The selected detection wavelengths were 520 nm for ANTCs, 320 nm for HCAs and 280 nm for the other PCs. HPLC–MS data analyses were used to corroborate peak assignment. The calculations of the relative individual phenolic contents were carried out by direct extrapolation from the calibration curve of selected reference standard. Total individual phenolic content (TIPC) was defined as the sum of the relative amount of the compounds in the methanolic extracts and expressed as milligrams per gram of dry extract (mg g^{-1} DE).

2.7. Total phenolic and flavonoid contents

2.7.1. Total phenolic content (TPC)

TPC was measured by the Folin-Ciocalteu method [124] with some adjustments [125]. Extracts were dissolved in methanol to yield a concentration (w/v) of 5 mg mL^{-1}. Each extract solution (50 µL) was mixed with 1.25 mL Folin-Ciocalteu reagent (FCR) (diluted 1:10 fold with distilled water) and 1 mL of sodium carbonate (7.5%) solution. The mixture was incubated for 30 minutes at room temperature (protected from light) and absorbance was measured at 765 nm (Perkin Elmer UV–vis Lambda 2, Germany). TPC was expressed as miligrams of gallic acid equivalents per gram of dry extract (mg GAE g^{-1} DE), based on the gallic acid calibration curve (50 - 600 mg L^{-1}).

2.7.2. Total flavonoid content (TFC)

TFC was determined by the aluminium chloride method [126] with some modifications [125]. In a 5-mL flask, 0.5 mL of extract solution (5 mg mL^{-1} in methanol), 1.5 mL of methanol, 2.8 mL of distilled water, 0.1 mL of potassium acetate solution (1 M) and 0.1 mL of aluminium chloride (10% in methanol) solution were added and mixed. After incubation for 30 min at room temperature (protected from light) the absorbance was read at 415 nm (Perkin Elmer UV–vis Lambda 2, Germany). Results were expressed as miligrams of rutin equivalent per gram of dry extract (mg RUE g^{-1} DE), based on the rutin calibration curve (10 – 200 mg L^{-1}).

2.8. *In vitro* enzyme inhibitory assays

2.8.1. Yeast α-glucosidase inhibitory assay

The inhibition of yeast α-glucosidase (AGLU) activity was determined by measuring the amount of *p*-nitrophenyl, hydrolyzed by the enzyme from *p*-nitrophenyl-α-D-glucopyranoside (*α*-*p*NPG). This assay performed using a previous methodology [18] with some adaptions [125]. In a 96-well plate, 50 μL of extract solution (sequential dilutions) was combined with 50 μL of enzyme solution (0.1 mg mL^{-1}) and 50 μL of *α*-*p*NPG solution (5 mM). All solutions were prepared in 0.1 M phosphate buffer (pH 6.9). The mixture was incubated at 37 °C for 20 minutes in the dark. Finally, 100 μL of sodium carbonate aqueous solution (0.1 M) was added and the absorbance was read at 405 nm (Victor^3 1420 multilable plate counter, Perkin-Elmer). Acarbose and 1-deoxynojirimycin (1-DNJ) were used as positive controls. Serial dilutions of these reference compounds were prepared in the above buffer and the same procedure for samples was used. AGLU control (C) was representative of the 100% enzyme activity and, in this case, extract was replaced by buffer. Appropriate sample blanks (SB) were also included, for each sample, for correcting the background absorbance. For this, buffer was used instead of the substrate. Blank to control (CB) consisted of the buffer (instead of extract and substrate), enzyme and sodium carbonate solution (added after incubation). Inhibition (%) of AGLU activity was calculated according to the following formula:

$$Inhibition\ (\%) = \frac{(A_C - A_{CB}) - (A_S - A_{SB})}{(A_C - A_{CB})} \times 100 \quad \textbf{(Equation 2)}$$

where A_C, A_{CB}, A_S, A_{SB} were the absorbance of control, blank control, sample and blank sample, respectively. The inhibitory activity was expressed as the IC_{50} value (mg mL^{-1} DE) determined from the least-squares regression line of the logarithmic concentrations plotted against percentage inhibition. This value corresponds to the concentration of extract able to reduce the enzyme activity by 50% with reference to the control.

2.8.2. Rat α-glucosidase inhibitory assay

For this assay, 0.5 g of intestinal acetone powder from rat was dissolved in 10 mL of phosphate buffer (0.1 M, pH 6.9) and sonicated for 10 min. After centrifugation (4000 rpm, 10 min, 4 °C)(Sigma 3K30), the resulting supernatant was diluted 5 times with above buffer and was used as the enzyme solution. It was prepared freshly for each experiment. The measurement of rat AGLU inhibition was performed as described in the previous section (*section* **2.8.1**). Acarbose and 1-DNJ were used as positive controls. Serial dilutions of these reference compounds were prepared in the above buffer and the same procedure for samples was used.

2.8.3. Almonds β-glucosidase inhibitory assay

The inhibition of β-glucosidase (BGLU) was carried out as above (*section* **2.8.1**) using *β-p*NPG as substrate. For this case, conduritol B epoxide (CBE) and 1-DNJ were used as positive controls. Serial dilutions of these reference compounds were prepared in phosphate buffer (0.1 M, pH 6.9) and the same procedure for samples was used.

2.8.4. Pancreatic α-amylase (AMY) inhibitory assay

The AMY inhibitory effect of the methanolic extracts was assayed by measuring the amount of hydrolysed starch by the enzyme, using iodine/iodate solution. The assay was performed as described before [18], with slight modifications [125]. Briefly, 20 µL of extract solution (serial dilutions) and 40 µL of starch solution (2 g L^{-1}) were mixed with 20 µL of AMY solution (0.1 mg mL^{-1}). All solutions were prepared in 0.1 M phosphate buffer (pH 6.9). After incubation, at 37 °C for 20 min, the reaction was stopped by the addition of 80 µL of HCl (0.4 M) followed by 100 µL of I_2 solution (5 mM in 5 mM KI) and the absorbance was read at 620 nm (Victor^3 1420 multilabel plate counter, Perkin-Elmer). Acarbose was used as positive control. Sequential dilutions were prepared in the above buffer and the same procedure for samples was used. The inhibitory activity was expressed as the IC_{50} value (mg mL^{-1} DE) and determined as described previously (*section* **2.8.1**).

2.8.5. Pancreatic lipase (PL) inhibitory assay

The inhibition of PL activity was determined by measuring the release of *p*-nitro-phenol, from *p*-nitrophenyl butyrate (*p*-NPB), by the enzyme. This assay was based on a previous procedure [22], with some modifications [125]. In resume, 40 µL of extract solution (serial dilutions) was mixed with 20 µL of *p*-NPB solution (10 mM) and 40 µL of the enzyme solution (2.5 mg mL^{-1}). Extracts and enzyme solution were prepared in phosphate buffer (0.1 M, pH 8). The enzyme substrate was dissolved in ethanol. After 20 minutes of incubation (37 °C) absorbance was read at 405 nm (Victor^3 1420 multilabel plate counter, Perkin-Elmer). A stock solution of orlistat (positive control) was prepared in DMSO (10 mg mL^{-1}) and further diluted with buffer. The experiment was conducted as described above. The inhibitory activity was expressed as the IC_{50} value (mg mL^{-1} DE) and determined as described previously (section 2.8.1).

2.8.6. Human aldose reductase (HAR) inhibitory assay

The inhibition of HAR activity was assayed spectrophotometrically by measuring the decrease in the absorption of NADPH due to its oxidation, adapted from a previous publication [127]. In a 96 well-plate (UV-transparent), 25 µL of extract solution (serial dilutions) were mixed with 25

µL of DL-glyceraldehyde (10 mM) and 25 µL of enzyme solution (1 mg mL^{-1}). All solutions were prepared in 0.1 M phosphate buffer containing 0.2 mM ammonium sulfate and 5 mM β-mercaptoethanol (pH 6.2). The reaction was initiated with the addition of 50 µL NADPH solution (0.5 mM) and incubation at 37 ºC for 20 minutes. The enzyme activity was measured at 340 nm (Victor^3 1420 multilabel plate counter, Perkin-Elmer) over 0 and 20 min of reaction. Quercetin was used as positive control. A stock solution was prepared in ethanol (10 mg mL^{-1}) and further diluted with above buffer. The absorbance of the sample mixture (S) was measured against control (C), representative of 100% enzyme activity (contained all components except for the extract). The inhibition (%) of aldose reductase activity was calculated by the following equation:

$$Inhibition\ (\%) = \frac{(A_{C\ 20min} - A_{C\ 0min}) - (A_{S\ 20min} - A_{S\ 0min})}{(A_{C\ 20min} - A_{C\ 0min})} \times 100 \quad \textbf{(Equation 3)}$$

where A_C, A_S, were the absorbance of control and the sample at 0 and 20 min of reaction. The inhibitory activity was expressed as the IC_{50} value (mg mL^{-1} DE) determined from the least-squares regression line of the logarithmic concentrations plotted against percentage inhibition. This value corresponds to the concentration of extract able to reduce the enzyme activity by 50% with reference to the control.

2.9. *In vitro* evaluation of anti-glycation potential of methanolic extracts

2.9.1. Bovine-serum albumin (BSA) glycation inhibition assay

Inhibition of BSA glycation was measured fluorimetrically in 96 black well-plates, with slight modifications from a published protocol [73]. Each well contained 20 µL of sample extracts (serial dilutions), 50 µL of BSA solution (10 mg mL^{-1}), 80 µL of phosphate buffer (0.1 M containing NaN_3, 3 mM; pH 7.4) and 50 µL of fructose or ribose solution (0.5 M). All solutions were prepared in the above buffer. Plates were incubated for 24 hours at 37 °C (in the dark) and then analyzed at an excitation wavelength of 355 nm and emission wavelength of 460 nm (Victor^3 1420 multilabel plate counter, Perkin-Elmer). Aminoguanidine (AMG) and quercetin were used as positive controls. A stock solution of quercetin was prepared in ethanol (10 mg mL^{-1}) and further diluted with buffer. A control (C), i.e., 100% AGEs formation, consisted of wells with buffer (instead of sample), BSA and sugar. To subtract intrinsic fluorescence resulting from incubation with BSA, a blank (SB) was made for each sample (replacing the sugar by buffer). A blank control (BC), with no AGE formation, consisted of wells with only BSA and buffer. The percentage (%) of inhibition of AGEs formation was calculated according to the following equation:

$$Inhibition\ (\%) = \frac{(F_C - F_{CB}) - (F_S - F_{SB})}{(F_C - F_{CB})} \times\ 100 \qquad \textbf{(Equation 4)}$$

where F_C, F_{CB}, F_S, F_{SB} were the fluorescence of control, blank control, sample and blank sample, respectively. The inhibitory activity was expressed as the IC_{50} value (mg mL^{-1} DE) determined from the least-squares regression line of the logarithmic concentrations plotted against percentage inhibition. This value corresponds to the concentration of extract able to reduce fluorescence by 50% with reference to the control.

2.10. *In vitro* Antioxidant Assays

2.10.1. ABTS radical cation ($ABTS^{\bullet+}$) scavenging assay

The antioxidant activity (AOA) of extracts was evaluated by the method of decolorization of $ABTS^{\bullet+}$ solution. First, 50 mL of ABTS aqueous solution (2 mM) was reacted with 200 µL of potassium persulfate solution (70 mM) [118]. This mixture was kept in the dark for at least 16 hours at room temperature and was stable in this form during two days [118].

Before usage, the $ABTS^{\bullet+}$ solution was diluted with phosphate buffered saline (PBS) solution (10 mM) to an initial absorbance of 0.700 ± 0.021 at 734 nm. This solution was freshly prepared for each analysis. For the evaluation of the radical scavenging activity, 40 µL of extract solution (5 mg mL^{-1} in MeOH) was added to 1.96 mL of $ABTS^{\bullet+}$ solution. PBS was used as a blank. The decrease of absorbance at 734 nm (Perkin Elmer UV–vis Lambda 2, Germany) was measured during 6 minutes [125]. Results were expressed based on the Trolox calibration curve (0.5 - 0.7 mM in ethanol) as millimole of Trolox equivalents per gram of dry extract (mmol TE g^{-1} DE).

2.10.2. $DPPH^{\bullet}$ radical scavenging activity

The measurement of decolorization of the $DPPH^{\bullet}$ radical solution followed a previous reported methodology [119] with some adaptations [125]. For each determination, 100 µL of extract solution (5 mg mL^{-1} in MeOH) was added to 3.5 mL of $DPPH^{\bullet}$ solution (0.06 mM in MeOH). Absorbance was measured at 516 nm (Perkin Elmer UV–vis Lambda 2, Germany), after 30 min of reaction in the dark (room temperature). Methanol was used as blank control. The radical scavenging activities were expressed as mmol TE g^{-1} DE, based on the Trolox calibration curve (0.2 – 1.2 mM).

2.10.3. Nitric oxide ($NO^{\bullet}$) radical scavenging activity

The anti-radical activity was determined spectrophotometrically, with slight modifications [125] from a previous publication [28]. In a 96-well plate, 50 µL of sodium nitroprusside solution (20 mM) was mixed with 50 µL of extract solution (5 mg mL^{-1}) for 60 min, at room temperature, under

light. All solutions were prepared in 0.1 M phosphate buffer (pH 7.4). After incubation, 50 µL of Griess reagent (1% sulfanilamide and 0.1% N-(1-naphthyl)ethylene-diamine dihydrochloride (NEDA) in 2% phosphoric acid), was added to each well. For the blank measurements, Griess reagent was replaced by 2% phosphoric acid solution. After 10 minutes, the absorbance was read at 550 nm (Victor^3 1420 multilabel plate counter, Perkin-Elmer) and the results were expressed as mmol TE g^{-1} DE, based on the Trolox calibration curve (4 - 40 mM in EtOH).

2.10.4. Superoxide Anion ($O_2^{\bullet-}$) radical scavenging activity

Superoxide anion radicals ($O_2^{\bullet-}$) were generated by the NADH/PMS system according to a described procedure [120]. In a 96 well-plate, 25 µL of extract solution (5 mg mL^{-1}) was mixed with 200 µL of a solution composed of EDTA (0.1 mM), nitroblue tetrazolium chloride (62 µM) and NADH (98 µM). The reaction was initiated by the addition of 25 µL of phenazine methosulfate (PMS) (33 µM, containing 0.1 mM EDTA) to each well. All solutions were prepared in 0.1 M phosphate buffer (pH 7.4). After 5 minutes, the absorbance was measured at 550 nm (Victor^3 1420 multilabel plate counter, Perkin-Elmer). For the individual blanks, buffer was used instead of PMS solution. The AOA was expressed as mmol TE g^{-1} DE, based on the Trolox calibration curve (4 – 40 mM in EtOH).

2.11. Cytotoxicity evaluation of the methanolic extracts

2.11.1. Cell Culture

Human Caco-2 cells were supplied by the European Collection of Authenticated Cell Cultures (ECACC; UK). Caco-2 cells were cultured in minimum essential medium (MEM) supplemented with 10% (v/v) fetal bovine serum (FBS), 1% (v/v) antibiotic mixture (10,000 units/mL of penicillin, 10,000 µg/mL of streptomycin, and 25 µg/mL of amphotericin B), 1% (v/v) non-essential aminoacids (NEAA) and 1% (v/v) L-glutamine (200 mM) in petri dishes. The cells were grown at 37 ºC in an incubator with 5% CO_2. Growth medium was changed 3 times per week.

2.11.2. Cell viability (resazurin reduction assay)

The cytotoxic effect of plant extracts was evaluated in Caco-2 cells, as a model of intestinal epithelial cells, by the resazurin reduction assay [128]. Caco-2 cells were seeded on 96-well flat-bottom plates at a concentration of 5 x 10^4 cells/well. Each well contained 100 µl of growth medium. Following a 24 h incubation (37 ºC, 5% CO_2), the growth medium was removed. Then, different concentrations of extract solutions (dissolved in PBS) were added to 200 µL of growth medium. The cells were incubated at 37 ºC and 5% CO_2 for 24 h. After this period, the growth medium was removed

and 150 µL of 10% v/v resazurin (0.1 mg mL^{-1}) in cell culture was added to each well. After 3 hours of incubation at 37 ºC and 5% CO_2, resorufin's fluorescence was measured (λex = 530nm, λem = 590nm; Victor^3 1420 multilabel plate counter, Perkin-Elmer). All tests were performed in duplicate (n = 8). The percentage (%) of cell viability was determined as follows:

$$Cell\ viability\ (\%) = \frac{F_C - F_S}{F_C} \times\ 100 \quad \textbf{(Equation 5)}$$

where F_C and F_S were the fluorescence of control (untreated cells) and samples respectively. Cytotoxicity was expressed as the IC_{50} value (mg mL^{-1} DE) determined from the least-squares regression line of the logarithmic concentrations plotted against percentage inhibition. This value corresponds to the concentration of extract able to reduce the fluorescence of treated cells by 50% with reference to the control (cells treated only with culture medium).

2.12. Statistical Analysis

All experiments were run at least in triplicate for each sample and results are given as the means ± standard deviations. Data was analysed using one-way analysis of variance (ANOVA) followed by Tukey's post hoc test using SPSS for Windows, IBM SPSS Statistics 20 (SPSS, Inc., USA). A value of $p < 0.05$ was considered statistically significant. Pearson correlation coefficients (r) were determined to corroborate relationships between selected parameters.

Chapter III – Results and Discussion

A. Phytochemical Composition

The initial work plan of this Ph.D. project consisted of a list of more than 30 plants species. As it will be explained in the next sections, the main goal was to evaluate the potential of targeted plants extracts/components as modulators of glucose and lipids metabolism, anti-glycatives and antioxidant agents. Considering the results of an initial screening (yeast α-glucosidase (AGLU) and α-amylase (AMY) assays (**Table S 4** – Supplementary Material), we decided to focus this investigation on berry-producing plants (BPPs) in regard to their higher inhibitory activities towards key carbohydrate-hydrolysing enzymes. Nevertheless, the remaining plant species were studied in parallell and, some of the obtained data, has been already published in scientific literature.

Hence, the anti-diabetic potential of six BPPs were evaluated in this study: four endemic from Madeira archipelago (*M. faya*, *R. grandifolius*, *S. lanceolata* and *V. padifolium*), one non-native species (*E. umbellata*) and one endemism from Azores archipelago (*V. padifolium*). Additionally, a sample of *M. faya* was collected at Ilha Terceira (Azores) to establish a comparison of the phenolic profiles and bioactivities.

In the next subsections, the results obtained for each plant species are presented divided by analysis/assay.

1. Physico-chemical analysis

In the present work, the total soluble solids (TSS) and moisture contents of selected BPPs were determined.

1.1. Total soluble solids (TSS) determination

The TSS content was determined for each berry species. The values ranged between 4.4 and 16.9 (**Table 6**), corresponding to *S. lanceolata* and *E. umbellata*, respectively.

Table 6- Content of total soluble solids (TSS) and total sugars of berries under study.

Berry species		**º Brix**		**Sucrose eq. (g L^{-1})**		**Total sugars (g 100 g^{-1} FW)**	
		2013	2014	2013	2014	2013	2014
E. umbellata		16.9	16.5	179.68	175.39	5.74	5.60
M. faya	MX	-	15.5	158.24	164.67	6.60	7.39
	FL	-	16.2	-	172.18	-	7.68
	ASJ	-	15.2	-	161.46	-	7.21
	BV	-	16.3	-	173.25	-	7.70
	SX	-	16.0	-	170.03	-	7.47
	RJ	-	16.2	-	172.18	-	7.23
	PM	-	15.7	-	166.82	-	6.27
	TC	-	13.4	-	142.17	-	7.14
R. grandifolius	FX	-	8.3	-	87.50	-	5.10
	MX	-	10.3	-	108.94	-	5.72
S. lanceolata		-	4.4	-	45.70	-	2.15
V. cylindraceum		-	11.4	-	120.73	-	4.16
V. padifolium		11.7	12.1	123.94	128.23	4.57	5.13

MX: Machico; FL: Faial; ASJ: Arco de São Jorge; BV: Boaventura; SX: Seixal; RJ: Ribeira da Janela; PM: Porto Moniz; TC: Ilha Terceira.

E. umbellata berries presented a higher TSS content as compared to previous works (14.5º Brix)[129]. Values of *M. faya* berries varied between 13.4 and 16.3 ºBrix; slightly higher than that found in different cultivars of *M. rubra* (8.74 – 11.67 ºBrix)[82]. Berries of *R. grandifolius* collected in Funchal (FX) showed a higher TSS content than Machico (MX) counterpart. These values are slightly lower than those reported for other *Rubus* species (10.2 – 12.0 º Brix) [88]. Previous analysis on *Sambucus nigra* and *S. canadenses* [130] showed superior values

(11.2 – 15.4 º Brix). According to literature [131–134], TSS content of *Vaccinium spp.* berries range between 6.0 and 15.5 ºBrix, which agrees with the obtained values in this analysis (**Table 6**).

1.2. Moisture content

The moisture content (%) of berries and leaves of analyzed berry-producing plants (BPPs) was determined after freeze-drying and the percentages are shown in **Table 7**.

Table 7- Moisture content (%) of berry-producing plants under study.

Plant species		**Berries**		**Leaves**	
		2013	2014	2013	2014
E. umbellata		31.95	35.42	16.99	17.84
M. faya	MX	-	45.48	-	31.42
	FL	-	46.37	-	24.08
	ASJ	-	45.29	-	29.91
	BV	-	45.05	-	22.93
	SX	-	44.51	-	27.48
	RJ	-	41.98	-	26.32
	PM	-	37.59	-	27.74
	TC	-	36.12	-	20.34
R. grandifolius	FX	-	58.31	-	48.33
	MX	-	52.50	-	47.41
S. lanceolata		-	47.06	-	25.17
V. cylindraceum		-	27.82	-	21.68
V. padifolium		28.79	40.0	10.79*	10.35*
				14.04**	13.76**

*Young Leaves; **Mature Leaves. MX: Machico; FL: Faial; ASJ: Arco de São Jorge; BV: Boaventura; SX: Seixal; RJ: Ribeira da Janela; PM: Porto Moniz; TC: Ilha Terceira.

Berries possessed a higher moisture content (27.82 – 58.31%) than leaves (10.35 – 48.33%). The highest values were observed for *R. grandifolius* samples, while berries of *V. cylindraceum* and young leaves (YLs) of *V. padifolium* showed the lowest contents (**Table 7**).

2. Determination of berries mineral content by inductively coupled plasma-mass spectrometry (ICP-MS)[4]

Berries represent a good source of both macro- and micronutrients (K, Ca, Mg, Fe, Cu, among others) [5,35,39]. Many elements are required in small amounts to maintain human health due to their nutritious value, as they play important roles in various important physiological and biochemical processes in the human system. These elements must be regularly provided through the diet [39,103]. In contrast, toxic metals can turn a potential foodstuff unfit for human consumption. It has also been proposed that the anti-diabetic activity of some plant-based products is the result of elevated levels of metals such as Mg, Mn, Ca, Cr and Zn, which are known to regulate blood sugar levels [135–137].

The inorganic content os targeted berries has not been previously described in scientific literature (except for *E. umbellata*). For an easier discussion, only the average concentrations (including different years and different locations) will be used (**Table 8**). The range of mineral concentrations (min – max value) for each species are shown in Supplementary Material (**Table S 5 - Table S 9**). When detected, the levels of different toxic elements (Ag, As, Cd, Hg, Pb, Sb, Sn, and Tl) were very low, so none of these berries would represent a risk to human health from this point of view.

The recommended dietary allowance (RDA) values for minerals provided by the Commission of the European Communities [138] have been used to calculate the amount of minerals ingested through the consumption of each of the analyzed berries. For this case, calculations were made considering a daily consumption of 30 g of fresh berries, which is a normal amount for similar foodstuffs. The obtained results are shown in **Table 9** and will be discussed in the following sub-sections.

[4] This part of the work has already been published [121].

Table 8 - Average mineral content of analysed berries (μg g^{-1} of FW) determined by inductively coupled plasma-mass spectrometry (ICP-MS). Data represent the mean ± standard deviation (n = 3). Reprinted (adapted) with permission from [121].

	E. umbellata	***M. faya***	***R. grandifolius***	***S. lanceolata***	***V. cylindraceum***	***V. padifolium***
Al	30 ± 30^{a}	80 ± 50^{a}	100 ± 100^{a}	4.7 ± 0.5^{a}	37 ± 3^{a}	25 ± 5^{a}
Ba	1.1 ± 0.1^{a}	0.5 ± 0.3^{a}	5 ± 1^{c}	3.3 ± 0.3^{b}	5.6 ± 0.5^{c}	3.1 ± 0.1^{b}
Ca	1000 ± 100^{a}	900 ± 100^{a}	1700 ± 400^{c}	1200 ± 100^{ab}	1400 ± 100^{c}	860 ± 80^{ab}
Cd	N.D.	N.D.	N.D.	N.D.	N.D.	Detected
Co	0.03 ± 0.01^{a}	0.2 ± 0.1^{b}	0.05 ± 0.01^{a}	0.016 ± 0.01^{a}	0.008 ± 0.01^{a}	0.08 ± 0.03^{a}
Cr	Detected	0.6 ± 0.5^{a}	0.6 ± 0.4^{a}	0.12 ± 0.01^{a}	0.08 ± 0.01^{a}	Detected
Cu	6.0 ± 0.9^{c}	1.6 ± 0.5^{a}	5 ± 1^{bc}	3.5 ± 0.3^{ab}	3.7 ± 0.3^{b}	4 ± 1^{bc}
Fe	32 ± 5^{a}	110 ± 50^{b}	120 ± 90^{b}	28 ± 5^{a}	19 ± 1^{a}	17 ± 3^{a}
K	7900 ± 300^{c}	4400 ± 500^{ab}	5000 ± 700^{b}	15100 ± 400^{d}	4700 ± 300^{ab}	3500 ± 400^{a}
Mg	420 ± 10^{a}	550 ± 100^{a}	1500 ± 200^{b}	1590 ± 50^{b}	420 ± 20^{a}	530 ± 10^{a}
Mn	11 ± 1^{a}	9 ± 3^{a}	30 ± 10^{b}	12 ± 1^{a}	131 ± 5^{c}	44 ± 5^{b}
Mo	0.7 ± 0.1^{b}	0.11 ± 0.05^{a}	0.12 ± 0.01^{a}	Detected	N.D.	N.D.
Na	70 ± 6^{a}	2000 ± 400^{c}	70 ± 10^{a}	65 ± 3^{a}	560 ± 30^{b}	60 ± 5^{a}
Ni	1.4 ± 0.2^{b}	1.6 ± 0.6^{b}	1.1 ± 0.3^{ab}	0.42 ± 0.05^{a}	0.36 ± 0.03^{a}	1.1 ± 0.1^{ab}
P	800 ± 100^{b}	330 ± 50^{a}	800 ± 200^{b}	2010 ± 70^{c}	760 ± 30^{b}	560 ± 40^{ab}
Pb	N.D.	Detected	N.D.	N.D.	N.D.	N.D.
Sb	N.D.	Detected	N.D.	N.D.	N.D.	N.D.
Ti	1.7 ± 0.3^{a}	20 ± 10^{a}	20 ± 20^{a}	0.69 ± 0.05^{a}	0.44 ± 0.03^{a}	0.5 ± 0.2^{a}
V	Detected	0.3 ± 0.2^{a}	0.4 ± 0.3^{a}	Detected	N.D.	Detected
Zn	10 ± 6^{ab}	4.4 ± 0.5^{ab}	9 ± 3^{b}	5.9 ± 0.4^{b}	5.3 ± 0.3^{b}	5.4 ± 0.9^{a}

Means in the same line not sharing the same letter are significantly different at $p < 0.05$ probability level.

Table 9 – Mineral percentage (%) contribution for RDA of analysed berry species. Data represent the mean ± standard deviation (n = 3). Reprinted (adapted) with permission from [121].

	RDA	% RDA					
	(mg)	***E. umbellata***	***M. faya***	***R. grandifolius***	***S. lanceolata***	***V. cylindraceum***	***V. padifolium***
Ca	800	3.8	3.4	6.5	4.4	5.4	3.2
Cu	1	18	4.8	15	10.5	11.1	12
Fe	14	6.9	23.6	25.7	6	4.1	3.6
K	2000	11.8	6.6	7.5	22.6	7.1	5.2
Mg	375	3.4	4.4	12	12.7	3.4	4.2
Mn	2	16.5	13.5	45	18	193	66
Mo	0.05	42	6.6	7.2	---	---	---
P	700	3.4	1.4	3.4	8.6	3.3	2.4
Zn	10	3	1.3	2.7	1.8	1.6	1.6

2.1. *Elaeagnus umbellata*

In general, the average levels of the most important nutritional elements varied between 7900 μg g^{-1} of K and 0.03 μg g^{-1} of Co. Concentrations decreased in the following order: K > Ca > P > Mg > Na > Fe > Mn > Cu > Ni > Mo > Co (**Table 8**). V was detected, although in amounts too low to be quantified. Some elements concentration was affected by the year of collection ($p < 0.05$), namely K, Mn, Mo, P and Zn (**Table S 6**). The latter decreased approximately 3-fold from 2013 to 2014. The contribution to the RDA (**Table 9**) was lower than 10 % for Ca, Fe, Mg, P, and Zn. However, contributions between 10-20 % were observed expected for Cu, K, and Mn, and higher than 40% for Mo.

Previous analysis on this species [102,103] have also reported K, P, Mg and Ca as the main minerals, but at lower concentrations that those here observed. Different cultivars and edaphoclimatic conditions might be the reason for the observed variations but accuracy of analytical method is a more reasonable explanation, since those authors used atomic absorption for quantification.

2.2. *Myrica faya*

For this species, the levels of nutritional elements decreased in the following order: K (4400 μg g^{-1}) > Na > Ca > Mg > P > Fe > Mn > Zn > Cu > Ni > V > Co > Mo (0.11 μg g^{-1}) (**Table 8**). Significant variations ($p < 0.05$) were found among berries collected in different locations (except for Ba and Cu levels) (**Table S 7**). Different soil compositions and climatic conditions might justify these

differences. Except for Mn (13%) and Fe (24%), all elements showed a contribution to the RDA lower than 10% (**Table 9**).

Similarly, K, Ca and Mg have been reported as dominant elements in *M. rubra* (bayberry) [139]. Levels of K in *M. faya* were superior than in *M. rubra* [139], but the remaining elements presented lower or similar concentrations.

2.3. *Rubus grandifolius*

In this case, the contents of nutritional elements decreased in the following order: K (5000 μg g^{-1}) > Ca > Mg > P > Fe > Na > Mn > Zn > Cu > Ni > V > Mo > Co (0.05 μg g^{-1}) (**Table 8**). Variations were found for Ba, Ca, K, Mg, Mn, P and Zn contents in samples collected in different locations ($p < 0.05$). Except for Ba and Mo, berries collected in Machico (MX) (600 m high) presented higher concentrations than Funchal (FX) counterparts (collected at 1000 m high) (**Table S 8**). This is probably due to the different soil characteristics. The contribution of *R. grandifolius* minerals to the RDA is significant for Cu (15%), Fe (26%), Mg (12%) and Mn (45%) (**Table 9**).

The concentration of minerals found in the present study, were higher than those reported for other *Rubus* species (blackberry and raspberry) [39,134].

2.4. *Sambucus lanceolata*

The levels of the nutritional elements in this case decreased in the following order: K (15100 μg g^{-1}) > P > Mg > Ca > Na > Fe > Mn > Zn > Cu > Ni > Co (0.016 μg g^{-1}) (**Table 8)**. In terms of contribution to the mineral RDA, P, Cu, K, Mg and Mn present percentages close or higher than 10 % (**Table 9**).

Inferior mineral levels were documented in *S. nigra* [39].

2.5. *Vaccinium cylindraceum*

For this species, the quantified levels of the inorganic elements decreased in the following order: K (4700 μg g^{-1}) > Ca > P > Na > Mg > Mn > Fe > Zn > Cu > Ni > Co (0.008 μg g^{-1}) (**Table 8**). Except for Cu (11%) and Mn (> 190 %)[5], the contribution to the RDA of most elements were below 10 % (**Table 9**).

[5]The highest level of intake at which unwanted side effects are mot expected has been established at 11 mg/day for adults (including pregnant and breast feeding women). So consumption of *V. cylindraceum* is not toxic for humans.

2.6. *Vaccinium padifolium*

Similar to previous species, K, Ca and P were the major components of *V. padifolium*. In this case, the concentrations of the nutritional elements decreased in the following order: K (3500 μg g^{-1}) > Ca > P > Mg > Na > Mn > Fe > Zn > Cu > Ni > Co (0.08 μg g^{-1}) (**Table 8**). Significant differences ($p < 0.05$) were observed for the contents of Al, Ca, K, Mg, Mn and P in berries collected in consecutive years (**Table S 9**). Additionally, variations were observed between species: *V. cylindraceum* showed higher contents of minerals (except for C, Cu, Mg and Ni) (**Table 8**). Genetic factors (species, cultivar) and edaphoclimatic conditions (soil conditions, climate, etc) are known to affect chemical composition of berries [35]. The contribution to the RDA of minerals was lower than 10 % for all elements (**Table 9**). Exceptions were observed for Cu (12 %) and Mn (66 %), which makes this species less interesting in terms of their mineral content than the previous ones. The levels of all minerals in analysed *Vaccinium spp*. berries were higher than some reports in *V. corymbosum* berries [39,134].

2.7. General discussion

In general, the highest levels of Ca and Fe were observed in *R. grandifolius*. Berries of *E. umbellata* presented the highest levels of Cu and Zn. *S. lanceolata* exhibited the highest content in K, Mg and P. *V. cylindraceum* berries showed the highest levels of Mn, much higher than in the other berries. For comparison basis, the levels of all the minerals were higher than some reports in strawberries and cherries [134], cranberries and blackcurrants [39].

In conclusion, the mineral composition was diverse among the different species. The analysed berries presented low concentrations of Co, Ni, Mo and Cu, but proved to be good sources of K, Ca, P, Na and Mg. Moreover, only very low contents of toxic elements were detected, if at all, ensuring the absence of risk for human health. In this sense, *R. grandifolius* and *S. lanceolata* stand out due to their highest contribution of dietary essential elements (Ca, Cu, Fe, K, Mg, Mn, P and Zn). Consumption of *E. umbellata*, *R. grandifolius*, and *S. lanceolata* may potentially contribute to a dietary control/management of hyperglycaemia in diabetic patients due to their appreciable Ca, Mg and Zn amounts. The high Mn content in *V. cylindraceum* could also be beneficial for glucose homeostasis. It has been suggested that minerals like Ca, Cr, Mg, Mn, and Zn are involved in insulin synthesis and secretion, increase insulin sensivity and glucose tolerance, scavenge free radicals and reduce lipid oxidation [34,135–137]**.** Hence, dietary supplementation of minerals with anti-diabetic effects, through berries intake, seems an interesting approach to prevent T2DM symptoms.

3. Extraction of Phenolic Compounds (PCs)

Prior to the phenolic characterization, the influence of different experimental variables on the extraction procedure (solvent type, concentration, and duration of extraction) was investigated to increase the extraction efficiency of PCs. Initially, the extraction process was optimized for leaves of *M. faya*, with acetone and methanol tested as solvents[6]. The concentration of extractor in water (70 - 100%, v/v) was also evaluated. The efficiency of the different extraction conditions was determined by means of TPC assay (*section* **2.7.1**) (expressed as mg GAE 100 g^{-1} FW).

Considering obtained data (**Figure 22 A-B**), pure methanol exhibited the highest phenolics amounts and was used to further evaluate the influence of extraction time (15, 30 and 60 min). Results indicated that increasing the extraction duration had a positive effect on the extraction efficiency **(Figure 22 C**), therefore, an extraction time of 60 min with 100% methanol was considered as optimum conditions.

Figure 22 - Extraction efficiency of different extraction conditions determined by TPC (mg/100 g DW) in *Myrica faya* leaves: (A) effect of solvent (methanol versus acetone); (B) effect of methanol concentration (v/v); (C) effect of extraction time. Data represent the mean ± standard deviation (n = 3). Reprinted (adapted) with permission from [106].

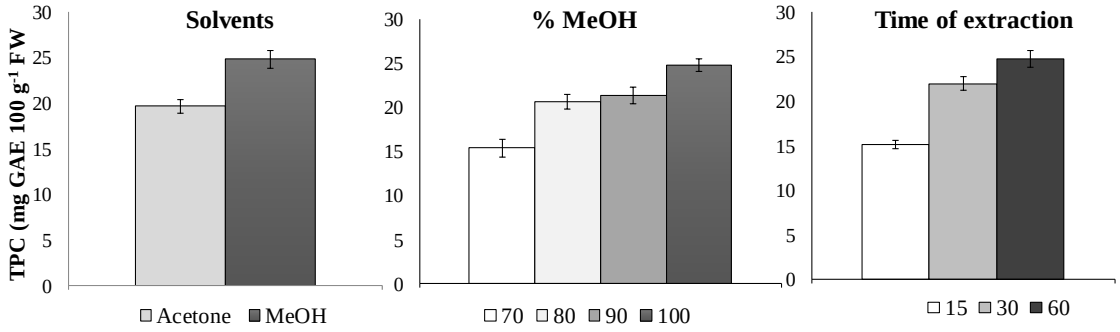

For berries, a solution composed of 80:20 MeOH/water (containing 7% acetic acid) was chosen instead. According to literature, anthocyanins (ANTCs) extraction is more efficient when using acidified aqueous mixtures of polar solvents, like methanol. This enhances extraction due to rupture of cellular membranes and simultaneously dissolve and stabilize ANTCs [36,37,43]. This same extraction procedure was further applied to berries and leaves of other BPPs (non-digested and digested) to maintain the homogeneity of the extraction process and facilitate comparison between all samples. The extraction percentage yields are shown in **Table 10**.

[6]This part of the work has already been published [106].

In general, extraction yields of berries were higher than those of leaves (**Table 10**). This could be due to the higher content of other non-phenolic components (sugars, organic acids, fibers, among others) that are co-extracted by polar solvents [37,43].

Table 10 – Extraction yield (%) of berry-producing plants (BPPs) under study (pre- and post *in vitro* gastrointestinal digestion).

Plant species		**Extraction Yield (%)**			
Year/ Collection area		Berries		Leaves	
		Non-Digested	Digested	Non-Digested	Digested
E. umbellata	2013	6.93	-	11.69	-
	2014	14.94	32.06	13.87	26.91
M. faya	MX	58.13	-	23.05	-
	FL	53.13	-	24.10	-
	ASJ	57.88	-	29.08	-
	BV	54.63	33.06	19.02	22.00
	SX	46.21	-	21.94	-
	RJ	53.59	-	22.30	-
	PM	51.25	-	23.64	-
	TC	42.35	-	18.07	-
S. lanceolata		16.34	37.70	14.63	10.74
R. grandifolius	FX	53.89	37.41	30.05	20.54
	MX	41.75	-	29.17	-
V. cylindraceum		52.54	40.19	35.08	18.35
V. padifolium	2013	50.49	-	30.57*	-
				33.72**	-
	2014	49.34	45.53	31.47*	20.50*
				26.47**	26.38**

*Young Leaves; **Mature Leaves. MX: Machico; FL: Faial; ASJ: Arco de São Jorge; BV: Boaventura; SX: Seixal; RJ: Ribeira da Janela; PM: Porto Moniz; TC: Ilha Terceira

4. HPLC-DAD-ESI/MS^n analysis of methanolic extracts

Berries contain a high amount of a diverse range of phythochemicals, most of which are PCs (anthocyanins (ANTCs), flavonols, flavan-3-ols, proanthocyanidins (PACs), ellagitannins and phenolic acids)[5,34–36,39].

The aim of this part of the work was to characterize the phytochemical composition, in particular PCs, of methanolic extracts by HPLC-DAD-ESI/MS^n. Identification of phytochemicals was achieved based on MS^n spectrum data, authentic standards (when available) and literature[7]. After identification of phytochemicals by HPLC-ESI$^-$/MS^n, the main PCs of analysed methanolic extracts were quantified by HPLC-DAD. For this analysis, a corresponding standard was used for calibration of each phenolic group to calculate relative individual concentrations (**Table 11**). It was not possible to quantify all identified compounds because some were present in trace amounts and did not permit a proper integration of peaks.

Table 11 – Regression curves and linearity of selected standards used for quantification purposes.

Standard	**Equation**		**R^2**	**Phenolic group**
	m	*b*		
Caffeic acid	0.437	0.383	0.997	Hydroxycinnamic acids
Protocatechuic acid	0.172	-0.678	0.998	Hydroxybenzoic acids
5-*O*-Caffeoylquinic acid	0.537	1.878	0.999	Caffeoylquinic acids
Cyanidin 3-*O*-glucoside	0.080	0.168	0.998	Anthocyanins
Quercetin hydrate	0.127	0.173	0.990	Flavonols
(+)-Catechin hydrate	0.063	0.201	0.996	Flavan-3-ols
Apigenin	0.433	-1.276	0.993	Flavones
Hesperidin	0.076	-0.295	0.997	Flavanones
Ellagic acid	0.145	0.059	0.995	Ellagic acid derivatives
Myricitrin	0.133	0.144	0.999	Myricetin derivatives

A great number of different PCs were identified and the structures of the most relevant are presented in **Figure 6** and **Figure 23.**

The quantification data is presented in the following sections, and discussion will be presented for each plant individually.

[7]For detailed information about the identification/characterization of phytochemicals in analysed methanolic extracts please check the Supplementary Material.

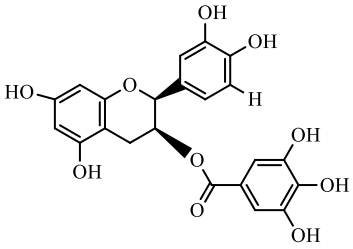

(epi)Catechin-*O*-gallate (ECG)

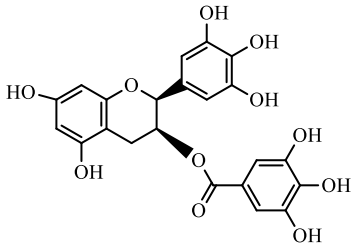

(epi)Gallocatechin-*O*-gallate (EGCG)

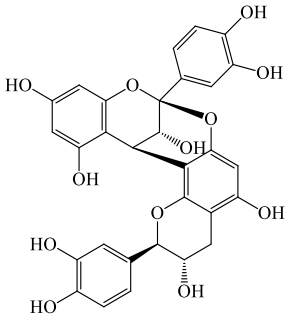

Proanthocyanin (A-type)

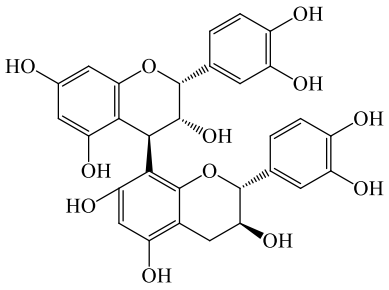

Proanthocyanin (B-type)

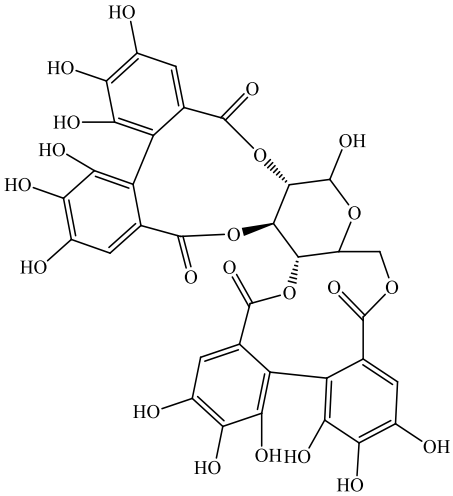

Pedunculagin

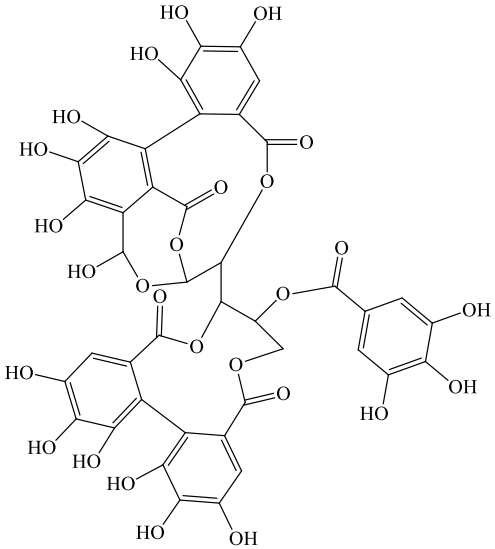

Casuarin

Figure 23 – Chemical structures of the main flavom-3-ols and ellagitannins identified in the analysed methanolic extracts.

4.1. *Elaeagnus umbellata*

The methanolic extracts of *E. umbellata* (berries and leaves) collected in two consecutive years were analysed. The distribution of phytochemicals in the different morphological parts are shown in **Figure 24** (only the most abundant compounds are numbered for the sake of clarity). A total of 85 phytochemicals were identified, including flavonoids, ellagitannins, phenolic acids, organic acids, saccharides and terpenoids (Supplementary Material - **Table S 10**).

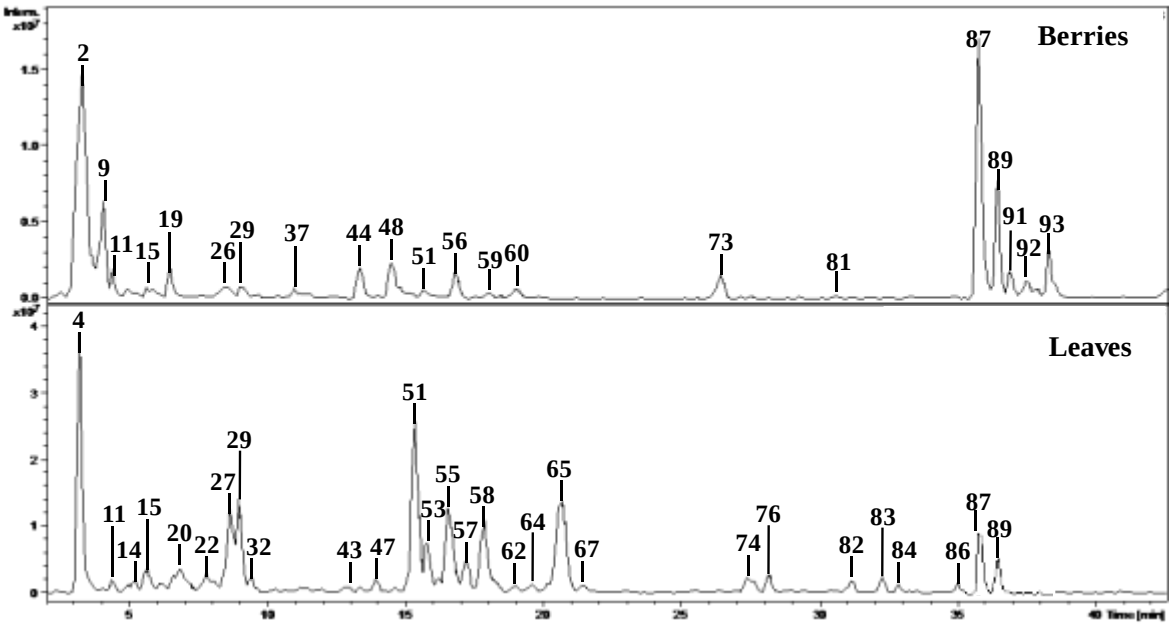

Figure 24 – Representative base peak chromatogram (BPC) of the HPLC-ESI$^-$/MS^n analysis of *E. umbellata* (collected in 2014) methanolic extracts (berries and leaves). For peak identification check **Table S 10** (Supplementary Material).

4.1.1. Pre-*in vitro* gastrointestinal digestion

In the present analysis, 38 main PCs were quantified in *E. umbellata* extracts and values ranged between 3.87 - 5.56 and 37.94 - 42.35 mg g^{-1} DE for berries and leaves, respectively (**Table 12**). Quantitative variations ($p < 0.05$) were found between berries and leaves collected in different years. Samples from 2014 contained, in general, higher phenolic contents (except for flavan-3-ols) (**Table 12**). Inter-annual discrepancies could be related to different climacteric conditions (solar radiation, rainfall and temperature) observed during 2013 and 2014. These factors could have a substantial impact on plants phenolic composition [35].

The compositional percentages of *E. umbellata* extracts (pre- and post *in vitro* digestion) are represented in **Figure 25**.

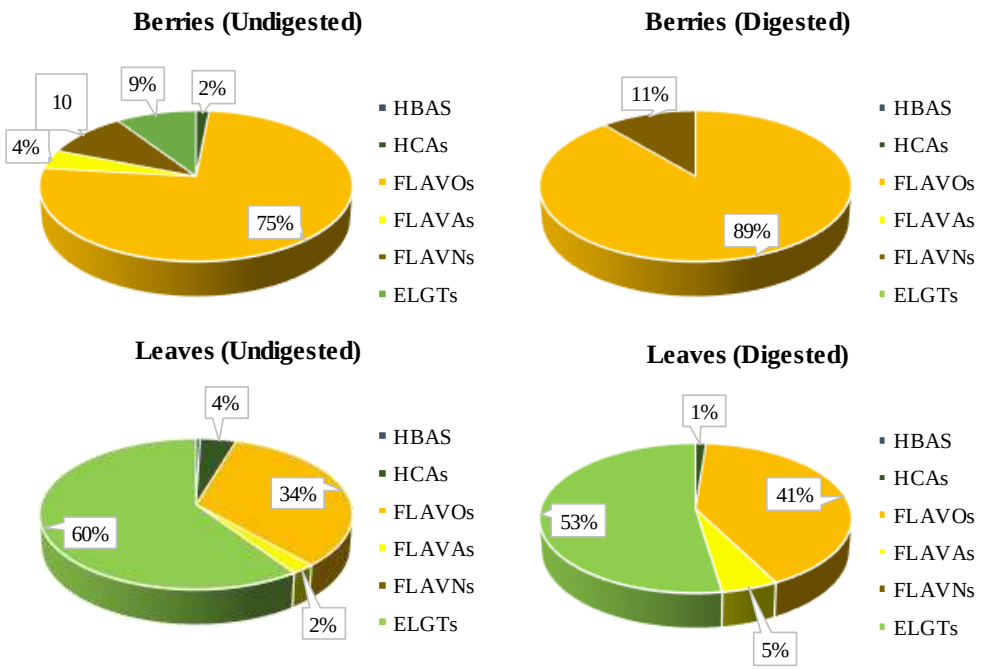

Figure 25 - Phenolic composition of *E. umbellata* extracts (pre- and post-*in vitro* digestion). In the case of undigested extracts the values represent the means from data of samples collected in two consecutive years. For more detailed data check **Table S 10**. HBAs: hydroxybenzoic acids; HCAs hydroxycinnamic acids; FLAVOs: flavonols; FLAVAs: flavan-3-ols; FLAVNs: flavones; ELGTs: ellagitannis.

Kaempferol-*O*-rutinoside (**87**) was the most abundant compound (18.06 – 37.18%) in berries; other compounds such as kaempferol-*O*-hexoside (**73**) (6.11 - 10.20%), dihydrokaempferol-*O*-hexoside (**37**) (8.67%), quercetin-*O*-pentoside (**49**) (8.38%) and kaempferol-*O*-rutinoside (**89**) (6.65%) were also relevant (**Table 12**). In the case of leaves, bis-HHDP-*O*-hexoside (**17**) (26.68 – 31.81%), galloyl-HHDP-*O*-hexoside (**22**) (12.77 – 15.49%) pendunculagin I (**15**) (10.25%) and quercetin-*O*-pentosyl(hexoside) (**51**) (10.25 – 12.53%) were the main phenolics.

Little is known about the phenolic composition of *E. umbellata*. In a previous work [104], catechin polymers were main compounds of berries aqueous/acetone extracts. However, these compounds were not found in the present analysis. From another study [105], gallic acid and kaempferol were quantified in leaves (0.95 and 0.81 mg g^{-1} DE, respectively). These discrepancies could be related to edaphoclimatic conditions and/or differences in the extraction methodology (procedure, solvents, etc).

Table 12 – Quantification (mg g^{-1} DE) of main phenolic compounds present in *E. umbellata* extracts (berries and leaves) collected in two consecutive years. Data represent the mean ± standard deviation (n = 3).

Nº	Assigned identification	Berries		Leaves	
Hydroxycinnamic acids		2013	2014	2013	2014
28	Sinapic acid-*O*-(pentosyl)hexoside	0.04 ± 0.01[b]	0.10 ± 0.01[a]	0.73 ± 0.03[c]	1.42 ± 0.04[d]
35	Sinapic acid-*O*-hexoside			0.15 ± 002[a]	0.18 ± 0.01[a]
41	Sinapic acid derivative			0.20 ± 0.01[a]	0.31 ± 0.01[b]
78	Caffeic acid derivative			0.04 ± 0.01	
85	Disinapoyl-*O*-hexoside			0.19 ± 0.01[a]	0.21 ± 0.02[a]
Total		**0.04 ± 0.01[b]**	**0.10 ± 0.01[a]**	**1.32 ± 0.08[c]**	**2.12 ± 0.10[d]**
Hydroxybenzoic acids					
68	Trigalloylglucose derivative			0.16 ± 0.01	
Total				**0.16 ± 0.01**	
Flavonols					
14	Q-*O*-(pentosyl)dihexoside			0.73 ± 0.03[b]	0.67 ± 0.03[a]
26	K-*O*-dihexoside-*O*-rhamnoside		0.05 ± 0.01		
33	I-*O*-glucuronide derivative	0.13 ± 0.01[a]	0.17 ± 0.01[b]		
37	Dihydro-K-*O*-hexoside	0.34 ± 0.01[b]	0.21 ± 0.01[a]		
38	I-*O*-(pentosyl)hexoside-*O*-rhamnoside	0.19 ± 0.01[a]	0.17 ± 0.01[a]		
43	Q-*O*-dihexoside			0.42 ± 0.01[c]	0.59 ± 0.02[d]
48	Q-*O*-(pentosyl)hexoside	0.22 ± 0.01[a]	0.20 ± 0.01[a]		
49	Q-*O*-pentoside	0.04 ± 0.01[a]	0.47 ± 0.01[b]		
51	Q-*O*-pentosyl(hexoside)			4.13 ± 0.06[a]	5.06 ± 0.29[b]
54	I-*O*-dihexoside			0.40 ± 0.02[a]	0.39 ± 0.02[a]
60	I-*O*-(pentosyl)hexoside	0.19 ± 0.01[b]	0.14 ± 0.01[a]		
61	Q-*O*-hexoside	0.09 ± 0.01[a]	0.13 ± 0.01[b]		
65	I-*O*-pentosyl(hexoside)			2.69 ± 0.11[a]	3.94 ± 0.17[b]
73	K-*O*-hexoside	0.40 ± 0.03[b]	0.34 ± 0.01[a]	0.53 ± 0.02[c]	0.51 ± 0.01[c]
74	I-*O*-hexoside			0.90 ± 0.03[a]	1.71 ± 0.08[b]
80	K-*O*-(coumaroyl)dihexoside		0.07 ± 0.01		
84	I-*O*-dihexoside derivative			0.19 ± 0.01[a]	0.94 ± 0.02[b]
87	K-*O*-(coumaroyl)hexoside	0.70 ± 0.03[a]	2.07 ± 0.01[c]	0.90 ± 0.15[b]	2.02 ± 0.05[c]
89	K-*O*-(coumaroyl)hexoside	0.23 ± 0.01[a]	0.37 ± 0.01[b]	0.35 ± 0.02[b]	0.62 ± 0.01[c]
Total		**2.51 ± 0.13[a]**	**4.38 ± 0.12[b]**	**11.26 ± 0.79[c]**	**16.44 ± 0.78[d]**
Flavones					
88	Diosmetin-*C*-dihexoside	0.08 ± 0.01[a]	0.09 ± 0.01[a]		

90	Diosmetin-*O*-dihexoside	0.13 ± 0.01[a]	0.11 ± 0.01[a]		
91	Diosmetin-*C*-dihexoside	0.25 ± 0.01[a]	0.24 ± 0.01[a]		
Total		**0.46 ± 0.03[a]**	**0.43 ± 0.02[a]**		
Flavan-3-ols					
16	Gallo(epi)catechin	0.23 ± 0.01[b]	0.15 ± 0.01[a]	0.91 ± 0.04[d]	0.85 ± 0.03[c]
Total		**0.23 ± 0.01[b]**	**0.15 ± 0.01[a]**	**0.91 ± 0.04[d]**	**0.85 ± 0.03[c]**
Ellagic acid derivatives/Ellagitannins					
13	Pedunculagin I			2.15 ± 0.04[b]	1.21 ± 0.03[a]
15	Pedunculagin I			4.07 ± 0.11[b]	3.28 ± 0.14[a]
17	Pedunculagin I			12.64 ± 0.45[b]	10.77 ± 0.23[a]
21	Galloyl-HHDP-*O*-hexoside	0.14 ± 0.01[a]	0.16 ± 0.01[a]		
22	Galloyl-HHDP-*O*-hexoside			5.07 ± 0.27[a]	6.25 ± 0.40[b]
24	Casuarinin	0.16 ± 0.01[a]	0.35 ± 0.01[b]		
40	Ellagic acid-*O*-hexoside			0.14 ± 0.01[a]	0.28 ± 0.02[b]
42	Ellagic acid-*O*-(acetyl)pentoside			2.01 ± 0.09[b]	1.15 ± 0.05[a]
Total		**0.30 ± 0.02[a]**	**0.50 ± 0.03[b]**	**26.09 ± 1.37[d]**	**22.93 ± 1.75[c]**
TIPC		**3.87 ± 0.28[a]**	**5.56 ± 0.39[b]**	**37.94 ± 1.63[c]**	**42.34 ± 2.95[c]**

HHDP: Hexahydroxydiphenoyl; K: Kaempferol; I: Isorhamnetin; Q: Quercetin. TIPC: total individual phenolic content. Bold values represent the sum of each type of components. Means in the same line not sharing the same letter are significantly different at $p < 0.05$ probability level.

4.1.2. Post *in vitro* gastrointestinal digestion

For this analysis, samples collected in 2014 were selected in detriment of those collected in previous year due to the higher TIPC (total individual phenolic content). After simulated digestion, qualitative and quantitative differences were found in *E. umbellata* in relation to native values ($p < 0.05$) (**Figure 25** and **Table 13**). Berries components were most unstable than in leaves (a reduction of 71.05% and 62.24% of TIPC, respectively). Hydroxycinnamic acids (HCAs) and ellagitannins were not quantifiable in digested berries extracts (**Figure 25** and **Table 13**). Flavonols and flavones suffered a degradation of 67.28% and 59.30%, respectively. Flavones and flavan-3-ols were not quantified after digestion of leaves (**Figure 25** and **Table 13**). HCAs content showed the highest loss (90.20%), followed by ellagitannins (62.59%) and flavonols (43.63%).

Regarding individual phenolic compounds, kaempferol-*O*-rutinoside (**87**) (60.76%) and quercetin-*O*-pentoside (**49**) (11.58%) remained the major component in berries (**Table 13**). A reduction of 52.70% and 60.00% was verified, respectively. In leaves, pedunculagin I (**17**) (25.52%) quercetin-*O*-pentosyl(hexoside) (**51**) (17.33%) and galloyl-HHDP-*O*-hexoside (**22**) (14.93%) were

still dominant (**Table 13**). These compounds showed a decrease of 62.51%, 43.10% and 61.68%, respectively, upon digestion.

Unfortunately, information regarding the stability of PCs in the gastrointestinal (GI) tract occurring in *E. umbellata* is lacking in the literature. However, this issue has been extensively studied for other berries species and losses of TIPC have also been reported (23.7-80.50%)[24,49,54,59,117,140,141].

Table 13 - Quantification of main polyphenolic compounds present in *E. umbellata* (mg g^{-1} DE) before and after *in vitro* gastrointestinal digestion. Data represent the mean ± standard deviation (n = 3).

Nº	**Assigned identification**	**Berries**		**Leaves**	
Hydroxycinnamic acids		Non-digested	Digested	Non-digested	Digested
28	Sinapic acid-*O*-(pentosyl)hexoside	0.10 ± 0.01[a]		1.42 ± 0.04[b]	
35	Sinapic acid-*O*-hexoside			0.18 ± 0.02[b]	0.08 ± 0.01[a]
41	Sinapic acid derivative			0.31 ± 0.01[b]	0.11 ± 0.01[a]
78	Caffeic acid derivative				
85	Disinapoyl-*O*-hexoside			0.21 ± 0.02	
Total		**0.10 ± 0.01[a]**		**2.13 ± 0.07[c]**	**0.20 ± 0.01[b]**
Flavonols					
14	Q-*O*-(pentosyl)dihexoside			0.67 ± 0.03[b]	0.22 ± 0.08[a]
26	K-*O*-dihexoside-*O*-rhamnoside	0.06 ± 0.01			
33	I-*O*-glucuronide derivative	0.17 ± 0.01			
37	Dihydro-K-*O*-hexoside	0.21 ± 0.01			
38	I-*O*-(pentosyl)hexoside-*O*-rhamnoside	0.17 ± 0.01			
43	Q-*O*-dihexoside			0.59 ± 0.02[b]	0.20 ± 0.01[a]
48	Q-*O*-(pentosyl)hexoside	0.19 ± 0.01			
49	Q-*O*-pentoside	0.47 ± 0.01[b]	0.19 ± 0.05[a]		
51	Q-*O*-pentosyl(hexoside)			5.05 ± 0.25[b]	2.37 ± 0.05[a]
54	I-*O*-dihexoside			0.39 ± 0.01[b]	0.12 ± 0.01[a]
60	I-*O*-(pentosyl)hexoside	0.14 ± 0.01			
61	Q-*O*-hexoside	0.13 ± 0.01			
65	I-*O*-pentosyl(hexoside)			3.94 ± 0.14[b]	1.27 ± 0.03[a]
73	K-*O*-hexoside	0.34 ± 0.01[c]	0.13 ± 0.02[a]	0.51 ± 0.02[d]	0.22 ± 0.01[b]
74	I-*O*-hexoside			1.71 ± 0.05[b]	0.73 ± 0.03[a]
79	I-*O*-dihexoside-*O*-glucuronide				
80	K-*O*-(coumaroyl)dihexoside	0.07 ± 0.01			
84	I-*O*-dihexoside derivative			0.94 ± 0.01[b]	0.22 ± 0.01[a]

87	K-*O*-rutinoside	2.07 ± 0.13^{c}	0.98 ± 0.03^{a}	2.02 ± 0.05^{c}	1.17 ± 0.31^{b}
89	K-*O*-rutinoside	0.37 ± 0.05^{c}	0.14 ± 0.01^{a}	0.62 ± 0.02^{d}	0.21 ± 0.02^{b}
Total		**4.38 ± 0.12^{b}**	**1.43 ± 0.08^{a}**	**16.45 ± 0.55^{d}**	**6.74 ± 0.43^{c}**
Flavones					
88	Diosmetin-*C*-dihexoside	0.09 ± 0.01			
90	Diosmetin-*O*-dihexoside	0.1 ± 0.01^{b}	0.06 ± 0.01^{a}		
91	Diosmetin-*C*-dihexoside	0.24 ± 0.01^{b}	0.11 ± 0.01^{a}		
Total		**0.43 ± 0.03^{b}**	**0.18 ± 0.02^{a}**		
Flavan-3-ols					
16	Gallo(epi)catechin	0.15 ± 0.01^{a}		0.85 ± 0.03^{b}	
Total		**0.15 ± 0.01^{a}**		**0.85 ± 0.03^{b}**	
Ellagic acid derivatives/ Ellagitannins					
13	Pedunculagin I			1.21 ± 0.03	
15	Pedunculagin I			3.28 ± 0.09^{b}	1.54 ± 0.13^{a}
17	Pedunculagin I			10.77 ± 0.13^{b}	4.03 ± 0.32^{a}
21	Galloyl-HHDP-*O*-hexoside	0.16 ± 0.01			
22	Galloyl-HHDP-*O*-hexoside			6.25 ± 0.04^{b}	2.39 ± 0.09^{a}
24	Casuarinin	0.35 ± 0.01			
40	Ellagic acid-*O*-hexoside			0.28 ± 0.01	
42	Ellagic acid-*O*-(acetyl)pentoside			1.15 ± 0.01^{b}	0.61 ± 0.03^{a}
Total		**0.50 ± 0.03^{a}**		**22.93 ± 0.30^{c}**	**8.58 ± 0.33^{b}**
TIPC		**5.56 ± 0.19^{b}**	**1.61 ± 0.09^{a}**	**42.35 ± 0.95^{d}**	**15.52 ± 0.84^{c}**

HHDP: Hexahydroxydiphenoyl; K: Kaempferol; I: Isorhamnetin; Q: Quercetin. TIPC: total individual phenolic content. Bold values represent the sum of each type of components. Means in the same line not sharing the same letter are significantly different at $p < 0.05$ probability level.

4.2. *Myrica faya*

4.2.1. Identification of phythochemicals

More than 160 phytochemicals were identified in *M. faya* extracts (berries and leaves) from different origins. ANTCs, other flavonoids, phenolic acids, organic acids, terpenoids, lignans and oxylipins were detected; similar to previous established profiles for *M. faya* [106] and *M. rubra* [82,142,143]. **Figure 26** and **Figure 27** show representative BPCs obtained during the analysis of *M. faya* extracts. Identification of phytochemicals is presented in Supplementary Material (**Table S 11** and **Table S 12**).

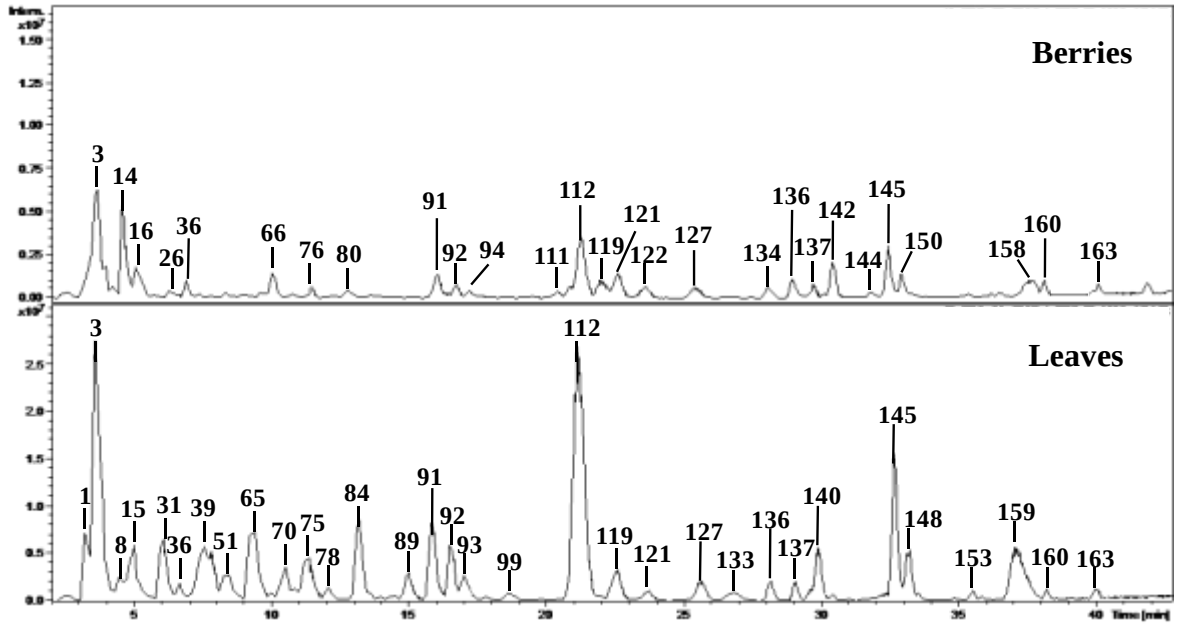

Figure 26 – Representative base peak chromatogram (BPC) of the HPLC-ESI$^-$/MS^n analysis of *M. faya* methanolic extracts (berries and leaves). For peak identification check **Table S 11** (Supplementary Material).

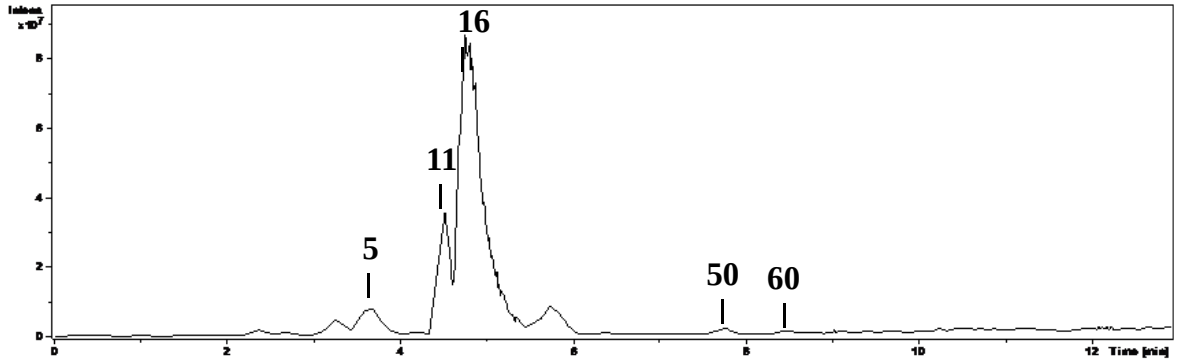

Figure 27 - Representative base peak chromatogram (BPC) of the HPLC-ESI$^+$/MS^n analysis of *M. faya* methanolic extracts (berries). For peak identification check **Table S 12** (Supplementary Material)**.**

4.2.2. Pre-*in vitro* gastrointestinal digestion

In this analysis, 66 main PCs were quantified in *M. faya* samples by HPLC-DAD (**Table 14** and **Table 15**). TIPC ranged between 83.48 – 102.35 and 34.52 – 43.63 mg g^{-1} DE for leaves and berries, respectively (**Table 14** and **Table 15**). Significant variations ($p < 0.05$) were observed in the phenolic composition of *M. faya* from different origins. These are possibly due to climacteric and soil conditions. Samples collected in the northeast part of the Island (Seixal (SX), Ribeira da Janela (RJ) and Porto Moniz (PM)) are subjected to different climacteric conditions than those in the west/northwest (Machico (MX), Faial (FL), Arco de São Jorge (ASJ) and Boaventura (BV)). Additionally, samples from a different archipelago (Terceira Island (TC), Azores archipelago) have grown under completely different environmental conditions, that are known to impact qualitative and quantitative measurements [35].

The compositional percentages of *M. faya* extracts (pre- and post *in vitro* digestion) are represented in **Figure 28**.

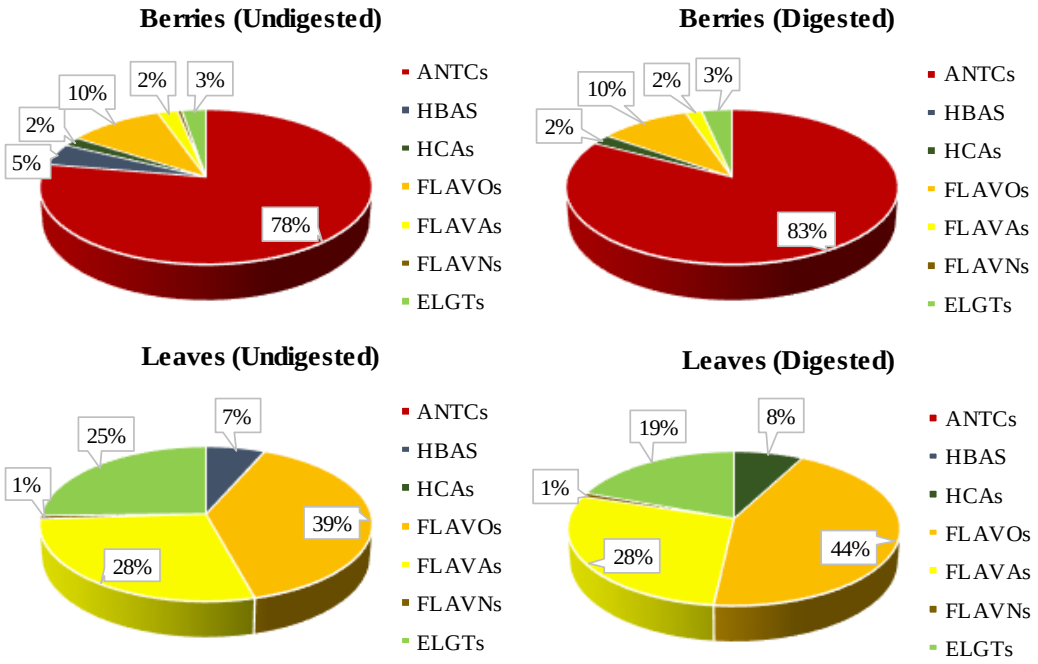

Figure 28 - Phenolic composition of *M. faya* extracts (pre- and post-*in vitro* digestion). In the case of undigested extracts, the values represent the means from data of samples collected in different locations. For more detailed data check Table 14 and Table 15. ANTCs: anthocyanins; HBAs: hydroxybenzoic acids; HCAs hydroxycinnamic acids; FLAVOs: flavonols; FLAVAs: flavan-3-ols; FLAVNs: flavones; ELGTs: ellagitannis.

Cyanidin-3-*O*-glucoside (C3G) (**16**) was the absolute predominant phenolic in berries (67.20 – 76.07%), which is in agreement with previous works on *M. faya* and *M. rubra* [65,82,106]. In

general, BV berries showed the highest phenolic amounts, while RJ and MX presented the lowest ($p < 0.05$) (**Table 14**). Myricitrin (MCT) (**112**) was the main compound in leaves (13.19 – 24.36%) (**Table 15**), as previous reported for *Myrica spp*. [106,117,142]. Digalloyl(epi)gallocatehcin dimer (**71**) (6.00 – 15.73%), casuarin (**53**) (4.58 – 9.70%) EGCG (**81**) (4.02 – 8.29%), and pedunculagin I (**31**) (2.26 – 6.32%) were also relevant. Overall, leaves from BV showed the highest phenolic contents and RJ the lowest ($p < 0.05$) (**Table 15**). Differences in phenolic contents were more notorious in leaves, in particular, for those collected in a different Island/archipelago: digalloyl(epi)gallocatehcin dimer (**71**) (15.73%), MCT (**112**) (13.19%) and EGCG-EGCG (**46**) (10.18%) were major in TC leaves (**Table 15**).

Previously analysis on *M. faya* [106] and *M. rubra* [65,82,142,143] showed similar phenolic compositions. However, different units make it difficult to establish a comparison with present data (**Table 14** and **Table 15**).

Table 14 - Quantification (mg g^{-1} DE) of main phenolic compounds present in *M. faya* extracts (berries) collected in eight different locations. Data represent the mean ± standard deviation (n = 3).

Nº	Assigned identification	MX	FL	ASJ	BV	SX	RJ	PM	TC
Anthocyanins									
5	Delphinidin-*O*-hexoside	0.26 ± 0.01^{c}	0.10 ± 0.02^{a}	0.24 ± 0.01^{b}	0.31 ± 0.01^{d}	0.31 ± 0.01^{d}	0.24 ± 0.01^{b}	0.35 ± 0.01^{e}	0.31 ± 0.01^{d}
11	Delphinidin-*O*-hexoside	2.02 ± 0.02^{d}	1.87 ± 0.05^{c}	2.10 ± 0.01^{e}	2.34 ± 0.01^{f}	1.37 ± 0.04^{a}	1.67 ± 0.01^{b}	1.40 ± 0.06^{a}	1.60 ± 0.07^{d}
16	Cyanidin-3-*O*-glucoside	24.47 ± 0.05^{b}	26.54 ± 0.46^{b}	33.19 ± 0.25^{f}	32.01 ± 0.18^{e}	28.53 ± 0.10^{d}	23.73 ± 0.30^{a}	27.33 ± 0.61^{b}	27.20 ± 0.05^{cd}
48	Cyanidin-*O*-pentoside			0.17 ± 0.01					
50	Cyanidin-*O*-hexoside	0.28 ± 0.01^{c}		0.23 ± 0.01^{b}	0.15 ± 0.01^{a}			0.34 ± 0.01^{d}	
69	Cyanidin-*O*-(acetyl)hexoside	0.21 ± 0.01^{a}		0.20 ± 0.01^{a}	0.30 ± 0.01^{b}			0.33 ± 0.01^{c}	0.21 ± 0.08^{a}
Total		**27.24 ± 0.10^{b}**	**28.51 ± 0.54^{b}**	**36.13 ± 0.27^{f}**	**35.11 ± 0.21^{e}**	**30.21 ± 0.07^{c}**	**25.64 ± 0.32^{a}**	**29.75 ± 0.69^{b}**	**29.32 ± 0.13^{d}**
Hydroxycinnamic acids									
10	Caffeoylisocitrate		0.41 ± 0.01^{d}		0.12 ± 0.01^{a}		0.20 ± 0.01^{b}	0.33 ± 0.01^{c}	
56	Coumaric acid-*O*-hexoside	0.01 ± 0.01^{a}	0.02 ± 0.01^{b}				0.01 ± 0.01^{a}		
63	5-*O*-CQA				0.29 ± 0.01^{b}	0.21 ± 0.01^{a}			
76	Dihydro-Co-*O*-hexoside								0.08 ± 0.01
164	B-*p*-tri-CoDOA	0.39 ± 0.01^{a}	0.69 ± 0.02^{d}	0.51 ± 0.01^{b}	0.54 ± 0.01^{c}	0.38 ± 0.02^{a}	0.48 ± 0.01^{b}	0.53 ± 0.01^{c}	0.79 ± 0.01^{e}
Total		**0.40 ± 0.01^{a}**	**1.12 ± 0.03^{f}**	**0.51 ± 0.01^{b}**	**0.95 ± 0.0^{2}**	**0.59 ± 0.02^{c}**	**0.69 ± 0.01^{d}**	**0.86 ± 0.02^{e}**	**0.87 ± 0.01^{e}**
Hydroxybenzoic acids									
4	Galloyl-*O*-hexoside	0.25 ± 0.01^{d}	0.21 ± 0.01^{c}	0.19 ± 0.0^{1}	0.16 ± 0.01^{a}	0.21 ± 0.01^{c}	0.22 ± 0.01^{c}	0.18 ± 0.01^{ab}	0.14 ± 0.01^{a}
12	Galloyl-*O*-hexoside	1.11 ± 0.03^{b}	1.03 ± 0.01^{a}	1.31 ± 0.02^{c}	1.45 ± 0.03^{d}	1.53 ± 0.04^{e}	1.30 ± 0.01^{c}	1.00 ± 0.01^{a}	1.08 ± 0.01^{f}
15	Galloylquinic acid			0.20 ± 0.01					
27	Digalloyl-*O*-hexoside	0.39 ± 0.01^{d}	0.27 ± 0.08^{bc}	0.20 ± 0.01^{b}	0.20 ± 0.01^{b}	0.27 ± 0.01^{c}	0.21 ± 0.01^{b}	0.10 ± 0.01^{a}	0.69 ± 0.01^{e}
88	Trigalloyl glucose		0.24 ± 0.01^{b}		0.06 ± 0.01^{a}				
161	Methyl gallate derivative								0.05 ± 0.01

Total		**1.75 ± 0.05^{b}**	**1.75 ± 0.03^{e}**	**1.90 ± 0.03^{e}**	**1.87 ± 0.04^{d}**	**2.01 ± 0.05^{ef}**	**1.73 ± 0.02^{c}**	**1.28 ± 0.01^{a}**	**1.96 ± 0.07^{g}**
Flavonols									
83	Dihydro-K-*O*-hexoside								0.29 ± 0.01
91	M-*O*-hexoside	0.22 ± 0.01^{c}	0.16 ± 0.01^{b}	0.26 ± 0.01^{de}	0.25 ± 0.01^{d}	0.29 ± 0.01^{f}	0.24 ± 0.01^{cd}	0.12 ± 0.01^{a}	0.25 ± 0.01^{d}
92	M-*O*-(galloyl)hexoside	0.14 ± 0.01^{cd}	0.21 ± 0.01^{e}	0.14 ± 0.01^{cd}	0.09 ± 0.01^{a}	0.10 ± 0.01^{b}	0.12 ± 0.01^{bc}	0.09 ± 0.01^{a}	0.12 ± 0.01^{bc}
108	M-*O*-pentoside		0.49 ± 0.01^{c}					0.11 ± 0.01^{a}	0.18 ±0.01^{b}
112	Myricitrin	1.36 ± 0.02^{c}	1.09 ± 0.02^{a}	1.13 ± 0.03^{a}	1.20 ± 0.02^{b}	1.53 ± 0.02^{d}	1.37 ± 0.03^{c}	1.38 ± 0.05^{c}	1.23 ± 0.02^{b}
121	Q-*O*-hexoside	0.07 ± 0.01^{a}		0.18 ± 0.01^{c}	0.12 ± 0.01^{b}	0.45 ± 0.01^{e}	0.17 ± 0.01^{c}	0.07 ± 0.01^{a}	0.28 ± 0.01^{d}
122	Q-*O*-(galloyl)hexoside	0.27 ± 0.01^{d}		0.10 ± 0.01^{a}	0.10 ± 0.01^{a}	0.17 ± 0.02^{b}	0.15 ± 0.01^{b}	0.19 ± 0.01^{c}	0.18 ± 0.01^{c}
127	Q-*O*-(galloyl)hexoside	0.20 ± 0.01^{b}		0.22 ± 0.01^{bc}	0.15 ± 0.01^{a}				0.21 ± 0.01^{b}
131	K-*O*-hexoside	0.15 ± 0.01^{a}	0.26 ± 0.01^{c}	0.25 ± 0.02^{c}	0.32 ± 0.01^{d}	0.27 ± 0.01^{c}	0.19 ± 0.01^{b}	0.14 ± 0.01^{a}	0.14 ± 0.01^{a}
136	K-*O*-hexoside	0.60 ± 0.01^{c}			0.20 ± 0.01^{a}	0.19 ± 0.01^{a}		0.27 ± 0.01^{b}	
137	Q-*O*-deoxyhexoside				0.24 ± 0.01^{a}			0.25 ± 0.01^{ab}	0.27 ± 0.01^{b}
139	K-*O*-(galloyl)hexoside	0.35 ± 0.01^{b}	0.47 ± 0.03^{c}	0.43 ± 0.01^{c}		0.27 ± 0.01^{a}	0.82 ± 0.01^{d}		0.84 ± 0.01^{d}
140	Dimethyl-M-*O*-pentoside							0.25 ± 0.01	
145	M-*O*-(galloyl)deoxyhexoside	0.42 ± 0.01^{e}	0.38 ± 0.01^{c}	0.35 ± 0.01^{cd}		0.30 ± 0.02^{b}	0.38 ± 0.01^{d}		0.19 ± 0.01^{a}
151	Q-*O*-(galloyl)deoxyhexoside	0.40 ± 0.01^{c}		0.21 ± 0.01^{a}	0.27 ± 0.01^{b}			0.60 ± 0.01^{e}	0.46 ± 0.01^{d}
153	Q-*O*-(galloyl)deoxyhexoside		0.38 ± 0.02^{b}	0.28 ± 0.01^{a}			1.13 ± 0.01^{d}	0.40 ± 0.01^{b}	1.09 ± 0.01^{c}
160	Quercetin								0.31 ± 0.01
Total		**4.34 ± 0.08^{e}**	**3.44 ± 0.15^{b}**	**3.61 ± 0.08^{c}**	**2.93 ± 0.05^{a}**	**3.57 ± 0.07^{bc}**	**4.57 ± 0.13^{e}**	**3.98 ± 0.08^{d}**	**6.26 ± 0.20^{f}**
Flavan-3-ols									
43	Gallo(epi)catechin	0.20 ± 0.01^{ab}	0.76 ± 0.03^{e}	0.12 ± 0.01^{a}	0.11 ± 0.01^{a}		0.12 ± 0.07^{a}	0.23 ± 0.01^{c}	0.34 ± 0.01^{d}
45	Gallocatechin dimer			0.16 ± 0.01^{a}	0.26 ± 0.01^{b}				
71	Digalloyl(epi)gallocatechin dimer		0.50 ± 0.01^{c}	0.38 ± 0.01^{b}	0.32 ± 0.01^{a}		0.37 ± 0.01^{b}	0.58 ± 0.01^{d}	

79	Catechin	0.16 ± 0.01[a]					0.25 ± 0.01[b]		
81	Gallo(epi)catechin-*O*-gallate	0.04 ± 0.01[a]	0.12 ± 0.01[c]		0.05 ± 0.01[ab]		0.06 ± 0.01[b]	0.05 ± 0.01[ab]	
87	Digallocatechin derivative		0.45 ± 0.01[c]			0.14 ± 0.01[a]			0.28 ± 0.01[b]
99	Gallo(epi)catechin-*O*-gallate		0.46 ± 0.01[b]			0.25 ± 0.01[a]			
Total		**0.40 ± 0.01[a]**	**2.29 ± 0.07[e]**	**0.66 ± 0.02[b]**	**0.74 ± 0.02[c]**	**0.39 ± 0.01[a]**	**0.80 ± 0.09[cd]**	**0.86 ± 0.02[d]**	**0.62 ± 0.01[b]**
Flavones									
86	Tricin-*O*-hexoside derivative	0.25 ± 0.01[c]						0.11 ± 0.01[a]	0.21 ± 0.01[b]
Total		**0.25 ± 0.01[c]**						**0.11 ± 0.01[a]**	**0.21 ± 0.01[b]**
Elagic acid derivatives/ Ellagitannins									
31	Pedunculagin I	0.11 ± 0.01[a]		0.39 ± 0.01[d]	0.46 ± 0.01[e]	0.24 ± 0.01[c]	0.24 ± 0.01[c]	0.18 ± 0.01[b]	
39	Pedunculagin I	0.13 ± 0.01[a]	0. 19 ± 0.01		0.17 ± 0.01[b]	0.37 ± 0.01[d]	0.42 ± 0.02[e]	0.23 ± 0.01[c]	0.47 ± 0.01[f]
53	Casuarinin	0.26 ± 0.01[d]			0.14 ± 0.01[a]	0.20 ± 0.01[b]	0.21 ± 0.01[b]	0.23 ± 0.01[bc]	
65	Casuarinin	0.18 ± 0.01[bc]	0.44 ± 0.01[e]		0.16 ± 0.01[b]			0.06 ± 0.01[a]	0.23 ± 0.01[d]
67	Casuarinin like ellagitannin			0.26 ± 0.01[d]	0.21 ± 0.01[b]		0.16 ± 0.01[a]		0.22 ± 0.01[bc]
80	HHDP-*O*-hexoside	0.05 ± 0.01[a]	0.14 ± 0.01[c]			0.25 ± 0.01[d]	0.06 ± 0.01[ab]		
89	Ellagitannin	0.10 ± 0.01[a]						0.12 ± 0.01[ab]	
93	Ellagic acid-*O*-pentoside			0.17 ± 0.01[a]		0.29 ± 0.01[c]		0.22 ± 0.02[b]	0.32 ± 0.02[cd]
Total		**0.83 ± 0.02[b]**	**0.77 ± 0.01[a]**	**0.82 ± 0.01[b]**	**1.14 ± 0.02[d]**	**1.35 ± 0.03[f]**	**1.09 ± 0.04[c]**	**1.04 ± 0.03[c]**	**1.24 ± 0.02[e]**
TIPC		**35.20 ± 0.66[a]**	**37.88 ± 0.77[b]**	**42.74 ± 0.90[d]**	**43.63 ± 0.78[d]**	**38.12 ± 0.92[bc]**	**34.52 ± 0.57[a]**	**37.88 ± 0.85[b]**	**40.48 ± 0.25[c]**

MX: Machico; FL: Faial; ASJ: Arco de São Jorge; BV: Boaventura; SX: Seixal; PM: Porto Moniz; TC: Terceira; B: benzoyl; HHDP: Hexahydroxydiphenoyl; CoDOA: coumaroyl-2,7-anhydro-3- deoxy-2-octulopyranosonic acid; K: Kaempferol; M: Myricetin; Q: Quercetin. TIPC: total individual phenolic content. Bold values represent the sum of each type of components. Means in the same line not sharing the same letter are significantly different at $p < 0.05$ probability level.

Table 15 – Quantification (mg g^{-1} DE) of main phenolic compounds present in *M. faya* extracts (leaves) collected in eight different locations. Data represent the mean ± standard deviation (n = 3).

Nº	Assigned identification	MX	FL	ASJ	BV	SX	RJ	PM	TC
Hydroxycinnamic acids									
56	Co-*O*-hexoside								0.21 ± 0.01
164	B-*p*-tri-CoDOA	0.07± 0.01^{cd}	0.03 ± 0.01^{a}	0.05 ± 0.01^{bc}	0.04 ± 0.01^{ab}		0.08 ± 0.01^{de}	0.04 ± 0.01^{ab}	0.03 ± 0.01^{a}
Total		**0.07± 0.01^{cd}**	**0.03 ± 0.01^{a}**	**0.05 ± 0.01^{bc}**	**0.04 ± 0.01^{ab}**		**0.08 ± 0.01^{de}**	**0.04 ± 0.01^{ab}**	**0.24 ± 0.01^{f}**
Hydroxybenzoic acids									
12	Galloyl-*O*-hexoside	3.13 ± 0.06^{e}	3.25 ± 0.10^{ef}	3.58 ± 0.04^{gh}	2.12 ± 0.03^{ab}	2.76 ± 0.01^{c}	1.99 ± 0.08^{a}	2.97 ± 0.05^{d}	3.45 ± 0.29^{g}
15	Galloylquinic acid	2.08 ± 0.09^{d}	2.65 ± 0.06^{f}	2.39 ± 0.05^{e}	1.42 ± 0.01^{a}	1.61 ± 0.01^{b}	2.02 ± 0.04^{d}	1.76 ± 0.07^{c}	3.19 ± 0.02^{g}
18	Gallic acid	1.67 ± 0.03^{d}			0.79 ± 0.02^{b}	0.83 ± 0.01^{bc}	0.94 ± 0.18^{c}	0.56 ± 0.02^{a}	
88	Trigalloyl-*O*-hexoside	0.22 ± 0.01^{c}	0.23 ± 0.01^{c}	0.25 ± 0.01^{cd}	0.16 ± 0.01^{b}	0.18 ± 0.01^{b}	0.12 ± 0.01^{a}	0.10 ± 0.01^{a}	0.49 ± 0.03^{e}
106	Tetragalloyl-*O*-hexoside			0.47 ± 0.02^{b}				0.12 ± 0.01^{a}	1.13 ± 0.03^{c}
Total		**7.10 ± 0.29^{e}**	**6.13 ± 0.35^{d}**	**6.69 ± 0.25^{d}**	**4.49 ± 0.09^{a}**	**5.38 ± 0.04^{bc}**	**5.07 ± 0.36^{b}**	**5.51 ± 0.23^{c}**	**8.36 ± 0.50^{f}**
Flavonols									
91	M-*O*-hexoside	3.11 ± 0.09^{d}	2.43 ± 0.18^{c}	3.58 ± 0.16^{e}	5.39 ± 0.17^{f}	3.10 ± 0.01^{d}	1.75 ± 0.06^{b}	1.17 ± 0.01^{a}	1.22 ± 0.04^{a}
92	M-*O*-(galloyl)hexoside	3.70 ± 0.04^{d}	2.84 ± 0.06^{b}	7.23 ± 0.32^{g}	9.77 ± 0.15^{h}	6.09 ± 0.08^{f}	3.38 ± 0.03^{c}	2.32 ± 0.08^{a}	4.19 ± 0.03^{e}
104	Rutin	0.64 ± 0.02^{d}	0.57 ± 0.01^{c}		0.23 ± 0.01^{a}	0.34 ± 0.01^{b}	0.78 ± 0.02^{e}	0.65 ± 0.01^{d}	
108	M-*O*-pentoside							0.57 ± 0.01^{b}	0.14 ± 0.01^{a}
112	Myricetin	15.91 ± 0.03^{b}	21.57 ± 0.53^{f}	19.59 ± 0.09^{e}	18.47 ± 0.38^{d}	23.55 ± 0.11^{g}	17.59 ± 0.09^{c}	21.66 ± 0.28^{f}	13.27 ± 0.31^{a}
121	Q-*O*-hexoside	0.20 ± 0.01^{b}	0.28 ± 0.01^{c}	0.12 ± 0.01^{a}	0.33 ± 0.01^{d}	0.19 ± 0.01^{b}	0.27 ± 0.01^{c}	0.35 ± 0.01^{d}	0.70 ± 0.01^{e}
122	Q-*O*-(galloyl)hexoside	2.00 ± 0.06^{cd}	1.97 ± 0.07^{c}	2.88 ± 0.05^{f}	2.66 ±0.03^{e}	3.75 ± 0.01^{g}	1.83 ± 0.07^{c}	1.52 ± 0.03^{b}	0.57 ± 0.02^{a}
131	K-*O*-hexoside	0.68 ± 0.03^{c}	0.62 ± 0.01^{b}	0.86 ± 0.02^{f}	0.77 ± 0.03^{e}	0.71 ± 0.02^{cd}	0.77 ± 0.01^{e}	0.60 ± 0.02^{b}	0.44 ± 0.01^{a}
137	Q-*O*-deoxyhexoside	0.60 ± 0.03^{ab}	0.79 ± 0.03^{c}	1.15 ± 0.01^{e}	1.42 ± 0.03^{f}	0.56 ± 0.01^{a}	0.91 ± 0.03^{d}	0.88 ± 0.03^{d}	0.57 ± 0.02^{a}
139	K-*O*-(galloyl)hexoside	0.37 ± 0.02^{a}	0.51 ± 0.01^{c}	0.83 ± 0.01^{e}	0.43 ± 0.01^{b}	0.55 ± 0.01^{c}	0.33 ± 0.01^{a}	0.55 ± 0.01^{c}	0.63 ± 0.01^{d}

140	Dimethyl-M-*O*-pentoside	0.32 ± 0.01^{c}			0.19 ± 0.01^{a}			0.25 ± 0.01^{b}	
145	M-*O*-(galloyl)hexoside	0.20 ± 0.01^{a}		0.24 ± 0.01^{b}	0.18 ± 0.01^{a}		0.42 ± 0.02^{d}	0.34 ± 0.01^{c}	
148	K-*O*-rhamnoside	0.76 ± 0.01^{b}	0.58 ± 0.01^{a}	0.90 ± 0.03^{c}	1.24 ± 0.04^{e}	0.60 ± 0.01^{a}	0.76 ± 0.03^{b}	1.11 ± 0.04^{d}	1.17 ± 0.02^{d}
150	M-*O*-(galloyl)deoxyhexoside	3.00 ± 0.08^{d}	2.89 ± 0.13^{c}	2.32 ± 0.07^{b}	1.17 ± 0.02^{a}	3.73 ± 0.04^{f}	2.92 ± 0.03^{cd}	2.26 ± 0.06^{b}	3.24 ± 0.11^{e}
151	Q-*O*-(galloyl)deoxyhexoside	1.16 ± 0.03^{a}	1.27 ± 0.46^{ab}	1.84 ± 0.02^{d}	3.61 ± 0.12^{e}		1.06 ± 0.10^{a}	1.40 ± 0.02^{c}	
152	Q-*O*-(acetyl)rhamnoside			0.23 ± 0.01^{b}	0.17 ± 0.01^{a}				0.36 ± 0.01^{c}
153	Q-*O*-(galloyl)deoxyhexoside	0.13 ± 0.01^{a}	0.16 ± 0.01^{ab}	0.22 ± 0.01^{c}		0.33 ± 0.01^{d}	0.25 ± 0.01^{c}	0.14 ± 0.01^{a}	0.13 ± 0.01^{a}
160	Quercetin								0.16 ± 0.01
Total		**32.78 ± 0.5^{b}**	**36.48 ± 1.53^{c}**	**41.99 ± 0.86^{d}**	**46.04 ± 1.13^{e}**	**43.50 ± 0.36^{d}**	**33.02 ± 0.52^{b}**	**35.77 ± 0.64^{c}**	**26.79 ± 0.63^{a}**
Flavan-3-ols									
32	Gallocatechin	0.26 ± 0.01^{b}	0.26 ± 0.03^{b}	0.42 ± 0.02^{e}		0.36 ± 0.02^{d}	0.20 ± 0.01^{a}	0.61 ± 0.01^{f}	0.31 ± 0.02^{c}
43	Gallocatechin	2.38 ± 0.01^{b}	3.30 ± 0.06^{c}		1.28 ± 0.05^{a}				
46	Gallo(epi)catechin-Gallo(epi)catechin-*O*-gallate	2.52 ± 0.01^{a}	3.63 ± 0.03^{b}	6.44 ± 0.04^{e}	5.84 ± 0.03^{d}	5.68 ± 0.10^{d}	4.69 ± 0.03^{c}	4.92 ± 0.12^{c}	10.24 ± 0.28^{f}
71	Digalloyl(epi)gallocatechin dimer	2.68 ± 0.39^{e}	2.28 ± 0.28^{d}	0.55 ± 0.02^{a}			3.33 ± 0.09^{b}	7.54 ± 0.26^{c}	
75	Digalloyl(epi)gallocatechin dimer	6.93 ± 0.19^{d}	5.51 ± 0.17^{a}	6.00 ± 0.13^{c}	10.63 ± 0.40^{g}	7.60 ± 0.07^{e}	8.29 ± 0.08^{f}	6.16 ± 0.18^{b}	15.82 ± 0.22^{h}
81	Gallo(epi)catechin-*O*-gallate	7.25 ± 0.07^{f}	6.74 ± 0.19^{de}	6.54 ± 0.12^{d}	7.20 ± 0.06^{f}	6.06 ± 0.01^{c}	6.36 ± 0.22^{d}	3.89 ± 0.10^{a}	4.41 ± 0.12^{b}
87	Digallo(epi)catechin derivative	2.03 ± 0.05^{c}	2.96 ± 0.12^{e}	2.04 ± 0.09^{c}	0.70 ± 0.02^{a}	2.77 ± 0.02^{d}	1.48 ± 0.11^{b}	2.99 ± 0.11^{e}	
99	Gallo(epi)catechin-*O*-gallate	2.16 ± 0.02^{c}	1.82 ± 0.01^{a}		3.43 ± 0.07^{d}	1.71 ± 0.07^{a}	2.00 ± 0.06^{b}	1.93 ± 0.03^{b}	
Total		**26.21 ± 0.67^{c}**	**26.50 ± 0.70^{c}**	**21.99 ± 0.61^{a}**	**28.08 ± 0.59^{d}**	**24.18 ± 0.52^{b}**	**26.35 ± 0.39^{c}**	**28.04 ± 0.96^{d}**	**30.78 ± 0.50^{e}**
Flavones									
86	Tricin-*O*-hexoside derivative		1.06 ± 0.01^{c}		0.87 ± 0.01^{b}				0.64 ± 0.01^{a}
94	Tricin-*O*-hexoside derivative	0.41 ± 0.01^{a}				0.43 ± 0.01^{a}			

Total		**0.41 ± 0.01^{a}**	**1.06 ± 0.01^{d}**		**0.87 ± 0.01^{c}**	**0.43 ± 0.01^{a}**			**0.64 ± 0.01^{b}**
Ellagic acid deriatives/Ellagitannins									
8	HHDP-*O*-hexoside		0.27 ± 0.01^{a}	0.46 ± 0.02^{c}	0.23 ± 0.01^{a}				0.33 ± 0.01^{b}
19	Pedunculagin I derivative								0.31 ± 0.01
22	Pedunculagin I					3.61 ± 0.13^{b}		2.24 ± 0.22^{a}	
31	Pedunculagin I	3.62 ± 0.01^{d}	4.09 ± 0.18^{e}	3.36 ± 0.07^{c}	3.07 ± 0.10^{b}	2.24 ± 0.01^{a}	3.00 ± 0.01^{b}	4.34 ± 0.16^{e}	6.44 ± 0.27^{f}
37	Casuarinin								1.07 ± 0.04
38	HHDP-*O*-hexoside			0.30 ± 0.01^{a}	0.47 ± 0.01^{b}			0.49 ± 0.01^{b}	
39	Pedunculagin I	3.23 ± 0.13^{b}	2.73 ± 0.16^{a}	4.45 ± 0.01^{e}	3.78 ± 0.18^{c}	3.45 ± 0.11^{b}	4.12 ± 0.18^{e}	3.96 ± 0.09^{cd}	5.94 ± 0.28^{f}
49	Ellagic acid derivative	2.89 ± 0.01^{c}	3.74 ± 0.13^{d}	2.63 ± 0.02^{ab}	2.61 ± 0.14^{e}	3.91 ± 0.11^{d}	2.58 ± 0.05^{a}	4.52 ± 0.11^{e}	2.50 ± 0.01^{a}
53	Casuarinin	1.44 ± 0.02^{d}	1.14 ± 0.05^{b}	2.00 ± 0.01^{e}	2.93 ± 0.01^{g}	2.19 ± 0.08^{f}	0.94 ± 0.04^{a}	2.80 ± 0.06^{g}	1.34 ± 0.04^{c}
62	Casuarinin	6.35 ± 0.05^{d}	6.56 ± 0.09^{e}	5.04 ± 0.23^{b}	5.74 ± 0.20^{c}	4.94 ± 0.04^{b}	3.82 ± 0.25^{a}	5.54 ± 0.33^{bc}	9.76 ± 0.27^{f}
65	Casuarinin	0.99 ± 0.01^{c}	1.37 ± 0.04^{d}			0.50 ± 0.01^{a}	1.64 ± 0.06^{e}		0.72 ± 0.01^{b}
73	Pedunculagin II								0.31 ± 0.01
80	HHDP-*O*-hexoside	0.95 ± 0.02^{c}	0.66 ± 0.03^{a}	0.84 ± 0.03^{b}	1.16 ± 0.03^{d}	1.18 ± 0.06^{d}	0.83 ± 0.03^{b}	0.90 ± 0.01^{c}	2.59 ± 0.05^{e}
89	Ellagitannin	1.44 ± 0.01^{d}	1.11 ± 0.05^{a}	2.46 ± 0.01^{f}	2.84 ± 0.12^{g}	1.19 ± 0.05^{b}	2.03 ± 0.02^{e}	1.31 ± 0.04^{c}	1.17 ± 0.06^{g}
93	Ellagic acid-*O*-pentoside			0.89 ± 0.01^{a}				1.15 ± 0.01^{b}	1.31 ± 0.07^{c}
Total		**20.91 ± 0.27^{b}**	**21.67 ± 0.86^{bc}**	**22.43 ± 0.28^{c}**	**22.83 ± 1.05^{c}**	**23.21 ± 0.59^{c}**	**18.96 ± 0.64^{a}**	**27.25 ± 0.79^{d}**	**33.79 ± 1.12^{e}**
TIPC		**87.48 ± 1.26^{b}**	**91.87 ± 1.46^{c}**	**93.15 ± 2.16^{c}**	**102.35 ± 2.00^{e}**	**96.70 ± 1.25^{d}**	**83.45 ± 1.91^{a}**	**96.61 ± 2.08^{d}**	**100.60 ± 1.49^{e}**

MX: Machico; FL: Faial; ASJ: Arco de São Jorge; BV: Boaventura; SX: Seixal; PM: Porto Moniz; TC: Terceira; B: benzoyl; HHDP: Hexahydroxydiphenoyl; CoDOA: coumaroyl-2,7-anhydro-3- deoxy-2-octulopyranosonic acid; K: Kaempferol; M: Myricetin; Q: Quercetin. TIPC: total individual phenolic content. Bold values represent the sum of each type of components. Means in the same line not sharing the same letter are significantly different at $p < 0.05$ probability level.

4.2.3. Post *in vitro* gastrointestinal digestion

In this case, BV samples were submitted to *in vitro* digestion due to the higher phenolic amounts and available plant material. Differences on the composition of *M. faya* extracts was observed after *in vitro* digestion ($p < 0.05$) (**Figure 28** and **Table 16**). TIPC of digested berries and leaves decreased 70.20% and 56.64%, respectively (**Table 16**).

HCAs and ANTCs were the most affected classes in berries (-71.27% and -69.71%, respectively); flavan-3-ols, ellagitannins and flavonols contents also decreased: -69.41%, -61.90% and -53.85%, respectively (**Table 16**). HCAs were not quantified in digested leaves (**Figure 28 and Table 16)**. Flavones were the most affected class (59.88%), while HBAs the least (-31.09%). Flavonols (-59.47%), ellagitannins (63.62%) and flavonols (57.14%) showed different degradation rates.

C3G (**16**) remained the main compound in berries (77.83%) (**Table 16**), although in minor amounts (-68.74%). MCT (**112**) (18.97%), digalloyl(epi)gallocatechin dimer (**71**) (10.63%) and EGCG (**81**) (6.20%) were still relevant in leaves. A reduction of 54.55%, 55.72% and 61.89% was verified, respectively, in their contents.

Previously [117], MCT and quercetin-*O*-deoxyhexoside contents of *M. rubra* leaves were significantly decreased upon *in vitro* digestion (80.32% and 56.09%, respectively).

Table 16 - Quantification of main phenolic compounds present in *M. faya* (mg g^{-1} DE) before and after *in vitro* gastrointestinal digestion. Data represent the mean ± standard deviation ($n = 3$).

Nº	**Assigned identification**	**Berries**		**Leaves**	
Anthocyanins		Non-Digested	Digested	Non-Digested	Digested
5	Delphinidin-*O*-hexoside	0.31 ± 0.01			
11	Delphinidin-*O*-hexoside	2.34 ± 0.01^{a}	0.63 ± 0.02^{a}		
16	Cyanidin-3-*O*-glucoside	32.01 ± 0.18^{b}	10.01 ± 0.16^{a}		
50	Cyanidin-*O*-hexoside	0.15 ± 0.01			
69	Cyanidin-*O*-(acetyl)hexoside	0.30 ± 0.01			
Total		**35.11 ± 0.65^{b}**	**10.64 ± 0.21^{a}**		
Hydroxycinnamic acids					
10	Caffeoylisocitrate	0.12 ± 0.01			
63	5-*O*-CQA	0.29 ± 0.02			
164	B-*p*-tri-CoDOA	0.54 ± 0.01^{d}	0.27 ± 0.01^{c}	0.04 ± 0.01^{b}	0.01 ± 0.01^{a}
Total		**0.95 ± 0.04^{d}**	**0.27 ± 0.01^{a}**	**0.04 ± 0.01^{b}**	**0.01 ± 0.01^{a}**
Hydroxybenzoic acids					
4	Galloyl-*O*-hexoside	0.16 ± 0.01			

12	Galloyl-*O*-hexoside	1.45 ± 0.51^{ab}		2.12 ± 0.37^{b}	1.05 ± 0.05^{a}
15	Galloylquinic acid			1.42 ± 0.21^{b}	0.61 ± 0.02^{a}
18	Gallic acid			0.79 ± 0.03^{a}	1.43 ± 0.06^{b}
27	Digalloyl-*O*-hexoside	0.20 ± 0.01			
88	Trigalloyl glucose	0.06 ± 0.01^{a}		0.16 ± 0.01^{b}	
Total		**1.87 ± 0.62^{a}**		**4.49 ± 0.19^{c}**	**3.09 ± 0.18^{b}**
Flavonols					
91	M-*O*-hexoside	0.25 ± 0.01^{b}	0.11 ± 0.01^{a}	5.39 ± 0.17^{d}	2.43 ± 0.03^{c}
92	M-*O*-(galloyl)hexoside	0.09 ± 0.01^{b}	0.06 ± 0.01^{a}	9.77 ± 0.35^{d}	3.80 ± 0.21^{c}
104	Rutin			0.23 ± 0.01^{b}	0.09 ± 0.01^{a}
112	Myricitrin	1.20 ± 0.01^{b}	0.51 ± 0.01^{a}	18.48 ± 0.79^{d}	8.40 ± 0.17^{c}
121	Q-*O*-hexoside	0.12 ± 0.01^{b}	0.06 ± 0.01^{a}	0.33 ± 0.01^{c}	0.12 ± 0.02^{b}
122	Q-*O*-(galloyl)hexoside	0.10 ± 0.01^{b}	0.05 ± 0.01^{a}	2.66 ± 0.33^{d}	1.03 ± 0.06^{c}
131	K-*O*-hexoside	0.32 ± 0.01^{c}	0.14 ± 0.01^{a}	0.77 ± 0.04^{d}	0.24 ± 0.02^{b}
136	K-*O*-hexoside	0.20 ± 0.01^{b}	0.10 ± 0.01^{a}	1.42 ± 0.47^{d}	0.62 ± 0.03^{c}
137	Q-*O*-deoxyhexoside	0.24 ± 0.01^{b}	0.11 ± 0.01^{a}	0.43 ± 0.02^{c}	0.19 ± 0.01^{a}
140	Dimethyl-M-*O*-pentoside			0.19 ± 0.01	
145	M-*O*-(galloyl)deoxyhexoside			0.18 ± 0.01^{b}	0.06 ± 0.01^{a}
148	K-*O*-rhamnoside			1.24 ± 0.08^{b}	0.43 ± 0.01^{a}
150	M-*O*-(galloyl)deoxyhexoside			1.17 ± 0.04^{b}	0.33 ± 0.01^{a}
151	Q-*O*-(galloyl)deoxyhexoside	0.27 ± 0.01^{b}	0.15 ± 0.01^{a}	3.61 ± 0.27^{d}	1.37 ± 0.10^{c}
152	Q-*O*-(acetyl)rhamnoside			0.17 ± 0.03^{b}	0.03 ± 0.01^{a}
160	Quercetin				0.60 ± 0.01
Total		**2.93 ± 0.09^{b}**	**1.29 ± 0.02^{a}**	**46.04 ± 3.74^{d}**	**17.97 ± 1.31^{c}**
Flavan-3-ols					
43	Gallo(epi)catechin	0.11 ± 0.01^{a}		1.28 ± 0.1^{c}	0.47 ± 0.03^{b}
45	Gallocatechin dimer	0.26 ± 0.01^{b}	0.10 ± 0.01^{a}		
46	Gallo(epi)catechin-Gallo(epi)catechin-*O*-gallate			5.84 ± 0.24^{b}	2.16 ± 0.50^{a}
71	Digalloyl(epi)gallocatechin dimer	0.32 ± 0.01^{b}	0.11 ± 0.01^{a}		
75	Digalloyl(epi)gallocatechin dimer			9.63 ± 0.68^{b}	4.71 ± 0.33^{a}
81	Gallo(epi)catechin-*O*-gallate	0.05 ± 0.01^{b}	0.02 ± 0.01^{a}	7.20 ± 0.25^{d}	2.74 ± 0.16^{c}
87	Digallo(epi)catechin derivative			0.70 ± 0.02^{b}	0.35 ± 0.02^{a}
99	Gallo(epi)catechin-*O*-gallate			3.43 ± 0.17^{b}	1.35 ± 0.27^{a}
Total		**0.74 ± 0.04^{b}**	**0.23 ± 0.02^{a}**	**28.08 ± 1.95^{d}**	**11.45 ± 0.61^{c}**
Flavones					
86	Tricin-*O*-hexoside derivative			0.87 ± 0.04^{b}	0.35 ± 0.02^{a}

Total				**0.87 ± 0.04^{b}**	**0.35 ± 0.02^{a}**
Ellagic acid derivativesEllagitannins					
8	HHDP-*O*-hexoside			0.23 ± 0.01	
31	Pedunculagin I	0.46 ± 0.01^{b}	0.19 ± 0.01^{a}	3.07 ± 0.15^{d}	1.18 ± 0.09^{c}
38	HHDP-*O*-hexoside			0.47 ± 0.20	
39	Pedunculagin I	0.17 ± 0.01b	0.04 ± 0.02a	3.78 ± 0.28^{d}	1.41 ± 0.08^{c}
49	Ellagic acid derivative			2.61 ± 0.32^{b}	0.97 ± 0.13^{a}
53	Casuarinin	0.14 ± 0.01^{b}	0.03 ± 0.01^{a}	2.93 ± 0.11^{d}	0.93 ± 0.04^{c}
62	Casuarinin			5.74 ± 0.43^{b}	1.96 ± 0.10^{a}
65	Casuarinin	0.16 ± 0.01^{b}	0.10 ± 0.01^{a}		
67	Casuarinin like ellagitannin	0.21 ± 0.01^{b}	0.05 ± 0.01^{a}		
75	Digalloyl(epi)gallocatechin dimer				
80	HHDP-*O*-hexoside			1.16 ± 0.08^{b}	0.40 ± 0.04^{a}
81	Gallo(epi)catechin-*O*-gallate				
89	Ellagitannin			2.84 ± 0.17^{b}	1.02 ± 0.17^{a}
93	Ellagic acid-*O*-pentoside		0.03 ± 0.01		
Total		**1.14 ± 0.05^{b}**	**0.43 0.02^{a}**	**22.83 ± 1.46^{d}**	**7.86 ± 0.75^{c}**
TIPC		**43.63 ± 0.92^{a}**	**12.86 ± 0.84^{a}**	**102.35 ± 2.00^{b}**	**42.83 ± 2.71^{a}**

B: benzoyl; HHDP: Hexahydroxydiphenoyl; CoDOA: coumaroyl-2,7-anhydro-3- deoxy-2-octulopyranosonic acid; K: Kaempferol; M: Myricetin; Q: Quercetin. TIPC: total individual phenolic content. Bold values represent the sum of each type of components. Means in the same line not sharing the same letter are significantly different at $p < 0.05$ probability level.

4.3. *Rubus grandifolius*

The phytochemical profile of *R. grandifolius* from two locations of Madeira Island (Funchal and Machico) was composed by 122 compounds, including ANTCs, other flavonoids, phenolic acids, terpenoids, coumarins and organic acids (Supplementary Material - **Table S 13** and **Table S 14**).

The BPCs of the methanolic extracts are shown in **Figure 29** - **Figure 31** (only the most abundant compounds are numbered for the sake of clarity).

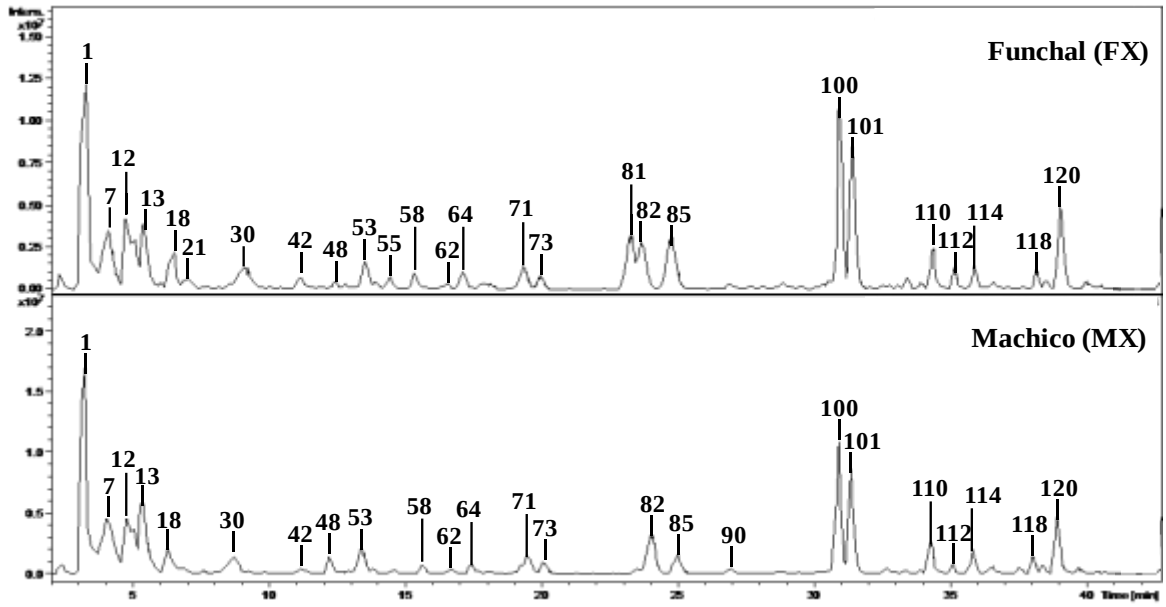

Figure 29 – Representative base peak chromatogram (BPC) of the HPLC-ESI$^-$/MS^n analysis of *R. grandifolius* methanolic extracts (berries) collected in two different locations. For peak identification check **Table S 13** (Supplementary Material).

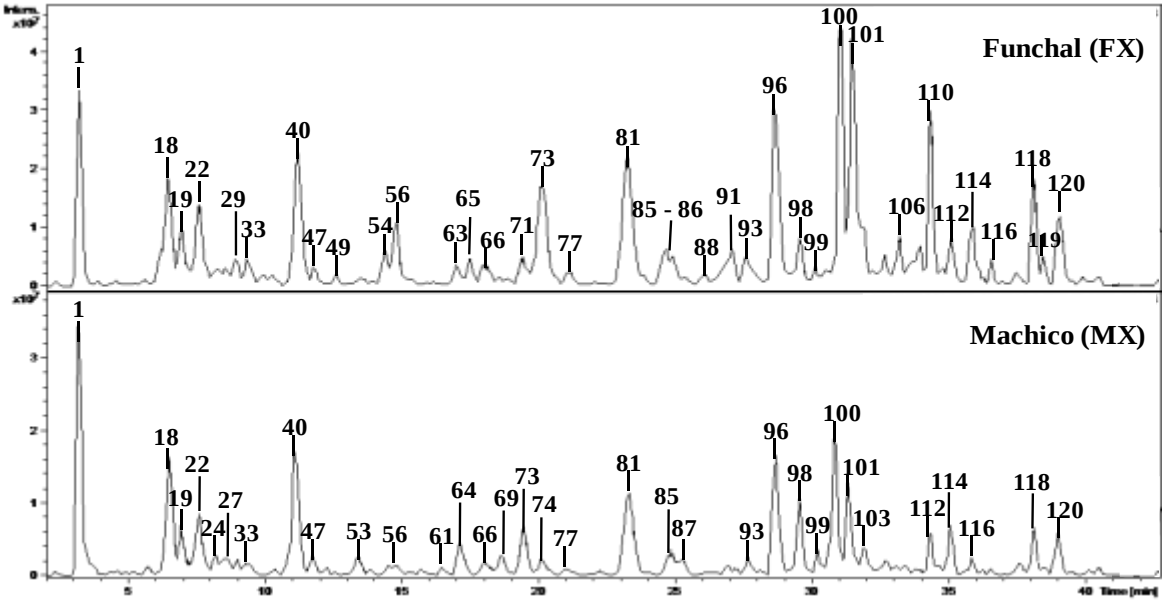

Figure 30 - Representative base peak chromatogram (BPC) of the HPLC-ESI^{-}/MS^{n} analysis of *R. grandifolius* methanolic extracts (leaves) collected in two different locations. For peak identification check **Table S 13** (Supplementary Material).

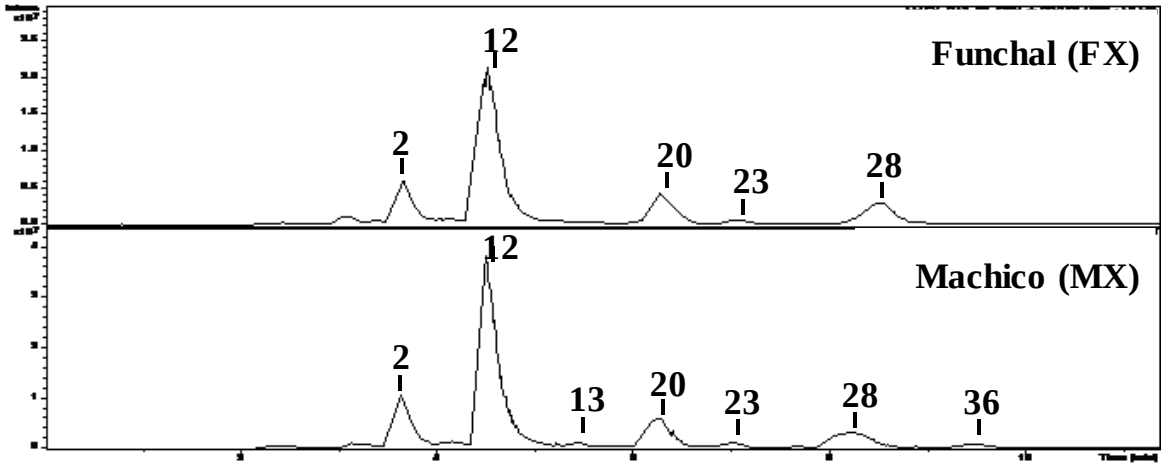

Figure 31 - Representative base peak chromatogram (BPC) of the HPLC-ESI^{+}/MS^{n} analysis of *R. grandifolius* methanolic extracts (berries) collected in two different locations. For peak identification check **Table S 14** (Supplementary Material).

4.3.1. Pre-*in vitro* gastrointestinal digestion

Fifty main PCs were quantified in *R. grandifolius* samples (**Table 17**). The phenolic composition of analysed extracts ranged from 92.96 – 97.47 and 118.01 – 137.41 mg g^{-1} DE, for berries and leaves, respectively (**Table 17**). Significant variations ($p < 0.05$) were observed from samples collected in different locations. In general, FX samples showed the highest amounts of PCs. Exceptions were observed for HCAs and flavan-3-ols contents in berries and leaves, respectively.

The compositional percentages of *R. grandifolius* extracts (pre- and post *in vitro* digestion) are represented in **Figure 32**.

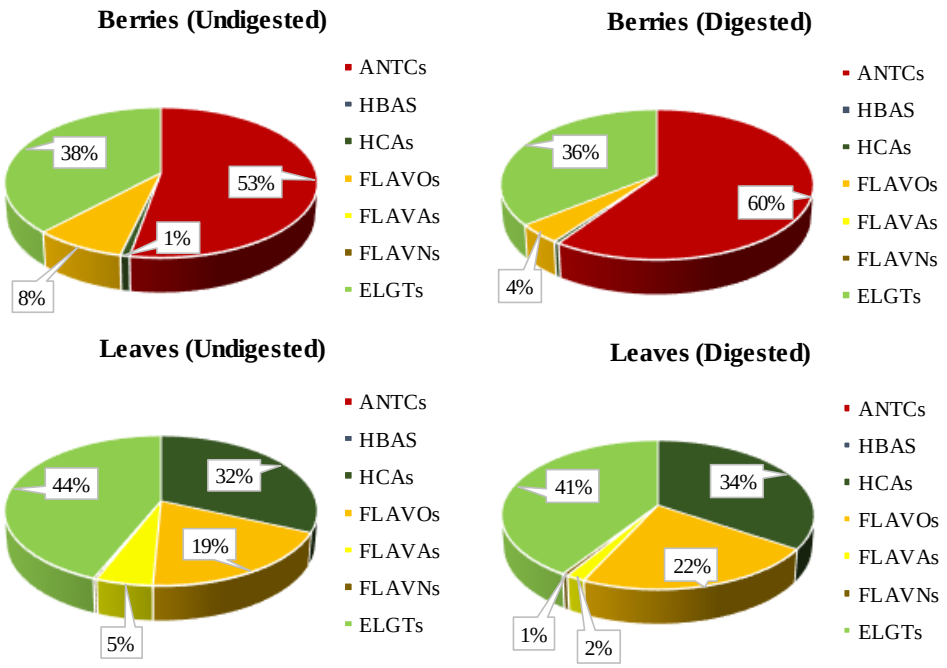

Figure 32 - Phenolic composition of *R. grandifolius* extracts (pre- and post-*in vitro* digestion). In the case of undigested extracts, the values represent the means from data of samples collected in different locations. For more detailed data check **Table 17** and **Table 18**. ANTCs: anthocyanins; HBAs: hydroxybenzoic acids; HCAs hydroxycinnamic acids; FLAVOs: flavonols; FLAVAs: flavan-3-ols; FLAVNs: flavones; ELGTs: ellagitannis.

C3G (**12**) was major compound in *R. grandifolius* (41 – 45%) (**Table 17**), which is also reported for other *Rubus* berries [88,114,144]. Ellagic acid-*O*-glucuronide (11.65 – 15.39%) (**48**) and casuarinin (20.97 – 22.30%) (**53**) were also present in high amounts (**Table 17**). Similar TIPC, ellagitannins, flavonoids and HCAs were documented in wild blackberries [114]. Casuarinin (**53**) was the main PC in leaves (33 – 43%) (**Table 17**), which is corroborative with literature data [34,87,88]. As oppose to present work, ellagintannins were not detected and only one ellagic acid derivative was

identified, previously, in *R. grandifolius* [107]. These discrepancies could be due differences in the period of collection and drying techniques. Quercetin-*O*-glucuronide (**81**) (9.56%), catechin (**39**) (8.91%), 3-*O*-CQA (**18**) (6.21 - 7.24%), caffeic acid derivative (**49**) (6.57%) and ellagic acid-*O*-hexoside (**74**) (5.7%) were also major compounds (**Table 17**).

Flavan-3-ols contents seemed significantly ($p < 0.05$) affected by the collection area: catechin (**39**) content in MX leaves were almost 8-fold higher. An explanation for the observed variations in the phenolic composition might be due to geographical differences of collection areas. Samples collected in Funchal grown at approximately 1400 m high (while Machico at about 500). Environmental factors like ligh/solar radiation, temperature, rainfall, among others, affect the phenolic composition [35]. At higher altitudes, plants are more subject to stress conditions that may induce intense higher synthesis of PCs as response to abiotic stress. It is known that the amounts of PCs in *Rubus* species is influenced by the collection area [31,87,88].

ANTCs, ellagitannins, flavonols and HCAs contents of berries (**Table 17**) were within those determined for other *Rubus spp*. [114]. Berries of *R. glaucus* and *R. adenotrichus* showed inferior TIPC (18.61 and 41.71 mg g^{-1} DE, respectively) than *R. grandifolius* [88]. TIPC of leaves was found within the range of other wild blackberries (83.02 – 334.24 mg g^{-1} DE)[87]. However, ellagitannins and flavonoids contents found in the present work were lower (51.59 – 255.01 and 8.68 – 61.27 mg g^{-1} DE, respectively), while HCAs amounts was in the upper limit (8.62 - 43.14 mg g^{-1} DE).

Table 17 - Quantification (mg g^{-1} DE) of main phenolic compounds present in *R. grandifolius* extracts (leaves and berries) collected in two different locations. Data represent the mean ± standard deviation ($n = 3$).

Nº	Assigned identification	Berries		Leaves	
Anthocyanins		FX	MX	FX	MX
2	Cyanidin-O-hexoside	5.19 ± 0.14^{b}	3.46 ± 0.05^{a}		
12	Cyanidin-3-*O*-glucoside	39.49 ± 0.44^{a}	40.94 ± 1.20^{a}		
13	Cyanidin-*O*-pentoside	2.86 ± 0.03^{b}	1.67 ± 0.06^{a}		
30	Cyanidin-*O*-(pentosyl)glucoside	4.76 ± 0.08^{b}	3.74 ± 0.13^{a}		
Total		**52.31 ± 0.72^{b}**	**48.81 ± 0.89^{a}**		
Hydroxycinnamic acids					
18	3-*O*-CQA		0.54 ± 0.02^{a}	9.96 ± 0.24^{c}	6.75 ± 0.32^{b}
19	Caffeic acid-*O*-hexoside			5.84 ± 0.13^{b}	3.09 ± 0.11^{a}
22	Caffeic acid-*O*-hexoside			6.41 ± 0.21^{b}	2.59 ± 0.08^{a}
24	Caffeic acid derivative			1.85 ± 0.05^{b}	1.27 ± 0.02^{a}
27	Salvianolic acid			1.55 ± 0.03^{a}	1.72 ± 0.03^{b}
29	5-*O*-CQA dimer	0.69 ± 0.02^{c}	0.35 ± 0.01^{a}	1.20 ± 0.02^{d}	0.58 ± 0.02^{b}

34	Ferulic acid-*O*-hexoside	0.04 ± 0.01			
40	Ferulic acid derivative			7.29 ± 0.12^{b}	3.97 ± 0.14^{a}
44	Caffeic acid-*O*-hexoside derivative			0.84 ± 0.02^{a}	1.09 ± 0.02^{b}
49	Caffeic acid derivative			6.42 ± 0.14^{a}	7.14 ± 0.12^{b}
54	Caffeic acid derivative			0.24 ± 0.01	
56	Caffeic acid-*O*-(galloyl)hexoside			1.99 ± 0.03^{b}	0.08 ± 0.01^{a}
65	Caffeic acid derivative			1.18 ± 0.03	
77	Caffeic acid derivative			0.25 ± 0.01^{b}	0.13 ± 0.01^{a}
93	Umbelliferone			0.46 ± 0.01^{b}	0.38 ± 0.02^{a}
96	Caffeic acid-*O*-dihexoside			4.76 ± 0.07^{b}	1.56 ± 0.06^{a}
98	Umbelliferone			0.72 ± 0.01^{b}	0.35 ± 0.01^{a}
104	Caffeic acid-*O*-(Co)hexoside			0.20 ± 0.01	
109	Umbelliferone			0.18 ± 0.01	
121	Coumaric acid				0.08 ± 0.01
Total		**0.72 ± 0.02^{a}**	**0.89 ± 0.02^{b}**	**51.69 ± 1.15^{d}**	**30.79 ± 0.95^{c}**
Flavonols					
55	Q-*O*-(pentosyl)hexoside	0.65 ± 0.02^{b}	0.58 ± 0.01^{a}		
62	I-*O*-glucuronide	0.47 ± 0.01^{a}	0.48 ± 0.01^{a}		
64	Rutin	0.44 ± 0.01^{a}	0.65 ± 0.01^{b}		2.14 ± 0.02^{c}
71	Q-*O*-hexoside	1.11 ± 0.02^{a}	2.02 ± 0.04^{b}	3.70 ± 0.09^{d}	2.14 ± 0.02^{c}
81	Q-*O*-glucuronide	1.74 ± 0.02^{b}	1.08 ± 0.02^{a}	13.13 ± 0.05^{d}	10.22 ± 0.20^{c}
82	3-Hydroxy-3-MG-Q-*O*-hexoside	1.21 ± 0.02^{b}	1.00 ± 0.02^{a}		
85	Q-*O*-pentoside	1.37 ± 0.02^{b}	0.60 ± 0.01^{a}	4.82 ± 0.08^{b}	2.84 ± 0.04^{a}
90	Q-*O*-(acetyl)hexoside	0.32 ± 0.01^{a}	0.30 ± 0.01^{a}	2.08 ± 0.06^{b}	1.99 ± 0.06^{b}
91	K-*O*-hexoside			1.75 ± 0.04^{a}	1.80 ± 0.02^{a}
92	I derivative	0.31 ± 0.01^{a}	0.38 ± 0.01^{a}		
114	K-*O*-(coumaroyl)hexoside	0.34 ± 0.01^{a}	0.48 ± 0.02^{b}	2.07 ± 0.04^{d}	0.71 ± 0.03^{c}
115	Quercetin	0.27 ± 0.01			
Total		**8.23 ± 0.16^{b}**	**7.81 ± 0.14^{a}**	**27.54 ± 0.49^{d}**	**21.98 ± 0.39^{c}**
Flavan-3-ols					
32	Procyanidin dimer (B type)				1.23 ± 0.02
39	Catechin			2.67 ± 0.07^{a}	9.68 ± 0.15^{b}
Total				**2.67 ± 0.07^{a}**	**10.91 ± 0.17^{b}**
Flavones					
99	Apigenin-*O*-glucuronide			0.39 ± 0.01^{a}	0.35 ± 0.01^{a}
Total				**0.39 ± 0.01^{a}**	**0.35 ± 0.01^{a}**
Ellagic acid derivatives/ Ellagitannins					

9	HHDP-*O*-hexoside				1.83 ± 0.04
15	Pedunculagin I			0.38 ± 0.01[a]	0.36 ± 0.01[a]
21	Pedunculagin I		1.99 ± 0.06[c]	0.51 ± 0.01[a]	1.01 ± 0.03[b]
37	Trigalloyl-*O*-hexoside			1.42 ± 0.04	
42	Ellagic acid-*O*-glucuronide	1.02 ± 0.02			
48	Ellagic acid-*O*-glucuronide	11.35 ± 0.18[a]	14.31 ± 0.31[b]		
53	Casuarinin	21.74 ± 0.72[b]	19.49 ± 0.34[a]	44.83 ± 0.77[c]	47.00 ± 0.67[d]
58	Ellagic acid-*O*-pentoside	0.44 ± 0.01[a]	0.40 ± 0.02[a]	0.73 ± 0.03[b]	
61	Ellagic acid derivative				0.27 ± 0.01
73	Ellagic acid-*O*-hexoside	0.20 ± 0.01[a]	0.25 ± 0.01[a]	7.86 ± 0.16[c]	1.01 ± 0.04[b]
113	Ellagic acid derivative	1.47 ± 0.02			
Total		**36.21 ± 0.95[a]**	**36.45 ± 0.73[a]**	**59.93 ± 1.10[c]**	**53.98 ± 0.80[b]**
TIPC		**97.47 ± 1.85[b]**	**92.96 ± 1.94[a]**	**137.41 ± 2.22[d]**	**118.01 ± 1.89[c]**

FX: Funchal; MX: Machico. HHDP: Hexahydroxydiphenoyl; MG: methlyglutaroyl; K: Kaempferol; I: Isorhamnetin; Q: Quercetin; Co: coumaroyl. TIPC: total individual phenolic content. Bold values represent the sum of each type of components. Means in the same line not sharing the same letter are significantly different at $p < 0.05$ probability level.

4.3.2. Post *in vitro* gastrointestinal digestion

In this case, FX samples were selected for the *in vitro* digestion. The phenolic profile of *R. grandifolius* was affected by simulated digestion (**Figure 28**), with a reduction ($p < 0.05$) on TIPC of 71.88% and 59.17% for berries and leaves, respectively (**Table 18**).

In berries, flavonols (-86.18%), HCAs (-80.07%), ellagitannins (-72.94%) and ANTCs (-68.80%) were substantially affected. Lower degradation rates (54.18 – 63.22%) were observed in leaves for flavan-3-ols, HCAS, flavanones, ellagitannins and flavonols contents. Main compounds of berries, C3G (**12**) (60.75%), casuarinin (**53**) (19.68%) and ellagic acid-*O*-glucuronide (**48**) (11.02%), showed lower amounts after simulated digestion (**Table 18**); a reduction of 62.32%, 71.88% and 69.83% was noted, respectively. Casuarinin (**53**) and quercetin-*O*-glucuronide (**81**), major phenolic in leaves (34.19% and 11.02% of TIPC), suffered losses of 62.62% and 49.07%, respectively.

Previous studies [56,141,145–147] reported the effect of *in vitro* digestion on *Rubus spp.*, but this is the first study on *R. grandifolius*. ANTCs were the most affected class (- 90%) in blackberries [56,141]. Ellagitannins (60 - 70%) and quercetin derivatives contents (20 – 60%) were also significantly reduced [56]. Lower degradation rates were verified for ANTCs in other study (4.7 – 68.30%)[147].

Table 18 - Quantification of main phenolic compounds (mg g^{-1} DE) present in *R. grandifolius* (Funchal, FX) before and after *in vitro* gastrointestinal digestion. Data represent the mean ± standard deviation (n = 3).

Nº	Assigned identification	Berries		Leaves	
Anthocyanins		Non-Digested	Digested	Non-Digested	Digested
2	Cyanidin-O-hexoside	5.19 ± 0.14^{b}	1.44 ± 0.10^{a}		
12	Cyanidin-3-*O*-glucoside	39.49 ± 1.78^{b}	14.87 ± 0.69^{a}		
13	Cyanidin-*O*-pentoside	2.86 ± 0.03			
30	Cyanidin-*O*-dioxaloylglucoside	4.76 ± 0.08			
Total		**52.31 ± 0.72^{b}**	**16.32 ± 1.79^{a}**		
Hydroxycinnamic acids					
18	3-*O*-CQA			9.96 ± 0.24^{b}	4.02 ± 0.03^{a}
19	Caffeic acid-*O*-hexoside			5.84 ± 0.13^{b}	2.51 ± 0.12^{a}
22	Caffeic acid-*O*-hexoside			6.41 ± 0.21^{b}	3.03 ± 0.06^{a}
24	Caffeic acid derivative			1.85 ± 0.05^{b}	0.55 ± 0.01^{a}
27	Salvianolic acid			1.55 ± 0.03^{b}	0.47 ± 0.01^{a}
29	5-*O*-CQA dimer	0.69 ± 0.02^{c}	0.14 ± 0.01^{a}	1.2 ± 0.02^{d}	0.31 ± 0.01^{b}
34	Ferulic acid-*O*-hexoside	0.04 ± 0.01			
40	Ferulic acid-*O*-hexoside			7.29 ± 0.12^{b}	2.38 ± 0.10^{a}
44	Caffeic acid-*O*-hexoside derivative			0.84 ± 0.02^{b}	0.23 ± 0.02^{a}
49	Caffeic acid derivative			6.42 ± 0.14^{b}	2.60 ± 0.15^{a}
54	Caffeic acid derivative			0.24 ± 0.01^{b}	0.10 ± 0.01^{a}
56	Caffeic acid-*O*-(galloyl)hexoside			1.99 ± 0.03^{b}	0.76 ± 0.02^{a}
65	Caffeic acid derivative			1.18 ± 0.03^{b}	0.04 ± 0.01^{a}
77	Caffeic acid derivative			0.25 ± 0.01	
93	Umbelliferone			0.46 ± 0.01	
96	Caffeic acid-*O*-dihexoside			4.76 ± 0.07^{b}	1.96 ± 0.09^{a}
98	Umbelliferone			0.72 ± 0.01^{b}	0.27 ± 0.02^{a}
104	Caffeic acid-*O*-(Co)hexoside			0.20 ± 0.01	
109	Umbelliferone			0.18 ± 0.01^{b}	0.08 ± 0.01^{a}
121	Coumaric acid				
Total		**0.72 ± 0.02^{a}**	**0.14 ± 0.01^{b}**	**51.69 ± 1.15^{d}**	**19.32 ± 0.93^{a}**
Flavonols					
55	Q-*O*-(pentosyl)hexoside	0.65 ± 0.02			
62	I-*O*-glucuronide	0.47 ± 0.01^{b}	0.14 ± 0.01^{a}		
64	Rutin	0.44 ± 0.01^{b}	0.16 ± 0.01^{a}		
71	Q-*O*-hexoside	1.11 ± 0.02^{b}	0.30 ± 0.01^{a}	3.7 ± 0.09^{d}	1.49 ± 0.03^{c}
81	Q-*O*-glucuronide	1.74 ± 0.02^{a}		13.13 ± 0.50^{c}	6.69 ± 0.35^{b}
82	3-Hydroxy-3-MG-Q-*O*-hexoside	1.21 ± 0.02^{b}	0.16 ± 0.03^{a}		
85	Q-*O*-pentoside	1.37 ± 0.02^{b}	0.19 ± 0.01^{a}	4.82 ± 0.08^{d}	1.93 ± 0.07^{c}
90	Q-*O*-(acetyl)hexoside	0.32 ± 0.01^{a}	0.98 ± 0.01^{c}	2.08 ± 0.06^{d}	0.84 ± 0.02^{b}
91	K-*O*-hexoside			1.75 ± 0.04^{b}	0.65 ± 0.03^{a}

92	I derivative	0.31 ± 0.01			
114	K-*O*-(coumaroyl)hexoside	0.34 ± 0.01^{b}	0.08 ± 0.01^{a}	2.07 ± 0.04^{d}	1.03 ± 0.03^{c}
115	Quercetin	0.27 ± 0.01			
Total		**8.23 ± 0.37^{b}**	**1.14 ± 0.05^{a}**	**27.54 ± 0.49^{d}**	**12.62 ± 0.54^{c}**
Flavan-3-ols					
39	Catechin			2.67 ± 0.07^{b}	0.98 ± 0.03^{a}
Total				**2.67 ± 0.07^{b}**	**0.98 ± 0.03^{a}**
Flavones					
99	Apigenin-*O*-glucuronide			0.73 ± 0.04^{b}	0.29 ± 0.01^{a}
Total				**0.73 ± 0.04^{b}**	**0.29 ± 0.01^{a}**
Ellagic acid derivatives/ Ellagitannins					
9	HHDP-*O*-hexoside				
15	Pedunculagin I			0.38 ± 0.01	
21	Pedunculagin I			0.51 ± 0.01^{b}	0.18 ± 0.05^{a}
37	Trigalloyl-*O*-hexoside			1.42 ± 0.04^{b}	0.53 ± 0.01^{a}
42	Ellagic acid-*O*-glucuronide	1.02 ± 0.02			
48	Ellagic acid-*O*-glucuronide	11.35 ± 0.18^{b}	3.42 ± 0.15^{a}		
53	Casuarinin	21.74 ± 0.72^{c}	6.11 ± 0.43^{a}	44.83 ± 0.77^{d}	16.76 ± 0.87^{b}
58	Ellagic acid-*O*-pentoside	0.44 ± 0.01^{c}	0.14 ± 0.02^{a}	0.73 ± 0.03^{d}	0.31 ± 0.01^{b}
61	Ellagic acid derivative				
70	Ellagic acid		0.12 ± 0.03^{a}		2.35 ± 0.09^{b}
74	Ellagic acid-*O*-hexoside	0.20 ± 0.01^{a}		7.86 ± 0.16^{c}	2.75 ± 0.12^{b}
113	Ellagic acid derivative	1.47 ± 0.02			
Total		**36.22 ± 0.96^{c}**	**9.80 ± 0.47^{a}**	**59.93 ± 1.11^{d}**	**22.89 ± 1.11^{b}**
TIPC		**97.47 ± 1.85^{c}**	**27.40 ± 1.54^{a}**	**137.41 ± 3.75^{d}**	**56.10 ± 2.83^{b}**

HHDP: Hexahydroxydiphenoyl; MG: methlyglutaroyl; K: Kaempferol; I: Isorhamnetin; Q: Quercetin; Co: coumaroyl. TIPC: total individual phenolic content. Bold values represent the sum of each type of components. Means in the same line not sharing the same letter are significantly different at $p < 0.05$ probability level.

4.4. *Sambucus lanceolata*[8]

Seventy-seven phytochemicals were identified in *S. lanceolata* namely ANTCs, other flavonoids, phenolic acids, oligosaccharides, organic acids, terpenoids, lignans and fatty acids (**Figure 33** and **Figure 34**). The characterization of the compounds is reported in Supplementary Material (**Table S 15** and **Table S 16**).

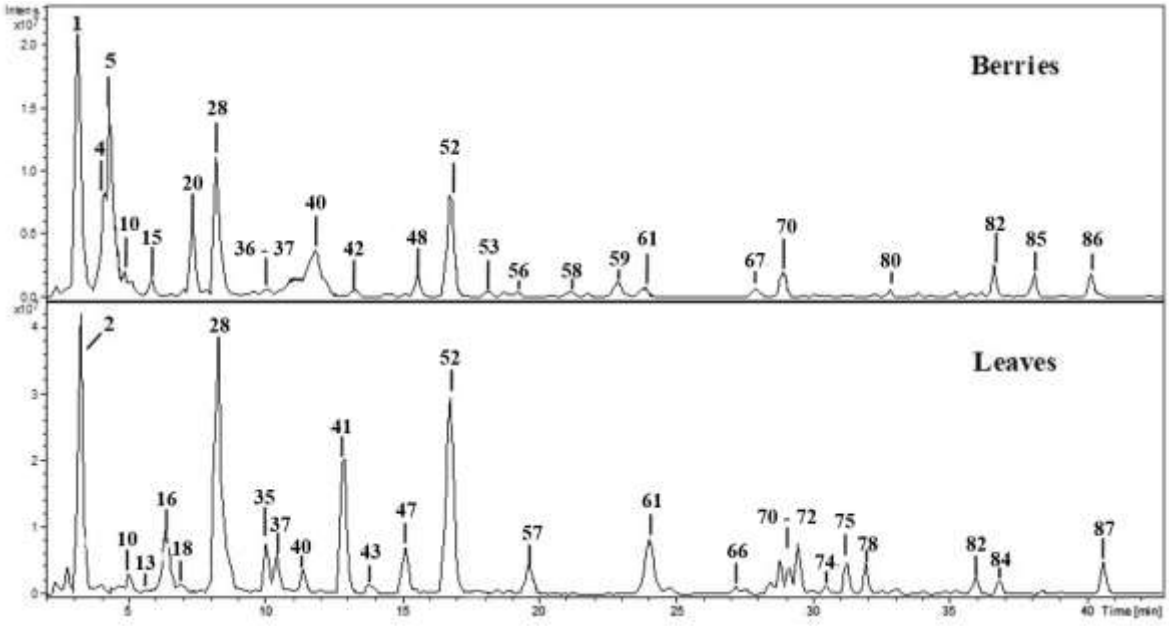

Figure 33 - Representative base peak chromatogram (BPC) of the HPLC-ESI$^-$/MS^n analysis of S. lanceolata methanolic extracts (berries and leaves). For peak assignment check **Table S 15** (Supplementary Material).

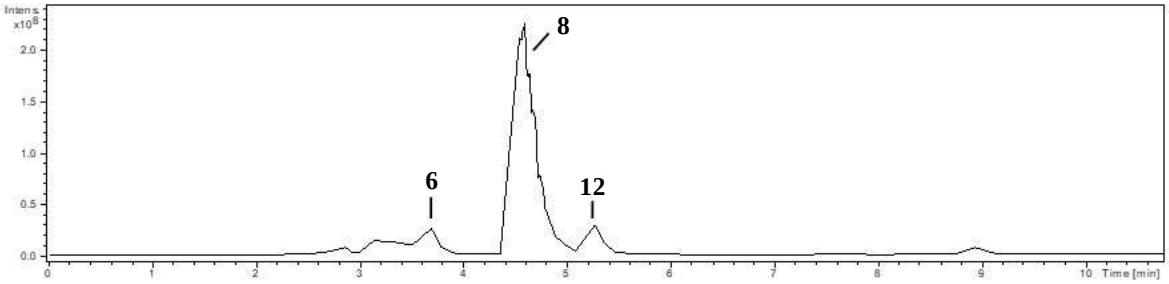

Figure 34 - Representative base peak chromatogram (BPC) of the HPLC-ESI$^+$/MS^n analysis of *S. lanceolata* (berries) methanolic extracts. For peak identification check **Table S 16** (Supplementary Material).

[8]This part of the work has been already published [123].

4.4.1. Pre-*in vitro* gastrointestinal digestion

Thirty-one PCs were quantified in *S. lanceolata* extracts (**Table 19**). In this case, berries showed a higher phenolic composition than leaves ($p < 0.05$) (**Table 19**). The same trend was observed for *S. nigra* [148]. However, leaves displayed superior contents of HCAs and flavonols ($p < 0.05$). The compositional percentages of *S. lanceolata* extracts (pre- and post *in vitro* digestion) are represented in **Figure 35**.

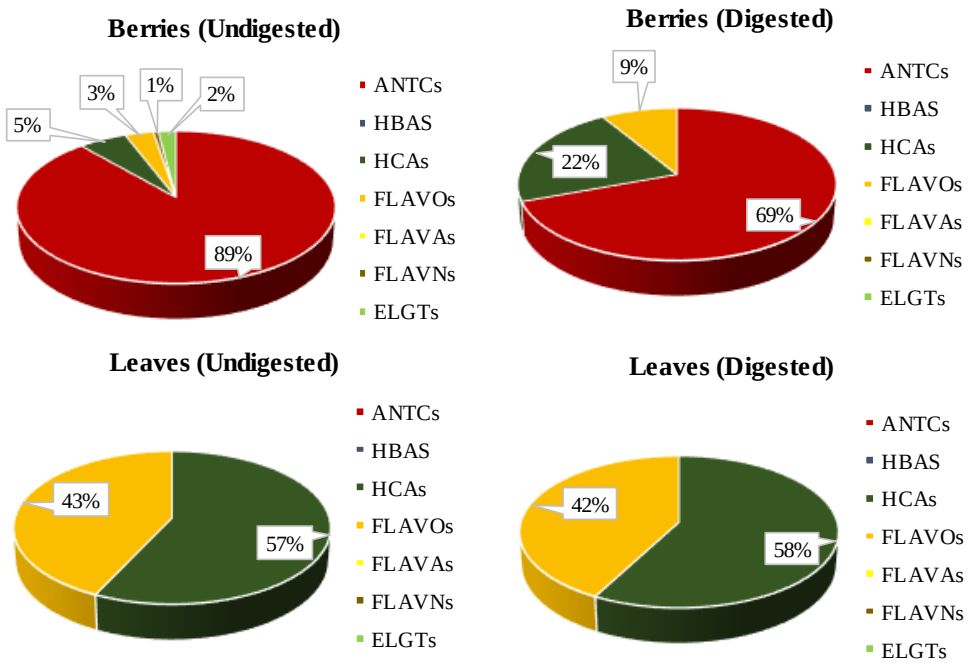

Figure 35 - Phenolic composition of *S. lanceolata* extracts (pre- and post-*in vitro* digestion). For more detailed data check Table 19. ANTCs: anthocyanins; HBAs: hydroxybenzoic acids; HCAs hydroxycinnamic acids; FLAVOs: flavonols; FLAVAs: flavan-3-ols; FLAVNs: flavones; ELGTs: ellagitannis.

Cyanidin-*O*-sambubioside (**8**) was dominant in berries (73.95%) (**Table 19**), as reported previously for other *Sambucus* species [24,148,149]. By contrast, C3G was dominant in other works [150,151]. Comparable C3G (0.4 – 0.7 mg g^{-1} DE) but lower ANTCs total amounts (8.8 – 13.4 mg g^{-1} DE) were documented in *S. nigra* [150,151]. 3-*O*-Caffeoylquinic acid (3-*O*-CQA) (**28**) (44.71%), rutin (**52**) (17.06%), and quercetin-*O*-(rhamnosyl)rutinoside (**41**) (14.67%) were representative in leaves (**Table 19**). TIPC of *S. lanceolata* berries was within the range found on *S. nigra* (0.7 – 27.4 mg g^{-1} DE) [148,150].

Table 19 - Quantification (mg g^{-1} DE) of main phenolic compounds of *S. lanceolata* extracts (berries and leaves) before and after *in vitro* gastrointestinal digestion. Data represent the mean ± standard deviation (n = 3).

Nº	Assigned identification	Berries		Leaves	
Anthocyanins		Non-digested	Digested	Non-digested	Digested
6	Cyandin-*O*-sambubioside	3.16 ± 0.04			
8	Cyandin-*O*-sambubioside	20.13 ± 0.11^{b}	3.10 ± 0.02^{a}		
12	Cyanidin-*O*-hexoside	0.85 ± 0.03			
Total		**24.13 ± 0.13^{b}**	**3.10 ± 0.02^{a}**		
Hydroxycinnamic acids					
4	Caffeoylisocitrate	0.15 ± 0.01^{b}	0.06 ± 0.01^{a}		
10	Hydroxytyrosol-*O*-hexoside	0.53 ± 0.02^{b}		1.03 ± 0.01^{c}	0.02 ± 0.01^{a}
21	Caffeic acid-*O*-hexoside			0.31 ± 0.01	
28	3-*O*-CQA	0.68 ± 0.03^{a}	0.77 ±0.01^{b}	11.58 ± 0.17^{d}	5.22 ± 0.07^{c}
36	CQA derivative			0.08 ± 0.01	
37	5-*O*-CQA	0.06 ± 0.01^{a}	0.14 ± 0.01^{b}	0.50 ± 0.01^{c}	0.15 ± 0.01^{b}
42	5-*O*-Feruloylquinic acid			0.06 ±0.01	
66	Coumaric acid derivative			0.28 ± 0.01^{b}	0.23 ± 0.01^{a}
68	Caffeic acid derivative			0.14 ± 0.01	
69	Coumaric acid derivative			0.20 ± 0.01^{b}	0.14 ± 0.01^{a}
70	Coumaric acid derivative			0.23 ± 0.01^{b}	0.12 ± 0.01^{a}
75	Coumaric acid derivative			0.16 ± 0.01^{b}	0.08 ± 0.01^{a}
78	Coumaric acid derivative			0.16 ± 0.01^{b}	0.09 ± 0.01^{a}
79	Ferulic acid derivative			0.06 ± 0.01^{b}	0.02 ± 0.01^{a}
Total		**1.51 ± 0.05^{b}**	**0.98 ± 0.01^{a}**	**14.78 ± 0.11^{d}**	**6.66 ± 0.07^{c}**
Flavonols					
41	Q-*O*-(rhamnosyl)rutinoside	0.10 ± 0.01^{a}		3.80 ± 0.04^{c}	2.12 ± 0.11^{b}
43	M derivative			0.46 ± 0.01^{b}	0.25 ± 0.01^{a}
46	Q-*O*-(pentosyl)hexoside	0.11 ± 0.01^{b}	0.07 ± 0.01^{a}	0.74 ± 0.01^{d}	0.41 ± 0.01^{c}
48	Q-*O*-(pentosyl)hexoside	0.13 ± 0.01			
52	Rutin	0.29 ± 0.01^{b}	0.19 ± 0.01^{a}	4.42 ± 0.01^{c}	1.90 ± 0.01^{b}
56	Q-*O*-hexoside	0.21 ± 0.01^{b}	0.12 ± 0.01^{a}		
60	I-*O*-rutinoside	0.08 ± 0.01^{b}	0.01 ± 0.01^{a}		
61	K-*O*-rutinoside			1.52 ± 0.03^{b}	0.36 ± 0.01^{a}
74	I-*O*-pentoside derivative			0.18 ± 0.01	
83	Quercetin	0.12 ± 0.01			
Total		**0.89 ± 0.01^{b}**	**0.39 ± 0.01^{a}**	**11.12 ± 0.08^{d}**	**4.87 ± 0.01^{c}**
Flavones					

20	Luteolin derivative	0.09 ± 0.01			
38	Tricin-*O*-hexoside	0.06 ± 0.01			
Total		**0.15 ± 0.03**			
Ellagic acid derivatives					
26	Ellagic acid-*O*-(pentosyl)hexoside derivative	0.16 ± 0.01			
81	Ellagic acid derivative	0.39 ± 0.01			
Total		0.55 ± 0.01			
TIPC		**27.22 ± 0.20^{d}**	**4.97 ± 0.02^{a}**	**25.90 ± 0.19^{c}**	**11.53 ± 0.07^{b}**

K: Kaempferol; I: Isorhamnetin; Q: Quercetin. TIPC: total individual phenolic content. Bold values represent the sum of each type of components. Means in the same line not sharing the same letter are significantly different at $p < 0.05$ probability level.

4.4.2. Post *in vitro* gastrointestinal digestion

Significant changes ($p < 0.05$) in the amounts of phenolic compounds of *S. lanceolata* were observed following *in vitro* digestion (**Figure 35** and **Table 19**). Berries were more affected than leaves, with 81.8% and 61.5% reduction of TIPC, respectively, upon simulated digestion.

The most significant reduction mainly concerned the ANTCs content in berries (-87.15%). Only cyanidin-*O*-sambuboside (**8**) was detected in the digested extract (**Table 19**) and its amount was reduced by 84.60%. Loss of HCAs (35.10%) and flavonols (56.18%) contents were also observed in berries, although, in lower extent. Ellagitannins and flavones were not quantified upon the digestion process (**Figure 35** and **Table 19**). An exception was observed for 3-*O*-CQA (**28**) which increased by 13% ($p < 0.05$), with reference to native amounts (**Table 19**). Similarly, Zhou and co-workers [152] reported an increase by 214% of 3-*O*-CQA after simulated digestion of *S. nigra*. These might be due to this compound being bound to proteins or fibre in the original matrix and, because of enzymatic action, it was released from these structures. In leaves, a similar reduction of HCAs an flavonols contents was observed (≈ 55%). 3-*O*-CQA (**28**) (45.27%), quercetin-*O*-(rhamnosyl)hexoside (**41**) (18.37%) and rutin (**52**) (16.48%) remained main compounds (**Table 19**), despite the observed reductions of 54.92%, 44.21% and 57.01%, respectively.

In vitro GID of *S. nigra* has been documented in the literature [24,152], however, none was conducted in *S. lanceolata* so far. Similar degradation rates were noted for ANTCs and TIPC of *S. nigra* (88.4% and 80.5%, respectively) [24].

4.6. *Vaccinium cylindraceum*[9]

Eighty-four phytochemicals were characterized in *V. cylindraceum* extracts (**Figure 36 and Figure 37**), including ANTCs, other flavonoids, phenolic acids, oligosaccharides, organic acids, terpenoids and coumarins (Supplementary Material **- Table S 17** and **Table S 18)**. This species was collected at Ilha das Flores (Azores archipelago) and it was selected for this study to establish a comparison with Madeira Island counterpart. A previous study [109] have focused only on the ANTCs composition of berries, hence, the complete phenolic profile of this species (berries and leaves) is here reported for the first time.

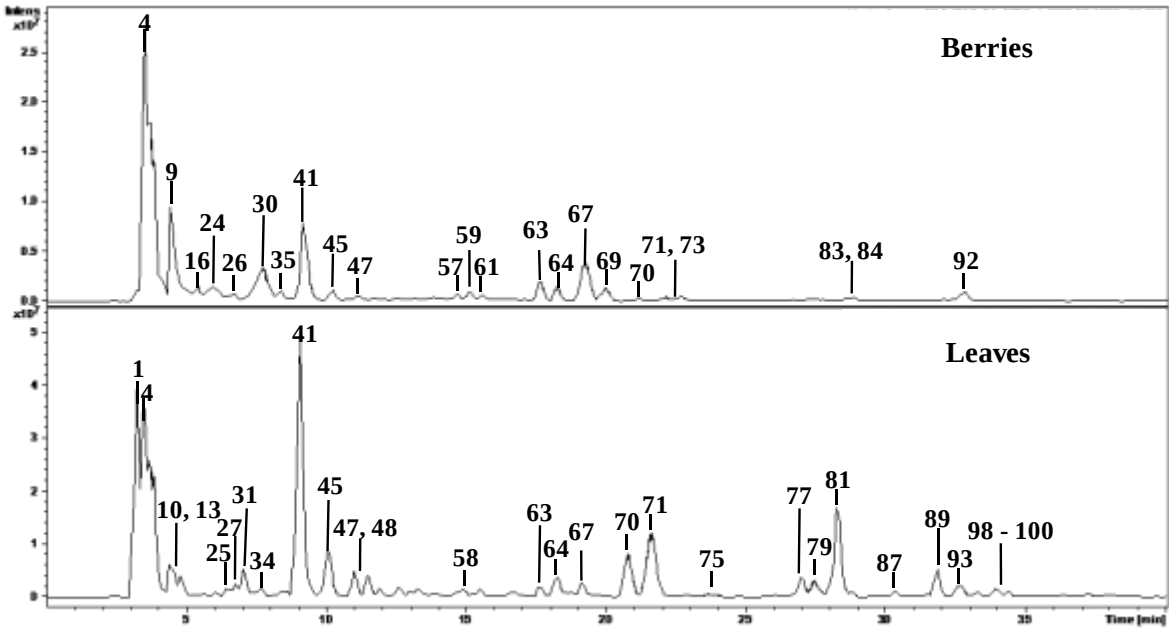

Figure 36 – Representative base peak chromatogram (BPC) of the HPLC-ESI$^-$/MS^n analysis of *V. cylindraceum* methanolic extracts (berries and leaves). For peak identification check **Table S 17** (Supplementary Material).

[9] This part of the work has been already published [234].

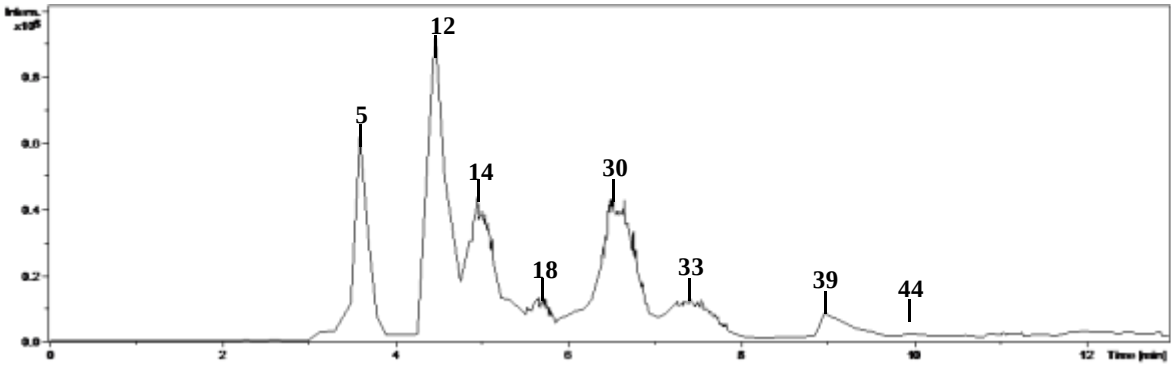

Figure 37 – Representative base peak chromatogram (BPC) of the HPLC-ESI^{+}/MS^{n} analysis of *V. cylindraceum* methanolic extracts (berries). For peak assignment check **Table S 18.**

4.6.1.Pre-*in vitro* gastrointestinal digestion

In this species, the contents of 44 PCs were determined by HPLC-DAD (**Table 20**). TIPC ranged between 84.13 to 103.37 mg g^{-1} DE for berries and leaves, respectively (**Table 20**). Similarly, leaves of other *Vaccinium* species possessed higher phenolic amounts than berries [79,80,84,132]. The compositional percentages of *V. cylindraceum* (pre- and post *in vitro* digestion) are shown in **Figure 38**.

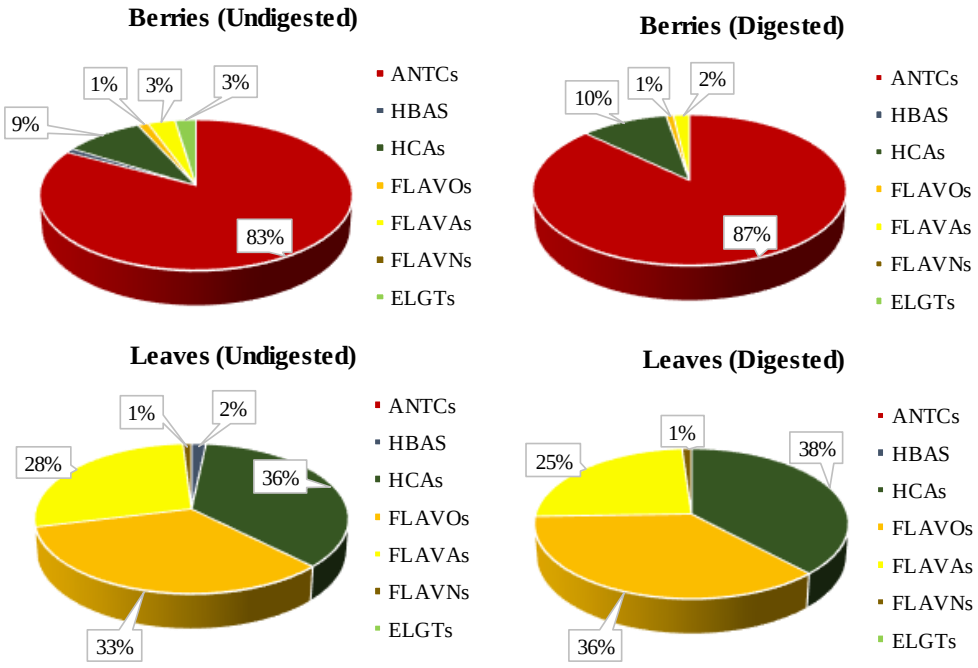

Figure 38 - Phenolic composition of *V. cylindraceum* extracts (pre- and post-*in vitro* digestion). For more detailed data check Table 20. ANTCs: anthocyanins; HBAs: hydroxybenzoic acids; HCAs hydroxycinnamic acids; FLAVOs: flavonols; FLAVAs: flavan-3-ols; FLAVNs: flavones; ELGTs: ellagitannis.

Delphinidin, petunidin and malvidin glycosides (**11**, **14** and **30**) were dominant ANTCs in berries (31.80%, 18.09% and 12.54%, respectively) (**Table 20**). In a previous study [109], malvidin glycosides showed superior amounts (31 – 46%) than delphinidin conjugates (20 – 30%) in *V. cylindraceum*. This slight variation could be related to different years of collection and sample preparation methodologies. 5-*O*-CQA (**41**) (36.85 %), kaempferol-*O*-hexoside (**81**) (11.27%), B-type PAC dimer (**45**) (10.94 %), quercetin-*O*-hexoside (**70**) (8.76 %) and catechin (**48**) (7.87 %) were relevant in leaves (**Table 20**). Alike phenolic compositions were reported for other *Vaccinium* species [63,79,84,85,132]. As oppose to previous works [63,79,84,86,132], flavan-3-ols were the most abundant flavonoids in analysed berries (**Table 20**).

Higher and lower TIPC were documented in literature (4.59 – 42.19 and 68.84 – 185.18 mg g^{-1} DE) for berries and leaves, respectively, of other *Vaccinium species* [63,80,131]. 5-*O*-CQA was also relevant in berries and leaves of *Vaccinium* spp. (0.72 – 12.96 and 104.00 mg g^{-1} DE, respectively) [63]. The highest TIPC found in literature were determined in *V. macrocarpon* extracts (91.10 – 137.44 and 215.49 – 388.94 mg g^{-1} DE in berries and leaves, respectively) [79].

Table 20 - Quantification (mg g^{-1} DE) of main phenolic compounds of *V. cylindraceum* extracts (berries and leaves) before and after *in vitro* gastrointestinal digestion. Data represent the mean ± standard deviation (*n* =3).

Nº	**Assigned identification**	**Berries**		**Leaves**	
Anthocyanins		Non-digested	Digested	Non-digested	Digested
3	Delphinidin-*O*-(pentosyl)hexoside	0.82 ± 0.03			
5	Delphinidin-*O*-hexoside	7.88 ± 0.03^{b}	2.42 ± 0.15^{a}		
11	Delphinidin-*O*-hexoside	26.81 ± 0.96^{b}	13.41 ± 0.35^{a}		
14	Petunidin-*O*-hexoside	15.25 ± 0.11^{b}	4.38 ± 0.21^{a}		
21	Delphinidin-*O*-rhamnoside	2.14 ± 0.09			
24	Peonidin-*O*-hexoside	2.04 ± 0.04			
30	Malvidin-*O*- hexoside	10.57 ± 0.07^{b}	4.23 ± 0.19^{a}		
33	Malvidin-*O*-pentoside	2.13 ± 0.09			
44	Malvidin-*O*-pentoside	0.63 ± 0.01			
Total		**68.17 ± 3.15^{b}**	**24.44 ± 1.17^{a}**		
Hydroxycinnamic acids					
7	Caffeoylisocitrate	0.35 ± 0.01			
35	Caffeic acid-*O*-hexoside	0.56 ± 0.03^{c}		0.49 ± 0.02^{b}	0.16 ± 0.01^{a}
41	5-*O*-Caffeoylquinic acid	5.57 ± 0.05^{b}	2.24 ± 0.17^{a}	33.11 ± 1.30^{d}	16.26 ± 0.98^{c}
47	Caffeoylquinic acid	0.03 ± 0.01^{a}	0.01 ± 0.01^{a}	1.03 ± 0.04^{c}	0.50 ± 0.02^{b}
49	Caffeoylshikimic acid	0.26 ± 0.01^{b}	0.11 ± 0.01^{a}		
54	5-*p*-Coumaroylquinic acid			0.55 ± 0.01^{b}	0.21 ± 0.02^{a}

58	5-*p*-Coumaroylquinic acid			0.78 ± 0.02^{b}	0.35 ± 0.02^{a}
59	Methyl-(5-caffeoyl)quinate	0.01 ± 0.01^{a}	0.07 ± 0.01^{b}	0.09 ± 0.01^{c}	
64	Coumaroyl iridoid	0.31 ± 0.01^{b}	0.12 ± 0.01^{a}	0.29 ± 0.01^{b}	0.11 ± 0.01^{a}
67	Coumaroyl iridoid	0.52 ± 0.02^{b}		0.55 ± 0.01^{b}	0.29 ± 0.02^{a}
75	Coumaric acid derivative			0.11 ± 0.01^{b}	0.06 ± 0.01^{a}
Total		**7.67 ± 0.11^{b}**	**2.86 ± 0.17^{a}**	**37.00 ± 1.51^{d}**	**17.83 ± 1.26^{c}**
Hydroxybenzoic acids					
25	Protocatechuic acid-*O*-hexoside	0.80 ± 0.02^{b}		0.60 ± 0.02^{a}	
34	Protocatechuic acid derivative			1.15 ± 0.02	
Total		**0.80 ± 0.02^{a}**		**1.74 ± 0.07^{b}**	
Flavonols					
61	Myricetin-*O*-hexoside	0.11 ± 0.01^{b}	0.06 ± 0.01^{a}		
68	Cinchonain Ib			0.24 ± 0.01^{b}	0.12 ± 0.01^{a}
69	Myricetin-*O*-(deoxy)hexoside	0.41 ± 0.01^{b}	0.18 ± 0.01^{a}	4.93 ± 0.11^{d}	2.13 ± 0.17^{c}
70	Quercetin-*O*-hexoside	0.13 ± 0.01^{a}		9.06 ± 0.30^{c}	5.04 ± 0.27^{b}
77	Cinchonain Ib			1.38 ± 0.03^{b}	0.55 ± 0.03^{a}
79	Cinchonain Ib			1.24 ± 0.05^{b}	0.64 ± 0.02^{a}
81	Kaempferol-*O*-hexoside			11.65 ± 0.24^{b}	5.14 ± 0.24^{a}
83	6-Hydroxy-7,4-dimethoxy-quercetin-*O*-hexoside	0.14 ± 0.01			
84	Isorhamentin-*O*-hexoside	0.14 ± 0.01			
86	Quercetin-*O*-(acetyl)hexoside	0.07 ± 0.01		0.16 ± 0.01^{b}	0.09 ± 0.01^{a}
93	Cinchonain Ib			4.49 ± 0.04^{b}	2.49 ± 0.14^{a}
97	Kaempferol-*O*-(acetyl)hexoside			0.21 ± 0.01^{b}	0.10 ± 0.01^{a}
100	6-Hydroxy-7,4-dimethoxy-quercetin-*O*-hexoside derivative			1.47 ± 0.04^{b}	0.76 ± 0.02^{a}
Total		**1.00 ± 0.01^{b}**	**0.24 ± 0.01^{a}**	**34.75 ± 1.74^{d}**	**17.07 ± 1.23^{c}**
Flavan-3-ols					
31	Procyanidin dimer (B type)			3.28 ± 0.08^{b}	0.93 ± 0.02^{a}
37	Procyanidin dimer (B type)			1.92 ± 0.03^{b}	0.65 ± 0.03^{a}
45	Procyanidin dimer (B type)	1.22 ± 0.03^{a}		11.31 ± 0.38^{c}	4.19 ± 0.23^{b}
48	Catechin	0.83 ± 0.04^{b}	0.52 ± 0.01^{a}	8.14 ± 0.21^{d}	5.50 ± 0.17^{c}
52	Procyanidin trimer (B type)	0.57 ± 0.02^{b}		4.08 ± 0.04^{c}	0.18 ± 0.02^{a}
Total		**2.62 ± 0.07^{b}**	**0.52 ± 0.01^{a}**	**28.73 ± 0.91^{d}**	**11.45 ± 0.92^{c}**
Flavanones					
87	Phlorizin			1.02 ± 0.04^{b}	0.51 ± 0.02^{a}
Total				**1.02 ± 0.04^{b}**	**0.51 ± 0.02^{a}**

Flavones					
50	Dimethoxy-hydroxytricin-*O*-hexoside			0.12 ± 0.01	
Total				**0.12 ± 0.01**	
Ellagic acid derivatives					
16	Tergallagic acid	1.15 ± 0.06			
28	Methyl-ellagic acid-*O*-pentoside	0.86 ± 0.01			
Total		**2.01 ± 0.06**			
TIPC		**84.13 ± 1.44^{c}**	**28.06 ± 0.13^{a}**	**103.37 ± 2.55^{d}**	**46.36 ± 2.03^{b}**

TIPC: total individual phenolic content. Bold values represent the sum of each type of components. Means in the same line not sharing the same letter are significantly different at $p < 0.05$ probability level.

4.6.2. Post *in vitro* gastrointestinal digestion

After simulated digestion, quantitative differences in relation to native values were observed ($p < 0.05$) (**Figure 38** and **Table 20**). Berries were more affected than in leaves, showing a reduction of 66.65% and 55.15% of TIPC, respectively.

Flavan-3-ols (-80.16%), flavonols (-76.00%), ANTCs (-64.15%) and HCAs (-62.69%) were the most unstable compounds in berries. Ellagic acid derivatives and HBAs were not determined after simulated digestion (**Figure 38** and **Table 20**). In leaves, flavan-3-ols contents were also highly affected (-60.15%). HCAs, flavanones and flavonols concentrations suffered similar reductions (46.54%, 50.43% and 50.87%, respectively). Flavones and HBAs were not quantifiable in digested leaves (**Figure 38** and **Table 20**).

Regarding main PCs in berries, petunidin-*O*-hexoside (**14**) malvidin-*O*-hexoside (**30**), 5-*O*-CQA (**41**) and delphinidin-*O*-hexoside (**11**) showed the highest decreases (71.27%, 60.00%, 59.70% and 50.00%, respectively) (**Table 20**). The dominant compounds of leaves were also affected: kaempferol-*O*-hexoside (**81**) (-55.88%), 5-*O*-CQA (**41**) (-50.93%), quercetin-*O*-hexoside (**70**) (-44.37%) and catechin (**48**) (-32.44%).

Other *Vaccinium* species have been submitted to GID studies [54,59,140,141,153]. Similarly, ANTCs were very unstable to GID, with losses from 35.60% to 96.9% [54,59,140,141,153]. By contrast, 5-*O*-CQA and quercetin-*O*-arabinoside seemed unaffected by the adverse conditions [54]. A reduction of TIPC (-50.59%) was reported for *V. vitis-idea*, PAC dimer (B type) being the most affected compound (-93%) [59]. Higher recoveries were also noted for quercetin glycosides (42 – 99%), after human digestion. In another study [153], only 3.10% of initial TIPC was recovered after simulated GID of blueberries (*Vaccinium spp*.).

4.7. *Vaccinium padifolium*[10]

The phytochemical profiles of different morphological parts of *V. padifolium* were determined by HPLC-ESI-MS^n (**Figure 39 and Figure 40**). A total of 102 phytochemicals were identified (Supplementary Material **– Table S 19** and **Table S 20**), such as ANTCs, other flavonoids, phenolic acids, oligosaccharides and organic acids. Previous works [112,113] have focused only on the ANTCs composition of berries, not the complete phenolic profile of this species (berries and leaves). In this case, leaves were separated into young leaves (YLs) and mature leaves (MLs) based on the coloration of their twigs.

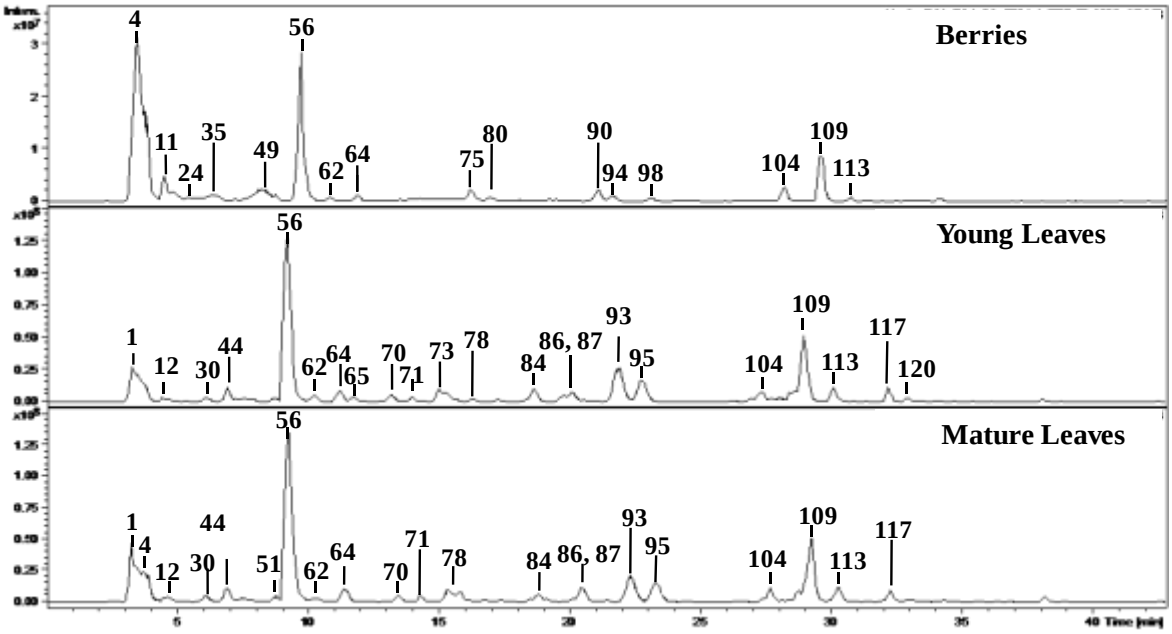

Figure 39 – Representative base peak chromatogram (BPC) of the HPLC-ESI$^-$/MS^n analysis of *V. padifolium* methanolic extracts (berries and leaves). For peak assignment please check **Table S 19** (Supplementary Material).

[10]This part of the work has already been published [234].

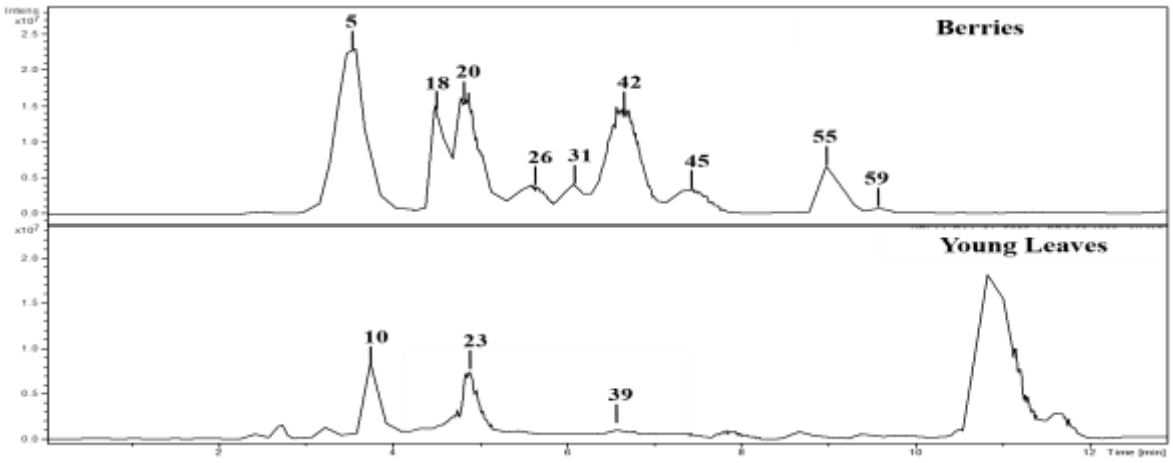

Figure 40 – Representative base peak chromatogram (BPC) of the HPLC-ESI^{+}/MS^{n} analysis of *V. padifolium* methanolic extracts (berries and leaves). For peak assignment please check **Table S 20** (Supplementary Material).

4.7.1. Pre-*in vitro* gastrointestinal digestion

Forty-six PCs were quantified by HPLC-DAD in *V. padifolium*, collected in two consecutive years (2013 - 2014). TIPC ranged between 82.09 to 134.42 mg g^{-1} DE, for berries and leaves, respectively (**Table 21**). The compositional percentages of *V. padifolium* extracts (pre- and post *in vitro* digestion) are shown in **Figure 41**.

Delphinidin-*O*-hexoside (**5 a**nd **16**) (14.61 – 15.16% and 32.41 – 32.61%, respectively), petunidin-*O*-hexoside (**20**) (11.04 – 11.89%), malvidin-*O*-hexoside (**46**) (9.84 – 10.46%) and 5-*O*-CQA (**57**) (9.40 – 9.68%) were dominant in berries (**Table 21**). Differences in the relative abundance of ANTCs were observed (malvidin > delphinidin > petunidin) in previous studies [112,113] on this species, which could be related to different sample preparation and extraction procedures. Moreover, in the present analysis, tri-glycosides of ANTCs were not detected. In general, berries collected in 2014 showed higher phenolic contents than samples collected in previous year ($p < 0.05$) (**Table 21**). This difference was highlighted in the case of ANTCs content ($p < 0.05$).

The amounts of remaining phenolic classes were slightly affected between 2013 and 2014. These variations could be attributed to different climacteric conditions (rainfall, solar radiation, thermal amplitude), that are known to affect the phytochemical composition [35].

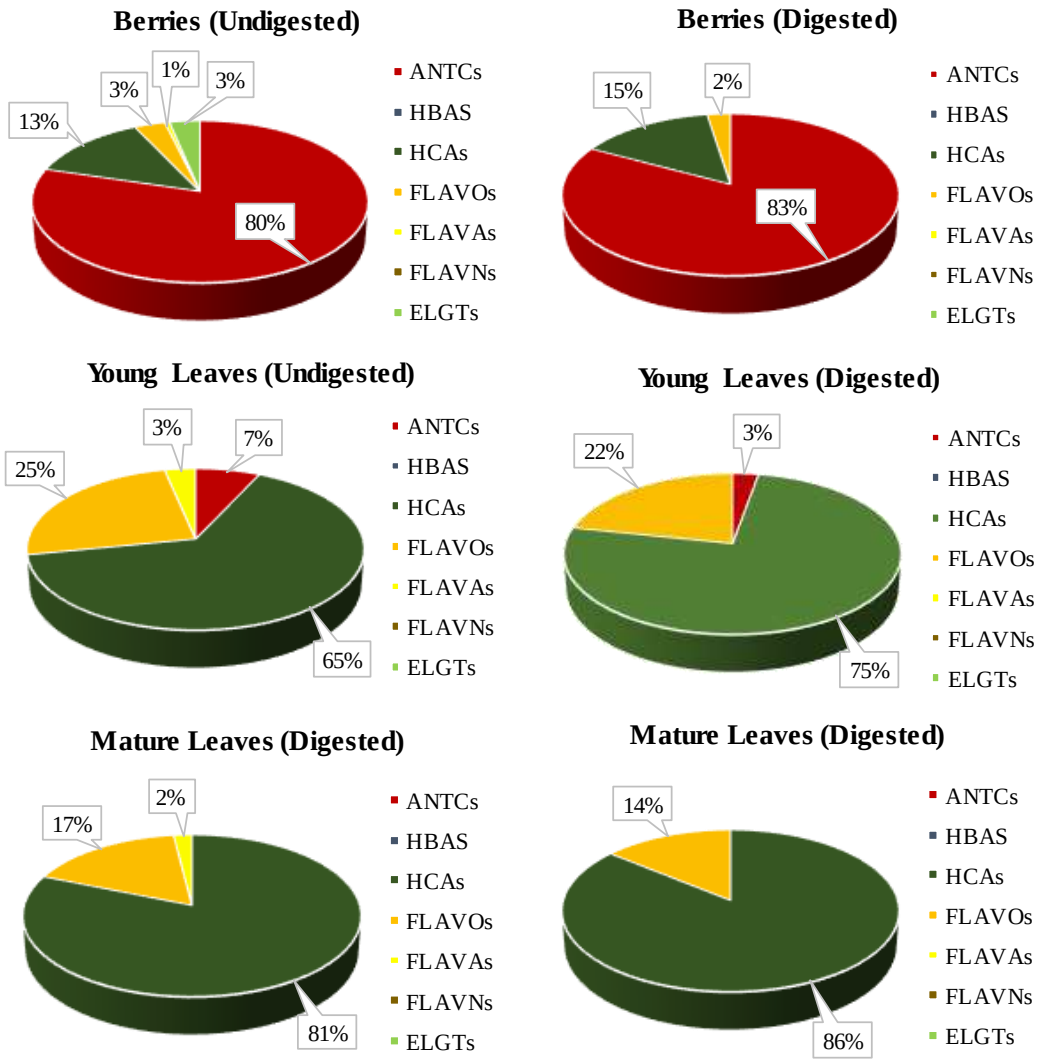

Figure 41 - Phenolic composition of *V. padifolium* extracts (pre- and post-*in vitro* digestion). In the case of undigested extracts, the values represent the means from data of samples collected in different years. For more detailed data check Table 21 and Table 22. ANTCs: anthocyanins; HBAs: hydroxybenzoic acids; HCAs hydroxycinnamic acids; FLAVOs: flavonols; FLAVAs: flavan-3-ols; FLAVNs: flavones; ELGTs: ellagitannis.

TIPC of leaves extracts are similar, although their individual phenolic composition was slightly different ($p < 0.05$) (**Figure 41** and **Table 21**). Leaves were rich sources of 5-*O*-CQA (**57**) (47.90 – 67.11%), but quercetin-*O*-hexoside (**93** and **95**) (5.40 – 16.46%) and a coumaric acid derivative (**113**) (6.87 – 10.03%) were also relevant. In general, YLs showed superior phenolic amounts than mature counterparts. Exception was noted in HCAs content, where 5-*O*-CQA content was 1.3 times-fold higher. Inter-annual variations ($p < 0.05$) were also observed and, in general, samples collected in 2014 had higher concentrations (**Table 21**). Previous works [84,154] observed also significant variations in phenolic compositions among *Vaccinium* species grown in consecutive

years. Environmental conditions, like precipitation and temperature, that influence phenotypic factors may have significant impact on phenolic composition. Unfortunately, this climacteric data was not available to justify the obtained results (**Table 21**). Cyanidin glycosides (**10** and **23**) (6.82 - 7.61%) were quantified only in YLs with considerably lower ($p < 0.05$) concentrations than in fruits (**Figure 41** and **Table 21**). Usually, ANTCs are present in red fruits, but cyanidin derivatives have also been quantified in leaves of other *Vaccinium* species (22.38 – 28.26 mg g^{-1} DE) [79,132]. According to literature [132], synthesis of ANTCs is activated/stimulated by the higher sun exposure of young leaves. Additionally, quercetin glycosides and HCAs play simultaneously a predominant role in defense against solar radiation [132].

V. padifolium extracts showed similar compositions to other *Vaccinium* species [84][63,79,85,86,132]. By comparison, inferior phenolic contents ($p < 0.05$) were found in berries and leaves of *V. cylindraceum* (**Table 20**). Exceptions were verified in flavonols and flavan-3-ols amounts ($p < 0.05$). In the latter group, amounts were 6 to 8-times higher than in *V. padifolium* (**Table 21**). HCAs content was superior in *V. padifolium*, mostly due to the higher 5-*O*-CQA amounts (almost 3 times-fold higher). Moreover, *V. padifolium* berries, collected in 2013, showed lower ANTCs and TIPC than *V. cylindraceum* ($p < 0.05$) (**Table 20** and **Table 21**). Genetic factors (species/cultivar) and different environmental conditions (since *V. padifolium* was collected in a different island/archipelago) could play an important role in the obtained results [35]. It is known that blueberries phenolic content is influenced by genotype and growing locations [154]. Overall, the amounts of quantified PCs were within the range reported for other *Vaccinium* species, as discussed previously (**section 4.6.1**).

Table 21 - Quantification (mg g^{-1} DE) of main phenolic compounds present in *V. padifolium* extracts (berries and leaves). Data represent the mean ± standard deviation (n = 3).

Nº	Assigned identification	Berries		Young Leaves		Mature Leaves	
Anthocyanins		2013	2014	2013	2014	2013	2014
3	Delphinidin-*O*-(pentosyl)hexoside	1.58 ± 0.01^{a}	1.88 ± 0.02^{b}				
5	Delphinidin-*O*-hexoside	12.03 ± 0.19^{a}	13.77 ± 0.20^{b}				
10	Cyanidin-3-*O*-glucoside			5.83 ± 0.24^{a}	6.65 ± 0.20^{b}		
16	Delphinidin-*O*-hexoside	26.78 ± 0.05^{a}	29.40 ± 0.22^{b}				
20	Petunidin-*O*-hexoside	9.76 ± 0.08^{a}	10.02 ± 0.40^{a}				
23	Cyanidin-*O*-pentoside			3.15 ± 0.06^{a}	3.58 ± 0.16^{b}		
34	Peonidin-*O*-hexoside	3.11 ± 0.03^{a}	3.62 ± 0.11^{b}				
42	Malvidin-*O*-hexoside	1.19 ± 0.02^{a}	1.36 ± 0.03^{b}				
45	Malvidin-*O*-pentoside	0.95 ± 0.02^{a}	1.08 ± 0.04^{b}				
46	Malvidin-*O*-hexoside	8.08 ± 0.24^{a}	9.49 ± 0.28^{b}				
52	Malvidin-*O*-hexoside	0.19 ± 0.01^{b}	0.13 ± 0.01^{a}				
Total		**63.67 ± 0.54^{c}**	**70.73 ± 1.01^{d}**	**8.98 ± 0.32^{a}**	**10.23 ± 0.47^{b}**		
Hydroxycinnamic acids							
17	Caffeoylquinic acid derivative			0.30 ± 0.01^{ab}	0.33 ± 0.01^{b}	0.32 ± 0.01^{b}	0.29 ± 0.01^{a}
30	3-*O*-Caffeoylquinic acid dimer			0.59 ± 0.01^{c}	0.65 ± 0.02^{d}	0.19 ± 0.01^{a}	0.22 ± 0.01^{b}
44	Caffeoylquinic acid derivative			0.33 ± 0.01^{a}	0.39 ± 0.01^{b}	0.35 ± 0.01^{a}	0.38 ± 0.01^{b}
48	Caffeoylquinic acid derivative			0.57 ± 0.01^{d}	0.48 ± 0.01^{c}	0.39 ± 0.01^{b}	0.27 ± 0.01^{a}
49	Caffeic acid-*O*-hexoside	0.37 ± 0.01^{a}	0.40 ± 0.02^{b}	0.58 ± 0.01^{c}	0.60 ± 0.02^{c}	0.65 ± 0.02^{c}	0.70 ± 0.02^{d}
57	5-*O*-Caffeoylquinic acid	7.72 ± 0.32^{a}	8.88 ± 0.10^{b}	63.07 ± 2.55^{c}	66.05 ± 0.52^{c}	86.47 ± 0.39^{d}	87.27 ± 1.11^{d}

64	Caffeoylquinic acid	0.17 ± 0.01^{a}	0.22 ± 0.01^{b}	2.67 ± 0.04^{c}	2.64 ± 0.05^{c}	1.91 ± 0.10^{d}	2.00 ± 0.08^{d}
70	5-*p*-Coumaroylquinic acid	0.24 ± 0.01^{a}	0.28 ± 0.01^{b}	1.48 ± 0.05^{d}	1.62 ± 0.04^{e}	1.36 ± 0.05^{c}	1.58 ± 0.10^{e}
73	Caffeoylquinic acid derivative			0.30 ± 0.01^{b}	0.33 ± 0.01^{b}	0.30 ± 0.02^{b}	0.24 ± 0.01^{a}
78	Caffeoylquinic acid derivative			0.73 ± 0.02^{b}	0.77 ± 0.02^{b}	0.24 ± 0.01^{a}	0.25 ± 0.01^{a}
82	Methyl-(5-caffeoyl)quinate	0.63 ± 0.01^{b}	0.24 ± 0.01^{a}	0.74 ± 0.03^{c}	0.78 ± 0.02^{c}	1.52 ± 0.08^{e}	0.96 ± 0.02^{d}
83	Coumaroyl iridoid	0.36 ± 0.01^{a}	0.34 ± 0.01^{a}	1.14 ± 0.02^{c}	1.06 ± 0.02^{c}	0.73 ± 0.02^{b}	0.75 ± 0.01^{b}
84	Coumaric acid derivative			1.36 ± 0.04^{b}	0.86 ± 0.01^{a}	2.01 ± 0.02^{d}	1.62 ± 0.02^{c}
103	4-B-9-*p*-Co- 2,7-anhydro-3-DOA	0.24 ± 0.01^{a}	0.23 ± 0.01^{a}	1.66 ± 0.04^{d}	1.05 ± 0.02^{b}	2.37 ± 0.08^{e}	1.44 ± 0.03^{c}
113	Coumaric acid derivative	0.76 ± 0.01^{a}	0.93 ± 0.02^{b}	9.81 ± 0.22^{c}	13.02 ± 0.24^{d}	12.91 ± 0.02^{d}	13.48 ± 0.06^{e}
114	Coumaric acid derivative	0.12 ± 0.01^{a}	0.13 ± 0.01^{a}	0.97 ± 0.04^{b}	1.18 ± 0.05^{c}	1.35 ± 0.05^{d}	1.40 ± 0.01^{d}
124	Coumaric acid derivative			0.24 ± 0.01^{c}	0.04 ± 0.01^{a}	0.11 ± 0.01^{b}	0.08 ± 0.02^{a}
Total		**10.59 ± 0.30^{a}**	**11.64 ± 0.14^{b}**	**86.54 ± 2.51^{c}**	**91.85 ± 0.86^{d}**	**113.16 ± 0.60^{e}**	**112.91 ± 1.08^{e}**
Flavonols							
80	Myricetin-*O*-hexoside	0.23 ± 0.01^{a}	0.29 ± 0.01^{b}				
86	Rutin			0.64 ± 0.02^{a}	0.71 ± 0.04^{bc}	0.78 ± 0.03^{c}	0.81 ± 0.06^{c}
93	Quercetin-*O*-hexoside			21.67 ± 0.98^{c}	17.98 ± 0.63^{b}	10.17 ± 0.02^{a}	10.68 ± 0.01^{a}
94	Myricetin-*O*-deoxyhexoside	0.50 ± 0.01^{a}	0.58 ± 0.01^{b}				
95	Quercetin-*O*-hexoside	0.80 ± 0.02^{a}	0.88 ± 0.02^{b}	9.04 ± 0.26^{f}	7.26 ± 0.20^{e}	6.94 ± 0.01^{d}	6.51 ± 0.16^{c}
101	Quercetin-*O*-pentoside			0.63 ± 0.02^{a}	0.65 ± 0.02^{ab}	0.60 ± 0.02^{a}	0.63 ± 0.02^{b}
105	Cinchonain-Ib			0.51 ± 0.05^{bc}	0.54 ± 0.01^{c}	0.42 ± 0.01^{a}	0.46 ± 0.01^{b}
107	Quercetin-*O*-(acetyl)hexoside					0.12 ± 0.01^{a}	0.15 ± 0.01^{b}
117	Kaempferol-*O*-(acetyl)hexoside			2.63 ± 0.09^{ab}	2.96 ± 0.05^{c}	2.71 ± 0.08^{b}	2.57 ± 0.02^{a}
120	Cinchonain-Ib			0.98 ± 0.02^{c}	0.65 ± 0.01^{b}	1.35 ± 0.02^{d}	0.60 ± 0.02^{a}
122	6-Hydroxy-7,4-dimethoxy-Q-*O*-(acetyl)hexoside	0.36 ± 0.01^{b}	0.20 ± 0.01^{a}				
123	Kaempferol-*O*-(acetyl)hexoside			0.25 ± 0.01^{a}	0.26 ± 0.01^{b}	0.42 ± 0.15^{c}	0.46 ± 0.02^{c}

125	6-Hydroxy-7,4-dimethoxyquercetin derivative	0.39 ± 0.01[a]	0.38 ± 0.01[a]				
Total		**2.77 ± 0.03[a]**	**2.90 ± 0.05[b]**	**36.74 ± 1.18[e]**	**31.39 ± 0.78[d]**	**23.85 ± 0.30[c]**	**23.14 ± 0.27[c]**
Flavan-3-ols							
65	Catechin			2.76 ± 0.01[c]	2.89 ± 0.07[d]	0.63 ± 0.02[a]	1.66 ± 0.06[b]
68	Procyanidin trimer (B type)			1.53 ± 0.07[b]	1.99 ± 0.06[c]	1.21 ± 0.04[a]	1.99 ± 0.03[c]
100	Procyanidin dimer (A type)	0.40 ± 0.01[a]	0.45 ± 0.01[b]				
Total		**0.40 ± 0.01[a]**	**0.45 ± 0.01[b]**	**4.29 ± 0.60[de]**	**4.88 ± 0.11[e]**	**1.84 ± 0.05[c]**	**3.65 ± 0.07[d]**
Ellagic acid derivatives							
35	Methyl-ellagic acid derivative	2.52 ± 0.16[a]	2.85 ± 0.13[b]				
40	Methyl-ellagic acid-*O*-pentoside	0.10 ± 0.01[a]	0.10 ± 0.02[a]				
Total		**2.62 ± 0.09[a]**	**2.95 ± 0.18[b]**				
TIPC		**82.10 ± 0.91[a]**	**90.72 ± 1.44[b]**	**131.66 ± 4.02[c]**	**134.42 ± 2.06[c]**	**128.85 ± 0.95[c]**	**129.70 ± 1.41[c]**

B:Benzoyl; Co: Coumaroyl, Q: Quercetin. TIPC: total individual phenolic content. Bold values represent the sum of each type of components. Means in the same line not sharing the same letter are significantly different at $p < 0.05$ probability level.

4.7.2. Post *in vitro* gastrointestinal digestion

For this analysis, samples collected in 2014 were selected in detriment of those collected in previous year. After simulated digestion, a decrease ($p < 0.05$) on the TIPC of *V. padifolium* was verified (**Table 22**): berries (64.03%) and leaves (54.12 – 56.50%).

Flavonols (-71.68%), ANTCs (-61.78%) and HCAs (-58.97%) contents were significantly affected, after *in vitro* digestion of berries (**Table 22**). Ellagic acid conjugates were not quantified in digested berries (**Figure 41** and **Table 22**). ANTCs (-83.94%), flavonols (-59.59 – 63.77%) and HCAs (-51.95 – 54.73%) were the most affected classes in leaves.

Regarding major PCs of berries, delphinidin-*O*-hexoside (**16**) (35.84%), delphinidin-*O*-hexoside (**5**) (15.86%), petunidin-*O*-hexoside (**20**) (13.84%) and 5-*O*-CQA (**57**) (10.90%) and showed a decrease of 60.22%, 62.40%, 59.93% and 54.91%, respectively, with respect to native amounts (**Table 22**). 5-*O*-CQA (**57**), the main compound of leaves (62.61 – 73.57%), also suffered losses on its initial content: 47.83% and 50.20% for young and mature leaves, respectively.

The impact of *in vitro* GID on *Vaccinium* species has been discussed previously (**section 4.6.2**), and, to our best knowledge this is the first study conducted on *V. padifolium*. By comparison with *V. cylindraceum*, submitted to equal digestive conditions (**section 4.6.2**), similar degradation rates were verified for phenolic contents of berries (66.65%) and leaves (54.12 – 56.51%). However, TIPC was slightly higher for *V. padifolium* digested extracts (**Table 22**), which could be due to its higher native amounts.

Table 22 - Quantification (mg g^{-1} DE) of main phenolic compounds present in *V. padifolium* extracts (berries and leaves) before and after *in vitro* gastrointestinal digestion. Data represent the mean ± standard deviation (n = 3).

Nº	Assigned identification	Berries		Young Leaves		Mature Leaves	
Anthocyanins		Non-Digested	Digested	Non-Digested	Digested	Non-Digested	Digested
3	Delphinidin-*O*-(pentosyl)hexoside	1.88 ± 0.02[b]					
5	Delphinidin-*O*-hexoside	13.77 ± 0.20[b]	5.18 ± 0.09				
10	Cyanidin-*O*-glucoside			6.65 ± 0.20[b]	1.64 ± 0.14		
16	Delphinidin-*O*-hexoside	29.40 ± 0.22[b]	11.69 ± 0.17				
20	Petunidin-*O*-hexoside	10.02 ± 0.40[a]	4.52 ± 0.11				
23	Cyanidin-*O*-pentoside			3.58 ± 0.16[b]			
34	Peonidin-*O*-hexoside	3.62 ± 0.11[b]	1.82 ± 0.06				
42	Malvidin-*O*-hexoside	1.36 ± 0.03[b]	0.59 ± 0.01				
45	Malvidin-*O*-pentoside	1.08 ± 0.04[b]					
46	Malvidin-*O*-hexoside	9.49 ± 0.28[b]	3.24 ± 0.03				
52	Malvidin-*O*-hexoside	0.13 ± 0.01[a]					
Total		**70.73 ± 1.01[d]**	**27.04 ± 0.42**	**10.23 ± 0.47[b]**	**1.64 ± 0.14**		
Hydroxycinnamic acids							
17	Caffeoylquinic acid derivative			0.33 ± 0.01[b]	0.14 ± 0.04	0.29 ± 0.01[a]	0.11 ± 0.02
30	3-*O*-Caffeoylquinic acid dimer			0.65 ± 0.02[d]	0.23 ± 0.03	0.22 ± 0.01[b]	0.09 ± 0.06
44	Caffeoylquinic acid derivative			0.39 ± 0.01[b]	0.09 ± 0.01	0.38 ± 0.01[b]	
48	Caffeoylquinic acid derivative			0.48 ± 0.01[c]		0.27 ± 0.01[a]	
49	Caffeic acid-*O*-hexoside	0.40 ± 0.02[b]	0.20 ± 0.01	0.60 ± 0.02[c]		0.70 ± 0.02[d]	
57	5-*O*-Caffeoylquinic acid	8.88 ± 0.10[b]	3.56 ± 0.03	66.05 ± 0.52[c]	34.46 ± 1.95	87.27 ± 1.11[d]	43.46 ± 1.59

64	Caffeoylquinic acid	0.22 ± 0.01^{b}	0.09 ± 0.01	2.64 ± 0.05^{c}	1.31 ± 0.05	2.00 ± 0.08^{d}	0.75 ± 0.03
70	5-*p*-Coumaroylquinic acid	0.28 ± 0.01^{b}	0.11 ± 0.01	1.62 ± 0.04^{e}	0.77 ± 0.05	1.58 ± 0.10^{e}	0.74 ± 0.02
73	Caffeoylquinic acid derivative			0.33 ± 0.01^{b}	1.00 ± 0.04	0.24 ± 0.01^{a}	
78	Caffeoylquinic acid derivative			0.77 ± 0.02^{b}	0.38 ± 0.02	0.25 ± 0.01^{a}	
82	Methyl-(5-caffeoyl)quinate	0.24 ± 0.01^{a}	0.06 ± 0.01	0.78 ± 0.02^{c}	0.30 ± 0.01	0.96 ± 0.02^{d}	0.44 ± 0.02
83	Coumaroyl iridoid	0.34 ± 0.01^{a}	0.09 ± 0.01	1.06 ± 0.02^{c}	0.36 ± 0.02	0.75 ± 0.01^{b}	
84	Coumaric acid derivative			0.86 ± 0.01^{a}	0.41 ± 0.02	1.62 ± 0.02^{c}	
103	4-B-9-*p*-Co- 2,7-anhydro-3-DOA	0.23 ± 0.01^{a}	0.06 ± 0.01	1.05 ± 0.02^{b}	0.34 ± 0.01	1.44 ± 0.03^{c}	0.63 ± 0.03
113	Coumaric acid derivative	0.93 ± 0.02^{b}	0.57 ± 0.02	13.02 ± 0.24^{d}	3.92 ± 0.16	13.48 ± 0.06^{e}	4.51 ± 0.09
114	Coumaric acid derivative	0.13 ± 0.01^{a}	0.05 ± 0.01	1.18 ± 0.05^{c}	0.42 ± 0.01	1.40 ± 0.01^{d}	0.36 ± 0.01
124	Coumaric acid derivative			0.04 ± 0.01^{a}	0.02 ± 0.01	0.08 ± 0.02^{a}	0.03 ± 0.01
Total		**11.64 ± 0.14^{b}**	**4.78 ± 0.17**	**91.85 ± 0.86^{d}**	**44.14 ± 2.32**	**112.91 ± 1.08^{e}**	**51.11 ± 2.88**
Flavonols							
80	Myricetin-*O*-hexoside	0.29 ± 0.01^{b}	0.08 ± 0.01				
86	Rutin			0.71 ± 0.04^{bc}	0.25 ± 0.02	0.81 ± 0.06^{c}	0.26 ± 0.01
93	Quercetin-*O*-hexoside		0.03 ± 0.01	17.98 ± 0.63^{b}	5.40 ± 0.29	10.68 ± 0.01^{a}	3.74 ± 0.20
94	Myricetin-*O*-deoxyhexoside	0.58 ± 0.01^{b}	0.20 ± 0.01				
95	Quercetin-*O*-hexoside	0.88 ± 0.02^{b}	0.33 ± 0.01	7.26 ± 0.20^{e}	2.44 ± 0.12	6.51 ± 0.16^{c}	2.57 ± 0.21
101	Quercetin-*O*-pentoside			0.65 ± 0.02^{ab}	0.27 ± 0.02	0.63 ± 0.02^{b}	0.28 ± 0.02
105	Cinchonain-Ib			0.54 ± 0.01^{c}	0.18 ± 0.01	0.46 ± 0.01^{b}	
107	Quercetin-*O*-(acetyl)hexoside		0.03 ± 0.01			0.15 ± 0.01^{b}	
117	Kaempferol-*O*-(acetyl)hexoside			2.96 ± 0.05^{c}	1.02 ± 0.05	2.57 ± 0.02^{a}	1.10 ± 0.06
120	Cinchonain-Ib			0.65 ± 0.01^{b}	0.25 ± 0.01	0.60 ± 0.02^{a}	0.22 ± 0.01
122	6-Hydroxy-7,4-dimethoxy-Q-*O*-(acetyl)hexoside	0.20 ± 0.01^{a}	0.10 ± 0.01		2.30 ± 0.16		
123	Kaempferol-*O*-(acetyl)hexoside			0.26 ± 0.01^{b}	0.57 ± 0.02	0.46 ± 0.02^{c}	0.23 ± 0.02

125	6-Hydroxy-7,4-dimethoxyquercetin derivative	0.38 ± 0.01[a]	0.05 ± 0.01				
Total		**2.90 ± 0.05[b]**	**0.82 ± 0.03**	**31.39 ± 0.78[d]**	**12.69 ± 0.54**	**23.14 ± 0.27[c]**	**8.38 ± 0.43**
Flavan-3-ols							
65	Catechin		0.20 ± 0.01	2.89 ± 0.07[d]		1.66 ± 0.06[b]	
68	Procyanidin trimer (B type)			1.99 ± 0.06[c]		1.99 ± 0.03[c]	
100	Procyanidin dimer (A type)	0.45 ± 0.01[b]					
Total		**0.45 ± 0.01[b]**		**4.88 ± 0.11[e]**		**3.65 ± 0.07[d]**	
Ellagic acid derivatives							
35	Methyl-ellagic acid derivative	2.85 ± 0.13[b]					
40	Methyl-ellagic acid-*O*-pentoside	0.10 ± 0.02[a]					
Total		**2.95 ± 0.18[b]**					
TIPC		**90.72 ± 1.44[b]**	**32.63 ± 1.54**	**134.42 ± 2.06[c]**	**59.62 ± 2.86**	**129.70 ± 1.41[c]**	**59.50 ± 3.98**

TIPC: total individual phenolic content. Bold values represent the sum of each type of components. Means not sharing the same letter are significantly different at $p < 0.05$ probability level. 4-B-9-*p*-Co- 2,7-anhydro-3-DOA: 4-Benzoyl-9-p-coumaroyl-2,7-anhydro-3-deoxy-2-octulopyranosonic acid.

4.1. General discussion

4.1.1. Pre-*in vitro* gastrointestinal digestion

The individual phenolic contents of six BPPs was determined by HPLC-DAD. For a better comparison between the phenolic profiles of different species, the results were all included and a brief discussion is presented in **Figure 42**.

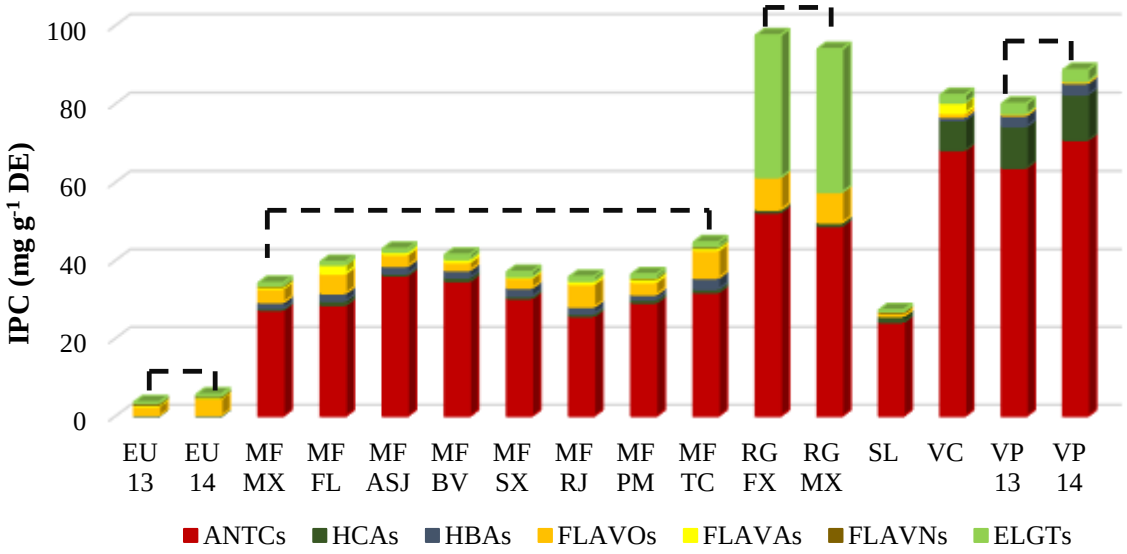

Figure 42 - Individual phenolic content (IPC) of analysed berries extracts (mg g^{-1} DE). Data represent the mean ± standard deviation (n = 3). EU: *E. umbellata*; MF: *M. faya*; RG: *R. grandifolius*; SL: *S. lanceolata*: VC: *V. cylindraceum*; VP: *V. padifolium*. ANTCs: anthocyanins; HCAs: hydroxycinnamic acids; HBAs: hydroxybenzoic acids; FLAVOs: flavonols; FLAVAs: flavan-3-ols; FLAVNs: flavones; ELLGTs: ellagic acid derivatives.

TIPC of different berries extracts varied between 3.87 and 97.47 mg g^{-1} DE, corresponding to *E. umbellata* and *R. grandifolius*, respectively (**Figure 42**). Phenolic profiles varied according to species. ANTCs were the main compounds in all berries extracts, except for *E. umbellata*, in which they were not detected. In this case, flavonols were main compounds (**Figure 42**). Based on ANTCs type, extracts could be divided in two sub-groups: cyanidin group (*M. faya*, *R. grandifolius* and *S. lanceolata*) and delphinidin/malvidin group (*Vaccinium spp.*). HCAs and ellagitannins were relevant in *Vaccinium* species and *R. grandifolius*, respectively (**Figure 42**).

In the case of leaves, TIPC ranged from 27.94 to 137.41 mg g^{-1} DE (**Figure 43**), for *S. lanceolata* and *R. grandifolius* (FX), respectively. The higher content of TIPC in leaves (except in *S. lanceolata*) could be justified to an increased expression of genes related to a biosynthesis of flavonoids due to growing and higher exposure to temperature, raditation and other weather

conditions that affect the accumulation of these compounds in plant tissues [79,132]. Additionnaly, the phenolic profiles of leaves were much more complex than berries.

Differences in phenolic compositions were found among species (**Figure 43**). ANTCs were only present in *V. padifolium* (YLs). HCAs were relevant in *Vaccinium* species and in *R. grandifolius*. Flavan-3-ols were representative in *V. cylindraceum* and *M. faya* extracts and, in a smaller extent, in *R. grandifolius* (MX). Ellagitannins were present in high amounts in *E. umbellata*, *M. faya* and *R. grandifolius* (**Figure 43**).

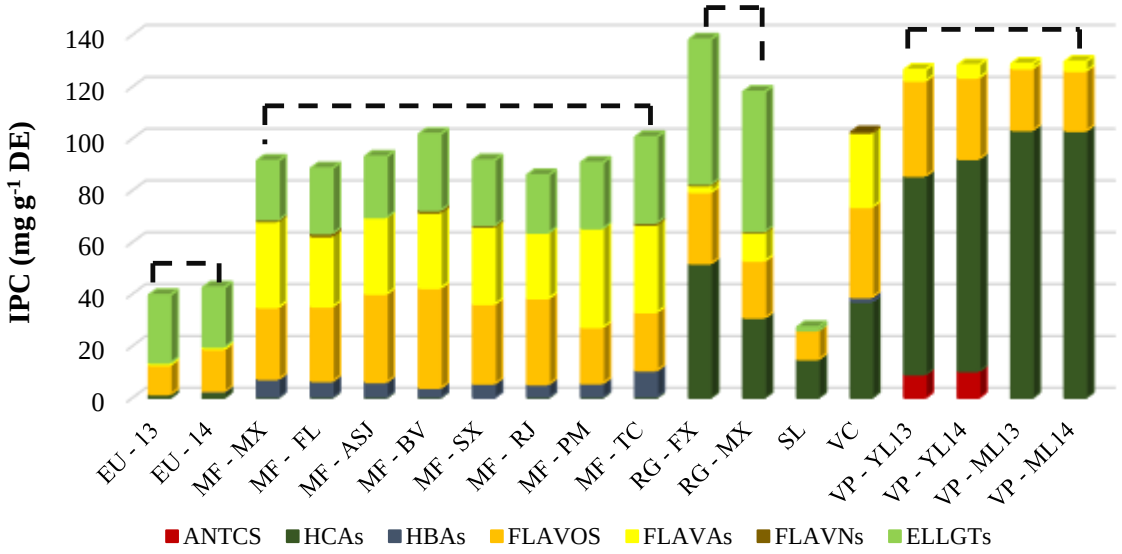

Figure 43 - Individual phenolic contents (IPC) of analysed leaves extracts (mg g^{-1} DE). Data represent the mean ± standard deviation (n = 3). EU: *E. umbellata*; MF: *M. faya*; RG: *R. grandifolius*; SL: *S. lanceolata*: VC: *V. cylindraceum*; VP: *V. padifolium*. ANTCs: anthocyanins; HCAs: hydroxycinnamic acids; HBAs: hydroxybenzoic acids; FLAVO: flavonols; FLAVA: flavan-3-ols; FLAVN: flavones; ELLG: ellagic acid derivatives.

4.1.2. Post *in vitro* gastrointestinal digestion

As mentioned, for the simulated digestion studies only samples collected in 2014 were selected. After subjected to *in vitro* digestion, a reduction of phenolic amounts ($p < 0.05$) was observed in all berries (**Figure 44**). TIPC ranged from 1.61 to 32.63 mg g^{-1} DE, corresponding to *E. umbellata* and *V. padifolium*. The decrease of TIPC ranged from 64.0% to 81.74% for *V. padifolium* and *S. lanceolata*, respectively (**Figure 44**). The latter species showed also the highest loss in ANTCs levels (-87.2%). Still, these compounds remained dominant in all berries (except on *E. umbellata* where flavonols were major). Ellagitannins and HCAs reamained relevant in *R. grandifolius* and *Vaccinium* berries, respectively. Some families present in native extracts (**Figure 44**), were not quantifiable after the digestion simulation, namely HCAS (*E. umbellata*), HBAs (*M. faya*, *V.*

cylindraceum and *V. padifolium*), flavones (*E. umbellata* and *S. lanceolata*), flavan-3-ols (*M. faya*) and ellagitannins (*E. umbellata*, *V. cylindraceum* and *V. padifolium*).

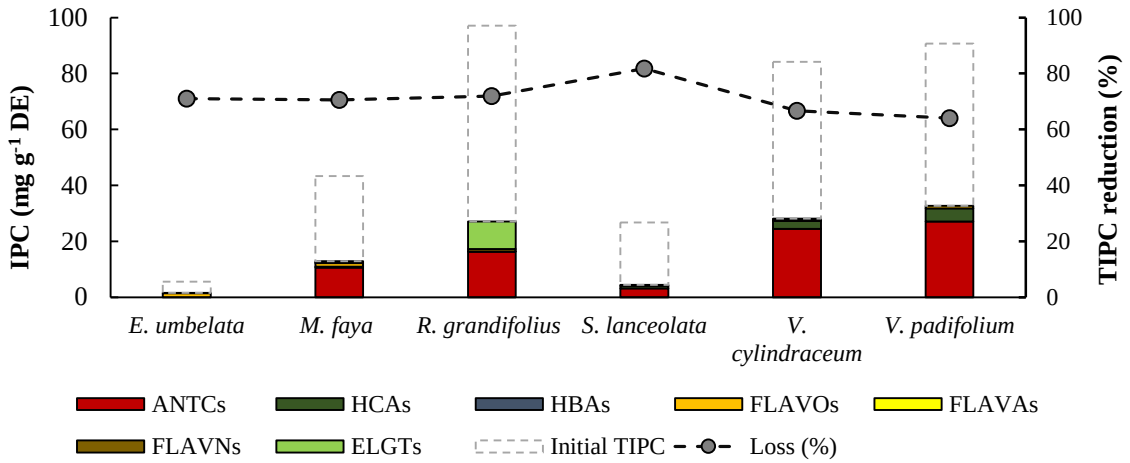

Figure 44 - Individual phenolic contents (mg g^{-1} DE) of digested berries extracts. ANT: anthocyanins; HCAs: hydroxycinnamic acids; HBAs: hydroxybenzoic acids; FLAVO: flavonols; FLAVA: flavan-3-ols; FLAVN: flavones; ELLG: ellagic acid derivatives.

A reduction of phenolic concentrations was also observed ($p < 0.05$) for leaves, although to a lesser extent than in berries (**Figure 45**). TIPC ranged from 11.53 to 59.62 mg g^{-1} DE, corresponding to *E. umbellata* and *V. padifolium*. Reduction of TIPC ranged between 54.12% and 63.35% for *V. padifolium* (MLs) and *E. umbellata* (**Figure 45**). HCAS remained dominant in *S. lanceolata* and *Vaccinium* leaves. Flavonols were still major in *M. faya* and become more relevant in *V. cylindraceum* after *in vitro* digestion. Ellagitannins continued as main compounds of *R. grandifolius*. Some phenolic groups present in native extracts (**Figure 43**), were not quantifiable after the digestion simulation, namely HCAS (*M. faya*), HBAs (*E. umbellata* and *V. cylindraceum*), flavan-3-ols (*E. umbellata* and *V. padifolium*) and ellagitannins (*S. lanceolata*) (**Figure 45**).

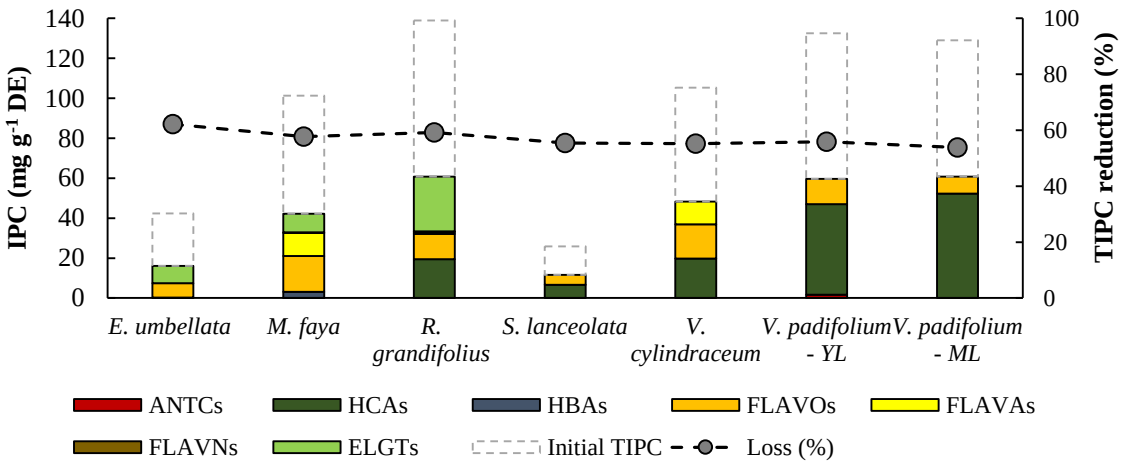

Figure 45 – Individual phenolic contents (mg g^{-1} DE) of digested leaves extracts. ANT: anthocyanins; HCAs: hydroxycinnamic acids; HBAs: hydroxybenzoic acids; FLAVO: flavonols; FLAVA: flavan-3-ols; FLAVN: flavones; ELLG: ellagic acid derivatives.

ANTCs were poorly recovered following the digestion of berries (60.28 – 87.15%). Declines from 28.10 to 99.9% of the initial ANTCs content are reported in literature, in different foodstuffs submitted to *in vitro* [24,48,49,53,54,56,58,140,141,145,147] and *in vivo* [59] digestion.

Flavan-3-ols were also highly affected by the digestion process (60.62 – 80.16%). The same trend was observed in different in chokeberry (- 28%), while pure (+)-catechin was recovered at only 42% [49]. In another study [55], (–)-epicatechin and B2-PAC from apples were completely degraded. Breakdown of oligomeric flavan-3-ols to (epi)catechin and further isomerization to catechin or degradation to unknown products is documented [52,55,59]. Moreover, B-type PACs seemed to be more affected by intestinal digestion than A-type due to their structural differences (**Figure 23**) [59].

5-*O*-CQA content decreased in analysed *Vaccinium* species (49.32 – 59.70%), which agrees with data on digested apples (41 – 77% reduction) [55]. This decline could be associate with the instability of CQAs in mild alkaline environments. By contrast, 5-*O*-CQA content increased by 24% in chokeberry [49], which was justified by regio-isomerization between CQAs under mild alkaline conditions. 5-*O*-CQA concentration remained constant during digestion of *V. angustifolium* [54].

A decrease on flavonols (-26%) was also observed in chokeberry [49], although in lower extent than present data (43.63 – 90.23%). On the contrary, quercetin content was improved by 2 and more than 4 times-fold in *Ribes uva-crispa* post *in vitro* digestion [155], while other PCs remained stable.

Ellagi- and gallotannins were strongly affected by *in vitro* digestion (50.93 – 72.94%), with reported reductions from 58.32 to 100% [47,51,52]. Ellagitannins are more stable throughout

digestion than are ANTCs, being hydrolysed to smaller components like ellagic acid [51,52,56]. For example, an increase of ellagic acid amounts was verified after *in vitro* digestion of pomegranate peel and strawberry-tree fruits (*Arbustus unedo*) (+ 113% and + 379%, respectively) [51,52], mainly due to the hydrolysis of ellagitannins.

Contradictory findings on the recovery of PCs after *in vitro* digestion are mainly due to differences in the type of food matrix and its initial state (frozen, freeze-dried, particle size, extract, etc). In fact, the stability and bioavailability of PCs during digestion depends mainly on the chemical environment (pH, ion strength, temperature, etc) than interaction with digestive enzymes [48,49,155]. Thus, stability of PCs from one fruit cannot be readily extended to other foodstuffs [47]. Discrepancies between studies could also result from the diversity of model conditions (time of digestion, concentration of salts/enzymes, pH, inclusion of various digestion steps, static *vs* dynamic models).

Before becoming bioavailable to exert their potential beneficial effects, PCs must be released from food matrix and hydrolysed/metabolised by intestinal enzymes and/or microflora [40,44,45]. During human digestion, dietary PCs are simultaneously exposed to different physical (temperature and agitation), chemical (pH) and biochemical (enzymes) conditions, which influences their bioavailability [40,46,47,49]. This environment results in several changes in their chemical structure/weight (hydrolysis, oxidation, epimerization and/or transformation/degradation) and solubility [44,49–51,56,146].

In the oral step, mastication along with the enzyme activity could facilitate the breakage of large molecules, which initially may be insoluble [44,50,51]. However, oral digestion has minimal modifications in the concentrations of PCs due to short exposure time and marginal effects of saliva [44,52]. Subsequently, the food bolus undergoes GID, where stomach and small intestine digestive enzymes, together play a key role in the release of PCs, making them available for absorption [55,57]. In general, PCs are very stable in the gastric media [41,47]. In fact, gastric digestion usually increases the amounts of PCs since the majority of these compounds appear to be released in the stomach [48,49,51,53,54,140,147,153]. However, polymerized flavan-3-ols seem to be highly susceptible to stomach conditions and are hydrolyzed into monomers or aglycones before being absorbed [41,52,55]. Most of the transformations of ingested PCs occur during the intestinal step, where they are exposed to mild alkaline conditions of digestive juices [40,41,47]. This leads to their hydrolysis and degradation and/or their conversion/break-down into other unknown or undetected metabolites [44,49,56]. Absorption and metabolism of PCs is highly variable and determined primarily by their

physicochemical characteristics, namely type of compound, molecular size, basic structure, degree of polymerization, acylation or glycosylation and solubility [1,2,16,44,50].

Among PCs, ANTCs seem the less efficiently absorbed in the lumen and their content may largely disappear after GID [40,47]. During the digestion process ANTCs can be found in different chemical forms due to dramatic pH variations [54,141]. In the oral phase, some minimal transformations are initiated in ANTCs [43]. When the food reaches the stomach (pH < 2), ANTCs are present in the form of stable flavylium cation and quinoidal form. This favorable chemical environment is responsible for their high recovery after gastric digestion [48,51–53,153]. However, the transition to the intestinal environment result in an intense degradation of ANTCs, due to their high unstability at mild-alkaline conditions [48,49,52–54,153]. At pH > 6, ANTCs are transformed to colourless carbinol and chalcone pseudobase, as a result of the chromophore desctruction [48,54,140,147]. At alkaline environments (pH > 7), ANTCs are further degraded upon C-ring fission and metabolized into low molecular weight compounds (protocatechuic acid, catechol, etc) [43,52,147]. In general, acylated anthocyanins are more stable than non-acylated forms; 3,5-diglycosides are more stable than 3-monoglycosides. This behavior is explained because the sugar moieties protect the molecule from degradation [43,52,54,140,147]. Also, increased aglycone hydroxyl methoxylation enhances stability, whereas anthocyanins with more hydroxylated aglycones are less stable [147]. C3G could contribute to the stabilization of other ANTCs due to sacrificial protection from oxidation [147]. The present data corroborate this explanation, since berries composed mainly by cyanidin derivatives (*S. lanceolata*, *M. faya* and *R. grandifolius*) showed the highest ANTCs degradation. Additionally, the superior loss verified in *S. lanceolata* berries is possibly due to the lower native amounts of ANTCs.

The non-ANTCs compounds are, overall, relatively stable at the intestinal environment [48,58,59,147]. The high pH values may induce structural changes in these molecules, namely deprotonation of hydroxyl groups and even degradation to other metabolites [47,48,53].

Additionally, it has become clear that stability/bioavailability of PCs is affected by interactions with other food constituents (proteins, lipids, carbohydrates, dietary fibers, minerals) that are released in the digestion process [45,47,49]. Some molecules have a very complex, porous structure which can trap PCs and, consequently, confer protection from oxidation during their passage through the GI tract [50,55]. For example, a higher recovery of ANTCs was observed in red cabbage (67.7%) versus the ANTCs-rich extract (13.2%), which suggested that vegetable components (like fibers) protected labile ANTCs from degradation under simulated digestion [156]. On the other hand, binding to proteins, dietary fibers and polysaccharies can limit their bioavailability by reducing their solubility and contact with digestive enzymes [45,47,50]. Food microstructure composition (matrix

type), namely variations in concentration within plant tissues, variations in cell wall structure and location of glycosides in cells can influence the release of PCs from the food matrix and impact also their bioavailability [44,54]. In this sense, the higher recoveries of PCs from leaves (**Figure 45**) could be related to the absence of pectinases and cellulases in the applied digestion model, which limited the degradation of PCs in leaves by comparison with berries. Finally, binding of PCs with components of the pancreatin/bile juices and digestive enzymes can lead to precipitation (insoluble complexes) and also mask compounds and make them undetectable with HPLC analysis [40,48,147].

In conclusion, the obtained results and previous reports confirm that dietary PCs are highly sensitive to *in vitro* digestion and suggest that, a substantial part of these compounds can be degraded and/or transformed into other unknown and/or undetected structural forms and, consequently, different bioavailability. In this case, the observed high losses (< 50%) could be partially attributed to the incomplete release/lower efficiency of aqueous extraction (i.e. digestion process) compared with initial chemical extraction using methanol. The same was verified by other authors [48,53]. Most of studies regarding plant-foods analysis usually refers to extraction of PCs in mixtures of aqueous and organic solvents. The amount of PCs extracted from the GID may differ quantitatively and qualitatively from those extracted by chemical methods; the latter extractor can lead to an overestimation of bioavailable PCs [48,53].

After examination of HPLC chromatograms from non-digested and digested extracts, the presence of new compounds resultant from digestion was not observed. The presence of PCs derivatives might be masked by other dominant compounds in analysed extracts and was not detected under current analytical conditions. Other possible scenario is the the lack of esterase activity on the commercial pancreatin, as reported by other authors [49,116]. In fact, the existence of degradation products derived from the catabolism of PCs have been documented only in studies that included microbiota fermentation or cell models [51,52,54,59].

Although the obtained data with *in vitro* GID simulation cannot be directly extrapolated to human conditions, this model was useful to predict the impact of this physiological process on bioavailability of PCs from BPPs. However, this model can be further improved to better reproduce the digestive process. Further investigations employing dialysis bags or including cellular models such as Caco-2, should be performed to study the bioaccessibility of PCs.

5. Total phenolic and total flavonoid contents

In this work, total phenolic and total flavonoids contents were also determined for the methanolic extracts (pre- and post *in vitro* digestion) and results are presented and discussed below.

5.1. Pre-*in vitro* gastrointestinal digestion

Total phenolic content (TPC) of analysed berries extracts ranged between 19.06 and 103.42 mg GAE g^{-1} DE (**Figure 46**), which corresponded to *E. umbellata* (2013) and *R. grandifolius* (FX). An opposite trend was found in other work [18], where blueberries, bilberries and lingonberries showed higher TPC than blackberries. Intra-species variations ($p < 0.05$) were observed between TPC of berries and leaves extracts from different years/collection. respectively.

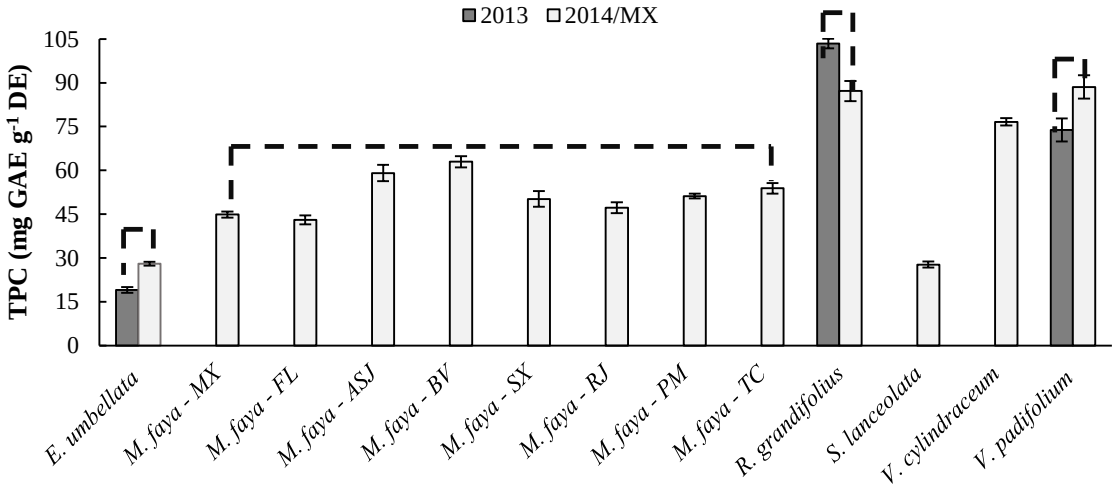

Figure 46 - Total phenolic content (TPC) of analysed berries extracts (mg GAE g^{-1} DE) determined by the Folin-Ciocalteu method. Data represent the mean ± standard deviation ($n = 3$).

TPC of leaves extracts ranged between 90.65 and 346.61 mg GAE g^{-1} DE (**Figure 47**), which corresponded to *S. lanceolata* and *V. padifolium* (YL 2013), respectively. Differences ($p < 0.05$) were found between TPC of *V. padifolium* leaves (YLs > MLs).

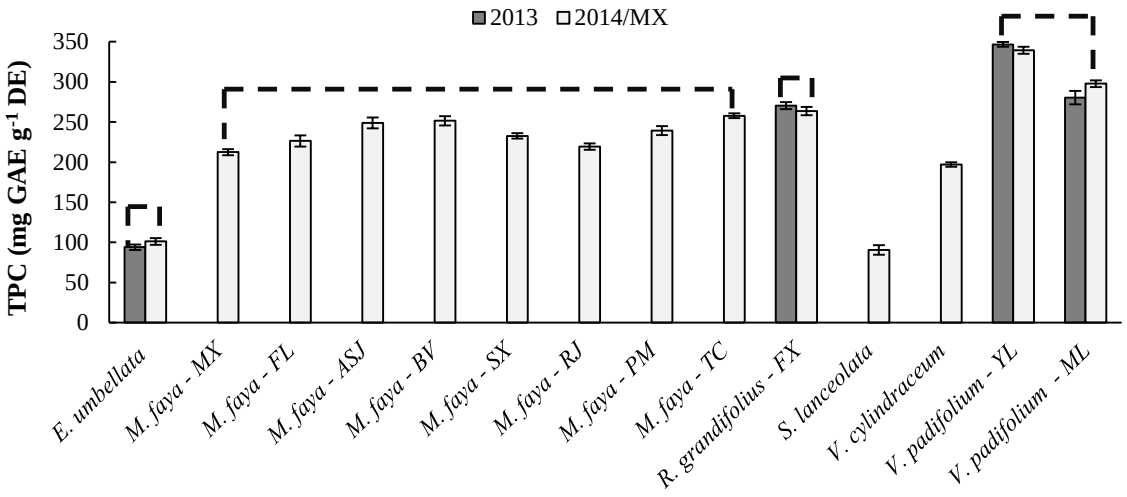

Figure 47 - Total phenolic content (TPC) of analysed leaves extracts (mg GAE g^{-1} DE) determined by the Folin-Ciocalteu method. Data represent the mean ± standard deviation (n = 3).

Total flavonoids content (TFC) of analysed berries extracts ranged between 6.69 and 14.67 mg RUE g^{-1} DE (**Figure 48**), which corresponded to *M. faya* (PM) and *R. grandifolius* (MX), respectively. Variations ($p < 0.05$) were also observed for different years/collection areas in TFC measurements

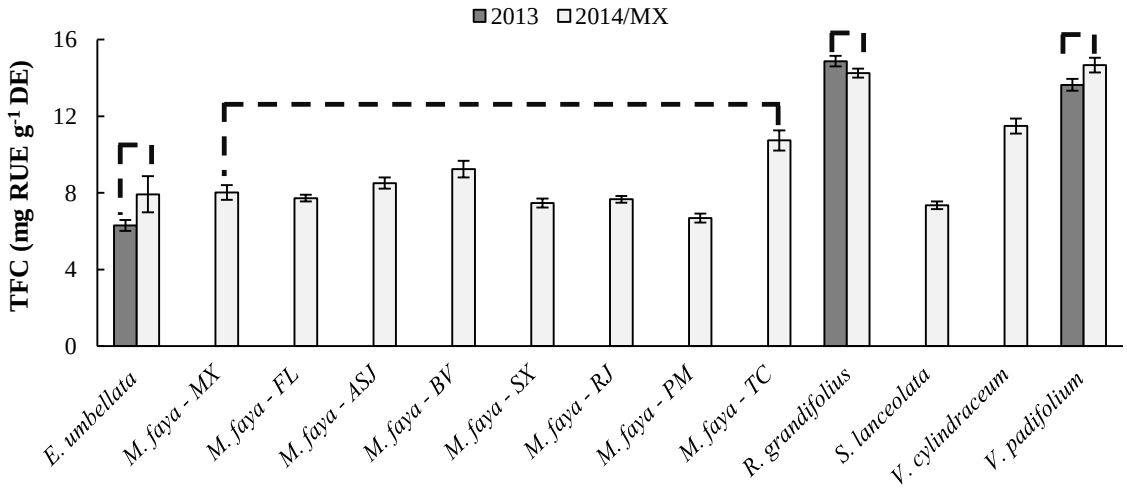

Figure 48 - Total flavonoid content (TFC) of analysed berries extracts (mg RUE g^{-1} DE) determined by the aluminium chloride method. Data represent the mean ± standard deviation (n = 3).

TFC of leaves extracts ranged between 35.41 and 134.06 mg RUE g^{-1} DE (**Figure 49**), which corresponded to *V. cylindraceum* and *V. padifolium* (YLs 2013), respectively. Variations ($p < 0.05$) were found between TFC of *V. padifolium* leaves (YLs > MLs).

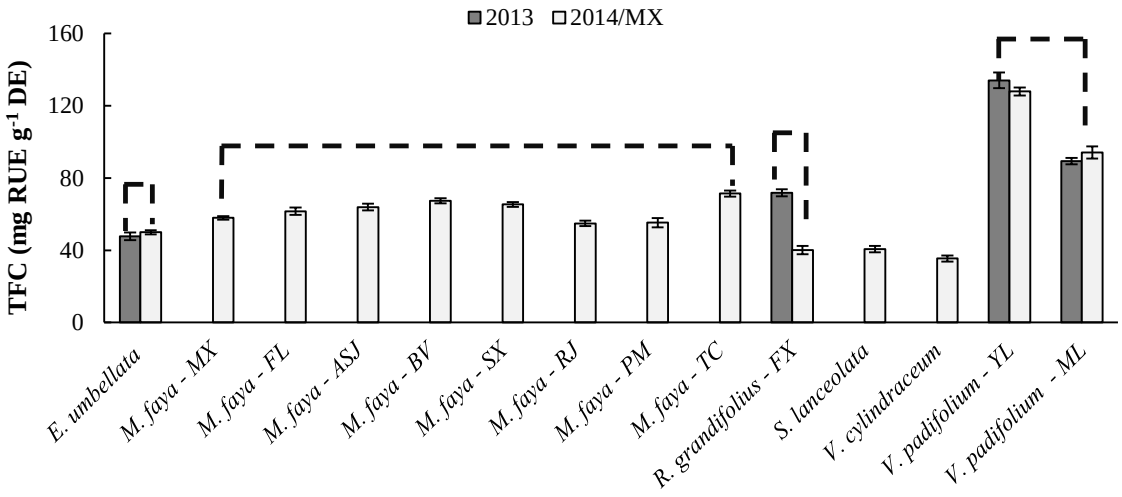

Figure 49 - Total flavonoid content (TFC) of analysed leaves extracts (mg RUE g^{-1} DE) determined by the aluminium chloride method. Data represent the mean ± standard deviation (n = 3).

Similar TPC but lower TFC values were found in *E. umbellata* berries (23.3 mg GAE g^{-1} DE and 3.6 mg QE g^{-1} DE, respectively)[103]. On another study [157], a lower TPC was reported (7.67 mg GAE g^{-1} DE). *M. rubra* had higher TPC (341 – 634 mg GAE g-1 DE) [62] and TFC (182.8 – 920 mg RUE g^{-1} DE) [62,117] than analysed *M. faya* extracts. Berries of *R. grandifolius* had hihgher TPC than other blackberries, cranberries, lingonberries and blueberries (3.27 – 83.13 mg GAE g^{-1} DE) [88,158–160]. Higher TPCs (49.2 – 90.6 mg GAE g^{-1} DE) were determined for other *Sambucus* species [151,161] compared with *S. lanceolata*. Inferior TPC [84,159] were described for different *Vaccinium* berries; while other studies [74,162] documented opposite results (100.5 - 630 mg GAE g^{-1} DE). TPC of YLs was comparable to that of other *Vaccinium* species [81,163,164], but lower TFC (63.24 – 114.21 mg catechin equivalent g^{-1} DE) was observed [163]. Variations in species/cultivar, sample preparation, extraction and methodologies could justify the discrepancies between obtained results and data from other studies.

5.2. Post *in vitro* gastrointestinal digestion

After *in vitro* GID, a significant ($p < 0.05$) reduction was observed for TPC. The decline ranged from 30.22% to 64.88%, corresponding to *S. lanceolata and E. umbellata*, respectively (**Figure 50**). TPC of digested berries ranged from 9.84 to 44.70 mg GAE g^{-1} DE.

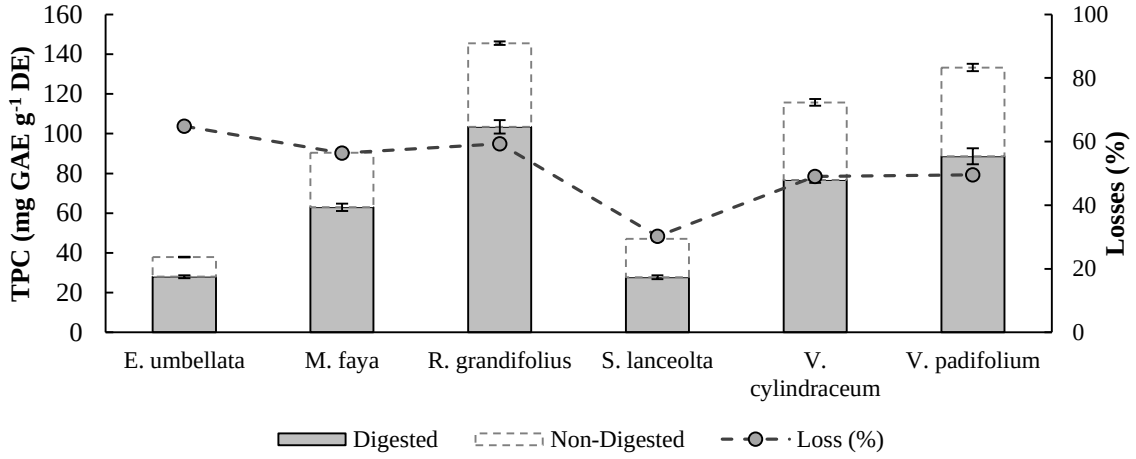

Figure 50 - Total phenolic content (TPC) (mg GAE g^{-1} DE) of analysed berries extracts (pre- and post *in vitro* digestion) determined by the Folin-Ciocalteu method. Data represent the mean ± standard deviation (n = 3).

In the case of digested leaves, a similar behaviour was observed. The decrease of TPC ranged from 52.90% to 64.40%, corresponding to *V. padifolium and E. umbellata*, respectively (**Figure 51**). The amounts ranged from 27.92 to 149.78 GAE g^{-1} DE.

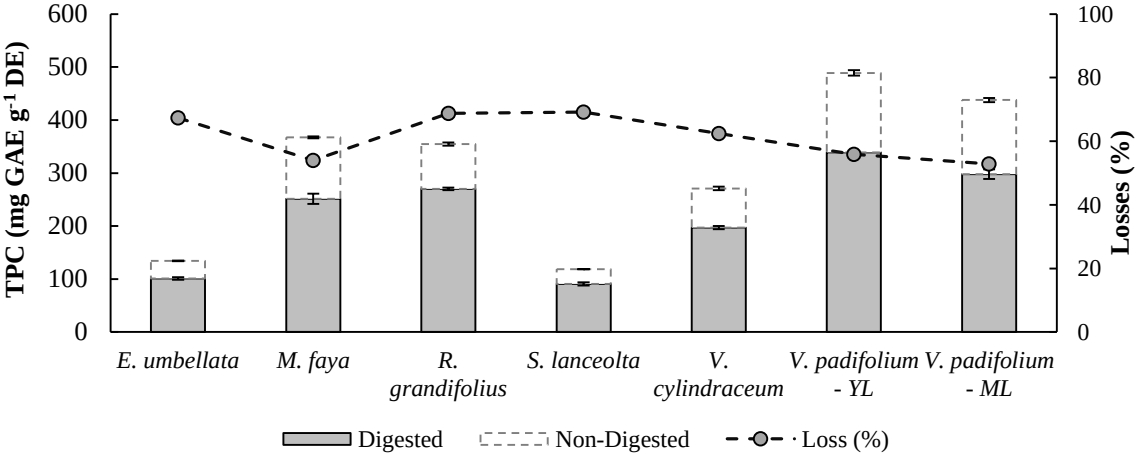

Figure 51 - Total phenolic content (TPC) (mg GAE g^{-1} DE) of analysed leaves extracts (pre- and post *in vitro* digestion) determined by the Folin-Ciocalteu method. Data represent the mean ± standard deviation (n = 3).

TFC was also significantly ($p < 0.05$) affected upon *in vitro* digestion. The decline of digested berries TFC ranged from 28.52% to 54.33%, corresponding to *R. grandifolius and M. faya*, respectively (**Figure 52**). The aomunts in digested berries ranged between 3.80 and 10.19 RUE g^{-1} DE.

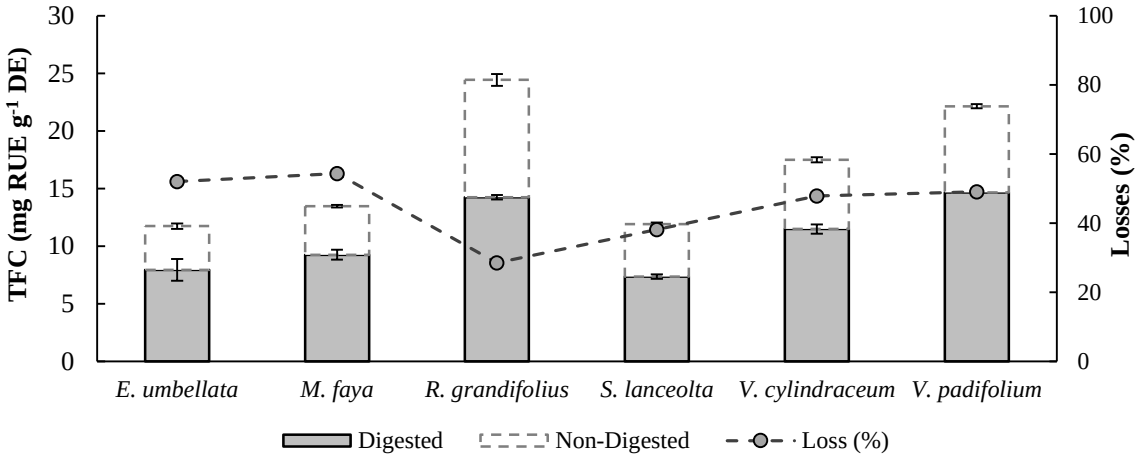

Figure 52 - Total flavonoid content (TFC) (mg RUE g^{-1} DE) of analysed berries extracts (pre- and post *in vitro* digestion) determined by the aluminium chloride method. Data represent the mean ± standard deviation (n = 3).

In the case of digested leaves, the decrease of TPC ranged from 26.10% to 73.81%, corresponding to *V. padifolium* (YLs) *and S. lanceolata*, respectively (**Figure 53**). The amounts ranged from 10.65 to 94.52 RUE g^{-1} DE.

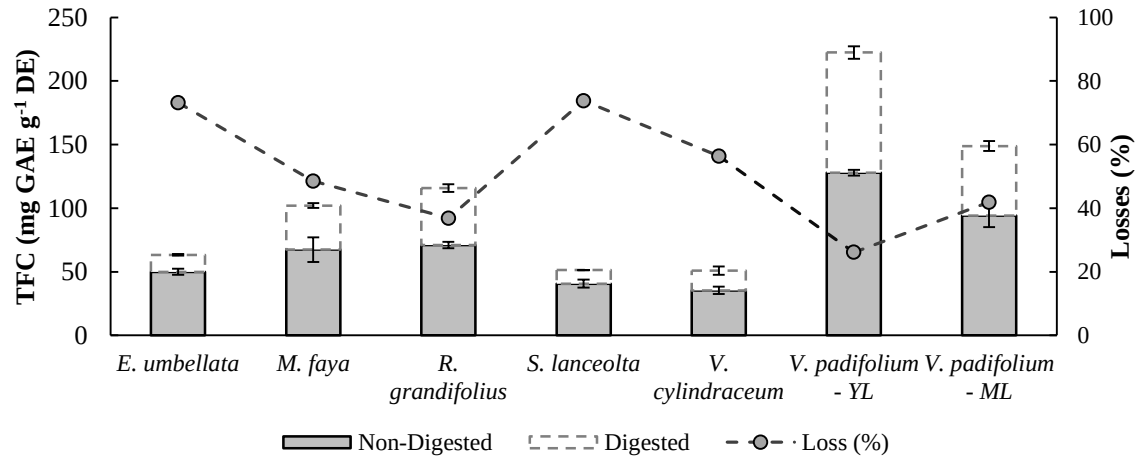

Figure 53 - Total flavonoid content (TFC) (mg RUE g^{-1} DE) of analysed leaves extracts (pre- and post *in vitro* digestion) determined by the Aluminium chloride method. Data represent the mean ± standard deviation (n = 3).

5.3. General discussion

TPC and TFC measurements are generally used by the scientific community and, despite their shortcomings, they are useful to compare results with available literature [18]. TPC and TFC are based in reduction reactions, so any reductant component of the sample will test positive and contribute to an increase on the overall value [29,36,78]. FCR is non-specific to PCs as it can be reduced by other compounds such as aromatic aminoacids, organic acids, sugars, thiols derivatives and vitamins (specially vitamin C) [18,36,47,55]. Additionally, these colorimetric assays do not yield information on the recovery of specific compounds or molecules [38,47,78]. Hence, TIPC, as discussed previously (**section 4**), is a much more accurate method to assess PCs content in natural products.

In the present work, TPC and TFC of methanolic extracts were significantly reduced after smiluated digestion. TPC and TFC of *M. rubra* was decreased by 13.2 – 43-0% [116] and 27.23% [117] for berries and leaves, respectively, upon *in vitro* digestion. Losses of 86% and 88.5% of TPC were previously reported *V. vitis-idea* and *R. idaeus*, respectively [59,147]. A decrease of 86.07% and 84.32% was reported for TPC and TFC, respectively, of digested blueberries (*Vaccinium spp*.) [153]. Similarly to present work, blackberries showed a greater TPC loss than blueberries (27% and 67%, respectively), upon GID [56,141]. In other study, a reduction of 86% of TPC was verified after digestion of chokeberry. [49]. By contrast, an increase of phenolic amounts was observed for blackberries (+ 35.1% TPC, + 31.9% TFC) and gooseberries (+ 21% TPC) subjected to *in vitro* digestion [146,155]. The chemical action during the digestive process can contribute to a higher extraction of non-PCs from food matrices [48,155]. FCR can potentially react with degradation products and macromolecule-bound PCs [55]. Additionally, interactions with matrix components (proteins, sugars) and other food components (vitamins) can overestimate TPC and TFC and lead to conflicting results [47].

Chapter III – Results and Discussion

B.Digestive Enzymes Inhibition

1. Inhibition of digestive enzymes responsible for the sugar metabolism

Berries have been widely studied for their potential to inhibit digestive enzymes involved in the glucose and lipids metabolism [5,16,18,21]. Retarding or inhibiting the digestion of these nutrients has therapeutic implications for controlling post-prandial hyperglycaemia and hyperlipidaemia [3,15,18,89,115]. In this view, the main aim of this part of the study was to evaluate the ability of berry-producing plants (BPPs) extracts to inhibit key digestive enzymes linked to type-2 diabetes melitus (T2DM) and obesity.

1.1. Glucosidases (GLUs)

The *in vitro* inhibitory activity of analysed extracts towards GLUs (α- and β-) was investigated using *p*-nitrophenyl-α-D-glucopyranoside (α-*p*NPG) and *p*-Nitrophenyl-β-D-glucopyranoside (β-*p*NPG) as substrates, respectively.

1.1.1. Yeast α-glucosidase

α-Glucosidases (AGLUs), including sucrase and maltase, are the main enzymes responsible for the breakdown of oligosaccharides and disaccharides into monosaccharides during digestion [2,4,16,20,91]. AGLU isolated from baker's yeast (*Saccharomyces cerevisae*) has been widely used for preliminary pharmacological screenings [31,65,85,98,115,162]. The inhibition of yeast AGLU by tested extracts was in a wide range with the IC_{50} values from 0.11 to 4.77 mg mL^{-1} (**Table 23**). Leaf extracts were the most potent inhibitors for AGLU ($p < 0.05$). Additionally, inter and intra-species differences ($p < 0.05$) were found in this assay. The order of the most potent inhibitors for berries extracts was as follows: *R. grandifolius* < *M. faya* < *V. padifolium* ≈ *V. cylindraceum* << *E. umbellata* < *S. lanceolata*. For the leaves, a slight different trend was observed: *R. grandifolius* < *M. faya* < *V. padifolium* (young leaves, YLs > mature leaves, MLs) < *V. cylindraceum* << *E. umbellata* << *S. lanceolata*.

In general, analysed extracts were more effective than commercial drug acarbose (**Figure 4**) (except for *E. umbellata* and *S. lanceolata*) (**Table 23**). Other studies also found acarbose to be less effective towards yeast AGLU than *Vaccinium* berries extracts [85,162]. 1-Deoxynojirimycin (1-DNJ) (**Figure 5**), a natural competitive GLUs inhibitor extracted from *Morus spp*. [33], showed stronger inhibitory activities ($p < 0.05$) than berries extracts (**Table 23**). Of course, it must be taken in account that this is a comparison of the activity of pure substances with that of plant extract where the amount of active substances is a small percentage of the sample, as shown in Chapter III.

No studies regarding the inhibition of digestive enzymes by *E. umbellata* and *S. lanceolata* or alike species were found in literature. *M. rubra* berries showed lower inhibitory activities towards

AGLU (IC_{50}: 2.08 – 3.17 mg mL^{-1})[65] than most of the analysed extracts. Different *Rubus* berries cultivars strongly inhibited yeast AGLU (IC_{50} = 0.001–0.034 mg mL^{-1}) [98,162]. Blackberries and blueberries studied by Tan and co-workers [115] displayed higher activities (IC_{50}: 0.031 – 0.057 mg mL^{-1}) than analysed samples. On another study, blackberry extracts showed lower activities towards yeast AGLU (≥ 26 mg mL^{-1})[31]. Different berry species (strawberries, black currants, blueberries and rowanberries) showed also the ability to modulate starch metabolism by inhibition of digestive enzymes [5,18,21,90,93,154].

Table 23 – *In vitro* inhibitory activities of analysed extracts towards α- and β-glucosidases (expressed as IC_{50} value, mg mL^{-1}). Data represent the mean ± standard deviation (*n* = 3).

Berries		**α-Glucosidase**		**β-Glucosidase**
		Yeast	**Rat**	
E. umbellata		3.14 ± 0.09^{q}	6.88 ± 0.33^{u}	18.70 ± 2.34^{x}
M. faya	MX	$0.76 \pm 0.02l^{m}$	4.51 ± 0.13^{r}	12.51 ± 0.20^{w}
	FL	0.75 ± 0.02^{l}	4.22 ± 0.11^{p}	12.05 ± 0.31^{uv}
	ASJ	0.69 ± 0.02^{k}	4.35 ± 0.15^{pq}	11.06 ± 0.15^{t}
	BV	0.72 ± 0.02^{k}	3.78 ± 0.11^{o}	11.45 ± 0.19^{u}
	SX	0.78 ± 0.01^{m}	4.40 ± 0.11^{q}	12.38 ± 0.30^{w}
	RJ	0.83 ± 0.02^{n}	4.63 ± 0.10^{s}	12.78 ± 0.20^{w}
	PM	0.71 ± 0.02^{k}	3.85 ± 0.12^{o}	12.10 ± 0.26^{v}
	TC	0.73 ± 0.03^{k}	3.91 ± 0.14^{o}	11.76 ± 0.20^{u}
R. grandifolius	FX	0.61 ± 0.02^{i}	3.26 ± 0.17^{n}	8.27 ± 0.15^{p}
	MX	0.68 ± 0.02^{k}	3.78 ± 0.23^{o}	8.79 ± 0.22^{q}
S. lanceolata		4.77 ± 0.27^{r}	7.95 ± 0.34^{v}	15.65 ± 0.6^{5}
V. cylindraceum		1.10 ± 0.04^{o}	4.36 ± 0.14^{pq}	9.88 ± 0.27^{s}
V. padifolium		1.03 ± 0.03^{o}	4.13 ± 0.10^{o}	9.36 ± 0.19^{r}
Leaves				
E. umbellata		1.98 ± 0.04^{p}	3.76 ± 0.09^{o}	9.38 ± 0.41^{r}
M. faya	MX	0.31 ± 0.02^{f}	1.41 ± 0.05^{k}	6.33 ± 0.10^{n}
	FL	0.27 ± 0.01^{e}	1.29 ± 0.08^{j}	6.48 ± 0.20^{n}
	ASJ	0.21 ± 0.01^{d}	1.13 ± 0.05^{i}	5.79 ± 0.21^{m}
	BV	0.20 ± 0.01^{cd}	1.16 ± 0.06^{i}	5.15 ± 0.17^{k}
	SX	0.27 ± 0.01^{e}	1.26 ± 0.03^{j}	5.41 ± 0.12^{l}
	RJ	0.33 ± 0.02^{f}	1.53 ± 0.04^{l}	6.86 ± 0.15^{o}
	PM	0.25 ± 0.01^{e}	1.35 ± 0.07^{jk}	5.55 ± 0.19^{lm}

	TC	0.18 ± 0.01^{c}	1.09 ± 0.06^{h}	4.86 ± 0.10^{j}
R. grandifolius	FX	0.11 ± 0.01^{a}	0.97 ± 0.03^{g}	3.24 ± 0.08^{g}
	MX	0.15 ± 0.01^{b}	0.89 ± 0.05^{g}	3.87 ± 0.12^{h}
S. lanceolata		3.73 ± 0.15^{q}	4.97 ± 0.25^{t}	11.28 ± 0.37^{t}
V. cylindraceum		0.85 ± 0.03^{m}	1.64 ± 0.06^{m}	4.59 ± 0.40^{ij}
V. padifolium	YLs	0.58 ± 0.01^{h}	0.80 ± 0.04^{f}	2.33 ± 0.19^{e}
	MLs	0.76 ± 0.02^{kl}	0.86 ± 0.02^{fg}	2.60 ± 0.12^{f}
Acarbose		2.06 ± 0.04^{p}	0.12 ± 0.01^{b}	N.I.
1-Deoxynojirimycin		0.65 ± 0.02^{i}	0.01 ± 0.01^{a}	0.45 ± 0.02^{b}
Conduritol B epoxide		-	-	8.94 ± 0.19^{q}
Cyanidin-3-*O*-glucoside		0.38 ± 0.02^{g}	0.23 ± 0.01^{d}	0.86 ± 0.03^{d}
5-*O*-Caffeoylquinic acid		0.36 ± 0.02^{g}	0.27 ± 0.02^{c}	0.39 ± 0.01^{c}
Myricitrin		0.63 ± 0.04^{i}	0.39 ± 0.02^{e}	0.35 ± 0.02^{a}

YLs: Young leaves. MLs: Mature leaves. N.I.: no inhibition. MX: Machico; FL: Faial; ASJ: Arco de S. Jorge; BV: Boaventura; SX: Seixal; RJ: Ribeira da Janela; PM: Porto Moniz; TC: Terceira; FX: Funchal. Means in the same column not sharing the same letter are significantly different at $p < 0.05$ probability level.

1.1.2. Rat intestinal α-glucosidase

In this study, rat AGLU was also tested to verify and compare any differences in the enzyme inhibitory action of berry-plants extracts, since it reasonably matches the human enzyme providing a better model to validate results [19]. At a first look, the IC_{50} values of analysed extracts were higher than in the microbial version of the enzyme; ranging from 0.82 to 7.95 mg mL^{-1} (**Table 23**). Other studies [165–167] also observed a decrease on the efficiency of extracts on mammalian enzyme when compared to the microbial equivalent. This suggests that most yeast AGLU inhibitors show a lower or no inhibitory effect on the mammalian equivalent. Additionally, a weak correlation ($r = 0.612$) was verified between results of both models. Again, statistical differences were verified among species and morphological parts ($p < 0.05$).

In this case, *R. grandifolius* berries showed the highest inhibitory activities (FX > MX) and the order of potency was as follows: *V. padifolium* ≈ *V. cylindraceum* ≈ *M. faya* > *E. umbellata* > *S. lanceolata*. Leaves of *V. padifolium* (YLs > MLs) were the most active, followed by *R. grandifolius* (MX > FX), *M. faya*, *V. cylindraceum*, *E. umbellata* and *S. lanceolata*. Positive controls (acarbose and 1-DNJ) showed the strongest activities ($p < 0.05$). Contrary to assayed extracts, these reference compounds displayed higher inhibitory activity over mammalian AGLU (about 17 and 65 times higher, respectively) than over the yeast counterpart (**Table 23**). Shai and co-workers [167] reported

a similar trend. Overall, obtained data confirm that inhibition of yeast AGLU does not translate into comparable inhibition of the mammalian enzyme [19,166,167]

. The divergent results are mainly due to the structural differences of the catalytic regions responsible for molecular recognition in the binding site of the enzymes [167]. AGLU are widely distributed in microorganisms, plants and animals and the catalytic region is known to differ greatly depending on their origin [168]. By analysis of the amino acid sequences containing the catalytic sites, these enzymes are generally classified into two groups: family I and family II. The first family consists of bacterial, yeast and insect enzymes and are composed of four catalytic regions, while family II (mold, plants and mammalians) have two catalytic sites responsible for the enzyme reaction [165]. These differences justify the discrepancies obtained in the present study (**Table 23**) and support the use of mammalian AGLU as a desirable model to search for new natural hypoglycaemic compounds.

Previously [10,89,93,94], different berry species have shown strong inhibitory activities towards rat AGLU. Unfortunately, results were expressed in total phenolic content basis which makes it difficult to establish a comparison.

1.1.3. Almond β-glucosidase (BGLU)

The inhibitory potential of BPPs extracts against BGLU was also evaluated. Although with a lower impact, BGLUs (galactosidase, lactase, etc) play also a role in the hydrolysis of dietary carbohydrates [19]. In the present study, almond BGLU from almonds was used due to the lack of a commercial version of this enzyme from animal origin. The IC_{50} values of analysed extracts ranged from 2.33 to 18.70 mg mL^{-1} (**Table 23**). Significant variations ($p < 0.05$) were observed between samples. Berries of *R. grandifolius* (FX > MX) were the most active sample, followed by *V. padifolium*, *V. cylindraceum*, *M. faya*, *S. lanceolata* and *E. umbellata*. The order of potency for leaves extracts was as follows: *V. padifolium* (YLs > MLs) > *R. grandifolius* (FX > MX) > *V. cylindraceum* ≈ *M. faya* > *S. lanceolata* > *E. umbellata*.

Acarbose was ineffective against BGLU activity, as documented previously [33]. Pure conduritol B epoxide (CBE)(**Figure 54**), an effective BGLU inhibitor [33], showed stronger activities ($p < 0.05$) than berries extracts (except for *R. grandifolius*), while pure 1-DNJ showed the best inhibitory activity among tested samples (**Table 23**).

Previously [169], Chinese quince (*Chaenomeles sinensis*) fruit extract showed also moderate BGLU inhibition.

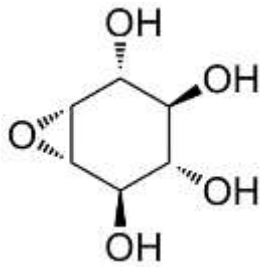

Figure 54 - Chemical strucutre of Conduritol B epoxide (CBE) (adapted from [33]).

1.2. Pancreatic α-Amylase (AMY)

Pancreatic AMY is responsible for the hydrolysis of large polysaccharides (starch, glycogen, amylose) into maltose, dextrin and maltotriose in the digestion system [2,3,16,19,61,95,96]. In this study, the *in vitro* inhibitory potential of BPPs extracts against AMY was investigated, using starch as substrate.

The IC_{50} values of assayed extracts ranged from 0.57 – 7.71 mg mL^{-1} (**Table 24**). Intra and inter-species variations were observed ($p < 0.05$). Berries of *R. grandifolius* (FX > MX) showed the highest activity, followed by *M. faya* > *V. padifolium* ≈ *V. cylindraceum* > *E. umbellata* > *S. lanceolata*. In the case of the leaves a slight different trend was verified: *M. faya* > *R. grandifolius* > *V. cylindraceum* > *V. padifolium* (YLs > MLs) > *E. umbellata* > *S. lanceolata*. Although the tested plant-extracts appeared to have strong glucosidases inhibitory potential, they showed lower potency against AMY. All samples were less effective ($p < 0.05$) than pure acarbose (**Table 24**).

V. arctostaphylos berries showed comparable IC_{50} values (1.91 mg mL^{-1}) [95] while leaves were more effective towards AMY (0.53 mg mL^{-1}) [96] than targeted *Vaccinium* species (**Table 24**). Black chokeberry extracts were less effective towards AMY (IC_{50} = 10.31 mg mL^{-1}) [97] than present samples (**Table 24**). *R. fruticosus* extracts were potent AMY inhibitors (0.054 mg mL^{-1}) [162]. Blackberry extract showed lower activity (1.56 mg mL^{-1}) [115] to *R. grandifolius*. Higher IC_{50} values for different blackberry extracts (≥ 95 mg mL^{-1}) [31]. On another study [98], raspberry extracts did not show any inhibitory activity towards AMY, which could be due to absence of tannins. Blackberries and blueberries showed lower inhibitions (1.26 – 156 mg mL^{-1}) [115] than analysed alike species.

Table 24 - *In vitro* inhibitory activities of analysed extracts and reference compounds towards porcine pancreatic α-amylase (expressed as IC_{50} value, mg mL^{-1}). Data represent the mean ± standard deviation (n = 3).

		Berries	Leaves
E. umbellata		4.01 ± 0.20^{s}	2.18 ± 0.13^{p}
M. faya	MX	1.38 ± 0.04^{l}	0.66 ± 0.02^{c}
	FL	1.25 ± 0.03^{k}	0.65 ± 0.03^{c}
	ASJ	1.19 ± 0.02^{j}	0.57 ± 0.02^{a}
	BV	1.08 ± 0.03^{i}	0.61 ± 0.02^{ab}
	SX	1.22 ± 0.03^{jk}	0.63 ± 0.02^{b}
	RJ	1.68 ± 0.02^{n}	0.67 ± 0.03^{c}
	PM	1.53 ± 0.04^{m}	0.76 ± 0.01^{e}
	TC	0.99 ± 0.02^{h}	0.58 ± 0.02^{a}
R. grandifolius	FX	0.94 ± 0.04^{g}	0.83 ± 0.03^{f}
	MX	0.97 ± 0.02^{gh}	0.72 ± 0.05^{de}
S. lanceolata		6.01 ± 0.54^{t}	7.71 ± 0.32^{u}
V. cylindraceum		2.78 ± 0.04^{r}	1.05 ± 0.03^{h}
V. padifolium		2.63 ± 0.09^{q}	1.75 ± 0.06^{n}*
			2.03 ± 0.04^{o}**
Acarbose		0.02 ± 0.01^{a}	
Cyanidin-3-*O*-glucosidase		0.97 ± 0.03^{gh}	
5-*O*-Caffeoylquinic acid		1.20 ± 0.04^{j}	
Myricitrin		2.02 ± 0.10^{o}	

*Young leaves; **Mature leaves. MX: Machico; FL: Faial; ASJ: Arco de S. Jorge; BV: Boaventura; SX: Seixal; RJ: Ribeira da Janela; PM: Porto Moniz; TC: Terceira; FX: Funchal. Means not sharing the same letter are significantly different at $p < 0.05$ probability level.

1.3. Pancreatic Lipase (PL)

PL is the most important enzyme responsible for the digestion of dietary fat, so its inhibition can lead to beneficial effects on overweight and obesity [18,64,170]. The inhibitory activity of berry-plants extracts towards PL was tested using *p*-nitrophenyl butyrate (*p*-NPB) as substrate. The IC_{50} values of samples varied from 1.49 to 9.68 mg mL^{-1} (**Table 25**). Significant differences ($p < 0.05$) were found among the analysed extracts in the inhibitory activities against PL. *R. grandifolius* berries were the most active, followed by *M. faya* > *V. padifolium* > *V. cylindraceum* > *S. lanceolata* > *E. umbellata*. In the case of leaves extracts the order of potency was as follows: *M. faya* > *V. padifolium*

≈ *R. grandifolius* ≈ *V. cylindraceum* > *E. umbellata* > *S. lanceolata*. In this case, the commercial drug orlistat (**Figure 4**) showed the strongest inhibitory activity ($p < 0.05$) (**Table 25**).

On another study, *M. rubra* leaves extracts were more active towards PL (IC_{50}: 0.25 – 0.73 mg mL^{-1})[23]. Black chokeberry extracts were less effective (IC_{50} = 85.45 mg mL^{-1}) [97] than analysed samples (**Table 25**). Blackberries and blueberries extracts showed potent inhibitory activities against PL (IC_{50}: 0.26 and 0.36 mg mL^{-1}, respectively)[115]. On another study [171], blackberry extract showed comparable activities (IC_{50}: 1.99 mg mL^{-1}) to *M. faya* leaves (**Table 25**). Again, raspberry extracts were ineffective towards PL since they have no tannins [98]. The potential of other berry species (strawberries, black currants, blueberries, blackberries, raspberries and rowanberries) to inhibit PL activity is documented in literature [5,18,21,64].

Table 25 - *In vitro* inhibitory activities of analysed extracts and reference compounds towards porcine pancreatic lipase (expressed as IC_{50} value, mg mL^{-1}). Data represent the mean ± standard deviation (n = *3*).

		Berries	**Leaves**
E. umbellata		9.68 ± 0.51^{t}	5.03 ± 0.22^{m}
M. faya	MX	5.75 ± 0.19^{op}	2.04 ± 0.07^{f}
	FL	5.30 ± 0.20^{n}	2.24 ± 0.05^{g}
	ASJ	4.83 ± 0.13^{l}	1.93 ± 0.10^{ef}
	BV	4.98 ± 0.10^{l}	1.60 ± 0.04^{d}
	SX	5.78 ± 0.15^{op}	1.68 ± 0.05^{d}
	RJ	6.15 ± 0.22^{q}	2.34 ± 0.08^{h}
	PM	5.46 ± 0.20^{n}	1.89 ± 0.06^{e}
	TC	5.26 ± 0.12^{mn}	1.49 ± 0.04^{c}
R. grandifolius	FX	4.45 ± 0.13^{k}	2.97 ± 0.09^{h}
	MX	3.97 ± 0.25^{j}	3.33 ± 0.08^{i}
S. lanceolata		7.75 ± 0.48^{s}	6.64 ± 0.25^{r}
V. cylindraceum		6.50 ± 0.34^{r}	4.20 ± 0.27^{k}
V. padifolium		5.97 ± 0.38^{pq}	2.18 ± 0.09^{g}*
			3.56 ± 0.25^{i}**
Orlistat		0.47 ± 0.02^{b}	
Cyanidin-3-*O*-glucoside		0.30 ± 0.01^{a}	
5-*O*-Caffeoylquinic acid		0.31 ± 0.01^{a}	
Myricitrin		0.51 ± 0.03^{b}	

*Young leaves; **Mature leaves; MX: Machico; FL: Faial; ASJ: Arco de S. Jorge; BV: Boaventura; SX: Seixal; RJ: Ribeira da Janela; PM: Porto Moniz; TC: Terceira; FX: Funchal. Means not sharing the same letter are significantly different at $p < 0.05$ probability level.

1.4. General Discussion

Phenolic compounds (PCs) are mainly known for their potential beneficial properties to human health, including antioxidant, antiproliferative, anti-inflammatory, anti-diabetic, anti-obesity, antibacterial, antiviral activities, among others [1,3,172]. Dietary PCs have also shown relevant anti-diabetic properties due to effectiveness to suppress post-prandial hyperglycaemia achieved by several mechanisms (**Figure 7**): enhancing of β-cell function, stimulation of insulin secretion, suppression of glucose release from the liver and improve glucose uptake in peripheral tissues by modulating intracellular signalling [5,6,16,172]. However, their main hypoglycaemic effect is primarily attributed to their binding to carbohydrate hydrolysing enzymes, which delays dietary carbohydrate intestinal breakdown and absorption. In humans, AMY and GLUs enzymes are responsible for the hydrolysis of polysaccharides and oligosaccharides, to produce glucose. [5,20,31,42]. These two enzymes can be acting at the same time, whereas the AGLU activity would be the rate-limiting step in starch hydrolysis [20]. Therefore, inhibition of the latter enzyme is more attractive within the search of new hypoglycaemic agents [14].

Similarly, the inhibitory activity of PCs towards PL is the main mechanism by which these compounds can prevent hyperlipidaemia and obesity [18,20,23,64]. The decreased digestion and absorption of dietary fats (triacylglycerols, fats and oils) lead to overall decreased caloric absorption, ultimately leading to weight loss [18,23]. In this view, inhibition of digestive enzymes by PCs is an effective and established approach to manage hyperglycaemia and hyperlipidaemia [18,21,31,32,90]. The use of synthetic drugs (like acarbose, miglitol, voglibose and orlistat) is very common, however, there have been reported undesired side effects from their intake (flatulence, diahrea, liver toxicity, abdominal pain, among others) [2,18,20,33,90] (**Table 1**). Therefore, PCs from natural products have been extensively evaluated as safe, cost-effective therapeutic agents for diabetes and obesity, throughout digestive enzyme activity inhibition [3,5,16,20,21,31,32,172].

Many studies have associated the increase in the consumption of PC-rich fruit and vegetables with the reduction on the risk of certain chronic diseases, including T2DM [18,85,94,171–173]. There is some evidence that berries have a favourable potential to inhibit key enzymes linked to T2DM and obesity, so their consumption seems highly beneficial aside from their nutritional value [5,18,21,31,32,61,65,89,93,154]. Additionally, leaves from BPPs are known to have similar phenolic composition to berries, but in higher amounts [34,80,87]. Therefore, leaves resulting from pruning and harvesting may be used as an alternative source of bioactive compounds for the development of food supplements, functional foods and/or nutraceuticals [34].

In the present work, different correlations were observed between total individual phenolic content (TIPC) of analysed extracts and inhibition of digestive enzymes: glucosidases ($r \geq -0.636$),

AMY ($r \geq$ -0.481) and PL ($r \geq$ -0.579) (**Table 26**). These low correlations could be justified by the diverse phenolic composition of analysed extracts (Chapter III). The same was verified in other studies [18,31,90,98,173].

Table 26 – Pearson's correlation coefficients (r) between digestive enzymes inhibitory assays and phenolic composition of analysed extracts. TIPC: total individual phenolic content; ANTCs: anthocyanins; HCAs: hydroxycinnamic acids; HBAs: hydroxybenzoic acids; FLAVOs: flavonols; FLAVAs: flavan-3ols; FLAVNs: flavanones; ELGTs: ellagitannins; Y: yeast; R: rat.

	TIPC	**ANTCs**	**HCAs**	**HBAs**	**FLAVOs**	**FLAVAs**	**FLAVNs**	**ELGTs**
Y-AGLU	-0.636	0.01	-0.076	-0.267	-0.431	-0.466	-0.187	**-0.449**
R-AGLU	-0.758	0.501	-0.405	-0.474	**-0.852**	-0.687	-0.326	-0.57
BGLU	-0.842	0.415	-0.558	-0.310	**-0.810**	-0.574	-0.218	-0.567
AMY	-0.481	0.069	0.045	-0.450	-0.405	-0.444	-0.227	**-0.437**
PL	-0.767	0.449	-0.18	-0.312	-0.811	-0.753	-0.348	**-0.597**
Berries	**TIPC**	**ANTCs**	**HCAs**	**HBAs**	**FLAVOs**	**FLAVAs**	**FLAVNs**	**ELGTs**
Y-AGLU	-0.477	**-0.525**	-0.041	-0.451	-0.170	-0.192	0.748	-0.231
R-AGLU	-0.589	**-0.550**	-0.101	-0.416	-0.362	-0.200	0.586	-0.379
BGLU	-0.889	**-0.869**	-0.381	-0.187	-0.185	-0.110	0.780	-0.562
AMY	-0.300	-0.216	-0.225	-0.429	**-0.510**	-0.136	0.424	-0.302
PL	-0.579	**-0.502**	0.073	-0.273	-0.397	-0.042	0.696	**-0.509**
Leaves	**TIPC**	**ANTCs**	**HCAs**	**HBAs**	**FLAVOs**	**FLAVAs**	**FLAVNs**	**ELGTs**
Y-AGLU	-0.776	-0.024	0.025	-0.466	**-0.676**	-0.569	-0.408	-0.498
R-AGLU	-0.908	-0.189	-0.245	-0.309	**-0.669**	-0.425	-0.319	-0.332
BGLU	-0.983	-0.371	**-0.618**	-0.079	-0.490	-0.061	-0.111	-0.187
AMY	-0.619	-0.050	-0.138	-0.458	**-0.660**	-0.577	-0.362	-0.471
PL	-0.583	-0.131	-0.207	-0.670	-0.653	**-0.692**	-0.442	-0.345

To further understand the main compounds responsible for the reported bioactivities, the conclusions about the analysis of correlation were divided for the whole tested materials (berries and leaves) and also to specific species (**Table 27**). In the case of berries, glucosidases seemed mainly inhibited by anthocyanins (ANTCs) ($r \geq$ -0.525), AMY by flavonols (r = -0.510) and PL by ellagitannins ($r \geq$ -0.509) (**Table 27**). Flavonols ($r \leq$ -0.669) and HCAs (r = -0.618) were the main inhibitors of glucosidases by leaves extracts, while flavonols (r = -0.660) and flavan-3-ols (r = -0.692) were key inhibitors of AMY and PL, respectively (**Table 27**). Correlations between TIPC and inhibitory activities by separated species (*M. faya*, *R. grandifolius* and *Vaccinium spp*.) was improved: glucosidases ($r \geq$ -0.919), AMY ($r \geq$ -0.709) and PL ($r \geq$ -0.850) (**Table 27**). This is due to the

similarities between samples and lower number of samples. A general analysis revealed that ellagitannins and flavan-3-ols were the main contributors for the observed activities of *M. faya* and *R. grandifolius* (**Table 27**). HCAs and flavonols were the main active compounds of *Vaccinium spp.* (**Table 27**).

Table 27 - Pearson's correlation coefficients (*r*) between digestive enzymes inhibitory assays and phenolic composition of analysed berry-producing plants. TIPC: total individual phenolic content; ANTCs: anthocyanins; HCAs: hydroxycinnamic acids; HBAs: hydroxybenzoic acids; FLAVOs: flavonols; FLAVAs: flavan-3ols; FLAVNs: flavanones; ELGTs: ellagitannins;Y: yeast; R: rat.

M. faya	**TIPC**	**ANTCs**	**HCAs**	**HBAs**	**FLAVOs**	**FLAVAs**	**FLAVNs**	**ELGTs**
Y-AGLU	-0.995	0.956	0.886	-0.861	-0.932	-0.975	-0.559	**-0.985**
R-AGLU	-0.992	0.966	0.850	-0.855	-0.943	-0.974	-0.553	**-0.979**
BGLU	-0.996	0.953	0.868	-0.859	-0.928	-0.980	-0.543	**-0.987**
AMY	-0.928	0.843	0.766	-0.823	-0.872	-0.879	-0.517	**-0.894**
PL	-0.993	0.947	0.857	-0.855	-0.929	-0.975	-0.540	**-0.979**
R. grandifolius	**TIPC**	**ANTCs**	**HCAs**	**HBAs**	**FLAVOs**	**FLAVAs**	**FLAVNs**	**ELGTs**
Y-AGLU	-0.947	0.988	-0.952	-	-0.982	-0.719	-	**-0.994**
R-AGLU	-0.919	0.982	-0.922	-	-0.961	-0.765	-	**-0.984**
BGLU	-0.939	0.992	-0.947	-	-0.979	0.736	-	**-0.996**
AMY	-0.709	0.906	-0.724	-	-0.802	**-0.947**	-	-0.881
PL	-0.850	0.890	-0.838	-	-0.812	-0.520	-	**-0.898**
Vaccinium spp.	**TIPC**	**ANTCs**	**HCAs**	**HBAs**	**FLAVOs**	**FLAVAs**	**FLAVNs**	**ELGTs**
Y-AGLU	-0.938	0.818	**-0.864**	0.622	-0.835	-0.158	0.037	0.824
R-AGLU	-0.937	0.962	-0.904	0.624	**-0.921**	-0.356	0.240	0.943
BGLU	-0.957	0.945	**-0.926**	0.650	-0.897	-0.297	0.178	0.930
AMY	-0.498	0.863	-0.427	0.155	**-0.943**	-0.860	0.179	0.814
PL	-0.938	0.851	**-0.867**	0.620	-0.865	-0.210	0.089	0.854

Present data suggested that enzyme inhibition is more influenced by specific phenolic types rather than the total amounts, which agrees with previous works [10,18,61,90]. Different concentrations, molecular weight, size, number and position of substitution (hydroxylation, glycosylation), polymerization, polarity and structural conformations of PCs play a role in enzyme inhibition [6,20]. The structural diversity influence their stability, solubility and binding ability with digestive enzymes [18]. Interaction between PCs and digestive enzymes occur between similar chemical groups (aromatic rings, hydroxyl groups, etc) by non-covalent binding, mainly van der-Waals forces, hydrogen binding, hydrophobic binding, and other electrostatic forces [20,174]. These

inhibitory interactions are mainly by non-competitive mode and are dependent on the chemical structure of PCs [20]. Overall, the PCs-enzymes affinity seem to increase with the complexity of the structures of the PCs (number of hydroxyl groups, polymerization) or the number of hydrophilic sites on the enzyme [6]. This is why flavonoids, usually, display higher inhibitory activities compared to phenolic acids [6,20]. In the case of tannins, their strong ability to bind to proteins can also originate insoluble and indigestible complexes, resulting in the deactivation of digestive enzymes [50,174].

Most studies are conducted with berries crude extracts with a high variety of compounds that may show synergistic and/or antagonistic effects and influence the assay measurements [61,64,65,85,89,93,97,98]. For example, among several fruits chokeberry extract was the most active PL inhibitor [18], while in other study [97] no inhibition was observed when chokeberry extract was used. Fractionation and /or purification of crude extracts improved their inhibitory activities towards digestive enzymes [10,64,115]. The inhibitory effect of individual PCs depends also on target enzyme [32]. For example, some extracts are potent GLUs inhibitors but have poor AMY or lipase inhibitory activities [20,21,32].

ANTCs present in berries seem the most important inhibitors of AGLU activity [18,21,32,89,92,93,98], but a range of different phenolic classes are also effective. Blueberry and blackcurrant extracts, which had the highest ANTCs content, were the most effective inhibitors of AGLU [21]. The extent of inhibition of AGLU is strongly influenced by chemical structure and the sugar units linked to the anthocyanidin [6,42]. Cyanidin showed inhibition of sucrase activity, although to a much lesser extent than its monoglycosides (being higher for cyanidin-3-galactoside), while cyanidin-3,5-diglucoside showed relatively no inhibition [60]. Hence, different glycoside nature at the 3-*O* position of cyanidin is an important factor for modulating the inhibition of AGLU. The mechanism of AGLU inhibition action by ANTCs is not fully understood but it seems competitive (just like acarbose) and results from the structural similarity between the normal substrate maltose and the glucosyl groups β-linked to the ANTC which bind to the active site but are not hydrolysed [32]. Another possibility is that the polar groups present in the active site of the enzyme interact with hydroxyl groups on ANTCs, changing the molecular configuration of the enzyme and its hydrophilic and hydrophobic properties, leading to a change in enzyme activity [42]. A synergistic inhibition due to combination of acarbose and cyanidin glycosides was shown for AGLU [60]. This combination may lead to a reduction of the dose of acarbose in the treatment of T2DM, consequently reducing side effects that occur by the acarbose intake [42]. 5-*O*-CQA is another potent AGLU inhibitor [21,89]. Inhibition of AGLU by CQAs appears to be non-competitive, suggesting binding to, or interaction with, the enzyme at a site other than the active site [5,21]. Interactions between different PCs (ANTCs, flavonols, HCAs) can also improve inhibition of AGLU [65,85,89,98]. For

example, the relatively higher AGLU inhibitory activities of fractionated extracts from *M. rubra* berries than those of the isolated compounds suggested synergistic effects between different compounds [65]. By contrast, it was suggested that the inhibitory effect of blueberries extracts towards AGLU are mainly attributed to phenolic acids rather than ANTCs [85].

While AGLU activity is largely modulated by a wide range of PCs, AMY inhibition seems more specific [5,21,89,98]. AMY activity is primarily affected by condensed (ellagitannins) and hydrolysable tannins (gallotannins and proanthocyanidins, PACs) [21,32,61,89,90,93]. In general, the larger and more complex tannins show higher degree of inhibition against AMY [6]. Raspberry extract was much more effective against AMY than equivalent extracts of blueberry [21,162], suggesting that ellagitannins were the main active components. This trend is similar to that observed in analysed extracts (*Rubus* >> *Vaccinium*)(**Table 24**). Although ANTCs are not crucial for AMY inhibition, their presence can modulate the effectiveness of tested extracts [5,61,97]. For example, a higher ellagitannins content in yellow raspberries did not increase AMY inhibition in comparison with red counterparts [61,90]. This suggested that a synergetic effect between ANTCs and ellagitannins occurred and potentiated the inhibitory activity of red raspberries [32,61]. The same authors reported also a synergetic interaction with combination of rowanberry PACs and acarbose, reducing the acarbose concentration required for AMY inhibition. The management of hyperglycaemia linked to T2DM through plant extracts that have high AGLU and moderate/lower AMY inhibition is desirable [90,115]. Excessive AMY inhibition can lead to abnormal bacterial fermentation of undigested starch in the colon and consequent stomach distention and discomfort (flatulence and diarrhea) [61,89,172]. Hence, berries with low AMY and high AGLU inhibitory activities are preferable candidates as part of a dietary approach to manage early stages of hyperglycaemia linked to T2DM.

The activity of PL seems to be most affected by flavan-3-ols (monomers and oligomers) [18,23,32,64]. The presence of the galloyl group in tannins seems important to enhance their inhibitory activity towards PL [6,32]. For example, polymers of epigallocatechin-3-*O*-gallate (ECGC) were the main hypolipidaemic agents from *M. rubra* leaves [23]. Additionally, extracts with the highest PACs content and degree of polymerization exhibited the strongest PL inhibitory activity [23]. Ellagitannins are also reported to be the main active compounds from for PL inhibition in *Rubus* berries [18,21,64,90,93]. Similar to present work, cloudberries, raspberries and artic bramble were more potent than blueberries against PL [93]. The inhibitory activity of different ANTCs-containing foodstuffs towards PL was positively correlated with their ANTCs content [171]. Among ANTCs, C3G showed the highest PL inhibitory activity (IC_{50} value = 1.17 mg mL^{-1} [97]. By contrast, McDougall and collaborators [64] suggested that just like for AMY, ANTCs are not necessary for PL

inhibition. Nevertheless, it is possible that synergistic interactions between ANTCs and other PCs could occur.

Considering that C3G, 5-*O*-CQA and MCT were the most abundant compounds of some extracts and they were available on the laboratory, their individual inhibitory potential towards digestive enzymes was further evaluated. C3G displayed significant inhibitory activities towards digestive enzymes, with lower IC_{50} values than positive controls in yeast AGLU and PL assays ($p < 0.05$). For rat AGLU and BGLU, C3G showed stronger activities than extracts (being comparable to 1-DNJ in the latter assay). In the case of AMY, its efficiency was similar to *R. grandifolius* berries extracts Previously, C3G has demonstrated potent inhibitory activities towards AGLU and LIP [60,65,89,93,97,171]. The positive effects of ANTCs, including C3G, on the management of T2DM are very well summarised in [42].

5-*O*-CQA was a powerful inhibitor of targeted enzymes, with higher efficiency than positive controls in yeast AGLU, BGLU and PL assays ($p > 0.05$). In the case of mammalian AGLU, it was more effective than extracts. For AMY, it showed comparable activities to *M. faya* berries extracts. 5-*O*-CQA seems a more effective inhibitor of GLUs and PL, as suggested by literature [89,115], even though Worsztynowickz and co-workers [97] found no inhibition of 5-*O*-CQA over PL activity. These findings add to the extensive list of mechanisms through wich CQA exerts a positive action on regulating glucose and lipid metabolism, as previously reviwed [175].

In the case of MCT standard, its higher potency was verified towards BGLU with lower IC_{50} values than positive controls and extracts. It showed comparable to 1-DNJ and *V. padifolium* (mature leaves) extracts in yeast AGLU and AMY assays. Previously [65], MCT was found to be a more effective AGLU inhibitor than C3G and quercetin glycosides. However, an opposite trend was described in the present work (**Table 23**). Nevertheless, our findings suggest that MCT is an active inhibitor of GLUs, although other compounds (like tannins) could also contributed for the measured activity of *M. faya* extracts. For example, fractions from *M. rubra* extracts showed higher inhibitory activities than isolated C3G and MCT, which indicated the involvement or the synergistic effects of different PCs for the inhibitory effects [65].

In general, the present data demonstrate that C3G > 5-*O*-CQA > MCT can be considered as main active hypoglycaemic and hypolypidaemic agents present in analysed extracts. Nevertheless, the action of other components cannot be ruled out since they could interact to additively or synergistically inhibit digestive enzymes. The following phase would be fractionation of extracts to better understand which classes and/or mixtures of PCs are more involved in the inhibitory activities of digestive enzymes.

All analysed extracts inhibited targeted digestive enzymes in a dose-dependent manner, although with different potencies. Overall, the most promising results were obtained from *R. grandifolius* berries extracts and, therefore, this species deserve a special attention as a dietary complementary approach for the control/management of diabetes and obesity. The unique phenolic composition (ANTCs and ellagitannins) in this species (Chapter III) could justify the present data. It is known that these particular classes of PCs could act synergistically to influence digestive enzymes activity [32,61,93]. In the case of *Vaccinium* berries, observed differences could be related to genotype × environment factors that affect the phenolic composition and, therefore, the anti-diabetic effects of blueberries [154].

As for leaves, the results varied according to the tested digestive enzyme. For yeast AGLU, *R. grandifolius* extracts displayed the best inhibitory activities. *V. padifolium* extracts were the strongest samples against AGLU from rat and BGLU, which could be attributed to their high contents in 5-*O*-CQA. Previously, a synergetic inhibition towards AGLU was observed for the combination of ANTCs and 5-*O*-CQA [18,21,89]. It is to be noted that higher effect of *V. cylindraceum* (leaves) on AMY in comparison with *V. padifolium* (**Table 24**) is a result of its higher flavan-3-ols content (Chapter III). The most active extracts towards AMY and PL were *M. faya*. The higher diversity of tannins (gallo- and ellagitannins) in *M. faya* by comparison with other species seems to be the main factor for the observed activities. The lower activities of *Vaccinium* extracts (**Table 24** and **Table 25**) was directly related to their low tannins content (Chapter III). In this view, leaves of *M. faya*, *R. grandifolius* and *Vaccinium* species are interesting alternative sources of bioactive compounds for the development of infusions, food supplements, nutraceuticals and/or functional foods with anti-diabetic purposes.

Although the analysed extracts seemed capable of decreasing post-prandial hyperglycaemia/hyperlipidaemia through inhibition of key digestive enzymes, it is unclear whether they would be effective *in vivo*. Despite some dissonant views [16], the available literature suggest that PCs-rich berries might provide a mechanism for regulating glucose digestion and absorption in the gut and thereby providing an effective management of pre-diabetes symptoms and associated complications. However, one crucial issue that needs to be clarified is whether the ingested PCs that go through gastrointestinal digestion (GID) still maintain their bioactivity. On Chapter III the stability of PCs from targeted BPPs was evaluated in a simulated digestion and a substantial decrease of PPs amounts was observed. However, it is known that most of PCs are stable on the gastric phase [48,49,51,53,54,140,147,153] and therefore reach the duodenum intact where they potentially exert their inhibitory activities towards intestinal digestive enzymes [21,32]. A shortcoming of this work was that the *in vitro* GID was not performed in separated phases (oral, gastric, intestinal) and in that

case the potential effect of post-gastric extracts towards digestive enzymes could be determined and compared with the undigested samples. Nevertheless, since the effects of oral and gastric digestion seem minimal on foodstuufs, it can be expected similar results to those found in undigested samples towards digestive enzymes since they reach the colon with minimal tranformations.

Large ingested PCs from berries (PACs, ellagitannins, etc) are not taken up into the circulation and remain resident in the small intestine where their potential interactions with digestive enzymes can be physiologically relevant [21,41]. However, it is possible that effects in the gastrointestinal (GI) tract may be short–lived due mild-alkaline intestinal conditions and interaction with salts and bile acids that promote their degradation and/or structural changes [49,51,54,56,146]. The few conducted *in vivo* studies indicated that berries PCs may modulate glucose availability through the inhibition of carbohydrate-hydrolysing enzymes, which could influence blood glucose control [5,16].

The obtained results are only indicative, therefore, more research is required to confirm that PCs of BPPs beneficially impact glycaemic responses *in vivo*, through digestive enzymes inhibition, and to understand and exploit the underlying mechanisms.

Chapter III – Results and Discussion

C. Aldose Reductase and Protein Glycation Inhibition

1. Inhibition of Human Aldose Reductase (HAR) activity

Inhibition of digestive enzymes (Chapter IV) is the first significant approach to control glucose levels in the bloodstream. However, the use of a single therapeutic procedure has unfortunately not been successful in overcoming all the complications caused by the high level of glucose in blood [2,4,14]. Hyperglycaemia-induced complications (retinopathy, neuropathy, nephropathy, etc) are mainly associated with the increased activity of the polyol pathway and accumulation of advanced glycation end-products (AGEs) that cause oxidative stress (OS) and vascular damages [66,69].

In this view, the first part of this chapter was to evaluate the ability of berry-producing plants (BPPs) extracts to inhibit HAR, using glyceraldehyde and NADPH as substrate and cofactor, respectively.

1.1. Pre-*in vitro* gastrointestinal digestion

The activity of HAR was reduced by the non-digested extracts in a dose-dependent manner, with IC_{50} values ranging between 0.29 and 4.46 mg mL^{-1} (**Table 28**). Significant differences ($p < 0.05$) were found in the inhibitory activities among analysed extracts (inter and intra-species). Leaves were the morphological part with strongest effects ($p < 0.05$). Among berries, *R. grandifolius* (FX > MX) showed the highest inhibitory activities, followed by *M. faya* > *V. padifolium* ≈ *V. cylindraceum* > *E. umbellata* >> *S. lanceolata* (**Table 28**). A slight different trend was observed for leaves: *R. grandifolius* (MX > FX) > *V. padifolium* (YLs > MLs) > *M. faya* > *V. cylindraceum* > *E. umbellata* >> *S. lanceolata*.

With regard to the activity of the standard compounds, all of them exhibited remarkable inhibition of HAR. Quercetin stands out by its superior inhibitory activity among tested samples ($p < 0.05$) (**Table 28**). Quercetin aglycone and its mono-glycosides were highly effective towards the activity of aldose reductase (AR) [68,69]. 5-*O*-CQA displayed a similar effect to quercetin and was more effective than other standards (cyanidin-3-*O*-glucoside, C3G > myricitrin, MCT). C3G and MCT showed comparable inhibitory activities to *M. faya* leaves extracts. In different studies, caffeoylquinic acids (CQAs) (3-*O*-CQA, 3,4-di-*O*-CQA, 1,3,5-tri-*O*-CQA and 3,4,5-tri-*O*-CQA) and C3G displayed a greater activity towards AR inhibition than quercetin [68,69]. Previously, MCT showed a lower effect than quercetin (IC_{50}: 3.80 and 0.15 µg mL^{-1}, respectively) [176], which agrees with the present data (**Table 28**).

Studies regarding the inhibition of AR by BPPs are scarce in literature, being mostly conducted with medicinal plants and isolated compounds. Two studies on blueberries (*V. myrtillus*

and *V. cyanococcus*) were found [69,173] and a low activity (IC_{50} = 16.80 mg mL^{-1} DE) was reported for the latter species [173].

Table 28 - *In vitro* inhibitory activities of analysed extracts towards human aldose reductase (expressed as IC_{50} value, mg mL^{-1}). Data represent the mean ± standard deviation (n = 3).

		Berries		**Leaves**	
		Non-Digested	Digested	Non-Digested	Digested
E. umbellata		2.19 ± 0.10^{s}	9.34 ± 0.50^{y}	0.86 ± 0.02^{k}	2.51 ± 0.10^{t}
M. faya	MX	0.91 ± 0.04^{k}	N.D.	0.50 ± 0.02^{fg}	N.D.
	FL	0.84 ± 0.03^{j}	N.D.	0.45 ± 0.02^{e}	N.D.
	ASJ	0.80 ± 0.02^{j}	N.D.	0.40 ± 0.03^{cd}	N.D.
	BV	0.72 ± 0.03^{i}	4.79 ± 0.17^{w}	0.37 ± 0.01^{c}	1.09 ± 0.03^{o}
	SX	0.98 ± 0.02^{n}	N.D.	0.40 ± 0.01^{cd}	N.D.
	RJ	1.05 ± 0.02^{o}	N.D.	0.52 ± 0.02^{g}	N.D.
	PM	0.88 ± 0.03^{k}	N.D.	0.43 ± 0.01^{de}	N.D.
	TC	0.74 ± 0.03^{i}	N.D.	0.36 ± 0.01^{c}	N.D.
R. grandifolius	FX	0.52 ± 0.02^{g}	1.97 ± 0.09^{r}	0.35 ± 0.01^{c}	0.89 ± 0.03^{k}
	MX	0.64 ± 0.03^{h}	N.D.	0.26 ± 0.01^{b}	N.D.
S. lanceolata		4.46 ± 0.17^{u}	12.41 ± 0.59^{z}	3.61 ± 0.14^{t}	9.07 ± 0.38^{x}
V. cylindraceum		0.90 ± 0.03^{kl}	3.50 ± 0.12^{u}	0.73 ± 0.03^{i}	1.70 ± 0.07^{k}
V. padifolium		0.93 ± 0.04^{l}	3.58 ± 0.11^{u}	0.29 ± 0.01^{b}*	0.93 ± 0.02^{m}*
				0.43 ± 0.02^{de}**	1.24 ± 0.04^{p}**
Reference Compounds					
Quercetin		0.10 ± 0.01^{a}	N.D.		
Cyanidin-3-glucoside		0.38 ± 0.01^{c}	N.D.		
5-*O*-Caffeoylquinic acid		0.13 ± 0.01^{a}	N.D.		
Myricetin		0.49 ± 0.02^{f}	N.D.		

*Young leaves; **Mature leaves. N.D.: Not determined. MX: Machico; FL: Faial; ASJ: Arco de S. Jorge; BV: Boaventura; SX: Seixal; RJ: Ribeira da Janela; PM: Porto Moniz; TC: Terceira; FX: Funchal. Means not sharing the same letter are significantly different at $p < 0.05$ probability level.

1.2. Post *in vitro* gastrointestinal digestion

After simulated gastrointestinal digestion (GID), the HAR inhibitory activity of analysed samples was significantly decreased ($p < 0.05$). The IC_{50} values ranged from 0.89 – 12.41 mg mL^{-1} (**Table 28**). The increase of IC_{50} values (from 2.28 up to 6.66-fold) mean that after *in vitro* GID extracts displayed much lower inhibitory activities against HAR. This should be linked with the reduced amounts of phenolic compounds (PCs) present in the digested extracts (Chapter III).

Moreover, possible alterations on the PCs structure could also justify the obtained results. Although in lower potency, PCs present in digested extracts still displayed inhibitory effects against HAR. Significant differences were between morphological parts and targeted species ($p < 0.05$). Berries of *R. grandifolius* showed the highest activity, followed by *V. padifolium* ≈ *V. cylindraceum* > *M. faya* > *E. umbellata* > *S. lanceolata*. For leaves, *R. grandifolius* was still the most active sample and the order of the most potent HAR inhibitors was as follows: *V. padifolium* > *M. faya* > *V. cylindraceum* > *E. umbellata* > *S. lanceolata*. No studies regarding the effect of simulated digestion in AR activity were found in literature to establish a comparison with present data.

1.3. General Discussion

A moderate correlation was observed between total individual phenolic content (TIPC) and HAR inhibitory activity (r = -0.605) (**Table 29**), higher than that ($r \geq 0.435$) presented by Wu and co-workers [173]. From this correlational analysis, it can be inferred that as for previous enzymatic assays (Chapter IV) the type of PCs is more important than total amounts for inhibition of HAR. In the case of berries, low correlations were observed (**Table 29**). Flavonols (r = -0.610) seemed key compounds for the observed inhibitory activities of berries and leaf extracts. Analysis by species, showed an improvement of correlation values (**Table 29**). Ellagitannins were main contributors for *M. faya* and *R. grandifolius*, while HCAs were relevant for *Vaccinium spp.* (**Table 29**). After *in vitro* digestion, TIPC x HAR correlations were improved (r = -0.825) compared to pre-digestion (**Table 29**), which might be linked to the small number of analysed samples. After digestion, anthocyanins (ANTCs) and flavonols were the main contributors for berries and leaves, respectively (**Table 29**).

HAR is the first enzyme in the polyol pathway, which in hyperglycaemia condition, reduces the excessive glucose to sorbitol with consumption of co-factor NADPH. Accumulation of sorbitol in tissues is implicated in the development of degenerative complications of type-2 diabetes (T2DM) (retinopathy, neuropathy, nephropathy, etc) due to osmotic stress (**Figure 8**) [66–68,173]. The increased activity of the polyol pathway also contributes to the formation of fructose (by oxidation of sorbitol) and dicarbonyls, which later conjugate with proteins and promotes AGEs formation (**Figure 8**) [12,66–68]. Moreover, depletion of NADPH could intensify cellular OS, since it is necessary for ghutathione regeneration (**Figure 8**) [4,12,17,67]. So, reduction of the polyol pathway activity by inhibition of HAR seems to offer the possibility of reducing long-term diabetic complications [3,6,67,68]. Currently, epalrestat (a carboxylic acid derivative) is the only commercial HAR inhibitor, available in Japan, China and India, for the treatment of diabetic neuropathy [67,100]. Other synthetic drugs (alrestatin, tolrestat, sorbinil, etc) have been developed, but show relatively low efficiency and

safety issues (liver toxicity) [69,100]. Thus, there is an urgent need for development of new effective agents [69].

Table 29 - Pearson's correlation coefficients (*r*) between human aldose reductase (HAR) inhibitory assay and phenolic composition of analysed berry-producing plants (BPPs) (pre- and post *in vitro* digestion). TIPC: total individual phenolic content; ANTCs: anthocyanins; HCAs: hydroxycinnamic acids; HBAs: hydroxybenzoic acids; FLAVOs: flavonols; FLAVAs: flavan-3ols; FLAVNs: flavanones; ELGTs: ellagitannins.

Pre-digestion	**TIPC**	**ANTCs**	**HCAs**	**HBAs**	**FLAVOs**	**FLAVAs**	**FLAVNs**	**ELGTs**
General	-0.605	0.089	-0.164	-0.366	**-0.464**	-0.394	-0.171	-0.424
Berries	-0.409	-0.357	0.085	-0.42	**0.517**	-0.244	0.399	-0.277
Leaves	-0.738	-0.121	-0.086	-0.31	**-0.661**	-0.403	-0.287	-0.402
M. faya	-0.962	0.879	0.768	-0.826	-0.887	-0.921	-0.574	**-0.945**
R. grandifolius	-0.856	0.917	-0.806	-	-0.867	-0.84	-	**-0.913**
Vaccinium spp.	-0.967	0.859	**-0.936**	0.782	-0.819	-0.13	0.005	0.892
Post-digestion	**TIPC**	**ANTCs**	**HCAs**	**HBAs**	**FLAVOs**	**FLAVAs**	**FLAVNs**	**ELGTs**
General	-0.825	-0.069	-0.446	-0.247	**-0.596**	-0.339	-0.19	-0.413
Berries	-0.864	**-0.804**	-0.326	-	0.026	-0.352	0.412	-0.489
Leaves	-0.781	-0.24	-0.367	-0.215	**-0.692**	-0.278	-0.358	0.32

Various natural compounds (PCs, alkaloids, terpenoids) have proven effective *in vitro* AR inhibitors [3,67,69]. The molecular structures of PCs have a great impact on the inhibition of HAR [68]. Kinetic studies suggest that PCs exert their HAR inhibition in both competitive and non-competitive binding [67,68,100]. Flavan-3-ols seem weaker than flavones, flavonols, and flavanones type compounds towards inhibition of AR. However, galloylation of catechins seem to improve their efficiency [68]. Ellagitannins were the main active compounds of Indian gooseberry, with activities comparable to that of quercetin [100]. Among PCs isolated from plant sources, quercetin, kaempferol, CQAs, (epi)gallocatechin-*O*-gallate (EGCG) and ellagic acid are the most promising AR inhibitors and have shown a great potential in the treatment of AR-dependent diabetic complications [3,67,69]**.**

The diverse phenolic composition of analysed extracts (Chapter III) seems to be linked to the different potencies against HAR activity. ANTCs, ellagitannins and 5-*O*-CQA seem to be the major contributors for the inhibition of HAR since *R. grandifolius* (berries and leaves) and *V. padifolium* (leaves) exhibited the most promising results.

2. Inhibition of Advanced Glycation End-Products (AGEs) Formation

Due to the close link between AGEs generation and the increased activity of the polyol pathway, the *in vitro* anti-glycation properties of BPPs extracts, as well as their major constituents, was also studied. In the present study, two models were assayed using ribose and fructose as glycation agents of bovine serum albumin (BSA).

2.1. Pre-*in vitro* gastrointestinal digestion

All analysed extracts inhibited AGEs formation through inhibition of BSA glycation (**Table 30**) in a dose-dependent manner. Different potencies were verified between extracts ($p < 0.05$) with the IC_{50} values ranging between 0.41 and 6.04 mg mL^{-1} DE (**Table 30**). Among berries, *R. grandifolius* (FX > MX) showed the highest inhibitory activities, followed by *V. padifolium* > *V. cylindraceum* > *M. faya* >> *E. umbellata* > *S. lanceolata* (**Table 30**). In the case of leaves the order of the most potent extract was as follows: *V. padifolium* (YL > ML) > *R. grandifolius* > *V. cylindraceum* > *M. faya* > *E. umbellata* > *S. lanceolata*. Leaves extracts showed the best inhibitory activities, regardless of the model ($p < 0.05$).

In the ribose model, all samples were more effective than aminoguanidine (AMG) (**Figure 55**), an investigational AGEs inhibitor drug ($p < 0.05$). The same behaviour was documented before for *V. macrocarpon* [76]. This is might be due to the fact that AMG is not effective in the early stage of protein glycation since it acts as a carbonyl scavenger [70,76,177].

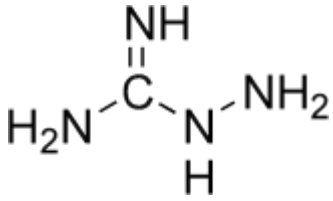

Figure 55 – Chemical structure of aminoguanidine (AMG), an experimental drug for the treatment of nephropathy.

For the fructose model, some differences were observed. In this case, higher glycation rates were found in BSA-ribose assay ($p < 0.05$). It is known that glycation ability occurs in the following increasing order: D-glucose < D-fructose < D-ribose [66,71,74]. This is explained by the almost planar structure of the aldofuranose ring of ribose which causes its instability and high rate of anomerization; the unstable ring is thus susceptible to reactions with nucleophiles, such as amino groups, giving rise to its high efficiency in protein glycation [71]. In the present study, a good correlation was observed between results of both models ($r = 0.850$).

AMG inhibitory activity was similar to that of *S. lanceolata* leaves, but higher than *E. umbellata* and *S. lanceolata* berries ($p < 0.05$) (**Table 30**). On a previous study [74], AMG was more effective than different extracts (blueberries, blackberries, strawberries, raspberries, cranberries, and grapes) in a fructose-BSA model. Such anti-glycation effects of different berries extracts were attributed to their carbonyls scavenging activity [74].

Despite the known antioxidant activity (AOA) of berries and anti-glycation activity of related PCs, only a few works have assessed their effects on AGEs generation. Previously [74], different berries extracts (blueberries, blackberries, strawberries, raspberries, cranberries, and grapes) were capable to inhibit AGEs generation. However, no IC_{50} values were documented. The potency of analysed extracts was inferior to those reported for other *Vaccinium* species (≤ 0.06 mg mL^{-1} DE) [75–77,159,164]. By contrast, cloudberry showed an IC_{50} value of 4.01 mg mL^{-1} DE [159] only inferior to that of *E. umbellata* and *S. lanceolata* (**Table 30**). In previous works, *Vaccinium* berries were more potent than *Rubus* species [74,159]. However, that was no the case for the species of the presen study (**Table 30**). Discrepancies can arise from different phytochemical compositions but the anti-glycation capacities mainly depends on the model system employed [72,177]. There is a great variety of methods with various combinations and dosages/type of protein and sugar, glycation agents (glyoxal, methylglyoxal, fructose, ribose, glucose, etc) as well as incubation periods and temperatures [177].

Standards of C3G, 5-*O*-CQA and MCT were also evaluated for their anti-glycation activities and demonstrated stronger activities than extracts ($p < 0.05$). In the ribose model, 5-*O*-CQA was the most effective (comparable to quercetin inhibitory activity) while C3G and MCT displayed similar effects. In the case of fructose assay, all standards showed alike inhibitory activities (slightly higher for C3G). A previous work [178] reported a similar trend on the inhibition of protein glycation among tested flavonoids (C3G > quercetin > MCT).

Table 30 - *In vitro* inhibitory activities of analysed extracts towards BSA glycation (expressed as IC_{50} value, mg mL^{-1}). Data represent the mean ± standard deviation (n = 3).

		Ribose		**Fructose**	
		Berries	Leaves	Berries	Leaves
E. umbellata		5.35 ± 0.21^{u}	2.38 ± 0.10^{n}	2.75 ± 0.15^{t}	1.22 ± 0.05^{m}
M. faya	MX	3.23 ± 0.08^{r}	1.53 ± 0.02^{j}	1.85 ± 0.03^{r}	0.77 ± 0.02^{i}
	FL	2.99 ± 0.09^{pq}	1.42 ± 0.04^{i}	1.72 ± 0.04^{q}	0.83 ± 0.01^{j}
	ASJ	2.72 ± 0.03^{o}	1.38 ± 0.02^{i}	1.59 ± 0.02^{o}	0.67 ± 0.01^{g}
	BV	2.67 ± 0.11^{o}	1.15 ± 0.05^{g}	1.66 ± 0.05^{p}	0.68 ± 0.02^{g}
	SX	3.07 ± 0.08^{q}	1.33 ± 0.04^{h}	1.80 ± 0.04^{r}	0.73 ± 0.01^{h}
	RJ	3.35 ± 0.09^{s}	1.58 ± 0.03^{j}	1.79 ± 0.03^{qr}	0.87 ± 0.02^{j}
	PM	2.94 ± 0.07^{p}	1.30 ± 0.04^{h}	1.74 ± 0.03^{q}	0.76 ± 0.01^{hi}
	TC	2.86 ± 0.05^{op}	1.21 ± 0.02^{g}	1.69 ± 0.02^{p}	0.65 ± 0.02^{g}
R. grandifolius	FX	1.77 ± 0.05^{k}	0.96 ± 0.05^{e}	0.88 ± 0.02^{k}	0.55 ± 0.01^{f}
	MX	1.87 ± 0.04^{l}	1.07 ± 0.04^{fg}	0.94 ± 0.04^{l}	0.68 ± 0.02^{g}
S. lanceolata		7.04 ± 0.30^{v}	4.47 ± 0.16^{t}	4.10 ± 0.15^{u}	2.30 ± 0.08^{s}
V. cylindraceum		2.35 ± 0.11^{n}	1.21 ± 0.11^{g}	1.53 ± 0.10^{o}	0.57 ± 0.01^{f}
V. padifolium		2.09 ± 0.11^{m}	0.75 ± 0.04^{c}*	1.35 ± 0.06^{n}	0.41 ± 0.01^{d}*
			0.88 ± 0.03^{d}**		0.49 ± 0.01^{e}**
Reference compounds					
Aminoguanidine		9.56 ± 0.36^{v}		2.29 ± 0.13^{s}	
Quercetin		0.11 ± 0.01^{a}		0.24 ± 0.02^{b}	
Cyanidin-3-glucoside		0.24 ± 0.01^{b}		0.18 ± 0.01^{a}	
5-*O*-Caffeoylquinic acid		0.14 ± 0.01^{a}		0.20 ± 0.01^{a}	
Myricetin		0.27 ± 0.02^{b}		0.22 ± 0.01^{ab}	

*Young leaves; **Mature leaves. MX: Machico; FL: Faial; ASJ: Arco de S. Jorge; BV: Boaventura; SX: Seixal; RJ: Ribeira da Janela; PM: Porto Moniz; TC: Terceira; FX: Funchal. Means from the same model not sharing the same letter are significantly different at $p < 0.05$ probability level.

2.2. Post *in vitro* gastrointestinal digestion

After simulated GID, the anti-glycation activity of analysed samples was significantly decreased ($p < 0.05$). The IC_{50} values of assayed extracts ranged from 0.41 – 11.21 mg mL^{-1} DE (**Table 31**) and significant differences were observed among samples ($p < 0.05$). The increase of IC_{50} values (from 1.74 up to 3.59-fold) suggested that digested extracts displayed lower anti-glycation activities. This is believed to be linked to the reduced levels of PCs present in the digested extracts

(Chapter III). Additionally, possible alterations on the PCs structure and could also justify the obtained results. Nevertheless, PCs present in digested extracts were still able to prevent the *in vitro* glycation of BSA. Digested *R. grandifolius* berries showed the highest activity in both assays, followed by *V. padifolium* ≈ *V. cylindraceum* > *M. faya* > *E. umbellata* > *S. lanceolata*. After GID, *V. padifolium* leaves remained the most potent extracts (YLs > MLs) > *R. grandifolius* > *M. faya* > *V. cylindraceum* > *E. umbellata* > *S. lanceolata*.

The strong correlation (r = 0.907) between the two sugar models was maintained after the *in vitro* digestion. Unfortunately, no studies regarding the effect of simulated digestion in AGEs formation were found in literature to establish a comparison with present data.

Table 31 – *In vitro* inhibitory activities of analysed extracts towards BSA-glycation, pre- and post *in vitro* gastrointestinal digestion (expressed as IC_{50} value, mg mL^{-1}). Data represent the mean ± standard deviation (n = 3).

		Ribose		**Fructose**	
Berries		Non-Digested	Digested	Non-Digested	Digested
E. umbellata		5.35 ± 0.21^{m}	9.34 ± 0.21^{r}	2.75 ± 0.15^{l}	6.31 ± 0.25^{p}
M. faya		2.67 ± 0.11^{i}	7.09 ± 0.31^{p}	1.47 ± 0.05^{h}	4.28 ± 0.12^{o}
R. grandifolius		1.77 ± 0.05^{e}	5.43 ± 0.24^{mn}	0.88 ± 0.02^{d}	3.16 ± 0.17^{m}
S. lanceolata		7.04 ± 0.34^{p}	11.21 ± 0.25^{s}	3.10 ± 0.15^{l}	8.15 ± 0.31^{q}
V. cylindraceum		2.35 ± 0.15^{h}	6.24 ± 0.30^{o}	1.53 ± 0.11^{hi}	3.63 ± 0.11^{n}
V. padifolium		2.09 ± 0.14^{h}	6.03 ± 0.21^{o}	1.35 ± 0.06^{g}	3.71 ± 0.13^{n}
Leaves					
E. umbellata		2.38 ± 0.10^{i}	5.69 ± 0.22^{n}	1.22 ± 0.05^{f}	3.25 ± 0.14^{m}
M. faya		1.15 ± 0.05^{d}	3.03 ± 0.07^{j}	0.61 ± 0.02^{c}	1.60 ± 0.03^{i}
R. grandifolius		0.96 ± 0.05^{c}	2.62 ± 0.10^{i}	0.55 ± 0.01^{b}	1.52 ± 0.06^{h}
S. lanceolata		4.47 ± 0.16^{l}	7.41 ± 0.33^{pq}	2.30 ± 0.08^{k}	4.48 ± 0.10^{o}
V. cylindraceum		1.21 ± 0.11^{d}	3.58 ± 0.12^{k}	0.57 ± 0.01^{b}	1.90 ± 0.04^{j}
V. padifolium	YLs	0.75 ± 0.04^{a}	1.92 ± 0.08^{f}	0.41 ± 0.01^{a}	1.09 ± 0.02^{e}
	MLs	0.88 ± 0.03^{b}	2.36 ± 0.09^{h}	0.49 ± 0.01^{a}	1.42 ± 0.05^{gh}

YLs; young leaves; MLs: mature leaves. Means from the same model not sharing the same letter are significantly different at $p < 0.05$ probability level.

2.3. General Discussion

In the present study, a good correlation was observed between TIPC and AGEs inhibitory activity ($r \geq -0.861$)(**Table 32**).

Table 32 - Pearson's correlation coefficients (*r*) between protein glycation inhibitory assays and phenolic composition of analysed berry-producing plants (BPPs) (pre-*in vitro* digestion). TIPC: total individual phenolic content; ANTCs: anthocyanins; HCAs: hydroxycinnamic acids; HBAs: hydroxybenzoic acids; FLAVOs: flavonols; FLAVAs: flavan-3ols; FLAVNs: flavanones; ELGTs: ellagitannins.

Pre-digestion	**TIPC**	**ANTCs**	**HCAs**	**HBAs**	**FLAVOs**	**FLAVAs**	**FLAVNs**	**ELGTs**
Ribose	-0.882	0.231	-0.390	-0.374	**-0.706**	-0.546	-0.190	-0.545
Fructose	-0.861	0.302	-0.370	-0.405	**-0.747**	-0.585	-0.240	-0.555
Berries	**TIPC**	**ANTCs**	**HCAs**	**HBAs**	**FLAVOs**	**FLAVAs**	**FLAVNs**	**ELGTs**
Ribose	-0.761	**-0.726**	-0.293	-0.340	-0.300	-0.192	0.619	-0.470
Fructose	-0.700	**-0.658**	-0.132	-0.304	-0.431	-0.127	0.623	-0.529
Leaves	**TIPC**	**ANTCs**	**HCAs**	**HBAs**	**FLAVOs**	**FLAVAs**	**FLAVNs**	**ELGTs**
Ribose	-0.892	-0.230	-0.311	-0.188	**-0.650**	-0.329	-0.238	-0.289
Fructose	-0.865	-0.219	-0.267	-0.256	**-0.687**	-0.392	-0.229	-0.244
M. faya	**TIPC**	**ANTCs**	**HCAs**	**HBAs**	**FLAVOs**	**FLAVAs**	**FLAVNs**	**ELGTs**
Ribose	-0.993	0.943	0.85	-0.844	-0.931	-0.970	-0.545	**-0.978**
Fructose	-0.994	0.957	0.865	-0.862	-0.940	-0.973	-0.529	**-0.982**
R. grandifolius	**TIPC**	**ANTCs**	**HCAs**	**HBAs**	**FLAVOs**	**FLAVAs**	**FLAVNs**	**ELGTs**
Ribose	-0.959	0.986	-0.964	-	-0.985	-0.690	-0.996	**-0.995**
Fructose	-0.994	0.957	0.865	-0.862	-0.990	-0.562	-0.529	**-0.982**
Vaccinium spp.	**TIPC**	**ANTCs**	**HCAs**	**HBAs**	**FLAVOs**	**FLAVAs**	**FLAVNs**	**ELGTs**
Ribose	-0.953	0.935	**-0.910**	-0.592	-0.900	-0.302	-0.190	0.907
Fructose	-0.906	0.966	-0.860	-0.533	**-0.945**	-0.427	-0.320	0.930

A moderate correlation ($r \geq -0.760$) was also found in a previous work [159], indicating that total amounts of PCs is more pertinent to anti-glycation actitivy than individual compositions [74,76,159]. In general, flavonols ($r \geq -0.706$) seem the main responsible for the inhibition of AGEs formation. ANTCs ($r \geq -0.658$) and flavonols ($r \geq -0.650$) were the main anti-glycation agents from berries and leaves, respectively (**Table 32**). Analysis by species revealed that ellagitannins ($r \geq -0.978$) seem the main contributors for results obtained for *M. faya* and *R. grandifolius*. HCAs ($r \geq -0.910$) were the key PCs for observed inhibitory activities of *Vaccinium* species (**Table 32**).

Table 33 - Pearson's correlation coefficients (*r*) between protein glycation inhibitory assays and phenolic composition of analysed berry-producing plants (BPPs) (post *in vitro* digestion). TIPC: total individual phenolic content; ANTCs: anthocyanins; HCAs: hydroxycinnamic acids; HBAs: hydroxybenzoic acids; FLAVOs: flavonols; FLAVAs: flavan-3ols; FLAVNs: flavanones; ELGTs: ellagitannins.

Post-digestion	**TIPC**	**ANTCs**	**HCAs**	**HBAs**	**FLAVOs**	**FLAVAs**	**FLAVNs**	**ELGTs**
Ribose	-0.918	0.220	**-0.695**	-0.201	-0.761	-0.360	-0.222	-0.342
Fructose	-0.929	0.202	**-0.654**	-0.292	-0.779	-0.410	-0.265	-0.379
Berries	**TIPC**	**ANTCs**	**HCAs**	**HBAs**	**FLAVOs**	**FLAVAs**	**FLAVNs**	**ELGTs**
Ribose	-0.812	-0.752	**-0.314**	-	-0.098	-0.293	0.220	-0.458
Fructose	-0.824	-0.767	**-0.275**	-	-0.028	-0.367	0.399	-0.479
Leaves	**TIPC**	**ANTCs**	**HCAs**	**HBAs**	**FLAVOs**	**FLAVAs**	**FLAVNs**	**ELGTs**
Ribose	-0.990	-0.461	**-0.741**	-0.016	-0.691	-0.153	-0.045	-0.105
Fructose	-0.953	-0.390	**-0.694**	-0.209	-0.687	-0.260	-0.341	-0.191

After *in vitro* digestion, TIPC x AGEs correlations were slightly improved ($r \geq -0.918$) (**Table 33**) compared to pre-digestion (**Table 32**); flavonols remained the main AGEs inhibitors ($r \geq -0.761$). ANTCs ($r \geq -0.752$) and HCAs ($r \geq -0.694$) were the main anti-glycation agents of berries and leaves, respectively (**Table 33**).

One of the inevitable consequences of hyperglycemia is the enhanced accumulation of AGEs due to prolonged exposure of plasma proteins (hemoglobin, serum albumin and transferrin) to elevated blood glucose [70]. Glycation is a series of non-enzymatic reactions between a reducing sugar and protein to yield, at a final stage, AGEs adducts [66,70–73]. Because the human body does not contain any enzymes capable of their structural degradation, AGEs tend to accumulate [179]. Consequently, AGEs lead to damage of protein structure and impairing intracellular physiological functions, while their extracellular presence result in abnormal protein cross-linking (**Figure 56**) [66,70,75]. Additionally, interaction with specific cell surface receptors (RAGEs) triggers the production of ROS, transcription factors (NF-kB) and pro-inflammatory agents (TNF-α, VEGF) [66,70,74,76,159,179]. The combination of these events leads to the increase of OS and a variety of diabetic complications, such as atherosclerosis, diabetic retinopathy, nephropathy, neuropathy, and wound healing (**Figure 56**) [66,70,74,76,159,179].

Thus, agents that inhibit the formation of AGEs have therapeutic potential in management of T2DM [66,70,72,180]. AMG (**Figure 55**) was the first synthetic AGE inhibitor explored in clinical trials [70]. It acts as a nucleophilic trap of reactive carbonyl intermediates such as glyoxal (GO),

methyl-glyoxal (MGO) and 3-deoxyglucosone (3-DG) (**Figure 9**) to form relatively non-toxic adducts, thus preventing their conversion to AGEs [70,177].

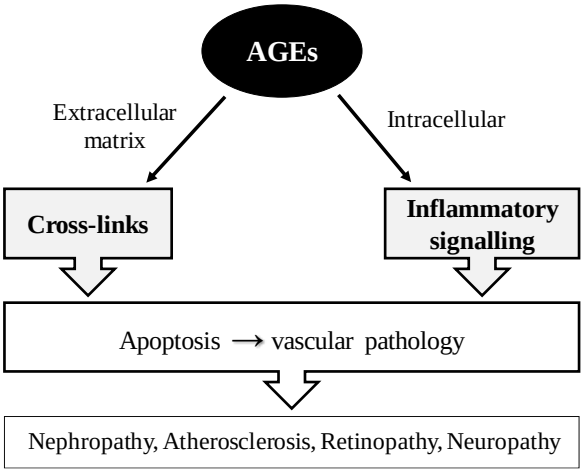

Figure 56 – Simplified mechanism of advanced glycation end-products (AGEs) pathology (adapted from [66]).

However, this drug was not ultimately approved for commercial production because of its low efficiency and hepatotoxic effect and is currently being used as a prototype for obtaining new anti-glycation compounds [70,74]. Hence, there is a great need to find/develop new compounds with higher anti-glycation therapeutics.

Terpenoids, PCs, polysaccharides, among other phytochemicals, have been proven to exhibit anti-glycation effects confirmed by *in vitro* and *in vivo* studies [3,66,70,180–182]. Therefore, inhibition of glycation by natural products can be utilized for pharmacological actions and possibly help in minimizing the pathogenesis of glycation-associated disorders [70,180].

The effective anti-glycation features of PCs are mainly associated with their antioxidant properties and capacity to scavenge reactive carbonyls, which are strongly linked to their molecular structure [6,66,72,74,75,77,159]. Hence, the observed anti-glycation activities (**Table 30 and Table 31**) are attributed to the different phenolic compositions of analysed extracts. Moreover, inhibition of HAR by PCs is beneficial to prevent production of AGEs since, in hyperglycaemia, the polyol pathway contributes to fructose formation (**Figure 8**) [66,67].

Berries intake has been suggested as a dietary approach to reduce or prevent the formation of AGEs [77,159,164,183]. The overall anti-glycation of berries seems related with the presence of other PCs including, but not limited, to ANTCs [74,76,77,159,164,177]. For example, quercetin and quercetin-3-*O*-galactoside ≈ cyanidin-3-*O*-galactoside were documented as main active principles of lingonberry extracts [77]. Hence, a variety of compounds may act synergistically to inhibit AGEs formation [75].

5-*O*-CQA and other CQAs are active anti-glycation compounds, more potent than AMG [70,177,179]. In fact, *V. padifolium* leaves (composed mainly of 5-*O*-CQA) showed the strongest inhibitions compared with other species with lower CQAs content (Chapter III). The anti-glycation effect of CQAs seems achieved by free radicals scavenging and preventing protein crosslinking through interaction with reactive dicarbonyl compounds [66,179].

In the case of flavonoids, hydroxylation on the positions 3', 4', 5 and 7 increases the AGEs inhibitiory ability of the compounds [6,66]. Quercetin is a potent anti-glycation agent [70,73,159] and proved to be the best tested inhibitor ($p < 0.05$) (followed closely by 5-*O*-CQA) (**Table 30**). Other authors found similar results [77,159]. Quercetin strongly inhibits AGEs formation through trapping MGO and GO [70,72,77,177]. Quercetin and other structural similar flavonols (kaempferol, myricetin, etc) seem more effective than other flavonoids and AMG towards inhibition of AGEs generation [70,72,73,184].

Flavan-3-ols have been reported to possess considerable anti-glycation activities, with more significant effects than ANTCs and quercetin [6,70,74,76,77,177]. In fact, proanthocyanidins(PACs)-rich extracts of different *Vaccinium* species have shown the greater inhibitions [74–76]. Trapping and scavenging carbonyls functions are the main anti-glycation mechanisms of PACs [72]. The presence of galloyl groups enhances the anti-glycation activity of flavan-3-ols [6,177], which could justify the inhibitory effects of *M. faya* (**Table 30**).

Both ellagic acids and ellagitannins showed significant inhibitory activities on AGEs generation [6,177]. Still, the total amounts of PCs seem more relevant for the anti-glycation activities than individual components [70,74,76,159], as oppose to enzymatic inhibitory assays.

In this study, AGEs formation was evaluated by BSA-ribose and fructose models. Although ribose presented a higher reactivity, inhibition of fructose-protein glycation is of greater importance since this model closer mimics the human system [74]. Fructose is produced through the oxidation of sorbitol (polyol pathway) (**Figure 8**). Hence, hyperglycaemia contributes for the accumulation of fructose in some cells and tissues (ocular lens, peripheral nerves, blood vessels, etc) [66,71,74].

In conclusion, the obtained results suggested that analysed extracts and major components exerted anti-diabetic activity by double action *i.e.* via simultaneous inhibition of polyol pathway and protein glycation. Furthermore, this study indicates the another potential therapeutic target of BPPs as possible protective agents against long-term diabetic complications, besides hypoglycaemic effects through modulation of digestive enzymes activity (Chapter IV). However, *in vivo* studies to provide a stronger basis for these evidences are needed before it can be established and incorporated in therapeutic measures.

Chapter III – Results and Discussion

D. Antioxidant Activity

1. Antioxidant Activity (AOA)

Type-2 diabetes melittus (T2DM) is associated with oxidative stress (OS), resulting from an imbalance between free-radical-generating and the antioxidant systems of the body [2,31,42,92]. The mythocondrial dysfunction, overactivity of the polyol pathway and increased AGEs formation, induced by hyperglycaemia, involves several oxidative processes that causes ROS production. Therefore, inhibition or reduction of ROS formation is proposed as a key mechanism for the management/control of hyperglycaemia associated with T2DM [42,65,185].

There are several methods reported for the overall measurement of the AOA of plant extracts [2,27,29,51]. In this work, the AOA of each sample (undigested and digested) was determined by four distinct *in vitro* assays using synthetic ($ABTS^{\bullet+}$ and $DPPH^{\bullet}$) and biological ($NO^{\bullet}$ and $O_2^{\bullet-}$) radicals. Results are shown in the following sections and their discussion will be separated by experimental assays.

1.1. ABTS Radical ($ABTS^{\bullet+}$) Scavenging Assay

1.1.1. Pre-*in vitro* gastrointestinal digestion

The AOA of tested samples was estimated as scavenging potential towards $ABTS^{\bullet+}$ (**Table 28**). Significant differences ($p < 0.05$) were observed among analysed extracts in this assay. The values varied from 0.59 to 8.72 mmol TE g^{-1} DE (**Table 28**). The order of the most potent berries extracts was as follows: *R. grandifolius* (FX > MX) > *V. padifolium* > *V. cylindraceum* > *M. faya* > *E. umbellata* > *S. lanceolata*. Leaves extracts were the most active samples (2.61 to 8.35 times fold): *M. faya* > *V. padifolium* (YLs) > *R. grandifolius* (FX > MX) > *V. padifolium* (MLs) > *E. umbellata* > *V. cylindraceum* > *S. lanceolata*.

Previously [106], higher and lower activities were documented for *M. faya* berries and leaves (2.50 and 4.81 mmol TE g^{-1} DE), respectively. Leaves of *M. rubra* showed inferior values (2.58 - 3.43 mmol TE g^{-1} DE)[117,186]. Other authors [65,82,116] have reported the *in vitro* antioxidant activities of *M. rubra* extracts, but in different units.

The AOA of *R. grandifolius* against $ABTS^{\bullet+}$ was reported in a previous work [107]. Contrary to obtained data (**Table 28**), berries were more active than leaves, which could be related to the lack of ellagitannins. By comparison, analysed berries presented higher activities than other *Rubus* species (0.01 - 0.09 mmol TE g^{-1} DE) [114]; but lower than leaves extracts (80.00 – 212.69 mmol TE g^{-1} DE)[87].

From a previous study (Mandrone et al., 2014), *S. nigra* berries extracts were more active towards $ABTS^{\bullet+}$ (1.74 – 2.20 mmol TE g^{-1} DE) than *S. lanceolata* (**Table 28**). A different trend was documented for *S. nigra* (0.33 mmol TE g^{-1} DE) by other authors [24,25].

By comparison, *V. myrtillus* and *V. macrocarpon* extracts presented lower scavenging activities (0.14– 0.35 and 0.79 – 0.96 mmol TE g^{-1} DE for berries and leaves, respectively) [80,131,158]. An opposite trend was observed in other work [79] for berries and leaves of *V. macrocarpon* (2.23 – 2.34 and 9.59 – 10.26 mmol TE g^{-1} DE, respectively).

Table 34 - *In vitro* antioxidant activities of analysed extracts measured by the $ABTS^{\bullet+}$ scavenging assay (expressed as mmol TE g^{-1} DE). Data represent the mean ± standard deviation (n = 3).

		Berries		**Leaves**	
		Non-Digested	Digested	Non-Digested	Digested
E. umbellata		0.68 ± 0.02^{d}	0.17 ± 0.01^{a}	4.71 ± 0.18^{r}	1.90 ± 0.04^{l}
M. faya	MX	1.20 ± 0.04^{gh}	N.D.	7.89 ± 0.37^{v}	N.D.
	FL	1.30 ± 0.04^{i}	N.D.	7.95 ± 0.19^{v}	N.D.
	ASJ	1.43 ± 0.05^{j}	N.D.	8.33 ± 0.17^{x}	N.D.
	BV	1.50 ± 0.04^{k}	0.61 ± 0.02^{c}	8.65 ± 0.22^{y}	3.64 ± 0.08^{q}
	SX	1.32 ± 0.04^{i}	N.D.	8.15 ± 0.24^{xw}	N.D.
	RJ	1.14 ± 0.04^{g}	N.D.	7.59 ± 0.32^{tu}	N.D.
	PM	1.36 ± 0.04^{i}	N.D.	7.95 ± 0.14^{v}	N.D.
	TC	1.45 ± 0.05^{j}	N.D.	8.82 ± 0.18^{y}	N.D.
R. grandifolius	FX	2.89 ± 0.04^{o}	0.80 ± 0.02^{e}	7.54 ± 0.20^{u}	3.46 ± 0.10^{p}
	MX	2.79 ± 0.13^{no}	N.D.	7.17 ± 0.13t	N.D.
S. lanceolata		0.59 ± 0.02^{c}	0.45 ± 0.01^{b}	2.92 ± 0.17^{o}	1.50 ± 0.05^{k}
V. cylindraceum		1.63 ± 0.03^{l}	0.92 ± 0.03^{f}	5.53 ± 0.17^{s}	2.67 ± 0.05^{n}
V. padifolium		2.10 ± 0.02^{m}	1.22 ± 0.06^{h}	7.91 ± 0.40^{vw}*	5.10 ± 0.21^{s}*
				7.08 ± 0.25^{t}**	3.47 ± 0.10^{p}**

*Young leaves; **Mature leaves. MX: Machico; FL: Faial; ASJ: Arco de S. Jorge; BV: Boaventura; SX: Seixal; RJ: Ribeira da Janela; PM: Porto Moniz; TC: Terceira; FX: Funchal. N.D.: not determined. Means not sharing the same letter are significantly different at $p < 0.05$ probability level.

1.1.2. Post *in vitro* gastrointestinal digestion

After *in vitro* digestion, the AOA of analysed extracts was reduced ($p < 0.05$). The values varied from 0.17 to 5.10 mmol TE g^{-1} DE (**Table 28**). AOA of berries was more affected by the *in vitro* GID (24.18 – 75.12% decrease) than leaves (35.49 – 59.57% decrease). The order of the most potent berries extracts was as follows: *V. padifolium* > *V. cylindraceum* > *R. grandifolius* > *M. faya*

> *S. lanceolata* > *E. umbellata*. Leaves extracts displayed the highest activities (1.82 to 11.32 times fold): *V. padifolium* (YLs) > > *M. faya* > *R. grandifolius* ≈ *V. padifolium* (MLs) > *V. cylindraceum* > *E. umbellata* > *S. lanceolata*.

Similarly to the present work (**Table 28**), the AOA of *M. rubra* and *S. nigra* berries was decreased after GID [24,25,116]. In the latter species, lower values (0.18 mmol TE g^{-1} DE) were obtained compared to that of digested *S. lanceolata* (**Table 28**). On another study [153], a decrease of AOA (-83%) was observed in *Vaccinium spp* digested berries.

1.2. DPPH• Radical Scavenging Assay

1.2.1. Pre-*in vitro* gastrointestinal digestion

The AOA of tested samples was estimated as scavenging potential towards DPPH• radical (**Table 35**). Significant differences ($p < 0.05$) were found among analysed extracts in this test. The values varied from 0.13 to 1.94 mmol TE g^{-1} DE (**Table 35**). Berries of *R. grandifolius* (FX > MX) showed the highest activity, followed by *V. padifolium* > *V. cylindraceum* > *M. faya* > *S. lanceolata* > *E. umbellata*. Leaves extracts were the strongest radical scavengers (1.52 to 3.39 times fold): *M. faya* > *R. grandifolius* (FX) > *V. padifolium* > *R. grandifolius* (MX) > *V. cylindraceum* > *E. umbellata* > *S. lanceolata*.

Previous studies [103,105,129,157] have reported the radical scavenging activity of *E. umbellata* extracts (berries, leaves and stems) against DPPH• radical. However, the results are expressed as the IC_{50} values which makes it impossible to establish a comparison with present data (**Table 35**).

In another work [106], similar and higher activities were documented for *M. faya* berries and leaves (1.90 and 4.07 mmol TE g^{-1} DE), respectively. Berries and leaves of *M. rubra* showed superior activities (2.92 – 3.97 and 3.00 – 4.93 mmol TE g^{-1} DE) [62,117,186] than analysed *M. faya* extracts (**Table 35**). Other works [65,82,116] have reported the *in vitro* antioxidant activities of *M. rubra* extracts, but in different units.

By comparison with literature [98,115,160], *R. grandifolius* berries presented higher activities than other *Rubus* species (0.30 - 0.63 mmol TE g^{-1} DE). After XAD-7 purification for removal of sugars and organic acids, higher values were obtained for blackberries (1.59 mmol TE g^{-1} DE)[115]. Previously works [31,98,107] on *Rubus* species have determined their antioxidant activities, but results were expressed in different units.

Berries of *S. nigra* were more active (0.62– 0.71 mmol TEg^{-1} DE)[150] than *S. lanceolata* (**Table 35**).

V. myrtillus and *V. macrocarpon* berries and leaves presented lower scavenging activity towards DPPH• radical (0.02– 0.40 and 0.39 – 0.60 mmol TE g^{-1} DE, respectively) [80,84,115,131,158] than analysed *Vaccinium* species (**Table 35**). However, after XAD-7 purification, superior values were obtained for blueberries (2.01 mmol TE g^{-1} DE)[115].

Table 35 – *In vitro* antioxidant activities of analysed extracts measured by the DPPH• radical scavenging assay (expressed as mmol TE g^{-1} DE). Data represent the mean ± standard deviation (n = 3).

		Berries		**Leaves**	
		Non-digested	Digested	Non-digested	Digested
E. umbellata		0.13 ± 0.01^{ab}	0.14 ± 0.01^{b}	0.84 ± 0.02^{s}	0.33 ± 0.01^{f}
M. faya	MX	0.35 ± 0.01^{g}	N.D.	1.72 ± 0.03^{v}	N.D.
	FL	0.43 ± 0.01^{i}	N.D.	1.75 ± 0.04^{vw}	N.D.
	ASJ	0.47 ± 0.01^{j}	N.D.	1.78 ± 0.04^{w}	N.D.
	BV	0.54 ± 0.02^{l}	0.20 ± 0.01^{c}	1.94 ± 0.04^{z}	0.59 ± 0.02^{m}
	SX	0.43 ± 0.01^{i}	N.D.	1.76 ± 0.01^{vw}	N.D.
	RJ	0.35 ± 0.01^{g}	N.D.	1.84 ± 0.03^{u}	N.D.
	PM	0.41 ± 0.01^{h}	N.D.	1.58 ± 0.04^{w}	N.D.
	TC	0.50 ± 0.02^{k}	N.D.	1.66 ± 0.02^{y}	N.D.
R. grandifolius	FX	0.77 ± 0.02^{q}	0.28 ± 0.01^{d}	1.68 ± 0.03^{y}	0.57 ± 0.01^{m}
	MX	0.73 ± 0.02^{r}	N.D.	1.11 ± 0.06^{t}	N.D.
S. lanceolata		0.22 ± 0.01^{c}	0.11 ± 0.01^{a}	0.41 ± 0.02^{h}	0.12 ± 0.01^{a}
V. cylindraceum		0.65 ± 0.02^{o}	0.28 ± 0.01^{d}	0.92 ± 0.03st	0.42 ± 0.01^{hi}
V. padifolium		0.70 ± 0.02^{p}	0.30 ± 0.01^{e}	1.61 ± 0.02^{x}*	0.69 ± 0.01^{op}*
				1.42 ± 0.03^{u}**	0.60 ± 0.01^{n}**

*Young leaves; **Mature leaves. MX: Machico; FL: Faial; ASJ: Arco de S. Jorge; BV: Boaventura; SX: Seixal; RJ: Ribeira da Janela; PM: Porto Moniz; TC: Terceira; FX: Funchal. N.D.: not determined. Means not sharing the same letter are significantly different at $p < 0.05$ probability level.

1.2.2. Post *in vitro* gastrointestinal digestion

After *in vitro* digestion, the AOA of analysed extracts was decreased ($p < 0.05$); values varied from 0.11 to 0.69 mmol TE g^{-1} DE (**Table 35**). In this case, leaves were more affected by the *in vitro* GID (52.22 – 71.28% decrease) than berries (50.78 – 66.10% decrease). The order of the most potent berries extracts was as follows: *V. padifolium* > *V. cylindraceum* ≈ *R. grandifolius* > *M. faya* > *E. umbellata* > *S. lanceolata*. Leaves extracts displayed the highest activities (2.03 to 3.48 times fold): *V. padifolium* > *M. faya* > *R. grandifolius* > *V. cylindraceum* > *E. umbellata* > *S. lanceolata*.

The AOA of digested *M. rubra* leaves decreased about 74.32% compared with initial values [117]. A slightly higher value was documented (0.65 mmol TE g^{-1} DE) compared to digested *M. faya* leaves (**Table 35**). In another work, a loss of AOA was verified after digestion of *M. rubra* berries [116]. A significant reduction (-57.60%) was observed after GID of *V. angustifolium* [54].

1.3. NO• Radical Scavenging Assay

1.3.1. Pre-*in vitro* gastrointestinal digestion

The AOA of tested samples was measured as scavenging potential towards NO• radical (**Table 36**). Significant differences ($p < 0.05$) were found between analysed extracts. The values varied from 0.08 to 0.95 mmol TE g^{-1} DE (**Table 36**). The order of potency of berries extracts was as follows: *R. grandifolius* (FX > MX) ≈ *V. padifolium* > *V. cylindraceum* > *M. faya* > *E. umbellata* ≈ *S. lanceolata*. Leaves displayed the highest activities (1.10 to 3.26 times fold): *R. grandifolius* (FX > MX) > *M. faya* > *V. padifolium* > *V. cylindraceum* > *E. umbellata* > *S. lanceolata*.

Previously [144,187], *S. nigra* and *R. adenotrichus* berries were also effective NO• scavengers, suggesting a potential beneficial effect against inflammation induced by OS. However, results were expressed as IC_{50} values and is difficult to establish a comparison with present data (**Table 36**).

Table 36 - *In vitro* antioxidant activities of analysed extracts measured by the NO radical scavenging assay (expressed as mmol TE g^{-1} DE). Data represent the mean ± standard deviation ($n = 3$).

		Berries		**Leaves**	
		Non-digested	Digested	Non-digested	Digested
E. umbellata		0.08 ± 0.01^{d}	0.02 ± 0.01^{a}	0.39 ± 0.01^{o}	0.14 ± 0.01^{g}
M. faya	MX	0.21 ± 0.02^{i}	N.D.	0.82 ± 0.02^{t}	N.D.
	FL	0.24 ± 0.02^{j}	N.D.	0.84 ± 0.02^{tu}	N.D.
	ASJ	0.31 ± 0.01^{l}	N.D.	0.89 ± 0.02^{vw}	N.D.
	BV	0.25 ± 0.01^{j}	0.10 ± 0.01^{e}	0.94 ± 0.01^{w}	0.42 ± 0.01^{o}
	SX	0.23 ± 0.01^{ij}	N.D.	0.84 ± 0.03^{t}	N.D.
	RJ	0.19 ± 0.01^{h}	N.D.	0.79 ± 0.02^{s}	N.D.
	PM	0.22 ± 0.02^{ij}	N.D.	0.85 ± 0.02^{u}	N.D.
	TC	0.28 ± 0.01^{k}	N.D.	0.88 ± 0.02^{v}	N.D.
R. grandifolius	FX	0.40 ± 0.01^{o}	0.12 ± 0.01^{f}	0.95 ± 0.02^{x}	0.43 ± 0.01^{p}
	MX	0.37 ± 0.01^{n}	N.D.	0.88 ± 0.01^{v}	N.D.
S. lanceolata		0.08 ± 0.01^{d}	0.03 ± 0.01^{b}	0.18 ± 0.01^{h}	0.06 ± 0.01^{c}

V. cylindraceum	0.36 ± 0.01^{n}	0.14 ± 0.01^{g}	0.69 ± 0.02^{qr}	0.32 ± 0.01^{l}
V. padifolium	0.39 ± 0.02^{o}	0.14 ± 0.01^{h}	0.84 ± 0.02^{tu}*	0.42 ± 0.02^{o}*
			0.80 ± 0.02^{s}**	0.37 ± 0.01^{n}**

*Young leaves; **Mature leaves. MX: Machico; FL: Faial; ASJ: Arco de S. Jorge; BV: Boaventura; SX: Seixal; RJ: Ribeira da Janela; PM: Porto Moniz; TC: Terceira; FX: Funchal. N.D.: not determined. Means not sharing the same letter are significantly different at $p < 0.05$ probability level.

1.3.2. Post *in vitro* gastrointestinal digestion

After simulated GID, the AOA of analysed extracts diminished ($p < 0.05$). The values varied from 0.02 to 0.42 mmol TE g^{-1} DE (**Table 36**). The AOA of berries was more affected by the *in vitro* digestion (52.22 – 71.28% decrease) than leaves (61.35 – 76.17% decrease). The order of the most potent berries extracts was as follows: *V. padifolium* ≈ *V. cylindraceum* > *R. grandifolius* > *M. faya* > *S. lanceolata* > *E. umbellata*. Leaves extracts displayed the highest activities (1.09 to 4.79 times fold): *R. grandifolius* > *V. padifolium* (YLs) > *M. faya* > *V. padifolium* (MLs) > *V. cylindraceum* > *E. umbellata* > *S. lanceolata*.

1.4. $O_2^{\bullet-}$ Radical Scavenging Assay

1.4.1. Pre-*in vitro* gastrointestinal digestion

The AOA of tested samples was measured as scavenging potential towards $O_2^{\bullet-}$ radical (**Table 37**). Significant variations ($p < 0.05$) were observed between analysed extracts in this assay. The values varied from 0.03 to 0.81 mmol TE g^{-1} DE (**Table 37**). The order of potency of berries extracts was as follows: *R. grandifolius* (FX > MX) > *V. padifolium* ≈ *V. cylindraceum* > *M. faya* > *S. lanceolata* > *E. umbellata*. Leaves extracts were the most effective (1.19 to 3.43 times fold higher): *V. padifolium* (YLs > MLs) > *M. faya* > *R. grandifolius* (MX > FX) > *V. cylindraceum* > *E. umbellata* > *S. lanceolata*.

Similarly, *V. angustifolium* berries extract was also effective to scavenge $O_2^{\bullet-}$ radical (59.06% inhibition at 10 µg mL^{-1}) [54].

1.4.2. Post *in vitro* gastrointestinal digestion

After *in vitro* GID, the AOA of analysed extracts was reduced ($p < 0.05$). The values varied from 0.01 to 0.29 mmol TE g^{-1} DE (**Table 37**). The AOA of berries was more affected by the *in vitro* GID (59.32 – 78.36% decrease) than leaves (51.15 – 63.34% decrease). A lower loss was reported for *V. angustifolium* berries after simulated digestion [54].

The order of the most potent berries extracts was as follows: *V. padifolium* > *V. cylindraceum* > *R. grandifolius* > *M. faya* > *S. lanceolata* > *E. umbellata*. Leaves extracts displayed the highest

activities (1.97 to 8.05 times fold): *V. padifolium* (YLs) > *M. faya* >*V. padifolium* (MLs) > *R. grandifolius* > *V. cylindraceum* > *E. umbellata* > *S. lanceolata*.

Table 37 - *In vitro* antioxidant activities of analysed extracts measured by the $O_2^{\bullet-}$ radical scavenging assay (expressed as mmol TE g^{-1} DE). Data represent the mean ± standard deviation (n = 3).

		Berries		**Leaves**	
		Non-digested	Digested	Non-digested	Digested
E. umbellata		0.03 ± 0.01^{c}	0.01 ± 0.01^{a}	0.22 ± 0.01^{n}	0.09 ± 0.01^{h}
M. faya	MX	0.19 ± 0.01^{kl}	N.D.	0.43 ± 0.01^{u}	N.D.
	FL	0.20 ± 0.01^{l}	N.D.	0.45 ± 0.02^{v}	N.D.
	ASJ	0.21 ± 0.01^{m}	N.D.	0.49 ± 0.02^{w}	N.D.
	BV	0.23 ± 0.02^{n}	0.06 ± 0.01^{e}	0.54 ± 0.02^{y}	0.28 ± 0.01^{o}
	SX	0.19 ± 0.01^{kl}	N.D.	0.47 ± 0.01^{v}	N.D.
	RJ	0.17 ± 0.01^{j}	N.D.	0.42 ± 0.02^{tu}	N.D.
	PM	0.18 ± 0.01^{k}	N.D.	0.45 ± 0.02^{v}	N.D.
	TC	0.21 ± 0.01^{m}	N.D.	0.51 ± 0.01^{x}	N.D.
R. grandifolius	FX	0.33 ± 0.01^{r}	0.07 ± 0.01^{f}	0.45 ± 0.02v	0.22 ± 0.01^{n}
	MX	0.31 ± 0.01^{q}	N.D.	0.41 ± 0.01t	N.D.
S. lanceolata		0.05 ± 0.01^{d}	0.02 ± 0.01^{b}	0.11 ± 0.01i	0.04 ± 0.01^{c}
V. cylindraceum		0.29 ± 0.01^{p}	0.08 ± 0.01^{g}	0.37 ± 0.02s	0.16 ± 0.01^{j}
V. padifolium		0.30 ± 0.01^{pq}	0.08 ± 0.01^{g}	0.62 ± 0.03z*	0.29 ± 0.01^{p}*
Leaves			N.D.	0.55 ± 0.02^{y}**	0.24 ± 0.01^{o}**

*Young leaves; **Mature leaves. MX: Machico; FL: Faial; ASJ: Arco de S. Jorge; BV: Boaventura; SX: Seixal; RJ: Ribeira da Janela; PM: Porto Moniz; TC: Terceira; FX: Funchal. N.D.: not determined. Means not sharing the same letter are significantly different at $p < 0.05$ probability level.

1.5. General Discussion

Hyperglycaemia condition induce OS mostly through glucose autoxidation, overactivity of the polyol pathway and increased non-enzymatic glycation of proteins [12,17,62,65,70,72,154]. An overproduction of ROS/RNS caused plays a key role in the initiation, promotion and progression of diabetic complications and other pathological conditions [2,17,24,27,28,31,42,56,92]. Once formed, free radicals overwhelm endogenous antioxidant defences (SOD, CAT, GPx, GR), rendering the affected cells and tissues more susceptible to oxidative damage by reacting with biological macromolecules (lipids, nucleic acids and proteins) leading to impaired cellular structure and

functions [2,12,17,26]. Among these reactive molecules, $NO^{\bullet}$, $O_2^{\bullet-}$ and $ONOO^-$ are the most widely studied species and play important roles in T2DM progression [12,17].

It has been suggested that a regular intake of berries would be beneficial to reduce chronic OS and inflammation commonly experienced in T2DM, due to their rich amounts of antioxidants [5,12,35,42,83]. Exogenous antioxidants, such as PCs, may be of great value in the prevention and/or reduction of OS by neutralization or trapping of free radicals [2,12,28,115,144,154]. The free hydroxyls groups of PCs can restore the chemical balance in free radicals by providing hydrogen or electrons and making the molecule stable [2,12,83]. Additionally, PCs can improve the endogenous antioxidant system and prevent the onset and development of long-term diabetic complications [1,15,27,172] (**Figure 18**). Hence, attention has been paid on the AOA of this class of phytochemicals [27].

In the present study, a strong correlation was observed between TIPC and AOA measured by four distinctive assays ($r \geq 0.795$); flavonols being the main contributors ($r \geq 0.764$) (**Table 38**). The same was found in previous works [18,48,51,74,76,80,82,84,92,116,131,141,154,159,160,188] suggesting that phenolic-richer extracts usually exhibit stronger inhibitory effects. The high antioxidant values of leaves are associated with the higher amounts of PCs, such as flavonols, flavan-3-ols, ellagitannins and phenolic acids (Chapter III). It is known that solar radiation, temperature, and other weather conditions affect accumulation of PCs in leaves due to the increased expression of genes related to their biosynthesis [79,80,132]. Anthocyanins (ANTCs) ($r \geq 0.775$) and flavonols ($r \geq 0.610$) were the key antioxidant agents of berries and leaves, respectively (**Table 38**). Ellagitannins ($r \geq 0.979$) and flavonols ($r \geq 0.947$), seem the main contributors for *M. faya* and *R. grandifolius* AOAs (**Table 38**). In the case of *Vaccinium* extracts, HCAs ($r \geq 0.851$) were the main antioxidant compounds (**Table 38**).

After *in vitro* digestion (**Table 39**), TIPC x AOA results was improved ($r \geq 0.879$) compared to pre-digestion (**Table 38**). Flavonols ($r \geq 0.754$) remained the main contributors for the observed activities. ANTCs ($r \geq 0.939$) and flavonols ($r \geq 0.686$) were the key antioxidant compounds of digested berries and leaves, respectively (**Table 39**). A strong correlation was also found by other authors after simulated digestion of berries [51,116,141].

Table 38 - Pearson's correlation coefficients (*r*) between antioxidant activity (AOA) assays and phenolic composition of analysed berry-producing plants (BPPs) (pre-*in vitro* digestion). TIPC: total individual phenolic content; ANTCs: anthocyanins; HCAs: hydroxycinnamic acids; HBAs: hydroxybenzoic acids; FLAVOs: flavonols; FLAVAs: flavan-3ols; FLAVNs: flavanones; ELGTs: ellagitannins.

Pre-Digestion	**TIPC**	**ANTCs**	**HCAs**	**HBAs**	**FLAVOs**	**FLAVAs**	**FLAVNs**	**ELGTs**
$ABTS^{\bullet+}$	0.795	-0.696	0.357	0.490	**0.933**	0.760	0.436	0.628
$DPPH^{\bullet}$	0.850	-0.554	0.355	0.640	**0.875**	0.751	0.424	0.585
$NO^{\bullet}$	0.935	-0.344	0.427	0.449	**0.791**	0.653	0.347	0.571
$O_2^{\bullet-}$	0.962	-0.276	0.424	0.376	**0.764**	0.601	0.298	0.622
Berries	**TIPC**	**ANTCs**	**HCAs**	**HBAs**	**FLAVOs**	**FLAVAs**	**FLAVNs**	**ELGTs**
$ABTS^{\bullet+}$	0.929	**0.723**	0.287	-0.195	0.441	-0.176	-0.496	0.878
$DPPH^{\bullet}$	0.862	**0.775**	0.282	0.195	0.369	0.051	-0.671	0.636
$NO^{\bullet}$	0.891	**0.913**	0.581	0.289	0.089	0.210	-0.658	0.438
$O_2^{\bullet-}$	0.957	**0.843**	0.387	0.012	0.328	0.031	-0.634	0.731
Leaves	**TIPC**	**ANTCs**	**HCAs**	**HBAs**	**FLAVOs**	**FLAVAs**	**FLAVNs**	**ELGTs**
$ABTS^{\bullet+}$	0.815	0.168	-0.020	0.472	**0.610**	0.468	0.432	0.460
$DPPH^{\bullet}$	0.863	0.197	0.084	0.491	**0.630**	0.484	0.377	0.310
$NO^{\bullet}$	0.913	0.292	0.254	0.280	**0.665**	0.386	0.332	0.395
$O_2^{\bullet-}$	0.921	0.309	0.292	0.236	**0.684**	0.358	0.305	0.320
M. faya	**TIPC**	**ANTCs**	**HCAs**	**HBAs**	**FLAVOs**	**FLAVAs**	**FLAVNs**	**ELGTs**
$ABTS^{\bullet+}$	0.975	-0.983	-0.893	0.858	0.957	0.981	0.562	**0.989**
$DPPH^{\bullet}$	0.977	-0.980	-0.889	0.863	0.951	0.985	0.547	**0.989**
$NO^{\bullet}$	0.964	-0.950	-0.872	0.843	0.398	0.973	0.563	**0.983**
$O_2^{\bullet-}$	0.973	-0.956	-0.805	0.836	0.951	0.969	0.553	**0.979**
R. grandifolius	**TIPC**	**ANTCs**	**HCAs**	**HBAs**	**FLAVOs**	**FLAVAs**	**FLAVNs**	**ELGTs**
$ABTS^{\bullet+}$	0.929	-0.998	0.943	-	**0.976**	0.752	-	0.998
$DPPH^{\bullet}$	0.984	-0.845	0.978	-	**0.947**	0.298	-	0.884
$NO^{\bullet}$	0.967	-0.986	0.973	-	**0.993**	0.670	-	0.996
$O_2^{\bullet-}$	0.987	-0.961	0.985	-	**0.995**	0.589	-	0.981
Vaccinium spp.	**TIPC**	**ANTCs**	**HCAs**	**HBAs**	**FLAVOs**	**FLAVAs**	**FLAVNs**	**ELGTs**
$ABTS^{\bullet+}$	0.964	-0.918	**0.922**	-0.661	0.886	0.254	0.132	-0.912
$DPPH^{\bullet}$	0.984	-0.782	**0.947**	-0.738	0.735	-0.014	-0.140	-0.798
$NO^{\bullet}$	0.922	-0.683	**0.851**	-0.685	0.696	-0.570	-0.181	-0.717

$O_2^{\bullet-}$	0.919	-0.749	**0.843**	-0.672	0.777	0.067	-0.059	-0.782

The AOA of berries is mainly due to the high amounts of phenolic acids and flavonoids [5,35,51,83]. ANTCs and 5-*O*-CQA are potent radical scavengers and known as the key contributors to the *in vitro* antioxidant properties of *Vaccinium spp*. [79,81,85,92,133]. The strong AOAs of *M. rubra* have been attributed to C3G and glycosides of quercetin and myricetin [62,65,82,99,185] and the same for *M. faya* can be speculated. Additionally, the presence of galloyl esters enhance such properties [185] and this could justify the obtained results. ANTCs and ellagitannins have been described in the literature as main contributors to antioxidant capacity of *Rubus* species [83,144,160]. ANTCs are known to possess high AOA and radical scavenging activity [133,144]. It is known that the AOA of berries is directly proportional to their ANTCs content [43], which could justify the observed potency among analysed berry species. Ellagitannins, characterised by the presence of several hydroxy functions in ortho position, exhibit a greater ability to donate an hydrogen atom and scavenging unpaired electrons as compared to other phenolic classes [87,144].

Table 39 - Pearson's correlation coefficients (*r*) between antioxidant activity (AOA) assays and phenolic composition of analysed berry-producing plants (BPPs) (post *in vitro* digestion). TIPC: total individual phenolic content; ANTCs: anthocyanins; HCAs: hydroxycinnamic acids; HBAs: hydroxybenzoic acids; FLAVOs: flavonols; FLAVAs: flavan-3ols; FLAVNs: flavanones; ELGTs: ellagitannins.

Post-digestion	**TIPC**	**ANTCs**	**HCAs**	**HBAs**	**FLAVOs**	**FLAVAs**	**FLAVNs**	**ELGTs**
$ABTS^{\bullet+}$	0.879	-0.444	0.756	0.303	**0.838**	0.334	0.299	0.312
$DPPH^{\bullet}$	0.943	-0.226	0.713	0.353	**0.754**	0.341	0.338	0.355
$NO^{\bullet}$	0.977	-0.144	0.690	0.346	**0.775**	0.482	0.326	0.308
$O_2^{\bullet-}$	0.953	-0.287	0.677	0.380	**0.816**	0.442	0.458	0.448
Berries	**TIPC**	**ANTCs**	**HCAs**	**HBAs**	**FLAVOs**	**FLAVAs**	**FLAVNs**	**ELGTs**
$ABTS^{\bullet+}$	0.954	**0.970**	0.816	-	-0.445	0.248	-0.698	0.139
$DPPH^{\bullet}$	0.968	**0.939**	0.576	-	-0.219	0.354	-0.511	0.360
$NO^{\bullet}$	0.996	**0.974**	0.709	-	-0.354	0.265	-0.576	0.310
$O_2^{\bullet-}$	0.985	**0.970**	0.633	-	-0.365	0.398	-0.636	0.318
Leaves	**TIPC**	**ANTCs**	**HCAs**	**HBAs**	**FLAVOs**	**FLAVAs**	**FLAVNs**	**ELGTs**
$ABTS^{\bullet+}$	0.864	0.721	0.642	0.158	**0.707**	0.009	0.266	0.107
$DPPH^{\bullet}$	0.989	0.481	0.592	0.266	**0.686**	0.129	0.367	0.196
$NO^{\bullet}$	0.961	0.349	0.580	0.271	**0.747**	0.368	0.394	0.142
$O_2^{\bullet-}$	0.945	0.319	0.510	0.295	**0.695**	0.268	0.540	0.345

The chemical structure of PCs plays a predominant role in their intrinsic reactivity towards ROS/RNS and hence the AOA [2,29,35,37,66,79]. The presence of aromatic rings and the highly conjugated system with multiple hydroxyl groups, makes PCs good electron or hydrogen atom donors to reactive species [2,66,83]. It seems that these effects are proportional to the number and position of hydroxyl groups on the aromatic rings in the molecules [2,35,53,54,79]. In fact, PCs displaying a catechol (*o*-dihydroxyphenyl) moiety are generally more potent than those containing a simple phenyl group [2,79,84].

Regarding phenolic acids, HCAs present a more potent AOA than HBAs mainly due to the larger distance between the carbonyl group and the aromatic ring. Additionally, the presence of a 7,8-double bond in HCAs also contributes for their higher antioxidant potencial [2].

The higher AOA of flavonoids relative to phenolic acids is linked to the increase number of hydroxyl groups in the aromatic rings [2,79]. The AOA of flavonoids is determined by the configuration of B-, A- and C-rings [2,35]. The presence of a 3',4'-*o*-catechol group in the B-ring significantly enhances the potency of flavonoids (**Figure 57**).

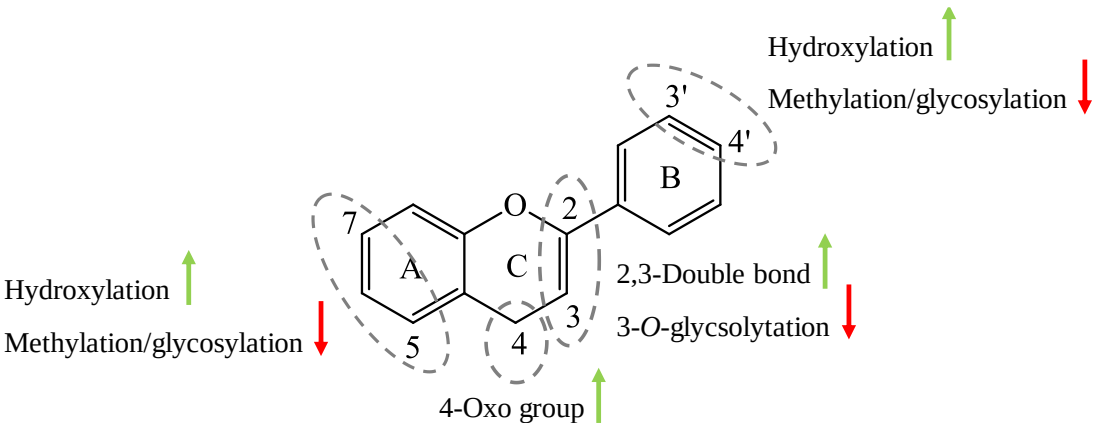

Figure 57 – Main structure-activity relationship of flavonoids (green arrows: enhances the antioxidant activity; red arrows: decreases the antioxidant activity) (adapted from [2]).

In the case of A-ring, a 5,7-m-dihydroxy group strongly increases the AOA of flavonoids (**Figure 57**) [2]. Increasing the number of hydroxyl groups in A- and B-rings improves the AOA, while methoxylation decreases it [2,35]. The conjugation of the B-ring catechol group along with a C-3 hydroxyl group in the C-ring is determinant for the potent AOA of flavonols and flavan-3-ols (**Figure 57**). This conformation allows the formation of intramolecular hydrogen bonds, thus aligning the B-ring with the heterocycle C-ring. This gives planarity to the structure of these compounds, promoting conjugation and electron dislocation to free radicals and improving AOA. By contrast, the absence of the 3-OH group impairs coplanarity and conjugation, thereby compromising the AOA, as

in the case of flavones and flavanones [2]. Furthermore, the presence of a double 2,3-double bond in conjugation with a 4-oxo function in the C-ring improves the AOA, due to electron delocalization into the B-ring (**Figure 57**) [2,35,117]. In this regard, flavonols seem potentially more active antioxidants than ANTCs [35]. In fact, with the exception of flavonols, in all other flavonoids classes the hydroxyl groups in B-ring are the main contributors for their AOAs [2,189]. For flavonols, the C-3 hydroxyl group is determinant for their antioxidant potency, which is potentiated by the 2,3-double bond in the C-ring [189].

Additionally, glycosylation usually decreases the antioxidant potential of PCs [2,35]. Generally, aglycones have strongest AOAs than their corresponding glycosides. The degree of polymerization also influences the AOA. For that reason, PACs (dimers and trimers) and ellagitannis are more potent free radical scavengers than monomeric flavonoids [2,87,144].

Several *in vitro* chemical-based assays have been developed to determine the AOA of natural products based on multiple reaction characteristics and different mechanisms [2,26,27,29,51]. Each methodology only provides an estimate of AOA that is subjective to its conditions and reagents [26,51]. To study the potential antioxidant effects of natural products, it is highly recommended to combine more than one test [26,27,51]. Therefore, the potential anti-radical activities of analysed extracts were evaluated through four distinctive *in vitro* methodologies. $ABTS^{\bullet+}$ and $DPPH^{\bullet}$ are simple and reproducible assays frequently used for preliminary screening of the AOA [27,29,150]. The higher obtained values in the ABTS assay are mainly due to differences in the sensitivity of the method and also because it measures both hydrophilic and lipophilic antioxidants [29]. Another positive aspect of this assay is that it is performed in aqueous media at physiological pH [26,27]. The benefit of employing $DPPH^{\bullet}$ assay is related to the higher stability of the radical and its commercial form being ready to use [27,29]. However, these two methodologies have been criticized for their lack of biological relevance, since they make use of artificial radicals [29]. Hence, $NO^{\bullet}$ and $O_2^{\bullet-}$ assays were also conducted in this study, involving biological radicals. These methodologies seem to provide more relevant information since these radicals are found in biological systems. Also, the observed simultaneous scavenging activity of extracts towards $NO^{\bullet}$ and $O_2^{\bullet-}$ suggest the prevention $OH^{\bullet-}$ and $ONOO^{-}$ generation, which are more reactive species linked to lipid peroxidation [12,27,28]. However, the results reported in the literature on the antioxidant potential may be considered as varied and difficult to compare, because of the differences in analytical methods and sample preparation, as well as variable forms of expression of the results. Additionally, the high variability in antioxidant capacity is highly dependent on the species/genotype, cultivar, edaphoclimatic conditions, agricultural

processes, harvest time and post-harvest practices which are important determinants of the phenolic composition [18,35,81].

Most of the studies evaluate the AOA of berries PCs in their native form, ignoring the intensive metabolism and chemical aterations occurring during digestion, with a consequential impact on their bioactivity. Thus, the physiochemical changes occurring in the GI tract should be considered when evaluating the potential AOA of PCs. Information on the changes of antioxidant effects of BPPs after GID are still scarce in the literature. It should be reminded that after the *in vitro* digestion, phenolic amounts of analysed samples decreased significantly (Chapter III), thus giving an overall loss in AOA. Since PCs are highly sensitive to the mild-alkaline conditions in the intestinal step, during GID studies a fraction of the PCs undergo structural transformations and/or extensive degradation and their bioactivities are affected [48,49,54,56,58,117]. The lower AOAs noted after digestion could arise from the quantitative decrease of the major PCs (Chapter III), as suggested in previous works [24,25,48,51,54,55,116,117,141].

The AOA of berries was, in general, more affected by GID than that of leaves. Notably, extracts with the highest initial AOA did not lead to the highest AOA after simulated digestion. Hence, the AOA after *in vitro* digestion seems dependent on the food matrix and the class of PCs since some compounds are more stable than others [40,141]. We speculate that the degradation of ANTCs after GID was the main cause for the reduced activities of berries extracts. The same was reported by several authors [25,48,54,56,58,59,117,140,141,156]. When exposed to mild-alkaline pH, PCs undergo structural transformations that result in metabolites with different chemical structures/properties and, in general, lower bioactivities than precursor molecules [40,48,49,51,54–56]. The pH variations during digestion may affect the racemisation of molecules creating enantiomers with different biological reactivity [51]. Finally, PCs may also interact with other phytochemicals or macromolecules liberated from the food matrix during digestion, altering their native antioxidant properties [35,53,54]. As a result of digestion process, the antioxidants could not react effectively or their reducing capacities are impaired [54,156]. Nevertheless, despite extensive degradation following digestion, analysed extracts were still active having the capacity to scavenge free radicals (although in minor extent) indicating their potential protective role in the progression of OS-related pathologies after passage through the alimentary tract.

The present work clearly demonstrated the *in vitro* AOA of analysed extracts. However, these results may not be relevant *in vivo* since the applied antioxidant assays do not considered the bioavailability of PCs [26,35]. Animal models and human studies are more appropriate but more

expensive and time-consuming [27,29]. Cell cultures systems have been suggested as intermediate testing methods used to obtain a more meaningful biological information and better correlation with *in vivo* performance [26,27,29,35]. Cellular AOA assays provide cost-effective and relatively fast approach that they take into consideration certain physicochemical aspects (uptake, distribution, and metabolism) that are crucial to the effectiveness of the antioxidant *in vivo* [26,27,29,116,117]. Hence, the antioxidant capacity of an extract is dependent on the bioavailability of their constituents, their synergistic interactions to yield the final antioxidant response at the cellular level [27,29]. Understanding the fate of dietary antioxidants in a real context will clarify the indirect mechanisms by which they may exert beneficial effects in human health [35].

Chapter III – Results and Discussion

E.Cytotoxicity Profiles

1. Cytotoxicity evaluation of the methanolic extracts

The anti-tumor activity of berries is widely documented [83], but no data are available supporting the extracts from analysed species (except for *E. umbellata*). Therefore, we decided to study the cytotoxic activity of selected berry-producing plants (BPPs) (before and after *in vitro* digestion) in human epithelial colorectal adenocarcinoma cells (Caco-2) and resazurin reduction assay. This assay assumes that only cells that are alive are metabolically active and can transform rezasurin into resorufin, which is a fluorescent molecule [128]. This part of the work was a first preliminary toxicological evaluation of the analysed extracts intended for development of formulations for human consumption.

Caco-2 cells culture is the most popular *in vitro* model across the pharmaceutical industry because it exhibits the same biological functions and structure as the human gut [19]. Hence, it is very useful to predict the uptake mechanisms and metabolism of bioactive compounds from foods and drugs [46,140]. Additionally, Caco-2 cell culture have also been coupled to *in vitro* digestion models to study the bioacessibility of food components [46,47].

1.1. Pre-*in vitro* gastrointestinal digestion

The exposure of cells to plant extracts (0.05 – 1.5 mg mL^{-1}) for 24 hours caused a decrease of cell viability in a dose-dependent manner in relation to control (100% of cell viability, cells cultured only in the presence of cell culture medium). Different degrees of potency were observed between morphological parts and species (**Table 40**). Leaves extracts were more effective than the fruit extracts, which presented higher IC_{50} values. The potency of berries extracts was as follows: *M. faya* > *V. padifolium* ≈ *V. cylindraceum* > *R. grandifolius* > *S. lanceolata* > *E. umbellata* (**Table 40**). For leaves, a different trend was observed: *M. faya* > *R. grandifolius* > *V. padifolium* ≈ *V. cylindraceum* > *E. umbellata* > *S. lanceolata*.

For a better understanding of these results, a comparison with alike berry species was established with literature data. Lower activities were documented for *E. umbellata* fruit and leaves extracts (76% and 93% inhibition at 1 mg mL^{-1}, respectively) in HepG2 cells [105]. Alike IC_{50} results were obtained for *M. rubra* leaves in Hep2-G cells [117]. *M. faya* leaves extract was more potent than those of *M. rubra* (IC_{50}: 0.14 – 0.61 mg mL^{-1})[186]. *S. nigra* berries extracts were less active against human colon (NCM460) cells (IC_{50} = 10.71 mg mL^{-1})[24]. Similar cytotoxicity effects were observed for *R. idaeus* (berries and shoots) in Caco-2, HL-60 and HeLa cell lines (0.11 – 0.30 mg mL^{-1})[190,191]. Blackberries and black raspberries extracts were more active against different cell lines

(IC_{50}: 0.05 – 0.19 mg mL^{-1}) [192] than analysed species (**Table 40**). Lower IC_{50} values were also found in literature for different *Vaccinium* berries and cell lines [192–195].

Table 40 – Cytotoxicity of analysed methanolic extracts towards Caco-2 cell lines after 24 hours of exposure. Values are expressed as IC_{50} (mg mL^{-1}).

	Berries		Leaves	
	Non-Digested	Digested	Non-Digested	Digested
E. umbellata	1.41 ± 0.08^{gh}	> 1.5	0.67 ± 0.05^{c}	> 1.5
M. faya	0.60 ± 0.02^{c}	1.48 ± 0.10^{h}	0.10 ± 0.01^{a}	1.04 ± 0.08^{e}
R. grandifolius	0.99 ± 0.04^{e}	1.45 ± 0.10^{gh}	0.17 ± 0.01^{ab}	1.30 ± 0.06^{g}
S. lanceolata	1.32 ± 0.09^{g}	> 1.5	0.83 ± 0.06^{d}	> 1.5
V. cylindraceum	0.80 ± 0.02^{d}	> 1.5	0.25 ± 0.02^{b}	1.21 ± 0.07^{f}
V. padifolium	0.80 ± 0.05^{d}	> 1.5	0.20 ± 0.02^{b}*	0.86 ± 0.06^{d}*
			0.23 ± 0.01^{b}**	1.11 ± 0.05^{ef}**

Data were obtained from two independent experiments with eight replicates (n = 8). *Young leaves; **Mature leaves. Means not sharing the same letter are significantly different at $p < 0.05$ probability level.

1.2. Post *in vitro* gastrointestinal digestion

The cytotoxicity effect of analysed extracts was reduced after *in vitro* gastrointestinal digestion (GID), with increased IC_{50} values (**Table 40**). Nevertheless, digested extracts were still able to affect cell viability at the assayed concentrations. For the berries extracts it was only possible to achieve 50% of inhibition within the tested concentrations for *M. faya* and *R. grandifolius*. An increase from 4 to 10 times-fold was verified for IC_{50} values of leaves extracts before and after *in vitro* digestion (**Table 40**). This time, YLs of *V. padifolium* showed the highest activities, followed by *M. faya* > *V. padifolium* (mature leaves) > *V. cylindraceum* > *R. grandifolius*. *S. lanceolata* and *E. umbellata* leaves showed the lowest effects (IC_{50} > 1.5 mg mL^{-1}).

The same behaviour was verified for similar berries species upon *in vitro* digestion. The first cytotoxic dose of *S. nigra* digested extract was verified at 2.55 mg mL^{-1}, at which cell viability was reduced by 10% [25]. In a follow-up investigation, the IC_{50} of digested *S. nigra* extract was increased from 10.71 to 12.7 mg mL^{-1} (+18.67%)[24]. The IC_{50} of digested *M. rubra* leaves extract was about 19 times higher than before digestion (from 0.09 to 1.73 mg mL^{-1})[117]; it was less effective than *M. faya* (**Table 40**). The cytotoxic effects of *V. angustifolium* extracts towards HT-29 and CRL-1790 cell lines were also decreased after simulated GID [54].

The significant decline of cell cytotoxicity and much higher IC_{50} values of analysed extracts is linked with the significant losses of phenolic compounds (PCs) upon simulated digestion [25,54,117].

1.3. General Discussion

In the present study, analysed extracts showed a cytotoxicity effect in a dose-dependent manner, suggesting that the inhibition of cell growth was associated with the phenolic composition. A moderate correlation was obtained for the total individual phenolic content (TIPC) x cytotoxic effects ($r \geq$ - 0.619)(**Table 41**), which suggests the role of individual or the combination of specific PCs in the presented activities. In general, flavonols were the main contributors (r = - 0.847) (**Table 41**). Anthocyanins (ANTCs) (r = - 0.728) and flavonols (r = - 0.897) seemed the key compounds responsible for the cytotoxic effects of berries and leaves extracts, respectively (**Table 41**).

Table 41 - Pearson's correlation coefficients (r) between cytotoxicity assay and phenolic composition of analysed berry-producing plants (BPPs) (pre- and post *in vitro* digestion). TIPC: total individual phenolic content; ANTCs: anthocyanins; HCAs: hydroxycinnamic acids; HBAs: hydroxybenzoic acids; FLAVOs: flavonols; FLAVAs: flavan-3ols; FLAVNs: flavanones; ELGTs: ellagitannins.

Pre-Digestion	TIPC	ANTCs	HBAs	HCAs	FLAVOs	FLAVAs	FLAVNs	ELGTs
General	-0.787	0.347	-0.327	-0.614	**-0.847**	0.575	-0.180	-0.289
Berries	-0.619	**-0.728**	-0.454	-0.711	0.070	-0.423	0.826	-0.042
Leaves	-0.922	-0.235	-0.445	-0.434	**-0.897**	-0.524	-0.539	-0.259

PCs are considered among most important plant secondary metabolites due to their potent activities to attenuate the initiation, progression and spread of cancers in *in vitro* cellular assays [196]. These anti-cancer properties are mainly attributed to their antioxidant and anti-inflammatory activities [83]. The potential anti-cancer mechanisms of dietary PCs are summarised in **Figure 58**. For a more detailed review please check reference [196].

Berries have been shown to have cytotoxic effects in human cancer cells [83,192]. Among berry phenolics, ANTCs have been shown to be major contributors toward the induction of apoptosis in cancer cells [83,190,192–194]. The cytotoxic and anti-proliferative effects of blueberries (*Vaccinium spp*.) are mainly attributed to their ANTCs content [54,83,193,194]. Their inhibitory effects include two main potential mechanisms, namely redox status modification (antioxidant and anti-inflammatory) and interference with multiple molecular events involved in carcinogenesis (cell-growth, apoptosis, angiogenesis, invasion and metastasis) (**Figure 58**) [194,196]. Non-acylated

mono-glycosylated ANTCs seem to possess higher inhibitory activities towards cell growth, while ANTCs with pelargonidin aglycone and tri-glycosylation have lower effects [196].

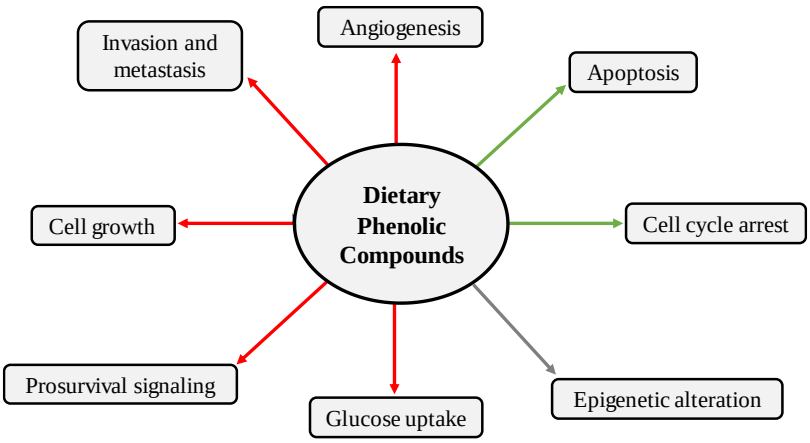

Figure 58 – Potential mechanisms of the anti-cancer activities of dietary phenolic compounds (red arrows: inhibition; green arrows: activation; grey arrow: regulation) (adapted from [196]).

It is also possible that these activities are due to synergetic action of ANTCs with other PCs, such as hydroxycinnamic acids (HCAs) or flavan-3-ols [83,194]. In fact, 5-*O*-CQA, the main compound of *Vaccinium* leaves, has shown significant anti-cancer properties involving different mechanisms such as cell growth reduction, cycle arrest, and apoptosis [193]. By contrast, ANTCs were not responsible for the cytotoxic effects induced by *S. nigra* extract in the cells of colonic mucosa [24]. On another study [195], the ANTCs-rich fraction of *V. vitis-idaea* was considerably less effective than the original extract, the cytotoxic activity being attributed to PACs instead.

Flavonoids were reported to exhibit anticancer effects through several mechanisms, such as inhibiting pro-carcinogen molecules, scavenging of electrophilic molecules, regulating cancer cell signaling pathways, promotion of apoptosis and modulating enzyme activities [117,196] (**Figure 58**). Myricitrin (MCT) is an effective inhibitor of cell proliferation and induced apoptosis in several cancer cell-lines [117,196]. The cytotoxicity of *M. faya* leaves may be related to the high amounts of this compounds. Quercetin and its conjugates (in particular quercetin-*O*-glucoside) have shown powerful cytotoxicity activities [196]. These compounds along with hydrolysable tannins were the main cytotoxic agents on *S. nigra* extracts [24].

Hydrolysable tannins (like (epi)gallocatechin-*O*-gallate) exhibited strong cytotoxic effects against different cancer cells types [24,185,186,196]. Their interaction with cell membrane affects various membrane-dependent cellular processes, such as cell proliferation, cell-cycle and apoptosis [186]. The cytotoxicity effect of *Rubus* species is mainly associated to its high ellagitannins content, which are known to affect nuclear morphology and induce cell apoptosis [190,191,195]. On a

previous study [191], sanguiin H-6 (ellagitannin) isolated from *R. idaeus* showed a high cytotoxic potential (IC_{50} = 0.02 - 0.04 mg mL^{-1}). ANTCs played also a role in the reported activities of *Rubus* berries [83].

Discrepancies with reported result could be due to factors such as cell type, cell density, assayed sample concentrations, stability and/or potential transformation of PCs given the pH of cell culture media, duration of cell exposure to samples, uptake of PCs or metabolites into cells, among others [192].

In the present study, the cytotoxicity effects of BPPs were associated with their phenolic composition/amounts. Considering the obtained results, analysed extracts seem safe to be applied in food/phytopharmaceuticals intended for human intake. However, this was only tested in one cancer cell line. Whether the cytotoxic effects are specific to cancer cell lines in general should be elucidated in future studies. Additionally, the molecular mechanisms involved in this study requires deeper investigation as well as the HPLC analysis of cell lysates to identify which compounds were absorbed by the cell-wall and contributed the most for the observed cytotoxic effects.

Chapter IV – Conclusions and Future Perspectives

1. Conclusions

The main goal of this dissertation was to study six berry-producing plants (BPPs) (native and non-native of Macaronesia region) and evaluate their potential in the control and management of T2DM and obesity, contributing to their economic and commercial valorisation and/or application in the development of phytopharmaceuticals or functional foods. Currently, there is none scientific evidence to clarify their anti-diabetic potential, which leads to the urgent need to perform biochemical studies which promote their consumption and use in large scale in the form of nutraceutical formulations.

From this work, the main conclusions we can withdraw are:

- The mineral composition is varied among the different berry species. The ICP-MS analysis indicated that analysed berries are good sources of essential minerals (K, Ca, P, Na and Mg). Additionally, *E. umbellata*, *R. grandifolius*, and *S. lanceolata* ingestion may potentially contribute to management/control of hyperglycaemia due to their relevant levels of Ca, Mg, and Zn.
- Analysed extracts presented diverse qualitative/quantitative phenolic compositions. In the case of berries, *E. umbellata* showed the lowest TIPC, while *R. grandifolius* the highest. ANTCs were absent in *E. umbellata*, while in the remaining cases they were the main PCs. Flavonols were dominant in *E. umbellata* berries. Based on ANTCs type, analysed berries can be divided into two main groups: cyanidin derivatives (*M. faya*, *R. grandifolius* and *S. lanceolata*) and delphinidin/malvidin derivatives (*Vaccinium spp*.). In the first case, the phenolic profile was composed mainly by one ANTC: C3G for *M. faya* and *R. grandifolius*; cyanidin-3-*O*-sambubioside for *S. lanceolata*. Regarding *Vaccinium* species, it presented a more complex composition: delphinidin, petunidin and malvidin glycosides. It is also worth highlighting the high content of ellagitannins in *R. grandifolius*.

  In the case of leaves, a more diverse and richer phenolic profile was found. Leaves of *S. lanceolata* showed the lowest phenolic amounts and *R. grandifolius* the highest. Ellagitannins were main compounds of *E. umbellata* and *R. grandifolius*. *M. faya* presented the most diverse phenolic composition: flavonols > flavan-3-ols ≈ ellagitannins. *S. lanceolata* was composed by HCAs and flavonols. *V. cylindraceum* had high amounts of flavan-3-ols and HCAs, being the latter category dominant in *V. padifolium*. Anthocyanins (cyanidin derivatives) were detected only in YLs of *V. padifolium*.
- Berries of *R. grandifolius* showed the best inhibitory effects towards digestive enzymes and HAR, which the conjugation of ANTCs and ellagitannins contributed greatly. In the case of leaves, different patterns were observed. For glucosidases (α- and β-), *V. padifolium* were the

most active samples. The high amounts of 5-*O*-CQA can justify the strongest inhibitory activities of *V. padifolium*. *M. faya* showed the most potent inhibitory activities towards AMY and PL. Hydrolysable and condensed tannins of *M. faya* seemed the most important inhibitory agents. Leaves of *R. grandifolius* showed the highest inhibitory activity towards HAR, which was attributed to the high ellagitannins content.

Regarding protein glycation, berries of *R. grandifolius* and leaves of *V. padifolium* showed the best inhibitory results (in both models). Again, ellagitannins and ANTCs could play a major role in berries; while the appreciable amounts of 5-*O*-CQA in *V. padifolium* leaves makes it the most important contributors.

- Berries of *R. grandifolius* displayed the strongest free radical scavenging activities in all assays, which ANTCs were the main contributors. In the case of leaves, *M. faya* were the most active against $ABTS^{\bullet+}$ and $DPPH^{\bullet}$ free radicals. *R. grandifolius* showed the highest anti-radical activities towards $NO^{\bullet}$; while *V. padifolium* was the most potent sample against $O_2^{\bullet-}$ formation. Ellagitannins, flavonols, flavan-3-ols and 5-*O*-CQA played a major role in the displayed activities.
- *M. faya* extracts (berries and leaves) showed the highest cytotoxicity effects towards Caco-2 cells. For this case, ANTCs and flavonols were the main compounds responsible for the observed activities.
- After simulated digestion, there was a considerable decrease in the amounts of PCs in all cases. Berries (in particular *S. lanceolata*) were more affected than leaves, which could be related with the higher susceptibility of ANTCs to the mild-alkaline conditions of the small intestine step. Flavan-3-ols and ellagitannins were also greatly affected by the *in vitro* digestion. Differences in food matrix microstructure may also have contributed for the observed differences on stability of berries and leaves submitted to GID.

  The antioxidant activities of analysed samples remained, although weakened after *in vitro* GID, and extracts were still able to modulate several processes relevant to the control of T2DM.

In conclusion, this study demonstrated the beneficial effects of different BPPs in the management/control of T2DM, since the performed assays related to physiologically important functions in the regulation of carbohydrates metabolism in the body, with anti-glycation and antioxidant properties. These beneficial properties are greatly attributed to the phenolic composition of analysed extracts. In this sense, berries could offer a good dietary strategy to prevent or ameliorate T2DM and associated disorders and provide benefits without the side effects presented by most

available drugs. In call cases, the leaves showed much higher activity than the berries. However, in terms of potential nutraceutical use it must be considered that berries are a food product than can be consumed in larger quantities than the leaves that are ingested in the form of infusions. Hence, leaves should be considered for inclusion in food or phytopharmaceutical supplements in the form of dragees or capsules, enriched or not with extract. Nevertheless, these results are only indicative and confirmatory studies in animals or humans are required to validate obtained data.

2. Future Perspectives

The work developed in this thesis opened some new questions and further studies are necessary to extend the knowledge about these BPPs and their bioactive properties.

- A complete separation/purification, characterization and identification of the main active fractions or compounds of the methanolic extracts must be performed. Additional extractions with less polar solvents (*n*-hexane, chloroform, and ethyl acetate) could also be developed to investigate other potential bioactive molecules (besides PCs) in targeted BPPs for the control and management of T2DM.
- *In silico* studies (molecular modelling and docking) could help to elucidate the type of interaction behaviour and mechanisms of action of extracts towards digestive and HAR enzymes with regards to the probable implications for synthesis of new natural-based drugs.
- Additional *in vitro* tests could be conducted to identify new therapeutic targets of analysed samples, namely DPP-4 inhibitory assay, glucose-6-phosphatase inhibitory assay, LDL oxidation inhibitory assay, angiotensin-converting enzyme (ACE) inhibitory assay, protein tyrosine phosphatase-1B (PTP-1B) inhibitory assay, etc. Cell-based assays, such as evaluation of glucose uptake by Caco-2, HepG2 cell lines, etc, or cellular protection against induced OS toxicity, could demonstrate other beneficial effects of extracts.
- The high AOA revealed by analysed samples requires deeper investigation. Cellular antioxidant assay (CAA) would give more relevant biological information and provides a better predictor for the AOA of extracts at cellular level. Further HPLC-MS analysis of cell lysates could help to identify which compounds were absorbed by the cells and contribute the most for the antioxidant effects.
- The cytotoxicity of extracts should also be tested in other cancer or normal cell lines to elucidate if these effects are specific to cancer cell lines or not. The anti-proliferative activities of extracts against cancer cells is another possible study.

- The *in vitro* digestion model could be improved and simulation of the different steps (oral, stomach and small intestine) should be performed separately to better understand the stability of PPs under different stages of GID.
- Finally, the most promising extracts should be further tested using STZ or ALX-induced diabetic rats/mice to validate their "real" impact on T2DM therapy.

References

1. Anhê FF, Desjardins Y, Pilon G, Dudonné S, Genovese MI, Lajolo FM, et al. Polyphenols and type 2 diabetes: a prospective review. PharmaNutrition. 2013;1(4):105–14.
2. Dias TR, Alves MG, Casal S, Oliveira PF, Silva BM. Promising potential of dietary (poly)phenolic compounds in the prevention and treatment of diabetes mellitus. Curr. Med. Chem. 2017;24(4):334–54.
3. Solayman M, Ali Y, Alam F, Asiful Islam M, Alam N, Ibrahim Khalil M, et al. Polyphenols: potential future arsenals in the treatment of diabetes. Curr. Pharm. Des. 2016;22:549–65.
4. El-Abhar HS, Schaalan MF. Phytotherapy in diabetes: review on potential mechanistic perspectives. World J. Diabetes. 2014;5(2):176–97.
5. Edirisinghe I, Burton-Freeman B. Anti-diabetic actions of berry polyphenols - review on proposed mechanisms of action. J. Berry Res. 2016;6(2):237–50.
6. Xiao J, Hogger P. Dietary polyphenols and type 2 diabetes: current insights and future perspectives. Curr Med Chem. 2015;22(1):23–38.
7. World Health Organization (WHO) Media Centre Diabetes Fact Sheet. 2017. Available from: www.who.int/mediacentre/factsheets/fs312/en/
8. IDF Diabetes Atlas - 8th Edition. International Diabetes Federation. 2017;150 pages.
9. Diabetes: factos e números - o ano de 2015. Relatório Anual do Observatório Nacional da Diabetes. Sociedade Portuguesa de Diabetologia. 2016;68 pages.
10. Kang B-H, Racicot K, Pilkenton S, Apostolidis E. *In-vitro* evaluation of bioactive fractions of blueberry extract for phenolic-mediated inhibition of carbohydrate hydrolyzing enzymes. Int. J. Appl. Res. Nat. Prod. 2016;9(2):33–8.
11. Arulselvan P, Ghofar HAA, Karthivashan G, Halim MFA, Ghafar MSA, Fakurazi S. Anti-diabetic therapeutics from natural source: a systematic review. Biomed. Prev. Nutr. 2014;4(4):607–17.
12. Marrazzo G, Barbagallo I, Galvano F, Gazzolo D, Frigiola A, Orazio ND, et al. Role of dietary and endogenous antioxidants in diabetes. Crit. Rev. Food Sci. Nutr. 2014;54:1599–616.
13. Singh R, Kaur N, Kishore L, Gupta GK. Management of diabetic complications: a chemical constituents based approach. J. Ethnopharmacol. 2013;150(1):51–70.
14. Hung H-Y, Qian K, Morris-Natschke SL, Hsu C-S, Lee K-H. Recent discovery of plant-derived anti-diabetic natural products. Nat. Prod. Rep. 2012;29(5):580.
15. Bahadoran Z, Mirmiran P, Azizi F. Dietary polyphenols as potential nutraceuticals in management of diabetes: a review. J. Diabetes Metab. Disord. 2013;12:43.
16. Kim Y, Keogh JB, Clifton PM. Polyphenols and Glycemic Control. Nutrients. 2016;8(1):17.
17. Tangvarasittichai S. Oxidative stress, insulin resistance, dyslipidemia and type 2 diabetes mellitus. World J. Diabetes. 2015;6(3):456–80.
18. Podsędek A, Majewska I, Redzynia M, Sosnowska D, Koziołkiewicz M. *In vitro* inhibitory effect on digestive enzymes and antioxidant potential of commonly consumed fruits. J. Agric. Food Chem. 2014;62(20):4610–7.
19. Williamson G. Possible effects of dietary polyphenols on sugar absorption and digestion. Mol. Nutr.

Food Res. 2013;57(1):48–57.

20. Martinez-Gonzalez AI, Díaz-Sánchez ÁG, Rosa LA de la, Vargas-Requena CL, Bustos-Jaimes I, Alvarez-Parrilla AE. Polyphenolic compounds and digestive enzymes: *in vitro* non-covalent interactions. Molecules. 2017;22:669–93.
21. McDougall GJ, Kulkarni NN, Stewart D. Current developments on the inhibitory effects of berry polyphenols on digestive enzymes. BioFactors. 2008;34(1):73–80.
22. Kim YS, Lee YM, Kim H, Kim J, Jang DS, Kim JH, et al. Anti-obesity effect of *Morus bombycis* root extract: anti-lipase activity and lipolytic effect. J. Ethnopharmacol. 2010;130(3):621–4.
23. Zhang Y, Chen S, Wei C, Chen J, Ye X. Proanthocyanidins from Chinese bayberry (*Myrica rubra* Sieb. et Zucc.) leaves regulate lipid metabolism and glucose consumption by activating AMPK pathway in HepG2 cells. J. Funct. Foods. 2017;29:217–25.
24. Olejnik A, Olkowicz M, Kowalska K, Rychlik J, Dembczyński R, Myszka K, et al. Gastrointestinal digested *Sambucus nigra* L. fruit extract protects *in vitro* cultured human colon cells against oxidative stress. Food Chem. 2016;197:648–57.
25. Olejnik A, Kowalska K, Olkowicz M, Rychlik J, Juzwa W, Myszka K, et al. Anti-inflammatory effects of gastrointestinal digested *Sambucus nigra* L. fruit extract analysed in co-cultured intestinal epithelial cells and lipopolysaccharide-stimulated macrophages. J. Funct. Foods. 2015;19:649–60.
26. Apak R, Özyürek M, Güçlü K, Çapanoğlu E. Antioxidant activity/capacity measurement. 3. Reactive oxygen and nitrogen species (ROS/RNS) scavenging assays, oxidative stress biomarkers, and chromatographic/chemometric assays. J. Agric. Food Chem.2016;64(5):1046–70.
27. López-Alarcón C, Denicola A. Evaluating the antioxidant capacity of natural products: A review on chemical and cellular-based assays. Anal. Chim. Acta. 2013;763:1–10.
28. Sousa C, Valentão P, Ferreres F, Seabra RM, Andrade PB. Tronchuda cabbage (*Brassica oleracea* L. var. *costata* DC): scavenger of reactive nitrogen species. J. Agric. Food Chem. 2008;56:4205–11.
29. Shahidi F, Zhong Y. Measurement of antioxidant activity. J. Funct. Foods. 2015;18:757–81.
30. Fan J, Johnson MH, Lila MA, Yousef G, De Mejia EG. Berry and citrus phenolic compounds inhibit dipeptidyl peptidase IV: implications in diabetes management. Aritlce ID 479505. Evidence-based Complement. Altern. Med. 2013;13 pages.
31. Sarkar D, Orwat J, Hurburt T, Woods F, Pitts JA, Shetty K. Evaluation of phenolic bioactive-linked functionality of blackberry cultivars targeting dietary management of early stages type-2 diabetes using *in vitro* models. Sci. Hortic. 2016;212:193–202.
32. McDougall GJ, Stewart D. The inhibitory effects of berry polyphenols on digestive enzymes. BioFactors. 2005;23(4):189–95.
33. Borges de Melo E, da Silveira Gomes A, Carvalho I. α- and β-Glucosidase inhibitors: chemical structure and biological activity. Tetrahedron. 2006;62(44):10277–302.
34. Ferlemi A-V, Lamari F. Berry leaves: an alternative source of bioactive natural products of nutritional and medicinal value. Antioxidants. 2016;5(17):20 pages.
35. Manganaris GA, Goulas V, Vicente AR, Terry LA. Berry antioxidants: small fruits providing large

benefits. J. Sci. Food Agric. 2014;94(5):825–33.

36. Hidalgo G-I, Almajano M. Red fruits: extraction of antioxidants, phenolic content, and radical scavenging determination: a review. Antioxidants; 2017;6(1):7.
37. Oroian M, Escriche I. Antioxidants: characterization, natural sources, extraction and analysis. Food Res. Int. 74:10–36.
38. Ignat I, Volf I, Popa VI. A critical review of methods for characterisation of polyphenolic compounds in fruits and vegetables. Food Chem. 2011;126(4):1821–35.
39. Nile SH, Park SW. Edible berries: bioactive components and their effect on human health. Nutrition.30(2):134–44.
40. Karaś M, Jakubczyk A, Szymanowska U, Złotek U, Zielińska E. Digestion and bioavailability of bioactive phytochemicals. Int. J. Food Sci. Technol. 2017;52(2):291–305.
41. Carbonell-Capella JM, Buniowska M, Barba FJ, Esteve MJ, Frígola A. Analytical methods for determining bioavailability and bioaccessibility of bioactive compounds from fruits and vegetables: a review. Compr. Rev. Food Sci. 2014;13(2):155–71.
42. Sancho RAS, Pastore GM. Evaluation of the effects of anthocyanins in type 2 diabetes. Food Res. Int. 2012;46(1):378–86.
43. Castañeda-Ovando A, Pacheco-Hernández M de L, Páez-Hernández ME, Rodríguez JA, Galán-Vidal CA. Chemical studies of anthocyanins: a review. Food Chem. 2009;113(4):859–71.
44. Parada J, Aguilera JM. Food microstructure affects the bioavailability of several nutrients. J. Food Sci. 2007;72(2).
45. Bohn T. Dietary factors affecting polyphenol bioavailability. Nutr. Rev. 2014;72(7):429–52.
46. Hur SJ, Lim BO, Decker EA, McClements DJ. *In vitro* human digestion models for food applications. Food Chem. 2011;125(1):1–12.
47. Alminger M, Aura A-M, Bohn T, Dufour C, El SN, Gomes A, et al. *In vitro* models for studying secondary plant metabolite digestion and bioaccessibility. Compr. Rev. Food Sci. 2014;13(4):413–36.
48. Tagliazucchi D, Verzelloni E, Bertolini D, Conte A. *In vitro* bio-accessibility and antioxidant activity of grape polyphenols. Food Chem. 2010;120(2):599–606.
49. Bermúdez-Soto M-J, Tomás-Barberán F-A, García-Conesa M-T. Stability of polyphenols in chokeberry (*Aronia melanocarpa*) subjected to *in vitro* gastric and pancreatic digestion. Food Chem. 2007;102(3):865–74.
50. Jakobek L. Interactions of polyphenols with carbohydrates, lipids and proteins. Food Chem. 2015 15;175:556–67.
51. Gullon B, Pintado ME, Fernández-López J, Pérez-Álvarez JA, Viuda-Martos M. *In vitro* gastrointestinal digestion of pomegranate peel (*Punica granatum*) flour obtained from co-products: changes in the antioxidant potential and bioactive compounds stability. J. Funct. Foods. 2015;19:617–28.
52. Mosele JI, Macià A, Romero MP, Motilva MJ. Stability and metabolism of *Arbutus unedo* bioactive

compounds (phenolics and antioxidants) under *in vitro* digestion and colonic fermentation. Food Chem. 2016;201:120–30.

53. Bouayed J, Hoffmann L, Bohn T. Total phenolics, flavonoids, anthocyanins and antioxidant activity following simulated gastro-intestinal digestion and dialysis of apple varieties: bioaccessibility and potential uptake. Food Chem. 2011;128(1):14–21.
54. Correa-Betanzo J, Allen-Vercoe E, McDonald J, Schroeter K, Corredig M, Paliyath G. Stability and biological activity of wild blueberry (*Vaccinium angustifolium*) polyphenols during simulated *in vitro* gastrointestinal digestion. Food Chem. 2014;165:522–31.
55. Bouayed J, Deußer H, Hoffmann L, Bohn T. Bioaccessible and dialysable polyphenols in selected apple varieties following *in vitro* digestion vs. their native patterns. Food Chem. 2012;131(4):1466–72.
56. Tavares L, Figueira I, Macedo D, McDougall GJ, Leitão MC, Vieira HLA, et al. Neuroprotective effect of blackberry (*Rubus* sp.) polyphenols is potentiated after simulated gastrointestinal digestion. Food Chem. 2012;131(4):1443–52.
57. Guerra A, Etienne-Mesmin L, Livrelli V, Denis S, Blanquet-Diot S, Alric M. Relevance and challenges in modeling human gastric and small intestinal digestion. Trends Biotechnol. 2012;30(11):591–600.
58. Liang L, Wu X, Zhao T, Zhao J, Li F, Zou Y, et al. *In vitro* bioaccessibility and antioxidant activity of anthocyanins from mulberry (*Morus atropurpurea* Roxb.) following simulated gastro-intestinal digestion. Food Res. Int. 2012;46(1):76–82.
59. Brown EM, Nitecki S, Pereira-Caro G, Mcdougall GJ, Stewart D, Rowland I, et al. Comparison of *in vivo* and *in vitro* digestion on polyphenol composition in lingonberries: potential impact on colonic health. BioFactors. 2014;40(6):611–23.
60. Akkarachiyasit S, Charoenlertkul P, Yibchok-Anun S, Adisakwattana S. Inhibitory activities of cyanidin and its glycosides and synergistic effect with acarbose against intestinal α-glucosidase and pancreatic α-amylase. Int. J. Mol. Sci. 2010;11(9):3387–96.
61. Grussu D, Stewart D, McDougall GJ. Berry polyphenols inhibit α-amylase *in vitro*: identifying active components in rowanberry and raspberry. J. Agric. Food Chem. 2011;59(6):2324–31.
62. Zhang X, Huang H, Zhao X, Lv Q, Sun C, Li X, et al. Effects of flavonoids-rich Chinese bayberry (*Myrica rubra* Sieb. et Zucc.) pulp extracts on glucose consumption in human HepG2 cells. J. Funct. Foods. 2015 Apr;14:144–53.
63. Martineau LC, Couture A, Spoor D, Benhaddou-Andaloussi A, Harris C, Meddah B, et al. Anti-diabetic properties of the Canadian lowbush blueberry *Vaccinium angustifolium* Ait. Phytomedicine. 2006;13(9–10):612–23.
64. McDougall GJ, Kulkarni NN, Stewart D. Berry polyphenols inhibit pancreatic lipase activity *in vitro*. Food Chem. 2009;115:193–9.
65. Yan S, Zhang X, Wen X, Lv Q, Xu C, Sun C, et al. Purification of flavonoids from chinese bayberry (*Morella rubra* Sieb. et Zucc.) fruit extracts and α-glucosidase inhibitory activities of different fractionations. Molecules.2016;21(9):1148.
66. Khangholi S, Majid FAA, Berwary NJA, Ahmad F, Aziz RBA. The mechanisms of inhibition of

advanced glycation end products formation through polyphenols in hyperglycemic condition. Planta Med. 2016;82:32–45.

67. Grewal AS, Bhardwaj S, Pandita D, Lather V, Sekhon BS. Updates on aldose reductase inhibitors for management of diabetic complications and non-diabetic diseases. Mini-Reviews Med. Chem. 2016;16(2):120–62.
68. Xiao J, Ni X, Kai G, Chen X. Advance in dietary polyphenols as aldose reductases inhibitors : structure-activity relationship aspect. Crit. Rev. Food Sci. Nutr. 2015;55:16–31.
69. Veeresham C, Rama Rao A, Asres K. Aldose reductase inhibitors of plant origin. Phytother. Res. 2014;28(3):317–33.
70. Chinchansure AA, Korwar AM, Kulkarni MJ, Joshi SP. Recent development of plant products with anti-glycation activity: a review. RSC Adv. 2015;5(39):31113–38.
71. Sompong W, Meeprom A, Cheng H, Adisakwattana S. A comparative study of ferulic acid on different monosaccharide-mediated protein glycation and oxidative damage in bovine serum albumin. Molecules;18(11):13886–903.
72. Yeh W, Hsia S, Lee W, Wu C. Polyphenols with antiglycation activity and mechanisms of action : a review of recent findings. J. Food Drug Anal. 2017;25:84–92.
73. Séro L, Sanguinet L, Blanchard P, Dang BT, Morel S, Richomme P, et al. Tuning a 96-well microtiter plate fluorescence-based assay to identify AGE inhibitors in crude plant extracts. Molecules.2013;18(11):14320–39.
74. Wang W, Yagiz Y, Buran TJ, Nunes CDN, Gu L. Phytochemicals from berries and grapes inhibited the formation of advanced glycation end-products by scavenging reactive carbonyls. Food Res. Int. 2011;44(9):2666–73.
75. McIntyre KL, Harris CS, Saleem A, Beaulieu LP, Chieu AT, Haddad PS, et al. Seasonal phytochemical variation of anti-glycation principles in lowbush blueberry (*Vaccinium angustifolium*). Planta Med. 2009;75(3):286–92.
76. Liu H, Liu H, Wang W, Khoo C, Taylor J, Gu L. Cranberry phytochemicals inhibit glycation of human hemoglobin and serum albumin by scavenging reactive carbonyls. Food Funct. 2011;2(8):475–82.
77. Beaulieu L-P, Harris CS, Saleem A, Cuerrier A, Haddad PS, Martineau LC, et al. Inhibitory effect of the Cree traditional medicine Wiishichimanaanh (*Vaccinium vitis-idaea*) on advanced glycation endproduct formation: identification of active principles. Phyther. Res. 2010;24(5):741–7.
78. Khoddami A, Wilkes M, Roberts T. Techniques for analysis of plant phenolic compounds. Molecules. 2013;18(2):2328–75.
79. Oszmiański J, Wojdyło A, Lachowicz S, Gorzelany J, Matłok N. Comparison of bioactive potential of cranberry fruit and fruit-based products versus leaves. J. Funct. Foods. 2016;22:232–42.
80. Teleszko M, Wojdyło A. Comparison of phenolic compounds and antioxidant potential between selected edible fruits and their leaves. J. Funct. Foods. 2015;14:736–46.
81. Venskutonis PR, Barnackas Š, Kazernavičiūtė R, Maždžierienė R, Pukalskas A, Šipailienė A, et al.

Variations in antioxidant capacity and phenolics in leaf extracts isolated by different polarity solvents from seven blueberry (*Vaccinium* L.) genotypes at three phenological stages. Acta Physiol. Plant. 2016;38(2):1–13.

82. Zhang X, Huang H, Zhang Q, Fan F, Xu C, Sun C, et al. Phytochemical characterization of chinese bayberry (*Myrica rubra* Sieb. et Zucc.) of 17 cultivars and their antioxidant properties. Int. J. Mol. Sci. 2015;16(6):12467–81.
83. Baby B, Antony P, Vijayan R. Antioxidant and anticancer properties of berries. Crit. Rev. Food Sci. Nutr. 2017;8398:1–17.
84. Bujor O-C, Le Bourvellec C, Volf I, Popa VI, Dufour C. Seasonal variations of the phenolic constituents in bilberry (*Vaccinium myrtillus* L.) leaves, stems and fruits, and their antioxidant activity. Food Chem. 2016;213:58–68.
85. Wu Y, Zhou Q, Chen X, Li X, Wang Y, Zhang J. Comparison and screening of bioactive phenolic compounds in different blueberry cultivars: evaluation of anti-oxidation and α-glucosidase inhibition effect. Food Res. Int. 2017;100(P1):312–24.
86. Vrhovsek U, Masuero D, Palmieri L, Mattivi F. Identification and quantification of flavonol glycosides in cultivated blueberry cultivars. J. Food Compos. Anal. 2012;25(1):9–16.
87. Oszmiański J, Wojdyło A, Nowicka P, Teleszko M, Cebulak T, Wolanin M. Determination of phenolic compounds and antioxidant activity in leaves from wild *Rubus* L. Species. Molecules. 2015;20(3):4951–66.
88. Mertz C, Cheynier V, Gunata Z, Brat P. Analysis of phenolic compounds in two blackberry species (*Rubus glaucus* and *Rubus adenotrichus*) by high-performance liquid chromatography with diode array detection and electrospray ion trap mass spectrometry. J. Agric. Food Chem. 2007;55(21):8616–24.
89. Boath AS, Stewart D, McDougall GJ. Berry components inhibit α-glucosidase *in vitro*: synergies between acarbose and polyphenols from black currant and rowanberry. Food Chem. 2012 1;135(3):929–36.
90. Cheplick S, Kwon Y-I, Bhowmik P, Shetty K. Clonal variation in raspberry fruit phenolics and relevance for diabetes and hypertension management. J. Food Biochem. 2007;31(5):656–79.
91. Kang B-H, Racicot K, Pilkenton SJ, Kwon Y-I, Apostolidis E. Blueberry extract inhibits carbohydrate-hydrolyzing enzymes and these inhibitory activities are not proanthocyanidin dependent. J. Korean Soc. Appl. Biol. Chem. 2015;58(1):127–36.
92. Wang SY, Camp MJ, Ehlenfeldt MK. Antioxidant capacity and α-glucosidase inhibitory activity in peel and flesh of blueberry (*Vaccinium* spp.) cultivars. Food Chem. 2012;132(4):1759–68.
93. Boath AS, Grussu D, Stewart D, McDougall GJ. Berry polyphenols inhibit digestive enzymes: a source of potential health benefits? Food Dig. 2012;2;3(1–3):1–7.
94. McDougall GJ, Shpiro F, Dobson P, Smith P, Blake A, Stewart D. Different polyphenolic components of soft fruits inhibit α-amylase and α-glycosidase. J. Agric. Food Chem. 2005;53(7):2760–6.
95. Nickavar B, Amin G. Bioassay-guided separation of an α-amylase inhibitor anthocyanin from *Vaccinium arctostaphylos* berries. J. Biosci. 2010;65 C(9–10):567–70.

96. Nickavar B, Amin G. Enzyme assay guided isolation of an α-amylase inhibitor flavonoid from *Vaccinium arctostaphylos* leaves. Iran. J. Pharm. Res. 2011;10(4):849–53.
97. Worsztynowicz P, Napierała M, Białas W, Grajek W, Olkowicz M. Pancreatic α-amylase and lipase inhibitory activity of polyphenolic compounds present in the extract of black chokeberry (*Aronia melanocarpa* L.). Process Biochem. 2014;49(9):1457–63.
98. Zhang L, Li J, Hogan S, Chung H, Welbaum GE, Zhou K. Inhibitory effect of raspberries on starch digestive enzyme and their antioxidant properties and phenolic composition. Food Chem. 2010;119(2):592–9.
99. Sun C-D, Zhang B, Zhang J-K, Xu C-J, Wu Y-L, Li X, et al. Cyanidin-3-glucoside-rich extract from Chinese bayberry fruit protects pancreatic β cells and ameliorates hyperglycemia in streptozotocin-induced diabetic mice. J. Med. Food. 2012;15(3):288–98.
100. Suryanarayana P, Kumar PA, Saraswat M, Petrash JM, Reddy GB. Inhibition of aldose reductase by tannoid principles of *Emblica officinalis*: implications for the prevention of sugar cataract. Mol. Vis. 2004;10:148–54.
101. Press JR, Short MJ. Flora of Madeira. London: HMSO; 1994.
102. Hussain I. Physiochemical and sensory characteristics of *Elaeagnus umbellata* (Thunb) fruit from Rawalakot (Azad Kashmir) Pakistan. African J. Food Sci. Technol. 2011;2(7):151–6.
103. Khattak KF. Free radical scavenging activity, phytochemical composition and nutrient analysis of *Elaeagnus umbellata* berry. J. Med. Plants Res. 2012;6(39):5196–203.
104. Pei R, Yu M, Bruno R, Bolling BW. Phenolic and tocopherol content of autumn olive (*Elaeagnus umbellate*) berries. J. Funct. Foods. 2015;16:305–14.
105. Kim M, Lim J, Yang S. Component analysis and anti-proliferative effects of ethanol extracts of fruits , leaves , and stems from *Elaeagnus umbellata* in HepG2 cells. J. Korean Soc. Food Sci. Nutr. 2016;45(6):828–34.
106. Spínola V, Llorent-Martínez EJ, Gouveia S, Castilho PC. *Myrica faya* : a new source of antioxidant phytochemicals. J. Agric. Food Chem. 2014;62:9722–9735.
107. Gouveia-Figueira SC, Castilho PC. Phenolic screening by HPLC–DAD–ESI/MSn and antioxidant capacity of leaves, flowers and berries of *Rubus grandifolius* Lowe. Ind. Crops Prod. 2015;73:28–40.
108. Rivera D, Obón C. The ethnopharmacology of Madeira and Porto Santo Islands, a review. J. Ethnopharmacol. 1995;46(2):73–93.
109. Lima EC, Baptista JB, Albuquerque LM. Antioxidant capacity versus total phenolic, total flavonoid and anthocyanin content of endemic azorean *Vaccinium cymindraceum*: comparison with commercial bilberry and highbush blueberry. Acta Hortic. 2009;810:901–10.
110. Schäfer H. Flora of the Azores. A Field Guide. Backhuys Publishers; 2005.
111. Base de Dados da Biodiversidade dos Açores. Universidade dos Açores. 2008. Available from: http://www.azoresbioportal.angra.uac.pt/imagens/Imagenes/GruposCAutores_11Jun08/Plantas_VascularesCAutores//Vacciniumcylindraceum_03_25.9.2003.jpg (last access 01/01/2018)

112. Cabrita L, Andersen ØM. Anthocyanins in blue berries of *Vaccinium padifolium*. Phytochem. 1999; 52(8):1693–6.
113. Cabrita L, Frøystein NÅ, Andersen ØM. Anthocyanin trisaccharides in blue berries of *Vaccinium padifolium*. Food Chem. 2000 Apr;69(1):33–6.
114. Oszmiański J, Nowicka P, Teleszko M, Wojdyło A, Cebulak T, Oklejewicz K. Analysis of phenolic compounds and antioxidant activity in wild blackberry fruits. Int. J. Mol. Sci. 2015;16(7):14540–53.
115. Tan Y, Chang SKC. Digestive enzyme inhibition activity of the phenolic substances in selected fruits, vegetables and tea as compared to black legumes. J. Funct. Foods. 2017;38:644–55.
116. Huang H, Sun Y, Lou S, Li H, Ye X. *In vitro* digestion combined with cellular assay to determine the antioxidant activity in Chinese bayberry (*Myrica rubra* Sieb. et *Zucc*.) fruits: a comparison with traditional methods. Food Chem. 2014;146:363–70.
117. Zhang Y, Chen S, Wei C, Gong H, Li L, Ye X. Chemical and cellular assays combined with in vitro digestion to determine the antioxidant activity of flavonoids from Chinese bayberry (*Myrica rubra* Sieb. et Zucc.) leaves. PLoS One. 2016;11(12):e0167484.
118. Re R, Pellegrini N, Proteggente A, Pannala A, Yang M, Rice-Evans C. Antioxidant activity applying an improved ABTS radical cation decolorization assay. Free Radic. Biol. Med. 1999;26(9):1231–7.
119. Dudonné S, Vitrac X, Coutière P, Woillez M, Mérillon J-M. Comparative study of antioxidant properties and total phenolic content of 30 plant extracts of industrial interest using DPPH, ABTS, FRAP, SOD, and ORAC assays. J. Agric. Food Chem. 2009;57:1768–74.
120. Ewing JF, Janero DR. Microplate superoxide dismutase assay employing a nonenzymatic superoxide generator. Anal. Biochem. 1995;232(2):243–8.
121. Llorent-Martínez EJ, Spínola V, Castilho PC. Evaluation of the inorganic content of six underused wild berries from Portugal: potential new sources of essential minerals. J. Food Compos. Anal. 2017;59:153–60.
122. Flores FP, Singh RK, Kerr WL, Pegg RB, Kong F. Total phenolics content and antioxidant capacities of microencapsulated blueberry anthocyanins during *in vitro* digestion. Food Chem. 2014;153:272–8.
123. Pinto J, Spínola V, Llorent-Martínez EJ, Fernández-de Córdova ML, Molina-García L, Castilho PC. Polyphenolic profile and antioxidant activities of Madeiran elderberry (*Sambucus lanceolata*) as affected by simulated *in vitro* digestion. Food Res. Int. 2017;100(P3):404–10.
124. Zheng W, Wang SY. Antioxidant activity and phenolic compounds in selected herbs. J. Agric. Food Chem. 2001 (11):5165–70.
125. Spínola V, Llorent-Martínez EJ, Gouveia-Figueira S, Castilho PC. *Ulex europaeus*: from noxious weed to source of valuable isoflavones and flavanones. Ind. Crops Prod. 2016;90:9–27.
126. Akkol EK, Göger F, Koşar M, Başer KHC. Phenolic composition and biological activities of *Salvia halophila* and *Salvia virgata* from Turkey. Food Chem. 2008;108(3):942–9.
127. Muthenna P, Suryanarayana P, Gunda SK, Petrash JM, Reddy GB. Inhibition of aldose reductase by dietary antioxidant curcumin: mechanism of inhibition, specificity and significance. FEBS Lett. 2009;583(22):3637–42.

128. Xiao S, Castro R, Maciel D, Gonçalves M, Shi X, Rodrigues J, et al. Fine tuning of the pH-sensitivity of laponite–doxorubicin nanohybrids by polyelectrolyte multilayer coating. Mater. Sci. Eng. C. 2016;60:348–56.

129. Ishaq S, Rathore HA, Sabir SM, Maroof MS. Antioxidant properties of *Elaeagnus umbellata* berry solvent extracts against lipid peroxidation in mice brain and liver tissues. Food Sci. Biotechnol. 2015;24(2):673–9.

130. Lee J, Finn CE. Anthocyanins and other polyphenolics in American elderberry (*Sambucus canadensis*) and European elderberry (*S. nigra*) cultivars. J Sci Food Agric. 2007;87(14):2665–75.

131. Oszmianski J, Kolniak-Ostek J, Lachowicz S, Gorzelany J, Matlok N. Phytochemical compounds and antioxidant activity in different cultivars of cranberry (*Vaccinium macrocarpon* L). J. Food Sci. 2017;82(11):2569–75.

132. Jaakola L, Määttä-Riihinen K, Kärenlampi S, Hohtola A. Activation of flavonoid biosynthesis by solar radiation in bilberry (*Vaccinium myrtillus* L.) leaves. Planta. 2004;218(5):721–8.

133. Garzón GA, Narváez CE, Riedl KM, Schwartz SJ. Chemical composition, anthocyanins, non-anthocyanin phenolics and antioxidant activity of wild bilberry (*Vaccinium meridionale* Swartz) from Colombia. Food Chem. 2010;122(4):980–6.

134. De Souza VR, Pereira PAP, Da Silva TLT, De Oliveira Lima LC, Pio R, Queiroz F. Determination of the bioactive compounds, antioxidant activity and chemical composition of Brazilian blackberry, red raspberry, strawberry, blueberry and sweet cherry fruits. Food Chem.; 2014;156:362–8.

135. McCarty MF. Nutraceutical resources for diabetes prevention - An update. Med. Hypotheses. 2005;64:151–8.

136. Barbagallo M, Dominguez LJ. Magnesium and type 2 diabetes. World J. Diabetes. 2015;6(10):1152–7.

137. Koh ES, Kim SJ, Yoon HE, Chung JH, Chung S, Park CW, et al. Association of blood manganese level with diabetes and renal dysfunction: a cross-sectional study of the Korean general population. BMC Endocr. Disord. 2014;14:24–36.

138. Commision of the European Communities. Directive 2008/100/EC on nutrition labelling for foodstuffs as regards recommended daily allowances, energy conversion factors and definitions. Off. J. Eur. Union. 2008;L285:9.

139. Fang Z, Zhang M, Tao G, Yunfei Sun A, Sun J. Chemical composition of clarified bayberry (*Myrica rubra* Sieb. et Zucc.) juice sediment. J Agric Food Chem. 2006;54(20):7710–6.

140. Liu Y, Zhang D, Wu Y, Wang D, Wei Y, Wu J, et al. Stability and absorption of anthocyanins from blueberries subjected to a simulated digestion process. Int. J. Food Sci. Nutr. 2014;65(4):440–8.

141. Marhuenda J, Alemán MD, Gironés-Vilaplana A, Pérez A, Caravaca G, Figueroa F, et al. Phenolic composition, antioxidant activity, and *in vitro* availability of four different berries. J. Chem. 2016; Article ID 5194901:7 pages.

142. Yang H, Ge Y, Sun Y, Liu D, Ye X, Wu D. Identification and characterisation of low-molecular-weight

phenolic compounds in bayberry (*Myrica rubra* Sieb. et Zucc.) leaves by HPLC-DAD and HPLC-UV-ESIM^S. Food Chem. 2011;128(4):1128–35.

143. Fang Z, Zhang M, Wang L. HPLC-DAD-ESIMS analysis of phenolic compounds in bayberries (*Myrica rubra Sieb. et Zucc.*). Food Chem. 2007;100(2):845–52.
144. Azofeifa G, Quesada S, Boudard F, Morena M, Cristol J-P, Pérez AM, et al. Antioxidant and anti-inflammatory *in vitro* activities of phenolic compounds from tropical highland blackberry (*Rubus adenotrichos*). J. Agric. Food Chem. 2013;61:5798–804.
145. Chen W, Xu Y, Zhang L, Su H, Zheng X. Blackberry subjected to *in vitro* gastrointestinal digestion affords protection against ethyl carbamate-induced cytotoxicity. Food Chem. 2016;212:620–7.
146. Chen W, Xu Y, Zhang L, Li Y, Zheng X. Wild raspberry subjected to simulated gastrointestinal digestion improves the protective capacity against ethyl carbamate-induced oxidative damage in Caco-2 cells. Oxid. Med. Cell. Longev. 2016; Article ID 3297363:12 pages.
147. McDougall GJ, Dobson P, Smith P, Blake A, Stewart D. Assessing potential bioavailability of raspberry anthocyanins using an *in vitro* digestion system. J. Agric. Food Chem. 2005;53(15):5896–904.
148. Dawidowicz AL, Wianowska D, Baraniak B. The antioxidant properties of alcoholic extracts from *Sambucus nigra* L. (antioxidant properties of extracts). LWT - Food Sci. Technol. 2006;39(3):308–15.
149. Sidor A, Gramza-Michałowska A. Advanced research on the antioxidant and health benefit of elderberry (*Sambucus nigra*) in food - a review. J. Funct. Foods. 2015;18:941–58.
150. Mandrone M, Lorenzi B, Maggio A, La Mantia T, Scordino M, Bruno M, et al. Polyphenols pattern and correlation with antioxidant activities of berries extracts from four different populations of Sicilian *Sambucus nigra* L. Nat. Prod. Res. 2014;28(16):1246–53.
151. Duymuş HG, Göger F, Başer KHC. *In vitro* antioxidant properties and anthocyanin compositions of elderberry extracts. Food Chem. 2014;155:112–9.
152. Zhou N, Zhu W, Yang F, Zhou K. *In vitro* gastrointestinal digestion model to monitor the antioxidant properties and bioavailability of phenolic antioxidants from elderberry. React. Oxyg. Species. 2016;2(6):421–31.
153. Jiao X, Li B, Zhang Q, Gao N, Zhang X, Meng X. Effect of *in vitro*-simulated gastrointestinal digestion on the stability and antioxidant activity of blueberry polyphenols and their cellular antioxidant activity towards HepG2 cells. Int. J. Food Sci. Technol. 2018;53(1):61–71.
154. Sarkar D, Agustinah W, Woods F, Coneva E, Vinson E, Shetty K. *In vitro* screening and evaluation of phenolic antioxidant-linked anti-hyperglycemic functions of rabbit-eye blueberry (*Vaccinium ashei*) cultivars. J. Berry Res. 2017;7(3):163–77.
155. Chiang C-J, Kadouh H, Zhou K. Phenolic compounds and antioxidant properties of gooseberry as affected by *in vitro* digestion. LWT - Food Sci. Technol. 2013;51(2):417–22.
156. Podsędek A, Redzynia M, Klewicka E, Koziolkiewicz M. Matrix effects on the stability and antioxidant activity of red cabbage anthocyanins under simulated gastrointestinal digestion. Biomed Res. Int. 2014;11 pages.
157. Tag H, Tsering J, Hui PK, Gogoi BJ, Veer V. Nutritional potential and traditional uses of high altitude

wild edible plants in eastern Himalayas, India.Int. Sci. Index. 2014;8(3):238–43.

158. Namiesnik J, Vearasilp K, Leontowicz H, Leontowicz M, Ham KS, Kang SG, et al. Comparative assessment of two extraction procedures for determination of bioactive compounds in some berries used for daily food consumption. Int. J. Food Sci. Technol. 2014;49(2):337–46.
159. Harris CS, Cuerrier A, Lamont E, Haddad PS, Arnason JT, Bennett SAL, et al. Investigating wild berries as a dietary approach to reducing the formation of advanced glycation endproducts: chemical correlates of *in vitro* antiglycation activity. Plant foods Hum. Nutr. 2014;69(1):71–7.
160. Bobinaitė R, Viškelis P, Šarkinas A, Venskutonis PR. Phytochemical composition, antioxidant and antimicrobial properties of raspberry fruit, pulp, and marc extracts. CyTA - J. Food. 2013;11(4):334–42.
161. Topuzović MD, Stanković MS, Jakovljević DZ, Bojović BM. Plant part variability of *Sambucus ebulus* L. secondary metabolites content and antioxidant activity. Agro Food Ind. Hi. Tech. 2016;27(2):60–3.
162. Salehi P, Asghari B, Esmaeili MA, Dehghan H, Ghazi I. α -Glucosidase and α -amylase inhibitory effect and antioxidant activity of ten plant extracts traditionally used in Iran for diabetes. J. Med. Plants Res. 2013;7(6):257–66.
163. Zhu L, Liu X, Tan J, Wang B. Influence of harvest season on antioxidant activity and constituents of rabbiteye blueberry (*Vaccinium ashei*) leaves. J. Agric. Food Chem. 2013;61(47):11477–83.
164. Ferrier J, Djeffal S, Morgan HP, Vander Kloet SP, Redžić S, Cuerrier A, et al. Antiglycation activity of *Vaccinium* spp. (Ericaceae) from the Sam Vander Kloet collection for the treatment of type II diabetes. Botany. 2012;90:401–6.
165. Kimura A, Lee JH, Lee IS, Lee HS, Park KH, Chiba S, et al. Two potent competitive inhibitors discriminating alpha-glucosidase family I from family II. Carbohydr. Res. 2004;339(6):1035–40.
166. Babu KS, Tiwari AK, Srinivas P V., Ali AZ, Raju BC, Rao JM. Yeast and mammalian α-glucosidase inhibitory constituents from Himalayan rhubarb *Rheum emodi* Wall.ex Meisson. Bioorganic Med. Chem. Lett. 2004;14(14):3841–5.
167. Shai J. L, Magano R. S, Lebelo L. S, Mogale M. A. Inhibitory effects of five medicinal plants on rat alpha-glucosidase: comparison with their effects on yeast alpha-glucosidase. J. Med. Plants Res. 2011;5(13):2863–7.
168. Oki T, Matsui T, Osajima Y. Inhibitory effect of alpha-glucosidase inhibitors varies according to its origin. J. Agric. Food Chem. 1999;47:550–3.
169. Sancheti S, Sancheti S, Seo S-Y. *Chaenomeles sinensis*: a potent α-and β-Glucosidase inhibitor. Am. J. Pharmacol. Toxicol. 2009;4(1):8–11.
170. Balaji M, Ganjayi MS, Hanuma Kumar GEN, Parim BN, Mopuri R, Dasari S. A review on possible therapeutic targets to contain obesity: the role of phytochemicals. Obes. Res. Clin. Pract. 2016;10(4):363–80.
171. Fabroni S, Ballistreri G, Amenta M, Romeo F V., Rapisarda P. Screening of the anthocyanin profile and *in vitro* pancreatic lipase inhibition by anthocyanin-containing extracts of fruits, vegetables,

legumes and cereals. J. Sci. Food Agric. 2016;96(14):4713–23.

172. Lin D, Xiao M, Zhao J, Li Z, Xing B, Li X, et al. An overview of plant phenolic compounds and their importance in human nutrition and management of type 2 diabetes. Molecules. 2016;21(10):1374–93.
173. Wu T, Luo J, Xu B. *In vitro* anti-diabetic effects of selected fruits and vegetables against glycosidase and aldose reductase. Food Sci. Nutr. 2015;3(6):495–505.
174. de Sales PM, de Souza PM, Simeoni LA, Magalhães PDO, Silveira D. α-Amylase inhibitors: a review of raw material and isolated compounds from plant source. J. Pharm. Sci. 2012;15(1):141–83.
175. Meng S, Cao J, Feng Q, Peng J, Hu Y. Roles of chlorogenic acid on regulating glucose and lipids metabolism: a review. Evidence-Based Complement. Altern. Med. 2013; Article ID 801457: 11 pages.
176. Matsuda H, Morikawa T, IwaoToguchida, Yoshikawa M. Structural requirements of flavonoids and related compounds for aldose reductase inhibitory activity. Chem. Pharm. Bull. 2002;50(6):788–95.
177. Xie Y, Chen X. Structures required of polyphenols for inhibiting advanced glycation end products formation. Curr. Drug Metab. 2013;14:414–31.
178. Matsuda H, Wang T, Managi H, Yoshikawa M. Structural requirements of flavonoids for inhibition of protein glycation and radical scavenging activities. Bioorganic Med. Chem. 2003;11(24):5317–23.
179. Kim J, Jeong I-H, Kim C-S, Lee YM, Kim JM, Kim JS. Chlorogenic acid inhibits the formation of advanced glycation end products and associated protein cross-linking. Arch. Pharm. Res. 2011;34(3):495–500.
180. Singh P, Jayaramaiah RH, Agawane SB. Potential dual role of eugenol in inhibiting advanced glycation end products in diabetes : proteomic and mechanistic insights. Sci. Rep. 2016;(6):18798.
181. Joglekar MM, Bavkar LN, Sistla S, Arvindekar AU. Effective inhibition of protein glycation by combinatorial usage of limonene and aminoguanidine through differential and synergistic mechanisms. Int. J. Biol. Macromol. 2017;99:563–9.
182. West BJ, Deng S, Uwaya A, Isami F, Abe Y, Yamagishi S, et al. Iridoids are natural glycation inhibitors. Glycoconj. J. 2016;33:671–81.
183. Wang W, Yagiz Y, Buran TJ, Nunes C do N, Gu L. Phytochemicals from berries and grapes inhibited the formation of advanced glycation end-products by scavenging reactive carbonyls. Food Res. Int. 2011;44(9):2666–73.
184. Li X, Zheng T, Sang S, Lv L. Quercetin inhibits advanced glycation end product formation by trapping methylglyoxal and glyoxal. J. Agric. Food Chem. 2014;62(50):12152–8.
185. Sun C, Huang H, Xu C, Li X, Chen K. Biological activities of extracts from Chinese bayberry (*Myrica rubra* Sieb. et Zucc.): a review. Plant Foods Hum. Nutr. 2013;68(2):97–106.
186. Zhang Y, Zhou X, Tao W, Li L, Wei C, Duan J, et al. Antioxidant and antiproliferative activities of proanthocyanidins from Chinese bayberry (*Myrica rubra* Sieb. et Zucc.) leaves. J. Funct. Foods. 2016;27:645–54.
187. Denev P, Ciz M, Ambrozova G, Lojek A, Yanakieva I, Kratchanova M. Solid-phase extraction of berries' anthocyanins and evaluation of their antioxidative properties. Food Chem. 2010;123(4):1055–61.

188. Chen L, Xin X, Yuan Q, Su D, Liu W. Phytochemical properties and antioxidant capacities of various colored berries. J. Sci. Food Agric. 2014;94(2):180–8.

189. Pérez-González A, Rebollar-zepeda AM, León-carmona JR, Galano A. Reactivity indexes and O-H bond dissociation energies of a large series of polyphenols : implications for their free radical scavenging activity. J. Mex. Chem. Soc. 2012;56(3):241–9.

190. Nowak A, Sójka M, Klewicka E, Lipińska L, Klewicki R, Kołodziejczyk K. Ellagitannins from *Rubus idaeus* L. exert geno- and cytotoxic effects against Human colon adenocarcinoma cell line Caco-2. J. Agric. Food Chem. 2017;65:2947–55.

191. Krauze-Baranowska M, Głód D, Kula M, Majdan M, Hałasa R, Matkowski A, et al. Chemical composition and biological activity of *Rubus idaeus* shoots – a traditional herbal remedy of Eastern Europe. BMC Complement. Altern. Med. 2014;14(1):480.

192. Seeram N, Adams L, Zhang Y, Rupo L, Sand D, Scheuller H, et al. Blackberry, black raspberry, bluerry, cranberry, red raspberry and strawberry extracts inhibit growth stimulate apoptsis of human cancer *in vitro*. J. Agric. Food Chem. 2006;54(ii):9329–39.

193. Maldonado-Celis ME, Arango-Varela SS, Rojano BA. Free radical scavenging capacity and cytotoxic and antiproliferative effects of *Vaccinium meridionale* Sw. agains colon cancer cell lines. Rev. Cuba. Plantas Med. 2014;19(2):172–84.

194. Massarotto G, Barcellos T, Garcia CSC, Brandalize APC, Moura S, Schwambach J, et al. Chemical characterization and cytotoxic activity of blueberry extracts (cv. Misty) cultivated in Brazil. J. Food Sci. 2016;81(8):H2076–84.

195. McDougall GJ, Ross HA, Ikeji M, Stewart D. Berry extracts exert different antiproliferative effects against cervical and colon cancer cells grown *in vitro*. J. Agric. Food Chem. 2008;56(9):3016–23.

196. Zhou Y, Zheng J, Li Y, Xu DP, Li S, Chen YM, et al. Natural polyphenols for prevention and treatment of cancer. Nutrients. 2016;8:515–50.

197. Engels C, Schieber A, Ganzle MG. Sinapic acid derivatives in defatted Oriental mustard (*Brassica juncea* L.) seed meal extracts using UHPLC-DAD-ESI-MS^n and identification of compounds with antibacterial activity. Eur. Food Res. Technol. 2012;234(3):535–42.

198. Spínola V, Pinto J, Castilho PC. Identification and quantification of phenolic compounds of selected fruits from Madeira Island by HPLC-DAD–ESI-MSn and screening for their antioxidant activity. Food Chem. 2015;173:14–30.

199. Calani L, Beghè D, Mena P, Del Rio D, Bruni R, Fabbri A, et al. Ultra-HPLC-MS(n) (poly)phenolic profiling and chemometric analysis of juices from ancient *Punica granatum* L. cultivars: a nontargeted approach. J. Agric. Food Chem. 2013;61(23):5600–9.

200. Bresciani L, Calani L, Cossu M, Mena P, Sayegh M, Ray S, et al. (Poly)phenolic characterization of three food supplements containing 36 different fruits, vegetables and berries. PharmaNutrition. 2015;3(2):11–9.

201. Gordon A, Jungfer E, da Silva BA, Maia JGS, Marx F. Phenolic constituents and antioxidant capacity

of four underutilized fruits from the Amazon region. J. Agric. Food Chem. 2011;59(14):7688–99.

202. Qiao X, He W, Xiang C, Han J, Wu L, Guo D, et al. Qualitative and quantitative analyses of flavonoids in *Spirodela polyrrhiza* by high-performance liquid chromatography coupled with mass spectrometry. Phytochem. Anal.;22(6):475–83.
203. Ferreres F, Magalhães SCQ, Gil-Izquierdo A, Valentão P, Cabrita ARJ, Fonseca AJM, et al. HPLC-DAD-ESI/MSn profiling of phenolic compounds from *Lathyrus cicera* L. seeds. Food Chem. 2017;214:678–85.
204. Ye M, Yan Y, Guo D-A. Characterization of phenolic compounds in the Chinese herbal drug Tu-Si-Zi by liquid chromatography coupled to electrospray ionization mass spectrometry. Rapid Commun. Mass Spectrom. 2005; (11):1469–84.
205. Cuyckens F, Claeys M. Mass spectrometry in the structural analysis of flavonoids. J. Mass Spectrom. 2004;39(1):1–15.
206. Mena P, Calani L, Dall'Asta C, Galaverna G, Garcia-Viguera C, Bruni R, et al. Rapid and comprehensive evaluation of (poly)phenolic compounds in pomegranate (*Punica granatum* L.) juice by UHPLC-MSn. Molecules. 2012;17(12):14821–40.
207. Verardo G, Duse I, Callea A. Analysis of underivatized oligosaccharides by liquid chromatography/electrospray ionization tandem mass spectrometry with post-column addition of formic acid. Rapid Commun. Mass Spectrom. 2009 (11):1607–18.
208. Harbaum B, Hubbermann EM, Wolff C, Herges R, Zhu Z, Schwarz K. Identification of flavonoids and hydroxycinnamic acids in pak choi varieties (Brassica campestris L. ssp. *chinensis* var. *communis*) by HPLC-ESI-MSn and NMR and their quantification by HPLC-DAD. J Agric Food Chem. 2007;55(20):8251–60.
209. Spínola V, Castilho PC. Phytochemical profile, chemotaxonomic studies and *in vitro* antioxidant activities of two endemisms from Madeira archipelago: *Melanoselinum decipiens* and *Monizia edulis* (Apiaceae). Chem. Biodivers. 2016;13(10):1290–306.
210. Sun J, Liu X, Yang T, Slovin J, Chen P. Profiling polyphenols of two diploid strawberry (*Fragaria vesca*) inbred lines using UHPLC-HRMS(^{n}.). Food Chem. 2014;146:289–98.
211. Gao J, Shi J, Lu X, Sun C, Pan Y. Differentiation of common diastereoisomeric ursane-type triterpenoids by high-performance liquid chromatography/tandem mass spectrometry. Rapid Commun. Mass Spectrom. 2011;25(10):1349–55.
212. Mikulic-Petkovsek M, Slatnar A, Stampar F, Veberic R. HPLC-MSn identification and quantification of flavonol glycosides in 28 wild and cultivated berry species. Food Chem. 2012;135(4):2138–46.
213. Mena P, Ascacio-Valdés JA, Gironés-Vilaplana A, Del Rio D, Moreno DA, García-Viguera C. Assessment of pomegranate wine lees as a valuable source for the recovery of (poly)phenolic compounds. Food Chem. 2014;145:327–34.
214. Latti AK, Kainulainen PS, Hayirlioglu-Ayaz S, Ayaz FA, Riihinen KR. Characterization of anthocyanins in caucasian blueberries (*Vaccinium arctostaphylos* L.) native to Turkey. J. Agric. Food Chem. 2009;57(12):5244–9.

215. Steingass CB, Glock MP, Schweiggert RM, Carle R. Studies into the phenolic patterns of different tissues of pineapple (*Ananas comosus* [L.] Merr.) infructescence by HPLC-DAD-ESI-MS (^{n}) and GC-MS analysis. Anal. Bioanal. Chem. 2015;407(21):6463–79.

216. Sentandreu E, Cerdán-Calero M, Halket JM, Navarro JL. Rapid screening of low molecular weight phenols from persimmon (*Diospyros kaki*) pulp using liquid chromatography-UV/Vis-electrospray mass spectrometry analysis. J. Sci. Food Agric. 2014;95:1648–54.

217. Fischer UA, Dettmann JS, Carle R, Kammerer DR. Impact of processing and storage on the phenolic profiles and contents of pomegranate (*Punica granatum* L.) juices. Eur. Food Res. Technol. 2011;233(5):797–816.

218. Ieri F, Pinelli P, Romani A. Simultaneous determination of anthocyanins, coumarins and phenolic acids in fruits, kernels and liqueur of *Prunus mahaleb* L. Food Chem. 2012;135(4):2157–62.

219. Del Bubba M, Checchini L, Chiuminatto U, Doumett S, Fibbi D, Giordani E. Liquid chromatographic/electrospray ionization tandem mass spectrometric study of polyphenolic composition of four cultivars of *Fragaria vesca* L. berries and their comparative evaluation. J. Mass Spectrom. 2012;47(9):1207–20.

220. Li J, Kuang G, Chen X, Zeng R. Identification of chemical composition of leaves and flowers from *Paeonia rockii* by UHPLC-Q-exactive orbitrap HRMS. Molecules. 2016;21(7):947.

221. Clifford MN, Knight S, Kuhnert N. Discriminating between the six isomers of dicaffeoylquinic acid by LC-MS^n. J. Agric. Food Chem. 2005;53(10):3821–32.

222. Simirgiotis MJ, Silva M, Becerra J, Schmeda-Hirschmann G. Direct characterisation of phenolic antioxidants in infusions from four Mapuche medicinal plants by liquid chromatography with diode array detection (HPLC-DAD) and electrospray ionisation tandem mass spectrometry (HPLC-ESI–MS). Food Chem. 2012;131(1):318–27.

223. Yang M, Wang X, Guan S, Xia J, Sun J, Guo H, et al. Analysis of triterpenoids in *Ganoderma lucidum* using liquid chromatography coupled with electrospray ionization mass spectrometry. J. Am. Soc. Mass Spectrom. 2007;18(5):927–39.

224. Mikulic-Petkovsek M, Ivancic A, Todorovic B, Veberic R, Stampar F. Fruit phenolic composition of different elderberry species and hybrids. J. Food Sci. 2015;80(10):C2180–90.

225. Gouveia SC, Castilho PC. Characterisation of phenolic acid derivatives and flavonoids from different morphological parts of *Helichrysum obconicum* by a RP-HPLC–DAD-(−)–ESI-MSn method. Food Chem. 2011;129(2):333–44.

226. Qiu X, Zhang J, Huang Z, Zhu D, Xu W. Profiling of phenolic constituents in *Polygonum multiflorum* Thunb. by combination of ultra-high-pressure liquid chromatography with linear ion trap-orbitrap mass spectrometry. J. Chromatogr. A. 2013;1292:121–31.

227. Eklund PC, Backman MJ, Kronberg LA, Smeds AI, Sjöholm RE. Identification of lignans by liquid chromatography-electrospray ionization ion-trap mass spectrometry. J. Mass Spectrom. 2008 ;43(1):97–107.

228. Simirgiotis MJ. Antioxidant capacity and HPLC-DAD-MS profiling of Chilean peumo (*Cryptocarya alba*) fruits and comparison with German peumo (*Crataegus monogyna*) from southern Chile. Molecules. 2013;18(2):2061–80.

229. Gu W-Y, Li N, Leung EL-H, Zhou H, Luo G-A, Liu L, et al. Metabolites software-assisted flavonoid hunting in plants using ultra-high performance liquid chromatography-quadrupole-time of flight mass spectrometry. Molecules. 2015;20(3):3955–71.

230. Zanutto F, Boldrin P, Varanda E, Souza S, Sano P, Vilegas W, et al. Characterization of flavonoids and naphthopyranones in methanol extracts of *Paepalanthus chiquitensis* Herzog by HPLC-ESI-IT-MS^n and their mutagenic activity. Molecules. 2013;18(1):244–62.

231. Sánchez-Rabaneda F, Jáuregui O, Lamuela-Raventós RM, Bastida J, Viladomat F, Codina C. Identification of phenolic compounds in artichoke waste by high-performance liquid chromatography–tandem mass spectrometry. J. Chromatogr. A. 2003;1008(1):57–72.

232. Stephens JM, Schlothauer RC, Morris BD, Yang D, Fearnley L, Greenwood DR, et al. Phenolic compounds and methylglyoxal in some New Zealand manuka and kanuka honeys. Food Chem. 2010;120(1):78–86.

233. Wang Y-F, Hu L-M, Liu Y-N, Pan X-P, Pan G-X, Chang Y-X, et al. A rapid method for qualitative and quantitative analysis of major constituents in dengzhanxixin injection by LC-DAD-ESI–MS^n. Chromatographia. 2010;71(9–10):845–53.

234. Spínola V, Pinto J, Castilho PC. Hypoglycemic, anti-glycation and antioxidant *in vitro* properties of two *Vaccinium* species from Macaronesia: a relation to their phenolic composition. J. Funct. Foods. 2018;40:595-605.

Supplementary Material

Table S 1 - Nomenclature of berry species mentioned in this thesis.

Scientific name	Common name
Adoxaceae family	
Sambucus nigra	Elderberry
Sambucus lanceolata	Madeira elderberry
Caprifoliaceae family	
Lonicera caerulea var. kamtschatica	Blue honeysuckle cv. Wojtek
Elaeagnaceae family	
Elaeagnus umbellata	Autumn olive
Elaeagnus angustifolia	Wild olive
Ericaceae family	
Vaccinium corymbosum	High-bush blueberry
Vaccinium angustifolium	Low-bush blueberry
Vaccinium myrtillus	Bilberry
Vaccinium macrocarpon	Cranberry (American)
Vaccinium oxycoccos	Cranberry (European)
Vaccinium vitis-idaea	Lingonberry
Vaccinium arctostaphylos	Whortleberry
Vaccinium cylindraceum	Azores blueberry
Vaccinium padifolium	Madeira blueberry
Glossulariaceae family	
Ribes nigrum	Black currant
Ribes rubrum	Red currant
Ribes uva-crispa	Gooseberry
Aronia melanocarpa	Black chokeberry
Aronia arbutifolia	Red chokeberry
Rosaceae family	
Fragaria × ananassa	Cultivated strawberry
Rubus articus	Artic bramble
Rubus fruticosus	Blackberry
Rubus idaeus	Red raspberry
Rubus chamaemorus	Cloudberries
Rubus grandifolius	Wild blackberries
Moraceae family	
Morus alba	Mulberry
Morus nigra	Black mulberry

Myricaceae family	
Myrica rubra	Bayberry
Myrica faya	Wax-myrtle
Phyllanthaceae family	
Emblica officinalis	Indian gooseberry

Table S 2 - Standard compounds and chemicals/reagents compounds used in this work.

Name	**Supplier**
Standard compounds	
Gallic acid (> 98%); Rutin (≥ 98%, HPLC)	Panreac (Barcelona, Spain)
Ellagic acid (≥ 96%); Luteolin (≥ 98%); Sinapic acid (> 99%)	Fluka (Lisbon, Portugal)
Caffeic acid (≥ 98%)	Sigma-Aldrich (St. Louis, MO, USA)
5-*O*-Caffeoylquininc acid (5-*O*-CQA, > 95%); 3,5-*O*-Dicaffeoylquinic acid (> 98%) Cyanidin-3-glucoside (C3G) chloride (> 98%), Hesperidin (95-99%)	Biopurify phytochemicals LTD (Chengdu, China)
Apigenin (≥ 99%); (+)-Catechin hydrated (>99%); Protocatechuic acid (≥ 99%); *p*-Coumaric acid (>99%); Ferulic acid (>99%)	Extrasynthese (Genay, France)
Quercetin dihydrate (> 99%)	Riedel-de Haen (Hanover, Germany)
Myricitrin (MCT) (> 98%)	Carbosynth (Berkshire, UK)
Cranberry fruit SRM-3281	National Institute of Standards and Technology (NIST)
Chemicals/Reagents	
Folin–Ciocalteu's phenol reagent (FCR); Sodium chloride (> 99.0%); Potassium chloride (99.5 – 100.5%); Potassium acetate (> 99.5%); Calcium chloride (99 - 105 %);	Panreac (Barcelona, Spain)
6-Hydroxy-2,5,7,8-tetramethylchroman-2-carboxylic acid (Trolox), 2,2′-azinobis-(3-ethylbenzthiazoline-6-sulfonic acid) (ABTS); 2,2-diphenyl-1-picrylhydrazyl (DPPH)	Fluka (Lisbon, Portugal)
N-(1-Naphthyl)ethylene-diamine dihydrochloride (NEDA, ≥ 98%); β-mercaptoethanol (≥ 99%); Quinic acid (98%); Phenazine methosulfate (PMS, ≥ 90%); Sulfanilamide (≥ 99%); β-Nicotinamide adenine dinucleotide reduced disodium salt hydrate (NADH, ≥94%); Ammonium sulphate (≥99%);	Sigma-Aldrich (St. Louis, MO, USA)

Potassium persulfate (99%); Sodium carbonate (100%); *α*-Glucosidase from *Saccharomyces cerevisiae* (type I); Intestinal acetone powder from rat source of *α*-glucosidase*; BGLU* from almonds*; α*-Amylase from porcine pancreas (type VI-B); Lipase (type II; from porcine pancreas); *p*-Nitrophenyl-α-D-glucopyranoside (*α-p*NPG); *p*-Nitrophenyl-*β*-D-glucopyranoside (*β-p*NPG); *p*-Nitrophenyl butyrate (*p*NPB); DL-Glyceraldehyde (≥98%); Bovine serum albumin (BSA, ≥ 98%); D-(-)-Ribose (≥ 99%); Aminoguanidine hydrochloride (AMG, ≥ 98%); Conduritol B epoxide (≥ 95 %); Acarbose; Orlistat; Formic acid (98%); Potassium dihydrogen phosphate (99.5%); Disodium hydrogen phosphate (99%); Ammonium chloride (99.8%); Mucin (type II; from porcine stomach); Pepsin (porcine gastric mucosa); Pancreatin (porcine pancreas); Porcine bile extract (contains glycine and taurine conjugates of hyodeoxycholic acid and other bile salts); Resazurin sodium salt; Phosphate buffered saline (10 x); In, P and Sn solutions (1000 µg mL^{-1}); Hydrogen peroxide solution for ultratrace analysis; Nitric acid solution (65%)	
Human aldose reductase (HAR)	Prozomix (Northumberland, UK)
1-Deoxynojirimycin (1-DNJ, 95-99%)	Biopurify phytochemicals LTD (Chengdu, China)
β-Nicotinamide adenine dinucleotide reduced tetrasodium salt hydrate (NADPH, ≥ 97%)	Calbiochem (EMD Milliipore Corp.; Billerica, MA, USA)
Nitroblue tetrazolium chloride (NBT, 90%); Kaempferol (> 99%)	Acros Organics (Geel, Belgium)
o-Phosphoric acid (85%)	BDH AnalaR (UK)
Aluminium chloride (98%); Hydrochloric acid (37%); Magnesium chloride hexahydrated (99%)	Riedel-de Haen (Hanover, Germany)
Acetic acid glacial (100%); Sucrose (> 95%)	Fischer Scientific (Bishop Meadow, UK)
Soluble starch (p.a.); D-(-)-Fructose (≥ 99%); Potassium iodate (99.5%); Sodium nitroprusside (99%); Ethylenediaminetetraacetic acid (EDTA, > 99%); Sodium azide (NaN_3, > 99%); Urea (≥ 99%)	Merck (Darmstadt, Germany)
Human Caucasian colon adenocarcinoma (Caco-2) cells	European Collection of Authenticated Cell Cultures (ECACC)

Minimum essential medium; Fetal bovine serum; Penicillin; Streptomycin; Amphotericin B; Non-essential amino acids; L-Glutamine	Life Technologies, Gibco (Paisley, UK)
Multi-element standard solution (100 µg mL-1)	SCP Science (Paris, France)
Solvents	
Acetonitrile (LC-MS grade, 99%)	Fischer Scientific (Bishop Meadow, UK)
Methanol (P.A.)	Fluka (Lisbon, Portugal)

Table S 3 - Operation conditions for ICP-MS analysis.

Plasma conditions	
RF power	1.2 kW
Plasma Ar flow rate	15 L min^{-1}
Auxiliary Ar flow rate	0.89 L min^{-1}
Carrier Ar flow rate	0.95 – 1.0 L min^{-1}
Torch horizontal alignment	- (0.5 – 1.0) mm
Torch vertical alignment	0.2 – 0.5 mm
Sampling depth	6.0 – 8.0 mm
Instrument	
Sampler cone	Nickel, 1.0 mm orifice diameter
Skimmer cone	Nickel, 0.4 mm orifice diameter
Isotopes	$^{107,109}Ag$, ^{27}Al, ^{75}As, ^{137}Ba, $^{43,44}Ca$, $^{111,114}Cd$, ^{59}Co, ^{53}Cr, $^{63,65}Cu$, ^{57}Fe, $^{199,202}Hg$, ^{115}In, ^{39}K, $^{24,25,26}Mg$, ^{55}Mn, $^{95,98}Mo$, ^{23}Na, $^{60,62}Ni$, ^{31}P, $^{206,208}Pb$, $^{121,123}Sb$, ^{82}Se, $^{116,118,120}Sn$, ^{47}Ti, $^{203,205}Tl$, ^{51}V, $^{66,68}Zn$

Table S 4 - Initial list of plant species under study. Initial screening for their inhibitory activities (at 5 mg mL^{-1} DE) towards digestive enzymes linked to sugar metabolism.

Family/Species		**Yeast α-glucosidase**	**Porcine α-Amylase**
Adoxaceae			
Sambucus lanceolata	Leaves	51%	11%
	Fruit	31%	6%
Aizoaceae			
Tetragonia tetragonoides	Leaves	20%	N.I.
	Stems	7%	N.I.

Amaranthanceae			
Beta vulgaris	Leaves	76%	23%
	Stems	28%	12%
Beta vulgaris (var. cicla)	Leaves	59 – 67%	13 – 27%
	Stems	13 – 25%	5 – 9%
Annonaceae			
Annona cherimolla	Leaves	21%	N.I.
Apiaceae			
*Melanoselinum decepiens**	Leaves	19%	N.I.
	Stems	9%	N.I.
*Monizia edulis**	Leaves	18 - 21%	N.I.
	Stems	11 - 14%	N.I.
Foenicum vulgare	Total aerial parts	21%	N.I.
Aquifoliaceae			
Ilex perado	Leaves	67%	18%
Araceae			
Arum italicum	Tubers	N.I.	N.I.
*Monstera deliciosa**	Fruits	13%	N.I.
Asteraceae			
Andryala glandulosa ssp.*	Leaves	56%	50%
*Argyranthemum pinnatifidum**	Leaves	64%	49%
	Flowers	69%	36%
*Artemisia argentea**	Leaves	43 – 47%	80%
	Flowers	46 – 48%	44%
*Calendula maderensis**	Leaves	16%	23%
	Flowers	21%	19%
*Cyanara cardunculus (var. ferocissima)**	Total aerial parts	10%	7%
*Helichrysum devium**	Leaves	45%	24%
	Flowers	57%	31%
*Helichrysum melaleucum**	Leaves	60%	22%
	Flowers	67%	27%
*Helichrysum monizii**	Total aerial parts	53%	21%
*Helichrysum obconicum**	Leaves	71%	31%

*Phagnalon lowei**	Leaves	65%	37%
	Flowers	79%	29%
Brassicaceae			
Sinapidendron spp	Leaves	13%	N.I.
	Flowers	7%	N.I.
*Rorippa nasturtium-aquaticum**	Total aerial parts	25%	17%
Convolvulaceae			
Ipomoea batatas	Total aerial parts	83%	31%
Elaeagnaceae			
Elaeagnus umbellata	Leaves	87 – 93%	54%
	Fruit	79 – 84%	39%
Ericaceae			
Vaccinium cylindraceum	Leaves	92%	55%
	Fruit	91%	83%
Vaccinnium padifolium	Leaves	97 – 99%	69%
	Fruit	90 – 93%%	62%
Fabaceae			
*Ulex europaeus**	Leaves	78%	65%
	Flowers	87%	68 %
Myricaceae			
Myrica faya	Leaves	>100%	72%
	Fruits	99%	86%
Myrtaceae			
Eugenia uniflora	Leaves	100%	88%
Polygonaceae			
*Rumex maderensis**	Leaves	82 %	17%
	Flowers	95%	21%
	Stems	69%	53%
Rosaceae			
Eriobotrya japonica	Leaves	93%	78%
	Fruit	84%	22%
Rubus grandifolius	Leaves	>100%	54%
	Fruit	≥ 99%	67%
Scrophulariaceae			
*Sibthorpia peregrina**	Leaves	74%	22%

Tropaeolaceae			
Tropaeolum majus	Leaves	30%	8%.
	Flowers	25%	3%

*This data has been already published in scientific literature.

Table S 5 - Mineral content of analysed berries collected in different years/collection areas determined by ICP-MS. Variation (min-max value) of minerals and trace elements concentration levels (μg g^{-1} of FW) in the analysed berry species. Reprinted (adapted) with permission from [121].

	E. umbellata	***M. faya***	***R. grandifolius***	***V. padifolium***
Ag	N.D.	N.D.	N.D.	N.D.
Al	13 - 86	11 - 200	15 – 260	20.0 – 30.9
As	N.D.	N.D. Detected	N.D.	N.D.
Ba	1.0 - 1.2	0.14 - 1.6	3.4 – 6.5	3.0 – 3.2
Ca	925 - 1150	750- 1140	1300 - 2100	770 - 940
Cd	N.D.	N.D.	N.D.	N.D.
Co	0.03 – 0.04	0.03– 0.31	0.04 – 0.06	0.03 – 0.14
Cr	Detected	Detected – 2.7	Detected – 1.1	Detected
Cu	5.2– 7.4	1.0 – 3.6	3.1 – 5.9	2.6 – 5.3
Fe	28 - 40	23 – 302	34 - 273	13.2 - 20.5
Hg	N.D.	N.D.	N.D.	N.D.
K	7600 - 8200	3400 – 5800	4300 - 5700	3000 - 3900
Mg	410 - 440	420 - 770	1350 - 1650	515 - 550
Mn	8.1 – 12.1	3.7 – 16	23.8 – 43.2	39 - 49
Mo	0.5 – 0.8	0.06 – 0.34	0.10 – 0.13	N.D.
Na	60 - 73	1300 - 2600	56 - 88	52 - 66
Ni	1.2 – 1.6	0.6 – 3.1	0.8 – 1.6	1.0 – 1.1
P	730 - 1000	275 – 440	610 - 950	510 - 610
Pb	N.D.	N.D. – 0.05	N.D.	N.D.
Sb	N.D.	N.D. – 0.6	N.D.	N.D.
Se	N.D.	N.D.	N.D.	N.D.
Sn	N.D.	N.D.	N.D.	N.D.
Ti	1.4 – 5.2	1.8 – 50.5	2.2 – 48.3	0.33 – 0.79
Tl	N.D.	N.D.	N.D.	N.D.
V	Detected	Detected – 0.79	Detected – 0.72	N.D.
Zn	4.5– 17.4	3.4 – 6.2	5.7 – 11.3	4.6 – 6.6

Table S 6 - Mineral content (μg g^{-1} of FW) of *E. umbellata* berries collected in consecutive years determined by ICP-MS. Data represent the mean ± standard deviation (n = 3). Reprinted (adapted) with permission from [121].

	2014	2013		2013	2014
Ag	N.D.	N.D.	**Mn**	9.08 ± 0.57[a]	11.83 ± 0.30[b]
Al	13.43 ± 0.44[a]	55.28 ± 31.42[b]	**Mo**	0.55 ± 0.07[a]	0.81 ± 0.04[b]
As	N.D.	N.D.	**Na**	65.26 ± 4.22[a]	73.73 ± 1.11[a]
Ba	1.17 ± 0.03 a	1.03 ± 0.02[a]	**Ni**	1.20 ± 0.01[a]	1.51 ± 0.10[b]
Ca	1038.17 ± 110.89[a]	974.52 ± 21.78[a]	**P**	757.44 ± 17.09[a]	967.82 ± 39.87[b]
Cd	N.D.	N.D.	**Pb**	N.D.	N.D.
Co	0.01 ± 0.01[a]	0.01 ± 0.01[a]	**Sb**	N.D.	N.D.
Cr	0.26 ± 0.02[b]	0.19 ± 0.01[a]	**Se**	N.D.	N.D.
Cu	5.26 ± 0.10[a]	6.68 ± 0.69[b]	**Sn**	N.D.	N.D.
Fe	36.11 ± 3.82[b]	28.48 ± 1.07[a]	**Ti**	1.77 ± 0.34[a]	1.71 ± 0.10[a]
Hg	N.D.	N.D.	**Tl**	N.D.	N.D.
K	7648.39 ± 7.71[a]	8228.94 ± 41.14[b]	**V**	0.09 ± 0.01[a]	0.08 ± 0.01[a]
Mg	415.03 ± 1.84[a]	430.21 ± 13.20[a]	**Zn**	5.06 ± 0.57[a]	15.85 ± 1.51[b]

Means in the same line not sharing the same letter are significantly different at $p < 0.05$ probability level.

Table S 7 - Mineral content (μg g^{-1} of FW) of *M. faya* berries collected in diferent locations of Madeira Island determined by ICP-MS. Data represent the mean ± standard deviation (n = 3). Reprinted (adapted) with permission from [121].

	Machico	Faial	Arco São Jorge	Boaventura	Seixal	Ribeira da Janela	Porto Moniz
Ag	N.D.	N.D.	N.D.	N.D.	N.D.	N.D.	N.D.
Al	71.45 ± 0.22^{b}	187.03 ± 11.08^{d}	169.57 ± 5.45^{d}	13.64 ± 0.44^{a}	12.84 ± 1.07^{a}	83.33 ± 0.38^{c}	67.87 ± 7.15^{b}
As	N.D.	N.D.	N.D.	N.D.	N.D.	N.D.	N.D.
Ba	0.82 ± 0.01^{d}	0.41 ± 0.01^{c}	0.97 ± 0.58^{e}	0.31 ± 0.01^{b}	0.16 ± 0.02^{a}	0.27 ± 0.02^{b}	0.30 ± 0.02^{b}
Ca	829.68 ± 25.58^{bc}	757.90 ± 4.40^{a}	800.80 ± 5.50^{b}	874.23 ± 22.28^{cd}	911.63 ± 87.18^{d}	1106.33 ± 29.43^{e}	940.23 ± 34.93^{de}
Cd	N.D.	N.D.	N.D.	N.D.	N.D.	N.D.	N.D.
Co	0.09 ± 0.01^{b}	0.20 ± 0.02^{d}	0.29 ± 0.02^{e}	0.06 ± 0.01^{a}	0.04 ± 0.01^{a}	0.31 ± 0.01^{e}	0.13 ± 0.01^{c}
Cr	0.28 ± 0.05^{b}	0.70 ± 0.05^{d}	2.67 ± 0.05^{e}	0.83 ± 0.51^{d}	0.09 ± 0.01^{a}	0.56 ± 0.07^{cd}	0.52 ± 0.05^{cd}
Cu	2.01 ± 0.03^{d}	1.61 ± 0.20^{c}	2.57 ± 1.00^{f}	1.28 ± 0.01^{a}	1.38 ± 0.02^{b}	2.17 ± 0.09^{e}	2.00 ± 0.05^{d}
Fe	108.65 ± 3.11^{b}	289.11 ± 14.05^{d}	277.23 ± 22.91^{d}	25.58 ± 2.26^{a}	26.02 ± 2.59^{a}	136.81 ± 19.61^{c}	100.82 ± 8.69^{b}
Hg	N.D.	N.D.	N.D.	N.D.	N.D.	N.D.	N.D.
K	5471.68 ± 64.08^{c}	3581.05 ± 162.80^{a}	4899.13 ± 23.38^{b}	5756.85 ± 25.30^{c}	3783.45 ± 257.95^{a}	3837.35 ± 92.40^{a}	3862.93 ± 226.33^{a}
Mg	474.16 ± 11.83^{b}	477.73 ± 23.76^{b}	735.82 ± 34.68^{e}	572.91 ± 15.98^{c}	479.46 ± 24.67^{b}	706.31 ± 2.81^{d}	460.19 ± 21.51^{a}
Mn	4.59 ± 0.08^{a}	10.31 ± 0.30^{c}	9.60 ± 0.52^{c}	10.15 ± 0.03^{c}	7.56 ± 0.19^{b}	15.46 ± 0.61^{d}	10.59 ± 0.69^{c}
Mo	0.32 ± 0.02^{e}	0.18 ± 0.01^{d}	0.14 ± 0.01^{c}	0.07 ± 0.01^{ab}	0.08 ± 0.01^{a}	0.10 ± 0.01^{b}	0.11 ± 0.01^{b}
Na	1718.89 ± 28.46^{b}	2493.98 ± 100.93^{d}	1309.28 ± 9.08^{a}	2253.63 ± 9.08^{c}	2130.15 ± 191.40^{c}	2304.50 ± 112.75^{cd}	1819.68 ± 175.05^{b}
Ni	2.31 ± 0.06^{c}	2.34 ± 0.14^{c}	2.78 ± 0.08^{d}	2.75 ± 0.33^{cd}	0.58 ± 0.03^{a}	1.51 ± 0.03^{b}	1.47 ± 0.06^{b}
P	339.35 ± 35.20^{b}	329.45 ± 15.40^{b}	388.30 ± 8.25^{c}	455.13 ± 15.68^{d}	282.43 ± 9.08^{a}	392.98 ± 2.48^{c}	335.50 ± 4.95^{b}
Pb	0.04 ± 0.01	N.D.	N.D.	N.D.	N.D.	N.D.	N.D.
Sb	0.02 ± 0.01^{a}	N.D.	0.13 ± 0.02^{b}	0.27 ± 0.06^{c}	N.D.	0.02 ± 0.01^{a}	0.53 ± 0.07^{d}
Se	N.D.	N.D.	N.D.	N.D.	N.D.	N.D.	N.D.

Sn	N.D.	N.D.	N.D.	N.D.	N.D.	N.D.	N.D.
Ti	12.13 ± 0.19^{c}	48.46 ± 2.04^{e}	26.46 ± 1.71^{d}	1.87 ± 0.11^{a}	2.12 ± 0.03^{b}	12.95 ± 0.03^{c}	12.93 ± 0.72^{c}
Tl	N.D.	N.D.	N.D.	N.D.	N.D.	N.D.	N.D.
V	0.27 ± 0.01^{b}	0.76 ± 0.04^{d}	0.65 ± 0.04^{c}	0.06 ± 0.01^{a}	0.07 ± 0.01^{a}	0.31 ± 0.02^{b}	0.26 ± 0.02^{b}
Zn	5.06 ± 0.50^{c}	4.18 ± 0.17^{a}	5.67 ± 0.55^{d}	5.14 ± 0.25^{c}	4.81 ± 0.08^{b}	4.62 ± 0.22^{bc}	4.18 ± 0.22^{a}

Means in the same line not sharing the same letter are significantly different at $p < 0.05$ probability level.

Table S 8 - Mineral content (μg g^{-1} of FW) of *R. grandifolius* berries collected in diferent locations of Madeira Island determined by ICP-MS. Data represent the mean ± standard deviation (n = 3). Reprinted (adapted) with permission from [121].

	Funchal	**Machico**		**Funchal**	**Machico**
Ag	N.D.	N.D.	**Mn**	24.99 ± 1.09[a]	42.62 ± 0.62[b]
Al	15.71 ± 1.30[a]	192.62 ± 77.14[b]	**Mo**	0.11 ± 0.01[a]	0.12 ± 0.01[a]
As	N.D.	N.D.	**Na**	58.88 ± 2.39[a]	82.51 ± 5.04[b]
Ba	6.11 ± 0.36[b]	3.41 ± 0.05[a]	**Ni**	0.95 ± 0.19[a]	1.29 ± 0.26[b]
Ca	1422.75 ± 83.79[a]	2055.84 ± 47.52[b]	**P**	629.79 ± 14.49[a]	902.54 ± 51.55[b]
Cd	N.D.	N.D.	**Pb**	N.D.	N.D.
Co	0.05 ± 0.01[a]	0.06 ± 0.01[a]	**Sb**	N.D.	N.D.
Cr	0.42 ± 0.02[a]	0.81 ± 0.29[b]	**Se**	N.D.	N.D.
Cu	3.70 ± 0.63[a]	5.71 ± 0.24[b]	**Sn**	N.D.	N.D.
Fe	35.28 ± 1.18[a]	214.13 ± 59.86[b]	**Ti**	2.18 ± 0.04[a]	34.18 ± 14.11[b]
Hg	N.D.	N.D.	**Tl**	N.D.	N.D.
K	4382.70 ± 107.94[a]	5597.38 ± 95.23[b]	**V**	0.06 ± 0.01[a]	0.55 ± 0.17[b]
Mg	1384.36 ± 16.30[a]	1664.47 ± 19.13[b]	**Zn**	6.41 ± 0.69[a]	10.75 ± 0.58[b]

Means in the same line not sharing the same letter are significantly different at $p < 0.05$ probability level.

Table S 9 - Mineral content (μg g^{-1} of FW) of *V. padifolium* berries collected in consecutive years i determined by ICP-MS. Data represent the mean ± standard deviation (n = 3). Reprinted (adapted) with permission from [121].

	2013	2014		2013	2014
Ag	N.D.	N.D.	**Mn**	48.05 ± 0.66[b]	40.26 ± 0.86a
Al	29.47 ± 1.22[b]	20.76 ± 1.09[a]	**Mo**	N.D.	N.D.
As	N.D.	N.D.	**Na**	57.09 ± 4.36[a]	62.34 ± 3.66a
Ba	3.07 ± 0.10[a]	3.14 ± 0.03[a]	**Ni**	1.12 ± 0.01[a]	1.06 ± 0.07[a]
Ca	930.60 ± 3.96[b]	785.73 ± 12.87[a]	**P**	583.44 ± 20.46[b]	532.29 ± 25.41[a]
Cd	N.D.	N.D.	**Pb**	N.D.	N.D.
Co	0.01 ± 0.01[a]	0.05 ± 0.01[a]	**Sb**	N.D.	N.D.
Cr	0.13 ± 0.01[a]	0.28 ± 0.01[b]	**Se**	N.D.	N.D.
Cu	3.88 ± 0.08[a]	3.93 ± 1.35[a]	**Sn**	N.D.	N.D.
Fe	13.66 ± 0.07[a]	19.54 ± 0.79[b]	**Ti**	0.40 ± 0.02[a]	0.67 ± 0.11[b]
Hg	N.D.	N.D.	**Tl**	N.D.	N.D.
K	3772.23 ± 96.03[a]	3148.86 ± 72.60[b]	**V**	N.D.	N.D.
Mg	538.86 ± 6.04[a]	533.61 ± 13.27[a]	**Zn**	5.97 ± 0.43[a]	4.88 ± 0.92[a]

Means in the same line not sharing the same letter are significantly different at $p < 0.05$ probability level

1. Identification of phytochemicals of methanolic extracts

The aim of this part of the work was to characterize the phytochemical composition of methanolic extracts by HPLC-ESI/MS^n. An essential step in these analyses was to determine the molecular weight of each compound. In general, in the negative ionization mode (ESI^-) MS^1 spectrum, the most intense peak corresponded to the deprotonated molecular ion [M-H]; this permitted to perform further MS^n analysis. Moreover, this assignment was more consistent if adduct ions and dimers were present. Most compounds were observed in their glycosylated form. The mass spectra of the conjugated phenolic compounds showed the aglycone ion as result of the loss of sugar moieties like glucuronyl, hexosyl, deoxyhexosyl, pentosyl, and rutinosyl (-176, −162, −146, −132 and −308 Da, respectively). Data from the positive ionization (ESI^+) mode was used for identification of ANTCs and confirmation purposes.

When reference substances were available, extract components were identified by comparing the HPLC retention time, UV and mass spectra, with those obtained for the standard. However, since the access to pure reference compounds was limited, characterization of most of the PCs was assigned based on comparison of the MS^n fragmentation patterns and UV-vis spectra with information available in scientific literature. Additionally, some derivatives of phytochemicals were putatively assigned, on the basis of analogous fragmentations.

The results of HPLC-DAD-ESI/MS^n screening will be presented for each plant individually. Compounds were numbered by their order of elution and this numeration was kept identical for berries and leaves, so the same compounds may have different numbers in different extracts. Identification will be presented in the next subsections, grouping the compounds by the family of the respective aglycones. Some of the compounds were present in all analysed extracts while some were absent. For clarity's sake, the discussion of available data for each compound will be presented for the first plant in which it appears and not repeated for subsequent plant species.

1.1. Elaeagnus umbellata

Following is a brief explanation for the identification of the compounds in *E.umbellata* extracts collected in 2013 and 2014 (**Table S 10**). For a more detailed explanation, please check the mentioned references.

1.1.1. Phenolic compounds

Compound **23** displayed $[M-H]^-$ ion at m/z 551 and MS^2 base peak at m/z 529 (by loss of 22 Da). Further MS^n fragmentation gave origin to product ions at m/z 169 and 125, typical of gallic acid (corroborative with analytical standard). With no more available information, **23** was tentatively characterized as a derivative.

Compounds **25** and **28** exhibited [M-H+HCOO]$^-$ ions at m/z 563. Sequential fragmentation gave origin to product ion at m/z 517. The 46 Da residue can be attributed to a formate adduct from the mobile phase. After loss of 132 Da, fragment ions at m/z 385 [M-H-sinapoyl+162]$^-$, 223 [M-H-sinapoyl]$^-$, 208 [M-H-sinapoyl-15]$^-$ and 164 [M-H-sinapoyl-44]$^-$ were detected [197]. Therefore, 25 was tentatively identified as sinapic acid-*O*-(pentosyl)hexoside. Sinapic acid-*O*-hexoside (compounds **29** and **35**) was also identified in analyzed extracts [197]. Compound **34**, with [M-H]$^-$ ion at m/z 489, showed a loss of 266 Da at MS^2. Fragment ion at m/z 223 was identified as sinapic acid [197], hence, **34** was tentatively characterized as a derivative. Similarly, compound **41** showed [M-H]- ion at m/z 503 and was identified as another derivative of sinapic acid. Compound **31**, with [M-H]$^-$ ion at m/z 565 was identified a caffeic acid-*O*-(sinapoyl-*O*-hexoside) [198]. Compounds **46** and **78** displayed [M-H]$^-$ ions at m/z 389 and 429, respectively. They followed different fragmentation patterns but had in common fragment ion at m/z 179 and 135, which are characteristic of caffeic acid (compared with analytical standard). Based only on the available data it was not possible to fully characterize these compounds; **46** and **78** were assigned as derivatives. 3,5-*O*-dicaffeoylquinic acid (compound **70**) was identified based on comparison with a reference standard solution.

Digalloyl-*O*-glucoside (compound **66**) was identified in leaves extract [199]. Compound **68** exhibited [M-H]$^-$ ion at m/z 689 and suffered a loss of 224 Da. The presence of product ions at m/z 635 at MS^2 and 465, 313, 169 and 125 at MS^3 was indicative of trigalloylglucose [200,201]. Hence, **68** was tentatively characterize as a derivative.

1.1.2. Flavonols

Several quercetin glycosides (compounds **14**, **27**, **30**, **43**, **48**, **49**, **51** and **61**) were characterized in the methanolic extracts of *E. umbellata*, based on literature data [84,200,202,203]. Compound **67**, with [M-H]$^-$ ion at m/z 839, yielded fragment ion at m/z 625 (by loss of 214 Da). Sequential fragmentation was corroborative with that of quercetin-*O*-dihexoside [200]. With no more available information, 67 was tentatively characterized as a derivative.

Kaempferol derivatives were abundant in the analyzed extracts. Their identification (compounds **26**, **36**, **37**, **50**, **69**, **73**, **76**, **87** and **89**) was achieved based on previous works [125,200,203]. Compound **63**, with [M-H]$^-$ ion at m/z 579, suffered a loss of 294 Da at MS^2. This could be attributed to a combined pentose (arabinose, xylose or apiose) plus hexose (glucose, mannose and galactose) (132 + 162 Da) moiety. Fragmentation of product ion at m/z 285 was consistent with MS^n data of kaempferol standard (fragment ions at m/z 257, 255, and 229). Hence, **63** was tentatively characterized as kaempferol-*O*-(pentosyl)hexoside.Compound **80** showed [M-H]$^-$ ion at m/z 755. It presented the same fragmentation pattern as compound **26**. However, due to the latter retention time, the loss of 146 Da is assigned to a coumaroyl residue rather than a rhamnosyl. Generally, flavonoid glycosides esterified with aromatic acids have higher retention times than their diglycosides, monoglycosides and aglycones [204]. Thus, **80** was tentatively characterized as kaempferol-*O*-(coumaroyl)dihexoside. Similarly, compounds **87** and **89** with [M-H]$^-$ ions at m/z 593, were tentatively characterized as kaempferol-*O*-(coumaroyl)hexoside. The loss of 308 Da is attributed to a

coumaroyl(hexoside) group (146 + 162 Da) instead of a rutinoside due to the presence of fragment ion at m/z 447 $[M-H-146]^-$.

Many isorhamnetin derivatives were found in this analysis (**Table S 10**). Compound **33** displayed $[M-H]^-$ ion at m/z 759 and suffered a loss of 210 Da at MS^2. Further fragmentation gave origin to product ion at m/z 491 (by loss of a 58 Da residue). Finally, it resulted in isorhamnetin aglycone at m/z 315 (after loss of 176 Da) and its typical fragment ions at m/z 299 and 271 [200]. With no more available information, **33** was tentatively characterized as derivative of isorhamnetin-*O*-glucuronide. Compound **38**, with $[M-H]^-$ ion at m/z 755, gave origin to MS^2 base peak at m/z 609 (by loss of 146 Da). Sequential fragmentation showed a loss of 294 Da to produce isorhamnetin aglycone (at m/z 315). Hence, **38** was tentatively identified as isorhamnetin-*O*-(pentosyl)hexoside-*O*-rhamnoside. Compounds **60** and **65** showed $[M-H]^-$ ions at m/z 609 and, by analogy, were characterized as isorhamnetin-*O*-(pentosyl)hexoside. Compound **75** displayed $[M-H]^-$ ion at m/z 845. It gave origin to MS^3 base peak at m/z 639, after loss of 206 Da. This residue can be attributed to a sinapoyl unit attached to the molecule [205]. Fragmentation pattern of product ion at m/z 639 matched that of isorhamnetin-*O*-dihexoside [200]. Thus, **75** was tentatively characterized as isorhamnetin-*O*-(sinapoyl)dihexoside. Isorhamnetin-*O*-dipentoside (compound **77**) was also characterized. After a combined loss of two pentoside units (132 + 132 Da) from $[M-H]^-$ ion at m/z 579, it gave origin to isorhamnetin (at m/z 315). Compound **79** presented $[M-H]^-$ ion at m/z 815. After loss of 176 Da, it gave origin to isorhamnetin-*O*-dihexoside at m/z 639 [200]; it was tentatively characterized as isorhamnetin-*O*-(glucuronyl)dihexoside-*O*-glucuronide. Compound **84**, with $[M-H]^-$ ion at m/z 805, suffered a loss of 166 Da at MS^2 to yield product ion at m/z 639 (previously identified as isorhamnetin-*O*-dihexoside). By analogy, **84** was tentatively identified as a derivative.

Compound **39** displayed $[M-H]^-$ ion at m/z 611. Fragmentation gave origin to product ions at m/z 317, 217 and 179 (after loss of 294 Da), characteristic of myricetin [200]. Hence, **39** was tentatively characterized as myricetin-*O*-(pentosyl)hexoside.

1.1.3. Flavones

Compounds **88** and **91** were characterized as diosmetin-8-*C*-dihexoside. They presented $[M-H]^-$ ions at m/z 581 and suffered a neutral loss of 120 Da to yield product ion at m/z 461. Sequential fragmentation showed another 120 Da loss, typical of *C*-glycosides flavonoids [205]. Based on previous publications [198,200], fragment ion at m/z 461 was identified as diosmetin-8-*C*-hexoside. Compound **90**, with $[M-H]^-$ ion at m/z 623, gave origin to MS^2 base peak at m/z 299 (after a combined loss of 324 Da). This main product ion was identified as diosmetin [198], hence, **90** was tentatively characterized as diosmetin-*O*-dihexoside.

1.1.4. Ellagic acid derivatives/Ellagitannins

Ellagitannins were common on *E. umbellata* extracts and their identification was achieved by comparison with literature [199,200,206]: hexahydroxydiphenoyl(HHDP)-*O*-glucose (compound **7** and **12**), bis-HHDP-*O*-glucose (compounds **10**, **13**, **15**, **17**, **20**), galloyl-HHDP-*O*-glucose (compounds **21**, **22** and **24**).

Compound **40** exhibited $[M-H]^-$ ion at m/z 463 was identified as ellagic acid-*O*-hexoside [107]. With an $[M-H]^-$ ion at m/z 475, compound **42** was tentatively characterized as ellagic acid-*O*-(acetyl)pentoside. The direct loss of 174 Da (132 + 42 Da) can be associated with a pentoside plus acetyl moiety.

1.1.5. Other compounds

Additionally, some non-phenolic compounds (saccharides, organic acids, terpenoids) were also identified in this analysis.Compound **1** displayed $[M-H]^-$ ion at m/z 179. Fragmentation yielded product ions at m/z 161, 143, 131, 119, 113 and 89, which was consisted with that of hexosides [207]. Similarly, compound **4** was characterized as a polymer of hexoses. Compound **2**, with $[M–H]^-$ ion at m/z 473, was identified as a trisaccharide, containing a pentose and two hexose units [125]. Other compounds with similar fragmentation ions (**19**, **47**, **52**, **53**, **55**, **57 - 59**, **62**, **64** and **94**) were tentatively characterized as saccharides.

Compound **3** showed $[M-H]^-$ ion at m/z 295. After loss of 116 Da, characteristic of malic acid derivatives [208], it gave origin to a hexose at m/z 179. Thus, **3** was tentatively characterized as hexosyl-malic acid. With an extra 295 Da moiety, compound **5** was identified as a dimmer. Compound **8** was identified as quinic acid, by comparison with analytical standard (data not shown). Compound **6**, with $[M-H]^-$ ion at m/z 533, was characterized as a derivative [106]. Malic and citric acids (compounds **10** and **11**) were identified based on literature data [198].

Compound **32** presented $[M-H+HCOO]^-$ at m/z 431 and suffered the loss of 46 Da (formate) to produce the ion at m/z 385, which was identified as a roseoside (vomifoliolglucoside) [209].

Compound **71** showed a [M-H]- ion at m/z 649. It suffered a loss of 180 Da to yield base peak at m/z 469. Further fragmentation resulted in product ion at m/z 187 (after loss of 282 Da). By comparison with literature [210], fragment ion at m/z 187 was identified as 2-methylaconitate. With no further information about its structure, **71** was tentatively characterized as a derivative.

Compound **81** exhibited $[M-H+HCOOH]^-$ ion at m/z 711. The combined loss of 208 Da (162 + 46 Da), generated product ion at m/z 503. Further fragmentation was corroborative with that of triterpene acid [211]. Hence, **81** was tentatively characterized as triterpene acid-*O*-hexoside (formate adduct).

Table S 10 - Characterization of phytochemicals of *E. umbellata* methanolic extracts by HPLC-ESI$^-$/MS^n.

No.	t_R (min)	[M-H]$^-$ (*m/z*)	HPLC-DAD-ESI/MS^n *m/z* (% base peak)	Assigned identity	Berries	Leaves	References
1	3.1	**179**	MS^2 [179]: 161 (76.9), 149 (17.8), 143 (76.5), 131 (24.7), 119 (47.6), 113 (57.6). 101 (27.8). 89 (100)	Hexose	✓	✓	[207]
2	3.2	**473**	MS^2 [473]: 342 (17.3), 341 (100), 221 (12.9), 179 (46.0), 132 (26.5) MS^3 [473→341]: 323(27.9), 281 (11.0), 179 (100), 161 (32.8), 143 (11.4) MS^4 [473→341→179]: 161 (13.5), 131 (53.7), 119 (37.6), 113 (19.6), 107 (23.3), 89 (100)	Oligosaccharide (Pentose + dihexose)	✓		[125]
3	3.3	**295**	MS^2 [295]: 235 (20.6), 205 (21.9); 179 (99.4). 161 (13.5), 133 (100); 115 (11.4) MS^3 [295→179]: 161 (581), 149 (12.1), 143 (72.6), 131 (25.7), 119 (50.8), 113 (23.3), 89 (100)	Hexosyl-malic acid	✓		
4	3.3	**683** [3M-H]$^-$	MS^2 [683]: 342 (14.4), 341 (100) MS^3 [683→341]: 179 (100), 161 (30.2), 143 (18.1), 119 (13.2), 113 (20.3), 101 (14.3) MS^4 [683→341→179]:161 (58.6), 143 (43.6), 131 (15.4), 119 (46.9), 113 (20.2), 101 (39.8), 89 (100), 71 (35.8), 59 (26.7)	Hexose polymer		✓	[207]
5	3.4	**591** [2M-H]$^-$	MS^2 [591]: 295 (100) MS^3 [591→295]: 235 (21.8), 205 (19.6), 179 (100); 161 (11.1), 143 (11.2), 133 (71.3), 119 (10.7), 113 (12.1), 89 (13.3)	Hexosyl-malic acid dimer	✓		
6	3.5	**533**	MS^2 [533]: 191 (100.0) MS^3 [533→191]: 153 (11.4), 127 (100.0), 111 (26.6), 93 (74.5), 85 (66.5)	Quinic acid derivative		✓	[106]
7	3.6	**481**	MS^2 [481]: 301 (100), 275 (19.2) MS^3 [481→301]: 257 (38.3), 245 (23.8), 185 (100)	HHDP-*O*-glucose		✓	[206]
8	3.7	**191**	MS^2 [191]: 173 (76.9), 171 (13.8), 127 (100.0), 111 (77.5), 109 (37.4), 93 (47.9), 87 (28.2), 85 (82.9), 81 (17.6) MS^3 [191→127]: 109 (21.1), 85 (100)	Quinic acid		✓	Standard
9	3.9	**133**	MS^2 [133]: 115 (100) MS^3 [133→115]: 71 (100)	Malic acid	✓	✓	[198]
10	4.0	**783**	MS^2 [783]: 765 (10.8), 721 (10.4), 481 (41.7), 301 (100), 275 (23.7) MS^3 [783→301]: 299 (100), 257 (22.8), 256 (24.5), 240 (14.6), 230 (21.0), 157 (10.1)	bis-HHDP-*O*-glucose (Pedunculagin I)		✓	[200]
11	4.4	**191**	MS^2 [191]: 173 (18.7), 111 (100) MS^3 [191→111]: 67 (100)	Citric acid	✓		[198]
12	4.6	**481**	MS^2 [481]:301 (100), 275 (12.8) MS^3 [481→301]:257 (100), 242 (54.5), 229 (41.9), 214 (51.5), 186 (72.9), 173 (84.1), 147 (38.0)	HHDP-*O*-glucose		✓	[206]
13	4.9	**783**	MS^2 [783]:765 (12.5), 721 (13.0), 481 (38.4), 301 (100), 275 (28.7) MS^3 [783→301]:299 (100), 284 (19.8), 257 (19.4), 245 (18.9), 229 811.7), 213 (77.9) MS^4 [783→301→299]: 281 (100)	bis-HHDP-*O*-glucose (Pedunculagin I)		✓	[200]
14	5.2	**757**	MS^2 [757]: 596 (25.2), 595 (100) MS^3 [757→595]: 445 (17.9), 301 (49.8), 300 (100), 271 (14.9), 255 (11.0) MS^4 [757→595→301]: 273 (11.5), 272 (27.2), 271 (100), 256 (11.6), 255 (30.0), 201 (11.0), 179 (32.4), 151 (40.1)	Quercetin-*O*-(pentosyl)dihexoside		✓	[202]
15	5.4	**783**	MS^2 [783]: 669 (11.6), 481 (11.3), 301 (100), 275 (18.5), 249 (22.4), 243 (12.6)	bis-HHDP-*O*-glucose (Pedunculagin I)	✓		[200]

16	5.7	**305**	MS^2 [305]: 261 (12.2), 221 (47,7), 219 (56.0), 179 (100), 165 (28.1), 137 (30.8), 125 (40.2) MS^3 [305→179]: 165 (66.9), 164 (53.2), 152 (35.0), 151 (100), 135 (76.1)	Gallo(epi)catechin	✓		[106]
17	5.8	**783**	MS^2 [783]:481 (30.5), 301 (100), 275 (17.8) MS^3 [783→301]: 300 (10.5), 285 (15.7), 283 (24.3), 273 (14.8), 257 (87.8), 245 (34.6), 241 (23.9), 229 (100), 213 (29.7) MS^4 [783→301→257]:185 (100)	bis-HHDP-*O*-glucose (Pedunculagin I)		✓	[200]
18	6.1	**583**	MS^2 [583]:538 (25.6), 537 (100) MS^3 [583→537]:491 (60.2), 406 (16.0), 405 (100), 293 (29.0), 243 (34.4), 225 (10.4), 191 (71.3), 168 (21.4), 161 (25.3), 149 (55.7)	Unknown		✓	
19	6.5	**451**	MS^2 [451]:405 (100) MS^3 [451→405]: 243 (46.7), 179 (25.7), 167 (20.5), 161 (12.7), 153 (44.0), 149 (100), 143 (11.6), 119 (22.2)	Saccharide	✓	✓	
20	7.0	**783**	MS^2 [783]: 481 (27.0), 301 (100), 275 (16.3) MS^3 [783→301]: 273 (25.5), 258 (23.9), 257 (100), 229 (35.8), 227 (22.3), 213 815.4), 202 (22.8), 186 (38.4), 169 (30.4), 145 (27.1)	bis-HHDP-*O*-glucose (Pedunculagin I)	✓	✓	[200]
21	7.4	**633**	MS^2 [633]: 614 (17.1), 463 (13.2), 301 (100), 273 (10.7), 271 (13.9) MS^3 [633→301]: 299 (53.5), 257 (100)	Galloyl-HHDP-*O*-hexoside	✓	✓	[199]
22	7.9	**633**	MS^2 [633]: 301 (100) MS^3 [633→301]: 286 (12.1), 275 (27.6), 258 (60.9), 257 (100), 245 (20.1), 230 (27.7), 229 (32.8), 202 (48.9), 201 (14.9), 186 (44.1)	Galloyl-HHDP-*O*-hexoside	✓	✓	[199]
23	8.0	**551**	MS^2 [551]: 529 (100) MS^3 [551→529]: 467 (100), 458 (20.6), 301 (10.6) MS^4 [551→529→467]: 301 (100), 299 (53.0), 289 (14.3), 285 (50.0), 277 (43.5), 169 (84.6), 125 (38.1)	Gallic acid derivative		✓	
24	8.3	**935**	MS^2 [935]: 917 (20.9), 659 (21.2), 633 (100), 615 (36.7), 571 (18.5), 329 (25.4), 301 (21.9), 299 (49.4) MS^3 [935→633]: 615 (76.5), 571 (70.3), 481 (44.3), 383 (31.7), 329 (76.1), 301 (28.7), 299 (100), 275 (26.5)	Galloyl-bis-HHDP hexoside (Casuarinin)	✓		[106]
25	8.5	**563**	MS^2 [563]: 517 (100) MS^3 [563→517]: 385 (93.1), 223 (89.7), 208 (100), 164 (52.3), MS^4 [563→517→208]: 164 (100)	Sinapic acid-*O*-pentosyl(hexoside) (formate adduct)	✓		
26	8.6	**755**	MS^2 [755]: 610 (23.7), 609 (100) MS^3 [755→609]: 430 (11.9), 429 (57.4), 285 (100), 284 (55.4), 257 (17.2), 255 (15.2) MS^4 [755→609→285]: 257 (64.6), 255 (79.8), 229 (43.9), 164 (18.6), 151 (100)	Kaempferol-*O*-dihexoside-*O*-rhamnoside	✓		[203]
27	8.7	**741**	MS^2 [741]: 595 (100), 446 (11.3), 271 (10.6) MS^3 [741→595]: 475 (33.1), 449 (22.3), 301 (44.4), 300 (100), 271 (15.5), 215 (11.0), 179 (11.1) MS^4 [741→595→300]: 271 (22.7), 255 (42.5), 179 (100)	Quercetin-*O*-(pentosyl)hexoside-*O*-rhamnoside	✓	✓	[203]
28	8.8	**563**	MS2 [563]: 518 (24.4), 517 (100) MS3 [563→517]: 387 (25.0), 385 (90.7), 365 (45.5), 293 (26.3), 223 (90.1), 208 (100), 164 (46.1)	Sinapic acid-*O*-(pentosyl)hexoside (formate adduct)		✓	
29	9.0	**385**	MS^2 [385]: 223 (100), 205 (73.6), 163 (10.5) MS^3 [385→223]: 208 (17.0), 164 (100), 149 (12.1)	Sinapic acid-*O*-hexoside	✓		[197]

30	9.1	**741**	MS^2 [741]: 595 (100), 446 (12.0), 300 (17.0) MS^3 [741→595]: 463 (20.2), 445 (43.7), 368 (19.3), 343 (36.2), 301 (38.0), 300 (100), 273 (42.1), 257 (10.1), 179 (15.4) MS^4 [741→595→300]: 271 (100), 179 (36.7)	Quercetin-*O*-(pentosyl)hexoside-*O*-rhamnoside	✓		[203]
31	9.3	**565**	MS^2 [565]: 520 (13.0), 519 (17.8), 403 (100), 385 (14.7), 325 (10.9), 223 (66.9), 221 (15.4), 179 (16.6) MS^3 [565→403]: 223 (89.5), 149 (27.5), 135 (100)	Caffeic acid-*O*-(sinapoyl-*O*-hexoside)	✓	✓	[198]
32	9.5	**431**	MS^2 [431]: 385 (100), 223 (13.5) MS^3 [431→385]: 223 (64.4), 206 (11.7), 205 (48.9), 161 (21.2), 153 (100), 138 (18.5) MS^4 [431→385→153]: 138 (100), 136 (56.9), 114 (40.8), 97 (26.7)	Roseoside (formate adduct)	✓	✓	[209]
33	9.8	**759**	MS^2 [759]: 651 (16.0), 639 (30.8), 621 (20.3), 579 (53.8), 549 (100) MS^3 [759→549]: 531 (21.1), 519 (49.8), 491 (100), 477 (83.4), 315 (52.0), 271 (15.2) MS^4 [759→549→491]: 315 (100), 300 (76.9), 299 (40.8), 271 (36.7)	Isorhamnetin-*O*-glucuronide derivative	✓		
34	10.5	**489**	MS^2 [489]: 446 (10.6), 295 (15.0), 283 (11.9), 265 (18.5), 223 (100), 208 (11.6), 205 (45.3), 190 (30.4), 175 (20.7), 164 (34.1), 149 (37.5) MS^3 [489→223]: 208 (77.7), 179 (100), 164 (43.9)	Sinapic acid derivative		✓	
35	10.6	**385**	MS^2 [385]: 325 (100), 295 (92.3), 265 (84.6), 223 (25.8) MS^3 [385→325]: 307 (34.3), 265 (82.0), 223 (100), 206 (48.1) MS^4 [385→325→223]:164 (100)	Sinapic acid-*O*-hexoside	✓	✓	[197]
36	10.7	**725**	MS^2 [725]: 622 (12.8), 580(35.0), 579 (100) MS^3 [725→579]: 521 (22.7), 447 (23.5), 429 (33.9), 326 (18.8), 285 (100), 257 (18.7), 255 (15.9)	Kaempferol-*O*-(pentosyl)hexoside-*O*-rhamnoside	✓		[203]
37	10.9	**449**	MS^2 [449]: 287 (100), 269 (32.4), 259 (53.9) MS^3 [449→287]: 259 (100), 243 (27.0), 201 (17.2), 173 (20.6), 151 (63.6), 125 (40.1), 119 (10.6)	Dihydrokaempferol-*O*-hexoside	✓		[125]
38	11.1	**755**	MS^2 [755]: 609 (100) MS^3 [755→609]: 459 (25.7), 315 (100), 300 (13.4), 299 (13.6), 271 (16.9), 243 (13.3) MS^4 [755→609→315]: 301 (21.1), 300 (100), 299 (91.8), 298 (16.1), 259 (20.9)	Isorhamnetin-*O*-(pentosyl)hexoside-*O*-rhamnoside	✓		
39	11.2	**611**	MS^2 [611]: 474 (15.9), 463 (22.8), 447 (17.0), 329 (12.3), 317 (100), 272 (11.0), 270(20.0), 251 (18.4) MS^3 [611→317]: 272 (76.2), 271 (100), 179 (25.0)	Myricetin-*O*-(pentosyl)hexoside	✓		
40	11.4	**463**	MS^2 [463]: 301 (100), 300 (35.6) MS^3 [463→301]: 300 (90.9), 257 (100), 229 (61.3), 207 (27.7), 172 (33.3)	Ellagic acid-*O*-hexoside		✓	[107]
41	11.8	**503**	MS^2 [503]: 223 (100), 205 (56.7), 191 (22.0), 164 (14.1), 149 (25.9) MS^3 [503→223]: 179 (100), 164 (65.5), 149 (76.1)	Sinapic acid derivative		✓	
42	12.7	**475**	MS^2 [475]: 301 (100), 275 (11.3) MS^3 [475→301]: 257 (100), 230 (22.3), 213 (27.5), 201 (29.8), 200 (29.0), 192 (34.7), 186 (14.7), 185 (34.0)	Ellagic acid-*O*-(acetyl)pentoside		✓	
43	13.0	**625**	MS^2 [625]: 505 (15.6), 463 (12.0), 445 (38.2), 301 (100), 300 (97.6), 271 (21.3), 255 (22.0) MS^3 [625→300]: 284 (13.6), 271 (100), 199 (13.4), 179 (50.6), 151 (41.5), 121 (15.5)	Quercetin-*O*-dihexoside		✓	[200]
44	13.2	**371**	MS^2 [371]: 249 (100) MS^3 [371→249]: 231 (41.1), 113 (100), 99 (12.5), 95 (27.3), 85 (49.4)	Unknown	✓	✓	[209]
45	13.9	**371**	MS^2 [371]: 249 (100) MS^3 [371→249]: 231 (47.1), 175 (10.9), 113 (100), 111 (12.2), 99 (20.5), 85 (36.3)	Unknown		✓	[209]
46	14.0	**389**	MS^2 [389]: 209 (100), 181 (19.1), 179 (76.2), 135 (35.8) MS^3 [389→209]: 135 (100)	Caffeic acid derivative	✓		

47	14.3	**725**	MS^2 [725]: 545 (100), 313 (12.9) MS^3 [725→545]: 351 (13.0), 313 (100), 295 (20.2), 249 (11.4), 247 (12.5), 231 (26.8), 229 (18.2), 187 (16.5), 179 (10.8), 161 (13.9) MS^4 [725→545→313]: 179 (100), 161 (85.9), 115 (40.7), 113 (63.4), 101 (63.4), 89 (49.0)	Saccharide		✓	
48	14.4	**595**	MS^2 [595]: 445 (14.8), 301 (46.2), 300 (100), 271 (20.6) MS^3 [595→301]: 271 (100), 257 (12.2), 255 (89.0), 243 (10.0), 179 (42.8), 151 (52.1)	Quercetin-*O*-(pentosyl)hexoside	✓	✓	[84]
49	14.8	**433**	MS^2 [433]: 301 (100), 300 (52.3 MS^3 [433→301]: 300 (100), 257 (40.7), 179 (53.8), 151 (55.5)	Quercetin-*O*-pentoside	✓		[84]
50	15.1	**609**	MS^2 [609]: 576 (57.3), 447 (72.2), 301 (48.2), 285 (100), 255 (25.1) MS^3 [609→285]: 255 (100)	Kaempferol-*O*-dihexoside	✓		[203]
51	15.1	**595**	MS^2 [595]: 445 (10.9), 301 (57.6), 300 (100), 271 (15.4), 255 (11.9) MS^3 [595→300]: 271 (100), 255 (59.9), 179 (36.9), 151 (34.4)	Quercetin-*O*-pentosyl(hexoside)		✓	[84]
52	15.5	**547**	MS^2 [547]:503 (10.6), 311 (100), 265 (10.9), 221 (13.6) MS^3 [547→311]: 293 (23.9), 275 (36.0), 251 (62.5), 233 (50.0), 221 (22.0), 179 (29.5), 161 (16.7), 149 (100), 113 (46.6)	Saccharide	✓		
53	15.7	**551**	MS^2 [551]: 505 (100) MS^3 [551→505]: 373 (100), 179 (22.3), 161 (54.4) MS^4 [551→505→373]: 161 (100), 119 (11.6), 113 (15.9)	Saccharide		✓	
54	16.1	**639**	MS^2 [639]: 477 (21.0), 315 (100), 300 (22.6), 299 (17.3), 271 (16.2) MS^3 [639→315]: 301 (11.0), 300 (100), 299 (22.6)	Isorhamnetin-*O*-dihexoside		✓	[200]
55	16.3	**547**	MS^2 [547]: 311 (100), 191 (14.1), 161 (21.8) MS^3 [547→311]: 293 (15.1), 251 (22.0), 179 (42.4), 161 (78.9), 149 (100), 119 (10.3), 101 (85.1)	Saccharide		✓	
56	16.6	**597**	MS^2 [597]:489 (15.1), 477 (49.4), 459 (17.2), 417 (15.9), 387 (67.8), 357 (100) MS^3 [597→357]: 209 (100), 139 (11.0), 123 (27.6) MS^3 [597→387]: 315 (100), 239 (37.1), 221 (14.8), 191 (18.5), 167 (12.0), 161 (11.0), 153 (10.4) MS^4 [597→357→209]: 165 (28.3), 164 (63.7), 123 (100), 121 (23.6) MS^4 [597→357→315]: 209 (41.4), 190 (21.3), 167 (100), 139 (28.5) 126 (37.7)	Unknown	✓		
57	17.1	**551**	MS^2 [551]: 505 (100) MS^3 [551→505]: 373 (100), 161 (22.7) MS^4 [551→505→373]: 179 (17.9), 161 (100), 143 (18.3), 113 (25.9)	Saccharide		✓	
58	17.4	**547**	MS^2 [547]: 311 (100), 179 (14.1), 161 (21.8) MS^3 [547→311]: 293 (15.1), 251 (22.0), 179 (42.4), 161 (78.9), 149 (100), 119 (10.3), 101 (85.1)	Saccharide		✓	
59	18.0	**415**	MS^2 [415]: 370 (51.9), 227 (75.2), 225 (81.0), 187 (67.1), 179 (100), 161 (23.9), 131 (14.5) MS^3 [415→179]: 161 (100), 143 (14.2), 119 (15.3)	Saccharide	✓		
60	18.9	**609**	MS^2 [609]: 578 (10.7), 477 (43.7), 357 (11.1), 315 (100), 314 (82.8), 300 (29.7) MS^3 [609→315]: 301 (20.6), 300 (100), 299 (72.2), 287 (10.1), 271 (58.1), 255 (39.7), 243 (39.6)	Isorhamnetin-*O*-(pentosyl)hexoside	✓		
61	19.0	**463**	MS^2 [463]: 415 (99.4), 301 (100), 299 (37.1) MS^3 [463→301]: 151 (100)	Quercetin-*O*-hexoside	✓		[84]
62	19.0	**549**	MS^2 [549]: 503 (100) MS^3 [549→503]: 417 (10.0), 371 (100), 353 (11.6), 191 (14.3), 173 (10.1), 161 (37.5), 149 (25.5), 143 (10.5)	Saccharide		✓	

			MS^4 [549→503→371]:161 (100)				
63	19.5	**579**	MS^2 [579]: 429 (28.1), 339 (10.6), 285 (100), 284 (47.0), 257 (12.3), 255 (14.9) MS^3 [579→285]: 257 (94.1), 255 (100), 229 (83.2), 199 (28.9), 151 (54.8)	Kaempferol-*O*-pentosyl(hexoside)		✓	
64	19.6	**549**	MS^2 [549]: 504 (16.9), 503 (100) MS^3 [549→503]: 372 (28.9), 371 (100), 293 (17.3), 179 (15.4), 161 (22.3) MS^4 [549→503→371]: 179 (49.8), 161 (100), 131 (15.8), 119 (23.3), 113 (55.1)	Saccharide (formate adduct)		✓	
65	20.4	**609**	MS^2 [609]: 577 (10.7), 459 (35.1), 315 (100), 300 (25.9), 299 (21.1), 271 (14.8) MS^3 [609→315]:300 (100), 299 (72.2), 271 (45.8), 255 (45.9), 243 (11.5)	Isorhamnetin-*O*-pentosyl(hexoside)		✓	
66	20.6	**483**	MS^2 [483]: 434 (15.8), 413 (21.6), 410 (31.9), 331 (50.3), 313 (32.7), 211 (90.9), 177 (75.7), 169 (100), 151 (24.1) MS^3 [483→169]: 125 (100)	Digalloyl-*O*-glucoside		✓	[199]
67	21.3	**839**	MS^2 [839]: 639 (14.4), 625 (100), 300 (11.5) MS^3 [839→625]: 505 (26.6), 463 (11.8), 445 (67.8), 301 (55.2), 300 (100), 299 (11.1), 271 (45.6), 179 (22.3) MS^4 [839→625→301]: 271 (100), 257 (11.4), 179 (66.0), 151 (26.6)	Quercetin-*O*-dihexoside derivative		✓	
68	24.5	**689**	MS^2 [689]: 635 (57.5), 519 (27.4), 465 (100), 313 (21.5) MS^3 [689→465]:313 (100), 295 (25.8), 169 (12.2), 125 (19.8) MS^4 [689→465→313]: 169 (100), 125 (21.5)	Trigalloylglucose derivative		✓	
69	24.7	**447**	MS^2 [447]: 285 (59.3), 284 (100), 255 (26.5) MS^3 [447→285]: 255 (100), 229 (21.4)	Kaempferol-*O*-hexoside		✓	[200]
70	25.8	**515**	MS^2 [515]: 353 (100) MS^3 [515→353]: 191 (100), 179 (29.3), 161 (10.8), 135 (15.7)	3,5-*O*-Dicaffeoylquinic acid	✓		Standard
71	25.7	**649**	MS^2 [649]: 469 (100) MS^3 [649→469]:425 (27.8), 237 (18.0), 231 (12.7), 205 (37.0), 187 (79.7), 161 (100) MS^4 [649→469→161]:129 (100) MS^4 [649→469→187]:143 (100)	2-Methylaconitate derivative		✓	
72	25.8	**477**	MS^2 [477]: 467 (20.9) 358 (26.0), 315 (100), 301 (14.9), 287 (42.3), 257 (10.9), 244 (14.0), 173 (42.9) MS^3 [477→315]: 300 (100), 285 (17.1), 271 (31.9)	Isorhamnetin-*O*-hexoside	✓		[212]
73	26.1	**447**	MS^2 [447]:327 (10.2), 285 (100), 255 (16.2) MS^3 [447→285]: 255 (100), 229 (10.9), 201 (25.3)	Kaempferol-*O*-hexoside	✓	✓	[200]
74	26.9	**477**	MS^2 [477]: 357 (10.3), 315 (100), 301 (10.5), 285 (27.4), 271 (14.1) MS^3 [477→315]: 301 (51.7), 300 (22.2), 299 (76.9), 286 (86.6), 285 (54.7), 271 (100), 257 (52.6), 243 (23.3)	Isorhamnetin-*O*-hexoside	✓	✓	[212]
75	27.0	**845**	MS^2 [845]: 653 (82.1), 639 (100), 515 (18.0), 459 (12.8), 413 (11.1), 330 (11.0), 315 (23.0), 300 (10.4) MS^3 [845→639]: 607 (12.6), 491 (21.9), 477 (14.4), 459 (40.4), 417 (18.4), 393 (21.1), 315 (100), 300 (41.9) MS^4 [845→639→315]: 301 (24.4), 300 (100), 299 (49.6), 257 (13.2)	Isorhamnetin-*O*-(sinapoyl)dihexoside		✓	
76	27.1	**447**	MS^2 [447]:285 (100), 284 (97.4), 255 (29.8) MS^3 [447→285]: 255 (100), 229 (10.3)	Kaempferol-*O*-hexoside		✓	[200]
77	27.9	**579**	MS^2 [579]: 533 (14.3), 315 (100), 299 (13.4), 271 (14.8) MS^3 [579→315]: 300 (100), 299 (15.1), 271 (34.9), 151 (15.6)	Isorhamnetin-*O*-dipentoside		✓	
78	28.0	**429**	MS^2 [429]: 249 (100), 205 (89.2), 179 (13.7), 161 (63.7), 135 (17.2)	Caffeic acid derivative		✓	
79	28.7	**815**	MS^2 [815]: 653 (63.0), 639 (100), 485 (11.4), 329 (11.0), 315 (18.9) MS^3 [815→639]: 607 (18.8), 580 (23.4), 491 (20.7), 459 (46.1), 433 (18.3), 357 (53.8), 315 (100), 301 (25.7), 300 (46.2), 299 (16.1), 271 (26.5)	Isorhamnetin-*O*-(glucuronyl)dihexoside-*O*-glucuronide		✓	

			MS^4 [815→639→315]: 300 (100), 299 (42.9), 285 (16.3)				
80	29.3	**755**	MS^2 [755]: 609 (100) MS^3 [755→609]: 429 (57.5), 285 (100), 284 (33.9), 255 (11.2) MS^4 [755→609→285]: 257 (25.0), 255 (100)	Kaempferol-*O*-(coumaroyl)dihexoside	✓		
81	30.5	**711**	MS^2 [711]:665 (10.5), 505 (10.2), 503 (100) MS^3 [711→503]: 485 (55.0), 453 (100), 421 (78.3), 417 (61.3), 410 (53.2), 409 (92.0), 380 (50.4) MS^4 [711→503→453]: 409 (100)	Triterpene acid-*O*-hexoside (formate adduct)	✓	✓	
82	31.1	**727**	MS^2 [727]: 681 (100), 619 (27.7) MS^3 [727→681]:619 (100) MS^4 [727→681→619]:457 (100), 425 (25.3)	Unknown		✓	
83	31.9	**711**	MS^2 [711]: 665 (100) MS^3 [711→665]:621 (100), 589 (27.5), 459 (13.4) MS^3 [711→665→621]: 590 (100), 459 (26.7), 428 (54.5); 459 (100)	Unknown		✓	
84	32.7	**805**	MS^2 [805]: 639 (100), 459 (30.1), 315 (87.2), 300 (26.0), 271 (11.4) MS^3 [805→315]: 300 (100), 299 (33.8), 287 (17.9), 151 (23.0)	Isorhamnetin-*O*-dihexoside derivative		✓	
85	33.0	**591**	MS^2 [591]:567 (52.0), 544 (30.7), 367 (24.9), 265 (28.4, 223 (100), 205 (28.1), 190 (14.9), 164 (12.8) MS^3 [591→223]:208 (88.8), 179 (17.0), 164 (100)	Disinapoyl-*O*-hexoside		✓	[197]
86	34.9	**581**	MS^2 [581]:559 (100), 558 (31.9) MS^3 [581→559]: 535 (21.4), 477 (10.4), 455 (20.2), 454 (100) MS^4 [581→559→454]: 373 (100)	Unknown		✓	
87	35.8	**593**	MS^2 [593]:447 (12.1), 284 (100), MS^3 [593→285]: 267 (19.1), 257 (56.0), 255 (32.7), 229 (31.2), 213 (28.1), 163 (20.6), 151 (100)	Kaempferol-*O*-(coumaroyl)hexoside	✓	✓	
88	36.2	**581**	MS^2 [581]: 461 (100), 341 (29.4) MS^3 [581→461]: 341 (100) MS^4 [581→461→341]: 299 (100), 284 (37.4), 271 (26.0), 151 (44.6)	Diosmetin-*C*-dihexoside	✓		
89	36.6	**593**	MS^2 [593]: 447 (10.5), 286 (12.5), 285 (100) MS^3 [593→285]: 257 (35.5), 241 (24.1), 229 (18.9), 213 (18.3), 151 (1000), 123 (11.9)	Kaempferol-*O*-(coumaroyl)hexoside	✓	✓	
90	36.8	**623**	MS^2 [623]: 461 (78.3), 323 (56.9), 315 (11.0), 301 (15.8), 299 (100), 285 (98.4), 256 (21.4) MS^3 [623→299]: 284 (100), 271 (40.4), 256 (47.3) MS^4 [623→299→284]: 256 (100), 151 (43.1)	Diosmetin-*O*-dihexoside	✓		
91	37.4	**581**	MS^2 [581]:461 (100), 341 (28.5) MS^3 [581→461]: 341 (100) MS^4 [581→461→341]: 299 (100), 284 (17.6), 151 (68.8)	Diosmetin-*C*-dihexoside	✓		
92	37.5	**613**	MS^2 [613]:492 (100), 476 (39.9), 466 (40.0), 462 (20.8), 342 (10.3) MS^3 [613→492]: 451 (16.5), 449 (100), 373 (22.8), 343 (47.3), 342 (62.6), 299 (14.3), 160 (11.7) MS^4 [613→492→449]: 303 (23.4), 299 (100), 149 (55.5), 145 (17.2)	Unknown	✓		
93	38.3	**613**	MS^2 [613]: 492 (100), 476 (39.9), 466 (40.0), 462 (20.8), 342 (10.3) MS^3 [613→492]: 451 (16.5), 449 (100), 373 (22.8), 357 (12.3), 343 (47.3), 342 (62.6), 299 (14.3), 288 (14.6), 145 (10.3) MS^4 [613→492→372]: 357 (100), 175 (51.1)	Unknown	✓		

			MS^4 [613→492→449]: 376 (23.8), 329 (25.8), 314 (49.6), 303 (23.0), 299 (21.5), 289 (14.1), 157 (100), 149 (14.1), 135 (16.8) MS^4 [612→492→449]: 275 (100), 233 (36.6), 174 (88.5), 145 (41.7), 134 (20.2)		
94	39.0	**533**	MS^2[533]: 487 (100) MS^3 [533→487]: 451 (24.4), 427 (53.3), 355 (46.0), 221 (51.3), 191 (45.1), 161 (41.7), 149 (100), 143 (52.8) MS^4 [533→487→149]:131 (12.4), 85 (100)	Saccharide	✓

t_R: retention time; HHDP: Hexahydroxydiphenoyl.

1.2. Myrica faya

Identification of phytochemicals of *M. faya* extracts is presented in **Table S 11** and **Table S 12**. Following is a brief explanation and for a more details about their characterization, please check the mentioned references.

1.2.1. Phenolic acids

Caffeoylisocitrate (compound **10**) and caffeic acid-*O*-hexoside (compounds **35** and **52**) were the only caffeic acid derivatives detected (**Table S11**).Compound **25** exhibited $[M-H]^-$ ion at m/z 333. After loss of 180 Da, it yielded protocatechuic acid at m/z 153 (by comparison with analytical standard). With no more data, it was tentatively characterized as a derivative. Compound **64**, $[M-H]^-$ ion at m/z 285, suffered a loss of 132 Da to produce protocatechuic acid at MS^2. Hence, it was identified as protocatechuic acid-*O*-pentoside. Compound **56** and **61** displayed $[M-H]^-$ ion at m/z 325 and were identified as coumaric acid-*O*-hexoside [84]. With an extra 112 Da residue, compound **138** was tentatively characterized as a derivative. Conjugates of coumaric acid with octulopyranosonic acid (compounds **142**, **144**, **163** and **165**) were identified in *M. faya* extracts based on a previous study [106]. Compound **63** showed a $[M-H]^-$ ion at m/z 353 and was plausibly identified as 5-*O*-caffeoylquinic acid (confirmed by a standard solution). Ferulic acid-*O*-hexoside (compound **68**), with $[M-H]^-$ ion at m/z 355, was identified [80]. With an additional 126 Da residue, compound **148** was tentatively identified as a derivative. Compound **105**, with $[M-H]^-$ ion at m/z 403, produced fragment ion at m/z 385 [M-H-sinapoylhexoside]$^-$ after loss of 18 Da (probably loss of a molecule of water); it was tentatively identified as a derivative.

Glycosides of gallic acid were very common in *M. faya* extracts (compounds **4**, **12**, **20**, **27** and **29**) and identified by comparison with literature (**Table S 11**). All these compounds presented different sugar residues esterified with gallic acid at m/z 169 (compound **18**), confirmed through a commercial standard. Compound **17** displayed $[M-H]^-$ ion at m/z 441. After suffering a neutral loss of 98 Da, it produced galloylquinic acid at m/z 343 (compound **15**) [200]. With no more available data, **17** was tentatively identified as a derivative. Compound **28**, with $[M-H]^-$ ion at m/z 391, exhibited gallic acid in its fragmentation pattern after a loss of 222 Da; it was tentatively characterized as a derivative. Compound **66** was tentatively identified as a *C*-glycoside flavonoid-(galloyl)hexoside. It presented an $[M-H]^-$ ion at m/z 451 and product ion at m/z 331 $[M-H-120]^-$, consistent with (galloyl)hexoside [213]. The 120 Da loss is attributed to *C*-glycoside flavonoids. Compound **78** displayed $[M-H]^-$ ion at m/z 609. After a neutral loss 290 Da, yielded MS^2 base peak at m/z 319. Additional fragmentation produced gallic acid; it was tentatively characterized as a derivative. Tri- and tetragalloyl-*O*-hexoside, with $[M-H]^-$ ions at m/z 635 and 787, were identified in *M. faya* extracts (compounds **88** and **106**, respectively). Compound **100**, with $[M-H]^-$ ion at m/z 553, suffered a loss of 384 Da to produce gallic acid. A full characterization was not achieved, hence, **100** was tentatively identified as a derivative. Compounds **111** and **116**, both with $[M-H]^-$ ions at m/z 413, yielded gallic acid in their fragmentation pattern, after two sequential neutral losses of 102 Da. With no more available data, they were also characterized as derivatives.

1.2.2. Flavonols

Several quercetin glycosides were present in *M. faya* extracts and identified by previous assignments (**Table S 11**). Quercetin (compound **161**), with $[M-H]^-$ ion at m/z 301, was confirmed by an analytical standard. Compound **120** showed $[M-H]^-$ ion at m/z 499. Further fragmentation gave origin to quercetin-*O*-hexoside core at m/z 463 [84]. The neutral loss of 36 Da could be attributed to two molecules of water (2 x 18 Da); **120** was tentatively identified as a derivative.

Compounds **107**, **113** and **118** showed $[M-H]^-$ ions at m/z 597. It exhibited fragment ions at m/z 477 $[M-H-120]^-$ and 357 $[M-H-120120]^-$, characteristic of *C*-glycoside flavonoids [205]. Glucaric acid was observed at m/z 209, with typical fragments at m/z 191 and 147 [198]. Thus, **107**, **113** and **118** were tentatively characterized as *C*-(glucaroyl)glycoside flavonoids.

Several myricetin conjugates (compounds **91**, **92**, **95**, **101**, **112**, **140**, **146** and **151**) were identified in *M. faya* extracts (**Table S 11**), with aglycone at m/z 317 [82]. Compound **125**, with $[M-H]^-$ ion at m/z 601, showed myricetin-*O*-pentoside at m/z 449 $[M-H-152]^-$ (compounds **108** and **114**) [79] at MS^2; it was tentatively characterized as myricetin-*O*-(galloyl)pentoside.

Compound **141** showed an $[M-H]^-$ ion at m/z 505. Isorhamnetin aglycone at m/z 315 (compound **150**) was observed after loss of 190 Da. With no further information, it was characterized as a derivative.

1.2.3. Flavan-3-ols

Catechin aglycone was observed (compound **79**) and confirmed by analytical standard. Compound **45**, with $[M-H]^-$ ion at m/z 611, displayed product ion at m/z 305 after loss of other 305 Da residue. This fragment was attributed to a gallo(epi)catechin unit [206]; **45** was identified as a dimer. Compound **115** showed $[M-H]^-$ ion at m/z 441 and was identified as catechin-*O*-gallate [200]. Compound **87** displayed a $[M-H]^-$ ion at m/z 569. It showed a MS^2 base peak at m/z 417 after loss of 152 Da (probably a galloyl residue). Further fragmentation resulted in product ion at m/z 305, which is consistent with gallocatechin [206]. The chemical nature of 112 Da residue could not be elucidated, hence, **87** was tentatively characterized as derivative of digalloyl(+)catechin.

1.2.4. Flavones

Compounds **77**, **82** and **86**, with $[M-H]^-$ ion at m/z 575, suffered a loss of 36 Da to yield product ion at m/z 539. After another loss of 48 Da, it presented a base peak at m/z 491 and fragment ions at m/z 329 and 314. This fragment pattern was consistent with tricin-*O*-hexoside [106]. Thus, compounds **77**, **82** and **86** were tentatively characterized as derivatives. Compound **85** displayed an $[M-H+HCOOH]^-$ ion at m/z 537 and it gave origin to tricin-*O*-hexoside (after loss of 46 Da). Other derivatives of tricin-*O*-hexoside (compounds **94**, **102**, **155,** and **157**) were also tentatively characterized in analysed samples.

Compound **147**, with $[M-H]^-$ ion at m/z 575, suffered a loss of 306 Da (162 Da + 144 Da) to give base peak ion at m/z 269. Further fragmentation of this product ion matched that of apigenin (by comparison with

analytical standard). The loss of 144 Da was attributed previously to a 3-hydroxy-3- methylglutaryl moiety [125]. Hence, **147** was characterized as apigenin-*O*-3-hydroxy-3- methylglutaryl(hexoside).

Compound **156**, with $[M-H]^-$ ion at m/z 555, displayed the same fragmentation pattern as described before for a derivative of baicalein [106].

1.2.5. Ellagic acid derivatives/Ellagitannins

In this analysis, ellagic acid conjugates formed the main group of phenolic compounds detected in *M. faya* (**Table S 11**). Compounds **19** and **25** displayed $[M-H]^-$ ions at m/z 815 and MS^2 base peak at m/z 783 $[M-H-32]^-$. Further fragmentation of this ion was consistent with bis-HHDP-*O*-glucoside [200]. Hence, these compounds were tentatively characterized as derivatives. Compound **36** exhibited $[M-H]^-$ ion at m/z 473. In its MS^2 fragmention yielded product ion at m/z 457 (by loss of 16 Da). Sequential fragmentation gave origin to ellagic acid at m/z 301 (by comparison with analytical standard). The loss of 156 Da could not be identified based in the available data. Hence, **36** was characterized as an ellagic acid derivative. Compound **67** was tentatively characterized as an ellagitannin. It exhibited an $[M-H]^-$ ion at m/z 949 and MS^2 base peak at m/z 917 (by loss of 32 Da). Further decarboxylation (-44 Da), gave origin to product ion at m/z 873, which fragmented into ellagic acid (at m/z 301). The presence of Casuarinin typical fragments (at m/z 935, 633 and 301) [87] indicates the potential presence of an ellagitannin.

1.2.6. Anthocyanins

Analysis performed in positive mode ionization (ESI^+) resulted in the identification of 14 anthocyanins in berries extracts (**Table S 12**). Cyanidin-*O*-hexoside (compound **13**) was plausibly identified by comparison with analytical standard. Other compounds (**6**, **16**, **33**, **42**, **47**, **50** and **60**) presented similar fragmentation patterns but this MS^n analysis did not allow to discriminate sugar moieties. Thus, they were characterized as isomers. With $[M-H]^-$ ion at m/z 419, compound **48** was identified as cyanidin-*O*-pentoside [188,214]. Glycosides of delphinidin and pelargonidin were also identified based on previous analysis on *M. rubra* [82].

1.2.7. Other compounds

Besides PCs, other phytochemicals were also identified in the analysed extracts, namely saccharides, lignans and oxylipins. Saccharides (compounds **124** and **128**) were tentatively identified based on typical hexose fragment ions (at m/z 179, 161, and 119). Compounds **119** and **123** exhibited $[M-H]^-$ ion at m/z 559. It showed a loss of 36 (probably two water molecules) to produce fragment ion at m/z 523. Further fragmentation was consistent with secoisolariciresinol-*O*-hexoside [209]. Thus, **119** and **123** were tentatively characterized as derivatives. Hexosides of phylligenin (compounds **126** and **132**) and conidendrin (compound **152**) were previously reported in *M. faya* [106]. Oxo-dihydroxy-octadecenoic acid has been previously characterized in *M faya* [106].

Table S 11 - Characterization of phytochemicals of *M. faya* methanolic extracts by HPLC-ESI$^-$/MS^n.

Nº	t_R (min)	[M-H]$^-$ (*m/z*)	HPLC-DAD-ESI/MS^n *m/z* (% base peak)	Assigned identity	Berries	Leaves	References
1	3.1	**683**	MS^2 [683]: 341 (100) MS^3 [683→341]: 179 (100), 161 (35.5), 143 (17.0), 119 (30.1), 113 (44.4), 101 (13.8)	Hexose polymer	✓	✓	[207]
2	3.5	**533**	MS^2 [533]: 191 (100) MS^3 [533→191]: 173 (100), 127 (64.9), 109 (32.8), 99 (50.1), 93 (59.0), 85 (42.1) MS^4 [533→191→173]: 109 (100)	Quinic acid derivative		✓	[106]
3	3.7	**191**	MS^2 [191]: 173 (69.3), 127 (100) MS^3 [191→127]: 109 (100)	Quinic acid	✓	✓	Standard
4	3.7	**331**	MS^2 [331]: 271 (30.5), 169 (100), 125 (29.7) MS^3 [331→169]: 125 (100)	Galloyl-*O*-hexoside	✓		[206]
7	3.9	**383** **[2M-H]**$^-$	MS^2 [383]: 191 (100) MS^3 [383→191]: 127 (100), 85 (69.8), 93 (58.4), 109 (60.4), 111 (43.0), 173 (24.5)	Quinic acid dimer		✓	[106]
8	3.9	**481**	MS^2 [481]: 301 (100) MS^3 [481→301]: 275 (100), 257 (29.3)	HHDP-*O*-hexoside	✓		[201]
9	4.1	**133**	MS^2 [133]: 115 (100)	Malic acid	✓		[206]
10	4.3	**353**	MS^2 [353]: 111 (76.1), 173 (100) MS^3 [353→173]: 111 (100)	Caffeoylisocitrate	✓		[215]
12	4.5	**331**	MS^2 [331]: 271 (30.5), 169 (100), 125 (29.7) MS^3 [331→169]: 125 (100)	Galloyl-*O*-hexoside	✓		[206]
14	4.8	**191**	MS^2 [133]: 115 (100)	Citric acid	✓		[206]
15	4.8	**343**	MS^2 [343]: 169 (100) MS^3 [343→169]: 125 (100)	Galloylquinic acid	✓	✓	[200]
17	5.0	**441**	MS^2 [441]: 343 (100), 169 (46.7) MS^3 [441→343]: 169 (100), 125 (77.3)	Galloylquinic acid derivative	✓		
18	5.0	**169**	MS^2 [169]: 125 (100)	Gallic acid	✓		Standard
19	5.2	**815**	MS^2 [815]: 783 (100), 481 (37.5), 301 (66.2), 299 (22.1) MS^3 [815→783]: 721 (32.0), 507 (33.8), 481 (100), 301 (77.2), 299 (25.8) MS^4 [815→783→ 481]: 437 (52.7), 419 (33.1), 329 (11.8), 299 (100)	bis-HHDP-*O*-hexoside (Pedunculagin I) derivative		✓	
20	5.2	**609**	MS^2 [609]: 493 (30.5), 331 (100), 169 (43.5) MS^4 [609→331]: 169 (100), 125 (43.7)	Diacyl-galloyl-*O*-hexoside		✓	[216]
21	5.3	**359**	MS^2 [359]: 197 (100), 181 (17.6) MS^3 [359→197]: 181 (100), 153 (13.3) MS^4 [359→197→182]: 166 (86.0), 153 (89.0), 123 (100)	Syringic acid-*O*-hexoside	✓		[84]
22	5.3	**783**	MS^2 [783]: 721 (22.5), 481 (100), 301 (66.2), 299 (22.1) MS^3 [783→481]: 437 (33.5), 419 (28.9), 301 (77.5), 299 (100), 275 (61.0)	bis-HHDP-*O*-hexoside (Pedunculagin I)		✓	[200]
23	5.6	**935**	MS^2 [935]: 917 (20.9), 799 (100), 633 (53.7), 615 (33.7) 481 (73.4), 301 (21.9), 299 (49.4) MS^3 [935→799]: 633 (62.5), 517 (15.0), 481 (100), 457 (36.7), 329 (76.1), 301 (58.7), 299 (100), 275 (22.2)	Galloyl-bis-HHDP-*O*-hexoside (Casuarinin)		✓	[87]
24	5.5	**815**	MS^2 [815]: 783 (100), 301 (47.2), 299 (33.1) MS^3 [815→783]: 721 (25.5), 481 (72.9), 301 (100), 299 (22.1)	bis-HHDP-*O*-hexoside (Pedunculagin I)derivative		✓	

25	5.6	**333**	MS^2 [333]: 153 (100), 109 (47.2) MS^3 [333→153]: 109 (100), 79 (65.2)	Protocatechuic acid derivative		✓	
26	5.7	**467**	MS^2 [467]: 458 (33.6), 301 (100), 299 (77.2) MS^3 [467→301]: 299 (100), 283 (43.2)	Ellagic acid derivative	✓		[217]
27	5.7	**483**	MS^2 [483]: 313 (15.2), 331 (100), 193 (10.6), 169 (47.2) MS^3 [483→331]: 169 (100), 125 (62.1)	Digalloyl-*O*-hexoside	✓	✓	[199]
28	5.8	**391**	MS^2 [391]: 169 (100), 125 (35.7)	Gallic acid derivative		✓	
29	5.8	**483**	MS^2 [483]: 313 (15.2), 331 (100), 193 (10.6), 169 (47.2) MS^3 [483→331]: 271 (33.3), 169 (100), 125 (62.1)	Digalloyl-*O*-hexoside		✓	[199]
30	5.9	**305**	MS^2 [305]: 261 (54.6), 221 (34.0), 219 (85.6), 204 (21.7), 179 (100), 166 (17.0), 139 (16.5), 137 (63.1) MS^3 [305→179]: 163 (100), 152 (45.5), 151 (77.3), 135 (32.1)	(+)Gallo(epi)catechin		✓	[206]
31	6.1	**783**	MS^2 [783]: 721 (22.5), 481 (87.6), 301 (100), 299 (22.1) MS^3 [783→301]: 299 (100), 275 (32.7)	bis-HHDP-*O*-hexoside (Pedunculagin I)	✓		[200]
32	6.2	**305**	MS^2 [305]: 179 (100) MS^3 [305→179]: 135 (100)	Gallocatechin		✓	[206]
35	6.5	**341**	MS^2 [341]: 179 (100), 161 (49.3), 135 (12.6) MS^3 [341→179]: 135 (100)	Caffeic acid-*O*-hexoside		✓	[84]
36	6.6	**473**	MS^2 [473]: 457 (100), 301 (62.4), 299 (19.2) MS^3 [473→457]: 301 (85.3), 299 (100), 289 (31.3), 273 (50.4)	Ellagic acid derivative		✓	
37	6.8	**935**	MS^2 [935]: 917 (20.9), 659 (21.2), 633 (100), 615 (36.7), 571 (18.5), 329 (25.4), 301 (21.9), 299 (49.4) MS^3 [935→633]: 615 (76.5), 571 (100), 481 (44.3), 383 (31.7), 329 (76.1), 301 (28.7), 299 (97.9), 275 (26.5)	Galloyl-bis-HHDP-*O*-hexoside (Casuarinin)		✓	[87]
38	6.7	**481**	MS^2 [481]: 301 (100), 275 (33.4) MS^3 [481→301]: 257 (100), 229 (33.8)	HHDP-*O*-hexoside	✓		[201]
39	7.0	**783**	MS^2 [783]: 481 (37.6), 301 (100), 299 (28.1) MS^3 [783→301]: 299 (100), 257 (47.7), 229 (33.4)	bis-HHDP-*O*-hexoside (Pedunculagin I)		✓	[200]
40	7.0	**315**	MS^2 [315]: 269 (60.9), 223 (20.6), 161 (47.3), 153 (100) MS^3 [315→153]: 135 (31.6), 109 (100), 79 (42.1)	Protocatechuic acid-*O*-hexoside	✓	✓	[199]
41	7.1	**935**	MS^2 [935]: 917 (20.9), 799 (43.2), 633 (100), 615 (33.7) 329 (25.4), 301 (21.9), 299 (49.4) MS^3 [935→799]: 633 (62.5), 517 (15.0), 481 (44.3), 457 (36.7), 329 (76.1), 301 (58.7), 299 (100), 275 (22.2)	Galloyl-bis-HHDP-*O*-hexoside (Casuarinin)		✓	[87]
43	7.2	**305**	MS^2 [305]: 179 (100) MS^3 [305→179]: 135 (100)	Gallocatechin		✓	[206]
44	7.2	**633**	MS^2 [633]: 481 (60.1), 331 (33.5), 301 (100), 299 (65.8), 275 (21.2) MS^3 [633→301]: 299 (82.3), 257 (100)	Galloyl HHDP-*O*-hexoside		✓	[199]
45	7.3	**611** $[2M-H]^-$	MS^2 [611]: 485 (33.2), 305 (100) MS^3 [611→305]: 287 (27.2), 219 (13.5), 179 (100)	Gallocatechin dimer		✓	
46	7.5	**761** $[2M-H]^-$	MS^2 [761]: 635 (17.8), 609 (69.0), 575 (36.6), 591 (51.2), 593 (33.8), 423 (100), 305 (38.4) MS^3 [761→423]: 305 (51.2), 297 (61.7), 283 (100), 255 (37.4), 241 (48.5)	Gallo(epi)catechin- Gallo(epi)catechin-*O*-gallate	✓	✓	[142]
49	7.9	**467**	MS^2 [467]: 458 (100), 343 (41.5), 249 (13.2) MS^3 [467→458]: 436 (17.8), 413 (25.1), 343 (32.2), 315 (28.1), 301 (100)	Ellagic acid derivative		✓	[217]

			MS^4 [467→458→301]: 299 (63.2), 289 (31.3), 273 (50.4)				
51	8.1	**633**	MS^2 [633]: 481 (60.1), 331 (33.5), 301 (100), 299 (65.8), 275 (21.2) MS^3 [633→301]: 299 (82.3), 257 (100)	Galloyl-HHDP-*O*-hexoside		✓	[199]
52	8.1	**341**	MS^2 [341]: 179 (100), 161 (49.3), 135 (12.6) MS^3 [341→179]: 135 (100)	Caffeic acid-*O*-hexoside	✓		[84]
53	8.1	**935**	MS^2 [935]: 917 (100), 799 (43.2), 633 (80.2), 615 (33.7) 329 (25.4), 301 (21.9), 299 (49.4) MS^3 [935→917]: 873 (62.5), 633 (100), 481 (44.3), 457 (36.7), 329 (76.1), 301 (58.7), 299 (100), 275 (22.2) MS^4 [935→917→301]: 299 (100), 283 (33.3), 273 (49.4), 167 (22.1)	Galloyl-bis-HHDP-*O*-hexoside (Casuarinin)		✓	[87]
54	8.2	**595**	MS^2 [595]: 385 (100), 355 (43.2), 313(80.2), 235 (33.7) MS^3 [595→385]: 341 (44.3), 355 (36.7), 313 (100), 235 (33.2), 223 (58.7), 175 (22.2)	5,7,4′-Trihydroxyflavanone 6,8-di-*C*-hexoside	✓	✓	[202]
55	8.3	**467**	MS^2 [467]: 458 (100), 343 (41.5), 249 (13.2) MS^3 [467→458]: 436 (17.8), 413 (25.1), 343 (32.2), 315 (28.1), 301 (100) MS^4 [467→458→301]: 299 (63.2), 289 (31.3), 273 (50.4)	Ellagic acid derivative	✓	✓	[217]
56	8.4	**325**	MS^2 [325]: 163 (100), 119 (13.2) MS^3 [325→163]: 119 (100)	Coumaric acid-*O*-hexoside		✓	[84]
57	8.4	**649**	MS^2 [649]: 497 (37.3), 463 (55.3), 301 (100) MS^3 [649→301]: 299 (62.3), 275 (33.5), 257 (100), 229 (42.7)	Galloyl-HHDP-*O*-gluconate (Lagerstannin C)		✓	[206]
58	8.5	**595**	MS^2 [595]: 475 (77.5), 385 (100), 355 (43.2), 313(80.2), 235 (33.7) MS^3 [595→385]: 367 (44.3), 341 (24.3), 339 (45.7), 355 (36.7), 313 (100), 235 (33.2), 223 (58.7), 175 (22.2)	5,7,4′-Trihydroxyflavanone 6,8-di-*C*-hexoside	✓		[202]
59	8.6	**633**	MS^2 [633]: 481 (60.1), 331 (33.5), 301 (100), 299 (65.8), 275 (21.2) MS^3 [633→301]: 299 (82.3), 257 (100)	Galloyl-HHDP-*O*-hexoside		✓	[206]
61	8.7	**325**	MS^2 [325]: 163 (100), 119 (13.2) MS^3 [325→163]: 119 (100)	Coumaric acid-*O*-hexoside		✓	[84]
62	8.8	**935**	MS^2 [935]: 917 (100), 799 (43.2), 633 (80.2), 615 (33.7) 329 (25.4), 301 (21.9), 299 (49.4) MS^3 [935→917]: 873 (62.5), 633 (100), 481 (44.3), 457 (36.7), 329 (76.1), 301 (58.7), 299 (100), 275 (22.2) MS^4 [935→917→301]: 299 (100), 283 (33.3), 273 (49.4), 167 (22.1)	Galloyl-bis-HHDP-*O*-hexoside (Casuarinin)		✓	[87]
63	9.1	**353**	MS^2 [353]: 191 (100) MS^3 [353→191]: 173 (24.7), 127 (100), 111 (16.1), 109 (28.7), 93 (46.4), 85 (50.1) MS^4 [353→191→127]: 109 (100), 85 (17.0)	5-*O*-caffeoylquinic acid	✓		Standard
64	9.2	**285**	MS^2 [285]: 269 (60.9), 223 (20.6), 161 (43.9), 153 (100) MS^3 [285→153]: 135 (29.6), 109 (100)	Protocathechuic acid-*O*-pentoside	✓	✓	
65	9.3	**935**	MS^2 [935]: 917 (56.7), 799 (43.2), 633 (100), 615 (33.7) 329 (25.4), 301 (21.9), 299 (49.4) MS^3 [935→633]: 481 (44.3), 457 (36.7), 329 (76.1), 301 (88.7), 299 (100), 275 (22.2) MS^4 [935→633→301]: 299 (100), 283 (33.3), 273 (49.4), 167 (22.1)	Galloyl-bis-HHDP-*O*-hexoside (Casuarinin)		✓	[87]
66	9.3	**451**	MS^2 [451]: 331 (60.9), 169 (100) MS^3 [451→331]: 169 (100), 125 (62.1)	*C*-glycoside flavonoid-(galloyl)hexoside	✓		
67	9.6	**949**	MS^2 [949]: 935 (33.8), 917 (100), 799 (43.2), 633 (77.5), 615 (33.7) 329 (25.4), 301 (21.9), 299 (49.4) MS^3 [949→917]: 873 (100), 799 (13.2), 633 (56.5), 615 (47.7) 329 (35.4), 301 (88.6) MS^4 [949→917→873]: 301 (92.5), 299 (100), 283 (41.3), 273 (34.5)	Casuarinin like ellagitannin		✓	

68	9.7	**355**	MS^2 [355]: 193 (100) MS^3 [355→193]: 149 (31.5), 134 (100)	Ferulic acid-*O*-hexoside	✓		[80]
70	9.9	**431**	MS^2 [431]: 385 (100), 223 (60.2), 186 (15.0) MS^3 [431→385]: 223 (79.7), 153 (100) MS^4 [431→385→153]: 109 (100)	Roseoside (formate adduct)	✓	✓	[106]
71	10.5	**913** **$[2M-H]^-$**	MS^2 [913]: 761 (100), 609 (69.0), 575 (36.6), 591 (51.2), 593 (33.8), 423 (55.8), 305 (38.4) MS^3 [913→761]: 609 (100), 305 (38.4), 297 (61.7), 283 (100), 255 (77.4) MS^4 [913→761→609]: 305 (100), 287 (27.2), 219 (13.5), 179 (100)	Digalloyl(epi)gallocatechin dimer	✓	✓	[201]
72	10.6	**489**	MS^2 [489]: 454 (32.3), 447 (36.5), 445 (39.0), 403 (38.6), 285 (100), 257 (25.8) MS^3 [489→285]: 257 (100), 255 (84.2), 243 (63.0), 239 (32.5), 229 (52.5), 197 (30.7), 163 (19.4)	Kaempferol-*O*-(acetyl)hexoside	✓		[87]
73	10.8	**785**	MS^2 [785]: 767 (38.9) 633 (37.5), 615 (26.5), 483 (71.3), 331 (19.3), 301 (100), 275 (21.1) MS^3 [785→301]: 283 (24.7), 257 (100), 229 (39.5)	Digalloyl-HHDP-*O*-hexoside (Pedunculagin II)		✓	[199]
75	11.0	**913** **$[2M-H]^-$**	MS^2 [913]: 761 (100), 609 (69.0), 575 (36.6), 591 (51.2), 593 (33.8), 423 (55.8), 305 (38.4) MS^3 [913→761]: 609 (100), 305 (38.4), 297 (61.7), 283 (100), 255 (77.4) MS^4 [913→761→609]: 305 (100), 287 (27.2), 219 (13.5), 179 (100)	Digalloyl(epi)gallocatechin dimer		✓	[201]
76	11.1	**327**	MS^2 [327]: 165 (100), 121 (24.2) MS^3 [327→165]: 147 (100), 121 (33.2), 113 (19.2)	Dihydro-*O*-coumaric acid-*O*-hexoside	✓		[218]
77	11.7	**575**	MS^2 [575]: 539 (100) MS^3 [575→539]: 491 (100), 329 (63.2), 314 (27.2) MS^4 [575→539→491]: 371 (12.9), 329 (100), 314 (27.2), 181 (31.5)	Tricin-*O*-hexoside derivative	✓		
78	11.7	**609**	MS^2 [609]: 319 (100), 169 (37.5) MS^3 [609→319]: 169 (84.7), 125 (100)	Gallic acid derivative		✓	
79	11.8	**289**	MS^2 [289]: 246 (20.6), 245 (100), 179 (20.7), 105 (32.6) MS^3 [289→245]: 227 (27.8), 203 (100), 185 (22.3), 175 (66.2), 161 (22.4)	Catechin		✓	Standard
80	11.9	**481**	MS^2 [481]: 301 (100) MS^3 [481→301]: 275 (100), 257 (29.3)	HHDP-*O*-hexoside	✓		[201]
81	12.4	**457**	MS^2 [457]: 331 (19.8), 319 (14.8), 305 (12.4), 193 (16.3), 169 (100) MS^3 [457→169]: 125 (100)	Gallo(epi)catechin-*O*-gallate	✓	✓	[142]
82	12.1	**575**	MS^2 [575]: 539 (100) MS^3 [575→539]: 491 (100), 329 (63.2), 314 (27.2) MS^4 [575→539→491]: 371 (12.9), 329 (100), 314 (27.2), 181 (31.5)	Tricin-*O*-hexoside derivative	✓		
83	12.3	**449**	MS^2 [449]: 421 (33.5), 327 (35.6), 287 (100) MS^3 [449→287]: 259 (100), 253 (63.2), 201 (27.1), 187 (19.5), 125 (22.7)	Dihydrokaempferol-*O*-hexoside		✓	[206]
84	12.4	**457**	MS^2 [457]: 331 (19.8), 319 (14.8), 305 (12.4), 193 (16.3), 169 (100) MS^3 MS^3 [457→169]: 125 (100)	Gallo(epi)catechin-*O*-gallate	✓	✓	[142]
85	12.6	**537**	MS^2 [537]: 491 (100) MS^3 [537→491]: 357 (35.6), 329 (100), 314 (54.2), 181 (28.4)	Tricin-*O*-hexoside (formate adduct)	✓		
86	13.1	**575**	MS^2 [575]: 539 (100) MS^3 [575→539]: 491 (100), 329 (63.2), 314 (27.2) MS^4 [575→539→491]: 371 (12.9), 329 (100), 314 (27.2), 181 (31.5)	Tricin-*O*-hexoside derivative	✓		
87	13.6	**569**	MS^2 [569]: 417 (100) MS^3 [569→417]: 305 (100)	Digallocatechin derivative		✓	

			MS^4 [569→417→305]: 261 (54.6), 221 (34.0), 219 (85.6), 204 (21.7), 179 (100), 169 (17.0), 137 (16.5), 125 (11.5)				
88	13.7	**635**	MS^2 [635]: 617 (35.2), 483 (52.7), 465 (100), 313 (25.8) MS^3 [635→465]: 313 (100), 169 (76.2), 125 (32.8) MS^4 [635→465→313]: 169 (100), 125 (55.1)	Trigalloyl-*O*-hexoside		✓	[201]
89	14.1	**467**	MS^2 [467]: 391 (53.2), 313 (32.4), 301 (100) MS^3 [467→301]: 287 (100), 275 (33.5), 257 (45.2)	Casurictin/Potentillin like ellagitannin		✓	[219]
90	14.1	**761**	MS^2 [761]: 635 (17.8), 609 (69.0), 575 (36.6), 591 (51.2), 593 (33.8), 423 (100), 305 (38.4) MS^3 [761→423]: 305 (51.2), 297 (61.7), 283 (100), 255 (77.4), 243 (36.5) MS^4 [761→423→284]: 255 (33.5), 241 (100)	Gallo(epi)catechin- Gallo(epi)catechin-*O*-gallate		✓	[142]
91	14.8	**479**	MS^2 [479]: 317 (100), 316 (92.3), 179 (16.0) MS^3 [479→317]: 287 (30.6), 271 (81.6), 193 (40.6), 179 (100)	Myricetin-*O*-hexoside	✓	✓	[142]
92	15.5	**631**	MS^2 [631]: 479 (39.7), 318 (12.7), 317 (100) MS^3 [631→317]: 179 (100), 151 (39.1)	Myricetin-*O*-(galloyl)hexoside	✓	✓	[106]
93	16.0	**433**	MS^2 [433]: 301 (100), 299 (52.9) MS^3 [433→301]: 299 (100), 257 (39.1), 229 (41.4)	Ellagic acid-*O*-pentoside	✓		[206]
94	16.6	**567**	MS^2 [567]: 491 (33.5), 329 (100) MS^3 [567→329]: 341 (25.8), 314 (100), 269 (52.7), 181 (18.4)	Tricin-*O*-hexoside derivative		✓	
95	16.9	**631**	MS^2 [631]: 479 (39.7), 318 (12.7), 317 (100) MS^3 [631→317]: 179 (100), 151 (39.1)	Myricetin-*O*-(galloyl)hexoside		✓	[106]
96	17.0	**197**	MS^2 [197]: 169 (100), 125 (37.2)	Ethyl-gallate	✓		[213]
97	17.1	**467**	MS^2 [467]: 423 (36.6), 313 (52.4), 169 (100) MS^3 [467→423]: 313 (27.5), 169 (100), 125 (51.5)	Gallic acid derivative		✓	[106]
98	17.3	**167**	MS^2 [167]: 151 (100)	Vanillic acid	✓		[125]
99	17.4	**457**	MS^2 [457]: 331 (19.8), 319 (14.8), 305 (12.4), 193 (16.3), 169 (100) MS^3 MS^3 [457→169]: 125 (100)	Gallo(epi)catechin-*O*-gallate		✓	[142]
100	17.4	**553**	MS^2 [553]: 169 (100) MS^3 [553→169]: 125 (100)	Gallic acid derivative		✓	
101	17.5	**631**	MS^2 [631]: 479 (39.7), 318 (12.7), 317 (100) MS^3 [631→317]: 179 (100), 151 (39.1)	Myricetin-*O*-(galloyl)hexoside		✓	[106]
102	17.7	**567**	MS^2 [567]: 491 (33.5), 329 (100) MS^3 [567→329]: 341 (25.8), 314 (100), 299 (47.9), 181 (18.4)	Tricin-*O*-hexoside derivative		✓	
103	18.0	**457**	MS^2 [457]: 331 (19.8), 319 (66.8), 305 (12.4), 193 (16.3), 169 (100) MS^3 [457→169]: 125 (100)	Gallo(epi)catechin-*O*-gallate		✓	[142]
104	18.3	**609**	MS^2 [609]: 539 (39.5), 301 (100), 300 (11.3), 255 (24.5) MS^3 [609→301]: 273 (35.1), 179 (100), 151 (77.7), 107 (19.0)	Quercetin-*O*-rutinoside (Rutin)	✓	✓	[200]
105	18.3	**403**	MS^2 [403]: 385 (31.4), 287 (29.3), 269 (12.8), 223 (100), 163 (13.5) MS3 [403→223]: 208 (69.4), 179 (100), 164 (32.3)	Sinapic acid-*O*-hexoside derivative	✓	✓	
106	18.5	**787**	MS^2 [787]: 617 (100), 483 (52.7), 465 (62.4), 313 (25.8) MS^3 [787→617]: 465 (100), 313 (59.7), 169 (76.2) MS^4 [635→617→465]: 313 (72.1), 295 (18.4), 169 (100), 125 (55.1)	Tetragalloyl-*O*-hexoside		✓	[201]
107	18.9	**597**	MS^2 [597]: 477 (45.0), 459 (15.3), 417 (25.2), 388 (17.3), 387 (53.6), 358 (20.0), 357 (100) MS^3 [597→357]: 300 (15.3), 209 (100), 123 (12.1),121 (25.4) MS^4 [597→357→209]: 191 (70.5), 165 (48.0), 147 (100)	*C*-(glucaroyl)glycoside flavonoid	✓	✓	
108	18.9	**449**	MS^2 [449]: 317 (100), 316 (92.3), 179 (16.0) MS^3 [449→317]: 287 (30.6), 271 (81.6), 193 (40.6), 179 (100)	Myricetin-*O*-pentoside	✓	✓	[79]

109	18.9	**477**	MS^2 [477]: 315 (100) MS^3 [477→315]: 301 (45.1), 300 (55.6), 299 (14.7), 285 (77.6), 271 (100), 255 (17.2), 243 (50.7)	Isorhamentin-*O*-hexoside		✓	[212]
110	19.0	**609**	MS^2 [609]: 255 (100), 539 (39.5), 301 (22.3), 301 (11.3), 255 (24.5) MS^3 [609→301]: 273 (35.1), 179 (100), 151 (77.7), 107 (19.0)	Quercetin-*O*-rutinoside (Rutin)		✓	[200]
111	19.3	**413**	MS^2 [413]: 311 (100), 169 (62.3) MS^3 [413→311]: 169 (100), 125 (37.8)	Gallic acid derivative	✓		
112	19.4	**463**	MS^2 [463]: 318 (10.1), 317 (100), 316 (64.5) MS^3 [463→317]: 288 (11.4), 287 (24.7), 272 (27.2), 271 (59.7), 270 (35.9), 179 (100), 151 (10.7)	Myricetin-*O*-deoxyhexoside (Myricitrin)	✓	✓	Standard
113	19.7	**597**	MS^2 [597]: 477 (45.0), 459 (15.3), 417 (25.2), 388 (17.3), 387 (53.6), 358 (20.0), 357 (100) MS^3 [597→357]: 300 (15.3), 209 (100), 123 (12.1),121 (25.4) MS^4 [597→357→209]: 191 (70.5), 165 (48.0), 147 (100)	*C*-(glucaroyl)glycoside flavonoid	✓	✓	
114	19.7	**449**	MS^2 [449]: 317 (100), 316 (92.3), 179 (16.0) MS^3 [449→317]: 287 (30.6), 271 (81.6), 193 (40.6), 179 (100)	Myricetin-*O*-pentoside		✓	[79]
115	20.1	**441**	MS^2 [441]: 289 (100), 290 (21.5), 169 (17.5), 331 (11.6) MS^2 [441→289]: 245 (100), 203 (39.7), 205 (43.4), 179 (28.3), 161 (27.4), 135 (17.6)	(epi)Catechin-*O*-gallate	✓	✓	[200]
116	20.2	**413**	MS^2 [413]: 311 (100), 169 (60.1) MS^3 [413→311]: 169 (100), 125 (35.3)	Gallic acid derivative	✓	✓	
117	20.5	**463**	MS^2 [463]: 301 (100) MS^3 [463→301]: 299 (51.4), 179 (59.7), 151 (100)	Quercetin-*O*-hexoside	✓	✓	[84]
118	20.6	**597**	MS^2 [597]: 477 (45.0), 459 (15.3), 417 (25.2), 388 (17.3), 387 (53.6), 358 (20.0), 357 (100) MS^3 [597→357]: 300 (15.3), 209 (100), 123 (12.1),121 (25.4) MS^4 [597→357→209]: 191 (70.5), 165 (48.0), 147 (100)	*C*-(glucaroyl)glycoside flavonoid	✓	✓	[106]
119	20.9	**559**	MS^2 [559]: 523 (100) MS^3 [559→523]: 508 (16.8), 488 (43.2), 361 (100), 343 (15.9), 299 (15.7), 165 (32.1), 147 (12.0) MS^4 [559→523→361]: 347 (43.1), 346 (96.1), 313 (80.4), 222 (47.1), 205 (85.0), 192 (84.3), 165 (100), 109 (94.8)	Secoisolariciresinol-*O*-hexoside derivative		✓	
120	21.3	**499**	MS^2 [499]: 463 (100), 301 (68.3) MS^3 [499→463]: 301 (100), 299 (51.4), 179 (59.7), 151 (100)	Quercetin-*O*-hexoside derivative	✓	✓	
121	22.2	**463**	MS^2 [463]: 301 (100) MS^3 [463→301]: 299 (51.4), 179 (59.7), 151 (100)	Quercetin-*O*-hexoside		✓	[84]
122	22.7	**615**	MS^2 [615]: 313 (14.7), 301 (100), 313 (16.6) MS^3 [615→301]: 179 (100), 193 (15.5), 151 (63.4) MS^4 [615→301→179]: 257 (11.5), 151 (100), 169 (64.3)	Quercetin-*O*-(galloyl)hexoside	✓	✓	[143]
123	22.8	**559**	MS^2 [559]: 523 (100) MS^3 [559→523]: 508 (16.8), 488 (43.2), 361 (100), 343 (15.9), 299 (15.7), 165 (32.1), 147 (12.0) MS^4 [559→523→361]: 347 (43.1), 346 (96.1), 313 (80.4), 222 (47.1), 205 (85.0), 192 (84.3), 165 (100), 109 (94.8)	Secoisolariciresinol-*O*-hexoside derivative		✓	
124	23.8	**415**	MS^2 [415]: 379 (100) MS^3 [415 → 379]: 247 (31.5), 179 (21.9), 149 (100), 143 (51.7), 131 (53.9)	Saccharide		✓	
125	23.9	**601**	MS^2 [601]: 449 (44.7), 317 (100), 316 (92.3), 179 (16.0) MS^3 [601→317]: 287 (30.6), 271 (81.6), 193 (40.6), 179 (100)	Myricetin-*O*-(galloyl)pentoside		✓	
126	24.6	**579**	MS^2 [579]: 534 (16.7), 533 (100), 372 (22.5), 371 (99.5)	Phylligenin-*O*-hexoside		✓	[106]

			MS^3 [579→533]: 372 (15.9), 371 (100) MS3 [579→371]: 342 (18.1), 341 (100), 340 (61.9), 297 (13.1) MS^4 [579→533→371]: 357 (29.2), 356 (100), 342 (18.3), 341 (68.7), 297 (13.1)	(formate adduct)			
127	24.7	**615**	MS^2 [615]: 301 (100) MS^3 [615→301]: 193 (15.5), 179 (100) MS^4 [615→301→179]: 169 (64.3), 151 (100), 125 (35.8)	Quercetin-*O*-(galloyl)hexoside		✓	[143]
128	25.5	**567**	MS^2 [567]: 247 (21.2), 179 (79.8), 161 (100) MS^3 [567→161]: 149 (100), 143 (51.7), 119 (33.9)	Saccharide		✓	
129	25.6	**615**	MS^2 [615]: 313 (16.6), 302 (14.7), 301 (100) MS^3 [615→301]: 179 (100), 151 (63.4) MS^4 [615→301→179]: 169 (64.3), 151 (100)	Quercetin-*O*-(galloyl)hexoside	✓	✓	[143]
130	26.2	**615**	MS^2 [615]: 301 (100) MS^3 [615→301]: 179 (100), 169 (47.6), 151 (63.4), 125 (65.2)	Quercetin-*O*-(galloyl)hexoside		✓	[143]
131	26.3	**447**	MS^2 [447]: 285 (91.8), 284 (100), 255 (22.0) MS^3 [447→285]: 257 (17.4), 255 (100), 227 (42.3), 239 (16.1), 223 (103.), 167 (46.0)	Kaempferol-*O*-hexoside	✓	✓	[82]
132	26.8	**579**	MS^2 [579]: 534 (16.7), 533 (100), 372 (22.5), 371 (99.5) MS^3 [579→533]: 372 (15.9), 371 (100) MS3 [579→371]: 342 (18.1), 341 (100), 340 (61.9), 297 (13.1) MS^4 [579→533→371]: 357 (29.2), 356 (100), 342 (18.3), 341 (68.7), 297 (13.1)	Phylligenin-*O*-hexoside (formate adduct)	✓		[106]
133	27.1	**525**	MS^2 [525]: 169 (100) MS^3 [525→169]: 125 (100)	Gallic acid derivative		✓	
134	27.5	**447**	MS^2 [447]: 315 (100) 300 (29.7), 299 (73.6) MS^3 [447→315]: 300 (100), 251 (10.4), 221 (27.3), 191 (48.1), 161 (49.8), 151 (13.5)	Isorhamnetin-*O*-pentoside	✓		[212]
135	27.6	**593**	MS^2 [593]: 285 (100), 286 (18.8) MS^3 [593→285]: 257 (100), 241 (58.8), 229 (35.9), 197 (17.6), 169 (23.2), 163 (39.6), 93 (30.3)	Kaempferol-*O*-rutinoside	✓		[200]
136	28.3	**447**	MS^2 [447]: 285 (91.8), 284 (100), 255 (22.0) MS^3 [447→285]: 257 (17.4), 255 (100), 227 (42.3), 239 (16.1), 223 (103.), 167 (46.0)	Kaempferol-*O*-hexoside	✓	✓	[82]
137	28.7	**447**	MS^2 [447]: 301 (100), 300 (24.9), 302 (14.8) MS^3 [447→301]: 273 (22.8), 271 (14.8), 255 (10.7), 211 (21.3), 179	Quercetin-*O*-deoxyhexoside	✓	✓	[142]
138	28.8	**437**	MS^2 [437]: 325 (100) MS^3 [437→325]: 163 (100), 119 (42.8)	Coumaric acid-*O*-hexoside derivative	✓		
139	29.2	**599**	MS^2 [599]: 313 (100), 285 (98.5), 314 (22.6), 286 (12.3) MS^3 [599→313]: 169 (100), 125 (36.0), 152 (34.0), 211 (29.3)	Kaempferol-*O*-(galloyl)hexoside	✓		[106]
140	30.1	**477**	MS^2 [477]: 331 (100) MS^3 [477→331]: 315 (100) MS^4 [477→331→315]: 193 (100)	Dimethylmyricetin-*O*-pentoside		✓	[201]
141	30.2	**505**	MS^2 [505]: 315 (100) 300 (29.7), 299 (73.6) MS^3 [505→315]: 300 (65.1), 271 (100), 251 (10.4), 221 (27.3), 191 (48.1), 161 (49.8), 151 (13.5)	Isorhamnetin derivative		✓	
142	30.4	**633**	MS^2 [633]: 488 (16.5), 487 (12.2), 470 (18.7), 469 (100), 347 (50.7) MS^3 [633→469]: 347 (76.0), 323 (56.3), 303 (20.4), 259 (33.1), 235 (15.7), 163 (100), 145 (50.9) MS^4 [633→469→163]: 119 (100)	Benzoyl-*p*-dicoumaryl- 2,7-anhydro-3-DOA	✓		[106]
143	30.4	**599**	MS^2 [599]: 313 (100), 285 (98.5), 314 (22.6), 286 (12.3) MS^3 [599→313]: 169 (100), 125 (36.0), 152 (34.0), 211 (29.3)	Kaempferol-*O*-(galloyl)deoxyhexoside	✓	✓	[106]

144	31.3	**633**	MS^2 [633]: 488 (16.5), 487 (12.2), 470 (18.7), 469 (100), 347 (50.7) MS^3 [633→469]: 347 (76.0), 323 (56.3), 303 (20.4), 259 (33.1), 235 (15.7), 163 (100), 145 (50.9), 119 (55.1)	Benzoyl-*p*-dicoumaryl- 2,7-anhydro-3-DOA	✓		[106]
145	31.7	**615**	MS^2 [615]: 463 (41.8), 318 (16.8), 317 (100) MS^3 [615→317]: 227 (11.6), 193 (16.2), 191 (12.6), 180 (12.4), 179 (100), 151 (33.3), 137 (16.7) MS^4 [615→317→179]: 151 (100)	Myricetin-*O*-(galloyl)deoxyhexoside	✓	✓	[82]
146	31.8	**575**	MS^2 [575]: 269 (100) MS^3 [575→269]: 241 (16.9), 225 (100), 149 (62.9)	Apigenin-*O*-3-hydroxy- 3-methylglutaroyl(hexoside)		✓	
147	32.1	**481**	MS^2 [481]: 463 (22.2), 355 (19.3), 193 (100) MS^3 [481→355]: 193 (100), 149 (46.5). 134 (100)	Ferulic acid-*O*-hexoside derivative	✓		
148	32.4	**431**	MS^2 [431]: 286 (16.7), 285 (100), 284 (28.4), 255 (10.5) MS^3 [431→285]: 257 (61.7), 255 (100), 239 (32.5), 229 (52.5), 197 (30.7), 163 (19.4)	Kaempferol-*O*-rhamnoside		✓	[106]
149	32.7	**315**	MS^2 [315]: 301 (100), 299 (28.6), 271 (77.1)	Isorhamnetin	✓		[212]
150	33.0	**615**	MS^2 [615]: 317 (100) MS^3 [615→317]: 227 (11.6), 193 (16.2), 191 (12.6), 180 (12.4), 179 (100), 151 (33.3)	Myricetin-*O*-(galloyl)deoxyhexoside	✓		[82]
151	34.9	**599**	MS^2 [599]: 553 (28.3), 485 (25.8), 447 (45.6), 301 (100), 299 (11.1), 297 (18.7) MS^3 [599→301]: 273 (15.5), 187 (12.9), 179 (57.7), 151 (100)	Quercetin-*O*-(galloyl)deoxyhexoside		✓	[106]
152	35.3	**489**	MS^2 [489]: 454 (32.3), 447 (36.5), 445 (39.0), 403 (38.6), 301 (100) MS^3 [489→301]: 271 (84.2), 243 (63.0), 151 (100)	Quercetin-*O*-(acetyl)rhamnoside	✓	✓	[106]
153	35.5	**599**	MS^2 [599]: 553 (28.3), 485 (25.8), 447 (45.6), 301 (100), 299 (33.1) MS^3 [599→301]: 273 (15.5), 187 (12.9), 179 (57.7), 151 (100)	Quercetin-*O*-(galloyl)deoxyhexoside	✓		[106]
154	36.2	**527**	MS^2 [527]: 491 (100) MS^3 [527→491]: 371 (12.9), 330 (28.5), 330 (20.3), 329 (100), 314 (10.7) MS^4 [527→491→329]: 314 (100)	Tricin-*O*-hexoside derivative	✓		
155	36.4	**555**	MS^2 [555]: 417 (21.7), 305 (32.9), 287 (27.1), 269 (100), 267 (22.4), 223 (54.3), 161 (22.2) MS^3 [555→269]: 251 (20.5), 241 (38.8), 227 (45.9), 226 (51.3), 225 (32.3), 223 (100), 197 (68.9), 195 (33.5), 179 (17.1)	Baicalein derivative		✓	[106]
156	36.7	**527**	MS^2 [527]: 491 (100) MS^3 [527→491]: 371 (12.9), 330 (28.5), 330 (20.3), 329 (100), 314 (50.7)	Tricin-*O*-hexoside derivative	✓		
157	36.8	**297**	MS^2 [297]: 183 (100) MS^3 [297→183]: 169 (100), 125 (52.7)	Methyl-gallate derivative	✓	✓	[220]
158	37.3	**563**	MS^2 [563]: 356 (11.0), 355 (100) MS^3[563→355]: 341 (12.8), 340 (100), 325 (43.4) MS^4 [563→355→340]: 326 (15.2), 325 (100), 296 (79.8), 281 (36.7), 212 (27.6)	Conidendrin-*O*-hexoside	✓	✓	[106]
159	37.6	**284**	MS^2 [284]: 242 (57.4), 222 (100), 142 (35.8) MS^3 [284→222]: 157 (100), 142 (41.5)	Unknown		✓	
160	38.0	**301**	MS^2 [301]: 271 (23.7), 179 (100), 151 (44.7)	Quercetin	✓		Standard
161	38.0	**297**	MS^2 [297]: 183 (100) MS^3 [297→183]: 169 (100), 125 (52.7)	Methyl-gallate derivative		✓	[220]
162	38.5	**779**	MS^2 [779]: 634 (26.5), 633 (100), 616 (26.2), 615 (74.3), 469 (38.7) MS^3[779→633]: 488 (18.7), 487 (17.9), 470 (35.0), 469 (100), 325 (17.3), 265 (11.1) MS^4 [779→633→469]: 307 (88.9), 163 (100), 145 (49.5), 119 (24.8)	Benzoyl-*p*-tricoumaryl- 2,7-anhydro-3-DOA	✓	✓	[106]
163	39.9	**327**	MS^2 [327]: 311 (27.9), 294 (13.1), 293 (18.7), 229 (100), 211 (72.1), 183 (14.5), 171 (12.4) MS^3 [327→229]: 211 (100), 209 (32.3), 165 (16.9), 127 (32.2), 125 (67.3)	Oxo-dihydroxy-octadecenoic acid	✓		[106]

164	40.0	**779**	MS^2 [779]: 633 (100), 615 (75.2), 469 (39.1) MS^3 [779→633]: 487 (19.3), 470 (33.2), 469 (100), 325 (18.5), 265 (13.5) MS^4 [779→633→469]: 307 (83.6), 163 (100), 145 (47.9), 119 (31.3)	Benzoyl-*p*-tricoumaryl- 2,7-anhydro-3-DOA	✓	[106]

t_R: retention time; HHDP: Hexahydroxydiphenoyl; DOA: deoxy-2-octulopyranosonic acid.

Table S 12 - Characterization of anthocyanins of *M. faya* (berries) methanolic extracts by HPLC-ESI^+/MS^n.

Nº	***t_R*** **(min)**	**$[M-H]^+$ (*m/z*)**	**HPLC-DAD-ESI/MS^n *m/z* (% base peak)**	**Assigned identity**	**References**
5	3.7	**465**	MS^2 [465]: 303 (100) MS^3 [465→303]: 257 (100), 229 (42.2), 201 (26.8), 159 (46.6), 150 (25.7)	Delphinidin-*O*-hexoside	[82]
6	3.9	**449**	MS^2 [449]: 287 (100) MS^3 [449→287]: 231 (100), 213 (50.5), 165 (16.5), 161 (32.1), 137 (59.6)	Cyanidin-*O*-hexoside	
11	4.2	**465**	MS^2 [465]: 303 (100) MS^3 [465→303]: 275 (16.9), 257 (100), 229 (29.4), 201 (25.3), 165 (24.3), 161 (21.8), 151 (10.3)	Delphinidin-*O*-hexoside	[82]
13	4.4	**449**	MS^2 [449]: 287 (100) MS^3 [449→287]: 231 (100), 213 (50.5), 165 (16.5), 161 (32.1), 137 (59.6)	Cyanidin-*O*-hexoside	
16	4.9	**449**	MS^2 [449]: 287 (100) MS^3 [449→287]: 231 (100), 213 (50.5), 165 (16.5), 161 (32.1), 137 (59.6)	Cyanidin-3-*O*-glucoside	Standard
33	6.3	**449**	MS^2 [449]: 287 (100) MS^3 [449→287]: 231 (100), 213 (50.5), 165 (16.5), 161 (32.1), 137 (59.6)	Cyanidin-*O*-hexoside	
34	6.4	**433**	MS^2 [433]: 271 (100) MS^3 [433→271]: 187 (100), 173 (12.6), 149 (30.0), 131 (10.3)	Pelargonidin-*O*-hexoside	[82]
42	7.2	**449**	MS^2 [449]: 287 (100) MS^3 [449→287]: 231 (100), 213 (50.5), 165 (16.5), 161 (32.1), 137 (59.6)	Cyanidin-*O*-hexoside	
47	7.5	**449**	MS^2 [449]: 287 (100) MS^3 [449→287]: 231 (100), 213 (50.5), 165 (16.5), 161 (32.1), 137 (59.6)	Cyanidin-*O*-hexoside	
48	7.5	**419**	MS^2 [419]: 317 (17.4), 303 (61.9), 287 (100) MS^3 [419→287]: 241 (82.2), 213 (100), 175 (57.6), 161 (87.3), 153 (78.9), 137 (24.6), 109 (19.2)	Cyanidin-*O*-pentoside	[188,214]
50	8.0	**449**	MS^2 [449]: 287 (100) MS^3 [449→287]: 231 (100), 213 (50.5), 165 (16.5), 161 (32.1), 137 (59.6)	Cyanidin-*O*-hexoside	
60	8.6	**449**	MS^2 [449]: 287 (100) MS^3 [449→287]: 231 (100), 213 (50.5), 165 (16.5), 161 (32.1), 137 (59.6)	Cyanidin-*O*-hexoside	
69	9.9	**491**	MS^2 [491]: 449 (41.4), 303 (31.9), 287 (100) MS^3 [491→287]: 241 (82.2), 213 (100), 175 (57.6), 161 (87.3), 153 (78.9), 137 (24.6), 109 (19.2)	Cyanidin-*O*-(acetyl)hexoside	[153]
74	10.9	**491**	MS^2 [491]: 449 (41.4), 303 (31.9), 287 (100) MS^3 [491→287]: 241 (82.2), 213 (100), 175 (57.6), 161 (87.3), 153 (78.9), 137 (24.6), 109 (19.2)	Cyanidin-*O*-(acetyl)hexoside	[153]

t_R: retention time

1.3. Rubus grandifolius

The phytochemical profile of *R. grandifolius* collected at two different locations of Madeira Island (Funchal and Machico) was established. Following is a brief explanation about the identification of phytochemicals **Table S 13** and **Table S 14** and for more details about the characterization, please check the mentioned references.

1.3.1. Phenolic acids

Glycosides of caffeic acid were identified in analysed samples (compounds **19**, **22**, **75**, **84**, **88** and **96**) (**Table S 13**). Compound **11**, with $[M-H]^-$ ion at m/z 371, showed a loss of 174 (probably a quinic acid moiety) to yield MS^2 base peak at m/z 197. This ion fragmentation was consistent with syringic acid [199], however, the presence of fragment ions at m/z 353, 191, 179 and 135 is also indicative of CQA [221]. Therefore, **11** was tentatively identified as caffeic/syringic acid derivative. Several derivatives of caffeic acid (compounds **24**, **49**, **54**, **65**, **67**, **69**, **77**, **102** and **109**) were detected in extracts. The tentatively characterization resulted from the observation of characteristic ions at m/z 179 and 135. Compound **31** exhibited an $[M-H]^-$ ion at m/z 457. It showed an MS^2 base peak at m/z 341$[M-H-116]^-$, consistent with caffeic acid-*O*-hexoside (compounds **19** and **22**)[84]. The loss of 116 Da is indicative of mallic acid, hence, **31** was tentatively characterized as caffeoylhexoside-mallic acid. By analogy, compound **44** with an $[M-H]^-$ ion at m/z 537, was characterized as a derivative of caffeic acid-*O*-hexoside. Compound **56** displayed $[M-H]^-$ ion at m/z 493 and was tentatively identified as caffeic acid-*O*-(galloyl)hexoside. The presence of product ions at m/z 341 $[M-H-152]^-$, 179 $[M-H-152-162]^-$ and 135 $[M-H-152-162-44]^-$ supported this characterization. Compound **104** exhibited an $[M-H]^-$ ion at m/z 487. At MS^2 fragmentation, it showed caffeic acid-*O*-hexoside and caffeic acid at m/z 341 $[M-H-146]^-$ and 179 $[M-H-146-162]^-$, respectively. At this retention time, the 146 Da loss is attributed to a coumaroyl unit. Hence, **104** was tentatively characterized as caffeic acid-*O*-(coumaroyl)hexoside. Discrimination of 3-*O* and 5-*O*-CQA isomers (compounds **14**, **18** and **29**) was explained in previous sample. Compounds **86** and **89** displayed both $[M-H]^-$ ions at m/z 515 and were identified as 4,5-*O* and 3,5-*O*-diCQAs, respectively. Their characterization was confirmed by analytical standards.

Salvianolic acid (compound **27**), with $[M-H]^-$ ion at m/z 537, was plausibly identified in leaves extracts [222].

Compound **52** displayed $[M-H]^-$ ion at m/z 493. Gallic acid was observed (at m/z 169) after two separated losses of 162 Da. Therefore, **52** was identified as galloyl-*O*-dihexoside. Compound **94** displayed $[M-H]^-$ ion at m/z 477. Protocatechuic acid was observed at m/z 153 $[M-H-162-162]^-$. Thus, **94** was identified as protocatechuic acid-*O*-dihexoside.

Identification of coumaric acid (compound **121**) was confirmed by an analytical standard.

1.3.2. Flavonols

Different quercetin glycosides were detected in analysed extracts (**Table S 13**), in all cases with aglycone at m/z 301 (compound **115**). Their characterization was explained in previous samples. Compound **81** exhibited an $[M-H]^-$ ion at m/z 477 and suffered a loss of 176 Da at MS^2. It was identified as quercetin-*O*-glucuronide [212]. Compound **82** with $[M-H]^-$ ion at m/z 607 was identified previously in *R. grandifolius* as 3-hydroxy-3-methylglutaroyl-quercetin-*O*-hexoside [107].

Compound **62** showed $[M-H]^-$ ion at m/z 491 and MS^2 base peak at m/z 315 $[M-H-176]^-$. It was identified as isorhamnetin-*O*-glucuronide [212]. Compound **92** showed an $[M-H]^-$ ion at m/z 533. Further fragmentation showed isorhamnetin aglycone at m/z 315 $[M-H-218]^-$; it was tentatively characterized as a derivative.

Kaempferol conjugates (compounds **76**, **80**, **83**, **91**, **97** and **114**) had in common aglycone at m/z 285 and were plausibly identified based on previous studies (**Table S 13**).

1.3.3. Flavan-3-ols

Catechin derivatives (compounds **45** – **47**) were common in samples collected in Machico. In all cases, they showed catechin aglycone (at m/z 289) (compound **39**) after loss of different moieties. Compound **32** displayed an $[M-H]^-$ ion at m/z 577 and it followed the same fragmentation pattern as described for PAC dimer (B type) [84]. Compound **72**, with $[M-H]^-$ ion at m/z 483, showed catechin aglycone after direct loss of 194 Da. The presence of fragment ion at m/z 451 was consisted with catechin-*O*-hexoside $[M-H-32]^-$ [219], hence, **72** was tentatively identified as a derivative.

1.3.4. Flavones

Compound **78** exhibited $[M-H]^-$ ion at m/z 523 and MS^2 base peak at m/z 475 $[M-H-48]^-$. Sequential fragmentation gave origin to product ion at m/z 329 $[M-H-146]^-$, which was consistent with tricin aglycone [106]. Based on the available data, **78** was tentatively characterized as a derivative of tricin-*O*-coumaroyl. Apigenin-*O*-glucuronide (compound **99**) was identified previously in other *Rubus* species [87].

1.3.5. Ellagic acid derivatives/ Ellagitannins

Ellagic acid alone was found in this analysis (compound **70**), but also attached to different sugar moieties: ellagic acid-*O*-glucuronide (compounds **42** and **48**), ellagic acid-*O*-pentoside (compounds **50** and **58**) and ellagic acid-*O*-hexoside (compound **73**) (**Table S 13**). Compound **61**, with an $[M-H]^-$ ion at m/z 513, showed ellagic acid at m/z 301 $[M-H-212]^-$. With no further information, **61** was identified as a derivative. Similarly, compound **113** showed $[M-H]^-$ ion at m/z 517 and was tentatively characterized as another derivative.

1.3.6. Other compounds

Compounds of non-phenolic nature were also present in methanolic extracts of *R. grandifolius* (saccharides, organic acids, terpenoids and coumarins). Oligosaccharides (compounds **1**, **6**, **35**, **43**, **51** and **60**) were characterized in *R. grandifolius* extracts based on their fragmentation pattern. Compound **4**, with $[M-H]^-$ ion at m/z 515, showed a loss of 174 Da at MS^2. This moiety could indicate the presence of quinic acid. Sequential fragmentation of product ion at m/z 341 was consistent with two units of hexose (compound **6**) [207]. Hence, **4** was tentatively characterized as dihexoside-quinic acid.

Organic acids (compounds **7** and **8**) were also identified in analysed extracts. Compound **16** exhibited an $[M-H]^-$ ion at m/z 369. It showed citric acid typical fragment ions (at m/z 191, 173 and 111) [206] and was tentatively characterized as a derivative.

Triterpene glycosides were abundant in this analysis. Characterization of triterpene acid-*O*-hexoside (formate adduct) (compounds **79**, **95**, **100**, **105**, **111** and **117**) was described in a previous sample. Compounds **101**, **113** and **121** displayed $[M-H]^-$ ions at m/z 603 and were identified previously in *R. grandifolius* [107] as ganoderic acid C2 hexoside. Compound **120** gave a $[M-H]^-$ ion at m/z 663 and in the MS^2 spectrum displayed base peak at m/z 501 (loss of 162 Da). Fragmentation pattern of this ion was described before for ganolucidic acid B [223], hence, **120** was identified as ganolucidi acid B hexoside. 12-Hydroxyganoderic acid C2 (compound **122**) was identified based on previous data [223]. Compound **108**, with $[M-H]^-$ ion at m/z 839, showed a MS^2 base peak at m/z 677 $[M-H-162]^-$. Sequential fragmentation yielded product ion at m/z 503 $[M-H-162-174]^-$, which originated fragment ions at m/z 485, 453 and 409. This pattern was consistent with that of a triterpene acid structure [211], thus, **108** was tentatively characterized as a derivative.
Fragmentation pattern of compounds **93**, **98** and **109**, with $[M-H]^-$ ions at m/z 547, was corroborative with umbelliferone, previously identified in this species [107].

1.3.7. Anthocyanins

Eleven anthocyanins were identified in *R. grandifolius* berries in positive mode (**Figure 31**), all conjugates of cyanidin (at m/z 287) (**Table S 14**). By contrast to a previous analysis [107], no delphinin and petunidin derivatives were found in analysed extracts. This could be mainly due to differences in extraction solvents.

Table S 13 - Characterization of phytochemicals of *R. grandifolius* methanolic extracts by HPLC-ESI$^-$/MS^n (FX: Funchal: MX: Machico).

Nº	t_R (min)	[M-H]$^-$ (*m/z*)	HPLC-DAD-ESI/MS^n *m/z* (% base peak)	Assigned identification	Berries		Leaves		References
					FX	MX	FX	MX	
1	3.2	**683**	MS^2 [683]: 341 (100) MS^3 [683→341]: 179 (100), 161 (23.0), 143 (33.1), 119 (16.9), 113 (45.2)	Hexose polymer	✓	✓	✓	✓	[207]
3	3.8	**353**	MS^2 [353]: 173 (100), 155 (11.5), 111 (21.5) MS^3 [353→173]: 155 (17.9), 111 (100)	Caffeoylisocitrate	✓	✓			[215]
4	3.4	**515**	MS^2 [515]: 341 (100) MS^3 [515→341]:179 (100), 161 (33.9), 149 (15.2), 119 (46.9), 131 (25.1), 113 (28.5)	Saccharide (Dihexose + Quinic acid)			✓	✓	
5	3.5	**533**	MS^2 [533]: 191 (100) MS^3 [533→191]: 173 (100), 153 (18.0), 127 (91.3), 109 (36.1), 93 (55.0), 85 (99.5)	Quinic acid derivative				✓	[106]
6	3.6	**341**	MS^2 [341]: 179 (100), 161 (34.0), 149 (23.7), 119 (33.5)	Saccharide (Dihexose)			✓		[207]
7	3.8	**191**	MS^2 [191]: 173 (100), 111 (36.5) MS^3 [191→173]: 155 (21.2), 111 (100)	Citric acid	✓	✓		✓	[206]
8	4.0	**133**	MS^2 [133]:115 (100) MS^3 [133→115]:71 (100)	Malic acid				✓	[206]
9	4.2	**481**	MS^2 [481]: 301 (100) MS^3 [481→301]: 275 (100), 257 (29.3)	HHDP-*O*-hexoside				✓	[201]
11	4.5	**371**	MS^2 [371]: 353 (82.6), 197 (49.2), 191 (47.7), 179 (12.8), 173 (48.5), 153 (22.8), 135 (100) MS^3 [371→197]: 179 (77.7), 153 (100), 135 (88.1)	Caffeic/Syringic acid derivative			✓	✓	
14	5.5	**707** [2M-H]$^-$	MS^2 [707]: 615 (27.4), 533 (48.1), 353 (100), 339 (37.7), 315 (38.3), 271 (62.7), 243 (11.2) MS^3 [707→353]: 191 (100), 179 (30.3)	3-*O*-Caffeoylquinic acid dimer				✓	[221]
15	5.7	**783**	MS^2 [783]: 617 (14,7), 481 (43.0), 301 (100), 275 (11.0) MS^3 [783→301]: 257 (100), 257 (47.0), 185 (86.0)	bis-HHDP-*O*-hexoside (Pedunculagin I)			✓	✓	[200]
16	5.7	**369**	MS^2 [369]: 191 (11.8), 173 (100), 111 (23.2) MS^3 [369→173]: 155 (16.1), 111 (100)	Citric acid derivative	✓	✓			
18	6.4	**353**	MS^2 [353]: 191 (100), 179 (43.5), 135 (17.2) MS^3 [353→191]: 173 (48.4), 127 (100), 109 (16.5), 93 (68.1), 85 (70.8)	3-*O*-Caffeoylquinic acid	✓	✓	✓	✓	[221]
19	6.7	**341**	MS^2 [341]: 251 (20.5), 233 (27.2), 203 (19.0), 179 (100), 161 (27.3), 135 (19.6) MS^3 [341→179]: 135 (100)	Caffeic acid-*O*-hexoside	✓	✓	✓	✓	[84]
21	6.9	**783**	MS^2 [783]: 618 (10.3), 617 (45.1), 481 (15.0), 302 (14.2), 301 (100), 257 (24.9) MS^3 [783→301]: 284 (70.2), 257 (100)	bis-HHDP-*O*-hexoside (Pedunculagin I)	✓	✓		✓	[200]
22	7.4	**341**	MS^2 [341]: 281 (93.1), 251 (100), 221 (31.9), 179 (76.6) MS^3 [341→179]: 135 (100)	Caffeic acid-*O*-hexoside			✓	✓	[84]
24	8.2	**297**	MS^2 [297]: 179 (100), 135 (15.9) MS^3 [297→179]: 135 (100)	Caffeic acid derivative			✓	✓	
27	8.7	**537**	MS^2 [537]: 353 (100), 191 (12.3), 165 (11.0) MS^3 [537→353]: 191 (100); 165 (58.0), 127 (100), 111 (51.5), 93 (53.9), 85 (45.5)	Salvianolic acid			✓	✓	[222]
29	9.0	**707**	MS^2 [707]: 354 (11.3), 353 (100)	5-*O*-Caffeoylquinic acid dimer			✓		

		$[2M-H]^-$	MS^3 [707→353]: 191 (31.7), 179 (12.2), 173 (100), 135 (38.4)						
31	9.2	**457**	MS^2 [457]: 439 (37.2), 341 (100), 281 (34.1), 179 (16.8) MS^3 [457→341]: 281 (80.1), 251 (100), 221 (20.9), 179 (50.9), 135 (35.0)	Caffeoylhexoside-mallic acid			✓	✓	
32	9.5	**577**	MS^2 [577]: 519 (11.4), 451 (32.6), 425 (100), 407 (96.4), 289 (20.0) MS^3 [577→425]: 407 (100), 339 (18.8), 285 (25.4)	Procyanidin (B type)				✓	[84]
33	9.5	**431**	MS^2 [431]: 385 (100), 223 (12.2) MS^3 [431→385]: 223 (33.1), 205 (40.5), 161 (13.3), 153 (100)	Roseoside (formate adduct)			✓	✓	[106]
34	9.6	**355**	MS^2 [355]: 193 (100) MS^3 [355→193]: 149 (62.1), 134 (100)	Ferulic acid-*O*-hexoside	✓				[80]
35	10.0	**565**	MS^2 [565]: 520 (19.7), 519 (100), 341 (10.8) MS^3 [565→519]: 388 (18.3), 341 (100), 179 (44.7), 161 (33.6), 113 (25.0)	Saccharide	✓		✓		
37	10.3	**635**	MS^2 [635]: 466 (24.3), 465 (100) MS^3 [635→465]: 314 (11.6), 313 (100), 241 (12.5), 235 (10.2), 211 (12.8), 169 (63.3) MS^4 [635→465→313]: 205 (22.6), 193 (46.6), 169 (100), 125 (35.6)	Trigalloyl-*O*-hexoside			✓		[201]
38	10.4	**373**	MS^2 [373]: 337 (100), 319 (23.0), 293 (10.4), 277 (27.9) MS^3 [373→337]: 293 (100), 277 (90.4), 237 (82.9), 219 (62.8), 177 (38.0), 165 (17,1)	Unknown				✓	
39	10.8	**289**	MS^2 [289]: 246 (20.6), 245 (100), 179 (20.7), 105 (32.6) MS^3 [289→245]: 227 (27.8), 203 (100), 185 (22.3), 175 (66.2), 161 (22.4)	Catechin			✓		Standard
40	11.0	**355**	MS^2 [355]: 309 (33.1), 161 (100) MS^3 [355→161]: 133 (100), 117 (10.9)	Ferulic acid derivative			✓	✓	
41	11.1	**565**	MS^2 [565]: 324 (11.8), 323 (100), 211 (15.2) MS^3 [565→323]: 280 (12.0), 262 (11.4), 211 (100), 139 (17.5), 124 (15.9)	Unknown	✓	✓			
42	11.2	**477**	MS^2 [477]: 302 (22.8), 301 (100) MS^3 [477→301]: 283 (57.6), 257 (100)	Ellagic acid-*O*-glucuronide	✓	✓			[107]
43	11.3	**637**	MS^2 [637]: 356 (10.0), 355 (100), 179 (18.3) MS^3 [637→355]: 161 (100), 149 (14.4), 119 (26.8)	Saccharide			✓		
44	11.6	**537**	MS^2 [537]: 519 (100), 341 (11.1), 281 (14.5), 179 (100) MS^3 [537→519]: 357 (12.9), 341 (76.0), 325 (51.4), 295 (77.4), 179 (100), 135 (49.7)	Caffeic acid-*O*-hexoside derivative			✓	✓	
45	11.7	**401**	MS^2 [401]: 301 (20.3), 289 (100), 215 (10.6) MS^3 [401→289]: 245 (100), 205 (52.2), 203 (13.2), 179 (16.6)	Catechin derivative				✓	
46	12.0	**513**	MS^2 [513]: 433 (20.2), 401 (100), 301 (14.1), 291 (10.3), 257 (8.8), 215 (15.0) MS^3 [513→401]: 301 (52.6), 289 (100), 215 (16.9), 195 (20.5) MS^4 [513→401→289]: 245 (100), 188 (15.6), 175 (26.0), 151 (18.6)	Catechin derivative				✓	
47	12.3	**557**	MS^2 [557]: 513 (19.6), 445 (100), 255 (21.5), 211 (14.5) MS^3 [557→445]: 383 (28.1), 301 (47.0), 289 (100), 257 (35.2), 247 (22.9), 215 (47.8), 205 (20.4), 196 (12.1) MS^4 [557→445→289]: 245 (100), 205 (71.4)	Catechin derivative				✓	
48	12.4	**477**	MS^2 [477]: 301 (100) MS^3 [477→301]: 257 (100), 245 (40.4)	Ellagic acid-*O*-glucuronide	✓	✓			[107]
49	12.5	**537**	MS^2 [537]: 519 (100) MS^3 [537→519]: 281 (69.6), 265 (22.3), 217 (22.1), 179 (100), 135 (47.6)	Caffeic acid derivative				✓	
50	12.5	**433**	MS^2 [433]: 301 (100), 300 (62,7) MS^3 [433→301]: 257 (100)	Ellagic acid-*O*-pentoside		✓			[200]
51	12.8	**393**	MS^2 [393]: 358 (25.2), 348 (21.5), 347 (100), 289 (14.9), 179 (21.5) MS^3 [393→347]: 329 (71.6), 161 (100), 119 (33.4)	Saccharide	✓				
52	13.1	**493**	MS^2 [493]: 449 (22.0), 331 (100), 315 (14.5), 299 (26.7), 287 (32.1), 271 (37.4), 169 (31.3)	Galloyl-*O*-dihexoside			✓	✓	

			MS^3 [493→331]: 169 (100), 125 (37.3)							
53	13.5	**935**	MS^2 [935]: 915 (15.2), 897 (31.2), 633 (100), 301 (80.2) MS^3 [935→633]: 469 (11.8), 315 (12.8), 302 (14.7), 301 (100) MS^4 [935→633→301]: 300 (17.5), 285 (29.8), 257 (56.1), 229 (100), 201 (50.9), 186 (53.5)	Galloyl-bis-HHDP-*O*-hexoside (Casuarinin)	✓	✓	✓	✓	[87]
54	14.4	**537**	MS^2 [537]: 519 (44.5), 490 (26.1), 489 (100), 323 (24.3) MS^3 [537→489]: 324 (12.3), 323 (100), 221 (26.7), 179 (26.6), 161 (12.7), 135 (53.0)	Caffeic acid derivative			✓	✓	
55	14.4	**595**	MS^2 [595]: 463 (100), 434 (12,1), 433 (47.5), 301 (18.5) MS^3 [595→463]: 301 (100), 179 (55.2), 151 (28.4)	Quercetin-*O*-(pentosyl)hexoside	✓	✓			[84]
56	14.9	**493**	MS^2 [493]: 433 (20.1), 425 (10.6), 341 (57.1), 232 (26.3), 281 (62.9), 251 (81.3), 221 (45.7), 179 (100) MS^3 [493→179]: 135 (100)	Caffeic acid-*O*-(galloylhexoside			✓	✓	
57	15.1	**595**	MS^2 [595]: 463 (15.5), 301 (100) MS^3 [595→301]: 271 (45.5), 179 (50.2), 151 (100)	Quercetin-*O*-(pentosyl)hexoside			✓	✓	[84]
58	15.4	**433**	MS^2 [433]: 301 (100) MS^3 [433→301]: 300 (74.7), 258 (12.1), 257 (100), 229 (49.4), 217 (17.3)	Ellagic acid-*O*-pentoside	✓	✓	✓	✓	[200]
59	15.7	**739**	MS^2 [739]: 629 (17.1), 587 (100), 569 (21.2), 449 (15.4), 435 (40.8), 417 (16.2), 339 (22.0), 289 (14.5) MS^3 [739→587]: 569 (54.8), 477 (32.4), 459 (30.9), 435 (93.1), 417 (100), 339 (43.4), 325 (35.1), 299 (21.0), 177 (23.0) MS^4 [739→587→339]: 337 (100), 177 (87.6)	Unknown				✓	
60	15.9	**457**	MS^2[457]: 296 (13.2), 295 (100) MS^3 [457→295]: 180 (18.7), 179 (37.0), 149 (24.7), 133 (39.4), 119 (100), 113 (57.4)	Saccharide			✓		
61	16.4	**513**	MS^2 [513]: 427 (100), 361 (49.5), 301 (52.4), 300 (19.1), 289 (80.4), 257 (29.7) MS^3 [513→301]: 257 (100)	Ellagic acid derivative				✓	
62	16.6	**491**	MS^2 [491]: 315 (100), 300 (25.6) MS^3 [491→315]: 301 (25.5), 300 (100)	Isorhamnetin-*O*-glucuronide	✓	✓			[212]
63	16.9	**549**	MS^2 [549]: 503 (100), 311 (28.7), 221 (15.1), 191 (22.3) MS^3 [549→503]: 459 (26.5), 311 (53.2), 293 (28.4), 281 (18.0), 275 (30.0), 251 (13.3), 239 (36.2), 221 (100), 191 (35.3), 161 (10.4), 143 (18.0)	Unknown			✓		
64	17.2	**609**	MS^2 [609]: 301 (100), 300 (50.8) MS^3 [609→301]: 179 (54.3), 151 (100)	Quercetin-*O*-rutinoside (Rutin)	✓	✓	✓	✓	[200]
65	17.5	**645**	MS^2 [645]: 475 (100), 301 (23.9) MS^3 [645→475]: 323 (97.1), 313 (100), 179 (29.7) MS^4 [645→475→323]: 179 (12.8), 161 (22.7), 135 (100)	Caffeic acid derivative			✓		
66	17.8	**509**	MS^2 [509]: 491 (100), 473 (30.0), 461 (42.3), 367 (64.3), 313 (22.7), 311 (36.1) MS^3 [509→367]: 339 (100), 313 (25.1), 149 (58.4) MS^3 [509→491]: 473 (100), 462 (25.7), 461 (87.1)	Unknown	✓	✓	✓	✓	
67	18.3	**477**	MS^2 [477]: 323 (100), 221 (22.4), 179 (25.6), 177 (15.0), 161 (14.0) MS^3 [477→323]: 275 (12.5), 263 (39.2), 221 (41.2), 203 (37.5), 179 (100), 179 (18.8), 177 (73.2), 135 (50.2)	Caffeic acid derivative			✓		
68	18.5	**451**	MS^2 [451]: 341 (100) MS^3 [451→341]: 323 (11.7), 231 (25.0), 219 (29.2), 217 (100), 189 (17.5), 177 (19.3) MS^4 [451→341→217]: 191 (88.7), 189 (100), 153 (10.1)	Unknown			✓	✓	
69	18.7	**463**	MS^2 [463]: 337 (11.4), 323 (98.1), 221 (19.4), 179 (32.9), 135 (12.5) MS^3 [463→323]: 263 (100), 245 (17.3), 221 (46.1), 179 (97.8) MS^4 [463→323→179]: 135 (100)	Caffeic acid derivative			✓	✓	

70	19.2	**301**	MS^2 [301]: 257 (100), 229 (61,8), 217 (22,0), 185 (95,4), 146 (47,3), 119 (25,7)	Ellagic acid		✓			Standard
71	19.2	**463**	MS^2 [463]: 302 (13,8), 301 (100) MS^3 [463→301]: 273 (12.3), 271 (32.7), 257 (11.7), 255 (19.3), 179 (82.4), 151 (100)	Quercetin-*O*-hexoside	✓	✓			[84]
72	19.8	**483**	MS^2 [483]: 451 (17.1), 341 (23.6), 289 (100) MS^3 [483→289]: 245 (100), 205 (20.1), 203 (56.8), 187 (22.5), 179 (10.6)	Catechin-*O*-hexoside derivative				✓	
73	20.0	**463**	MS^2 [463]: 323 (100), 301 (96.1) MS^3 [463→301]: 257 (100)	Ellagic acid-*O*-hexoside	✓	✓	✓	✓	[206]
74	20.3	**463**	MS^2 [463]: 301 (100) MS^3 [463→301]: 271 (12.2), 179 (83.8), 151 (100)	Quercetin-*O*-hexoside			✓	✓	[84]
75	20.6	**503**	MS^2 [503]: 471 (13.4), 341 (13.9), 329 (29.7), 323 (21.4), 179 (100), MS^3 [503→179]: 135 (100)	Caffeic acid-*O*-dihexoside			✓		[87]
76	20.9	**593**	MS^2 [593]: 285 (100), 255 (18.1) MS^3 [593→285]: 257 (100), 241 (40.5), 229 (53.4), 227 (22.9), 199 (22.8), 195 (35.6), 185 (17.0)	Kaempferol-*O*-rutinoside				✓	[200]
77	21.0	**491**	MS^2 [491]: 323 (100), 179 (12.6) MS^3 [491→323]: 263 (30.2), 251 (22.2), 221 (84.5), 203 (43.1), 179 (100), 135 (94.9)	Caffeic acid derivative			✓	✓	
78	21.2	**523**	MS^2 [523]: 476 (28.0), 475 (100) MS^3 [523→475]: 460 (14.3), 443 (24.2), 415 (14.5), 399 (10.1), 387 (11.2), 341 (34.0), 329 (100), 327 (25.2), 315 (43.3), 297 (10.7), 283 (38.7), 271 (15.6), 195 (18.9) MS^4 [523→475→329]: 315 (16.3), 314 (100), 298 (10.0), 296 (10.7), 282 (10.4), 164 (15.4), 149 (26.5)	Tricin-*O*-coumaroyl derivative			✓	✓	
79	22.1	**711**	MS^2 [711]: 665 (11.9), 503 (100) MS^3 [711→503]: 439 (100), 427 (70.9), 409 (44.2), 368 (20.4) MS^4 [711→503→439]: 421 (31.1), 411 (47.2), 409 (100), 393 (25.0), 384 (75.0)	Triterpene acid-*O*-hexoside (formate adduct)			✓	✓	
80	22.9	**461**	MS^2 [461]: 285 (100) MS^3 [461→285]: 267 (46.0), 255 (43.2), 217 (67.8), 213 (23.4), 199 (18.5), 175 (100), 129 (78.3)	Kaempferol-*O*-glucuronide			✓	✓	[212]
81	23.0	**477**	MS^2 [477]: 302 (15.7), 301 (100) MS^3 [477→301]: 229 (12.3), 179 (74.2), 151 (100)	Quercetin-*O*-glucuronide	✓	✓	✓	✓	[212]
82	23.6	**607**	MS^2 [607]: 505 (15.6), 464 (17.8), 463 (100) MS^3 [607→463]: 301 (100), 300 (372) 179 (90.5), 151 (30.0)	3-Hydroxy-3-methylglutaroyl-quercetin-*O*-hexoside	✓	✓			[107]
83	24.0	**593**	MS^2 [593]: 286 (13.4), 285 (100) MS^3 [593→285]: 267 (35.6), 257 (100), 255 (12.9), 241 (35.1), 229 (75.6), 223 (32.8), 213 (36.9), 197 (44.1), 195 (25.3), 167 (32.1), 163 (34.4), 151 (17.5)	Kaempferol-*O*-rutinoside			✓	✓	[200]
84	24.1	**503**	MS^2 [503]: 459 (28.0), 341 (14.5), 323 (100), 251 (10.5), 179 (52.2), 177 (10.6), 161 (15.1) MS^3 [503→179]: 135 (100)	Caffeic acid-*O*-dihexoside			✓		[87]
85	24.5	**433**	MS^2 [433]: 301 (100), 300 (90.7) MS^3 [433→301]: 271 (100), 257 (13.7), 255 (51.9), 179 (67.5), 151 (60.8)	Quercetin-*O*-pentoside	✓	✓	✓	✓	[200]
86	24.8	**515**	MS^2 [515]: 353 (100), 335 (13.7), 191 (11.1), 179 (22.0), 173 (40.1) MS^3 [515→353]: 191 (39.9), 179 (62.6), 173 (100), 135 (22.3)	4,5-*O*-Dicaffeoylquinic acid			✓		Standard
87	25.1	**321**	MS^2 [321]: 303 (100), 259 (11.2), 215 (11.5) 179 (59.1), 159 (22.1), 135 (10.6) MS^3 [321→303]: 241 (56.9), 259 (100), 215 (25.1), 187 (10.0), 149 (11.7)	Unknown				✓	
88	26.2	**503**	MS^2 [503]: 341 (10.4), 323 (100), 221 (10.9), 179 (29.9) MS^3 [503→323]: 263 (20.4), 221 (34.4), 179 (100), 135 (29.9)	Caffeic acid-*O*-dihexoside			✓	✓	[87]
89	26.8	**515**	MS^2 [515]: 353 (100) MS^3 [515→353]: 191 (100), 179 (44.7), 135 (12.5) MS^4 [515→353→191]: 173 (56.0), 127 (100), 111 (56.7), 85 (61.7)	3,5-*O*-Dicaffeoylquinic acid			✓	✓	Standard
90	26.9	**505**	MS^2 [505]: 463 (53.7), 301 (100)	Quercetin-*O*-(acetyl)hexoside	✓	✓			[224]

			MS^3 [505→301]: 273 (19.4), 255 (37.2), 179 (79.1), 151 (100)						
91	27.2	**447**	MS^2 [447]: 285 (100), 284 (68.1), 255 (28.9) MS^3 [447→285]: 255 (100)	Kaempferol-*O*-hexoside			✓	✓	[200]
92	27.3	**533**	MS^2 [533]: 315 (100), 300 (34.4), 299 (21.0) MS^3 [533→315]: 271 (100)	Isorhamnetin derivative	✓				
93	27.7	**547**	MS^2 [547]: 341 (100), 281 (67.2), 251 (33.6), 221 (15.3), 179 (30.5) MS^3 [547→341]: 281 (100), 251 (75.8), 221 (21.8), 179 (68.2), 135 (57.3)	Umbelliferone			✓	✓	[107]
94	27.9	**477**	MS^2 [477]: 433 (18.8), 315 (100) MS^3 [477→315]: 153 (100), 109 (36.0)	Protocatechuic acid-*O*-dihexoside			✓	✓	
95	28.2	**711**	MS^2 [711]: 503 (100) MS^3 [711→503]: 487 (13.2), 485 (100), 383 (24.8), 343 (19.7) MS^4 [711→503→485]: 419 (100), 411 (64.5), 409 (78.1), 381 (47.3), 347 (53.8), 343 (50.9), 135 (43.2)	Triterpene acid-*O*-hexoside (formate adduct)				✓	
96	28.7	**503**	MS^2 [503]: 341 (96.6), 281 (71.5), 251 (73.6), 221 (40.0), 179 (100) MS^3 [503→341]: 323 (11.9), 281 (36.0), 251 (57.4), 221 (29.6), 179 (100), 135 (30.0)	Caffeic acid-*O*-dihexoside			✓	✓	[87]
97	28.9	**417**	MS^2 [417]: 285 (100), 255 (10.8) MS^3 [417→285]: 255 (100), 229 (10.2), 227 (29.4), 163 (13.3)	Kaempferol-*O*-pentoside			✓	✓	[107]
98	29.5	**547**	MS^2 [547]: 387 (12.0), 341 (19.6), 281 (20.0), 179 (26.3), 161 (100) MS^3 [547→341]: 281 (100), 179 (57.4), 135 (27.5)	Umbelliferone			✓	✓	[107]
99	30.0	**445**	MS^2 [445]: 314 (14.5), 269 (100), 175 (16.2) MS^3 [445→269]: 225 (49.5), 201 (40.7), 169 (100)	Apigenin-*O*-glucuronide			✓	✓	[87]
100	30.7	**711**	MS^2 [711]: 665 (10.7), 504 (30.2), 503 (100) MS^3 [711→503]: 486 (29.9), 485 (100), 454 (10.7), 453 (32.7) MS^4 [711→503→485]: 441 (100), 421 (16.5), 403 (11.8), 385 (19.2)	Triterpene acid-*O*-hexoside (formate adduct)	✓	✓	✓	✓	
101	31.3	**679**	MS^2 [679]: 517 (100), 499 (31.3), 455 (13.7) MS^3 [679→517]: 499 (100), 481 (13.9), 473 (19.6), 455 (42.2), 441 (31.6), 437 (42.1), 397 (13.4), 379 (17.1) MS^4 [679→517→499]: 481 (14.5), 455 (70.6), 441 (100), 437 (16.0), 425 (15.5), 409 (11.4), 397 (46.3), 393 (11.1), 381 (13.7), 379 (10.9)	Ganoderic acid C2 hexoside	✓	✓	✓	✓	[107]
102	31.5	**459**	MS^2 [459]: 297 (100), 135 (19.6) MS^3 [459→297]: 179 (14.4), 135 (100)	Caffeic acid derivative			✓	✓	
103	31.9	**451**	MS^2 [451]: 341 (100) MS^3 [451→341]: 231 (22.1), 219 (24.4), 217 (100), 189 (18.5), 177 (16.2) MS^4 [451→341→217]: 191 (97.0), 189 (100), 145 (10.9)	Unknown				✓	
104	32.3	**487**	MS^2 [487]: 451 (31.7), 341 (70.6), 323 (61.3), 281 (36.9), 251 (35.3), 179 (100) MS^3 [487→179]: 135 (100)	Caffeic acid-*O*-(coumaroyl)hexoside			✓	✓	
105	32.7	**711**	MS^2 [711]: 665 (14.1), 503 (100) MS^3 [711→503]: 485 (100), 443 (10.8), 441 (11.6) MS^4 [711→503→485]: 441 (38.1), 405 (18.3), 403 (25.3), 393 (100), 387 (58.2), 363 (26.1)	Triterpene acid-*O*-hexoside (formate adduct)		✓		✓	
106	32.8	**493**	MS^2 [493]: 447 (80.1), 179 (48.3), 177 (14.8), 161 (100) MS^3 [493→161]: 133 (49.9), 129 (29.5), 111 (100)	Unknown			✓		
107	33.4	**695**	MS^2 [695]: 487 (100) MS^3 [695→487]: 469 (100), 427 (11.4), 407 (21.3) MS^4 [695→487→469]: 451 (43.9), 437 (28.5), 423 (59.6), 407 (100), 405 (44.2), 371 (21.5)	Unknown			✓	✓	

108	33.4	**839**	MS^2 [839]: 677 (100), 503 (36.5) MS^3 [839→677]: 503 (100) MS^4 [839→677→503]: 485 (100), 453 (30.2), 441 (19.0), 428 (10.8), 409 (25.4), 403 (11.7)	Triterpene acid derivative		✓				
109	33.7	**547**	MS^2 [547]: 281 (32.0), 251 (27.6), 221 (12.6), 179 (59.7), 161 (100) MS^3 [547→179]: 135 (100)	Umbelliferone			✓			[107]
110	34.0	**709**	MS^2 [709]: 501 (100) MS^3 [709→501]: 471 (11.9), 457 (60.5), 455 (14.2), 439 (30.3), 421 (100), 403 (72.8), 387 (11.2), 361 (13.9)	Unknown	✓	✓	✓	✓		
111	34.8	**711**	MS^2 [711]: 665 (12.6), 503 (100), 501 (29.7) MS^3 [711→503]: 485 (100), 453 (18.3), 439 (15.4) MS^4 [711→503→485]: 453 (44.0), 439 (20.1), 421 (57.5), 419 (100), 403 (15.2), 385 (25.3)	Triterpene acid-*O*-hexoside (formate adduct)			✓	✓		
112	35.2	**679**	MS^2 [679]: 519 (11.5), 517 (100) MS^3 [679→517]: 499 (100), 473 (20.0), 455 (10.8) MS^4 [679→517→499]: 455 (52.1), 441 (27.1), 419 (35.3), 403 (100), 379 (36.0)	Ganoderic acid C2 hexoside	✓	✓	✓	✓	[107]	
113	35.7	**517**	MS^2 [517]: 301 (100), 300 (25.8) MS^3 [517→301]: 283 (97.8), 257 (100)	Ellagic acid derivative	✓					
114	35.9	**593**	MS^2 [593]: 447 (11.4), 285 (100) MS^3 [593→285]: 257 (97.8), 255 (23.7), 241 (100), 229 (14.8), 213 (40.2)	Kaempferol-*O*-(coumaroyl)hexoside	✓	✓	✓	✓	[212]	
115	36.2	**301**	MS^2 [301]: 273 (15.0), 235 (10.8), 179 (40.4), 151 (100)	Quercetin	✓	✓				Standard
116	37.3	**695**	MS^2 [695]: 649 (10.4), 487 (100), 485 (12.4) MS^3 [695→487]: 467 (28.5), 425 (55.3), 423 (100), 391 (39.0) MS^3 [695→487]: 469 (100), 427 (33.7), 425 (40.7), 423 (17.0), 373 (16.5)	Unknown	✓	✓	✓	✓		
117	37.5	**711**	MS^2 [711]: 503 (100) MS^3 [711→503]: 485 (100), 459 (13.0), 455 (18.2), 441 (53.2) MS^4 [711→503→485]: 455 (29.5), 440 (100), 423 (12.1)	Triterpene acid-*O*-hexoside (formate adduct)			✓	✓		
118	37.9	**709**	MS^2 [709]: 501 (100) MS^3 [709→501]: 483 (11.3), 471 (100), 453 (32.3) MS^4 [709→501→471]: 453 (100), 428 (11.0), 423 (13.9), 325 (18.6)	Unknown			✓	✓		
119	38.5	**663**	MS^2 [663]: 503 (12.4), 501 (100), 483 (56.9), 439 (15.8) MS^3 [663→501]: 483 (100), 465 (10.2), 457 (22.8), 455 (30.9) MS^4 [663→501→483]: 465 (100), 455 (22.0), 437 (22.6), 391 (87.2), 367 (65.7)	Ganolucidic acid B hexoside	✓	✓	✓	✓	[223]	
120	38.9	**679**	MS^2 [679]: 633 (10.7), 517 (62.4), 499 (22.2), 471 (100) MS^3 [679→517]: 499 (100), 473 (72.6), 455 (15.1) MS^4 [679→517→499]: 455 (89.8), 442 (81.9), 437 (20.5), 425 (13.0), 397 (26.5), 395 (50.2), 393 (85.1), 381 (100)	Ganoderic acid C2 hexoside	✓	✓	✓	✓	[107]	
121	39.9	**163**	MS^2 [163]: 119 (100)	Coumaric acid				✓		Standard
122	40.1	**533**	MS^2 [533]: 485 (100), 471 (15.4) MS^3 [533→485]: 467 (100), 441 (83.8), 425 (22.3), 423 (30.2), 381 (31.2), 310 (14.0) MS^4 [533→485→441]: 423 (100), 379 (49.0)	12-Hydroxyganoderic acid C2			✓	✓		[223]

t_R: retention time; HHDP: Hexahydroxydiphenoyl

Table S 14 - Characterization of anthocyanins of *R. grandifolius* (berries) methanolic extracts by HPLC-ESI$^+$/MS^n (FX: Funchal: MX: Machico).

Nº	t_R (min)	$[M-H]^+$ (*m/z*)	HPLC-DAD-ESI/MS^n *m/z* (% base peak)	Assigned identification	Berries		References
					FX	MX	
2	3.6	**449**	MS^2 [449]: 317 (17,4), 303 (61.9), 287 (100) MS^3 [449→287]: 241 (82.2), 213 (100), 175 (57.6), 161 (87.3), 153 (78.9)	Cyanidin-*O*-hexoside	✓	✓	
10	4.3	**581**	MS^2 [581]: 449 (51.9), 287 (100) MS^3 [581→287]: 241 (82.2), 213 (100), 175 (57.6), 161 (87.3), 153 (78.9), 137 (24.6), 109 (19.2)	Cyanidin-*O*-pentosyl(hexoside)		✓	[214]
12	4.4	**449**	MS^2 [449]: 317 (17.4), 303 (61.9), 287 (100) MS^3 [449→287]: 241 (82.2), 213 (100), 175 (57.6), 161 (87.3), 153 (78.9), 137 (24.6), 109 (19.2)	Cyanidin-3-*O*-glucoside	✓	✓	Standard
13	5.4	**419**	MS^2 [419]: 317 (17.4), 303 (61.9), 287 (100) MS^3 [419→287]: 241 (82.2), 213 (100), 175 (57.6), 161 (87.3), 153 (78.9), 137 (24.6), 109 (19.2)	Cyanidin-*O*-pentoside	✓		[214]
17	6.2	**449**	MS^2 [449]: 317 (17.4), 303 (61.9), 287 (100) MS^3 [449→287]: 241 (82.2), 213 (100), 175 (57.6), 161 (87.3), 153 (78.9), 137 (24.6), 109 (19.2)	Cyanidin-*O*-hexoside	✓	✓	
20	6.6	**419**	MS^2 [419]: 317 (17.4), 303 (61.9), 287 (100) MS^3 [419→287]: 241 (82.2), 213 (100), 175 (57.6), 161 (87.3), 153 (78.9), 137 (24.6), 109 (19.2)	Cyanidin-*O*-pentoside	✓	✓	[214]
23	7.5	**449**	MS^2 [449]: 317 (17.4), 303 (61.9), 287 (100) MS^3 [449→287]: 241 (82.2), 213 (100), 175 (57.6), 161 (87.3), 153 (78.9), 137 (24.6), 109 (19.2)	Cyanidin-*O*-hexoside	✓	✓	
26	8.7	**449**	MS^2 [449]: 317 (17.4), 303 (61.9), 287 (100) MS^3 [449→287]: 241 (82.2), 213 (100), 175 (57.6), 161 (87.3), 153 (78.9), 137 (24.6), 109 (19.2)	Cyanidin-*O*-hexoside	✓		
28	8.9	**535**	MS^2 [535]: 449 (51.3), 287 (100) MS^3 [535→287]: 257 (100), 213 (55.1), 175 (57.6), 161 (87.3), 153 (78.9), 137 (24.6), 109 (19.2)	Cyanidin-*O*-(malonyl)hexoside	✓	✓	[188]
30	9.1	**593**	MS^2 [593]: 287 (100) MS^3 [593→287]: 257 (82.2), 213 (100), 175 (57.6), 161 (87.3), 153 (78.9), 137 (24.6), 109 (19.2)	Cyanidin-*O*-dioxaloylglucoside	✓	✓	[188]
36	10.3	**491**	MS^2 [491]: 449 (31.4), 287 (100) MS^3 [491→287]: 241 (82.2), 213 (100), 175 (57.6), 161 (87.3), 153 (78.9), 137 (24.6), 109 (19.2)	Cyanidin-*O*-(acetyl)hexoside		✓	[153]

t_R: retention time

1.4. Sambucus lanceolata

In total, 77 phytochemicals were tentatively identified in *S. lanceolata*. Following is a brief explanation for the characterization of the compounds reported in **Table S 15** and **Table S 16**. For a more detailed explanation, please check the mentioned references.

1.4.1. Phenolic acids

Compounds **28** and **37** displayed $[M-H]^-$ ions at *m/z* 353. Using the hierarchical key for the identification of CQAs [221], **28** was identified as 3-*O*-CQA and **37** as 5-*O*-CQA (confirmed by analytical standard), respectively. With an extra 98 Da residue, compound **36** was tentatively characterized as a derivative of CQA.

Compound **11** exhibited $[M-H]^-$ ion at m/z 397 and MS^2 base peak at m/z 361 $[M-H-36]^-$. Syringic acid (at m/z 197) [199] was observed at MS^4; so **11** was tentatively identified as a derivative.

Hexosides of ferulic, caffeic and coumaric acids (**17, 21** and **25**, respectively) were detected in leaves [80,84]. Several coumaric acid derivatives (compounds **50**, **66**, **69**, **70**, **73**, **75** and **78**) were tentatively identified based on typical 163→119 transition. Compounds **68** and **79** were tentatively characterized as derivatives of caffeic and ferulic acids, respectively. It was not possible to achieve a full characterization for the previous compounds. Compound **24**, with $[M-H]^-$ ion at m/z 433, yielded sinapic acid-*O*-hexoside at m/z 385 $[M-H-48]^-$ [197]; it was tentatively characterized as a derivative. 5-*O*-Feruloylquinic acid (compound **42**) was identified according to the hierarchical scheme for CQAs identification [221].

1.4.2. Flavonols

Several conjugates of quercetin, isorhamnetin and kaempferol were identified in *S. lanceolata* extracts based on previous reports (**Table S 15**). Compounds **74** and **80** displayed $[M-H]^-$ ions at m/z 615. After loss of 168 Da it showed product ion at m/z 447, consistent with isorhamnetin-*O*-pentoside [212]. They were tentatively characterized as derivatives. Compound **43** displayed $[M-H]^-$ ion at m/z 679. It suffered a direct loss of 344 Da to produce fragment ion at m/z 335. Myricetin aglycone was observed at m/z 317 after loss of 36 Da (probably two molecules of water); it was tentatively identified as a derivative.

1.4.3. Flavones

Compound **20** was characterized as a luteolin derivative**.** It showed an $[M-H]^-$ ion at m/z 597 and produce luteolin aglycone at m/z 285 (confirmed by reference compound) after direct loss of 312 Da.

1.4.4. Flavan-3-ols

Procyanidin dimer (B-type) (compound **23)** was characterized based on bibliographic data [224], whereas the identification of catechin (compound **29**) was confirmed by an analytical standard.

1.4.5. Flavanones

Compound **49** exhibited $[M-H]^-$ ion at m/z 567 and was identified as a derivative of dimethoxylflavanone [225].

1.4.6. Ellagic acid derivatives/Ellagitannins

Compound **44** was identified as tetramethylellagic acid-*O*-hexoside [210]. Compound **51**, with $[M-H]^-$ ion at m/z 595, showed ellagic acid at m/z 301 $[M-H-294]^-$. Hence, it was characterized as ellagic acid-*O*-(pentosyl)hexoside. With extra 32 Da residues, compounds **26** and **34** were tentatively characterized as derivatives. Compound **81** showed an $[M-H]^-$ ion at m/z 645. Ellagic acid aglycone was observed at MS^3, after a direct loss of 344 Da. With no more available data, **81** was identified as a derivative of ellagic acid.

1.4.7. Other compounds

The fragmentation of compound **10** matched that of hydrxytyrosol-*O*-hexoside [200].

Other non-phenolic compounds were characterized in *S. lanceolata* extracts, namely saccharides, organic acids, anthraquinone, lignans and fatty acids. Oligosaccharides (compounds **1**, **2**, **32**, **40**, **53**, **57**, **58** and **67**) were characterized based on their fragmentation data.

Compound **9**, with $[M-H]^-$ ion at m/z 371, suffered a loss of 180 Da (probably 162 + 18 Da) to produce quinic acid; it was characterized as a derivative. Compounds **13**, **16** and **18** exhibited $[M-H]^-$ ions at m/z 515 and their fragmentation pattern was consistent to 3,5-di-*O*-CQA [221]. However, this class of compounds tend to elute in a latter retention time (by comparison with analytical standards). The successive losses of 162 Da were assigned to hexosides instead of caffeoyl residues. Thus, **13**, **16** and **18** were tentatively characterized as quinic acid-*O*-dihexoside.

Compound **11**, with $[M-H]^-$ ion at m/z 617, suffered losses of 36 Da to yield MS^2 base peak at m/z 581. This product ion was further fragment and showed emodin aglycone at m/z 269 [226] after loss of 312 Da. Hence, **11** was tentatively identified as a derivative.

Compound **19** showed an $[M-H+HCOO]^-$ ion at m/z 463. Syringaresinol aglycone at was observed m/z 417 [199] after loss of 46 Da.

Compounds **31** and **33** were characterized as formate adducts of dihydroxy-roseoside and roseoside (drovomifoliol-*O*-glucoside) considering previous information [106,209]. Compound **72** displayed $[M-H]^-$ ion at m/z 561 and MS^2 base peak at m/z 357 $[M-H-204]^-$. Fragmentation of this ion was consistent with pinoresinol [227]; so **69** was tentatively characterized as pinoresinol-*O*-(acetyl)hexoside.

The characterization of oxo-dihydroxy-octadecenoic and trihydroxy-octadecenoic acids (compounds **85** and **86**) has been previously explained [106].

1.4.8. Anthocyanins

Three anthocyanins (compounds **6**, **8** and **12**) were identified in *S. lanceolata* extracts (**Table S 16**) in positive mode, all cyanidin glycosides. These compounds have been previously described in elderberry (*S. nigra*) [24,151].

Table S 15 - Characterization of phytochemicals of *S. lanceolata* (berries and leaves) methanolic extracts by HPLC-ESI$^-$/MS^n.

Nº	t_R (min)	[M-H]$^-$ (*m/z*)	HPLC-DAD-ESI/MS^n *m/z* (% base peak)	Assigned identity	Berries	Leaves	References
1	3.0	**473**	MS^2 [473]: 341 (100) MS^3 [473→341]: 179 (100), 161 (23.0), 143 (33.1), 131 (10.3), 119 (16.9), 113 (45.2)	Oligosaccharide (Pentose + dihexose)	✓		[125]
2	3.2	**683**	MS^2 [683]: 341 (100) MS^3 [683→341]: 179 (100), 161 (23.0), 143 (33.1), 119 (16.9), 113 (45.2)	Hexose polymer		✓	[207]
3	3.3	**533**	MS^2 [533]: 191 (100) MS^3 [533→191]: 173 (100), 153 (18.0), 127 (91.3), 109 (36.1), 93 (55.0), 85 (99.5)	Quinic acid derivative		✓	[106]
4	3.5	**353**	MS^2 [353]: 173 (100), 111 (76.2) MS^3 [353→173]: 111 (100)	Caffeoylisocitrate	✓		[215]
5	3.7	**191**	MS^2 [191]: 173 (100), 111 (38.3) MS^3 [191→173]: 111 (100)	Citric acid	✓		[198]
7	3.8	**133**	MS^2 [133]: 115 (100) MS^3 [133→115]: 71 (100)	Malic acid		✓	[198]
9	4.7	**371**	MS^2 [371]: 353 (45.8), 341 (18.6), 191 (100), 173 (19.3) MS^3 [371→191]: 173 (50.3), 127 (68.5), 111 (45.1), 109 (54.8), 93 (84.1), 85 (100)	Quinic acid derivative		✓	
10	4.9	**315**	MS^2 [315]: 153 (100), 135 (14.7), 123 (21.6) MS^3 [315→153]: 123 (100)	Hydroxytyrosol-*O*-hexoside	✓	✓	[200]
11	5.2	**397**	MS^2 [397]: 559 (81.8), 361 (100), 359 (89.8), 234 (32.8), 198 (82.8), 197 (25.9) MS^3 [397→361]: 197 (100), 168 (11.0), 139 (47.7) MS^4 [397→361→197]: 182 (100), 167 (16.4), 123 (12.8)	Syringic acid derivative		✓	
13	5.5	**707** [2M-H]$^-$	MS^2 [707]: 674 (66.2), 671 (25.0), 533 (47.8), 515 (35.1), 413 (41.6), 353 (100), 324 (15.3), 321 (10.4), 269 (60.1), 205 (37.0) MS^3 [707→353]: 191 (100), 173 (20.5)	Quinic acid-*O*-dihexoside dimer	✓	✓	
14	5.8	**617**	MS^2 [617]: 581 (100) MS^3 [617→581]: 269 (100) MS^4 [617→581→269]: 241 (94.7), 225 (67.5), 214 (16.2), 201 (25.6), 169 (22.7), 155 (15.7)	Emodin derivative	✓		
15	5.9	**401**	MS^2 [401]: 239 (100). 179 (25.4) MS^3 [401→239]: 179 (100) MS^4 [401→239→179]: 164 (100), 137 (67.6)	Unknown	✓		
16	6.5	**707** [2M-H]$^-$	MS^2 [707]: 515 (100) MS^3 [707→515]: 323 (100), 191 (82.0), 173 (55.3)	Quinic acid-*O*-dihexoside dimer		✓	
17	6.7	**355**	MS^2 [355]: 193 (100) MS^3 [355→193]: 178 (39.2), 149 (100), 134 (20.0)	Ferulic acid-*O*-hexoside		✓	[80]

18	6.9	**707** $[2M-H]^-$	MS^2 [707]: 533 (100), 515 (32.3), 353 (48.3), 341 (26.8), 323 (18.8), 271 (22.7), 242 (18.0) MS^3 [707→353]: 191 (100), 135 (29.3)	Quinic acid-*O*-dihexoside dimer		✓	
19	7.0	**463**	MS^2 [463]: 417 (100), 235 (13.3), 181 (10.8) MS^3 [463→417]: 235 (41.0), 181 (100), 166 (41.2), 161 (24.4) MS^4 [463→417→181]: 166 (100)	Syringaresinol (formate adduct)	✓		
20	7.2	**597**	MS^2 [597]: 487 (14.9), 285 (100), 241 (14.9) MS^3 [597→285]: 243 (28.4), 241 (100), 217 (27.2), 215 (16.5), 199 (15.6), 149 (38.6)	Luteolin derivative	✓		
21	7.6	**341**	MS^2 [341]: 251 (20.5), 233 (27.2), 203 (19.0), 179 (100), 161 (27.3), 135 (19.6) MS^3 [341→179]: 135 (100)	Caffeic acid-*O*-hexoside		✓	[84]
22	7.7	**391**	MS^2 [391]: 373 (15.0), 283 (14.1), 217 (100), 199 (10.1), 173 (10.8), 111 (42.0) MS^3 [391→217]: 111 (100)	Citric acid derivative	✓		[198]
23	7.8	**577** $[2M-H]^-$	MS^2 [577]: 451 (18.4), 425 (96.8), 407 (100), 351 (11.8), 289 (23.2) MS^3 [577→425]: 407 (100), 339 (16.4) MS^4 [577→425→407]: 390 (17.1), 321 (16.9), 283 (100), 271 (17.6), 255 (25.6)	Procyanidin dimer (B type)	✓		[224]
24	7.8	**433**	MS^2 [433]: 403 (96.5), 385 (100), 340 (44.0), 271 (37.0), 223 (49.7), 199 (16.6), 179 (74.6), 164 (25.8) MS^3 [433→385]: 223 (100), 179 (35.7)	Sinapic acid-*O*-hexoside derivative		✓	
25	7.9	**325**	MS^2 [325]: 163 (100), 119 (18.4) MS^3 [325→163]: 119 (100)	Coumaric acid-*O*-hexoside		✓	[84]
26	7.9	**627**	MS^2 [627]: 595 (100) MS^3 [627→595]: 433 (10.5), 343 (13.5), 301 (100), 283 (12.8), 257 (58.6) MS^4 [627→595→301]: 257 (100)	Ellagic acid-*O*-(pentosyl)hexoside derivative	✓		
27	8.3	**707** $[2M-H]^-$	MS^2 [707]: 353 (100) MS^3 [707→353]: 191 (100) MS^4 [707→353→191]: 173 (12.7), 127 (67.7), 109 (19.9), 93 (100), 85 (11.5)	3-*O*-Caffeoylquinic acid dimer	✓	✓	
28	8.4	**353**	MS^2 [353]: 485 (57.5), 297 (39.2), 289 (35.0), 271 (70.7), 241 (13.6), 191 (100),179 (48.0) MS^3 [353→191]: 173 (63.1), 127 (100), 111 (47.1), 109 (42.7), 93 (48.5), 85 (50.9)	3-*O*-Caffeoylquinic acid	✓	✓	[221]
29	8.6	**289**	MS^2 [289]: 271 (13.4), 245 (100), 231 (15.4), 205 (31.1), 179 (18.7), 167 (15.2), 151 (16.3) MS^3 [289→245]: 203 (100), 188 (13.0)	Catechin	✓		Standard
30	8.7	**341**	MS^2 [341]: 251 (20.5), 233 (27.2), 203 (19.0), 179 (100), 161 (27.3), 135 (19.6) MS^3 [341→179]: 135 (100)	Caffeic acid-*O*-hexoside	✓		[84]
31	8.9	**433**	MS^2 [433]: 387 (100), 179 (25.4), 161 (22.2), 143 (10.1) MS^3 [433→387]: 207 (100), 189 (12.8), 179 (56.0), 161 (49.7), 159 (25.8), 131 (16.5)	Dihydroxy-roseoside (formate adduct)		✓	[209]
32	9.4	**427**	MS^2 [427]: 381 (100) MS^3 [427→381]: 249 (100), 161 (25.2) MS^4 [427→381→249]: 161 (100), 113 (19.3), 101 (18.7), 97 (12.5), 85 (24.3)	Saccharide	✓		
33	9.5	**431**	MS^2 [431]: 385 (100). 223 (12.2) MS^3 [431→385]: 223 (33.1), 205 (40.5), 161 (13.3), 153 (100)	Roseoside (formate adduct)		✓	[106]
34	9.9	**627**	MS^2 [627]: 595 (100) MS^3 [627→595]: 433 (10.5), 343 (13.5), 301 (100), 283 (12.8), 257 (58.6) MS^4 [627→595→301]: 257 (100)	Ellagic acid-*O*-(pentosyl)hexoside derivative	✓		
35	10.0	**435**	MS^2 [435]: 389 (33.9), 227 (100) MS^3 [435→227]: 101 (100)	Unknown		✓	

36	10.1	**451**	MS^2 [451]: 353 (57.6), 191 (100) MS^3 [451→353]: 191 (100), 135 (12.7)	Caffeoylquinic acid derivative	✓		
37	10.4	**353**	MS^2 [353]: 191 (100) MS^3 [353→191]: 339 (10.1), 173 (36.6), 127 (100), 111 (47.0), 93 (42.1), 85 (69.5)	5-*O*-Caffeoylquinic acid		✓	Standard
38	10.6	**537**	MS^2 [537]: 491 (100), 179 (19.9) MS^3 [537→491]: 476 (14.9), 357 (78.0), 329 (100), 314 (11.1), 301 (36.7), 297 (27.0), 255 (22.2), 181 (88.8), 150 (13.8) MS^4 [537→491→329]: 314 (100), 283 (68.0), 264 (29.5), 183 (32.3), 164 (17.8)	Tricin-O-hexoside (formate adduct)	✓		
39	11.2	**435**	MS^2 [435]: 390 (27.4), 389 (100) MS^3 [435→389]: 436 (51.6), 321 (23.4), 311 (27.9), 161 (43.8), 159 (100), 147 (31.4), 143 (11.3), 113 (58.1)	Unknown		✓	
40	11.5	**539**	MS^2 [539]: 491 (10.3), 179 (100), 161 (11.1) MS^3 [539→179]: 161 (43.1), 131 (34.5), 119 (48.5), 113 (24.2), 101 (50), 89 (100)	Saccharide	✓		
41	12.8	**755**	MS^2 [755]: 609 (34.4), 591 (66.6), 489 (23.9), 343 (14.0), 301 (100), 271 (25.3) MS^3 [755→301]: 271 (100), 255 (56.5), 179 (19.3), 151 (19.2)	Quercetin-*O*-(rhamnosyl)rutinoside	✓	✓	[198]
42	13.1	**367**	MS^2 [367]: 191 (100), 173 (15.8) MS^3 [367→191]: 127 (100), 111 (30.1), 93 (20.6), 85 (38.4)	5-*O*-Feruloylquinic acid	✓	✓	[221]
43	13.7	**679**	MS^2 [679]: 649 (10.4), 647 (19.8), 619 (16.2), 575 (23.2), 335 (100), 275 (11.2), 273 (30.4) MS^3 [679→335]: 317 (100), 299 (14.3), 273 (64.7), 245 (11.8), 229 (21.6) MS^4 [679→335→317]: 273 (100), 229 (58.2), 213 (63.1), 186 (40.9), 151 (20.4)	Myricetin derivative	✓		
44	14.0	**521**	MS^2 [521]: 359 (100), 344 (11.0) MS^3 [521→359]: 344 (100), 313 (16.6) MS^4 [521→359→344]: 329 (22.2), 313 (100), 265 (29.6), 255 (13.7), 219 (12.7), 203 (25.2), 189 (18.3), 159 (54.9)	Tetramethyl-ellagic acid-*O*-hexoside	✓		[210]
45	14.3	**611**	MS^2 [611]: 431 (100), 251 (83.9), 207 (19.7) MS^3 [611→431]: 269 (16.6), 251 (100), 207 (24.2), 189 (12.7) MS^4 [611→431→251]: 208 (49.3), 189 (100)	Unknown		✓	
46	14.6	**595**	MS^2[595]: 548 (11.7), 511 (11.9), 475 (14.7), 463 (35.6), 445 (26.9), 301 (34.5), 300 (100), 295 (13.9), 271 (49.2), 255 (15.1), 227 (19.0) MS^3 [595→301]: 271 (48.8), 255 (23.9), 179 (100), 151 (51.0)	Quercetin-*O*-(pentosyl)hexoside	✓		[84]
47	15.1	**739**	MS^2 [739]: 593 (15.3), 575 (100), 327 (12.7), 284 (45.6), 255 (11.5) MS^3 [739→575]: 547 (11.2), 429 (53.6), 393 (73.8), 369 (26.8), 339 (100), 327 (30.5), 323 (20.3), 309 (49.3), 297 (22.9), 285 (22.2), 283 (17.5), 227 (25.5), 192 (10.2)	Unknown		✓	
48	15.4	**595**	MS^2[595]: 548 (11.7), 511 (11.9), 475 (14.7), 463 (35.6), 445 (26.9), 301 (34.5), 300 (100), 295 (13.9), 271 (49.2), 255 (15.1), 227 (19.0) MS^3 [595→301]: 271 (48.8), 255 (23.9), 179 (100), 151 (51.0)	Quercetin-*O*-(pentosyl)hexoside	✓		[84]
49	15.8	**567**	MS^2 [567]: 535 (13.9), 521 (15.8), 447 (14.8), 341 (100), 330 (11.9), 329 (86.0) MS^3 [567→341]: 325 (40.5), 324 (29.4), 312 (10.5) MS^4 [567→341→325]: 311 (100), 309 (10.8), 145 (15.5)	Dimethoxylflavanone derivative	✓	✓	[225]
50	16.1	**323**	MS^2 [323]: 305 (64.0), 203 (41.0), 163 (100), 145 (57.5), 119 (22.5) MS^3 [323→163]: 119 (100)	Coumaric acid derivative	✓		
51	16.3	**595**	MS^2 [595]: 475 (10.7), 343 (30.2), 301 (100), 283 (24.7), 255 (13.9) MS^3 [595→301]: 258 (16.9), 257 (100), 255 (35.6)	Ellagic acid-*O*-(pentosyl)hexoside	✓		
52	16.8	**609**	MS^2 [609]: 301 (100), 300 (19.2) MS^3 [609→301]: 271 (34.7), 255 (26.2), 229 (27.4), 179 (85.0), 151 (100)	Quercetin-*O*-rutinoside (Rutin)	✓	✓	[200]
53	17.9	**521**	MS^2 [521]: 341 (35.1), 271 (14.3), 179 (100)	Saccharide	✓		

			MS^3 [521→179]: 88 (100)				
54	18.5	**463**	MS^2 [463]: 316 (100) MS^3 [463→316]: 287 (22.8), 272 (21.9), 271 (100), 242 (11.8), 179 (43.3), 163 (11.6), 151 (48.6)	Myricetin-*O*-deoxyhexoside		✓	Standard
55	18.6	**405**	MS^2 [405]: 226 (13.0), 225 (100), 181 (16.5) MS^3 [405→225]: 182 (10.1), 181 (100) MS^4[405→225→181]: 163 (100)	Unknown	✓		
56	19.0	**463**	MS^2 [463]: 301 (100), 300 (18.0) MS^3 [463→301]: 271 (12.8), 257 (62.3), 255 (25.1), 213 (13.5), 193 (22.8), 179 (92.8), 151 (100)	Quercetin-*O*-hexoside	✓		[84]
57	19.7	**415**	MS^2 [415]: 370 (23.1), 281 (11.6), 255 (11.5), 179 (100), 162 (10.0), 143 (32.0), 119 (11.2) MS^3 [415→179]: 161 (24.1), 143 (81.2), 131 (77.8), 119 (100), 97 (27.7), 89 (18.1)	Saccharide		✓	
58	21.0	**567**	MS^2 [567]: 521 (100), 179 (78.5) MS^3 [567→179]: 161 (100), 149 (11.7), 113 (33.5)	Saccharide	✓		
59	22.8	**663**	MS^2[663]: 647 (35.2), 633 (48.4), 615 (27.2), 605 (100), 587 (28.3), 573 (30.7), 508 (16.3) MS^3 [663→587]: 570 (30.2), 569 (100), 558 (27.0), 551 (11.0), 5111 (25.7), 446 (23.3), 415 (23.2), 281 (31.3)	Unknown	✓	✓	
60	23.7	**623**	MS^2 [623]: 315 (100), 300 (20.9), 271 (18.4), 255 (10.9) MS^3 [623→315]: 301 (18.3), 300 (100)	Isorhamnetin-*O*-rutinoside	✓		[224]
61	24.0	**593**	MS^2 [593]: 285 (100) MS^3 [593→285]: 267 (75.3), 257 (100), 255 (31.0), 241 (47.8), 229 (65.4), 213 (52.0), 199 (23.0), 197 (38.4), 195 (17.6), 174 (14.3), 169 (15.9), 163 (38.8)	Kaempferol-*O*-rutinoside	✓	✓	[224]
62	25.8	**505**	MS^2 [505]: 463 (14.4), 301 (100), 300 (38.0), 271 (18.3), 151 (16.5) MS^3 [505→301]: 271 (22.5), 255 (70.6), 179 (29.2), 151 (100)	Quercetin-*O*-(acetyl)hexoside	✓		[212]
63	26.0	**549**	MS^2 [549]: 505 (100) MS^3 [549→505]: 463 (100), 301 (88.4), 300 (21.0) MS^4 [549→505→301]: 179 (54.1), 151 (100)	Quercetin-*O*-(malonyl)hexoside	✓		[212]
64	26.3	**447**	MS^2 [447]: 285 (100), 255 (28.2), 221 (25.2), 157 (20.0), 151 (17.2) MS^3 [447→285]: 255 (100), 243 (31.6), 239 (14.0), 187 (20.2)	Kaempferol-*O*-hexoside	✓		[82]
65	27.0	**477**	MS^2 [477]: 406 (20.4), 315 (100), 300 (19.9), 286 (41.9), 271 (33.6), 270 (36.1), 205 (22.5), 176 (28.4), 151 (29.7) MS^3 [477→315]: 300 (14.4), 299 (13.1), 285 (100), 271 (71.2)	Isorhamnetin-*O*-hexoside	✓		[224]
66	27.2	**815**	MS^2 [815]: 507 (100) MS^3 [815→507]: 345 (57.6), 288 (19.2), 287 (19.2), 201 (15.5), 163 (100) MS^4 [815→507→163]: 119 (100)	Coumaric acid derivative		✓	
67	27.7	**447**	MS^2 [447]: 375 (100), 207 (18.3) MS^3 [447→375]: 327 (18.0), 195 (64.9), 191 (20.9), 179 (100), 146 (24.9) MS^4 [447→375→179]: 164 (48.7), 161 (100), 147 (47.5), 146 (32.9), 122 (18.9)	Saccharide	✓		
68	28.4	**523**	MS^2 [523]: 361 (57.9), 303 (100), 217 (10.9), 179 (76.8) MS^3 [523→179]: 135 (100)	Caffeic acid derivative		✓	
69	28.7	**653**	MS^2 [653]: 507 (100) MS^3 [653→507]: 345 (59.3), 287 (44.6), 163 (100) MS^4 [653→507→163]: 119 (100)	Coumaric acid derivative		✓	
70	29.0	**699**	MS^2 [699]: 653 (53.7), 507 (100) MS^3 [699→507]: 345 (66.2), 287 (31.1), 163 (100) MS^4 [699→507→163]: 119 (100)	Coumaric acid derivative		✓	

71	29.3	**663**	MS^2 [663]: 632 (23.4), 631 (64.9), 587 (100), 569 (19.0) MS^3 [663→587]: 569 (100), 557 (11.8), 327 (15.0) MS^4[663→587→569]: 551 (56.4), 509 (45.2), 447 (23.4), 429 (10.6), 327 (100), 309 (35.7), 280 (12.6), 215 (25.4)	Unknown	✓	✓	
72	29.6	**561**	MS^2 [561]: 545 (10.2), 533 (11.1), 358 (43.9), 357 (100) MS^3 [561→357]: 342 (17.5), 151 (34.8), 136 (100)	Pinoresinol-*O*-(acetyl)hexoside	✓		
73	29.9	**551**	MS^2 [551]: 520 (11.5), 507 (22.0), 505 (60.7), 480 (21.3), 449 (16.7), 325 (39.2), 265 (100), 243 (44.4), 235 (25.6), 206 (24.6), 187 (15.3), 163 (53.4) MS^3 [551→265]: 187 (10.5), 163 (100), 119 (80.3)	Coumaric acid derivative		✓	
74	30.5	**615**	MS^2 [615]: 447 (100), 429 (68.3) MS^3 [615→447]: 403 (39.8), 315 (40.4), 271 (65.5), 207 (89.3), 193 (74.9), 189 (36.9), 177 (71.9), 263 (46.0), 161 (100), 153 (73.8), 143 (36.4), 135 (63.6)	Isorhamnetin-*O*-pentoside derivative	✓	✓	
75	31.2	**507**	MS^2 [507]: 345 (99.0), 287 (42.2), 163 (100), 145 (14.7) MS^3 [507→163]: 119 (100)	Coumaric acid derivative		✓	
76	31.5	**433**	MS^2 [433]: 271 (100), 151 (13.5) MS^3 [433→271]: 227 (11.5), 169 (10.6), 151 (100)	Naringenin-*O*-hexoside	✓		[224]
77	31.7	**519**	MS^2 [519]: 315 (100) MS^3 [519→315]: 301 (16.9), 300 (100), 271 (18.6), 255 (14.0) MS^4 [519→315→300]: 271 (100), 255 (78.5)	Isorhamnetin-*O*-(acetyl)hexoside	✓		[224]
78	32.0	**507**	MS^2 [507]: 345 (97.5), 163 (100) MS^3 [507→163]: 119 (100)	Coumaric acid derivative		✓	
79	32.5	**537**	MS^2[537]: 522 (32.7), 519 (20.6), 491 (36.3), 375 (66.2), 362 (12.7), 317 (54.6), 285 (20.6), 202 (34.0), 193 (100) MS^3 [537→193]: 134 (100)	Ferulic acid derivative		✓	
80	33.0	**615**	MS^2 [615]: 447 (100), 429 (80.7), 297 (11.3) MS^3 [615→447]: 315 (47.9), 271 (55.7), 225 (15.4), 179 (12.1), 163 (47.6), 159 (61.9), 152 (75.8)	Isorhamnetin-*O*-pentoside derivative	✓	✓	
81	34.1	**645**	MS^2 [645]: 613 (23.4), 570 (12.4), 569 (15.1), 343 (25.5), 325 (13.3), 301 (100), 258 (22.6), 257 (54.2), 242 (11.0) MS^3 [645→301]: 258 (16.8), 257 (100)	Ellagic acid derivative	✓	✓	
82	36.5	**629**	MS^2 [629]: 598 (35.5), 597 (80.0), 579 (12.2), 554 (31.2), 553 (100), 535 (38.8) MS^3 [629→331]: 313 (100), 182 (65.4), 150 (47.1), 125 (27.9) MS^3 [629→553]: 535 (100), 523 (11.0), 413 (10.2), 293 (23.2) MS^4 [629→553→535]: 517 (40.2), 503 (18.3), 437 (15.0), 413 (18.0), 412 (39.5), 293 (100), 277 (10.3), 215 (26.6)	Unknown		✓	
83	37.1	**301**	MS^2 [301]: 257 (11.6), 229 (22.2), 179 (70.3), 151 (100), 121 (10.3)	Quercetin	✓		Standard
84	37.5	**631**	MS^2 [631]: 599 (100), 581 (18.9), 555 (21.5), 537 (24.6), 508 (31.2) MS^3 [631→599]: 581 (68.9), 555 (20.8), 537 (34.0), 477 (100), 460 (10.3), 459 (26.9) MS^4 [631→599→477]: 462 (48.1), 459 (100), 444 (36.6), 434 (26.0), 403 (30.3), 337 (34.1), 293 (15.1)	Unknown	✓	✓	
85	37.8	**327**	MS^2 [327]: 291 (49.0), 229 (100), 221 (23.7), 211 (49.0), 209 (19.6), 193 (15.0), 171 (76.0), 165 (10.9), 155 (10.4) MS^3 [327→171]: 127 (100), 125 (15.6) MS^4 [327→171→127]: 83 (100)	Oxo-dihydroxy-octadecenoic acid	✓		[106]
86	40.0	**329**	MS^2 [329]: 311 (25.3), 293 (18.7), 229 (100), 211 (74.2), 171 (25.4)	Trihydroxy-octadecenoic acid	✓		[106]

			MS^3 [329→229]: 213 (17.8), 211 (69.1), 209 (21.8), 193 (20.7), 185 (14.1), 183 (14.1), 171 (19.8), 167 (37.9), 125 (100)		
87	40.5	**629**	MS^2 [629]: 597 (88.2), 554 (27.6), 553 (100), 535 (32.4) MS^3 [629→597]: 579 (60.9), 567 (13.5), 555 (13.0), 553 (100), 535 (50.1)	Unknown	✓

t_R: retention time

Table S 16 - Characterization of anthocyanins of *S. lanceolata* (berries) methanolic extracts by HPLC-ESI^+/MS^n.

Nº	***t*$_R$ (min)**	**$[M+H]^+$ (*m/z*)**	**HPLC-DAD-ESI/MS^n *m/z* (% base peak)**	**Assigned identity**	**References**
6	3.7	**581**	MS^2 [581]: 287 (100) MS^3 [581→287]: 257 (34.3), 241 (100), 232 (31.0), 213 (46.6), 200 (36.7), 189 (83.5), 185 (34.5), 171 (11.6), 162 (10.3), 157 (42.9), 149 (16.5), 143 (54.8), 137 (51.3), 128 (54.5), 111 (93.5)	Cyanidin-*O*-sambubioside	[151]
8	4.5	**581**	MS^2 [581]: 287 (100) MS^3 [581→287]: 257 (34.3), 241 (100), 232 (31.0), 213 (46.6), 200 (36.7), 189 (83.5), 185 (34.5), 171 (11.6), 162 (10.3), 157 (42.9), 149 (16.5), 143 (54.8), 137 (51.3), 128 (54.5), 111 (93.5)	Cyanidin-*O*-sambubioside	[151]
12	5.2	**449**	MS^2 [449]: 287 (100) MS^3 [449→287]: 269 (15.2), 259 (29.3), 231 (34.1), 213 (100), 193 (18.9), 169 (25.5), 161 (14.2), 151 (11.4), 143 (15.2), 137 (52.7)	Cyanidin-*O*-hexoside	

t_R: retention time

1.5. Vaccinium cylindraceum

The phytochemical profile of different morphological parts of *V. cylindraceum* are here described for the first time. This species was collected at Ilha das Flores (Azores archipelago) and it was selected to establish a comparison with Madeira Island counterpart. Following is a brief explanation for the characterization of the compounds reported in **Table S 17** and **Table S 18**. For a more detailed explanation, please check the mentioned references.

1.5.1. Phenolic acids

Phenolic acids (hydroxybenzoic and hydroxycinnamic acids) were identified in analysed extracts. Compound **25** exhibited $[M-H]^-$ ion at m/z 315 and was identified as protocatechuic acid-*O*-hexoside [199]. On the same basis, compound **34**, with an extra 36 Da, was tentatively characterized as a derivative.

Derivatives of ferulic and coumaric acids (compounds **75** and **85**, respectively) were identified based on their typical fragments at m/z 163 and 193. Coumaroyl iridoids (compounds **64**, and **67**), with $[M-H]^-$ ions at m/z 535, were identified previously on *V. myrtillus* [84]. The presence of 3-*O*- and 5-*O*-CQAs (compounds **23**, **27**, **40** and **41**) was confirmed by comparison of their MS^n spectra with standards and literature [221]. Other compounds (**13**, **36** and **47**) showed typical fragment ions at m/z 353 and 191, but their full identification was not achieved; being tentatively characterized as CQAs and derivatives. 5-*p*-Coumaroylquinic acids (compounds **54** and **58**) were also identified following literature data [221]. Compound **59** showed $[M-H]^-$ ions at m/z 367 and could be assigned to feruloylquinic acid [221]. However the presence of caffeic acid instead of quinic acid in the MS^n spectra led to the assignment of the compound as methyl-(5-caffeoyl)quinate [228].

1.5.2. Ellagic acid derivatives

Tergallagic acid and methyl-ellagic acid-*O*-pentoside (compounds **16** and **28**, respectively) were plausibly identified [88,213]. Compounds **29**, with $[M-H]^-$ ion at m/z 465, was tentatively characterized as a derivative.

1.5.3. Flavones

Compound **66**, with $[M-H]^-$ ion at m/z 461, showed tricin aglycone at m/z 324 $[M-H-132]^-$ [106]; **66** was identified as tricin-*O*-pentoside. Compounds **50** and **53,** both with $[M-H]^-$ ions at m/z 539, suffered a loss of 48 Da to yield tricin-*O*-hexoside (at m/z 491) [106]. This residue could be attributed to dimethoxy-hydroxy (2 x 15 Da + 18 Da). Thus, **50** and **53** were tentatively identified as dimethoxy-hydroxy-tricin-*O*-hexoside.

1.5.4. Flavan-3-ols

Procyanidin dimers (A- and B-types) and trimers (compounds **31**, **37**, **45**, **52**, **56**, **66** and **73**) were identified previously in *V. mytrillus* [84]. Compound **46,** with $[M-H]^-$ ion at m/z 469, showed catechin at m/z 289 $[M-H-180]^-$ (compound **48**); it was tentatively characterized as a derivative. Compound **98** showed $[M-H]^-$

ion at m/z 613 and its fragmentation pattern was consistent with a bis-dihydroxylphenylpropanoid-substituted catechin [229].

1.5.5. Flavonols

Several quercetin glycosides were identified in analyzed extracts (**Table S 17**). Compound **83**, with $[M-H]^-$ ion at m/z 507, was identified as 6-hydroxy-7,4-dimethoxyquercetin-*O*-hexoside, respectively [230]. By analogy, compounds **91** and **95**, both with $[M-H]^-$ ions at m/z 549, were tentatively characterized as 6-hydroxy-7,4-dimethoxyquercetin-*O*-(acetyl)hexoside. Compound **92** exhibited $[M-H]^-$ ion at m/z 491. After loss of 146 Da, it showed 6-hydroxy-7,4-dimethoxyquercetin core (at m/z 345) [230]. The possibility of a rhamnosyl group $[M-H-146]^-$ was excluded due to its high retention time; being this moiety attributed to a coumaroyl group. Hence, **92** was tentatively characterized as 6-hydroxy-7,4-dimethoxy-quercetin-*O*-coumaroyl. By analogy, compound **100**, with $[M-H]^-$ ion at m/z 585, was tentatively characterized as a derivative of 6-hydroxy-7,4-dimethoxy-quercetin. Different myricetin glycosides (compounds **61** and **69**) were identified based on the nature of its moieties [79,142].

Cinchonain-I (compounds **68**, **77**, **79** and **93**) were identified based on earlier reports on *V. myrtillus* [84].

Five kaempferol glycosides were identified in this analysis (**Table S 17**). Compound **90**, with $[M-H]^-$ ion at m/z 533, showed a loss of 44 Da at MS^2 to yield kaempferol-*O*-(acetyl)hexoside core at m/z 489 (compounds **89** and **97**) [87]. Hence, **90** was tentatively characterized as kaempferol-*O*-(malonyl)hexoside.

1.5.6. Other compounds

Compound **20**, with $[M-H]^-$ ion at m/z 351, displayed hydrxytyrosol-*O*-hexoside core at m/z 315 $[M-H-36]^-$ (compound **22**) [200]. It was tentatively characterized as a derivative.

Additionally, some other non-phenolic compounds were also identified in this analysis, such as organic acids, terpenoids, coumarins, chalcones and saccharides. Based on their fragmentation pattern, compounds **10** and **32** were characterized as saccharides. Citric acid derivatives (compounds **19** and **26**) were identified in analysed extracts, based on their fragmentation products. Compound **51** exhibited $[M-H]^-$ ion at m/z 553 and produced glucaric acid at m/z 209, [198] after losses of different unidentified residues. Thus, **51** was tentatively characterized as a derivative. Compound **72** showed $[M-H]^-$ ion at m/z 579 and produced syringaresinol at m/z 417 $[M-H-162]^-$ [199] during its fragmentation pattern. Hence, **72** was identified as syringaresinol-*O*-hexoside. Compound **55** exhibited $[M-H]^-$ ion at m/z 739 and after loss of different moieties, gave origin to esculin at m/z 339 $[M-H-152-248]^-$ [231]. Hence, 55 was characterized as esculin-*O*-(malonyl)hexoside gallate. Phloretin-*O*-hexoside (compound **87**) was found previously in *V. macrocarpon* [79]. Characterization of triterpene acids (compounds **88** and **96)** was described in a previous sample.

1.5.7. Anthocyanins

The presence of anthocyanins was confirmed by analysis in positive mode (ESI^+) in berries extracts (**Table S 18**). Sixteen glycosylated anthocyanins were characterized based on their aglycones at m/z 303, 317,

287, 331 and 301, which are characteristic of delphinidin, petunidin, cyanidin, malvidin and peonidin, respectively. Compound **39** exhibited $[M-H]^+$ ion at m/z 477. After loss of 146 Da (rhamnosyl unit) it gave origin to delphinidin (at m/z 331) [200]. Hence, it was identified as delphinidin-*O*-rhamnoside.

Table S 17 - Characterization of phytochemicals of *V. cylindraceum* (berries and leaves) methanolic extracts by HPLC-ESI$^-$/MS^n.

Nº	t_R (min)	[M-H]$^-$ (*m/z*)	HPLC-DAD-ESI/MS^n *m/z* (% base peak)	Assigned identity	Berries	Leaves	References
1	3.4	**683**	MS^2 [683]: 342 (14.2), 341 (100) MS^3 [683→341]: 179 (100), 161 (21.8), 143 (21.1), 119 (22.5), 115 (10.89; 113 (41.0), 101 (16.3) MS^4 [683→341→179]: 161 (69.4), 143 (100), 131 (43.0), 119 (60.9), 113 (17.4), 101 (18.6), 89 (66.6), 71 (23.5)	Hexose polymer		✓	[207]
2	3.5	**533**	MS^2 [533]: 191 (100) MS^3 [533→191]: 173 (69.7), 127 (100), 111 (42.1), 109 (25.4), 93 (30.7), 85 (89.5)	Quinic acid derivative		✓	[106]
4	3.6	**191**	MS^2 [191]: 173 (34.4), 127 (100), 111 (18.0), 93 (76.7) MS^3 [191→127]: 85 (100)	Quinic acid	✓	✓	Standard
7	4.3	**353**	MS^2 [353]: 111 (76.1), 173 (100) MS^3 [353→173]: 111 (100)	Caffeoylisocitrate	✓		[215]
9	4.4	**191**	MS^2 [191]: 173 (18.5), 111 (100) MS^3 [191→111]: 67 (100)	Citric acid	✓		[206]
10	4.4	**337**	MS^2 [337]: 277 (100), 225 (20.1), 179 (90.6), 161 (11.3), 143 (12.2), 119 (17.0), 113 (11.6) MS^3 [337→179]: 161 (5.7), 143 (51.9), 131 (13.3), 119 (19.7), 89 (100)	Saccharide		✓	
13	4.8	**369**	MS^2 [369]: 353 (24.0), 341 (17.3), 225 (16.9), 191 (100), 179 (72.6) MS^3 [369→191]: 173 (69.7), 127 (100), 93 (70.1), 85 (70.5)	Caffeoylquinic acid derivative		✓	
16	5.2	**451**	MS^2 [451]: 325 (22.1), 302 (23.3), 301 (100), 257 (12.2), 175 (12.6) MS^3 [451→301]: 283 (34.4), 273 (32.9), 259 (90.2), 258 (47.7), 257 (100), 233 (40.9), 175 (24.7), 157 (16.7), 149 (77.9) MS^4 [451→301→257]: 215 (100), 173 (40.3)	Tergallagic acid	✓		[213]
19	5.4	**205**	MS^2 [205]: 191 (77.2), 111 (100), 173 (34.0) MS^3 [205→111]: 67 (100)	Citric acid derivative		✓	
20	5.5	**351**	MS^2 [351]: 315 (100), 313 (33.5), 153 (22.7) MS^3 [351→315]: 153 (100), 123 (29.4)	Hydroxytyrosol-*O*-hexoside derivative		✓	
22	5.7	**315**	MS^2 [315]: 153 (100) MS^3 [315→153]: 123 (100), 109 (32.2), 107 (13.4)	Hydroxytyrosol-*O*-hexoside	✓	✓	[200]
23	5.9	**707** [2M-H]$^-$	MS^2 [707]: 515 (15.4), 353 (100), 323 (16.6), 321 (12.2) MS^3 [707→353]: 191 (100), 179 (36.2) MS^4 [707→353→191]: 173 (83.9), 127 (38.0), 111 (94.0), 93 (100), 85 (77.1)	3-*O*-Caffeoylquinic acid dimer		✓	[221]
25	6.4	**315**	MS^2 [315]: 108 (14.4), 152 (24.1), 153 (100) MS^3 [315→153]: 109 (100)	Protocatechuic acid-*O*-hexoside	✓	✓	[199]
26	6.6	**391**	MS^2 [391]: 373 (22.6), 216 (25.1), 217 (71.5), 191 (22.2), 111 (100), 173 (42.2)	Citric acid derivative	✓		[198]
27	6.6	**707** [2M-H]$^-$	MS^2 [707]: 515 (23.9), 353 (100), 323 (10.9) MS^3 [707→353]: 191 (100), 179 (50.2) MS^4 [707→353→191]: 173 (100), 93 (23.8), 87 (100)	3-*O*-Caffeoylquinic acid dimer		✓	[221]
28	6.8	**447**	MS^2 [447]: 568 (15.0), 559 (13.0), 341 (10.9), 327 (12.7), 315 (58.8), 314 (100), 313 (15.1), 302 (11.1), 301 (17.9), 300 (18.5), 256 (10.5) MS^3 [447→315]: 300 (85.8), 299 (100), 285 (16.6), 271 (85.5), 255 (41.3), 231 (25.7), 211 (24.1), 199 (28.5)	Methyl-ellagic acid-*O*-pentoside	✓		[88]
29	6.9	**465**	MS^2 [465]: 421 (10.2), 419 (15.1), 315 (100), 313 (62.7), 301 (89.8), 257 (18.1)	Methyl-ellagic acid derivative	✓		

			MS^3 [465→315]: 301 (59.2), 283 (31.6), 257 (100)				
31	7.1	**577** [2M-H]$^-$	MS^2 [577]: 425 (91.2), 407 (100), 289 (25.3), 203 (14.0) MS^3 [577→407]: 389 (98.3), 335 (100), 297 (79.0), 283 (25.0) MS^3 [577→425]: 407 (100), 381 (27.3), 339 (52.7), 299 (16.4), 299 (14.9) MS^4 [577→425→407]: 389 (34.5), 285 (100), 284 (20.5), 281 (24.7), 256 (29.5)	Procyanidin dimer (B type)		✓	[84]
32	7.4	**451**	MS^2 [451]: 405 (100), 289 (24.5) MS^3 [451→405]: 243 (99.7), 179 (100), 161 (73.8), 131 (82.4), 113 (88.2)	Saccharide (formate adduct)		✓	
34	7.7	**613**	MS^2 [613]: 459 (16.2), 406 (15.4), 405 (100), 297 (54.6) MS^3 [613→405]: 297 (12.2), 153 (100), 135 (16.4) MS^4 [613→405→153]: 109 (100)	Protocatechuic acid derivative		✓	
35	8.1	**341**	MS^2 [341]: 179 (100), 135 (43.5) MS^3 [341→179]: 135 (100)	Caffeic acid-*O*-hexoside	✓	✓	[84]
36	8.3	**533**	MS^2 [533]: 515 (10.2), 359 (74.1), 243 (51.2), 191 (100) MS^3 [533→191]: 173 (100), 127 (23.6), 109 (53.7), 93 (42.9)	Caffeoylquinic acid derivative		✓	
37	8.4	**577** [2M-H]$^-$	MS^2 [577]: 559 (12.6), 451 (22.3), 426 (37.9), 425 (100), 407 (95.1), 381 (10.9), 289 (30.8), 243 (10.8) MS^3 [577→407]: 389 (32.1), 374 (14.1), 363 (31.5), 285 (100), 283 (48.4), 257 (38.8), 243 (77.9), 228 (13.3)	Procyanidin dimer (B type)		✓	[84]
38	9.0	**461**	MS^2 [461]: 416 (51.8), 415 (32.0), 341 (33.2), 329 (95.6), 328 (100), 301 (15.1), 299 (14.6), 272 (16.0) MS^3 [461→329]: 315 (12.3), 314 (100), 313 (34.6), 313 (41.7), 299 (13.3), 285 (24.9) MS^4 [461→329→314]: 300 (61.2), 299 (100), 267 (25.3), 226 (33.3)	Tricin-*O*-pentoside	✓		
40	9.1	**707** [2M-H]$^-$	MS^2 [707]: 353 (100) MS^3 [707→353]: 191 (100) MS^4 [707→353→191]: 173 (83.4), 127 (100), 111 (24.1), 93 (47.7), 85 (65.6)	5-*O*-Caffeoylquinic acid dimer	✓	✓	
41	9.4	**353**	MS^2 [353]: 191 (100) MS^3 [353→191]: 173 (24.7), 127 (100), 111 (16.1), 109 (28.7), 93 (46.4), 85 (50.1) MS^4 [353→191→127]: 109 (100), 85 (17.0)	5-*O*-Caffeoylquinic acid	✓	✓	Standard
42	9.7	**433**	MS^2 [433]: 387 (100) MS^3 [433→387]: 205 (100), 153 (95.6), 131 (24.9), 113 (61.1) MS^3 [433→387]: 225 (52.4), 179 (80.9), 161 (28.7), 143 (100), 113 (19.5) MS^4 [433→387→205]: 201 (76.8), 147 (100)	Dihydroxy-roseoside (formate adduct)		✓	[209]
43	10.1	**431**	MS^2 [431]: 385 (100), 161 (20.2), 139 (10.6) MS^3 [431→385]: 337 (28.8), 233 (22.7), 224 (100), 223 (10.3), 205 (18.3), 186 (54.8), 161 (76.0), 153 (85.4)	Roseoside (formate adduct)	✓	✓	[106]
45	10.3	**577** [2M-H]$^-$	MS^2 [577]: 425 (91.2), 407 (100), 289 (25.3), 203 (14.0) MS^3 [577→407]: 389 (98.3), 335 (100), 297 (79.0), 283 (25.0) MS^3 [577→425]: 407 (100), 381 (27.3), 339 (52.7), 299 (16.4), 299 (14.9) MS^4 [577→425→407]: 389 (34.5), 285 (100), 284 (20.5), 281 (24.7), 256 (29.5)	Procyanin dimer (B type)	✓	✓	[84]
46	10.8	**469**	MS^2 [469]: 423 (69.2), 415 (23.7), 315 (34.8), 289 (100), 229 (22.2) MS^3 [469→289]: 245 (77.4), 231 (45.0), 205 (86.6), 203 (100), 179 (25.5), 125 (17.0), 123 (20.0)	Catechin derivative		✓	
47	11.1	**353**	MS^2 [353]: 191 (100) MS^3 [353→191]: 173 (85.0), 171 (56.1), 127 (100), 111 (65.4), 109 (53.2), 93 (52.2), 85 (48.4)	Caffeoylquinic acid	✓	✓	
48	11.6	**289**	MS^2 [289]: 245 (100), 205 (38.2), 203 (18.1), 179 (16.1) MS^3 [289→245]: 227 (100), 203 (88.8), 188 (19.3), 175 (37.7), 159 (20.2)	Catechin	✓	✓	Standard

49	11.7	**335**	MS^2 [335]: 291 (19.1), 179 (74.5), 161 (100), 135 (52.0)	Caffeoylshikimic acid	✓		[84]
50	12.1	**539**	MS^2 [539]: 491 (100) MS^3 [539→491]: 456 (18.2), 357 (100), 166 (45.4) MS^3 [539→491]: 448 (21.5), 358 (15.3), 357 (43.3), 329 (100), 314 (12.7) MS^3 [539→491]: 357 (100), 329 (95.4), 314 (32.9), 297 (13.3) MS^4 [539→491→329]: 314 (100), **299**, 283 (37.5), 265 (21.4), 164 (36.1), 149 (92.9)	Dimethoxy-hydroxytricin-*O*-hexoside	✓	✓	
51	12.2	**553**	MS^2 [553]: 389 (100), 347 (10.8) MS^3 [553→389]: 209 (100), 191 (75.8), 179 (35.5), 165 (97.6), 147 (52.3), 135 (54.7), 119 (46.0), 109 (24.1)	Glucaric acid derivative		✓	
52	12.7	**865** $[3M-H]^-$	MS^2 [865]: 847 (10.9), 739 (40.9), 695 (100), 578 (23.8), 577 (79.2), 575 (33.0), 543 (31.0), 525 (11.8), 451 (49.7), 449 (27.1), 425 (24.1), 408 (10.4), 407 (64.6), 405 (24.6), 289 (12.2), 287 (39.7) MS^3 [865→695]: 676 (24.4), 677 (54.8), 658 (25.3), 568 (17.2), 543 (100), 529 (30.6), 526 (31.7), 525 (97.6), 451 (33.0), 407 (22.3), 405 (14.9), 391 (13.7), 363 (21.5), 289 (13.1), 256 (31.9), 243 (84.5) MS^4 [865→695→525]: 403 (100), 361 (50.0)	Procyanidin trimer (B type)	✓	✓	[84]
53	12.9	**539**	MS^2 [539]: 343 (12.6), 491 (100), 492 (29.8) MS^3 [539→491]: 329 (100.0), 357 (50.0) MS^4 [539→491→329]: 314 (100), 299 (43.2)	Dimethoxy-hydroxytricin-*O*-hexoside	✓	✓	
54	13.0	**337**	MS^2 [337]: 191 (100) MS^3 [337→191]: 173 (27.3), 171 (19.3), 127 (100), 111 (17.2), 109 (39.1), 93 (37.3), 85 (57.7)	5-*p*-Coumaroylquinic acid		✓	[221]
55	13.3	**739**	MS^2 [739]: 629 (10.5), 587 (100), 451 (21.4), 435 (41.1), 339 (23.4), 289 (16.9) MS^3 [739→587]: 569 (69.7), 477 (50.9), 449 (24.5), 417 (33.3), 339 (100), 177 (15.7) MS^4 [739→587→339]: 177 (100)	Esculin-*O*-(malonyl)hexoside gallate		✓	
56	13.8	**577** $[2M-H]^-$	MS^2 [577]: 425 (100), 407 (94.0), 289 (93.3), 287 (20.3), 245 (15.0), 231 (11.3) MS^3 [577→289]: 271 (28.4), 245 (100), 203 (14.7), 179 (26.7), 165 (34.2), 151 (48.4), 125 (70.4)	Procyanidin dimer (B type)		✓	[84]
57	14.6	**575**	MS^2 [575]: 431 (100), 432 (13.7) MS^3 [575→431]: 143 (38.7), 159 (11.5), 161 (79.9), 221 (14.9), 268 (25.9), 269 (100) MS^4 [575→431→269]: 113 (100), 158 (10.0), 161 (34.4)	Unknown	✓		
58	15.0	**337**	MS^2 [337]: 191 (100) MS^3 [337→191]: 173 (85.7), 127 (100), 111 (24.6), 93 (41.7), 85 (63.8)	5-*p*-Coumaroylquinic acid		✓	[221]
59	15.3	**367**	MS^2 [367]: 349 (10.7), 191 (36.5), 179 (36.5), 135 (33.3) MS^3 [367→179]: 135 (100)	Methyl-(5-caffeoyl)quinate	✓	✓	[228]
60	15.5	**391**	MS^2 [391]: 329 (16.6), 289 (41.5), 221 (16.2), 161 (26.7), 143 (35.0), 125 (100) MS^3 [391→289]: 125 (100)	Unknown		✓	
61	16.7	**479**	MS^2 [479]: 318 (17.4), 317 (83.0), 316 (100) MS^3 [479→317]: 288 (30.0), 287 (98.1), 273 (12.0), 272 (34.3), 271 (100), 255 (100), 179 (84.8), 151 (36.2) MS^4 [479→317→271]: 179 (100), 151 (44.5)	Myricetin-*O*-hexoside	✓		[142]
62	17.2	**739**	MS^2 [739]: 629 (16.6), 587 (100), 569 (44.0), 435 (37.1), 339 (32.0) MS^3 [739→587]: 569 (100), 417 (99.0), 339 (75.0), 325 (22.6), 229 (23.6) MS^4 [739→587→339]: 229 (32.8), 178 (17.3), 177 (100), 117 (23.4) MS^4 [739→587→417]: 376 (63.9), 308 (69.0), 281 (100), 255 (10.9), 182 (10.5)	Unknown		✓	
63	18.1	**431**	MS^2 [431]: 369 (12.1), 351 (36.9), 311 (100), 269 (34.0), 143 (32.4), 125 (66.8)	Apigenin-8-*C*-hexoside	✓	✓	[209]

			MS^3 [431→311]: 283 (83.6), 212 (100), 197 (78.6), 183 (71.0), 165 (53.8), 163 (48.6), 119 (94.9)				
64	18.2	**535**	MS^2 [535]: 491 (18.5), 373 (60.7), 329 (90.6), 191 (66.6), 163 (100) MS^3 [535→329]: 311 (12.0), 285 (41.0), 163 (100), 145 (36.9), 119 (38.8) MS^4 [535→329→163]: 119 (100)	Coumaroyl iridoid	✓	✓	[84]
65	19.5	**609**	MS^2 [609]: 301 (100), 300 (30.3) MS^3 [609→301]: 273 (12.0), 272 (16.3), 271 (23.7), 255 (14.2), 193 (10.6), 179 (83.1), 151 (100), 107 (16.3)	Quercetin-*O*-rutinoside (Rutin)		✓	[200]
66	19.6	**577** $[2M-H]^-$	MS^2 [577]: 425 (100), 407 (63.1), 289 (12.8) MS^3 [577→425]: 407 (100), 273 (20.2) MS^4 [577→425→407]: 285 (100), 281 (79.3), 253 (27.9), 237 (41.0), 200 (22.8)	Procyanidin dimer (B type)		✓	[84]
67	19.8	**535**	MS^2 [535]: 491 (13.0), 373 (52.5), 372 (18.4), 371 (73.5), 330 (15.9), 329 (95.0), 311 (28.6), 267 (11.4), 239 (15.9), 191 (100), 166 (13.6), 165 (54.3), 164 (11.5), 163 (92.1) MS^3 [535→329]: 267 (41.7), 165 (86.7), 164 (12.2), 163 (100), 147 (18.2), 145 (13.2), 123 (19.0), 119 (26.1)	Coumaroyl iridoid	✓	✓	[84]
68	20.4	**451**	MS^2 [451]: 341 (100) MS^3 [451→341]: 323 (13.3), 297 (10.5), 217 (100), 177 (15.0) MS^4 [451→341→217]: 191 (100), 189 (90.7)	Cinchonain-Ib		✓	[84]
69	21.6	**463**	MS^2 [463]: 318 (12.2), 317 (100) MS^3 [463→317]: 288 (23.9), 287 (44.6), 272 (98.2), 271 (100), 269 (50.5), 232 (29.3), 179 (96.3), 151 (44.6)	Myricetin-*O*-deoxyhexoside	✓		Standard
70	22.6	**463**	MS^2 [463]: 302 (11.4), 301 (100), 300 (30.1) MS^3 [463→301]: 271 (27.4), 255 (37.0), 179 (96.0), 151 (100)	Quercetin-*O*-hexoside	✓	✓	[84]
71	24.1	**463**	MS^2 [463]: 302 (11.4), 301 (100), 300 (30.1) MS^3 [463→301]: 271 (27.4), 255 (37.0), 179 (96.0), 151 (100)	Quercetin-*O*-hexoside	✓	✓	[84]
72	24.3	**579**	MS^2 [579]: 417 (100) MS^3 [579→417]: 403 (15.1), 372 (10.2), 181 (100), 166 (41.3), 151 (15.6) MS^4 [579→417→181]: 172 (12.3), 166 (100)	Syringaresinol-*O*-hexoside		✓	
73	24.5	**575** $[2M-H]^-$	MS^2 [575]: 449 (100), 424 (21.8), 423 (46.9), 289 (1.,4), 285 (17.4) MS^3 [575→449]: 287 (100)	Procyanidin dimer (A type)	✓		[84]
74	26.1	**433**	MS^2 [433]: 301 (100), 300 (92.7) MS^3 [433→301]: 273 (11.4), 272 (38.0), 271 (100), 256 (15.9), 255 (62.7), 179 (78.7), 151 (95.5) MS^4 [433→301→271]: 245 (32.8), 243 (23.1), 229 (100), 227 (14.7), 211 (24.0), 199 (13.0), 185 (13.0), 163 (18.5), 158 (10.7)	Quercetin-*O*-pentoside		✓	[84]
75	26.1	**417**	MS^2 [417]: 371 (32.5), 331 (12.4), 307 (100), 163 (10.3), 119 (10.5) MS^3 [417→307]: 163 (45.7), 145 (100), 119 (25.3)	Coumaric acid derivative		✓	
76	26.7	**593**	MS^2 [593]: 285 (100) MS^3 [593→285]: 267 (49.6), 257 (100), 241 (52.0), 229 (41.3), 213 (70.2), 197 (57.2), 163 (68.9)	Kaempferol-*O*-rutinoside		✓	[224]
77	26.9	**451**	MS^2 [451]: 341 (100) MS^3 [451→341]: 323 (17.0), 231 (21.2), 218 (15.5), 217 (100), 177 (20.1) MS^4 [451→341→217]: 191 (39.8), 189 (12.5), 189 (100)	Cinchonain Ib		✓	[84]
78	27.3	**433**	MS^2 [433]: 301 (100) MS^3 [433→301]: 271 (100), 255 (58.5), 179 (95.7), 151 (55.0)	Quercetin-*O*-pentoside	✓	✓	[84]
79	27.5	**451**	MS^3 [451→341]: 323 (17.0), 231 (21.2), 218 (15.5), 217 (100), 177 (20.1) MS^4 [451→341→217]: 191 (39.8), 189 (12.5), 189 (100)	Cinchonain-Ib		✓	[84]

80	28.4	**505**	MS^2 [505]: 301 (100) MS^3 [505→301]: 271 (74.7), 179 (54.1), 151 (100)	Quercetin-*O*-(acetyl)hexoside	✓		[224]
81	28.7	**447**	MS^2 [447]: 327 (15.5), 285 (100), 255 (31.1) MS^3 [447→285]: 255 (100), 227 (41.6), 210 (28.7), 184 (53.7), 163 (23.6)	Kaempferol-*O*-hexoside		✓	[200]
82	28.9	**447**	MS^2 [447]: 301 (100), 300 (22.1), 285 (11.1) MS^3 [447→301]: 272 (12.8), 179 (100), 151 (69.6)	Quercetin-*O*-rhamnoside	✓		[84]
83	29.8	**507**	MS^2 [507]: 345 (100), 301 (13.7) MS^3 [507→345]: 331 (12.5), 330 (100), 317 (12.9), 315 (58.2), 301 (97.4), 274 (13.0), 273 (35.4), 259 (15.2), 241 (10.6) MS^3 [507→345→301]: 286 (79.4), 273 (20.6), 270 (33.9), 269 (100), 258 (23.7), 241 (78.8)	6-Hydroxy-7,4-dimethoxyquercetin-*O*-hexoside	✓		[230]
84	29.9	**477**	MS^2 [477]: 357 (19.5), 315 (100), 285 (15.9), 271 (18.2) MS^3 [477→315]: 299 (45.5), 287 (15.1), 286 (36.2), 285 (100), 272 (16.6), 271 (68.6), 257 (14.0), 243 (28.7)	Isorhamnetin-*O*-hexoside	✓		[224]
85	30.0	**467**	MS^2 [467]: 355 (13.1), 265 (100), 235 (23.1), 193 (30.9) MS^3 [467→265]: 221 (13.4), 217 (29.5), 193 (100), 178 (55.5) MS^4 [467→265→193]: 149 (100)	Ferulic acid derivative		✓	
86	30.4	**505**	MS^2 [505]: 445 (67.4), 301 (100), 271 (17.0) MS^3 [505→301]: 271 (74.7), 255 (81.4), 151 (100)	Quercetin-*O*-(acetyl)hexoside	✓	✓	[224]
87	30.9	**435**	MS^2 [435]: 273 (100) MS^3 [435→273]: 167 (100), 123 (35.1)	Phloretin-*O*-hexoside (Phlorizin)		✓	[79]
88	31.5	**711**	MS^2 [711]: 665 (12.3), 504 (27.2), 503 (100) MS^3 [711→503]: 486 (31.5), 485 (100), 454 (11.8), 453 (31.2) MS^4 [711→503→485]: 453 (100); 387 (100)	Triterpene acid-*O*-hexoside (formate adduct)		✓	
89	31.9	**489**	MS^2 [489]: 285 (100) MS^3 [489→285]: 255 (68.4), 257 (100), 229 (40.1), 213 (23.2), 197 (26.0)	Kaempferol-*O*-(acetyl)hexoside		✓	[87]
90	32.4	**533**	MS^2 [533]: 489 (100) MS^3 [533→489]: 285 (100), 267 (18.9), 257 (53.1), 241 (21.6), 229 (34.1), 213 (10.7), 167 (12.3)	Kaempferol-*O*-(malonyl)hexoside		✓	
91	32.7	**549**	MS^2 [549]: 345 (100), 330 (13.5) MS^3 [549→345]: 330 (100), 315 (30.5), 302 (14.4) MS^4 [549→345→330]: 315 (100), 287 (39.3), 271 (14.2)	6-Hydroxy-7,4-dimethoxy-quercetin-*O*-(acetyl)hexoside	✓		
92	32.9	**491**	MS^2 [491]: 345 (100), 323 (12.4) MS^3 [491→345]: 330 (100), 315 (27.7), 301 (28.2), 287 (15.3), 274 (20.3), 273 (38.4), 245 (12.1) MS^4 [491→345→330]: 315 (100), 287 (35.2), 271 (23.9)	6-Hydroxy-7,4-dimethoxy-quercetin-*O*-coumaroyl	✓		
93	32.9	**451**	MS^2 [451]: 341 (100) MS^3 [451→341]: 231 (12.9), 217 (100), 189 (15.8), 177 (12.4) MS^4 [451→341→217]: 191 (100), 190 (10.8), 189 (93.8)	Cinchonain-Ib		✓	[84]
94	32.9	**439**	MS^2 [439]: 424 (72.8), 359 (100), 343 (10.9), 315 (29.4), 300 (16.7), 203 (12.1) MS^3 [439→359]: 345 (47.8), 343 (15.9), 311 (100) MS^4 [439→359→345]: 159 (100)	Unknown	✓		
95	33.0	**549**	MS^2 [549]: 345 (100), 330 (13.5) MS^3 [549→345]: 330 (100), 315 (30.5), 302 (14.4) MS^4 [549→345→330]: 315 (100), 287 (38.8), 271 (14.2)	6-Hydroxy-7,4-dimethoxy-quercetin-*O*-(acety)lhexoside	✓		
96	33.2	**711**	MS^2 [711]: 665 (12.3), 504 (27.2), 503 (100) MS^3 [711→503]: 486 (31.5), 485 (100), 454 (11.8), 453 (31.2)	Triterpene acid-*O*-hexoside (formate adduct)		✓	

			MS^4 [711→503→485]: 453 (28.7), 439 (100), 423 (19.9), 421 (18.7), 419 (54.8), 387 (15.4)			
97	33.4	**489**	MS^2 [489]: 285 (100) MS^3 [489→285]: 255 (68.4), 257 (100), 229 (40.1), 213 (23.2), 197 (26.0)	Kaempferol-*O*-(acetyl)hexoside	✓	[87]
98	34.8	**613**	MS^2 [613]: 503 (100), 461 (11.7), 393 (12.6), 341 (10.2) MS^3 [613→503]: 393 (100), 379 (12.2), 351 (25.8), 341 (96.7), 307 (16.7) MS^4 [613→503→393]: 375 (15.6), 304 (25.8), 285 (47.1), 255 (22.3), 241 (63.5), 239 (100), 229 (69.1), 225 (18.2), 197 (12.1)	bis-Dihydroxylphenylpropanoid-substituted catechin	✓	[229]
99	35.0	**543**	MS^2 [543]: 497 (100) MS^3 [543→497]: 335 (100), 273 (12.3), 161 (41.8) MS^4 [543→497→335]: 333 (40.9), 317 (29.5), 273 (100), 257 (63.4), 237 (40.4), 152 (57.3), 137 (45.5)	Unkown	✓	
100	35.3	**585**	MS^2 [585]: 371 (41.2), 359 (45.4), 357 (71.0), 345 (100) MS^3 [585→345]: 330 (100), 299 (14.2) MS^4 [585→345→330]: 315 (35.6), 297 (100), 256 (37.4), 251 (14.5), 213 (16.4)	6-Hydroxy-7,4-dimethoxy-quercetin-*O*-hexoside derivative	✓	
101	40.3	**517**	MS^2 [517]: 499 (17.0), 487 (26.3), 470 (29.8), 469 (100), 451 (17.1) MS^3 [517→469]: 452 (28.4), 451 (100), 407 (13.3) MS^4 [517→469→451]: 408 (32.9), 407 (27.5), 390 (19.9), 378 (100), 375 (24.5)	Unknown	✓	

t_R: retention time

Table S 18 - Characterization of anthocyanins present on *V. cylindraceum* (berries) methanolic extracts by HPLC-ESI^+/MS^n.

Nº	t_R **(min)**	$[M-H]^+$ **(*m/z*)**	**HPLC-DAD-ESI/MS^n** ***m/z* (% base peak)**	**Assigned identity**	**References**
3	3.5	**597**	MS^2 [597]: 303 (100) MS^3 [597→303]: 257 (59.9), 229 (4100), 201 (26.8), 159 (46.6), 150 (25.7)	Delphinidin-*O*-(pentosyl)hexoside	[214]
5	3.6	**465**	MS^2 [465]: 303 (100) MS^3 [465→303]: 257 (100), 229 (42.2), 201 (26.8), 159 (46.6), 150 (25.7)	Delphinidin-*O*-hexoside	[200]
6	3.8	**435**	MS^2 [435]: 303 (100) MS^3 [435→303]: 257 (100), 229 (42.2), 201 (26.8), 159 (46.6), 150 (25.7)	Delphinidin-*O*-pentoside	[188,214]
8	4.3	**449**	MS^2 [449]: 317 (17.4), 303 (61.9), 287 (100) MS^3 [449→287]: 241 (82.2), 213 (100), 175 (57.6), 161 (87.3), 153 (78.9), 137 (24.6), 109 (19.2)	Cyanidin-*O*-glucoside	Standard
11	4.6	**465**	MS^2 [465]: 303 (100) MS^3 [465→303]: 275 (16.9), 257 (100), 229 (29.4), 201 (25.3), 165 (24.3), 161 (21.8), 151 (10.3)	Delphinidin-*O*-hexoside	[200]
12	4.7	**435**	MS^2 [435]: 303 (100) MS^3 [435→303]: 257 (100), 229 (42.2), 213 (54.2), 201 (26.8), 159 (46.6), 150 (25.7)	Delphinidin-*O*-pentoside	[188,214]
14	4.8	**479**	MS^2 [479]: 317 (100) MS^3 [479→317]: 303 (100), 274 (57.3), 257 (14.4), 245 (24.3), 229 (34.4), 218 (33.1), 203 (27.1), 150 (27.2)	Petunidin-*O*-hexoside	[200]
15	4.9	**449**	MS^2 [449]: 317 (17.4), 303 (61.9), 287 (100) MS^3 [449→287]: 241 (82.2), 213 (100), 175 (57.6), 161 (87.3), 153 (78.9), 137 (24.6), 109 (19.2)	Cyanidin-*O*-hexoside isomer	
17	5.2	**479**	MS^2 [479]: 317 (100) MS^3 [479→317]: 303 (100), 274 (57.3), 257 (14.4), 245 (24.3), 229 (34.4), 218 (33.1), 203 (27.1), 150 (27.2)	Petunidin-*O*-hexoside	[200]

18	5.3	**449**	MS^2 [449]: 317 (100), 303 (47.7) MS^3 [449→317]: 303 (100), 274 (57.3), 257 (14.4), 245 (24.3), 229 (34.4), 218 (33.1), 203 (27.1), 150 (27.2)	Petunidin-*O*-pentoside	[214]
21	5.4	**449**	MS^2 [449]: 303 (100) MS^3 [449→303]: 257 (100), 229 (42.2), 201 (26.8), 159 (46.6), 150 (25.7) MS^4 [449→303→257]: 229 (100), 213 (54.2), 201 (19.9), 147 (21.1), 117 (10.1)	Delphinidin-*O*-rhamnoside	[214]
24	6.2	**463**	MS^2 [463]: 301 (100) MS^3 [463→301]: 287 (100), 268 (0.3), 258 (50.0), 230 (50.4), 213 (36.7), 202 (26.4), 187 (14.4), 177 (11.1), 147 (11.0)	Peonidin-*O*-hexoside	[200]
30	6.9	**493**	MS^2 [493]: 331 (100) MS^3 [493→331]: 315 (53.1), 299 (100), 287 (21.3), 271 (15.9), 242 (13.4), 179 (27.7)	Malvidin-*O*-hexoside	[200]
33	7.4	**463**	MS^2 [463]: 331 (100) MS^3 [463→331]: 315 (53.1), 299 (100), 287 (21.3), 271 (15.9), 242 (13.4), 179 (27.7)	Malvidin-*O*-pentoside	[188,214]
39	9.0	**477**	MS^2 [477]: 331 (100) MS^3 [477→331]: 315 (100), 299 (66.5), 298 (28.1), 287 (50.3), 271 (15.9), 242 (13.4), 179 (27.7)	Malvidin-*O*-rhamnoside	
44	10.2	**463**	MS^2 [463]: 331 (100) MS^3 [463→331]: 315 (100), 299 (66.5), 298 (28.1), 287 (50.3), 271 (15.9), 242 (13.4), 179 (27.7)	Malvidin-*O*-pentoside	[188,214]

t_R: retention time

1.6. Vaccinium padifolium

The phytochemical profiles of different morphological parts of *V. padifolium*, collected in 2013 and 2014, were determined by HPLC-ESI-MS^n. Following is a brief explanation for the characterization of the compounds identified in *V. padifolium* extracts (**Table S 19 and Table S 20**). For a more detailed explanation, please check the mentioned references.

1.6.1. Phenolic acids

Phenolic acids (hydroxybenzoic and hydroxycinnamic acids) were identified in analysed species. Compound **37** exhibited $[M-H]^-$ ion at m/z 447 and protocatechuic acid at m/z 153 $[M-H-294]^-$; it was identified as protocatechuic acid-*O*-(pentosyl)hexoside.

Hexosides of caffeic, ferulic, coumaric and syringic acids were detected (**Table S 19**). Syringic acid conjugates were not detected in *V. cylindraceum* extracts. Several coumaric acid derivatives (compounds **85**, **89**, **97**, **110**, **114**, **115**, **125** and **129**) were tentatively characterized based typical 163→119 transition. Coumaroyl iridoids were also detected in this species (compounds **84**, **88** and **91**). Compound **107**, with $[M-H+HCOO]^-$ ion at m/z 629, yielded MS^2 base peak at m/z 421 $[M-H-208]^-$. Further fragmentation resulted in methyl-syringate core at m/z 211 [232]. The loss of 211 Da at MS^3 is indicative of a dimer of this compound. Hence, **107** was tentatively characterized as di(methyl-syringate)-*O*-hexoside. Compound **104** showed $[M-H]^-$ ion at m/z 469 and was identified as 4-benzoyl-9-*p*-coumaroyl-2,7-anhydro-3-deoxy-2-octulopyranosonic acid [233].

3-*O*- and 5-*O*-CQAs isomers (compounds **30**, **56** – **58**) were also identified in *V. padifolium*. Other compounds (**17**, **44**, **47**, **48**, **50**, **64**, **65**, **79** and **93**) **18**, **20**, **51**, **55**, **61**, **76** and **78**) with typical fragment ions at m/z 353 and 191, were tentatively characterized as CQAs and derivatives. 5-*p*-Coumaroylquinic acids (compounds **71** and **78**) and methyl-(5-caffeoyl)quinate (compounds **76** and **83**) were were characterized previously.

1.6.2. Ellagic acid derivatives/Ellagitannins

Compounds **39**, with $[M-H]^-$ ion at m/z 495, was tentatively characterized as derivative of methyl-ellagic acid. It showed methyl-ellagic acid core at m/z 315 after loss of 180 Da.

1.6.3. Flavones

Tricin-*O*-pentoside, dimethoxy-hydroxy-tricin-*O*-hexoside and tricin-*O*-hexoside (compounds **54**, **68** and **70**, respectively) were previously explained.

1.6.4. Flavan-3-ols

Catechin oligomers (compounds **43**, **63**, **69** and **101**) and other catechin derivatives (compounds **122** and **127**) were previously characterized.

1.6.5. Flavonols

Several quercetin glycosides were identified in analyzed extracts (**Table S19**). Quercetin-*O*-hexoside derivatives (compounds **75, 77** and **120**) exhibited quercetin-*O*-hexoside core (at m/z 463) (compounds **94**, **96** and **99**) after loss of different unidentified moieties.

Compounds **137** displayed $[M-H]^-$ ion at m/z 653 and was identified as of 6,3-dimethoxyquercetin-3-*O*-β-D-6-(*p*-coumaroyl)glucopyranoside [230]. Other conjugates of 6-hydroxy-7,4-dimethoxyquercetin (at m/z 345) (compounds 113, 123, 126 and 128) were previously identified in *V. cylindraceum*. Myricetin glycosides (compounds **81**, **90** and **95**) were identified based on the nature of its moieties [79,142].

Laricitrin-*O*-hexoside (compounds **98**) was identified according to literature [212]. By analogy, compound **112** showed an $[M-H]^-$ ion at m/z 447 and was tentatively characterized as laricitrin-*O*-rhamnoside. These compounds were absent in *V. cylindraceum* extracts.

Cinchonain-I (compounds **92**, **106** and **121**) was also present in this *Vaccinium* species.

Different kaempferol glycosides were detected in this analysis (**Table S 19**) based on previous analysis.

1.6.6. Other compounds

Other non-phenolic compounds (saccharides, organic acids and lignans) were also identified in the methanolic extracts. Compounds **1** and **12** were characterized as saccharides. Compound **14** exhibited $[M-H]^-$ ions at m/z 389 and glucaric acid core at m/z 209 [198] after loss of different unidentified moieties. It was tentatively characterized as derivative.

1.6.7. Anthocyanins

Twenty-eight glycosylated anthocyanins were characterized by HPLC-ESI^+/MS^n in *V. padifolium*, distributed in berries and YLs extracts (**Table S 20**). Different glycosides of delphinidin, petunidin, cyanidin, malvidin and peonidin were present in analysed extracts. Their characterization was explained previously.

Table S 19 - Characterization of phytochemicals of *V. padifolium* (berries and leaves) methanolic extracts by HPLC-ESI$^-$/MS^n.

Nº	t_R (min)	[M-H]$^-$ (*m/z*)	HPLC-DAD-ESI/MS^n *m/z* (% base peak)	Assigned identity	Berries		Young Leaves		Mature Leaves		References
					2013	2014	2013	2014	2013	2014	
1	3.4	**683**	MS^2 [683]: 342 (14.2), 341 (100) MS^3 [683→341]: 179 (100), 161 (21.8), 143 (21.1), 119 (22.5), 115 (10.89; 113 (41.0), 101 (16.3) MS^4 [683→341→179]: 161 (69.4), 143 (100), 131 (43.0), 119 (60.9), 113 (17.4), 101 (18.6), 89 (66.6), 71 (23.5)	Hexose polymer	✓	✓	✓	✓	✓	✓	[207]
2	3.5	**533**	MS^2 [533]: 191 (100) MS^3 [533→191]: 173 (69.7), 127 (100), 111 (42.1), 109 (25.4), 93 (30.7), 85 (89.5)	Quinic acid derivative			✓	✓	✓	✓	[106]
4	3.6	**191**	MS^2 [191]: 173 (34.4), 127 (100), 111 (18.0), 93 (76.7) MS^3 [191→127]: 85 (100)	Quinic acid	✓	✓	✓	✓	✓	✓	Standard
6	3.8	**383** [2M-H]$^-$	MS^2 [383]: 191 (100) MS^3 [383→191]: 127 (100)	Quinic acid dimer	✓						[106]
8	4.1	**133**	MS^2 [133]: 115 (100) MS^3 [133→115]: 71 (48.1)	Malic acid	✓	✓					[206]
11	4.4	**191**	MS^2 [191]: 173 (18.5), 111 (100) MS^3 [191→111]: 67 (100)	Citric acid	✓	✓					[206]
12	4.4	**337**	MS^2 [337]: 277 (100), 225 (20.1), 179 (90.6), 161 (11.3), 143 (12.2), 119 (17.0), 113 (11.6) MS^3 [337→179]: 161 (5.7), 143 (51.9), 131 (13.3), 119 (19.7), 89 (100)	Saccharide			✓		✓	✓	
14	4.5	**389**	MS^2 [389]: 228 (25.9), 227 (18.3), 209 (56.8), 191 (100), 179 (20.4), 147 (78.7), 135 (51.9), 121 (20.9) MS^3 [389→191]: 147 (100)	Glucaric acid derivative	✓						
15	4.6	**405**	MS^2 [405]: 191 (100) MS^3 [405→191]: 111 (100)	Citric acid derivative	✓	✓					[198]
17	4.7	**371**	MS^2 [371]: 353 (35.1), 191 (100), 179 (14.2) MS^3 [371→191]: 173 (29.6), 127 (100), 111 (37.5), 109 (41.1), 93 (38.8), 85 (35.4)	Caffeoylquinic acid derivative			✓	✓	✓	✓	
22	5.0	**481**	MS^2 [481]: 355 (48.3), 301 (100), 239 (10.3), 175 (21.5) MS^3 [481→301]: 283 (100), 273 (47.1), 273 (10.2), 257 (45.8), 233 (65.8), 191 (34.7), 175 (88.4)	HHDP-*O*-hexoside	✓	✓					[201]
24	5.2	**451**	MS^2 [451]: 325 (22.1), 302 (23.3), 301 (100), 257 (12.2), 175 (12.6) MS^3 [451→301]: 283 (34.4), 273 (32.9), 259 (90.2), 258 (47.7), 257 (100), 233 (40.9), 175 (24.7), 157 (16.7), 149 (77.9) MS^4 [451→301→257]: 215 (100), 173 (40.3)	Tergallagic acid	✓	✓					[213]
27	5.4	**359**	MS^2 [359]: 197 (100), 181 (17.6) MS^3 [359→197]: 181 (100), 153 (33.3) MS^4 [359→197→181]: 166 (86.0), 153 (100)	Syringic acid-*O*-hexoside			✓		✓		[84]
28	5.5	**351**	MS^2 [351]: 315 (100), 313 (33.5), 153 (22.7)	Hydroxytyrosol-*O*-hexoside derivative			✓	✓	✓	✓	

			MS^3 [351→315]: 153 (100), 123 (29.4)								
29	5.7	**315**	MS^2 [315]: 153 (100) MS^3 [315→153]: 123 (100), 109 (32.2), 107 (13.4)	Hydroxytyrosol-*O*-hexoside			✓	✓	✓	✓	
30	5.9	**707** $[2M-H]^-$	MS^2 [707]: 515 (15.4), 353 (100), 323 (16.6), 321 (12.2) MS^3 [707→353]: 191 (100), 179 (36.2) MS^4 [707→353→191]: 173 (83.9), 127 (38.0), 111 (94.0), 93 (100), 85 (77.1)	3-*O*-Caffeoylquinic acid dimer			✓	✓	✓		[221]
33	6.1	**359**	MS^2 [359]: 197 (100), 182 (17.6) MS^3 [359→197]: 182 (100), 153 (13.3) MS^4 [359→197→182]: 167 (86.0), 153 (89.0), 123 (100)	Syringic acid-*O*-hexoside			✓		✓		[84]
35	6.3	**495**	MS^2 [495]: 369 (15.6), 316 (20.5), 315 (100), 271 (15.4) MS^3 [495→315]: 301 (44.6), 300 (100), 283 (34.4), 271 (67.2), 256 (45.2), 233 (16.0), 229 (38.7), 149 (17.8)	Methyl-ellagic acid derivative	✓	✓					
37	6.7	**447**	MS^2 [447]: 429 (17.4), 315 (100), 271 (26.8), 177 (63.9), 163 (24.2), 153 (32.2), 149 (22.6) MS^3 [447→315]: 153 (100), 109 (46.0)	Protocatechuic acid-*O*-(pentosyl)hexoside			✓	✓	✓	✓	
38	6.7	**515**	MS^2 [515]: 455 (38.8), 447 (11.6), 395 (27.2), 353 (100), 323 (47.0), 191 (56.4) MS^3 [515→353]: 191 (100) MS^4 [515→353→191]: 173 (47.2), 127 (100)	Quinic acid-*O*-dihexoside	✓						
40	6.8	**447**	MS^2 [447]: 568 (15.0), 559 (13.0), 341 (10.9), 327 (12.7), 315 (58.8), 314 (100), 313 (15.1), 302 (11.1), 301 (17.9), 300 (18.5), 256 (10.5) MS^3 [447→315]: 300 (85.8), 299 (100), 285 (16.6), 271 (85.5), 255 (41.3), 231 (25.7), 211 (24.1), 199 (28.5)	Methyl-ellagic acid-*O*-pentoside	✓	✓					[88]
41	6.9	**465**	MS^2 [465]: 421 (10.2), 419 (15.1), 315 (100), 313 (62.7), 301 (89.8), 257 (18.1) MS^3 [465→315]: 301 (59.2), 283 (31.6), 257 (100)	Methyl-ellagic acid derivative	✓	✓					
43	7.1	**577** $[2M-H]^-$	MS^2 [577]: 425 (91.2), 407 (100), 289 (25.3), 203 (14.0) MS^3 [577→407]: 389 (98.3), 335 (100), 297 (79.0), 283 (25.0) MS^3 [577→425]: 407 (100), 381 (27.3), 339 (52.7), 299 (16.4), 299 (14.9) MS^4 [577→425→407]: 389 (34.5), 285 (100), 284 (20.5), 281 (24.7), 256 (29.5)	Procyanidin dimer (B type)			✓	✓			[84]
44	7.3	**707**	MS^2 [707]: 533 (100), 515 (74.4), 463 (63.3), 353 (38.9), 323 (78.8), 321 (12.6) MS^3 [707→463]: 289 (80.4), 271 (17.9), 191 (100), 173 (19.4), 127 (33.4)	Caffeoylquinic acid derivative	✓	✓	✓	✓	✓	✓	
47	7.7	**527**	MS^2 [527]: 353 (34.6), 191 (100), 179 (17.6) MS^3 [527→353]: 191 (100), 135 (25.1), 127 (15.4)	Caffeoylquinic acid derivative				✓		✓	
48	8.1	**533**	MS^2 [533]: 515 (10.2), 353 (74.1), 243 (51.2), 191 (100) MS^3 [533→191]: 173 (55.0), 127 (79.2), 111 (36.7), 93 (100)	Caffeoylquinic acid derivative			✓	✓	✓	✓	
49	8.3	**341**	MS^2 [341]: 179 (100), 135 (43.5) MS^3 [341→179]: 135 (100)	Caffeic acid-*O*-hexoside	✓	✓	✓	✓	✓	✓	[84]
50	8.5	**385**	MS^2 [385]: 354 (17.9), 353 (89.0), 191 (100)	Caffeoylquinic acid derivative			✓	✓	✓	✓	

			MS^3 [385→191]: 173 (100), 111 (38.5), 109 (16.3), 93 (72.6), 85 (38.5)									
51	8.5	**325**	MS^2 [325]: 163 (100) MS^3 [325→163]: 119 (100)	Coumaric acid-*O*-hexoside			✓	✓		✓	✓	[84]
53	8.9	**463**	MS^2 [463]: 417 (100), 364 (13.2), 181 (12.7) MS^3 [463→417]: 255 (17.4), 181 (100), 166 (25.5) MS^4 [463→417→181]: 166 (100)	Syringaresinol (Formate adduct)						✓	✓	
54	9.0	**461**	MS^2 [461]: 416 (51.8), 415 (32.0), 341 (33.2), 329 (95.6), 328 (100), 301 (15.1), 299 (14.6), 272 (16.0) MS^3 [461→329]: 315 (12.3), 314 (100), 313 (34.6), 313 (41.7), 299 (13.3), 285 (24.9) MS^4 [461→329→314]: 300 (61.2), 299 (100), 267 (25.3), 226 (33.3)	Tricin-*O*-pentoside	✓	✓						
56	9.2	**353**	MS^2 [353]: 191 (100) MS^3 [353→191]: 173 (24.7), 127 (100), 111 (16.1), 109 (28.7), 93 (46.4), 85 (50.1) MS^4 [353→191→127]: 109 (100), 85 (17.0)	5-*O*-Caffeoylquinic acid	✓	✓	✓	✓		✓	✓	Standard
57	9.6	**353**	MS^2 [353]: 191 (100) MS^3 [353→191]: 173 (10.0), 171 (57.5), 155 (91.2), 127 (98.3), 111 (44.4), 109 (12.3), 85 (18.6)	5-*O*-Caffeoylquinic acid isomer						✓	✓	
60	10.1	**431**	MS^2 [431]: 385 (100), 161 (20.2), 139 (10.6) MS^3 [431→385]: 337 (28.8), 233 (22.7), 224 (100), 223 (10.3), 205 (18.3), 186 (54.8), 161 (76.0), 153 (85.4)	Roseoside (formate adduct)	✓	✓	✓	✓		✓	✓	[106]
62	10.3	**577** $[2M-H]^-$	MS^2 [577]: 425 (91.2), 407 (100), 289 (25.3), 203 (14.0) MS^3 [577→407]: 389 (98.3), 335 (100), 297 (79.0), 283 (25.0) MS^3 [577→425]: 407 (100), 381 (27.3), 339 (52.7), 299 (16.4), 299 (14.9) MS^4 [577→425→407]: 389 (34.5), 285 (100), 284 (20.5), 281 (24.7), 256 (29.5)	Procyanin dimer (B type)	✓	✓	✓	✓		✓	✓	[84]
63	10.8	**707** $[2M-H]^-$	MS^2 [707]: 353 (100) MS^3 [707→353]: 191 (100) MS^4 [707→353→191]: 127 (100), 111 (40.2), 109 (65.8), 93 (31.8)	Caffeoylquinic acid dimer						✓	✓	
64	11.1	**353**	MS^2 [353]: 191 (100) MS^3 [353→191]: 173 (85.0), 171 (56.1), 127 (100), 111 (65.4), 109 (53.2), 93 (52.2), 85 (48.4)	Caffeoylquinic acid	✓	✓	✓	✓		✓	✓	
65	11.6	**289**	MS^2 [289]: 245 (100), 205 (38.2), 203 (18.1), 179 (16.1) MS^3 [289→245]: 227 (100), 203 (88.8), 188 (19.3), 175 (37.7), 159 (20.2)	Catechin	✓	✓	✓	✓		✓	✓	Standard
66	11.8	**517**	MS^2 [517]: 473 (51.6), 343 (85.7), 255 (79.0), 233 (12.5), 193 (12.2), 191 (100) MS^3 [517→191]: 173 (100), 127 (43.7), 111 (25.9)	Quinic acid derivative				✓		✓	✓	
67	12.1	**539**	MS^2 [539]: 491 (100) MS^3 [539→491]: 456 (18.2), 357 (100), 166 (45.4) MS^3 [539→491]: 448 (21.5), 358 (15.3), 357 (43.3), 329 (100), 314 (12.7) MS^3 [539→491]: 357 (100), 329 (95.4), 314 (32.9), 297 (13.3)	Dimethoxy-hydroxytricin-*O*-hexoside			✓	✓		✓	✓	

			MS^4 [539→491→329]: 314 (100), **299**, 283 (37.5), 265 (21.4), 164 (36.1), 149 (92.9)									
68	12.7	**865** $[3M-H]^-$	MS^2 [865]: 847 (10.9), 739 (40.9), 695 (100), 578 (23.8), 577 (79.2), 575 (33.0), 543 (31.0), 525 (11.8), 451 (49.7), 449 (27.1), 425 (24.1), 408 (10.4), 407 (64.6), 405 (24.6), 289 (12.2), 287 (39.7) MS^3 [865→695]: 676 (24.4), 677 (54.8), 658 (25.3), 568 (17.2), 543 (100), 529 (30.6), 526 (31.7), 525 (97.6), 451 (33.0), 407 (22.3), 405 (14.9), 391 (13.7), 363 (21.5), 289 (13.1), 256 (31.9), 243 (84.5) MS^4 [865→695→525]: 403 (100), 361 (50.0)	Procyanidin trimer (B type)		✓	✓	✓	✓	✓	[84]
69	12.8	**491**	MS^2 [491]: 329 (100), 330 (24.1), 331 (10.9), 345 (27.3) MS^3 [491→329]: 314 (100), 299 (19.6), 285 (18.6), 270 (35.7) MS^4 [491→329→314]: 271 (18.0), 283 (15.0), 298 (23.8), 299 (100), 300 (10.1)	Tricin-*O*-hexoside		✓					[106]
70	13.0	**337**	MS^2 [337]: 191 (100) MS^3 [337→191]: 173 (27.3), 171 (19.3), 127 (100), 111 (17.2), 109 (39.1), 93 (37.3), 85 (57.7)	5-*p*-Coumaroylquinic acid	✓	✓	✓	✓	✓	✓	[221]
71	13.8	**791**	MS^2 [791]: 679 (100), 619 (29.6), 517 (43.8) MS^3 [791→679]: 619 (28.4), 589 (15.1), 559 (18.4), 517 (100), 473 (14.9), 191 (10.4) MS^4 [791→679→517]: 473 (90.4), 353 (24.2), 191 (100)	Caffeyolquinic acid derivative			✓	✓	✓	✓	
72	14.2	**625**	MS^2 [625]: 463 (16.9), 301 (100) MS^3 [625→301]: 272 (41.6), 256 (79.0), 255 (62.9), 179 (100), 151 (89.1)	Quercetin-*O*-dihexoside	✓	✓	✓	✓	✓	✓	[200]
73	15.0	**791**	MS^2 [791]: 679 (100), 619 (91.4), 589 (23.9), 517 (46.4) MS^3 [791→679]: 619 (100), 589 (55.6), 517 (66.9), 353 (18.9), 191 (19.9) MS^4 [791→679→619]: 517 (88.1), 353 (22.4), 299 (60.7), 256 (15.8), 227 (16.1), 191 (100)	Caffeyolquinic acid derivative			✓	✓	✓	✓	
74	15.0	**643**	MS^2 [643]: 463 (100) MS^3 [643→463]: 301 (100) MS^4 [643→463→301]: 229 (14.5), 179 (100), 151 (23.8)	Quercetin-*O*-hexoside derivative			✓				
75	15.3	**367**	MS^2 [367]: 349 (10.7), 191 (36.5), 179 (36.5), 135 (33.3) MS^3 [367→179]: 135 (100)	Methyl-(5-caffeoyl)quinate	✓	✓	✓	✓	✓	✓	[228]
76	15.9	**635**	MS^2 [635]: 463 (100), 301 (12.9) MS^3 [635→463]: 301 (100), 151 (45.1)	Quercetin-*O*-hexoside derivative	✓	✓	✓	✓	✓	✓	
77	16.2	**337**	MS^2 [337]: 191 (100) MS^3 [337→191]: 173 (14.2), 127 (100), 109 (41.2), 93 (31.3)	5-*p*-Coumaroylquinic acid			✓				[221]
78	16.3	**791**	MS^2 [791]: 679 (100), 619 (59.4), 589 (14.0), 559 (10.6), 517 (37.2) MS^3 [791→679]: 619 (72.9), 589 (18.5), 559 (17.1), 517 (100), 353 (11.6) MS^4 [791→679→517]: 353 (35.4), 289 (47.9), 255 (71.0), 191 (100), 173 (10.7)	Caffeoylquinic acid derivative			✓	✓	✓	✓	

79	16.4	**595**	MS^2 [595]: 445 (18.4), 301 (47.4), 301 (100), 271 (16.1), 255 (10.8) MS^3 [595→301]: 271 (100), 255 (74.5), 193 (51.5), 179 (19.8), 151 (50.0)	Quercetin-*O*-(pentosyl)hexoside			✓	✓	✓	✓	[84]
80	16.7	**479**	MS^2 [479]: 318 (17.4), 317 (83.0), 316 (100) MS^3 [479→317]: 288 (30.0), 287 (98.1), 273 (12.0), 272 (34.3), 271 (100), 255 (100), 179 (84.8), 151 (36.2) MS^4 [479→317→271]: 179 (100), 151 (44.5)	Myricetin-*O*-hexoside	✓	✓					[142]
81	17.2	**739**	MS^2 [739]: 629 (16.6), 587 (100), 569 (44.0), 435 (37.1), 339 (32.0) MS^3 [739→587]: 569 (100), 417 (99.0), 339 (75.0), 325 (22.6), 229 (23.6) MS^4 [739→587→339]: 229 (32.8), 178 (17.3), 177 (100), 117 (23.4) MS^4 [739→587→417]: 376 (63.9), 308 (69.0), 281 (100), 255 (10.9), 182 (10.5)	Unknown			✓	✓	✓	✓	
82	17.9	**367**	MS^2 [367]: 191 (17.0), 179 (100), 161 (17.5), 135 (62.7) MS^3 [367→179]: 135 (100)	Methyl-(5-caffeoyl)quinate	✓	✓	✓	✓	✓	✓	[228]
83	18.2	**535**	MS^2 [535]: 491 (18.5), 373 (60.7), 329 (90.6), 191 (66.6), 163 (100) MS^3 [535→329]: 311 (12.0), 285 (41.0), 163 (100), 145 (36.9), 119 (38.8) MS^4 [535→329→163]: 119 (100)	Coumaroyl iridoid	✓	✓	✓	✓	✓	✓	[84]
84	18.4	**455**	MS^2 [455]: 325 (48.1), 265 (97.1), 235 (100), 163 (39.3) MS^3 [455→235]: 163 (100), 119 (46.7) MS^3 [455→265]: 205 (100), 163 (86.4), 119 (30.0)	Coumaric acid derivative			✓	✓	✓	✓	
85	19.0	**355**	MS^2 [355]:194 (11.5), 193 (100) MS^3 [355→193]:162 (35.8), 134 (100)	Ferulic acid-*O*-hexoside		✓					[80]
86	19.5	**609**	MS^2 [609]: 301 (100), 300 (30.3) MS^3 [609→301]: 273 (12.0), 272 (16.3), 271 (23.7), 255 (14.2), 193 (10.6), 179 (83.1), 151 (100), 107 (16.3)	Quercetin-*O*-rutinoside (Rutin)	✓	✓	✓	✓	✓	✓	[200]
87	19.8	**535**	MS^2 [535]: 491 (13.0), 373 (52.5), 372 (18.4), 371 (73.5), 330 (15.9), 329 (95.0), 311 (28.6), 267 (11.4), 239 (15.9), 191 (100), 166 (13.6), 165 (54.3), 164 (11.5), 163 (92.1) MS^3 [535→329]: 267 (41.7), 165 (86.7), 164 (12.2), 163 (100), 147 (18.2), 145 (13.2), 123 (19.0), 119 (26.1)	Coumaroyl iridoid	✓	✓	✓	✓	✓	✓	[84]
88	19.9	**455**	MS^2 [455]: 385 (20.1), 325 (25.3), 265 (72.6), 235 (100), 163 (38.1), 145 (11.0) MS^3 [455→235]: 163 (100) MS^3 [455→265]: 205 (100), 163 (33.3), 119 (15.8)	Coumaric acid derivative	✓	✓	✓	✓	✓	✓	
89	19.9	**449**	MS^2 [449]: 317 (51.4), 316 (100), 271 (16.2), 241 (11.6) MS^3 [449→317]: 271 (100), 243 (22.0), 242 (21.4), 179 (62.8), 151 (29.5)	Myricetin-*O*-pentoside	✓	✓					[79]
90	20.2	**535**	MS^2 [535]: 491 (45.3), 371 (100), 329 (79.5), 191 (91.8), 163 (92.8), 161 (11.7) MS^3 [535→329]: 163 (83.8), 147 (17.5), 119 (100)	Coumaroyl iridoid	✓	✓					[84]
91	20.4	**451**	MS^2 [451]: 341 (100)	Cinchonain-Ib			✓	✓	✓		[84]

			MS^3 [451→341]: 323 (13.3), 297 (10.5), 217 (100), 177 (15.0) MS^4 [451→341→217]: 191 (100), 189 (90.7)									
92	20.9	**689**	MS^2 [689]: 527 (100), 353 (59.7), 191 (10.5) MS^3 [689→527]: 353 (99.6), 191 (100), 179 (22.8) MS^4 [689→527→353]: 191 (100)	Caffeoylquinic acid derivative			✓	✓				
93	21.5	**463**	MS^2 [463]: 302 (11.4), 301 (100), 300 (30.1) MS^3 [463→301]: 271 (27.4), 255 (37.0), 179 (96.0), 151 (100)	Quercetin-*O*-hexoside			✓	✓	✓	✓		[84]
94	21.6	**463**	MS^2 [463]: 318 (12.2), 317 (100) MS^3 [463→317]: 288 (23.9), 287 (44.6), 272 (98.2), 271 (100), 269 (50.5), 232 (29.3), 179 (96.3), 151 (44.6)	Myricetin-*O*-deoxyhexoside	✓	✓						Standard
95	22.6	**463**	MS^2 [463]: 302 (11.4), 301 (100), 300 (30.1) MS^3 [463→301]: 271 (27.4), 255 (37.0), 179 (96.0), 151 (100)	Quercetin-*O*-hexoside	✓	✓	✓	✓	✓	✓		[84]
96	23.3	**535**	MS^2 [535]: 517 (11.5), 473 (17.0), 371 (23.2), 355 (100), 329 (70.2), 311 (36.1), 163 (16.3), 147 (22.6) MS^3 [535→355]: 163 (96.3), 147 (18.7), 119 (22.1)	Coumaric acid derivative				✓	✓	✓		
97	23.8	**493**	MS^2 [493]: 456 (10.3), 331 (100), 330 (36.2) MS^3 [493→331]: 316 (100), 315 (16.2), 193 (11.4), 179 (46.3), 151 (10.3) MS^4 [493→331→316]: 299 (15.4), 273 (24.9), 271 (31.4), 270 (72.4), 203 (94.6), 179 (80.2), 151 (100)	Laricitrin-*O*-hexoside	✓	✓						[212]
98	24.1	**463**	MS^2 [463]: 302 (11.4), 301 (100), 300 (30.1) MS^3 [463→301]: 271 (27.4), 255 (37.0), 179 (96.0), 151 (100)	Quercetin-*O*-hexoside	✓	✓						[84]
99	24.3	**579**	MS^2 [579]: 417 (100) MS^3 [579→417]: 403 (15.1), 372 (10.2), 181 (100), 166 (41.3), 151 (15.6) MS^4 [579→417→181]: 172 (12.3), 166 (100)	Syringaresinol-*O*-hexoside			✓		✓	✓		
100	24.5	**575** $[2M-H]^-$	MS^2 [575]: 449 (100), 424 (21.8), 423 (46.9), 289 (1.,4), 285 (17.4) MS^3 [575→449]: 287 (100)	Procyanidin dimer (A type)	✓	✓						[84]
101	26.1	**433**	MS^2 [433]: 301 (100), 300 (92.7) MS^3 [433→301]: 273 (11.4), 272 (38.0), 271 (100), 256 (15.9), 255 (62.7), 179 (78.7), 151 (95.5) MS^4 [433→301→271]: 245 (32.8), 243 (23.1), 229 (100), 227 (14.7), 211 (24.0), 199 (13.0), 185 (13.0), 163 (18.5), 158 (10.7)	Quercetin-*O*-pentoside					✓	✓		[84]
102	26.7	**593**	MS^2 [593]: 285 (100) MS^3 [593→285]: 267 (49.6), 257 (100), 241 (52.0), 229 (41.3), 213 (70.2), 197 (57.2), 163 (68.9)	Kaempferol-*O*-rutinoside			✓	✓	✓	✓		[224]
103	27.0	**469**	MS^2 [469]: 326 (10.1), 325 (83.8), 265 (80.8), 235 (100), 163 (16.7) MS^3 [469→235]: 163 (100) MS^4 [469→235→163]: 119 (100)	4-Benzoyl-9-*p*-coumaroyl- 2,7-anhydro-3-DOA	✓	✓	✓	✓	✓	✓		[233]
104	27.3	**433**	MS^2 [433]: 301 (100) MS^3 [433→301]: 271 (100), 255 (58.5), 179 (95.7), 151 (55.0)	Quercetin-*O*-pentoside	✓	✓	✓	✓	✓	✓		[84]
105	27.5	**451**	MS^3 [451→341]: 323 (17.0), 231 (21.2), 218 (15.5), 217 (100), 177 (20.1) MS^4 [451→341→217]: 191 (39.8), 189 (12.5), 189 (100)	Cinchonain-Ib			✓	✓	✓	✓		[84]
106	27.7	**629**	MS^2 [629]: 421 (100)	Di(methyl-syringate)-*O*-hexoside			✓					

			MS^3 [629→421]: 211 (100), 196 (25.5), 181 (44.4), 153 (33.7) MS^4 [629→421→211]: 197 (65.7), 196 (100)	(formate adduct)								
107	28.4	**505**	MS^2 [505]: 301 (100) MS^3 [505→301]: 271 (74.7), 179 (54.1), 151 (100)	Quercetin-*O*-(acetyl)hexoside			✓	✓		✓	✓	[224]
108	28.7	**447**	MS^2 [447]: 327 (15.5), 285 (100), 255 (31.1) MS^3 [447→285]: 255 (100), 227 (41.6), 210 (28.7), 184 (53.7), 163 (23.6)	Kaempferol-*O*-hexoside	✓	✓						[200]
109	28.9	**437**	MS^2 [437]: 325 (45.5), 267 (13.0), 265 (76.2), 235 (100), 163 (25.8) MS^3 [437→235]: 163 (100), 119 (12.5)	Coumaric acid derivative			✓	✓		✓	✓	
110	28.6	**653**	MS^2 [653]: 593 (10.7), 491 (33.4), 345 (100), 330 (38.9), 315 (17.7) MS^3 [653→345]: 330 (100), 329 (17.6), 315 (42.4), 287 (31.8), 285 (17.4), 271 (41.9)	6,3-Dimethoxyquercetin-3-*O*-β-D-6-(*p*-coumaroyl)glucopyranoside	✓	✓	✓	✓		✓	✓	[230]
111	29.8	**477**	MS^2 [477]: 437 (10.2), 331 (100), 315 (13.1), 287 (14.6), 271 (10.1) MS^3 [477→331]: 316 (100), 298 (12.4), 287 (10.8), 272 (11.6), 151 (13.1) MS^4 [477→331→316]: 287 (100), 179 (89.3)	Laricitrin-*O*-rhamnoside	✓	✓						
112	29.8	**507**	MS^2 [507]: 345 (100), 301 (13.7) MS^3 [507→345]: 331 (12.5), 330 (100), 317 (12.9), 315 (58.2), 301 (97.4), 274 (13.0), 273 (35.4), 259 (15.2), 241 (10.6) MS^3 [507→345→301]: 286 (79.4), 273 (20.6), 270 (33.9), 269 (100), 258 (23.7), 241 (78.8)	6-Hydroxy-7,4-dimethoxyquercetin-*O*-hexoside	✓	✓						[230]
113	30.0	**437**	MS^2 [437]: 325 (45.5), 267 (13.0), 265 (76.2), 235 (100), 163 (25.8) MS^3 [437→235]: 163 (100) MS^3 [437→265]: 205 (100), 163 (72.5), 119 (78.5)	Coumaric acid derivative	✓	✓	✓	✓		✓	✓	
114	30.1	**473**	MS^2 [473]: 438 (20.3), 437 (100), 325 (58.2), 265 (19.2), 235 (41.0) MS^3 [473→437]: 325 (78.6), 265 (87.5), 236 (20.3), 235 (100), 205 (14.2), 163 (23.2) MS^4 [473→437→235]: 163 (100), 119 (13.5)	Coumaric acid derivative	✓	✓	✓	✓		✓	✓	
115	30.4	**505**	MS^2 [505]: 445 (67.4), 301 (100), 271 (17.0) MS^3 [505→301]: 271 (74.7), 255 (81.4), 151 (100)	Quercetin-*O*-(acetyl)hexoside	✓	✓	✓	✓		✓	✓	[224]
116	31.8	**417**	MS^2 [417]: 285 (100) MS^3 [417→285]: 267 (18.9), 257 (53.1), 255 (100), 241 (21.6), 229 (39.0)	Kaempferol-*O*-pentoside	✓	✓	✓	✓		✓	✓	[107]
117	31.9	**489**	MS^2 [489]: 285 (100) MS^3 [489→285]: 255 (68.4), 257 (100), 229 (40.1), 213 (23.2), 197 (26.0)	Kaempferol-*O*-(acetyl)hexoside	✓	✓	✓	✓		✓	✓	[87]
118	32.4	**533**	MS^2 [533]: 489 (100) MS^3 [533→489]: 285 (100), 267 (18.9), 257 (53.1), 241 (21.6), 229 (34.1), 213 (10.7), 167 (12.3)	Kaempferol-*O*-(malonyl)hexoside	✓	✓	✓	✓		✓	✓	
119	32.5	**563**	MS^2 [563]: 531 (100), 463 (79.7) MS^3 [563→531]: 463 (100), 301 (18.9) MS^4 [563→531→463]: 301 (99.3), 179 (100), 151 (18.2)	Quercetin-*O*-hexoside derivative	✓	✓	✓	✓		✓	✓	

120	32.8	**451**	MS^2 [451]: 341 (100) MS^3 [451→341]: 231 (12.9), 217 (100), 189 (15.8), 177 (12.4) MS^4 [451→341→217]: 191 (100), 190 (10.8), 189 (93.8)	Cinchonain-Ib	✓	✓	✓	✓		✓	✓		[84]
121	33.0	**613**	MS^2 [613]: 503 (100), 461 (11.7), 393 (12.6), 341 (10.2) MS^3 [613→503]: 393 (100), 379 (12.2), 351 (25.8), 341 (96.7), 307 (16.7) MS^4 [613→503→393]: 375 (15.6), 304 (25.8), 285 (47.1), 255 (22.3), 241 (63.5), 239 (100), 229 (69.1), 225 (18.2), 197 (12.1)	bis-Dihydroxylphenylpropanoid-substituted catechin			✓	✓		✓	✓		[229]
122	33.1	**549**	MS^2 [549]: 345 (100), 330 (13.5) MS^3 [549→345]: 330 (100), 315 (30.5), 302 (14.4) MS^4 [549→345→330]: 315 (100), 287 (38.8), 271 (14.2)	6-Hydroxy-7,4-dimethoxy-quercetin-*O*-(acety)lhexoside	✓	✓							
123	33.4	**489**	MS^2 [489]: 285 (100) MS^3 [489→285]: 255 (68.4), 257 (100), 229 (40.1), 213 (23.2), 197 (26.0)	Kaempferol-*O*-(acetyl)hexoside			✓	✓		✓	✓		[87]
124	33.9	**471**	MS^2 [471]: 307 (100), 163 (23.8), 145 (18.7) MS^3 [471→307]: 247 (24.2), 201 (30.7), 187 (28.5), 163 (59.9), 159 (15.2), 145 (100), 119 (25.1)	Coumaric acid derivative	✓	✓	✓	✓		✓	✓		
125	34.5	**585**	MS^2 [585]: 555 (16.0), 537 (73.0), 371 (41.1), 359 (37.0), 357 (79.5), 345 (100) MS^3 [585→345]: 330 (100) MS^4 [585→345→330]: 297 (100), 255 (63.7), 213 (43.6)	6-Hydroxy-7,4-dimethoxyquercetin derivative			✓	✓		✓	✓		
126	34.8	**613**	MS^2 [613]: 503 (100), 461 (11.7), 393 (12.6), 341 (10.2) MS^3 [613→503]: 393 (100), 379 (12.2), 351 (25.8), 341 (96.7), 307 (16.7) MS^4 [613→503→393]: 375 (15.6), 304 (25.8), 285 (47.1), 255 (22.3), 241 (63.5), 239 (100), 229 (69.1), 225 (18.2), 197 (12.1)	bis-Dihydroxylphenylpropanoid-substituted catechin			✓	✓		✓	✓		[229]
127	35.3	**585**	MS^2 [585]: 371 (41.2), 359 (45.4), 357 (71.0), 345 (100) MS^3 [585→345]: 330 (100), 299 (14.2) MS^4 [585→345→330]: 315 (35.6), 297 (100), 256 (37.4), 251 (14.5), 213 (16.4)	6-Hydroxy-7,4-dimethoxyquercetin derivative			✓	✓		✓	✓		
128	35.5	**479**	MS^2 [479]: 307 (100), 289 (11.6), 235 (44.8), 163 (54.2), 145 (10.4) MS^3 [479→307]: 259 (17.1), 235 (31.4), 217 (19.7), 215 (15.6), 163 (100), 119 (18.1)	Coumaric acid derivative						✓	✓		
129	38.0	**763**	MS^2 [763]: 343 (100), 328 (13.5) MS^3 [763→343]: 328 (100), 183 (17.1), 164 (14.7) MS^4 [763→343→328]: 236 (31.2), 224 (25.3), 212 (33.1), 183 (61.1), 183 (86.0), 182 (100), 164 (67.3), 138 (32.7), 121 (16.0)	Unknown			✓	✓		✓	✓		

t_R: retention time; HHDP: hexahydroxydiphenoyl; DOA: deoxy-2-octulopyranosonic acid

Table S 20 - Characterization of anthocyanins of *V. padifolium* (berries and leaves) methanolic extracts by HPLC-ESI$^+$/MS^n.

Nº	t_R (min)	[M-H]$^-$ (*m/z*)	HPLC-DAD-ESI/MS^n *m/z* (% base peak)	Assigned identity	Berries		Young Leaves		References
					2013	2014	2013	2014	
3	3.5	**597**	MS^2 [597]: 303 (100) MS^3 [597→303]: 257 (59.9), 229 (4100), 201 (26.8), 159 (46.6), 150 (25.7)	Delphinidin-*O*-(pentosyl)hexoside	✓	✓			[214]
5	3.6	**465**	MS^2 [465]: 303 (100) MS^3 [465→303]: 257 (100), 229 (42.2), 201 (26.8), 159 (46.6), 150 (25.7)	Delphinidin-*O*-hexoside	✓	✓			[200]
7	3.8	**435**	MS^2 [435]: 303 (100) MS^3 [435→303]: 257 (100), 229 (42.2), 201 (26.8), 159 (46.6), 150 (25.7)	Delphinidin-*O*-pentoside	✓				[188,214]
9	4.1	**479**	MS^2 [479]: 317 (100) MS^3 [479→317]: 302 (100), 275 (12.6), 274 (50.0), 246 (15.4), 229 (11.7), 228 (10.3)	Petunidin-*O*-hexoside	✓	✓			[200]
10	4.3	**449**	MS^2 [449]: 317 (17.4), 303 (61.9), 287 (100) MS^3 [449→287]: 241 (82.2), 213 (100), 175 (57.6), 161 (87.3), 153 (78.9), 137 (24.6), 109 (19.2)	Cyanidin-3-*O*-glucoside			✓	✓	Standard
13	4.4	**597**	MS^2 [597]: 303 (100) MS^3 [597→303]: 257 (100), 229 (42.2), 201 (26.8), 159 (46.6), 150 (25.7)	Delphinidin-*O*-(pentosyl)hexoside		✓			[214]
16	4.6	**465**	MS^2 [465]: 303 (100) MS^3 [465→303]: 275 (16.9), 257 (100), 229 (29.4), 201 (25.3), 165 (24.3), 161 (21.8), 151 (10.3)	Delphinidin-*O*-hexoside	✓				[200]
18	4.7	**435**	MS^2 [435]: 303 (100) MS^3 [435→303]: 257 (100), 229 (42.2), 213 (54.2), 201 (26.8), 159 (46.6), 150 (25.7)	Delphinidin-*O*-pentoside	✓	✓			[188,214]
19	4.8	**611**	MS^2 [611]: 317 (100) MS^3 [611→317]: 303 (100), 274 (57.3), 257 (14.4), 245 (24.3), 229 (34.4), 218 (33.1), 203 (27.1), 150 (27.2)	Petunidin-*O*-(pentosyl)hexoside	✓				[214]
20	4.8	**479**	MS^2 [479]: 317 (100) MS^3 [479→317]: 303 (100), 274 (57.3), 257 (14.4), 245 (24.3), 229 (34.4), 218 (33.1), 203 (27.1), 150 (27.2)	Petunidin-*O*-hexoside					[200]
21	4.9	**449**	MS^2 [449]: 317 (17.4), 303 (61.9), 287 (100) MS^3 [449→287]: 241 (82.2), 213 (100), 175 (57.6), 161 (87.3), 153 (78.9), 137 (24.6), 109 (19.2)	Cyanidin-*O*-hexoside	✓	✓	✓	✓	
23	5.1	**419**	MS^2 [419]: 317 (17.4), 303 (61.9), 287 (100) MS^3 [419→287]: 241 (82.2), 213 (100), 175 (57.6), 161 (87.3), 153 (78.9), 137 (24.6), 109 (19.2)	Cyanindin-*O*-pentoside			✓	✓	[188,214]
25	5.2	**479**	MS^2 [479]: 317 (100) MS^3 [479→317]: 303 (100), 274 (57.3), 257 (14.4), 245 (24.3), 229 (34.4), 218 (33.1), 203 (27.1), 150 (27.2)	Petunidin-*O*-hexoside	✓	✓			[200]
26	5.3	**449**	MS^2 [449]: 317 (100), 303 (47.7) MS^3 [449→317]: 303 (100), 274 (57.3), 257 (14.4), 245 (24.3), 229 (34.4), 218 (33.1), 203 (27.1), 150 (27.2)	Petunidin-*O*-pentoside	✓	✓			[214]
28	5.4	**449**	MS^2 [449]: 303 (100) MS^3 [449→303]: 257 (100), 229 (42.2), 201 (26.8), 159 (46.6), 150 (25.7) MS^4 [449→303→257]: 229 (100), 213 (54.2), 201 (19.9), 147 (21.1), 117 (10.1)	Delphinidin-*O*-rhamnoside					[214]
31	5.9	**493**	MS^2 [493]: 331 (100)	Malvidin-*O*-hexoside	✓	✓			[200]

			MS^3 [493→331]: 315 (100), 299 (66.5), 298 (28.1), 287 (50.3), 271 (15.9), 242 (13.4), 179 (27.7)						
32	6.0	**449**	MS^2 [449]: 317 (100), 303 (47.7) MS^3 [449→317]: 303 (100), 274 (57.3), 257 (14.4), 245 (24.3), 229 (34.4), 218 (33.1), 203 (27.1), 150 (27.2)	Petunidin-*O*-pentoside	✓	✓			[214]
34	6.2	**463**	MS^2 [463]: 301 (100) MS^3 [463→301]: 287 (100), 268 (0.3), 258 (50.0), 230 (50.4), 213 (36.7), 202 (26.4), 187 (14.4), 177 (11.1), 147 (11.0)	Peonidin-*O*-hexoside	✓	✓			[200]
36	6.6	**627**	MS^2 [627]: 465 (100), 303 (28.9) MS^3 [627→465]: 303 (54.7), 257 (100), 229 (42.2), 213 (54.2), 201 (26.8), 159 (46.6), 150 (25.7)	Delphinidin-*O*-dihexoside			✓		[206]
39	6.7	**449**	MS^2 [449]: 317 (17.4), 303 (61.9), 287 (100) MS^3 [449→287]: 241 (82.2), 213 (100), 175 (57.6), 161 (87.3), 153 (78.9), 137 (24.6), 109 (19.2)	Cyanidin-*O*-hexoside			✓	✓	
42	6.9	**493**	MS^2 [493]: 331 (100) MS^3 [493→331]: 315 (53.1), 299 (100), 287 (21.3), 271 (15.9), 242 (13.4), 179 (27.7)	Malvidin-*O*-hexoside	✓	✓			[200]
45	7.4	**463**	MS^2 [463]: 331 (100) MS^3 [463→331]: 315 (53.1), 299 (100), 287 (21.3), 271 (15.9), 242 (13.4), 179 (27.7)	Malvidin-*O*-pentoside	✓	✓			[188,214]
46	7.5	**493**	MS^2 [493]: 331 (100) MS^3 [493→331]: 315 (53.1), 299 (100), 287 (21.3), 271 (15.9), 242 (13.4), 179 (27.7)	Malvidin-O-hexoside	✓	✓			[200]
52	8.8	**493**	MS^2 [493]: 331 (100) MS^3 [493→331]: 315 (53.1), 299 (100), 287 (21.3), 271 (15.9), 242 (13.4), 179 (27.7)	Malvidin-*O*-hexoside	✓	✓			[200]
55	9.0	**477**	MS^2 [477]: 331 (100) MS^3 [477→331]: 315 (100), 299 (66.5), 298 (28.1), 287 (50.3), 271 (15.9), 242 (13.4), 179 (27.7)	Malvidin-*O*-rhamnoside	✓				
58	9.6	**493**	MS^2 [493]: 331 (100) MS^3 [493→331]: 299 (100), 287 (21.3), 271 (15.9), 242 (13.4), 179 (27.7)	Malvidin-*O*-hexoside		✓			[200]
59	10.0	**477**	MS^2 [477]: 331 (100) MS^3 [477→331]: 315 (100), 299 (66.5), 298 (28.1), 287 (50.3), 271 (15.9), 242 (13.4), 179 (27.7)	Malvidin-*O*-rhamnoside	✓	✓			
61	10.2	**463**	MS^2 [463]: 331 (100) MS^3 [463→331]: 315 (100), 299 (66.5), 298 (28.1), 287 (50.3), 271 (15.9), 242 (13.4), 179 (27.7)	Malvidin-*O*-pentoside	✓				[188,214]

t_R: retention time